

TRANSFORMER
AND INDUCTOR DESIGN
HANDBOOK
Third Edition, Revised and Expanded

COLONEL WM. T. MCLYMAN
Kg Magnetics, Inc.
Idyllwild, California, U.S.A.

Although great care has been taken to provide accurate and current information, neither the author(s) nor the publisher, nor anyone else associated with this publication, shall be liable for any loss, damage, or liability directly or indirectly caused or alleged to be caused by this book. The material contained herein is not intended to provide specific advice or recommendations for any specific situation.

Trademark notice: Product or corporate names may be trademarks or registered trademarks and are used only for identification and explanation without intent to infringe.

Library of Congress Cataloging-in-Publication Data

A catalog record for this book is available from the Library of Congress.

ISBN: 0-8247-5393-3

This book is printed on acid-free paper.

Headquarters

Marcel Dekker, Inc.
270 Madison Avenue, New York, NY 10016, U.S.A.
tel: 212-696-9000; fax: 212-685-4540

Distribution and Customer Service

Marcel Dekker, Inc.
Cimarron Road, Monticello, New York 12701, U.S.A.
tel: 800-228-1160; fax: 845-796-1772

Eastern Hemisphere Distribution

Marcel Dekker AG
Hutgasse 4, Postfach 812, CH-4001 Basel, Switzerland
tel: 41-61-260-6300; fax: 41-61-260-6333

World Wide Web

<http://www.dekker.com>

The publisher offers discounts on this book when ordered in bulk quantities. For more information, write to Special Sales/Professional Marketing at the headquarters address above.

Copyright © 2004 by Marcel Dekker, Inc. All Rights Reserved.

Neither this book nor any part may be reproduced or transmitted in any form or by any means, electronic or mechanical, including photocopying, microfilming, and recording, or by any information storage and retrieval system, without permission in writing from the publisher.

Current printing (last digit):

10 9 8 7 6 5 4 3 2 1

PRINTED IN THE UNITED STATES OF AMERICA

ELECTRICAL AND COMPUTER ENGINEERING

A Series of Reference Books and Textbooks

FOUNDING EDITOR

Marlin O. Thurston

Department of Electrical Engineering
The Ohio State University
Columbus, Ohio

1. Rational Fault Analysis, *edited by Richard Saeks and S. R. Liberty*
2. Nonparametric Methods in Communications, *edited by P. Papantoni-Kazakos and Dimitri Kazakos*
3. Interactive Pattern Recognition, *Yi-tzue Chien*
4. Solid-State Electronics, *Lawrence E. Murr*
5. Electronic, Magnetic, and Thermal Properties of Solid Materials, *Klaus Schröder*
6. Magnetic-Bubble Memory Technology, *Hsu Chang*
7. Transformer and Inductor Design Handbook, *Colonel Wm. T. McLyman*
8. Electromagnetics: Classical and Modern Theory and Applications, *Samuel Seely and Alexander D. Poularikas*
9. One-Dimensional Digital Signal Processing, *Chi-Tsong Chen*
10. Interconnected Dynamical Systems, *Raymond A. DeCarlo and Richard Saeks*
11. Modern Digital Control Systems, *Raymond G. Jacquot*
12. Hybrid Circuit Design and Manufacture, *Roydn D. Jones*
13. Magnetic Core Selection for Transformers and Inductors: A User's Guide to Practice and Specification, *Colonel Wm. T. McLyman*
14. Static and Rotating Electromagnetic Devices, *Richard H. Engelmann*
15. Energy-Efficient Electric Motors: Selection and Application, *John C. Andreas*
16. Electromagnetic Compossibility, *Heinz M. Schlicke*
17. Electronics: Models, Analysis, and Systems, *James G. Gottling*
18. Digital Filter Design Handbook, *Fred J. Taylor*
19. Multivariable Control: An Introduction, *P. K. Sinha*
20. Flexible Circuits: Design and Applications, *Steve Gurley, with contributions by Carl A. Edstrom, Jr., Ray D. Greenway, and William P. Kelly*
21. Circuit Interruption: Theory and Techniques, *Thomas E. Browne, Jr.*
22. Switch Mode Power Conversion: Basic Theory and Design, *K. Kit Sum*
23. Pattern Recognition: Applications to Large Data-Set Problems, *Sing-Tze Bow*
24. Custom-Specific Integrated Circuits: Design and Fabrication, *Stanley L. Hurst*
25. Digital Circuits: Logic and Design, *Ronald C. Emery*
26. Large-Scale Control Systems: Theories and Techniques, *Magdi S. Mahmoud, Mohamed F. Hassan, and Mohamed G. Darwish*
27. Microprocessor Software Project Management, *Eli T. Fathi and Cedric V. W. Armstrong (Sponsored by Ontario Centre for Microelectronics)*
28. Low Frequency Electromagnetic Design, *Michael P. Perry*
29. Multidimensional Systems: Techniques and Applications, *edited by Spyros G. Tzafestas*
30. AC Motors for High-Performance Applications: Analysis and Control, *Sakae Yamamura*

31. Ceramic Motors for Electronics: Processing, Properties, and Applications, *edited by Relva C. Buchanan*
32. Microcomputer Bus Structures and Bus Interface Design, *Arthur L. Dexter*
33. End User's Guide to Innovative Flexible Circuit Packaging, *Jay J. Miniet*
34. Reliability Engineering for Electronic Design, *Norman B. Fuqua*
35. Design Fundamentals for Low-Voltage Distribution and Control, *Frank W. Kussy and Jack L. Warren*
36. Encapsulation of Electronic Devices and Components, *Edward R. Salmon*
37. Protective Relaying: Principles and Applications, *J. Lewis Blackburn*
38. Testing Active and Passive Electronic Components, *Richard F. Powell*
39. Adaptive Control Systems: Techniques and Applications, *V. V. Chalam*
40. Computer-Aided Analysis of Power Electronic Systems, *Venkatachari Rajagopalan*
41. Integrated Circuit Quality and Reliability, *Eugene R. Hnatek*
42. Systolic Signal Processing Systems, *edited by Earl E. Swartzlander, Jr.*
43. Adaptive Digital Filters and Signal Analysis, *Maurice G. Bellanger*
44. Electronic Ceramics: Properties, Configuration, and Applications, *edited by Lionel M. Levinson*
45. Computer Systems Engineering Management, *Robert S. Alford*
46. Systems Modeling and Computer Simulation, *edited by Naim A. Kheir*
47. Rigid-Flex Printed Wiring Design for Production Readiness, *Walter S. Rigling*
48. Analog Methods for Computer-Aided Circuit Analysis and Diagnosis, *edited by Takao Ozawa*
49. Transformer and Inductor Design Handbook: Second Edition, Revised and Expanded, *Colonel Wm. T. McLyman*
50. Power System Grounding and Transients: An Introduction, *A. P. Sakis Meliopoulos*
51. Signal Processing Handbook, *edited by C. H. Chen*
52. Electronic Product Design for Automated Manufacturing, *H. Richard Stillwell*
53. Dynamic Models and Discrete Event Simulation, *William Delaney and Erminia Vaccari*
54. FET Technology and Application: An Introduction, *Edwin S. Oxner*
55. Digital Speech Processing, Synthesis, and Recognition, *Sadaoki Furui*
56. VLSI RISC Architecture and Organization, *Stephen B. Furber*
57. Surface Mount and Related Technologies, *Gerald Ginsberg*
58. Uninterruptible Power Supplies: Power Conditioners for Critical Equipment, *David C. Griffith*
59. Polyphase Induction Motors: Analysis, Design, and Application, *Paul L. Cochran*
60. Battery Technology Handbook, *edited by H. A. Kiehne*
61. Network Modeling, Simulation, and Analysis, *edited by Ricardo F. Garzia and Mario R. Garzia*
62. Linear Circuits, Systems, and Signal Processing: Advanced Theory and Applications, *edited by Nobuo Nagai*
63. High-Voltage Engineering: Theory and Practice, *edited by M. Khalifa*
64. Large-Scale Systems Control and Decision Making, *edited by Hiroyuki Tamura and Tsuneo Yoshikawa*
65. Industrial Power Distribution and Illuminating Systems, *Kao Chen*
66. Distributed Computer Control for Industrial Automation, *Dobrovoje Popovic and Vijay P. Bhatkar*
67. Computer-Aided Analysis of Active Circuits, *Adrian Ioinovici*
68. Designing with Analog Switches, *Steve Moore*

69. Contamination Effects on Electronic Products, *Carl J. Tautscher*
70. Computer-Operated Systems Control, *Magdi S. Mahmoud*
71. Integrated Microwave Circuits, *edited by Yoshihiro Konishi*
72. Ceramic Materials for Electronics: Processing, Properties, and Applications, Second Edition, Revised and Expanded, *edited by Relva C. Buchanan*
73. Electromagnetic Compatibility: Principles and Applications, *David A. Weston*
74. Intelligent Robotic Systems, *edited by Spyros G. Tzafestas*
75. Switching Phenomena in High-Voltage Circuit Breakers, *edited by Kunio Nakanishi*
76. Advances in Speech Signal Processing, *edited by Sadaoki Furui and M. Mohan Sondhi*
77. Pattern Recognition and Image Preprocessing, *Sing-Tze Bow*
78. Energy-Efficient Electric Motors: Selection and Application, Second Edition, *John C. Andreas*
79. Stochastic Large-Scale Engineering Systems, *edited by Spyros G. Tzafestas and Keigo Watanabe*
80. Two-Dimensional Digital Filters, *Wu-Sheng Lu and Andreas Antoniou*
81. Computer-Aided Analysis and Design of Switch-Mode Power Supplies, *Yim-Shu Lee*
82. Placement and Routing of Electronic Modules, *edited by Michael Pecht*
83. Applied Control: Current Trends and Modern Methodologies, *edited by Spyros G. Tzafestas*
84. Algorithms for Computer-Aided Design of Multivariable Control Systems, *Stanoje Bingulac and Hugh F. VanLandingham*
85. Symmetrical Components for Power Systems Engineering, *J. Lewis Blackburn*
86. Advanced Digital Signal Processing: Theory and Applications, *Glenn Zelniker and Fred J. Taylor*
87. Neural Networks and Simulation Methods, *Jian-Kang Wu*
88. Power Distribution Engineering: Fundamentals and Applications, *James J. Burke*
89. Modern Digital Control Systems: Second Edition, *Raymond G. Jacquot*
90. Adaptive IIR Filtering in Signal Processing and Control, *Phillip A. Regalia*
91. Integrated Circuit Quality and Reliability: Second Edition, Revised and Expanded, *Eugene R. Hnatek*
92. Handbook of Electric Motors, *edited by Richard H. Engelmann and William H. Middendorf*
93. Power-Switching Converters, *Simon S. Ang*
94. Systems Modeling and Computer Simulation: Second Edition, *Naim A. Kheir*
95. EMI Filter Design, *Richard Lee Ozenbaugh*
96. Power Hybrid Circuit Design and Manufacture, *Haim Taraseiskey*
97. Robust Control System Design: Advanced State Space Techniques, *Chia-Chi Tsui*
98. Spatial Electric Load Forecasting, *H. Lee Willis*
99. Permanent Magnet Motor Technology: Design and Applications, *Jacek F. Gieras and Mitchell Wing*
100. High Voltage Circuit Breakers: Design and Applications, *Ruben D. Garzon*
101. Integrating Electrical Heating Elements in Appliance Design, *Thor Hegbom*
102. Magnetic Core Selection for Transformers and Inductors: A User's Guide to Practice and Specification, Second Edition, *Colonel Wm. T. McLyman*
103. Statistical Methods in Control and Signal Processing, *edited by Tohru Katayama and Sueo Sugimoto*
104. Radio Receiver Design, *Robert C. Dixon*
105. Electrical Contacts: Principles and Applications, *edited by Paul G. Slade*

106. Handbook of Electrical Engineering Calculations, *edited by Arun G. Phadke*
107. Reliability Control for Electronic Systems, *Donald J. LaCombe*
108. Embedded Systems Design with 8051 Microcontrollers: Hardware and Software, *Zdravko Karakehayov, Knud Smed Christensen, and Ole Winther*
109. Pilot Protective Relaying, *edited by Walter A. Elmore*
110. High-Voltage Engineering: Theory and Practice, Second Edition, Revised and Expanded, *Mazen Abdel-Salam, Hussein Anis, Ahdab El-Morshedy, and Roshdy Radwan*
111. EMI Filter Design: Second Edition, Revised and Expanded, *Richard Lee Ozenbaugh*
112. Electromagnetic Compatibility: Principles and Applications, Second Edition, Revised and Expanded, *David Weston*
113. Permanent Magnet Motor Technology: Design and Applications, Second Edition, Revised and Expanded, *Jacek F. Gieras and Mitchell Wing*
114. High Voltage Circuit Breakers: Design and Applications, Second Edition, Revised and Expanded, *Ruben D. Garzon*
115. High Reliability Magnetic Devices: Design and Fabrication, *Colonel Wm. T. McLyman*
116. Practical Reliability of Electronic Equipment and Products, *Eugene R. Hnatek*
117. Electromagnetic Modeling by Finite Element Methods, *João Pedro A. Bastos and Nelson Sadowski*
118. Battery Technology Handbook: Second Edition, *edited by H. A. Kiehne*
119. Power Converter Circuits, *William Shepherd and Li Zhang*
120. Handbook of Electric Motors: Second Edition, Revised and Expanded, *edited by Hamid A. Toliyat and Gerald B. Kliman*
121. Transformer and Inductor Design Handbook: Third Edition, Revised and Expanded, *Colonel Wm. T. McLyman*

Additional Volumes in Preparation

Energy-Efficient Electric Motors: Third Edition, Revised and Expanded, *Ali Emadi*

To My Wife, Bonnie

Foreword

Colonel McLyman is a well-known author, lecturer, and magnetic circuit designer. His previous books on transformer and inductor design, magnetic core characteristics, and design methods for converter circuits have been widely used by magnetics circuit designers.

In this book, Colonel McLyman has combined and updated the information found in his previous books. He has also added several new subjects such as rotary transformer design, planar transformer design, and planar construction. The author covers magnetic design theory with all of the relevant formulas along with complete information on magnetic materials and core characteristics. In addition, he provides real-world, step-by-step design examples.

This book is a must for engineers working in magnetic design. Whether you are working on high “rel” state-of-the-art design or high-volume or low-cost production, this book is essential. Thanks, Colonel, for a well-done, useful book.

*Robert G. Noah
Application Engineering Manager (Retired)
Magnetics, Division of Spang and Company
Pittsburgh, Pennsylvania, U.S.A.*

Preface

I have had many requests to update *Transformer and Inductor Design Handbook*, because of the way power electronics has changed over the past few years. This new edition includes 21 chapters, with new topics such as: The forward converter, flyback converter, quiet converter, rotary transformers, and planar transformers, with even more design examples than the previous edition.

This book offers a practical approach, with design examples for design engineers and system engineers in the electronics and aerospace industries. Transformers are found in virtually all electronic circuits. This book can easily be used to design lightweight, high-frequency aerospace transformers or low-frequency commercial transformers. It is, therefore, a design manual.

The conversion process in power electronics requires the use of transformers, components that frequently are the heaviest and bulkiest item in the conversion circuit. Transformer components also have a significant effect on the overall performance and efficiency of the system. Accordingly, the design of such transformers has an important influence on overall system weight, power conversion efficiency, and cost. Because of the interdependence and interaction of these parameters, judicious trade-offs are necessary to achieve design optimization.

Manufacturers have, for years, assigned numeric codes to their cores to indicate their power-handling ability. This method assigns to each core a number called the area product, A_p , that is the product of its window area, W_a , and core cross-section area, A_c . These numbers are used by core suppliers to summarize dimensional and electrical properties in their catalogs. The product of the window area, W_a , and the core area, A_c , gives the area Product, A_p , a dimension to the fourth power. I have developed a new equation for the power-handling ability of the core, the core geometry, K_g . K_g has a dimension to the fifth power. This new equation provides engineers with faster and tighter control of their design. It is a relatively new concept, and magnetic core manufacturers are now beginning to include it in their catalogs.

Because of their significance, the area product, A_p , and the core geometry, K_g , are treated extensively in this handbook. A great deal of other information is also presented for the convenience of the designer. Much of the material is in tabular form to assist the designer in making the trade-offs best suited for a particular application in a minimum amount of time.

Designers have used various approaches in arriving at suitable transformer and inductor designs. For example, in many cases a rule of thumb used for dealing with current density is that a good working level is 1000 circular mils per ampere. This is satisfactory in many instances; however, the wire size used to meet this requirement may produce a heavier and bulkier inductor than desired or required. The information

presented here will make it possible to avoid the use of this and other rules of thumb, and to develop a more economical and better design. While other books are available on electronic transformers, none of them seems to have been written with the user's viewpoint in mind. The material in this book is organized so that the student engineer or technician—starting at the beginning of the book and continuing through the end—will gain a comprehensive knowledge of the state of the art in transformer and inductor design.

No responsibility is assumed by the author or the publisher for any infringement of patent or other rights of third parties that may result from the use of circuits, systems, or processes described or referred to in this handbook.

Acknowledgments

In gathering the material for this book, I have been fortunate in having the assistance and cooperation of several companies and many colleagues. I wish to express my gratitude to all of them. The list is too long to mention them all. However, there are some individuals and companies whose contributions have been especially significant. Colleagues who have retired from Magnetics include Robert Noah and Harry Savisky, who helped so greatly with the editing of the final draft. Other contributions were made by my colleagues at Magnetics, Lowell Bosley and his staff for sending up-to-date catalogs and sample cores. I would like to thank colleagues at Micrometals Corp., Jim Cox and Dale Nicol, and George Orenchak of TSC International. I would like to give special thanks to Richard (Oz) Ozenbaugh of Linear Magnetics Corp. for his assistance in the detailed derivations of many of the equations and his efforts in checking the design examples. I also give special thanks to Steve Freeman of Rodon Products, Inc., for building and testing the magnetics components used in the design examples.

I am also grateful to: Dr. Vatche Vorperian of Jet Propulsion Laboratory (JPL) for his help in generating and clarifying equations for the Quiet Converter; Jerry Fridenberg of Fridenberg Research, Inc., for modeling circuits on his SPICE program; Dr. Gene Wester of JPL for his input; and Kit Sum for his assistance in the energy-storage equations. I also thank the late Robert Yahiro for his help and encouragement over the years.

Colonel Wm. T. McLyman

About the Author

Colonel Wm. T. McLyman recently retired as a Senior Member of the Avionics Equipment Section of the Jet Propulsion Laboratory (JPL) affiliated with the California Institute of Technology in Pasadena, California. He has 47 years of experience in the field of Magnetics, and holds 14 United States Patents on magnetics-related concepts. Through his 30 years at JPL, he has written over 70 JPL Technical Memorandums, New Technology Reports, and Tech-Briefs on the subject of magnetics and circuit designs for power conversion. He has worked on projects for NASA including the Pathfinder Mission to Mars, Cassini, Galileo, Magellan, Viking, Voyager, MVM, Hubble Space Telescope, and many others.

He has been on the lecture circuit for over 20 years speaking in the United States, Canada, Mexico, and Europe on the design and fabrication of magnetic components. He is known as a recognized authority in magnetic design. He is currently the President of his own company, Kg Magnetics, Inc., which specializes in power magnetics design.

He recently completed a book entitled, *High Reliability Magnetic Devices: Design and Fabrication* (Marcel Dekker, Inc.). He also markets, through Kg Magnetics, Inc., a magnetics design and analysis software computer program called "Titan" for transformers and inductors (see Figure 1). This program operates on Windows 95, 98, 2000, and NT.

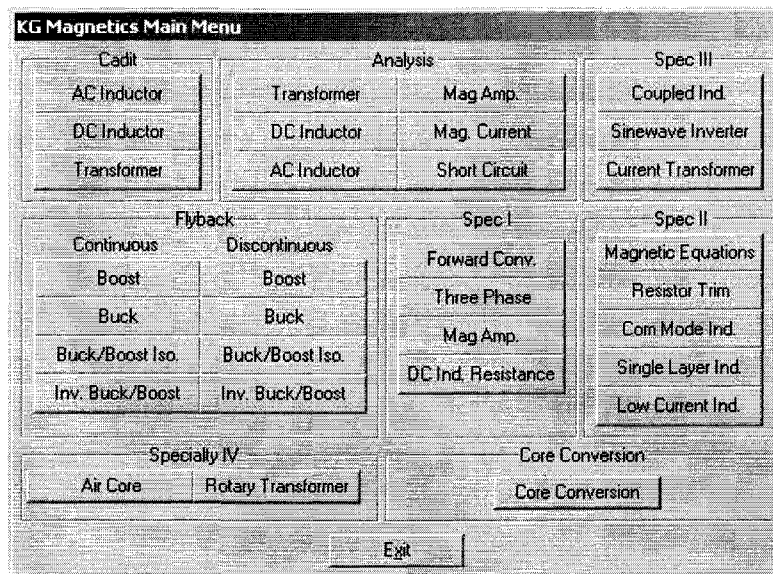


Figure 1. Computer Design Program Main Menu.

Colonel Wm. T. McLyman, (President)
Kg Magnetics, Inc.
Idyllwild, California 92549, U.S.A.
www.kgmagnetics.com; colonel@kgmagnetics.com

Contents

Foreword Robert G. Noah

Preface

About the Author

Symbols

Chapter 1

Fundamentals of Magnetics

Chapter 2

Magnetic Materials and Their Characteristics

Chapter 3

Magnetic Cores

Chapter 4

Window Utilization, Magnet Wire, and Insulation

Chapter 5

Transformer Design Trade-Offs

Chapter 6

Transformer-Inductor Efficiency, Regulation, and Temperature Rise

Chapter 7

Power Transformer Design

Chapter 8

DC Inductor Design Using Gapped Cores

Chapter 9

DC Inductor Design Using Powder Cores

Chapter 10

AC Inductor Design

Chapter 11

Constant Voltage Transformer (CVT)

Chapter 12

Three-Phase Transformer Design

Chapter 13

Flyback Converter, Transformer Design

Chapter 14

Forward Converter, Transformer Design, and Output Inductor Design

Chapter 15

Input Filter Design

	Chapter 16
Current Transformer Design	
	Chapter 17
Winding Capacitance and Leakage Inductance	
	Chapter 18
Quiet Converter Design	
	Chapter 19
Rotary Transformer Design	
	Chapter 20
Planar Transformers	
	Chapter 21
Derivations for the Design Equations	

Symbols

α	regulation, %
A_c	effective cross section of the core, cm^2
A_p	area product, cm^4
A_t	surface area of the transformer, cm^2
A_w	wire area, cm^2
$A_{w(B)}$	bare wire area, cm^2
$A_{w(I)}$	insulated wire area, cm^2
A_{wp}	primary wire area, cm^2
A_{ws}	secondary wire area, cm^2
A-T	amp turn
AWG	American Wire Gage
B	flux, tesla
B_{ac}	alternating current flux density, tesla
ΔB	change in flux, tesla
B_{dc}	direct current flux density, tesla
B_m	flux density, tesla
B_{max}	maximum flux density, tesla
B_o	operating peak flux density, tesla
B_{pk}	peak flux density, tesla
B_r	residual flux density, tesla
B_s	saturation flux density, tesla
C	capacitance
C_n	new capacitance
C_p	lumped capacitance
CM	circular mils
D_{AWG}	wire diameter, cm
$D_{(min)}$	minimum duty ratio
$D_{(max)}$	maximum duty ratio
D_x	dwell time duty ratio
E	voltage
E_{Line}	line to line voltage
E_{Phase}	line to neutral voltage
Energy	energy, watt-second

ESR	equivalent series resistance
η	efficiency
f	frequency, Hz
F	fringing flux factor
F_m	magneto-motive force, mmf
F.L.	full load
G	winding length, cm
γ	density, in grams-per-cm ²
ε	skin depth, cm
H	magnetizing force, oersteds
H_c	magnetizing force required to return flux to zero, oersteds
ΔH	delta magnetizing force, oersteds
H_o	operating peak magnetizing force
H_s	magnetizing force at saturation, oersteds
I	current, amps
I_c	charge current, amps
ΔI	delta current, amps
I_{dc}	dc current, amps
I_{in}	input current, amps
I_{Line}	input line current, amps
I_{Phase}	input phase current, amps
I_m	magnetizing current, amps
I_o	load current, amps
$I_{o(max)}$	maximum load current, amps
$I_{o(min)}$	minimum load current, amps
I_p	primary current, amps
I_s	secondary current, amps
$I_{s(Phase)}$	secondary phase current, amps
$I_{s(Line)}$	secondary line current, amps
J	current density, amps per cm ²
K_c	copper loss constant
K_c	quasi-voltage waveform factor
K_e	electrical coefficient

K_f	waveform coefficient
K_g	core geometry coefficient, cm^5
K_j	constant related to current density
K_s	constant related to surface area
K_u	window utilization factor
K_{up}	primary window utilization factor
K_{us}	secondary window utilization factor
K_{vol}	constant related to volume
K_w	constant related to weight
L	inductance, henry
L_c	open circuit inductance, henry
L_p	primary inductance, henry
l	is a linear dimension
$L_{(crit)}$	critical inductance
λ	density, grams per cm^3
l_g	gap, cm
l_m	magnetic path length, cm
l_t	total path length, cm
mks	meters-kilogram-seconds
MLT	mean length turn, cm
mmf	magnetomotive force, F_m
MPL	magnetic path length, cm
mW/g	milliwatts-per-gram
μ	permeability
μ_i	initial permeability
μ_Δ	incremental permeability
μ_m	core material permeability
μ_o	permeability of air
μ_r	relative permeability
μ_e	effective permeability
n	turns ratio
N	turns
N.L.	no load

N_L	inductor turns
N_n	new turns
N_p	primary turns
N_s	secondary turns
P	watts
P_{cu}	copper loss, watts
P_{fe}	core loss, watts
P_g	gap loss, watts
ϕ	magnetic flux
P_{in}	input power, watts
P_L	inductor copper loss, watts
P_o	output power, watts
P_p	primary copper loss, watts
P_s	secondary copper loss, watts
P_{Σ}	total loss (core and copper), watts
P_t	total apparent power, watts
P_{VA}	primary volt-amps
R	resistance, ohms
R_{ac}	ac resistance, ohms
R_{cu}	copper resistance, ohms
R_{dc}	dc resistance, ohms
R_e	equivalent core loss (shunt) resistance, ohms
R_g	reluctance of the gap
R_m	reluctance
R_{mt}	total reluctance
R_o	load resistance, ohms
$R_{o(R)}$	reflected load resistance, ohms
$R_{in(equiv)}$	reflected load resistance, ohms
R_p	primary resistance, ohms
R_R	ac/dc resistance ratio
R_s	secondary resistance, ohms
R_t	total resistance, ohms
ρ	resistivity, ohm-cm

S_1	conductor area/wire area
S_2	wound area/usable window
S_3	usable window area/window area
S_4	usable window area/usable window area + insulation area
S_{np}	number of primary strands
S_{ns}	number of secondary strands
S_{VA}	secondary volt-amps
T	total period, seconds
t_{off}	off time, seconds
t_{on}	on time, seconds
t_w	dwelt time, seconds
T_r	temperature rise, °C
U	multiplication factor
VA	volt-amps
V_{ac}	applied voltage, volts
V_c	control voltage, volts
$V_{c(pk)}$	peak voltage, volts
V_d	diode voltage drop, volts
V_{in}	input voltage, volts
$V_{in(max)}$	maximum input voltage, volts
$V_{in(min)}$	minimum input voltage, volts
V_n	new voltage, volts
V_o	output voltage, volts
V_p	primary voltage, volts
$V_{p(rms)}$	primary rms voltage, volts
$V_{s(LL)}$	secondary line to line voltage, volts
$V_{s(LN)}$	secondary line to neutral voltage, volts
$V_{r(pk)}$	peak ripple voltage
V_s	secondary voltage, volts
ΔV_{CC}	capacitor voltage, volts
ΔV_{CR}	capacitor ESR voltage, volts
ΔV_p	delta primary voltage, volts
ΔV_s	delta secondary voltage, volts

W	watts
W/kg	watts-per-kilogram
W_a	window area, cm^2
W_{ap}	primary window area, cm^2
W_{as}	secondary window area, cm^2
$W_{a(eff)}$	effective window area, cm^2
$w-s$	watt-seconds
W_t	weight, grams
W_{tcu}	copper weight, grams
W_{tfe}	iron weight, grams
X_L	inductive reactance, ohms

Chapter 1

Fundamentals of Magnetism

Introduction

Considerable difficulty is encountered in mastering the field of magnetics because of the use of so many different systems of units – the centimeter-gram-second (cgs) system, the meter-kilogram-second (mks) system, and the mixed English units system. Magnetics can be treated in a simple way by using the cgs system. There always seems to be one exception to every rule and that is permeability.

Magnetic Properties in Free Space

A long wire with a dc current, I , flowing through it, produces a circulatory magnetizing force, H , and a magnetic field, B , around the conductor, as shown in Figure 1-1, where the relationship is:

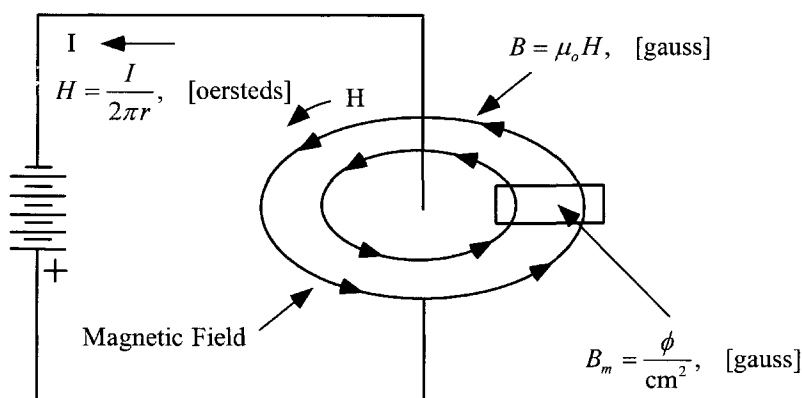


Figure 1-1. A Magnetic Field Generated by a Current Carrying Conductor.

The direction of the line of flux around a straight conductor may be determined by using the “right hand rule” as follows: When the conductor is grasped with the right hand, so that the thumb points in the direction of the current flow, the fingers point in the direction of the magnetic lines of force. This is based on so-called conventional current flow, not the electron flow.

When a current is passed through the wire in one direction, as shown in Figure 1-2(a), the needle in the compass will point in one direction. When the current in the wire is reversed, as in Figure 1-2(b), the needle will also reverse direction. This shows that the magnetic field has polarity and that, when the current I , is reversed, the magnetizing force, H , will follow the current reversals.

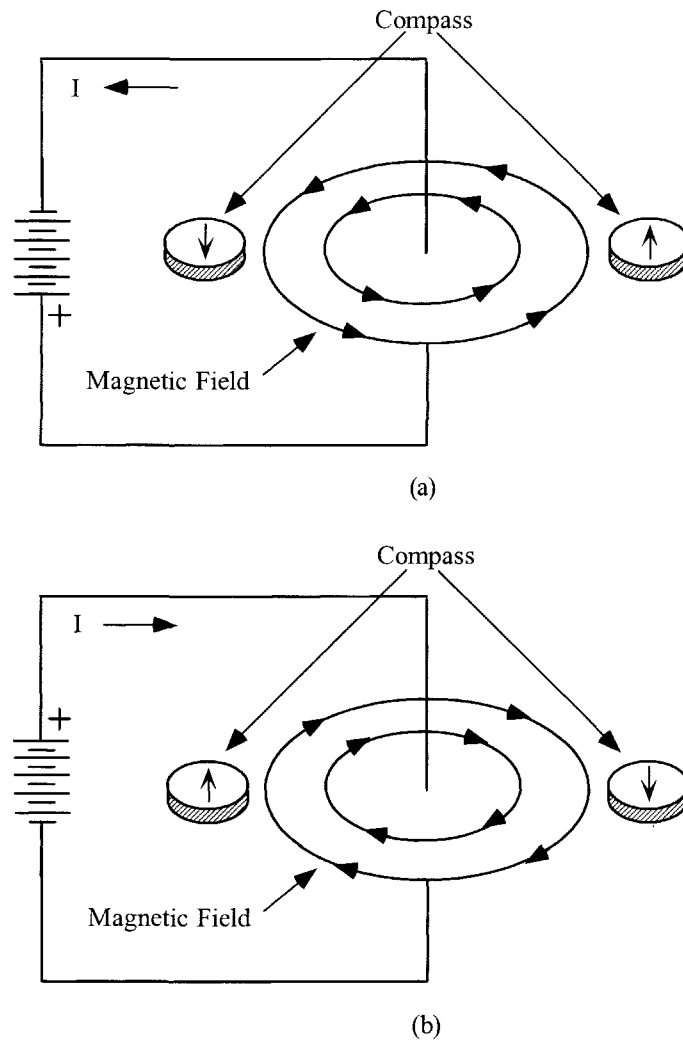


Figure 1-2. The Compass Illustrates How the Magnetic Field Changes Polarity.

Intensifying the Magnetic Field

When a current passes through a wire, a magnetic field is set up around the wire. If the conductors, as shown in Figure 1-3, carrying current in the same direction are separated by a relatively large distance, the magnetic fields generated will not influence each other. If the same two conductors are placed close to each other, as shown in Figure 1-4, the magnetic fields add, and the field intensity doubles.

$$\gamma = \frac{B^2}{8\pi\mu}, \quad [\text{energy density}] \quad [1-1]$$

If the wire is wound on a dowel, its magnetic field is greatly intensified. The coil, in fact, exhibits a magnetic field exactly like that of a bar magnet, as shown in Figure 1-5. Like the bar magnet, the coil has a north pole and a neutral center region. Moreover, the polarity can be reversed by reversing the current, I , through the coil. Again, this demonstrates the dependence of the magnetic field on the current direction.

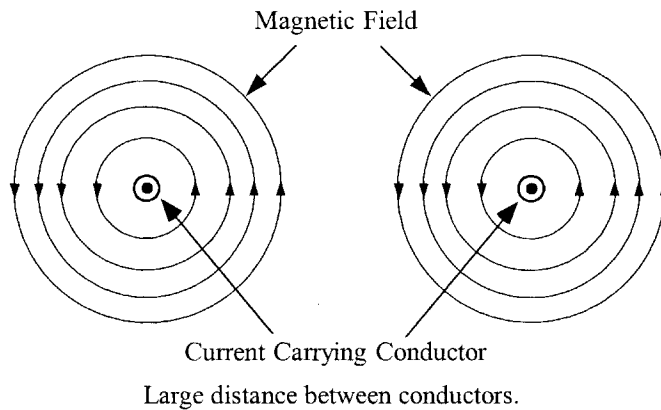


Figure 1-3. Magnetic Fields Produced Around Spaced Conductors.

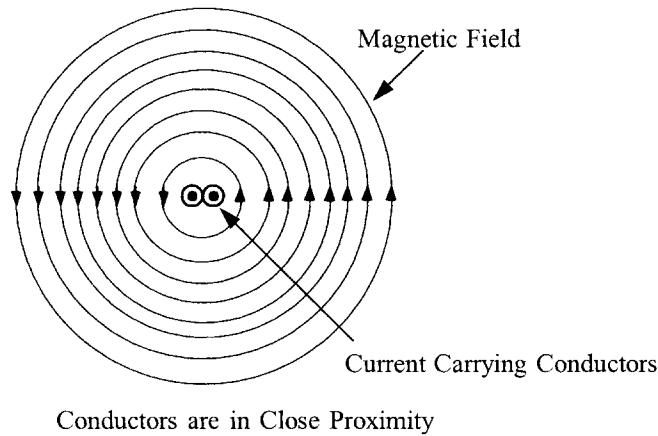


Figure 1-4. Magnetic Fields Produced Around Adjacent Conductors.

The magnetic circuit is the space in which the flux travels around the coil. The magnitude of the flux is determined by the product of the current, I , and the number of turns, N , in the coil. The force, NI , required to create the flux is magnetomotive force (mmf). The relationship between flux density, B , and magnetizing force, H , for an air-core coil is shown in Figure 1-6. The ratio of B to H is called the permeability, μ , and for this air-core coil the ratio is unity in the cgs system, where it is expressed in units of gauss per oersteds, (gauss/oersteds).

$$\begin{aligned} \mu_o &= 1 \\ B &= \mu_o H \end{aligned} \quad [1-2]$$

If the battery, in Figure 1-5, were replaced with an ac source, as shown in Figure 1-7, the relationship between B and H would have the characteristics shown in Figure 1-8. The linearity of the relationship between B and H represents the main advantage of air-core coils. Since the relationship is linear, increasing H increases B , and therefore the flux in the coil, and, in this way, very large fields can be produced with large currents. There is obviously a practical limit to this, which depends on the maximum allowable current in the conductor and the resulting rise.

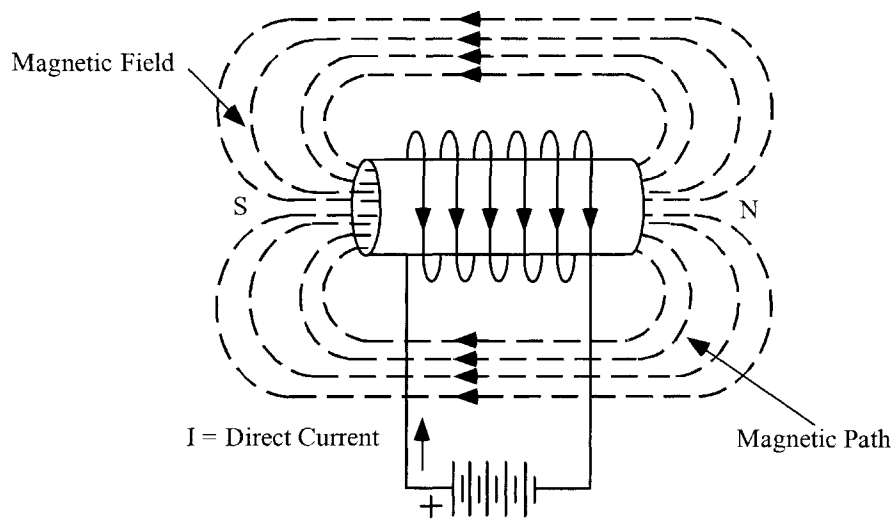


Figure 1-5. Air-Core Coil with dc excitation

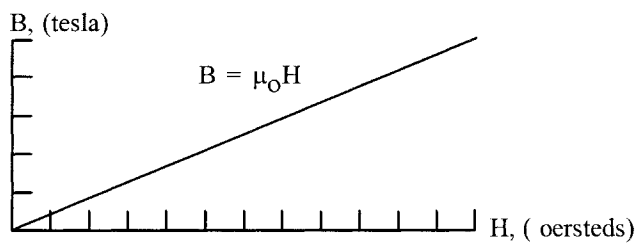


Figure 1-6. Relationship Between B and H with dc Excitation.

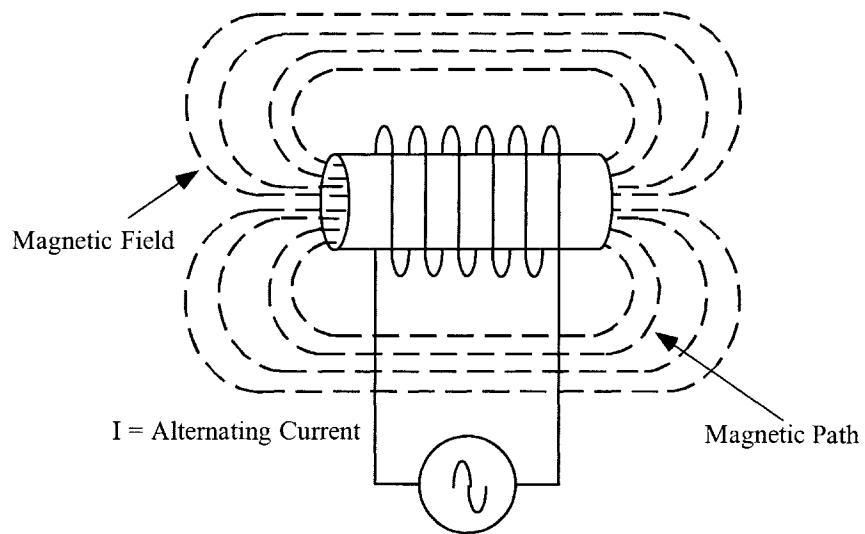


Figure 1-7. Air-Core Coil Driven from an ac Source.

Fields of the order of 0.1 tesla are feasible for a 40° C temperature rise above room ambient temperature. With super cooled coils, fields of 10 tesla have been obtained.

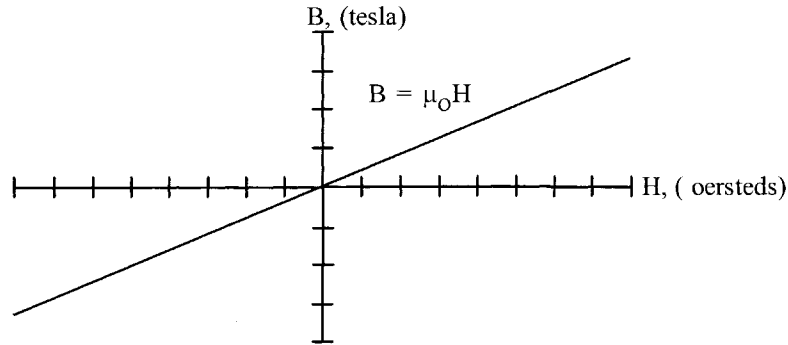


Figure 1-8. Relationship Between B and H with ac Excitation.

Simple Transformer

A transformer in its simplest form is shown in Figure 1-9. This transformer has two air coils that share a common flux. The flux diverges from the ends of the primary coil in all directions. It is not concentrated or confined. The primary is connected to the source and carries the current that establishes a magnetic field. The other coil is open-circuited. Notice that the flux lines are not common to both coils. The difference between the two is the leakage flux; that is, leakage flux is the portion of the flux that does not link both coils.

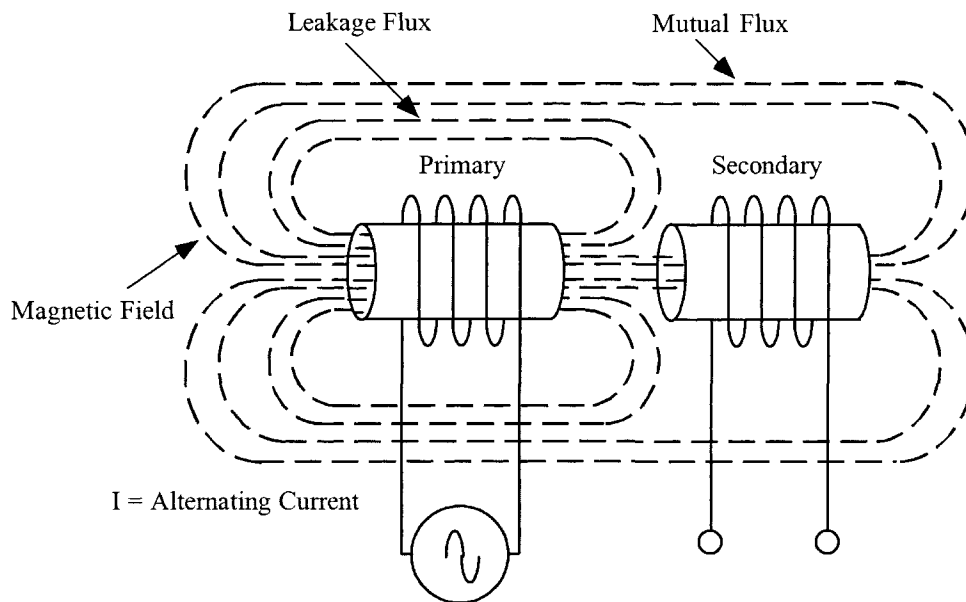


Figure 1-9. The Simplest Type of Transformer.

Magnetic Core

Most materials are poor conductors of magnetic flux; they have low permeability. A vacuum has a permeability of 1.0, and nonmagnetic materials, such as air, paper, and copper have permeabilities of the same order. There are a few materials, such as iron, nickel, cobalt, and their alloys that have high permeability, sometimes ranging into the hundreds of thousands. To achieve an improvement over the air-core, as shown in Figure 1-10, a magnetic core can be introduced, as shown in Figure 1-11. In addition to its high permeability, the advantages of the magnetic core over the air-core are that the magnetic path length (MPL) is well-defined, and the flux is essentially confined to the core, except in the immediate vicinity of the winding. There is a limit as to how much magnetic flux can be generated in a magnetic material before the magnetic core goes into saturation, and the coil reverts back to an air-core, as shown in Figure 1-12.

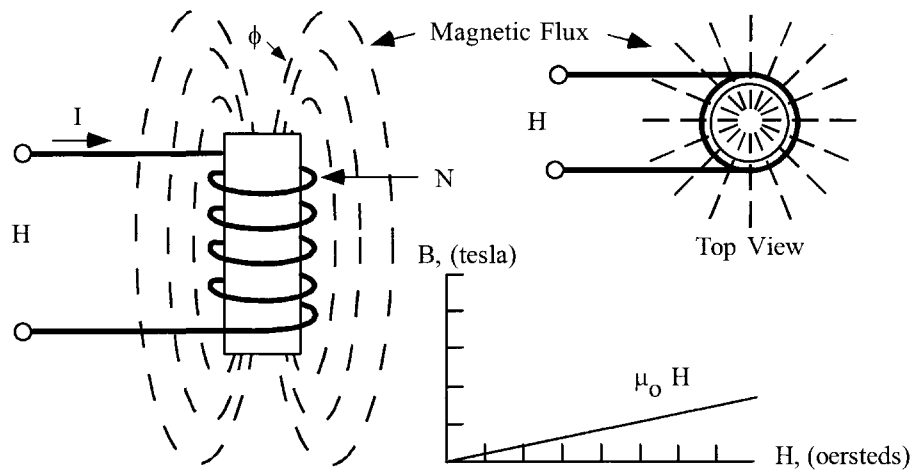


Figure 1-10. Air-Core Coil Emitting Magnetic Flux when Excited.

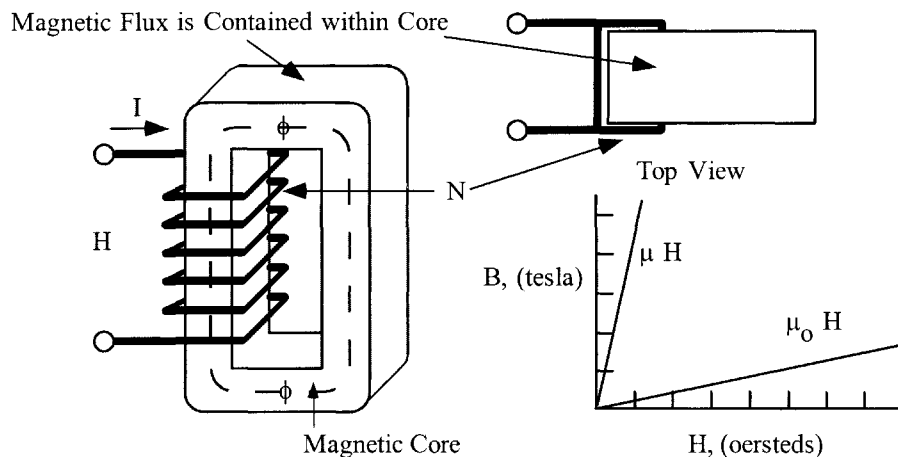


Figure 1-11. Introduction of a Magnetic Core.

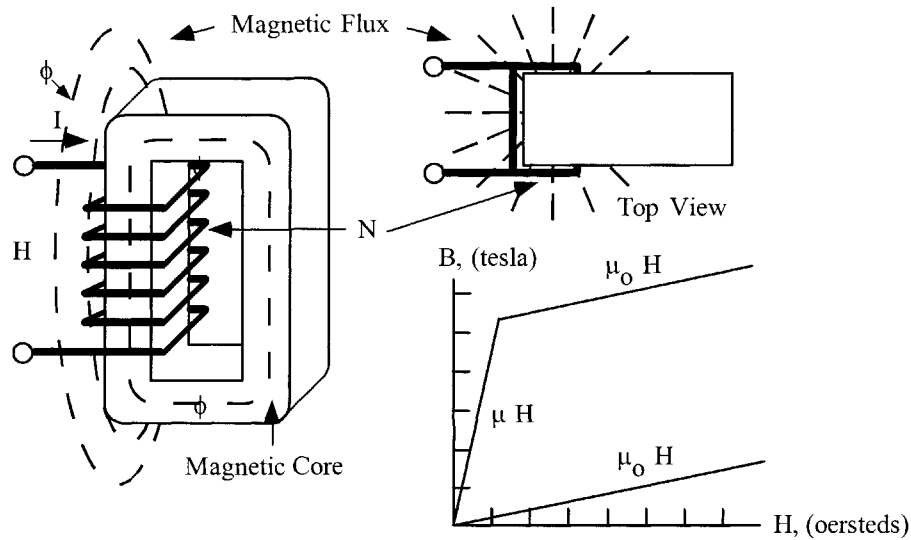


Figure 1-12. Excited Magnetic Core Driven into Saturation.

Fundamental Characteristics of a Magnetic Core

The effect of exciting a completely demagnetized, ferromagnetic material, with an external magnetizing force, H , and increasing it slowly, from zero, is shown in Figure 1-13, where the resulting flux density is plotted as a function of the magnetizing force, H . Note that, at first, the flux density increases very slowly up to point A, then, increases very rapidly up to point B, and then, almost stops increasing. Point B is called the knee of the curve. At point C, the magnetic core material has saturated. From this point on, the slope of the curve is:

$$\frac{B}{H} = 1, \text{ [gauss/oersteds] [1-3]}$$

The coil is now behaving as if it had an air-core. When the magnetic core is in hard saturation, the coil has the same permeability as air, or unity. Following the magnetization curve in Figure 1-14, Figures 1-15 through Figures 1-16 show how the flux in the core is generated from the inside of the core to the outside until the core saturates.

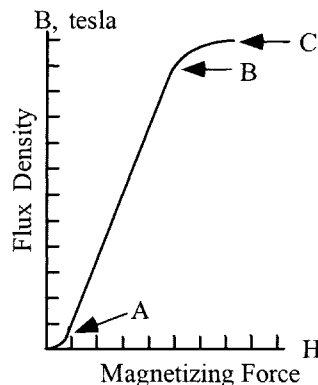


Figure 1-13. Typical Magnetization Curve.

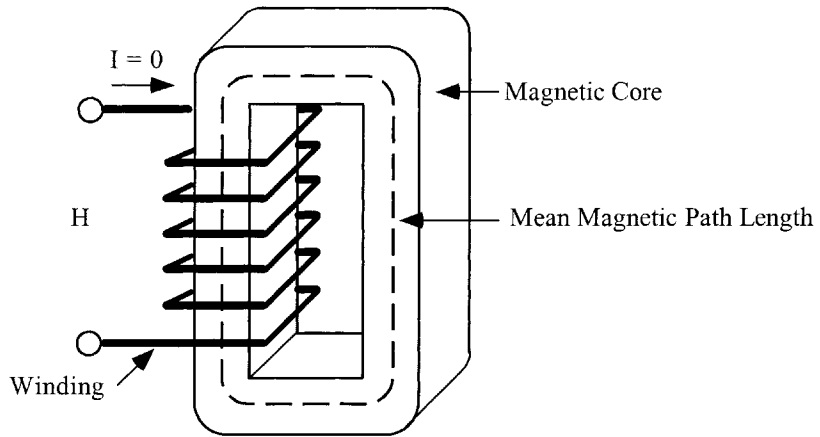


Figure 1-14. Magnetic Core with Zero Excitation.

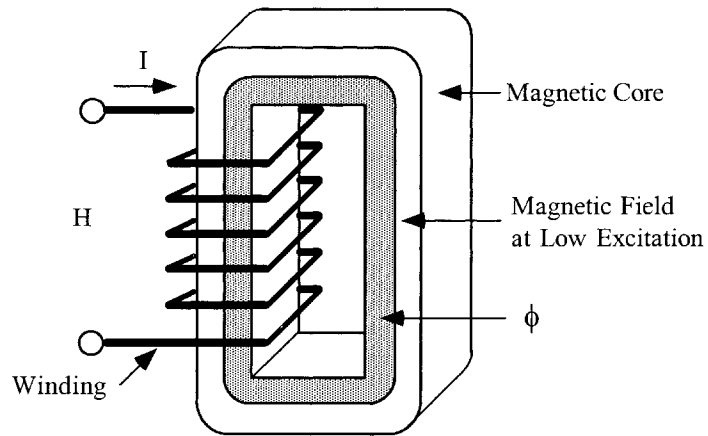


Figure 1-15. Magnetic Core with Low Excitation.

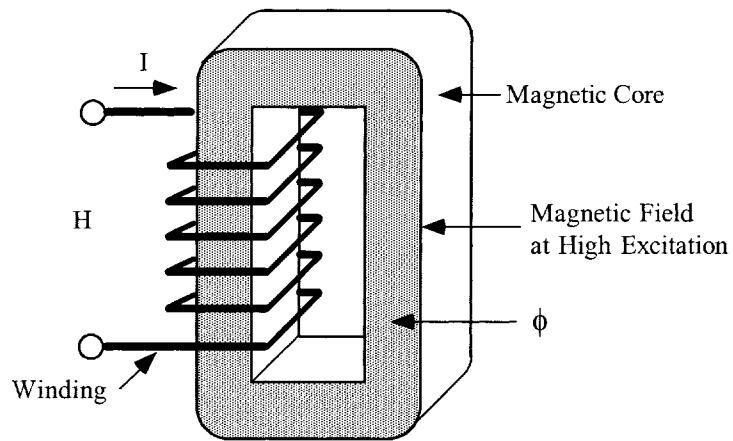


Figure 1-16. Magnetic Core with High Excitation.

Hysteresis Loop (B-H Loop)

An engineer can take a good look at the hysteresis loop and get a first order evaluation of the magnetic material. When the magnetic material is taken through a complete cycle of magnetization and demagnetization, the results are as shown in Figure 1-17. It starts with a neutral magnetic material, traversing the B-H loop at the origin X. As H is increased, the flux density B increases along the dashed line to the saturation point, B_s . When H is now decreased and B is plotted, B-H loop transverses a path to B_r , where H is zero and the core is still magnetized. The flux at this point is called remanent flux, and has a flux density, B_r .

The magnetizing force, H, is now reversed in polarity to give a negative value. The magnetizing force required to reduce the flux B_r to zero is called the coercive force, H_c . When the core is forced into saturation, the retentivity, B_{rs} , is the remaining flux after saturation, and coercivity, H_{cs} , is the magnetizing force required to reset to zero. Along the initial magnetization curve at point X, the dashed line, in Figure 1-17, B increases from the origin nonlinearly with H, until the material saturates. In practice, the magnetization of a core in an excited transformer never follows this curve, because the core is never in the totally demagnetized state, when the magnetizing force is first applied.

The hysteresis loop represents energy lost in the core. The best way to display the hysteresis loop is to use a dc current, because the intensity of the magnetizing force must be so slowly changed that no eddy currents are generated in the material. Only under this condition is the area inside the closed B-H loop indicative of the hysteresis. The enclosed area is a measure of energy lost in the core material during that cycle. In ac applications, this process is repeated continuously and the total hysteresis loss is dependent upon the frequency.

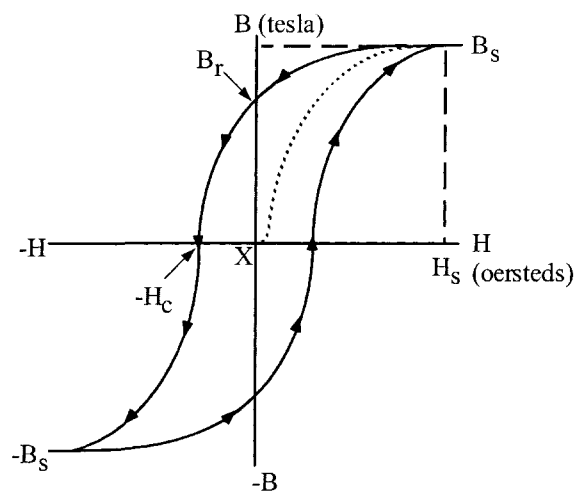


Figure 1-17. Typical Hysteresis Loop.

Permeability

In magnetics, permeability is the ability of a material to conduct flux. The magnitude of the permeability at a given induction is the measure of the ease with which a core material can be magnetized to that induction. It is defined as the ratio of the flux density, B, to the magnetizing force, H. Manufacturers specify permeability in units of gauss per oersteds.

$$\text{Permeability} = \frac{B}{H}, \left[\frac{\text{gauss}}{\text{oersteds}} \right] \quad [1-4]$$

The absolute permeability, μ_0 in cgs units is unity 1 (gauss per oersteds) in a vacuum.

$$\text{cgs: } \mu_0 = 1, \left[\frac{\text{gauss}}{\text{oersteds}} \right] = \left[\frac{\text{tesla}}{\text{oersteds}} (10^4) \right] \quad [1-5]$$

$$\text{mks: } \mu_0 = 0.4\pi(10^{-8}), \left[\frac{\text{henrys}}{\text{meter}} \right]$$

When B is plotted against H, as in Figure 1-18, the resulting curve is called the magnetization curve. These curves are idealized. The magnetic material is totally demagnetized and is then subjected to gradually increasing magnetizing force, while the flux density is plotted. The slope of this curve, at any given point gives the permeability at that point. Permeability can be plotted against a typical B-H curve, as shown in Figure 1-19. Permeability is not constant; therefore, its value can be stated only at a given value of B or H.

There are many different kinds of permeability, and each is designated by a different subscript on the symbol μ .

μ_0	Absolute permeability, defined as the permeability in a vacuum.
μ_i	Initial permeability is the slope of the initial magnetization curve at the origin. It is measured at very small induction, as shown in Figure 1-20.
μ_Δ	Incremental permeability is the slope of the magnetization curve for finite values of peak-to-peak flux density with superimposed dc magnetization as shown in Figure 1-21.
μ_e	Effective permeability. If a magnetic circuit is not homogeneous (i.e., contains an air gap), the effective permeability is the permeability of hypothetical homogeneous (ungapped) structure of the same shape, dimensions, and reluctance that would give the inductance equivalent to the gapped structure.
μ_r	Relative permeability is the permeability of a material relative to that of free space.
μ_n	Normal permeability is the ratio of B/H at any point of the curve as shown in Figure 1-22.
μ_{\max}	Maximum permeability is the slope of a straight line drawn from the origin tangent to the curve at its knee as shown in Figure 1-23.
μ_p	Pulse permeability is the ratio of peak B to peak H for unipolar excitation.
μ_m	Material permeability is the slope of the magnetization curve measure at less than 50 gauss as shown in Figure 1-24.

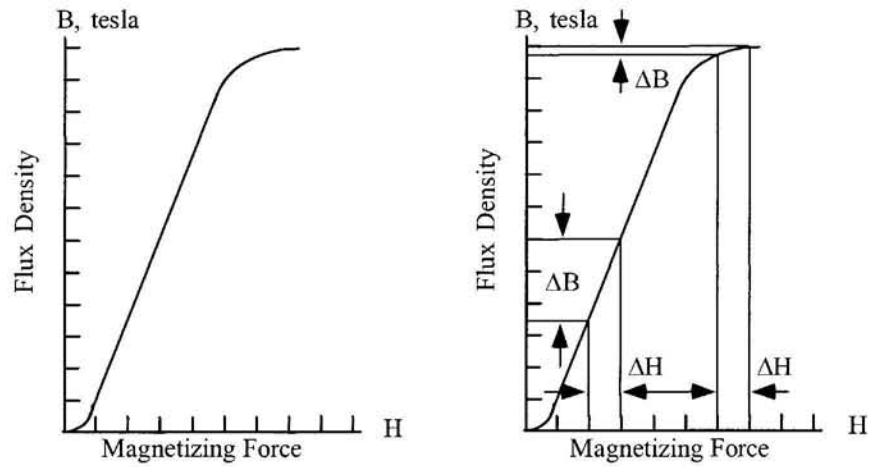


Figure 1-18. Magnetizing Curve.

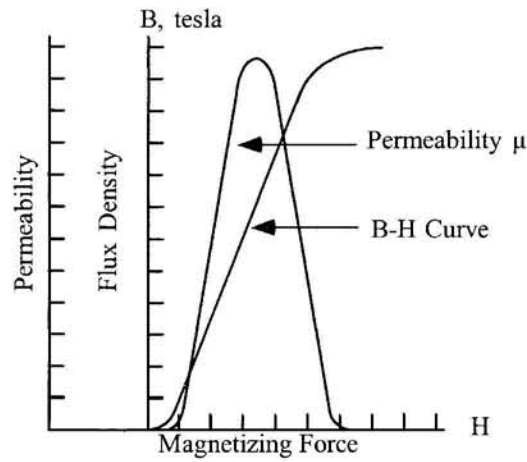


Figure 1-19. Variation of Permeability μ along the Magnetizing Curve.

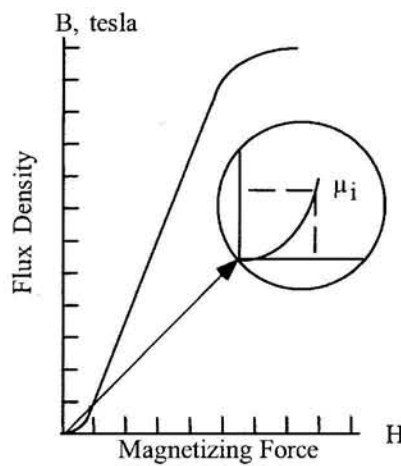


Figure 1-20. Initial Permeability.

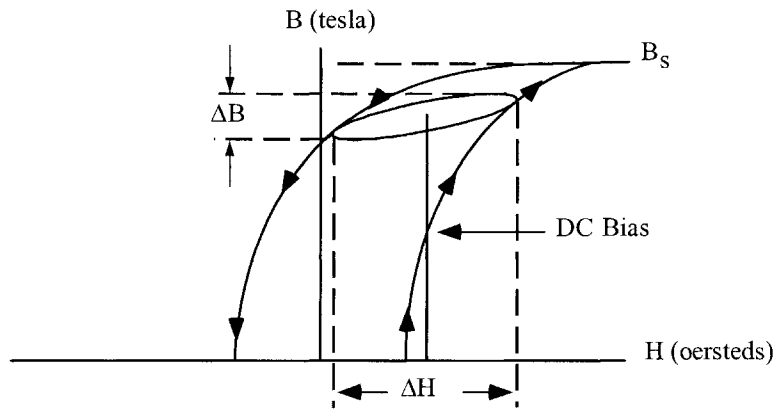


Figure 1-21. Incremental Permeability.

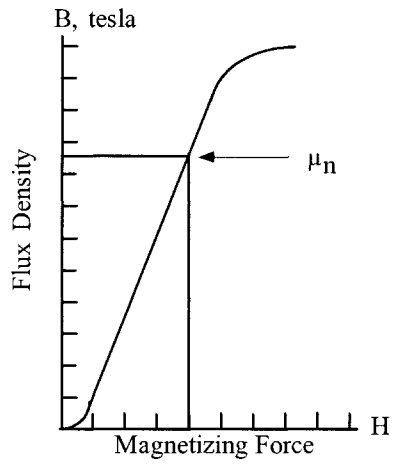


Figure 1-22. Normal Permeability.

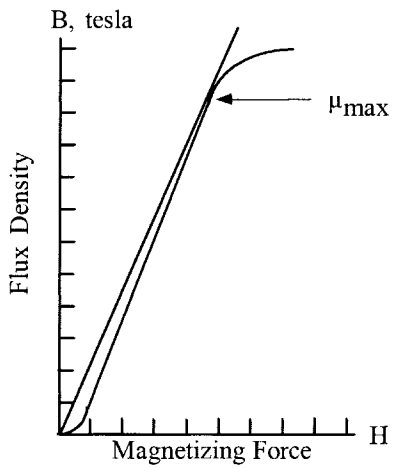


Figure 1-23. Maximum Permeability.

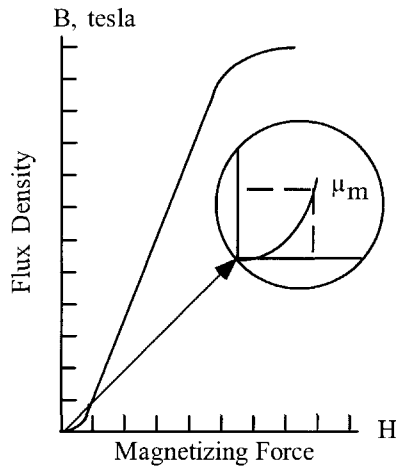


Figure 1-24. Material Permeability.

Magnetomotive Force (mmf) and Magnetizing Force (H)

There are two force functions commonly encountered in magnetics: magnetomotive force, mmf, and magnetizing force, H. Magnetomotive force should not be confused with magnetizing force; the two are related as cause and effect. Magnetomotive force is given by the equation:

$$\text{mmf} = 0.4\pi NI, \quad [\text{gilberts}] \quad [1-6]$$

Where, N is the number of turns and I is the current in amperes. Whereas mmf is the force, H is a force field, or force per unit length:

$$H = \frac{\text{mmf}}{\text{MPL}}, \quad \left[\frac{\text{gilberts}}{\text{cm}} = \text{oersteds} \right] \quad [1-7]$$

Substituting,

$$H = \frac{0.4\pi NI}{\text{MPL}}, \quad [\text{oersteds}] \quad [1-8]$$

Where, MPL = magnetic path length in cm.

If the flux is divided by the core area, A_c , we get flux density, B, in lines per unit area:

$$B = \frac{\phi}{A_c}, \quad [\text{gauss}] \quad [1-9]$$

The flux density, B, in a magnetic medium, due to the existence of a magnetizing force H, depends on the permeability of the medium and the intensity of the magnetic field:

$$B = \mu H, \quad [\text{gauss}] \quad [1-10]$$

The peak, magnetizing current, I_m , for a wound core can be calculated from the following equation:

$$I_m = \frac{H_o (MPL)}{0.4\pi N}, \text{ [amps]} \quad [1-11]$$

Where H_o is the field intensity at the peak operating point. To determine the magnetizing force, H_o , use the manufacturer's core loss curves at the appropriate frequency and operating flux density, B_o , as shown in Figure 1-25.

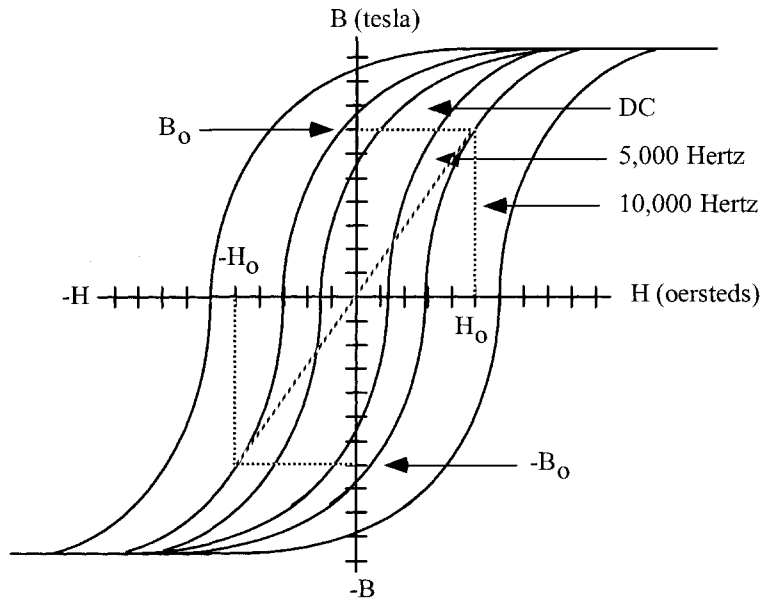


Figure 1-25. Typical B-H Loops Operating at Various Frequencies.

Reluctance

The flux produced in a given material by magnetomotive force (mmf) depends on the material's resistance to flux, which is called reluctance, R_m . The reluctance of a core depends on the composition of the material and its physical dimension and is similar in concept to electrical resistance. The relationship between mmf, flux, and magnetic reluctance is analogous to the relationship between emf, current, and resistance, as shown in Figure 1-26.

$$\begin{aligned} emf (E) &= IR = \text{Current} \times \text{Resistance} \\ mmf (F_m) &= \Phi R_m = \text{Flux} \times \text{Reluctance} \end{aligned} \quad [1-12]$$

A poor conductor of flux has a high magnetic resistance, R_m . The greater the reluctance, the higher the magnetomotive force that is required to obtain a given magnetic field.

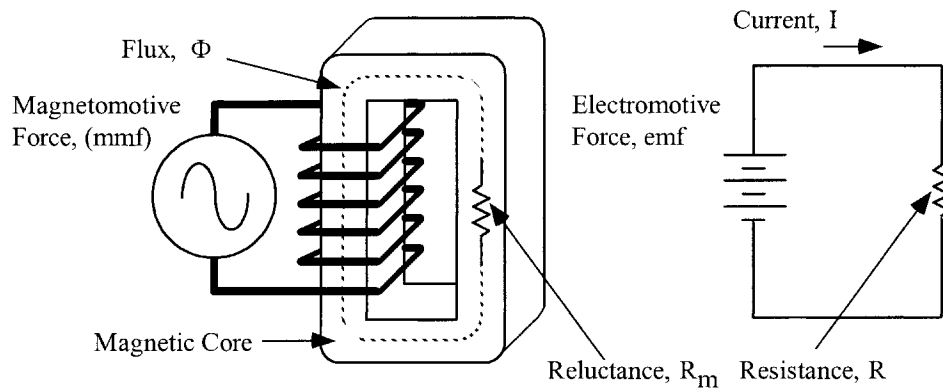


Figure 1-26. Comparing Magnetic Reluctance and Electrical Resistance.

The electrical resistance of a conductor is related to its length l , cross-sectional area A_w , and specific resistance ρ , which is the resistance per unit length. To find the resistance of a copper wire of any size or length, we merely multiply the resistivity by the length, and divide by the cross-sectional area:

$$R = \frac{\rho l}{A_w}, \quad [\text{ohms}] \quad [1-13]$$

In the case of magnetics, $1/\mu$ is analogous to ρ and is called reluctivity. The reluctance R_m of a magnetic circuit is given by:

$$R_m = \frac{MPL}{\mu_r \mu_o A_c} \quad [1-14]$$

Where MPL, is the magnetic path length, cm.

A_c is the cross-section of the core, cm^2 .

μ_r is the permeability of the magnetic material.

μ_o is the permeability of air.

A typical magnetic core is shown in Figure 1-27 illustrating the magnetic path length MPL and the cross-sectional area, A_c , of a C core.

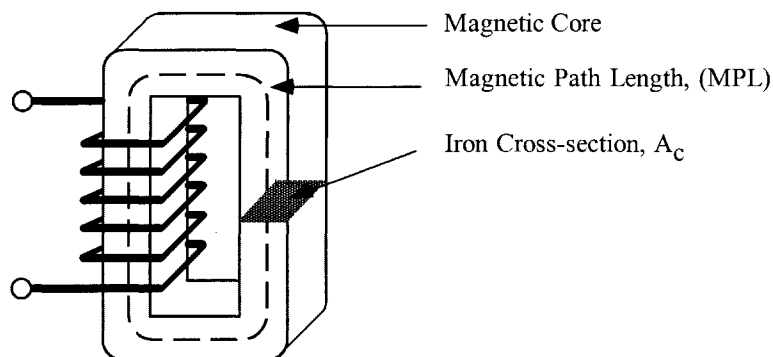


Figure 1-27. Magnetic Core Showing the Magnetic Path Length (MPL) and Iron Cross-section A_c .

Air Gap

A high permeability material is one that has a low reluctance for a given magnetic path length (MPL) and iron cross-section, A_c . If an air gap is included in a magnetic circuit as shown in Figure 1-28, which is otherwise composed of low relativity material like iron, almost all of the reluctance in the circuit will be at the gap, because the relativity of air is much greater than that of a magnetic material. For all practical purposes, controlling the size of the air gap controls the reluctance.

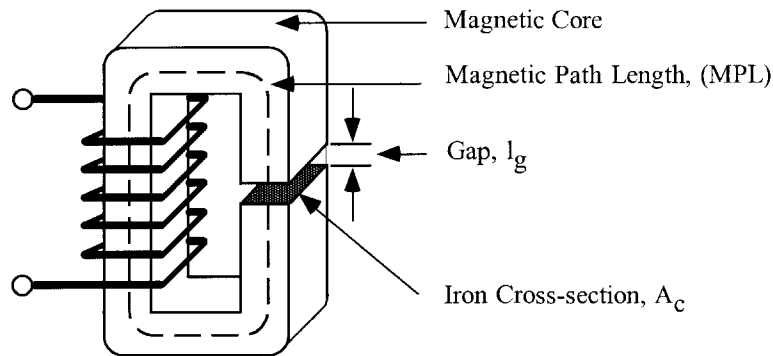


Figure 1-28. A Typical Magnetic Core with an Air Gap.

An example can best show this procedure. The total reluctance of the core is the sum of the iron reluctance and the air gap reluctance, in the same way that two series resistors are added in an electrical circuit. The equation for calculating the air gap reluctance, R_g , is basically the same as the equation for calculating the reluctance of the magnetic material, R_m . The difference is that the permeability of air is 1 and the gap length, l_g , is used in place of the magnetic path length (MPL). The equation is as follows:

$$R_g = \left(\frac{1}{\mu_o} \right) \left(\frac{l_g}{A_c} \right) \quad [1-15]$$

But, since $\mu_o = 1$, the equation simplifies to:

$$R_g = \frac{l_g}{A_c} \quad [1-16]$$

Where:

l_g is the gap length, cm.

A_c is the cross-section of the core, cm^2 .

μ_o is the permeability of air.

The total reluctance, R_{mb} , for the core shown in Figure 1-28 is therefore:

$$R_{mt} = R_m + R_g$$

$$R_{mt} = \frac{MPL}{\mu_r \mu_o A_c} + \frac{l_g}{\mu_o A_c} \quad [1-17]$$

Where μ_r is the relative permeability, which is used exclusively with magnetic materials.

$$\mu_r = \frac{\mu}{\mu_o} = \frac{B}{\mu_o H}, \quad \left[\frac{\text{gauss}}{\text{oersteds}} \right] \quad [1-18]$$

The magnetic material permeability, μ_m , is given by:

$$\mu_m = \mu_r \mu_o \quad [1-19]$$

The reluctance of the gap is higher than that of the iron even when the gap is small. The reason is because the magnetic material has a relatively high permeability, as shown in Table 1-1. So the total reluctance of the circuit depends more on the gap than on the iron.

Table 1-1. Material Permeability

Material Permeability, μ_m	
Material Name	Permeability
Iron Alloys	0.8K to 25K
Ferrites	0.8K to 20K
Amorphous	0.8K to 80K

After the total reluctance, R_t , has been calculated, the effective permeability, μ_e , can be calculated.

$$R_{mt} = \frac{l_t}{\mu_e A_c}$$

[1-20]

$$l_t = l_g + MPL$$

Where l_t is the total path length and μ_e is the effective permeability.

$$R_{mt} = \frac{l_t}{\mu_e A_c} = \frac{l_g}{\mu_o A_c} + \frac{MPL}{\mu_o \mu_r A_c} \quad [1-21]$$

Simplifying yields:

$$\frac{l_t}{\mu_e} = \frac{l_g}{\mu_o} + \frac{MPL}{\mu_o \mu_r} \quad [1-22]$$

Then:

$$\mu_e = \frac{l_t}{\frac{l_g}{\mu_o} + \frac{MPL}{\mu_o \mu_r}} \quad [1-23]$$

$$\mu_e = \frac{l_g + MPL}{\frac{l_g}{\mu_o} + \frac{MPL}{\mu_o \mu_r}}$$

If $l_g \ll \text{MPL}$, multiply both sides of the equation by $(\mu_r \mu_0 \text{MPL}) / (\mu_r \mu_0 \text{MPL})$.

$$\mu_e = \frac{\mu_o \mu_r}{1 + \mu_r \left(\frac{l_g}{\text{MPL}} \right)} \quad [1-24]$$

The classic equation is:

$$\mu_e = \frac{\mu_m}{1 + \mu_m \left(\frac{l_g}{\text{MPL}} \right)} \quad [1-25]$$

Introducing an air gap, l_g , to the core cannot correct for the dc flux, but can sustain the dc flux. As the gap is increased, so is the reluctance. For a given magnetomotive force, the flux density is controlled by the gap.

Controlling the dc Flux with an Air Gap

There are two similar equations used to calculate the dc flux. The first equation is used with powder cores. Powder cores are manufactured from very fine particles of magnetic materials. This powder is coated with an inert insulation to minimize eddy currents losses and to introduce a distributed air gap into the core structure.

$$\begin{aligned} \mu_r &= \mu_e \\ B_{dc} &= (\mu_r) \left(\frac{0.4\pi N I}{\text{MPL}} \right), \quad [\text{gauss}] \quad [1-26] \\ \mu_r &= \frac{\mu_m}{1 + \mu_m \left(\frac{l_g}{\text{MPL}} \right)} \end{aligned}$$

The second equation is used, when the design calls for a gap to be placed in series with the magnetic path length (MPL), such as a ferrite cut core, a C core, or butt stacked laminations.

$$\begin{aligned} \mu_r &= \mu_e \\ B_{dc} &= (\mu_r) \left(\frac{0.4\pi N I}{\text{MPL}} \right), \quad [\text{gauss}] \quad [1-27] \end{aligned}$$

Substitute $(\text{MPL}\mu_m) / (\text{MPL}\mu_m)$ for 1:

$$\mu_r = \frac{\mu_m}{1 + \mu_m \left(\frac{l_g}{\text{MPL}} \right)} = \frac{\mu_m}{\frac{\text{MPL}\mu_m}{\text{MPL}\mu_m} + \mu_m \left(\frac{l_g}{\text{MPL}} \right)} \quad [1-28]$$

Then, simplify:

$$\mu_r = \frac{MPL}{\frac{MPL}{\mu_m} + l_g} \quad [1-29]$$

$$B_{dc} = \left(\frac{MPL}{\frac{MPL}{\mu_m} + l_g} \right) \left(\frac{0.4\pi NI}{MPL} \right), \text{ [gauss]} \quad [1-30]$$

Then, simplify:

$$B_{dc} = \frac{0.4\pi NI}{l_g + \frac{MPL}{\mu_m}}, \text{ [gauss]} \quad [1-31]$$

Types of Air Gaps

Basically, there are two types of gaps used in the design of magnetic components: bulk and distributed. Bulk gaps are maintained with materials, such as paper, Mylar, or even glass. The gapping materials are designed to be inserted in series with the magnetic path to increase the reluctance, R , as shown in Figure 1-29.

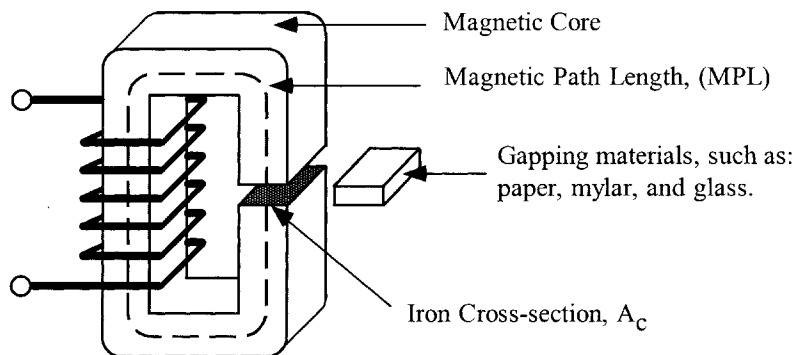


Figure 1-29. Placement of the Gapping Materials.

Placement of the gapping material is critical in keeping the core structurally balanced. If the gap is not proportioned in each leg, then the core will become unbalanced and create even more than the required gap. There are designs where it is important to place the gap in an area to minimize the noise that is caused by the fringing flux at the gap. The gap placement for different core configurations is shown in Figure 1-30. The standard gap placement is shown in Figure 1-30A, C, and D. The EE or EC cores shown in Figure 1-30B, are best-suited, when the gap has to be isolated within the magnetic assembly to minimize fringing flux noise. When the gap is used as shown in Figure 1-30A, C, and D, then, only half the thickness of the calculated gap dimension is used in each leg of the core.

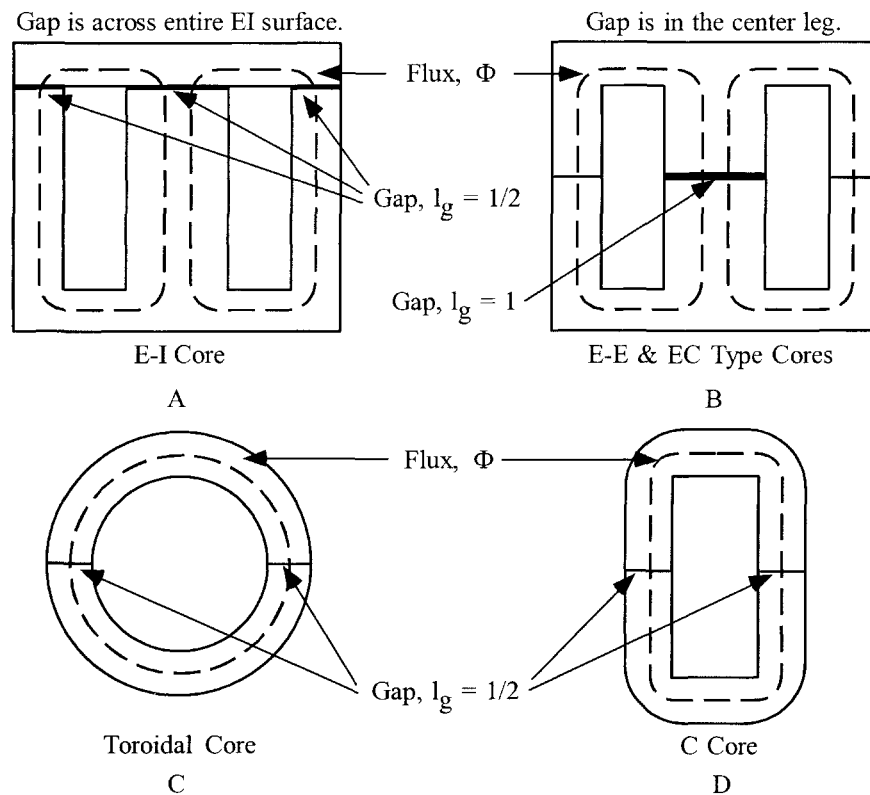


Figure 1-30. Gap Placement using Different Core Configurations.

Fringing Flux

Introduction

Fringing flux has been around since time began for the power conversion engineer. Designing power conversion magnetics that produce a minimum of fringing flux has always been a problem. Engineers have learned to design around fringing flux, and minimize its effects. It seems that when engineers do have a problem, it is usually at the time when the design is finished and ready to go. It is then that the engineer will observe something that was not recognized before. This happens during the final test when the unit becomes unstable, the inductor current is nonlinear, or the engineer just located a hot spot during testing. Fringing flux can cause a multitude of problems. Fringing flux can reduce the overall efficiency of the converter, by generating eddy currents that cause localized heating in the windings and/or the brackets. When designing inductors, fringing flux must to be taken into consideration. If the fringing flux is not handled correctly, there will be premature core saturation. More and more magnetic components are now designed to operate in the sub-megahertz region. High frequency has really brought out the fringing flux and its parasitic eddy currents. Operating at high frequency has made the engineer very much aware of what fringing flux can do to hamper a design.

Material Permeability, (μ_m)

The B-H loops that are normally seen in the manufacturers' catalogs are usually taken from a toroidal sample of the magnetic material. The toroidal core, without a gap, is the ideal shape to view the B-H loop of a given material. The material permeability, μ_m , will be seen at its highest in the toroidal shape, as shown in Figure 1-31.

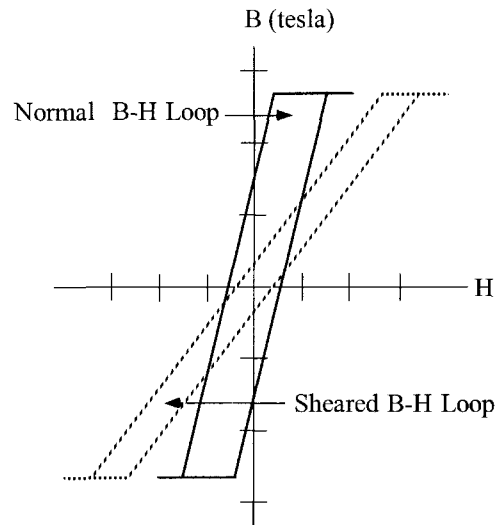


Figure 1-31. The Shearing of an Idealized B-H Loop Due to an Air Gap.

A small amount of air gap, less than 25 microns, has a powerful effect by shearing over the B-H loop. This shearing over of the B-H loop reduces the permeability. High permeability ferrites that are cut, like E cores, have only about 80 percent of the permeability, than that of a toroid of the same material. This is because of the induced gap, even though the mating surfaces are highly polished. In general, magnetic materials with high-permeability, are sensitive to temperature, pressure, exciting voltage, and frequency. The inductance change is directly proportional to the permeability change. This change in inductance will have an effect on the exciting current. It is very easy to see, that inductors that are designed into an LC, tuned circuit, must have a stable permeability, μ_e .

$$L = \frac{0.4\pi N^2 A_c \Delta\mu (10^{-8})}{MPL}, \text{ [henrys]} \quad [1-32]$$

Air Gaps

Air gaps are introduced into magnetic cores for a variety of reasons. In a transformer design a small air gap, l_g , inserted into the magnetic path, will lower and stabilize the effective permeability, μ_e .

$$\mu_c = \frac{\mu_m}{1 + \mu_m \left(\frac{l_g}{MPL} \right)} \quad [1-33]$$

This will result in a tighter control of the permeability change with temperature, and exciting voltage. Inductor designs will normally require a large air gap, l_g , to handle the dc flux.

$$l_g = \frac{0.4\pi N I_{dc} (10^{-4})}{B_{dc}}, \quad [\text{cm}] \quad [1-34]$$

Whenever an air gap is inserted into the magnetic path, as shown in Figure 1-32, there is an induced, fringing flux at the gap.

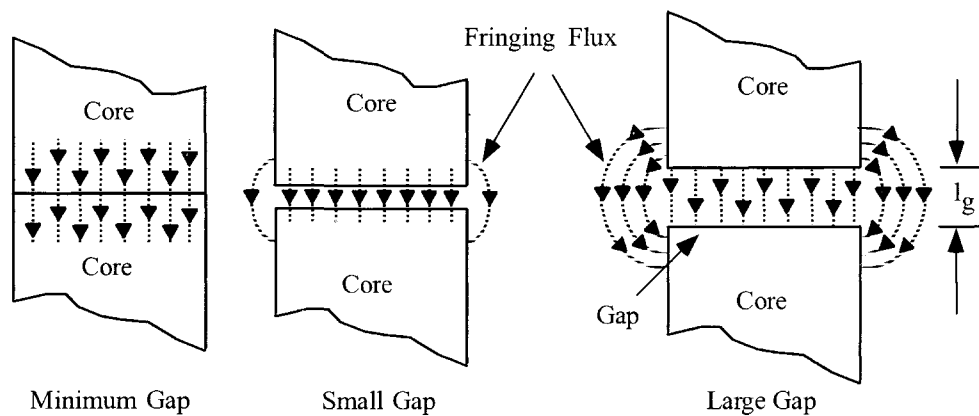


Figure 1-32. Fringing Flux at the Gap.

The fringing flux effect is a function of gap dimension, the shape of the pole faces, and the shape, size, and location of the winding. Its net effect is to shorten the air gap. Fringing flux decreases the total reluctance of the magnetic path and, therefore, increases the inductance by a factor, F , to a value greater than the one calculated.

Fringing Flux, F

Fringing flux is completely around the gap and re-enters the core in a direction of high loss, as shown in Figure 1-33. Accurate prediction of gap loss, P_g , created by fringing flux is very difficult to calculate.

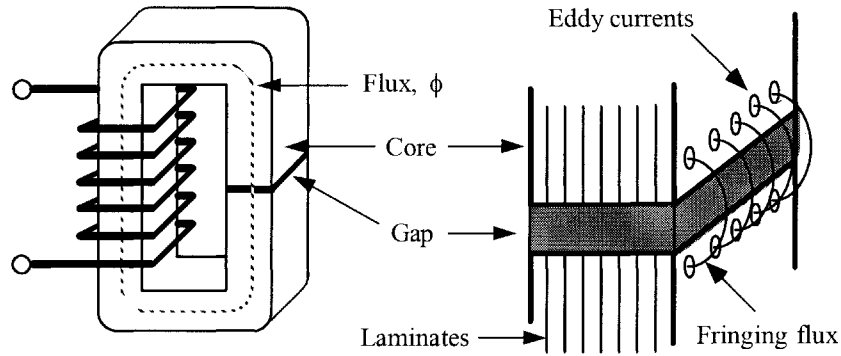


Figure 1-33. Fringing Flux, with High Loss Eddy Currents.

This area around the gap is very sensitive to metal objects, such as clamps, brackets and banding materials. The sensitivity is dependent on the intensity of the magnetomotive force, gap dimensions and the operating frequency. If a metal bracket or banding material is used to secure the core, and it passes over the gap, two things can happen: (1) If the material ferromagnetic is placed over the gap, or is in close proximity so it conducts the magnetic field, this is called “shorting the gap.” Shorting the gap is the same as reducing the gap dimension, thereby producing a higher inductance, than designed, and could drive the core into saturation. (2) If the material is metallic, (such as copper, or phosphor bronze), but not ferromagnetic, it will not short the gap or change the inductance. In both cases, if the fringing flux is strong enough, it will induce eddy currents that will cause localized heating. This is the same principle used in induction heating.

Gapped, dc Inductor Design

The fringing flux factor, F , has an impact on the basic inductor design equations. When the engineer starts a design, he or she must determine the maximum values for B_{dc} and for B_{ac} , which will not produce magnetic saturation. The magnetic material that has been selected will dictate the saturation flux density. The basic equation for maximum flux density is:

$$B_{\max} = \frac{0.4\pi N \left(I_{dc} + \frac{\Delta I}{2} \right) (10^{-4})}{l_g + \frac{MPL}{\mu_m}}, \quad [\text{tesla}] \quad [1-35]$$

The inductance of an iron-core inductor, carrying dc and having an air gap, may be expressed as:

$$L = \frac{0.4\pi N^2 A_c (10^{-8})}{l_g + \frac{MPL}{\mu_m}}, \quad [\text{henrys}] \quad [1-36]$$

The inductance is dependent on the effective length of the magnetic path, which is the sum of the air gap length, l_g , and the ratio of the core magnetic path length to the material permeability, (MPL/μ_m) . The final determination of the air gap size requires consideration of the fringing flux effect which is a function of the

gap dimension, the shape of the pole faces, and the shape, size, and location of the winding. The winding length, or the G dimension of the core, has a big influence on the fringing flux. See, Figure 1-34 and Equation 1-37.

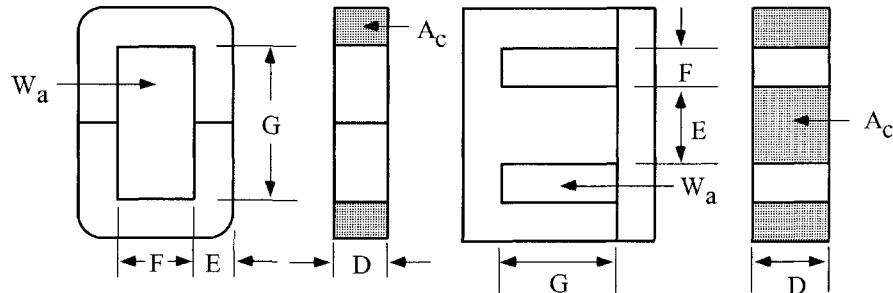


Figure 1-34. Dimensional, Call Out for C and E Cores.

The fringing flux decreases the total reluctance of the magnetic path length and, therefore, increases the inductance by a factor of F to a value greater than that calculated. The fringing flux factor is:

$$F = \left(1 + \frac{l_g}{\sqrt{A_c}} \ln \frac{2G}{l_g} \right) \quad [1-37]$$

After the inductance has been calculated using Equation 1-36, the fringing flux factor has to be incorporated into Equation 1-36. Equation 1-36 can now be rewritten to include the fringing flux factor, as shown:

$$L = F \left(\frac{0.4\pi N^2 A_c (10^{-8})}{l_g + \frac{\text{MPL}}{\mu_m}} \right), \quad [\text{henrys}] \quad [1-38]$$

The fringing flux factor, F, can now be included into Equation 1-35. This will check for premature, core saturation.

$$B_{\max} = F \left(\frac{0.4\pi N \left(I_{dc} + \frac{\Delta I}{2} \right) (10^{-4})}{l_g + \frac{\text{MPL}}{\mu_m}} \right), \quad [\text{tesla}] \quad [1-39]$$

Now that the fringing flux factor, F, is known and inserted into Equation 1-38. Equation 1-38 can be rewritten to solve for the required turns so that premature core saturation will not happen.

$$N = \sqrt{\frac{L \left(l_g + \frac{MPL}{\mu_m} \right)}{0.4\pi A_c F (10^{-8})}}, \quad [\text{turns}] \quad [1-40]$$

Fringing Flux and Coil Proximity

As the air gap increases, the fringing flux will increase. Fringing flux will fringe out away from the gap by the distance of the gap. If a coil was wound tightly around the core and encompasses the gap, the flux generated around the magnet wire will force the fringing flux back into the core. The end result will not produce any fringing flux at all, as shown in Figure 1-35. As the coil distance moves away from the core, the fringing flux will increase until the coil distance from the core is equal to the gap dimension.

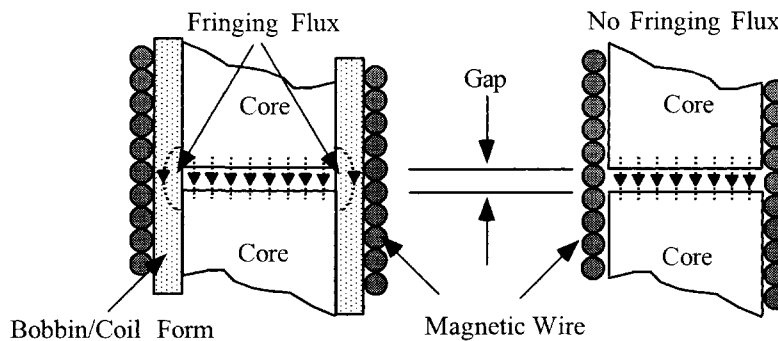


Figure 1-35. Comparing a Tightly-Wound Coil, and a Coil Wound on a Coil Form.

Fringing Flux, Crowding

Flux will always take the path of highest permeability. This can best be seen in transformers with interleave laminations. The flux will traverse along the lamination until it meets its mating, I or E. At this point, the flux will jump to the adjacent lamination and bypass the mating point, as shown in Figure 1-36.

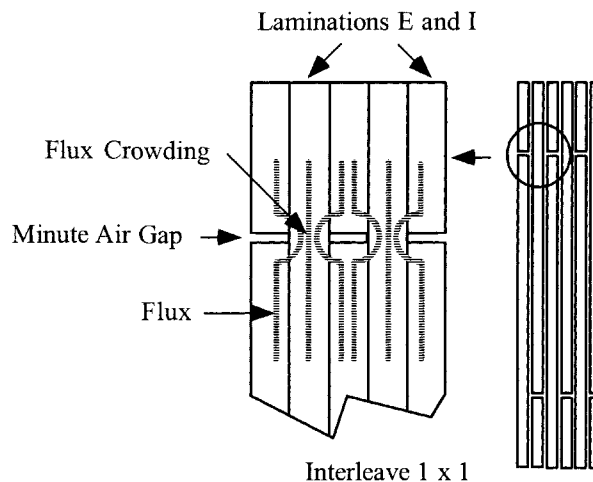


Figure 1-36. Flux Crowding in Adjacent Laminations.

This phenomena can best be seen by observing the exciting current at low, medium and high flux levels, as shown in Figure 1-37. At low levels of excitation, the exciting current is almost square, due to the flux taking the high permeability path, by jumping to the adjacent lamination, as shown in Figure 1-36. As the excitation is increased, the adjoining lamination will start to saturate, and the exciting current will increase and become nonlinear. When the adjacent lamination approaches saturation, the permeability drops. It is then that the flux will go in a straight line and cross the minute air gap, as shown in Figure 1-36.

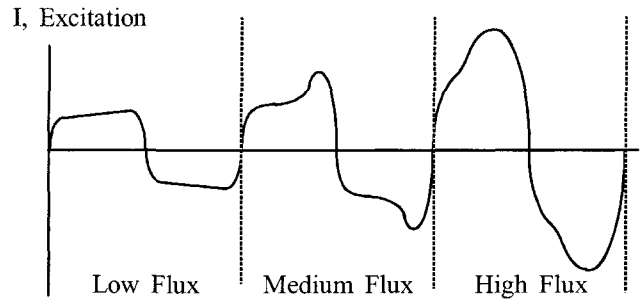


Figure 1-37. Exciting Current, at Different Levels of Flux Density, B.

Fringing Flux and Powder Cores

Designing high frequency converters, using low permeability powder cores, will usually require very few turns. Low perm power cores (less than 60), exhibit fringing flux. Powder cores with a distributed gap will have fringing flux that shorts the gap and gives the impression of a core with a higher permeability. Because of the fringing flux and a few turns, it is very important to wind uniformly and in a consistent manner. This winding is done to control the fringing flux and get inductance repeatability from one core to another, as shown in Figures 1-38 and 1-39.

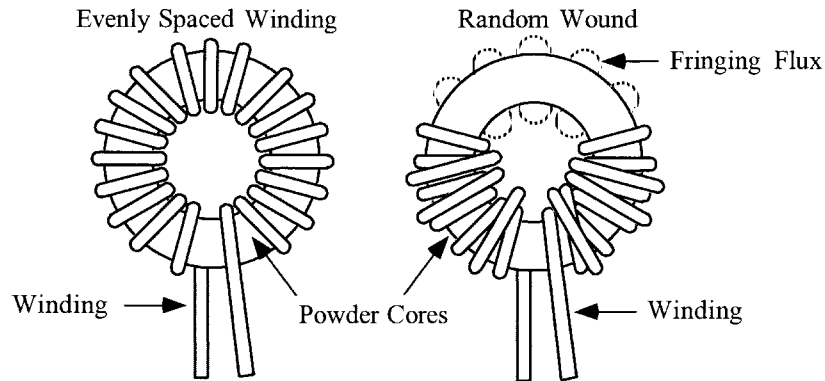


Figure 1-38. Comparing Toroidal, Winding Methods.

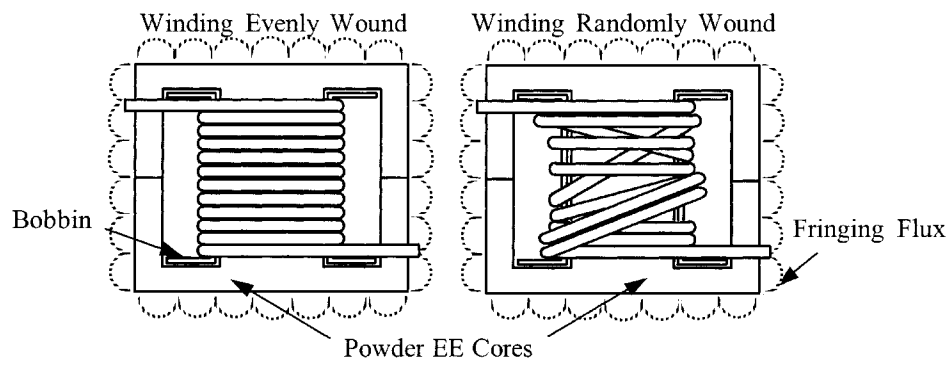


Figure 1-39. Comparing EE Cores, Winding Methods.

Chapter 2

Magnetic Materials and Their Characteristics

Introduction

The magnetic material is the paramount player in the design of magnetic components. The magnetics design engineer has three standard words when making the normal design trade-off study: cost, size, and performance. He will be happy to stuff any two into the bag. The magnetics engineer is now designing magnetic components that operate from below the audio range to the megahertz range. He is normally asked to design for maximum performance, with the minimum of his parasitic friends' capacitance and leakage inductance. Today, the magnetic materials the engineer has to work with are silicon steel, nickel iron (permalloy), cobalt iron (permendur), amorphous metallic alloys, and ferrites. These also have spin-off material variants, such as moly-permalloy powder, sendust powder, and iron powder cores. From this group of magnetic materials, the engineer will make trade-offs with the magnetic properties for his design. These properties are: saturation B_s , permeability μ , resistivity ρ (core loss), remanence B_r , and coercivity H_c .

Saturation

A typical hysteresis loop of a soft magnetic material is shown in Figure 2-1. When a high magnetizing force is encountered, a point is reached where further increase in, H , does not cause useful increase in, B . This point is known as the saturation point of that material. The saturation flux density, B_s , and the required magnetizing force, H_s , to saturate the core are shown with dashed lines.

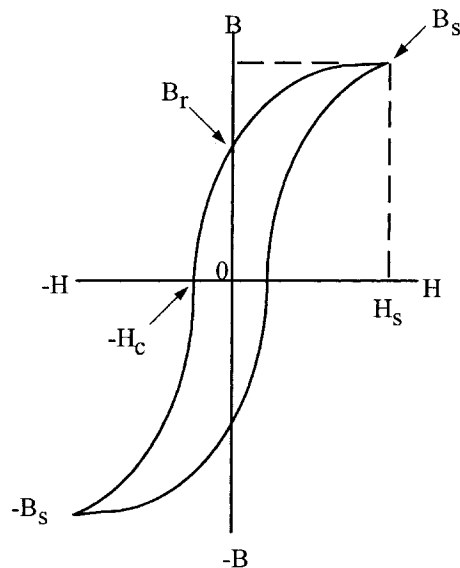


Figure 2-1. Typical B-H or Hysteresis Loop of a Soft Magnetic Material.

Remanence Flux, B_r , and Coercivity H_c

In Figure 2-1 the hysteresis loop clearly shows the remanence flux density, B_r . The remanence flux is the polarized flux remaining in the core after the excitation has been removed. The magnetizing force, $-H_c$, is called coercivity. It is the amount of magnetizing force required to bring the remanence flux density back to zero.

Permeability, μ

The permeability of a magnetic material is a measure of the ease in magnetizing the material. Permeability, μ , is the ratio of the flux density, B , to the magnetizing force, H .

$$\mu = \frac{B}{H}, \quad [\text{permeability}] \quad [2-1]$$

The relationship between B and H is not linear, as shown in the hysteresis loop in Figure 2-1. Then, it is evident that the ratio, B/H , (permeability), also varies. The variation of permeability with flux density, B , is shown in Figure 2-2. Also, it shows the flux density at which the permeability is at a maximum.

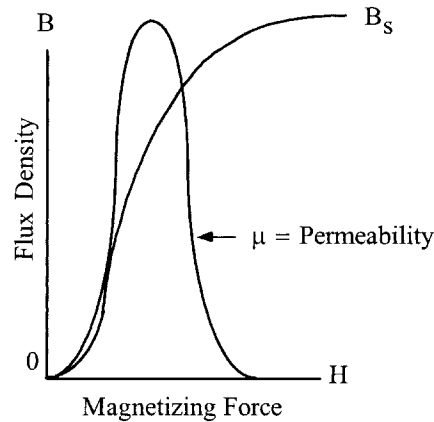


Figure 2-2. Variation in Permeability μ with B and H .

Hysteresis Loss, Resistivity, ρ , (core loss)

The enclosed area within the hysteresis, shown in Figure 2-1, is a measure of the energy lost in the core material during that cycle. This loss is made up in two components: (1) the hysteresis loss and (2) eddy current loss. The hysteresis loss is the energy loss when the magnetic material is going through a cycling state. The eddy current loss is caused when the lines of flux pass through the core, inducing electrical currents in it. These currents are called eddy currents and produce heat in the core. If the electrical resistance of the core is high, the current will be low; therefore, a feature of low-loss material is high electrical resistance. In the norm, when designing magnetic components, the core loss is a major design

factor. Core loss can be controlled by selecting the right material and thickness. Selecting the correct material, and operating within its limits, will prevent overheating that could result in damage to the wire insulation and/or the potting compound.

Introduction to Silicon Steel

Silicon steel was one of the first alloys to be used in transformers and inductors. It has been greatly improved over the years and is probably, pound for pound, the most, widely used magnetic material. One of the drawbacks in using steel in the early years was, as the material became older, the losses would increase. With the addition of silicon to the steel, the advantages were twofold: it increased the electrical resistivity, therefore reducing the eddy current losses, and it also improved the material's stability with age.

Silicon steel offers high saturation flux density, a relatively good permeability at high flux density, and a moderate loss at audio frequency. One of the important improvements made to the silicon steel was in the process called cold-rolled, grain-oriented, AISI type M6. This M6 grain-oriented steel has exceptionally low losses and high permeability. It is used in applications requiring high performance and the losses will be at a minimum.

Introduction to Thin Tape Nickel Alloys

High permeability metal alloys are based primarily on the nickel-iron system. Although Hopkinson investigated nickel-iron alloys as early as 1889, it was not until the studies by Elmen, starting in about 1913, on properties in weak magnetic fields and effects of heat-treatments, that the importance of the Ni-Fe alloys was realized. Elmen called his Ni-Fe alloys, "Permalloys," and his first patent was filed in 1916. His preferred composition was the 78Ni-Fe alloy. Shortly after Elmen, Yensen started an independent investigation that resulted in the 50Ni-50Fe alloy, "Hipernik," which has lower permeability and resistivity but higher saturation than the 78-Permalloy, (1.5 tesla compared to 0.75 tesla), making it more useful in power equipment.

Improvements in the Ni-Fe alloys were achieved by high temperature anneals in hydrogen atmosphere, as first reported by Yensen. The next improvement was done by using grain-oriented material and annealing it, in a magnetic field, which was also in a hydrogen atmosphere. This work was done by Kelsall and Bozorth. Using these two methods, a new material, called Supermalloy, was achieved. It has a higher permeability, a lower coercive force, and about the same flux density as 78-Permalloy. Perhaps the most important of these factors is the magnetic anneal, which, not only increases permeability, but also provides a "square" magnetization curve, important in high frequency power conversion equipment.

In order to obtain high resistance, and therefore lower core losses for high frequency applications, two approaches have been followed: (1) modification of the shape of metallic alloys and (2) development of magnetic oxides. The result was the development of thin tapes and powdered alloys in the 1920's, and thin films in the 1950's. The development of thin film has been spurred by the requirements of aerospace, power conversion electronics from the mid 1960's to the present.

The Ni-Fe alloys are available in thicknesses of 2 mil, 1 mil, 0.5 mil, 0.25 and 0.125 mil. The material comes with a round or square B-H loop. This gives the engineer a wide range of sizes and configurations from which to select for a design. The iron alloy properties for some of the most popular materials are shown in Table 2-1. Also, given in Table 2-1, is the Figure number for the B-H loop of each of the magnetic materials.

Table 2-1 Magnetic Properties for Selected Iron Alloys Materials.

Iron Alloy Material Properties								
Material Name	Composition	Initial Permeability μ_i	Flux Density Tesla B_s	Curie Temp. °C	dc, Coercive Force, Hc Oersteds	Density grams/cm ³ δ	Weight Factor x	Typical B-H Loop Figures
Silicon	3% Si 97% Fe	1.5 K	1.5-1.8	750	0.4-0.6	7.63	1.000	(2-3)
Supermendur*	49% Co 49% Fe 2% V	0.8 K	1.9-2.2	940	0.15-0.35	8.15	1.068	(2-4)
Orthonol	50% Ni 50% Fe	2 K	1.42-1.58	500	0.1-0.2	8.24	1.080	(2-5)
Permalloy	79% Ni 17% Fe 4% Mo	12 K-100 K	0.66-0.82	460	0.02-0.04	8.73	1.144	(2-6)
Supermalloy	78% Ni 17% Fe 5% Mo	10 K-50 K	0.65-0.82	460	0.003-0.008	8.76	1.148	(2-7)
* Field Anneal.								
x Silicon has unity weight factor.								

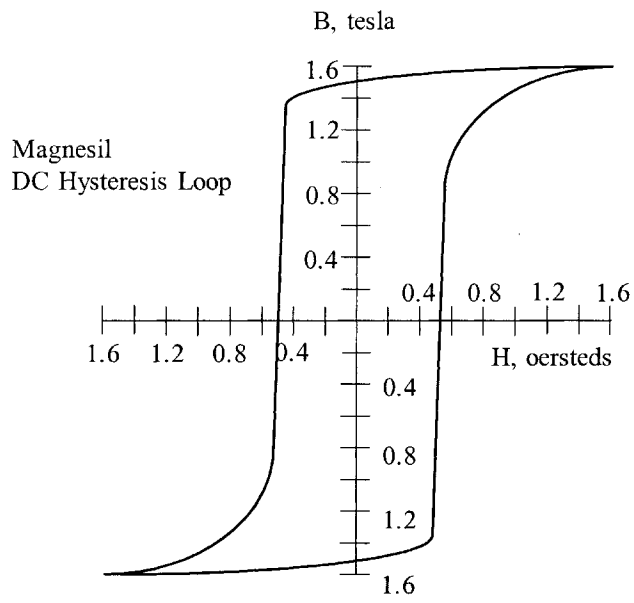


Figure 2-3. Silicon B-H Loop: 97% Fe 3% Si.

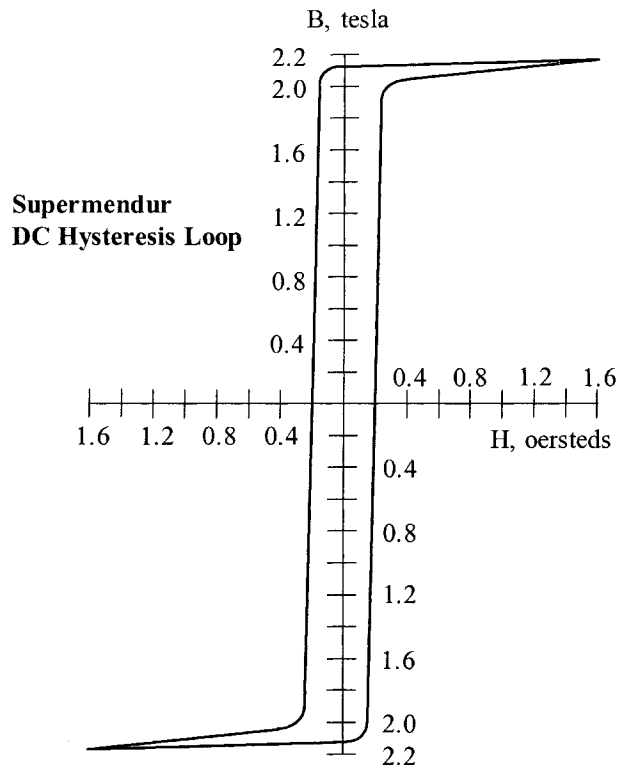


Figure 2-4. Supermendur B-H Loop: 49% Fe 49% Co 2% V.

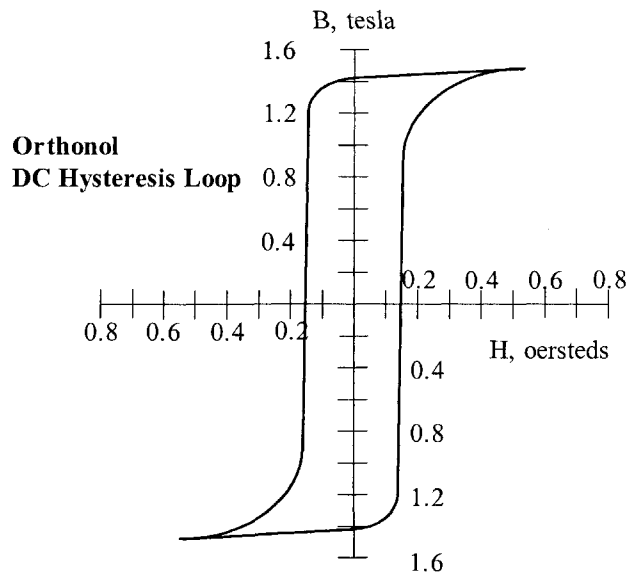


Figure 2-5. Orthonol B-H loop: 50% Fe 50% Ni.

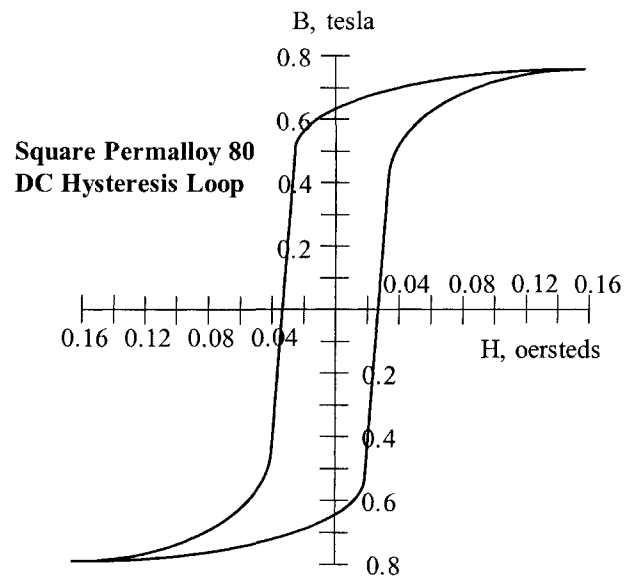


Figure 2-6. Square Permalloy 80 B-H loop: 79% Ni 17% Fe 4% Mo.

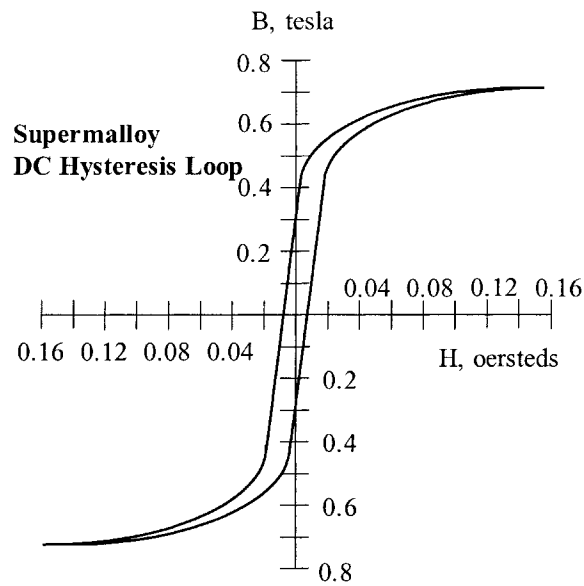


Figure 2-7. Supermalloy B-H Loop: 78% Ni 17% Fe 5% Mo.

Introduction to Metallic Glass

The first synthesis of a metallic glass drawing wide attention among material scientists, occurred in 1960. Klement, Willens and Duwez reported that a liquid, AuSi alloy, when rapidly quenched to liquid nitrogen temperature, would form an amorphous solid. It was twelve years later that Chen and Polk produced ferrous-based metallic glasses in useful shapes with significant ductility. Metallic glasses have since survived the transition from laboratory curiosities to useful products, and currently are the focus of intensive technological and fundamental studies.

Metallic glasses are generally produced, by liquid quenching, in which a molten metal alloy is rapidly cooled, at rates on the order of 10^5 degrees/sec., through the temperature at which crystallization normally occurs. The basic difference between crystalline (standard magnetic material) and glassy metals is in their atomic structures. Crystalline metals are composed of regular, three-dimensional arrays of atoms which exhibit long-range order. Metallic glasses do not have long-range structural order. Despite their structural differences, crystalline and glassy metals of the same compositions exhibit nearly the same densities.

The electrical resistivities of metallic glasses are much larger, (up to three times higher), than those of crystalline metals of similar compositions. The magnitude of the electrical resistivities and their temperature coefficients in the glassy and liquid states are almost identical.

Metallic glasses are quite soft magnetically. The term, "soft," refers to a large response of the magnetization to a small-applied field. A large magnetic response is desirable in such applications as transformers and inductors. The obvious advantages of these new materials are in high frequency applications with their high induction, high permeability and low core loss.

There are four amorphous materials that have been used in high frequency applications: 2605SC, 2714A, 2714AF and Vitroperm 500F. Material 2605SC offers a unique combination of high resistivity, high saturation induction, and low core loss, making it suitable for designing high frequency dc inductors. Material 2714A is a cobalt material that offers a unique combination of high resistivity, high squareness ratio B_r/B_s , and very low core loss, making it suitable for designing high frequency aerospace transformers and mag-amps. The Vitroperm 500F is an iron based material with a saturation of 1.2 tesla and is well-suited for high frequency transformers and gapped inductors. The high frequency core loss for the nanocrystal 500F is lower than some ferrite, even operating at a high flux density. The amorphous properties for some of the most popular materials are shown in Table 2-2. Also, given in Table 2-2, is the Figure number for the B-H loop of each of the magnetic materials.

Table 2-2. Magnetic Properties for Selected Amorphous Materials.

Amorphous Material Properties								
Material Name	Major Composition	Initial Permeability μ_i	Flux Density Tesla B_s	Curie Temperature °C	dc, Coercive Force, Hc Oersteds	Density grams/cm ³ δ	Weight Factor x	Typical B-H Loop Figures
2605SC	81% Fe 13.5% B 3.5% Si	1.5K	1.5-1.6	370	0.4-0.6	7.32	0.957	(2-8)
2714A	66% Co 15% Si 4% Fe	0.8K	0.5-0.65	205	0.15-0.35	7.59	0.995	(2-9)
2714AF	66% Co 15% Si 4% Fe	2K	0.5-0.65	205	0.1-0.2	7.59	0.995	(2-10)
Nanocrystal Vitroperm 500F*	73.5% Fe 1% Cu 15.5% Si	30K-80K	1.0-1.2	460	0.02-0.04	7.73	1.013	(2-11)
* Vitroperm is the trademark of Vacuumschmelze.								
x Silicon has a unity weight factor. See Table 2-1.								

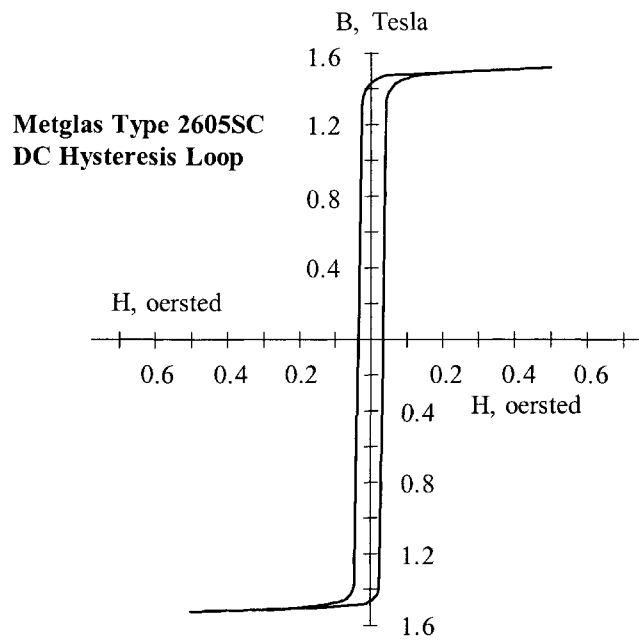


Figure 2-8. Amorphous 2605SC B-H Loop: 81% Fe 13.5% B 3.5% Si.

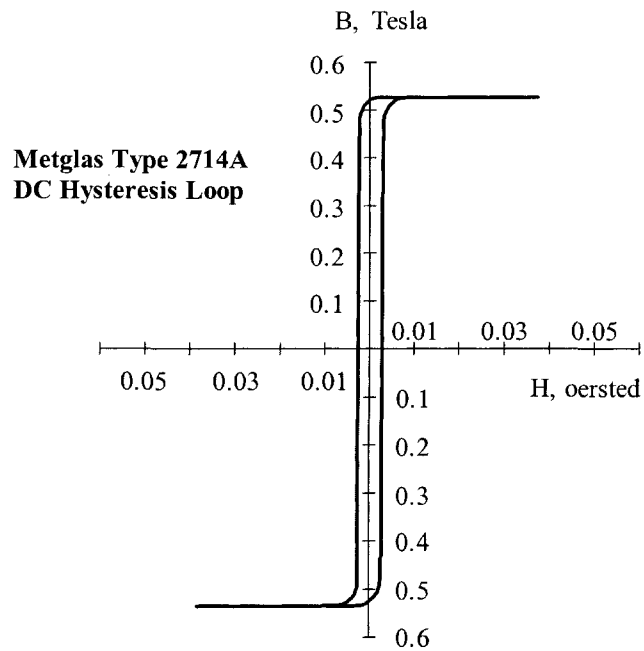


Figure 2-9. Amorphous 2714A B-H Loop: 66% Co 15% Si 4% Fe.

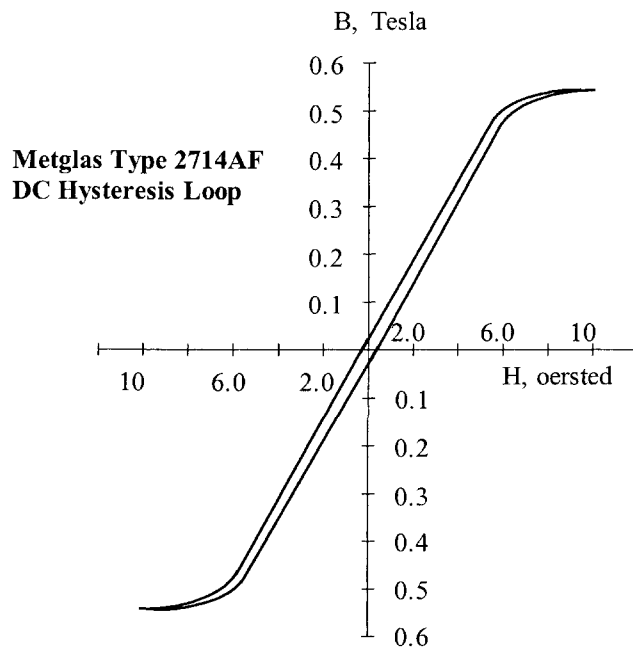


Figure 2-10. Amorphous 2714AF B-H Loop: 66% Co 15% Si 4% Fe.

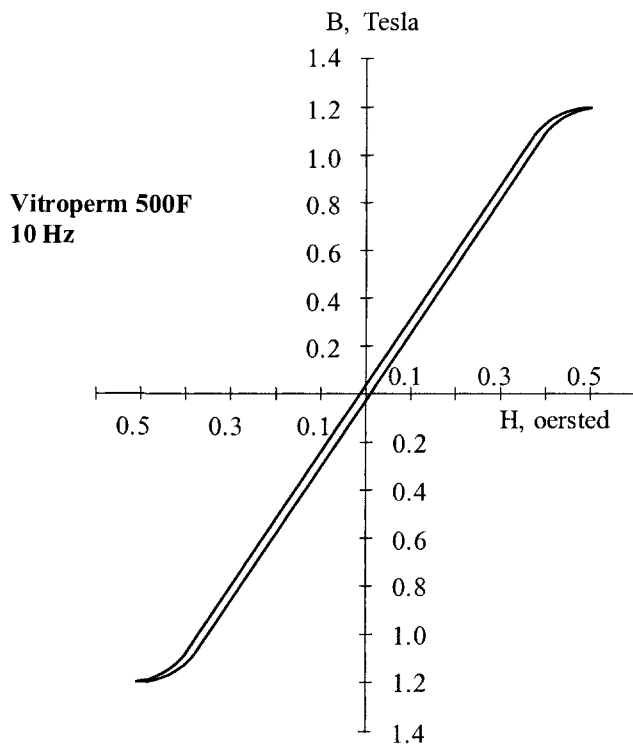


Figure 2-11. Vitroperm 500F B-H loop: 73.5% Fe 15.5% Si 1% Cu.

Introduction to Soft Ferrites

In the early days of electrical industry, the need for the indispensable magnetic material was served by iron and its magnetic alloys. However, with the advent of higher frequencies, the standard techniques of reducing eddy current losses, (using laminations or iron powder cores), was no longer efficient or cost effective.

This realization stimulated a renewed interest in "magnetic insulators," as first reported by S. Hilpert in Germany, in 1909. It was readily understood that, if the high electrical resistivity of oxides could be combined with desired magnetic characteristics, a magnetic material that was particularly well-suited for high frequency operation would result.

Research to develop such a material was being performed by scientists in various laboratories all over the world, such as V. Kato, T. Takei, and N. Kawai in the 1930's in Japan, and by J. Snoek of the Philips' Research Laboratories in the period 1935-1945 in The Netherlands. By 1945, Snoek had laid down the basic fundamentals of the physics and technology of practical ferrite materials. In 1948, the Neel Theory of ferromagnetism provided the theoretical understanding of this type of magnetic material.

Ferrites are ceramic, homogeneous materials composed of oxides; iron oxide is their main constituent. Soft ferrites can be divided into two major categories; manganese-zinc and nickel-zinc. In each of these categories, changing the chemical composition, or manufacturing technology, can manufacture many different Mn-Zn and Ni-Zn material grades. The two families of Mn-Zn and Ni-Zn ferrite materials complement each other, and allow the use of soft ferrites from audio frequencies to several hundred megahertz. Manufacturers do not like to handle manganese-zinc in the same area, or building with nickel-zinc, because one contaminates the other, which leads to poor performance yields. The basic difference between Manganese-Zinc and Nickel-Zinc is shown in Table 2-3. The biggest difference is Manganese-Zinc has a higher permeability and Nickel-Zinc has a higher resistivity. Shown in Table 2-4 are some of the most popular ferrite materials. Also, given in Table 2-4, is the Figure number for the B-H loop of each of the materials.

Table 2-3. Comparing Manganese-Zinc and Nickel-Zinc Basic Properties.

Basic Ferrite Material Properties					
Materials	Initial Permeability μ_i	Flux Density B_{max} Tesla	Curie Temperature, $^{\circ}C$	dc, Coercive Force, H_c Oersteds	Resistivity $\Omega - cm$
Manganese Zinc	750-15 K	0.3-0.5	100-300	0.04-0.25	10-100
Nickel Zinc	15-1500	0.3-0.5	150-450	0.3-0.5	10^6

Manganese-Zinc Ferrites

This type of soft ferrite is the most common, and is used in many more applications than the nickel-zinc ferrites. Within the Mn-Zn category, a large variety of materials are possible. Manganese-zinc ferrites are primarily used at frequencies less than 2 MHz.

Nickel-Zinc Ferrites

This class of soft ferrite is characterized by its high material resistivity, several orders of magnitude higher than Mn-Zn ferrites. Because of its high resistivity, Ni-Zn ferrite is the material of choice for operating from 1-2 MHz to several hundred megahertz.

The material permeability, μ_m , has little influence on the effective permeability, μ_e , when the gap dimension is relatively large, as shown in Table 2-5.

Table 2-4. Magnetic Properties for Selected Ferrite Materials.

Ferrites Material Properties							
*Magnetics Material Name	Initial Permeability μ_i	Flux Density Tesla $B_s@15 \text{ Oe}$	Residual Flux Tesla B_r	Curie Temperature $^{\circ}\text{C}$	dc, Coercive Force, H_c Oersteds	Density grams/cm ³ δ	Typical B-H Loop Figures
K	1500	0.48T	0.08T	>230	0.2	4.7	(2-12)
R	2300	0.50T	0.12T	>230	0.18	4.8	(2-13)
P	2500	0.50T	0.12T	>230	0.18	4.8	(2-13)
F	5000	0.49T	0.10T	>250	0.2	4.8	(2-14)
W	10,000	0.43T	0.07T	>125	0.15	4.8	(2-15)
H	15,000	0.43T	0.07T	>125	0.15	4.8	(2-15)

*Magnetics, a Division of Spang & Company

Table 2-5. Permeability, and its Effect on Gapped Inductors.

Comparing Material Permeabilities					
*Material	μ_m	Gap, inch	Gap, cm	**MPL, cm	μ_e
K	1500	0.04	0.101	10.4	96
R	2300	0.04	0.101	10.4	98
P	2500	0.04	0.101	10.4	99
F	3000	0.04	0.101	10.4	100

*The materials are from Magnetics, a Division of Spang and Company
 **Core , ETD44

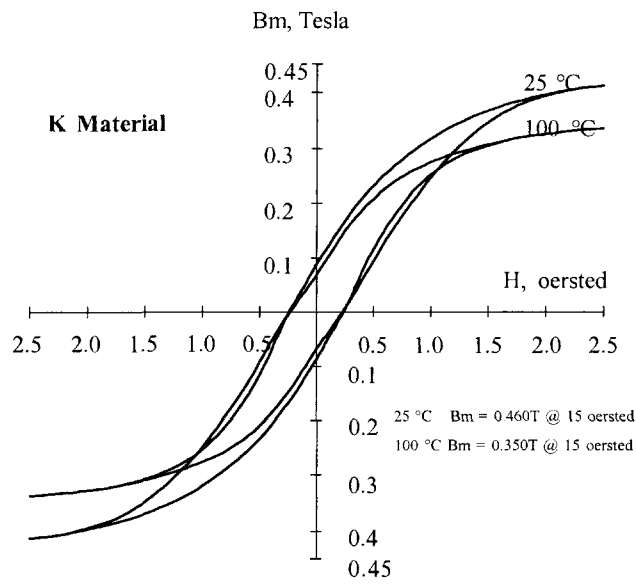


Figure 2-12. Ferrite B-H loop, K Material at 25 and 100 °C.

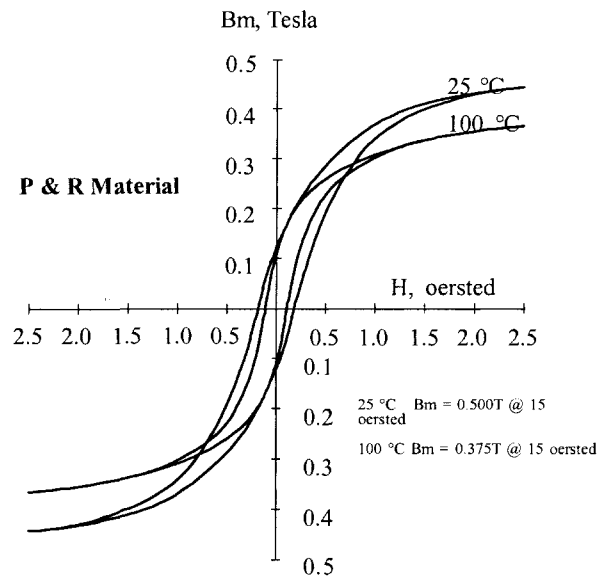


Figure 2-13. Ferrite B-H loop, P & R Material at 25 and 100 °C.

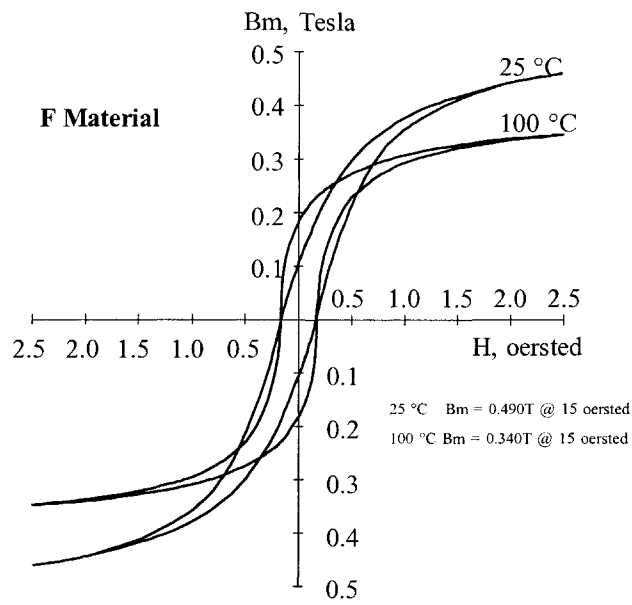


Figure 2-14. Ferrite B-H loop, F Material at 25 and 100 ° C.

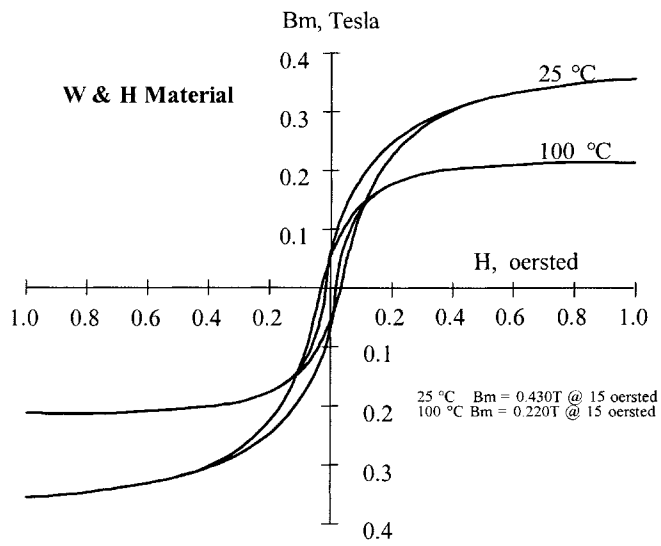


Figure 2-15. Ferrite B-H loop, W & H Material at 25 and 100 ° C.

Ferrite Cross Reference

The cross-reference, Table 2-6, has been put together using some of the leading ferrite manufacturers. The ferrite materials have been organized and referenced under Magnetics materials. This is because Magnetics has one of the broadest lines of standard ferrite materials.

Table 2-6. Ferrite Materials, Manufacturers' Cross-Reference.

Ferrite Material Cross Reference							
Permeability	1500	2300	2500	3000	5000	10000	15000
Application	Power	Power	Power	Power	Filter	Filter	Filter
Manufacturer's	Material Designation						
Magnetics	1 K	2 R	3 P	F	J	W	H
Ferroxcube	3F35	3F3	3C94	3C81	3E27	3E5	3E7
Permeability, μ_i	1400	2000	2300	2700	6000	10000	15000
Fair-Rite			78		75	76	
Permeability, μ_i			2300		5000	10000	
Siemens	N49	N87	N67	T41	T35	T38	T46
Permeability, μ_i	1300	2200	2100	3000	6000	10000	15000
TDK Corp.	PC50	PC40	PC44	H5A	HP5	H5C2	H5C3
Permeability, μ_i	1400	2300	2400	3300	5000	10000	15000
MMG		F44	F5	F5C	F-10	F-39	
Permeability, μ_i		1900	2000	3000	6000	10000	
Ceramic Mag	MN67	MN80	MN80	MN8CX	MN60	MC25	MC15K
Permeability, μ_i	1000	2000	2000	3000	6000	10000	15000
Token		HBM	B25	B3100	H5000	H12000	
Permeability, μ_i							
Ferrite Int.	TSF-5099	TSF-7099	TSF-7070	TSF-8040	TSF-5000	TSF-010K	
Permeability, μ_i	2000	2000	2200	3100	5000	10000	

1. High Frequency power material 250 kHz & up.
2. Lowest loss at 80°-100°C, 25 kHz to 250 kHz.
3. Lowest loss at 60°C-80°C.

Introduction to Molypermalloy Powder Cores

The nickel-iron (Ni-Fe) high permeability magnetic alloys (permalloy) were discovered in 1923 and 1927. Permalloy alloys were successfully used in powder cores, greatly contributing to the carrier wave communications of the time.

In the early 1940's, a new material, trademarked Molybdenum Permalloy Powder (MPP), was developed into cores by the Bell Telephone Laboratory and the Western Electric Company. This new material was developed for loading coils, filtering coils, and transformers at audio and carrier frequencies in the telephone facility. The use of such cores has been extended to many industrial and military circuits. The stability of permeability and core losses with time, temperature, and flux level, are particularly important to engineers designing tuned circuits and timing circuits. This new material has given reliable and superior performance over all past powder core materials.

Molybdenum permalloy powder, [2 Molybdenum (Mo)-82 Nickel (Ni)-16 Iron (Fe)], is made by grinding hot-rolled and embrittled cast ingots; then, the alloy is insulated and screened to a fineness of 120 mesh for use in audio frequency applications, and 400 mesh for use at high frequencies.

In the power conversion field, the MPP core has made its greatest impact in switching power supplies. The use of MPP cores and power MOSFET transistors has permitted increased frequency, resulting in greater compactness and weight reduction in computer systems. The power supply is the heart of the system. When the power supply is designed correctly, using a moderate temperature rise, the system will last until it becomes obsolete. In these power systems there are switching inductors, smoothing choke coils, common mode filters, input filters, output filters, power transformers, current transformers and pulse transformers. They cannot all be optimally designed, using MPP cores. But, in some cases, MPP cores are the only ones that will perform in the available space with the proper temperature rise.

Introduction to Iron Powder Cores

The development of compressed iron powder cores as a magnetic material for inductance coils, stemmed from efforts of Bell Telephone Laboratory engineers to find a substitute for fine iron-wire cores. The use of iron powder cores was suggested by Heaviside, in 1887, and again, by Dolezalek in 1900.

The first iron powder cores of commercially valuable properties were described by Buckner Speed, in U.S. Patent No. 1274952, issued in 1918. Buckner Speed and G.W. Elman published a paper in the A.I.E.E. Transactions, "Magnetic Properties of Compressed Powdered Iron," in 1921. This paper describes a

magnetic material, which is well-suited to the construction of cores in small inductance coils and transformers, such as those used in a telephone system. These iron powder cores were made from 80 Mesh Electrolytic Iron Powder. The material was annealed, then, insulated by oxidizing the surface of the individual particles. In this way, a very thin and tough insulation of grains of iron was obtained; this did not break down when the cores were compressed. A shellac solution was applied to the insulated powder as a further insulator and binder. This was how toroidal iron powder cores were manufactured by Western Electric Company until about 1929. Today's iron powder cores are manufactured in much the same way, using highly pure iron powder and a more exotic insulator and binder. The prepared powder is compressed under extremely high pressures to produce a solid-looking core. This process creates a magnetic structure with a distributed air-gap. The inherent high saturation flux density of iron, combined with the distributed air-gap, produces a core material with initial permeability of less than 100, and with high-energy storage capabilities.

The dc current does not generate core loss, but an ac or ripple current does generate core loss. Iron powder material has higher core loss than some other, more expensive, core materials. Most dc-biased inductors have a relatively small percentage of ripple current and, thus, core loss will be minimal. However, core loss will sometimes become a limiting factor in applications with a relatively high percentage of ripple current at very high frequency. Iron powder is not recommended for inductors with discontinuous current or transformers with large ac flux swings.

Low cost, iron powder cores are typically used in today's, low and high frequency power switching conversion applications, for differential-mode, input and output power inductors. Because iron powder cores have such low permeability, a relatively large number of turns are required for the proper inductance, thus keeping the ac flux at a minimum. The penalty for using iron powder cores is usually found in the size and efficiency of the magnetic component.

There are four standard powder materials available for power magnetic devices: Molypermalloy (MPP) Powder Cores with a family of curves, as shown in Figure 2-20; High flux (HF) Powder Cores with a family of curves, as shown in Figure 2-21; Sendust Powder Cores, *(Kool M μ), with a family of curves, as shown in Figure 2-22; and Iron Powder Cores, with a family of curves, as shown in Figure 2-23. The powder cores come in a variety of permeabilities. This gives the engineer a wide range in which to optimize the design. The powder core properties for the most popular materials are shown in Table 2-7. Also, given in Table 2-7, is the Figure number for the B-H loop of each of the powder core materials. In Table 2-8 is a listing of the most popular permeabilities for each of the powder core materials.

*Trademark of Magnetics Division, Spang and Company.

Table 2-7. Powder Core Material Properties.

Powder Core Material Properties							
Material Name	Composition	Initial Permeability μ_i	Flux Density Tesla B_s	Curie Temperature °C	dc, Coercive Force, Hc Oersteds	Density grams/cm ³ δ	Typical B-H Loop Figures
MPP	80% Ni 20% Fe	14-550	0.7	450	0.3	8.5	(2-16)
High Flux	50% Ni 50% Fe	14 - 160	1.5	360	1	8	(2-17)
Sendust (Kool M μ)	85% Fe 9% Si 6% Al	26 - 125	1	740	0.5	6.15	(2-18)
Iron Powder	100% Fe	4.0 - 100	0.5 - 1.4	770	5.0 - 9.0	3.3 - 7.2	(2-19)

Table 2-8. Standard Powder Core Permeabilities.

Standard Powder Core Permeabilities				
Powder Material	MPP	High Flux	Sendust (Kool M μ)	Iron Powder
Initial Permeability, μ_i				
10				X
14	X	X		
26	X	X	X	
35				X
55				X
60	X	X	X	X
75			X	X
90			X	
100				X
125	X	X	X	
147	X	X		
160	X	X		
173	X			
200	X			
300	X			
550	X			

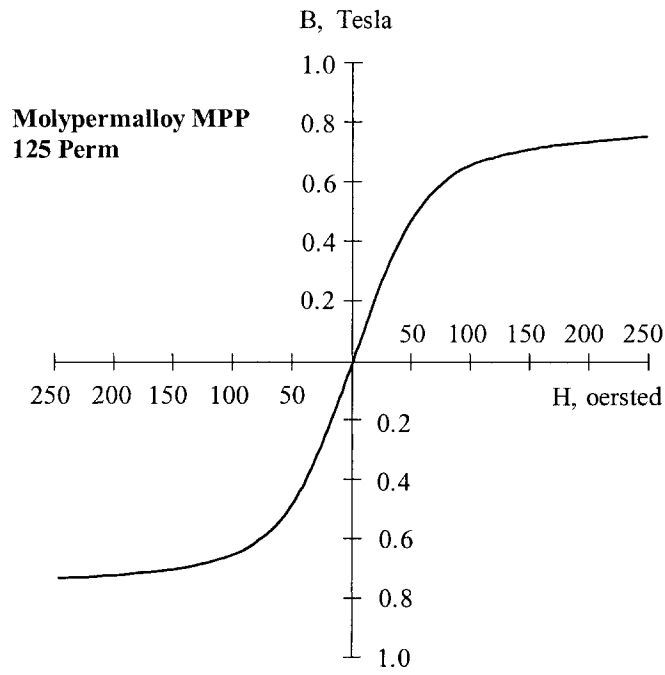


Figure 2-16. Molypermalloy Powder Core, 125 Perm.

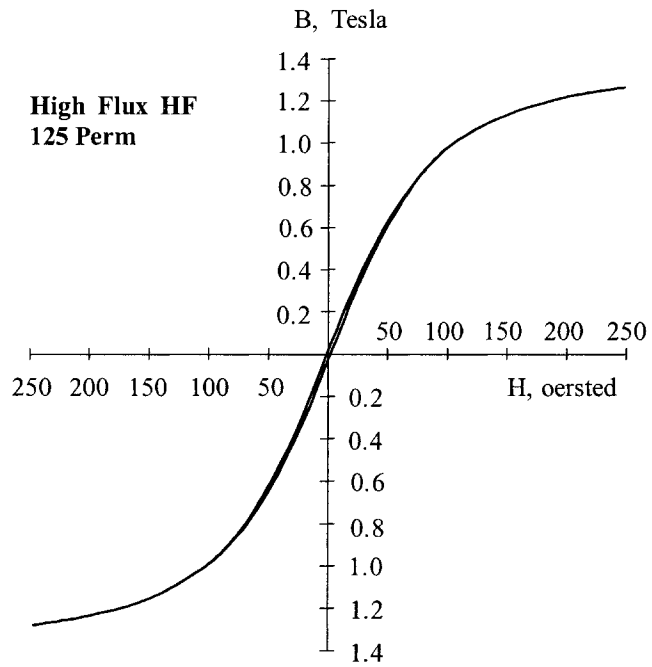


Figure 2-17. High Flux Powder Core, 125 Perm.

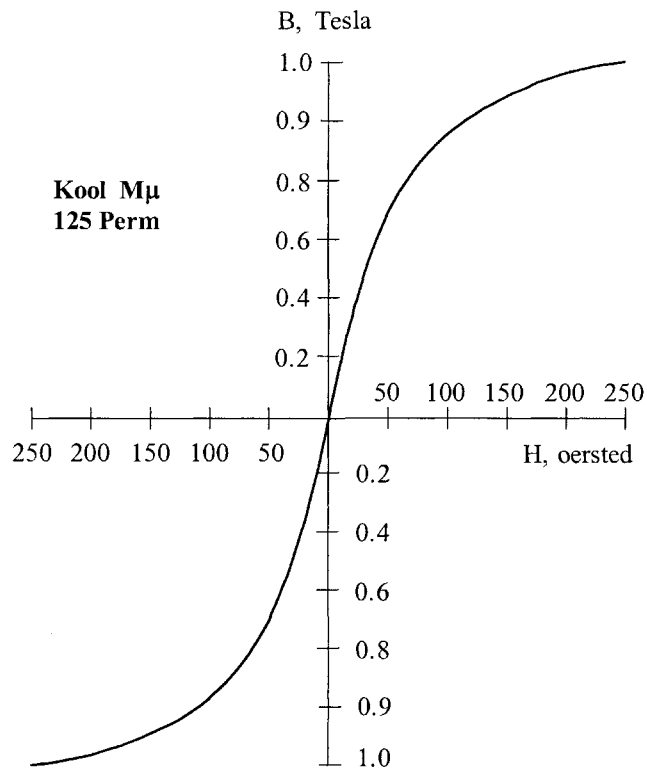


Figure 2-18. Sendust (Kool M μ) Powder Core, 125 Perm.

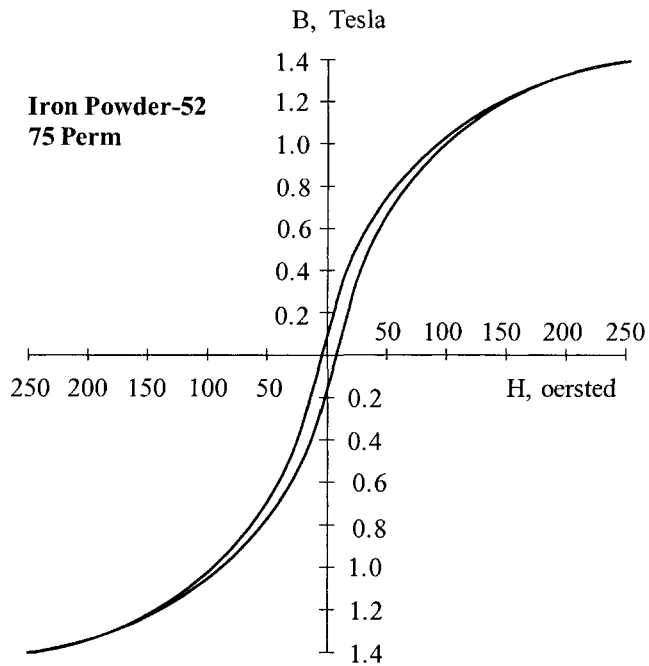


Figure 2-19. Iron Powder (-52) Core, 75 Perm.

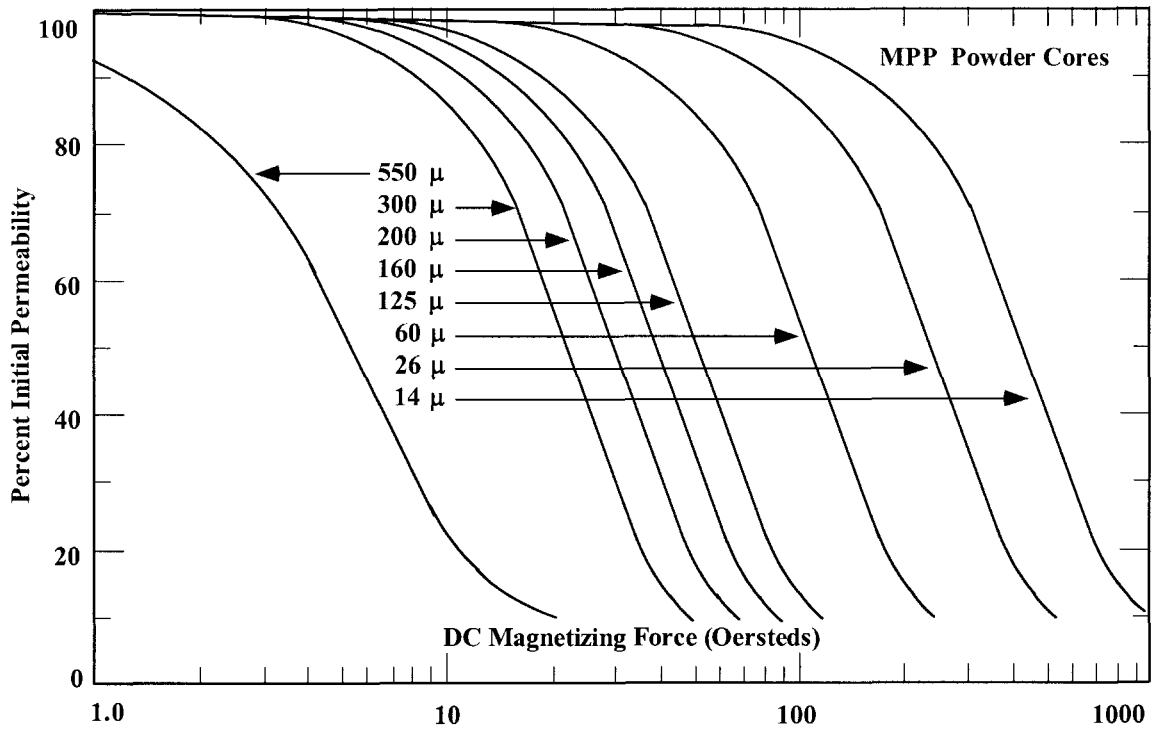


Figure 2-20. Permeability Versus dc Bias for Molypermalloy Powder Cores.

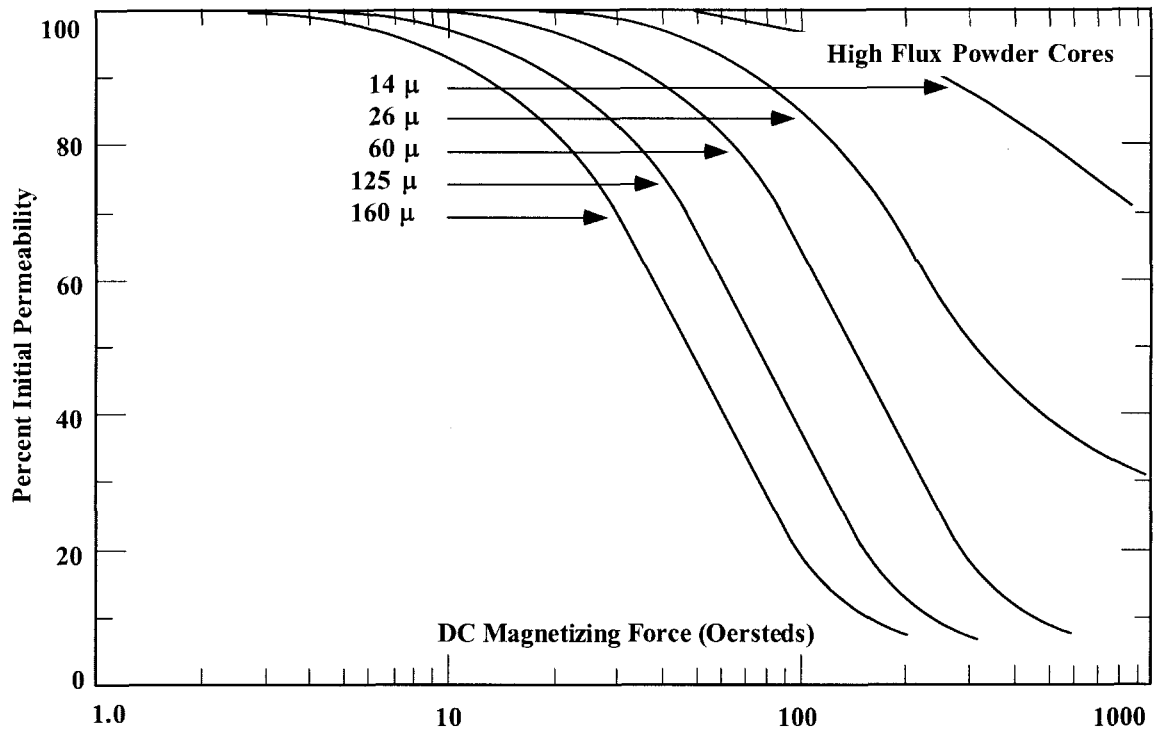


Figure 2-21. Permeability Versus dc Bias for High Flux Powder Cores.

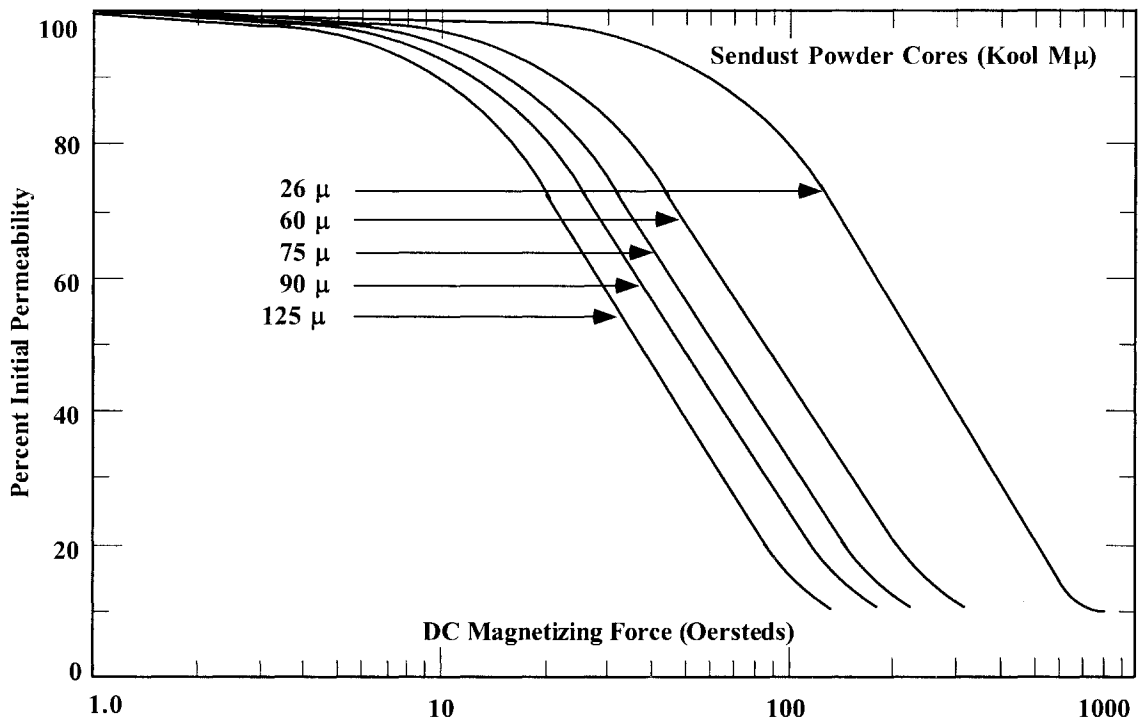


Figure 2-22. Permeability Versus dc Bias for Sendust Powder Cores.

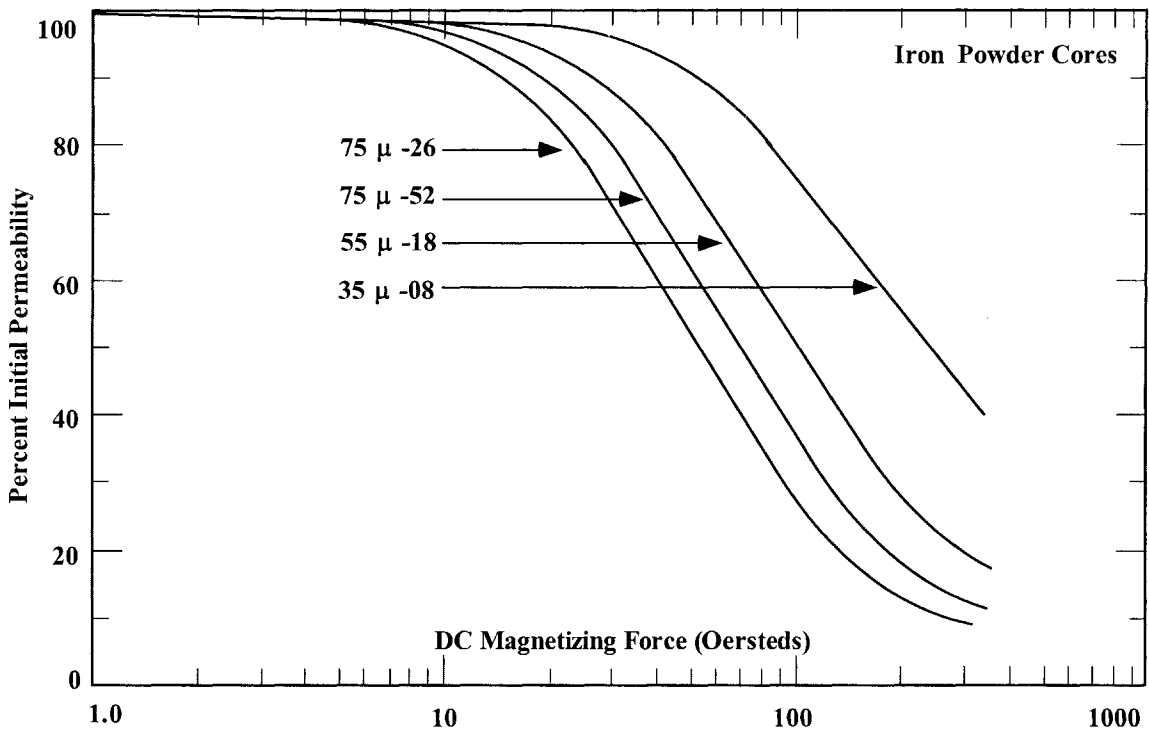


Figure 2-23. Permeability Versus dc Bias for Iron Powder Cores.

Core Loss

The designer of power magnetic components, such as transformer and inductors, requires specific knowledge about the electrical and magnetic properties of the magnetic materials used in these components. There are two magnetic properties that are of interest, the dc and the ac. The dc B-H hysteresis loop is a very useful guide for comparing the different types of magnetic materials. It is the ac magnetic properties that are of interest to the design engineer. One of the most important ac properties is the core loss. The ac core loss is a function of the magnetic material, magnetic material thickness, magnetic flux density B_{ac} , frequency f , and operating temperature. Thus, the choice of the magnetic material is based upon achieving the best characteristic using the standard trade-off such as cost, size, and performance.

All manufacturers do not use the same units when describing their core loss. The user should be aware of the different core loss units when comparing different magnetic materials. A typical core loss graph is shown in Figure 2-24. The vertical scale is core loss, and the horizontal scale is flux density. The core loss data is plotted at different frequencies, as shown in Figure 2-24.

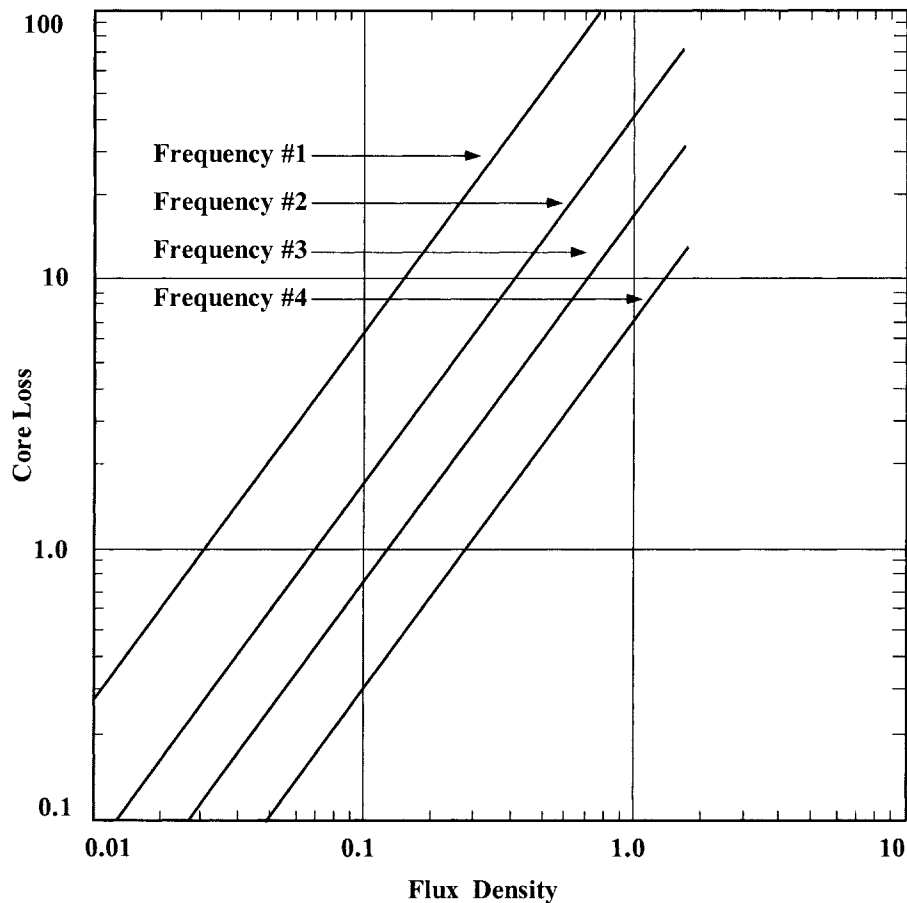


Figure 2-24. Typical Graph for Plotting Core Loss at Different Frequencies.

Vertical Scale

Here is a list of core loss units used by manufacturers:

1. watts per pound
2. watts per kilogram
3. milliwatts per gram
4. milliwatts per cubic centimeter (cm³)

Horizontal Scale

Here is a list of flux density units used by manufacturers:

1. gauss
2. kilogauss
3. tesla
4. millitesla

The data can be plotted or presented in either hertz or kilohertz.

Core Loss Equations

Manufacturers are now presenting the core loss in the form of an equation such as:

$$\text{watts/kilogram} = k f^{(m)} B^{(n)} \quad [2-2]$$

Here, again, the units will change from one manufacturer to another. In the following tables the manufacturers core loss data has been organized with the same units for all core losses. The data was modified to put the data in metric units, gauss to tesla and, watts per pound to watts per kilogram. The coefficients for Magnetics Inc. molypermalloy powder cores, (MPP), using Equation [2-2] are shown in Table 2-9. The coefficients for Magnetics Inc. High Flux powder cores, (HF), using Equation [2-2] are shown in Table 2-10. The coefficients for Magnetics Inc. Sendust powder cores, (Kool-M μ), using Equation [2-2] are shown in Table 2-11. The coefficients for iron alloy materials using Equation [2-2] are shown in Table 2-12.

Table 2-9. Core Loss Coefficients for MPP Powder Cores.

Core Loss Equation Factors				
Magnetics MPP Powder Cores				
Material	Permeability μ	Coefficient k	Coefficient (m)	Coefficient (n)
MPP	14	0.005980	1.320	2.210
MPP	26	0.001190	1.410	2.180
MPP	60	0.000788	1.410	2.240
MPP	125	0.001780	1.400	2.310
MPP	147-160-173	0.000489	1.500	2.250
MPP	200-300	0.000250	1.640	2.270
MPP	550	0.001320	1.590	2.360

Table 2-10. Core Loss Coefficients for High Flux Powder Cores.

Core Loss Equation Factors				
Magnetics HF Powder Cores				
Material	Permeability μ	Coefficient k	Coefficient (m)	Coefficient (n)
High Flux	14	$4.8667(10^{-7})$	1.26	2.52
High Flux	26	$3.0702(10^{-7})$	1.25	2.55
High Flux	60	$2.0304(10^{-7})$	1.23	2.56
High Flux	125	$1.1627(10^{-7})$	1.32	2.59
High Flux	147	$2.3209(10^{-7})$	1.41	2.56
High Flux	160	$2.3209(10^{-7})$	1.41	2.56

Table 2-11. Core Loss Coefficients for Sendust Powder Cores.

Core Loss Equation Factors				
Magnetics Kool-Mu Powder Cores				
Material	Permeability μ	Coefficient k	Coefficient (m)	Coefficient (n)
Sendust	26	0.000693	1.460	2.000
Sendust	60	0.000634		
Sendust	75	0.000620		
Sendust	90	0.000614		
Sendust	125	0.000596		

Table 2-12. Core Loss Coefficients for Iron Alloy Cores.

Core Loss Equation Factors					
Iron Alloy					
Material	Thickness mil's	Frequency Range	Coefficient k	Coefficient (m)	Coefficient (n)
50/50 Ni-Fe	1.00		0.0028100	1.210	1.380
	2.00		0.0005590	1.410	1.270
	4.00		0.0006180	1.480	1.440
Supermendur	2.00	400 Hz	0.0236000	1.050	1.300
	4.00		0.0056400	1.270	1.360
Permalloy 80	1.00		0.0000774	1.500	1.800
	2.00		0.0001650	1.410	1.770
	4.00		0.0002410	1.540	1.990
Supermalloy	1.00		0.0002460	1.350	1.910
	2.00		0.0001790	1.480	2.150
	4.00		0.0000936	1.660	2.060
Silicon	1.00		0.0593000	0.993	1.740
	2.00		0.0059700	1.260	1.730
	4.00		0.0035700	1.320	1.710
	12.00		0.0014900	1.550	1.870
	14.00		0.0005570	1.680	1.860
24 M27 non-or		50-60 Hz	0.0386000	1.000	2.092

The coefficients for amorphous materials, using Equation [2-2] are shown in Table 2-13. The coefficients for Magnetics ferrite materials, using Equation [2-2] are shown in Table 2-14. The coefficients for Micrometals iron powder materials, using Equation [2-3] are shown in Table 2-15.

$$\text{watts/kilogram} = k \left(\frac{f B_{ac}^3 (10^9)}{(a) + 681(b) B_{ac}^{0.7} + 2.512(10^6)(c) B_{ac}^{1.35}} \right) + 100(d) f^2 B_{ac}^2 \quad [2.3]$$

Table 2-13. Core Loss Coefficients for Amorphous Materials.

Core Loss Equation Factors				
Amorphous				
Material	Thickness mils	Coefficient k	Coefficient (m)	Coefficient (n)
2605SC	0.80	8.79(10 ⁻⁶)	1.730	2.230
2714A	0.80	10.1(10 ⁻⁶)	1.550	1.670
Vitroperm 500	0.80	0.864(10 ⁻⁶)	1.834	2.112

Table 2-14. Core Loss Coefficients for Magnetics Ferrites Materials.

Core Loss Equation Factors				
Magnetic's Ferrite Core Materials				
Material	Frequency Range	Coefficient k	Coefficient (m)	Coefficient (n)
K	f < 500kHz	2.524(10 ⁻⁴)	1.60	3.15
K	500kHz <= f < 1.0 MHz	8.147(10 ⁻⁸)	2.19	3.10
K	f => 1.0 MHz	1.465(10 ⁻¹⁹)	4.13	2.98
R	f < 100kHz	5.597(10 ⁻⁴)	1.43	2.85
R	100kHz <= f < 500kHz	4.316(10 ⁻⁵)	1.64	2.68
R	f => 500kHz	1.678(10 ⁻⁶)	1.84	2.28
P	f < 100kHz	1.983(10 ⁻³)	1.36	2.86
P	100kHz <= f < 500kHz	4.855(10 ⁻⁵)	1.63	2.62
P	f => 500kHz	2.068(10 ⁻¹⁵)	3.47	2.54
F	f <= 10kHz	7.698(10 ⁻²)	1.06	2.85
F	10kHz < f < 100kHz	4.724(10 ⁻⁵)	1.72	2.66
F	100kHz <= f < 500kHz	5.983(10 ⁻⁵)	1.66	2.68
F	f => 500kHz	1.173(10 ⁻⁶)	1.88	2.29
J	f <= 20kHz	1.091(10 ⁻³)	1.39	2.50
J	f > 20kHz	1.658(10 ⁻⁸)	2.42	2.50
W	f <= 20kHz	4.194(10 ⁻³)	1.26	2.60
W	f > 20kHz	3.638(10 ⁻⁸)	2.32	2.62
H	f <= 20kHz	1.698(10 ⁻⁴)	1.50	2.25
H	f > 20kHz	5.3720(10 ⁻⁵)	1.62	2.15

Table 2-15. Core Loss Coefficients for Iron Powder Cores.

Core Loss Equation Factors					
Micrometals Iron Powder Cores					
Material	Permeability μ	Coefficient (a)	Coefficient (b)	Coefficient (c)	Coefficient (d)
Mix-08	35	0.01235	0.8202	1.4694	$3.85(10^{-7})$
Mix-18	55	0.00528	0.7079	1.4921	$4.70(10^{-7})$
Mix-26	75	0.00700	0.4858	3.3408	$2.71(10^{-6})$
Mix-52	75	0.00700	0.4858	3.6925	$9.86(10^{-7})$

Selection of Magnetic Materials

Transformers used in static inverters, converters, and transformer-rectifier, (T-R), supplies, intended for aerospace and electronics industry power applications, are usually square loop tape, toroidal design. The design of reliable, efficient, and lightweight devices for this use has been seriously hampered by the lack of engineering data, describing the behavior of both the commonly used and more exotic core materials, with higher-frequency square wave excitation.

A program was carried out at the Jet Propulsion Laboratory, JPL, to develop these data from measurements of the dynamic B-H loop characteristics of the tape core materials presently available from various industry sources. Cores were produced in both toroidal and C forms, and were tested in both ungapped (uncut) and gapped (cut) configurations. This section describes the results of that investigation.

Typical Operation

A transformer used for inverters, converters, and transformer-rectifier supplies operates from a power bus, which could be dc or ac. In some power applications, a commonly used circuit is a driven transistor switch arrangement, such as that shown in Figure 2.25.

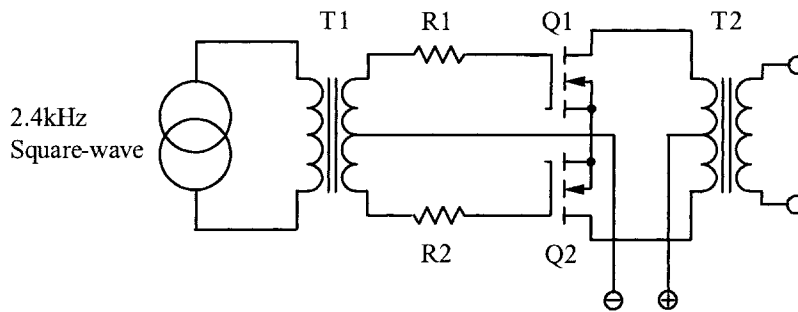


Figure 2-25. Typical Driven Power MOSFET Inverter.

One important consideration affecting the design of suitable transformers is that care must be taken to ensure that operation involves balanced drive to the transformer primary. In the absence of balanced drive, a net dc current will flow in the transformer primary, which causes the core to saturate easily during alternate half-cycles. A saturated core cannot support the applied voltage, limited mainly by its on resistance. The resulting high current, in conjunction with the transformer leakage inductance, results in a high-voltage spike during the switching sequence, which could be destructive to the power MOSFET. To provide balanced drive, it is necessary to exactly match the MOSFETs for $R_{DS(on)}$. But, this is not always sufficiently effective. Also, exact matching of the MOSFETs is a major problem in a practical sense.

Material Characteristics

Many available core materials approximate the ideal square loop characteristic, illustrated by the B-H curve, as shown in Figure 2-26. Representative, dc B-H loops for commonly available core materials, are shown in Figure 2-27. Other characteristics are tabulated in Table 2-16.

Many articles have been written about inverter and converter transformer design. Usually, authors' recommendations represent a compromise among material characteristics, such as those tabulated in Table 2-16, and displayed in Figure 2-27. These data are typical of commercially available core materials that are suitable for the particular application.

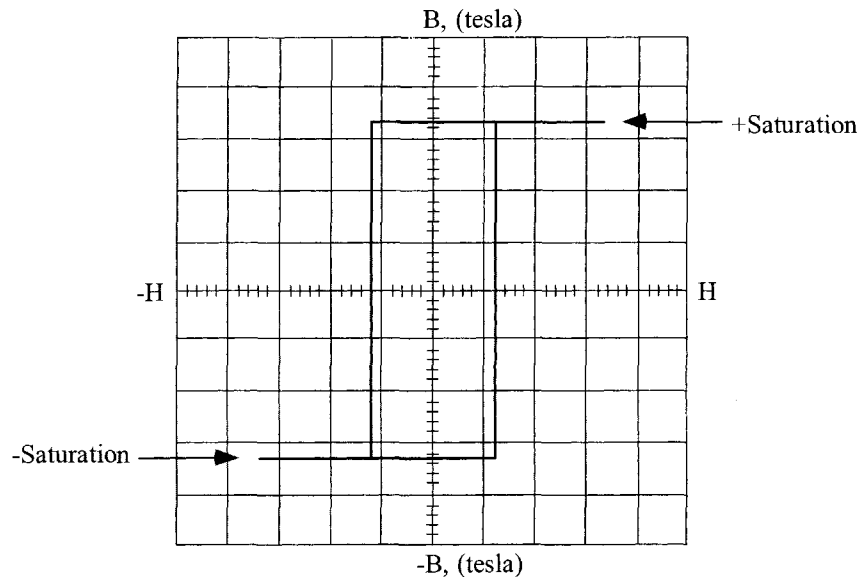


Figure 2-26. Ideal Square B-H Loop.

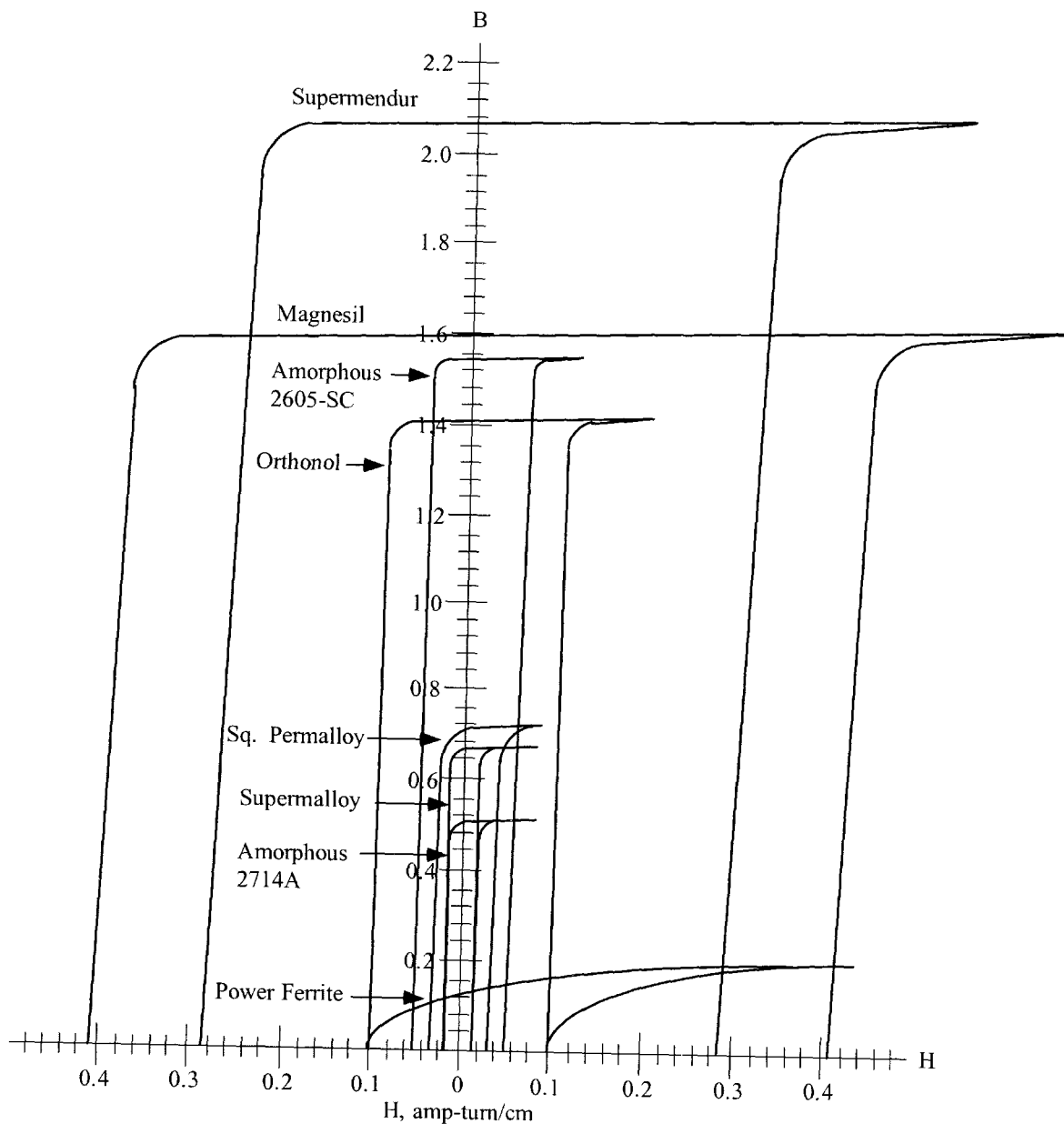


Figure 2-27. Typical dc B-H Loops of Magnetic Materials.

As can be seen, the material that provides the highest flux density (supermendur) would result in the smallest component size, and this would influence the choice if size were the most important consideration. The ferrite material, (see the ferrite curve in Figure 2-27), has the lowest flux density. This results in the largest transformer. Magnetic materials selected for transformers or inductors cannot be chosen by flux alone. There are other parameters, such as frequency and core configuration that must be taken into consideration.

Table 2-16. Magnetic Core Material Characteristics.

Magnetic Core Material Characteristics						
Material Name	Composition	Initial Permeability μ_i	Flux Density Tesla B_s	Curie Temperature °C	dc, Coercive Force, Hc Oersteds	Density grams/cm ³ δ
Magnesil	3% Si 97% Fe	1.5 K	1.5-1.8	750	0.4-0.6	7.3
Supermendur*	49% Co 49% Fe 2% V	0.8 K	1.9-2.2	940	0.15-0.35	8.15
Orthonol	50% Ni 50% Fe	2 K	1.42-1.58	500	0.1-0.2	8.24
Sq. Permalloy	79% Ni 17% Fe 4% Mo	12 K-100 K	0.66-0.82	460	0.02-0.04	8.73
Supermalloy	78% Ni 17% Fe 5% Mo	10 K-50 K	0.65-0.82	460	0.003-0.008	8.76
Amorphous 2605-SC	81% Fe 13.5% B 3.5% Fe	3K	1.5-1.6	370	0.03-0.08	7.32
Amorphous 2714A	66% Co 15% Si 4% Fe	20K	0.5-0.58	205	0.008-0.02	7.59
Ferrite	MnZn	0.75-15K	0.3-0.5	100-300	0.04-0.25	4.8
* Field Anneal.						

Usually, inverter transformer design is aimed at the smallest size, the highest efficiency and adequate performance under the widest range of environmental conditions. Unfortunately, the core material that can produce the smallest size has the lowest efficiency, and the highest efficiency materials result in the largest size. Thus, the transformer designer must make tradeoffs between allowable transformer size and the minimum efficiency that can be tolerated. Then, the choice of core material will be based upon achieving the best characteristic on the most critical or important design parameter, and upon acceptable compromises on the other parameters.

After analysis of a number of designs, most engineers choose size rather than efficiency as the most important criterion, and select an intermediate loss factor on core material for their transformers. Consequently, as the frequency is increased, ferrites have become the most popular material.

Magnetic Material Saturation Defined

To standardize the definition of saturation, several unique points on the B-H loop are defined, as shown in Figure 2-28.

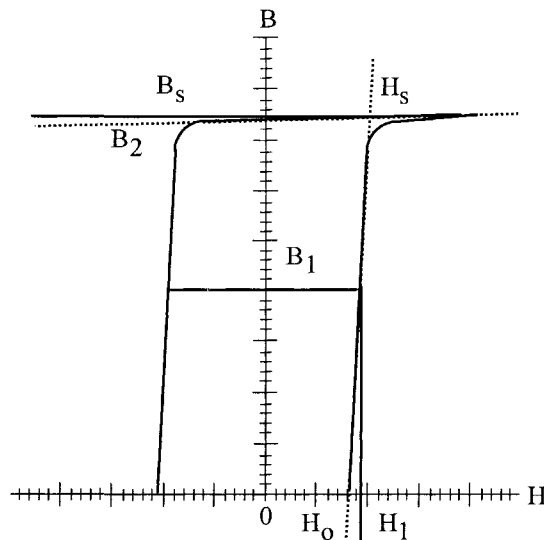


Figure 2-28. Defining the B-H Loop.

The straight line through $(H_0, 0)$ and (H_s, B_s) may be written as:

$$B = \left(\frac{\Delta B}{\Delta H} \right) (H - H_0) \quad [2-4]$$

The line through $(0, B_2)$ and (H_s, B_s) has essentially zero slope and may be written as:

$$B = B_2 \approx B_s \quad [2-5]$$

Equations [2-1] and [2-2] together define saturation conditions as follows:

$$B_s = \left(\frac{\Delta B}{\Delta H} \right) (H_s - H_o) \quad [2-6]$$

Solving Equation [2-3] for H_s yields:

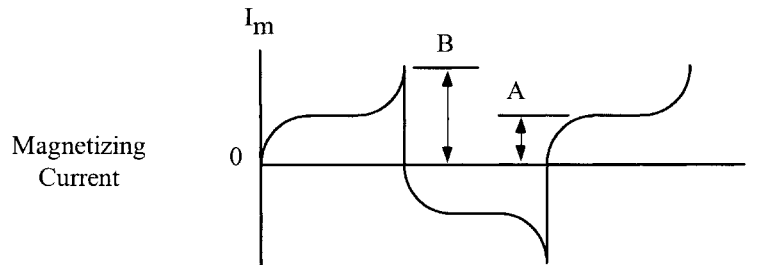
$$H_s = H_o + \frac{B_s}{\mu_o} \quad [2-7]$$

Where by definition:

$$\mu_o = \frac{\Delta B}{\Delta H} \quad [2-8]$$

By definition, saturation occurs when the peak exciting current (B) is twice the average exciting current (A) as shown in Figure 2-29. Analytically, this means that:

$$H_{pk} = 2H_s \quad [2-9]$$



By definition, saturation occurs when $B = 2A$

Figure 2-29. Defining the Excitation Current.

Solving Equation [2-1] for H_1 , we obtain:

$$H_1 = H_o + \frac{B_1}{\mu_o} \quad [2-10]$$

To obtain the pre-saturation dc margin (ΔH), Equation [2-4] is subtracted from Equation [2-6]:

$$\Delta H = H_s - H_1 = \left(\frac{B_s - B_1}{\mu_o} \right) \quad [2-11]$$

The actual unbalanced dc current must be limited to:

$$I_{dc} \leq \left(\frac{\Delta H(\text{MPL})}{N} \right), \text{ [amperes]} \quad [2-12]$$

Where, N is the number of turns

MPL is the mean magnetic path length.

Combining Equations [2-7] and [2-8] gives:

$$I_{dc} \leq \left(\frac{(B_s - B_1)(\text{MPL})}{\mu_o N} \right), \text{ [amperes]} \quad [2-13]$$

As mentioned earlier, in an effort to prevent core saturation, the drive to the switching power MosFet must be symmetrical and the power MosFet on resistance $R_{DS(on)}$ must be matched. The effect of core saturation, using an uncut or ungapped core, is shown in Figure 2-30, which illustrates the effect on the B-H loop transversed with a dc bias. Figure 2-31 shows typical B-H loops of 50-50 nickel-iron material excited from an ac source, with progressively reduced excitation; the vertical scale is 0.4 T/cm. It can be noted that the minor loop remains at one extreme position within the B-H major loop after reduction of excitation. The unfortunate effect of this random minor loop positioning is that, when conduction begins again in the transformer winding after shutdown, the flux swing could begin from the extreme ends rather than from the normal zero axis. The effect of this is to drive the core into saturation, with the production of spikes that can destroy transistors.

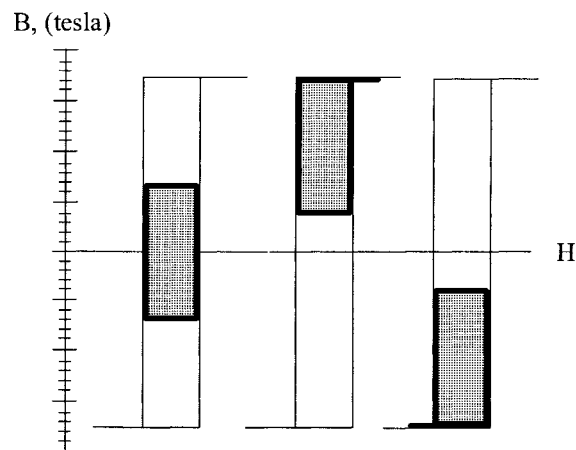


Figure 2-30. B-H Loop with dc Bias.

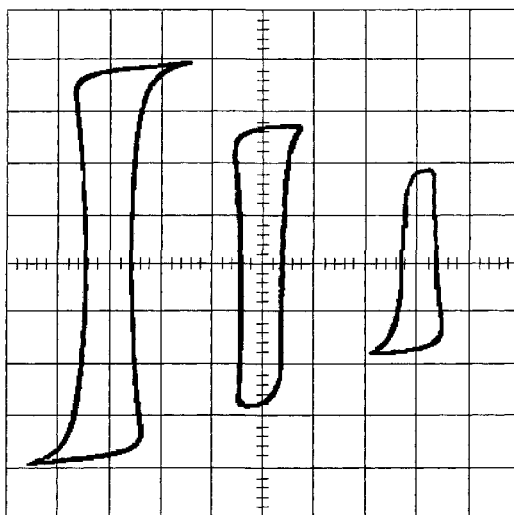


Figure 2-31. Typical Square Loop Material with dc Bias.

Test Conditions

The test fixture, schematically illustrated in Figure 2-32, was built to affect comparison of dynamic B-H loop characteristics of various core materials. Cores were fabricated from various core materials in the basic core configuration, designated No. 52029 for toroidal cores, manufactured by Magnetics Inc. The materials used were those most likely to be of interest to designers of inverter or converter transformers. Test conditions are listed in Table 2-17.

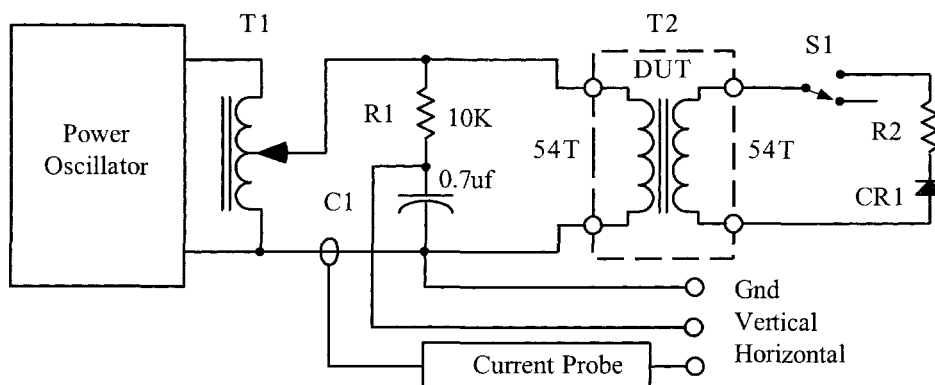


Figure 2-32. B-H Loop with dc Bias.

Winding Data were derived from the following:

$$N = \frac{V(10^4)}{4.0B_m f A_c}, \text{ [turns] [2-14]}$$

Table 2-17. Materials and Test Conditions.

Test Conditions					
Core Number*	Trade Name	B _s Tesla	Turns N	Frequency kHz	MPL cm
52029-2A	Orthonol	1.45	54	2.4	9.47
52029-2D	Sq. Permalloy	0.75	54	2.4	9.47
52029-2F	Supermalloy	0.75	54	2.4	9.47
52029-2H	48 Alloy	1.15	54	2.4	9.47
52029-2K	Magnesil	1.6	54	2.4	9.47

*Magnetics toroidal cores.

The test transformer, represented in Figure 2-32, consists of 54-turn primary and secondary windings, with square wave excitation on the primary. Normally, switch S1 is open. With switch S1 closed, the secondary current is rectified by the diode to produce a dc bias in the secondary winding.

Cores were fabricated from each of the materials by winding a ribbon of the same thickness on a mandrel of a given diameter. Ribbon termination was affected by welding in the conventional manner. The cores were vacuum impregnated, baked, and finished as usual.

Figures 2-33 – 2-36 show the dynamic B-H loops obtained for various core materials. In each of these Figures, switch S1 was in the open position, so there was no dc bias applied to the core and windings.

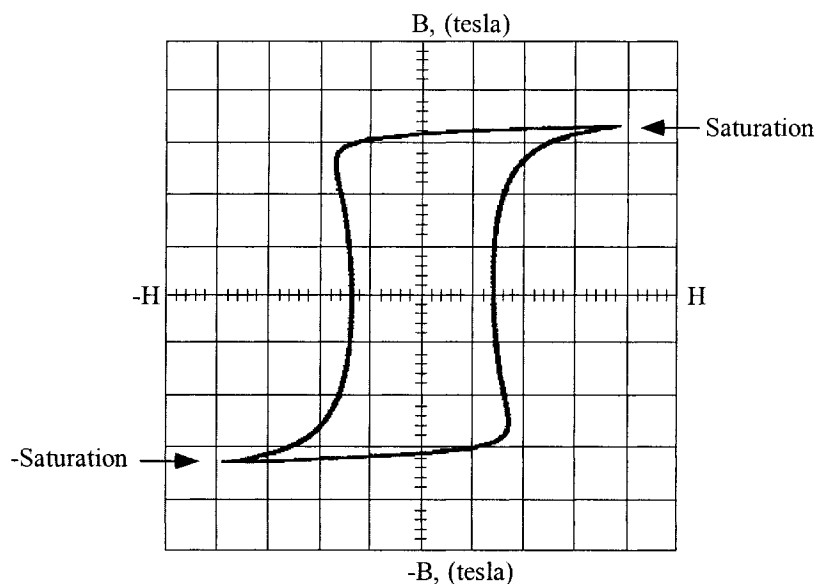


Figure 2-33. Magnesil (K) B-H Loop, B = 0.5 T/cm, H = 100 ma/cm.

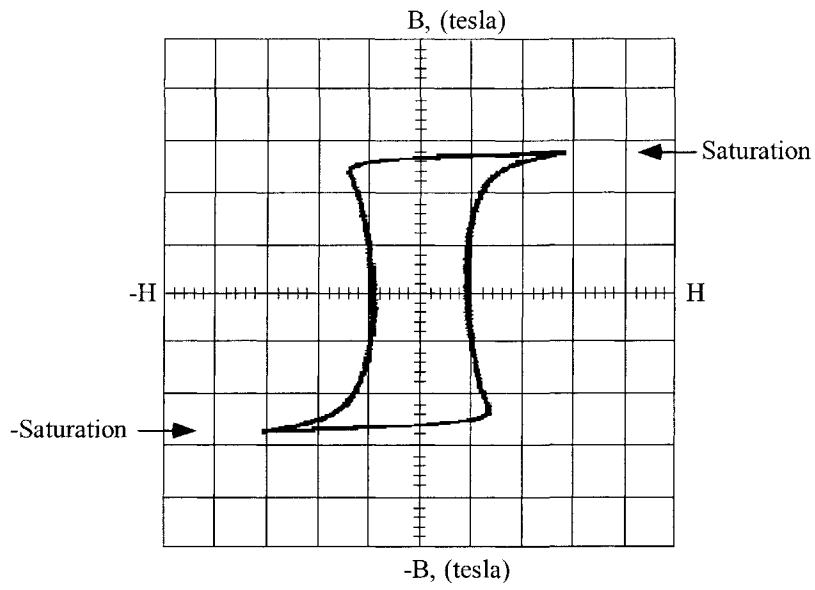


Figure 2-34. Orthonol (2A) B-H Loop, $B = 0.5 \text{ T/cm}$, $H = 50 \text{ ma/cm}$.

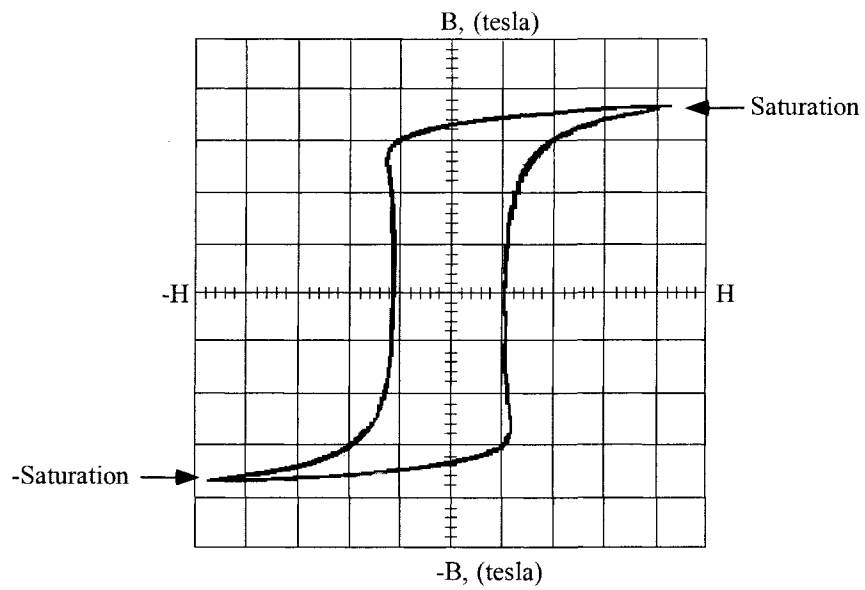


Figure 2-35. Square Permalloy (2D) B-H Loop, $B = 0.2 \text{ T/cm}$, $H = 20 \text{ ma/cm}$.

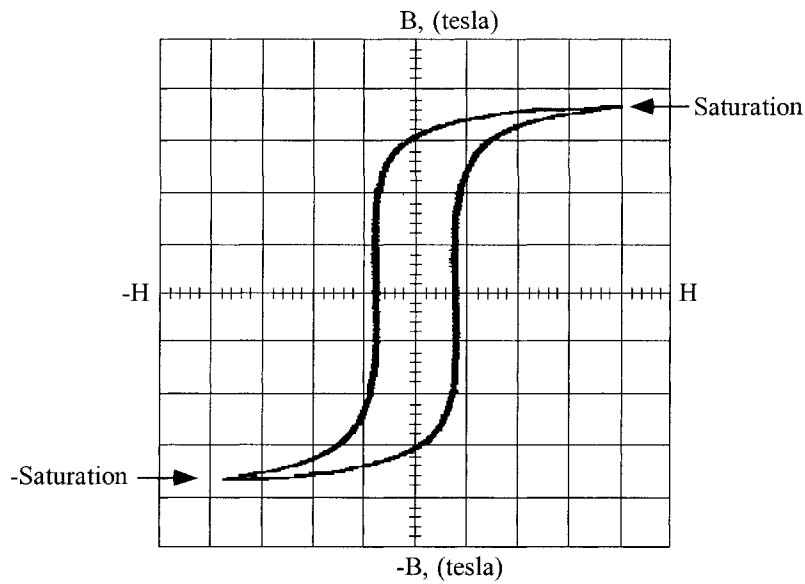


Figure 2-36. Supermalloy (2F) B-H Loop, $B = 0.2 \text{ T/cm}$, $H = 10 \text{ ma/cm}$.

Figures 2-37 to 2-40 show the dynamic B-H loop patterns obtained for various core materials when the test conditions are included in a sequence, in which S1 was in open condition (A), then in closed condition (B), and then, opened again, in condition (C). It is apparent from this data that, with a small amount of dc bias, the minor dynamic B-H loop can traverse the major B-H loop from saturation to saturation. Note that after the dc bias has been removed, the minor B-H loops remained shifted to one side or the other. Because of the ac coupling of the integrator to the oscilloscope, the photographs in these figures do not present a complete picture of what really happens during the flux swing.

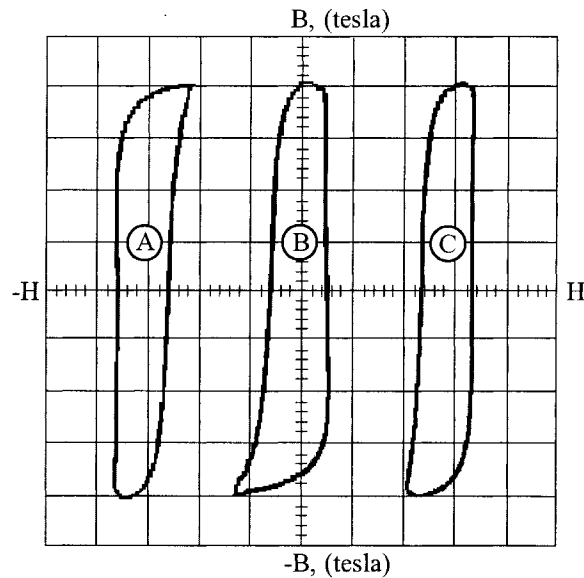


Figure 2-37. Magnesil (2K) B-H Loop, $B = 0.3 \text{ T/cm}$, $H = 200 \text{ ma/cm}$.

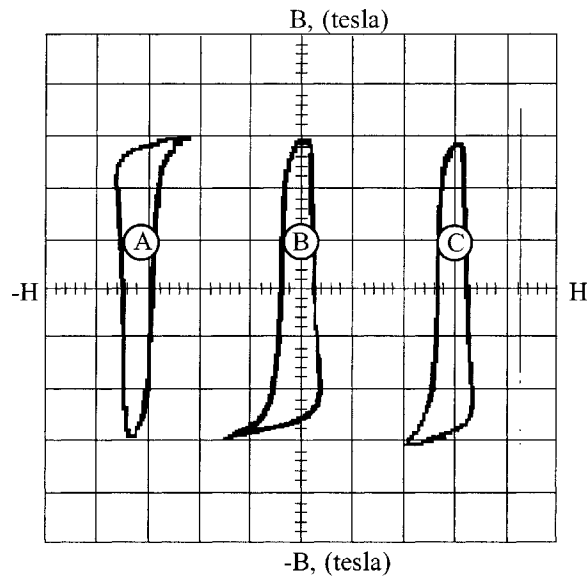


Figure 2-38. Orthonol (2A) B-H Loop, $B = 0.2 \text{ T/cm}$, $H = 100 \text{ ma/cm}$.

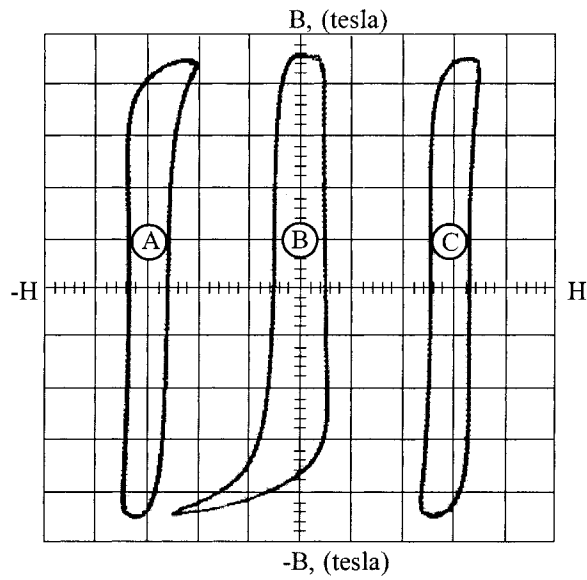


Figure 2-39. Sq. Permalloy (2D) B-H Loop, $B = 0.1 \text{ T/cm}$, $H = 20 \text{ ma/cm}$.

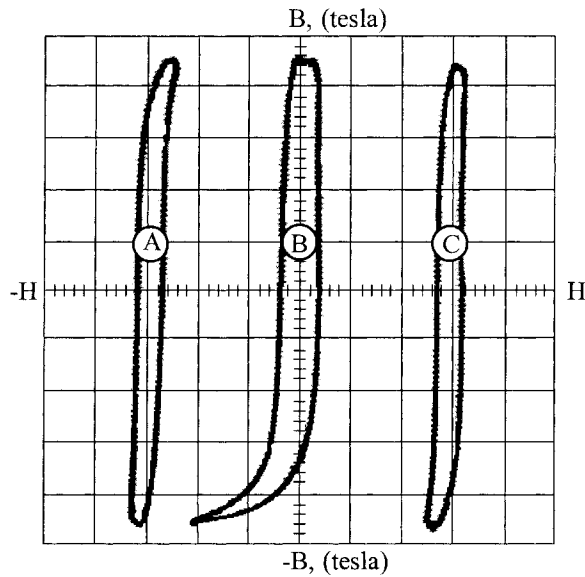


Figure 2-40. Supermalloy (2F) B-H Loop, $B = 0.1 \text{ T/cm}$, $H = 10 \text{ ma/cm}$.

Magnetic Material Saturation Theory

The domain theory of the nature of magnetism is based on the assumption that all magnetic materials consist of individual molecular magnets. These minute magnets are capable of movement within the material. When a magnetic material is in its unmagnetized state, the individual magnetic particles are arranged at random, and effectively neutralize each other. An example of this is shown in Figure 2-41, where the tiny magnetic particles are arranged in a disorganized manner. (The north poles are represented by the darkened ends of the magnetic particles.) When a material is magnetized, the individual particles are aligned or oriented in a definite direction, as shown in Figure 2-42.

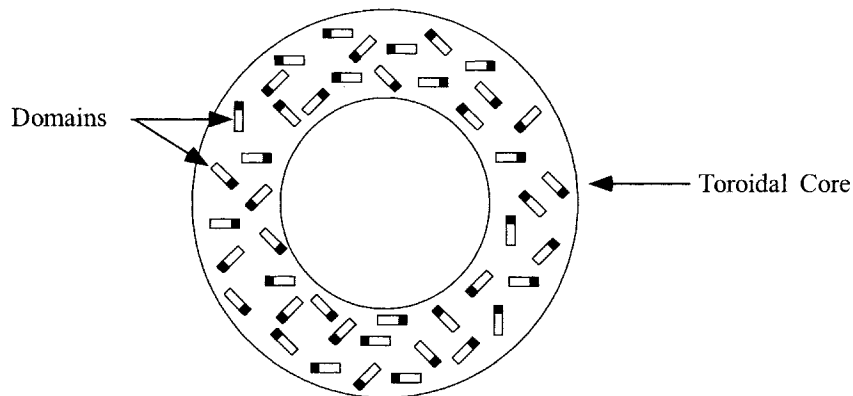


Figure 2-41. Magnetic Domains, Arranged in a Random Manner.

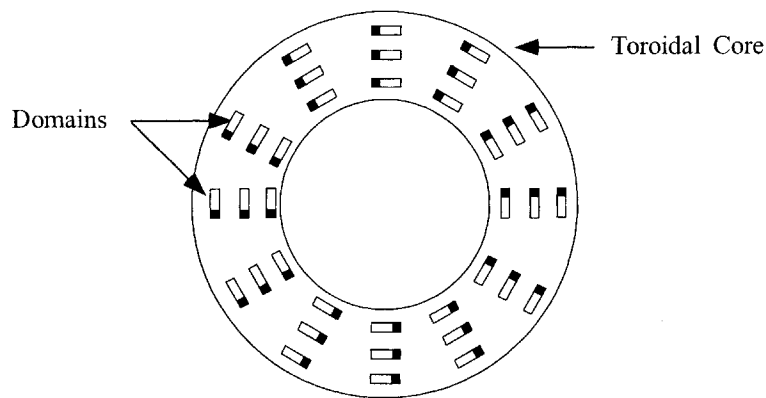


Figure 2-42. Magnetic Domains, Aligned in a Definite Direction.

The degree of magnetization of a material depends on the degree of alignment of the particles. The external magnetizing force can continue to affect the material up to the point of saturation, the point at which essentially all of the domains are lined up in the same direction.

In a typical toroidal core, the effective air gap is less than 10^{-6} cm. Such a gap is negligible in comparison to the ratio of mean length to permeability. If the toroid was subjected to a strong magnetic field (enough to saturate), essentially all of the domains would line up in the same direction. If suddenly the field were removed at B_m , the domains would remain lined up, and be magnetized along that axis. The amount of flux density that remains is called the residual flux, B_r . The result of this effect was shown earlier in Figures 2-37 through 2-40.

Air Gap Effect

An air gap introduced into the core has a powerful demagnetizing effect, resulting in a “shearing over” of the hysteresis loop, and a considerable decrease in permeability of high-permeability materials. Direct current excitation follows the same pattern. However, the core bias is considerably less affected than the magnetization characteristics by the introduction of a small air gap. The magnitude of the air gap effect also depends on the length of the mean magnetic path and on the characteristics of the uncut core. For the same air gap, the decrease in permeability will be less with a greater magnetic flux path, but more pronounced in a high-permeability core with a low coercive force

Effect of Gapping

Figure 2-43 shows a comparison of a typical toroidal core B-H loop, without and with a gap. The gap increases the effective length of the magnetic path. When voltage E is impressed across primary winding, N_p , of a transformer, the resulting current, I_m , will be small because of the highly inductive circuit, as shown in Figure 2-44. For a particular core size, maximum inductance occurs when the air gap is minimum.

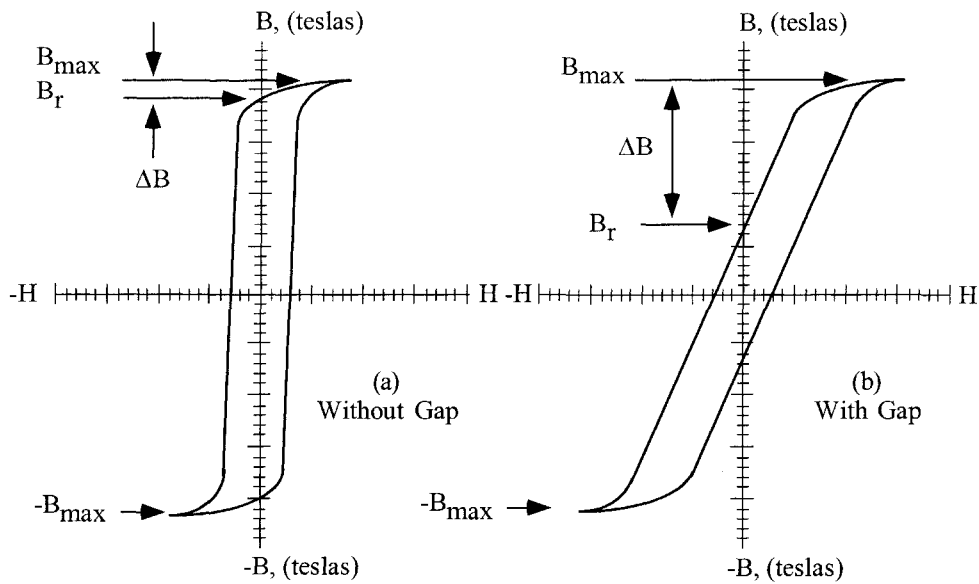


Figure 2-43. Comparing Magnetic Materials with and Without a Gap.

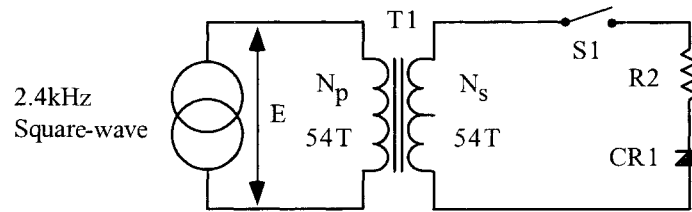


Figure 2-44. Implementing dc Unbalance.

When S1 is closed, an unbalanced dc current flows in the secondary, N_s turns, and the core is subjected to a dc magnetizing force, resulting in a flux density that may be expressed as:

$$B_{dc} = \frac{0.4\pi N_s I_{dc} (10^{-4})}{l_g + \frac{MPL}{\mu_r}}, \quad [\text{tesla}] \quad [2-15]$$

In converter and inverter design, this dc flux is augmented by the ac flux swing, which is:

$$B_{ac} = \frac{E(10^4)}{K_f f A_c N}, \quad [\text{tesla}] \quad [2-16]$$

If the sum of B_{dc} and B_{ac} shifts operations above the maximum operating flux density of the core material, the incremental permeability, (μ_{ac}) , is reduced. This condition lowers the impedance and increases the flow

of magnetizing current, I_m . This condition can be remedied by introducing into the core assembly an air gap which causes a decrease in dc magnetization in the core. However, the size of the air gap that can be incorporated has a practical limitation. Since the air gap lowers impedance, it results in increased magnetizing current I_m , which is inductive. The resultant voltage spikes produced by such currents apply a high stress to the switching transistors and may cause failure. This stress can be minimized by tight control of lapping and etching of the gap to keep the gap to a minimum.

From Figure 2-43, it can be seen that the B-H curves depict maximum flux density, B_m , and residual flux, B_r , for ungapped and gapped cores, and that the useful flux swing is designated, ΔB , which is the difference between, B_m and B_r . It will be noted, in Figure 2-43(a), that B_r approaches B_m , but, in Figure 2-43(b), there is a much greater, ΔB , between them. In either case, when excitation voltage is removed at the peak of the excursion of the B-H loop, flux falls to the B_r point. It is apparent that introducing an air gap reduces B_r to a lower level, and increases the useful flux density. Thus, insertion of an air gap in the core eliminates, or markedly reduces, the voltage spikes produced by the leakage inductance, due to the transformer saturation.

Two types of core configurations were investigated in the ungapped and gapped states. Figure 2-45 shows the type of toroidal core that was cut, and Figure 2-46 shows the type of C core that was cut. Toroidal cores are virtually gapless, when conventionally fabricated. To increase the gap, the cores were physically cut in half, and the cut edges were lapped, acid etched to remove cut debris, and banded to form the cores. A minimum air gap, on the order of less than 25 μm , was established.

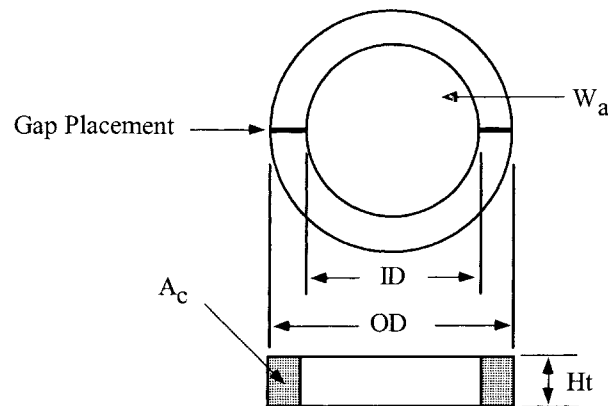


Figure 2-45. Typical cut Toroidal Core.

As will be noted from Figures 2-47 through 2-50, which show the B-H loops of the uncut and cut cores, the results obtained indicated that the effect of gapping was the same for both the C cores and the toroidal cores subjected to testing. It will be noted, however, that gapping of the toroidal cores produced a lowered squareness characteristic for the B-H loop, as shown in Table 2-18. This data was obtained from Figures 2-47 through 2-50. ΔH values extracted from the same figures, as shown in Figure 2-51, are tabulated in Table 2-19.

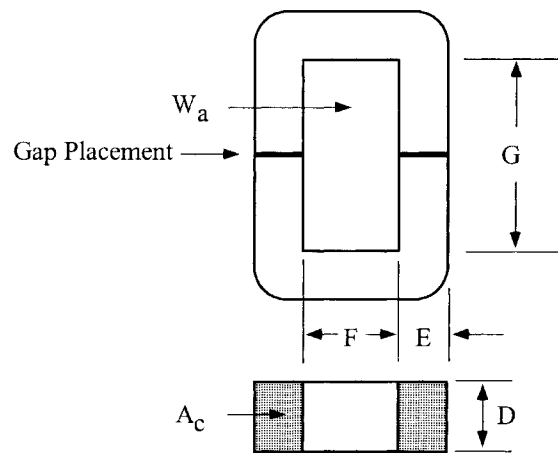


Figure 2-46. Typical Middle Cut C Core.

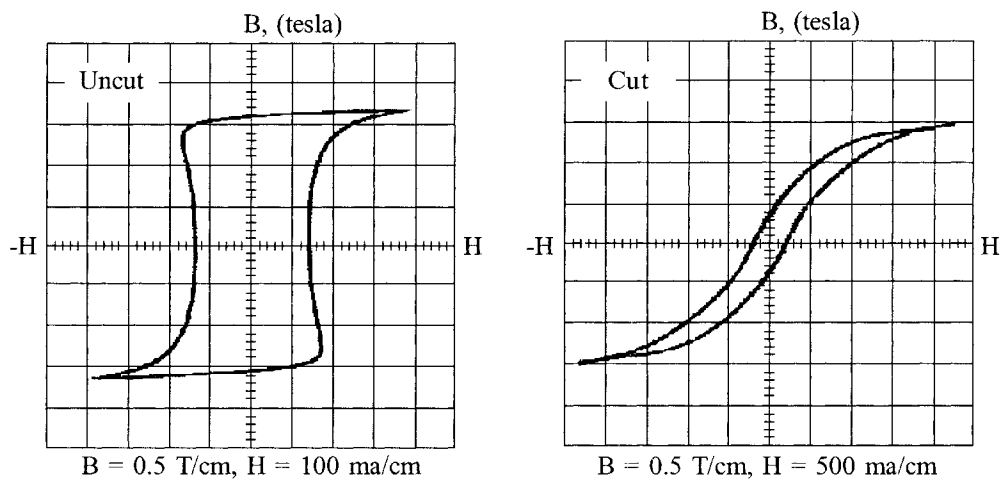


Figure 2-47. Magnesil (K) B-H Loop, Uncut and Cut with Minimum Gap.

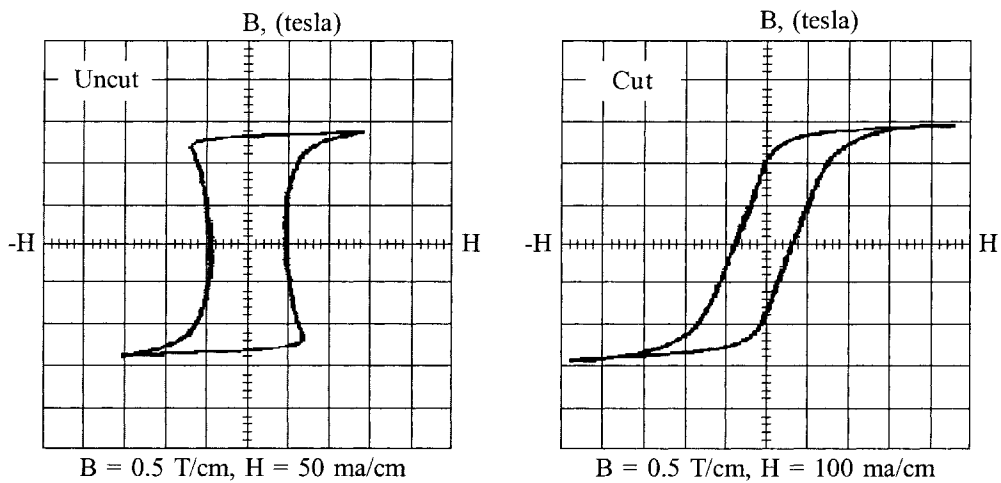


Figure 2-48. Orthonal (A) B-H Loop, Uncut and Cut with Minimum Gap.

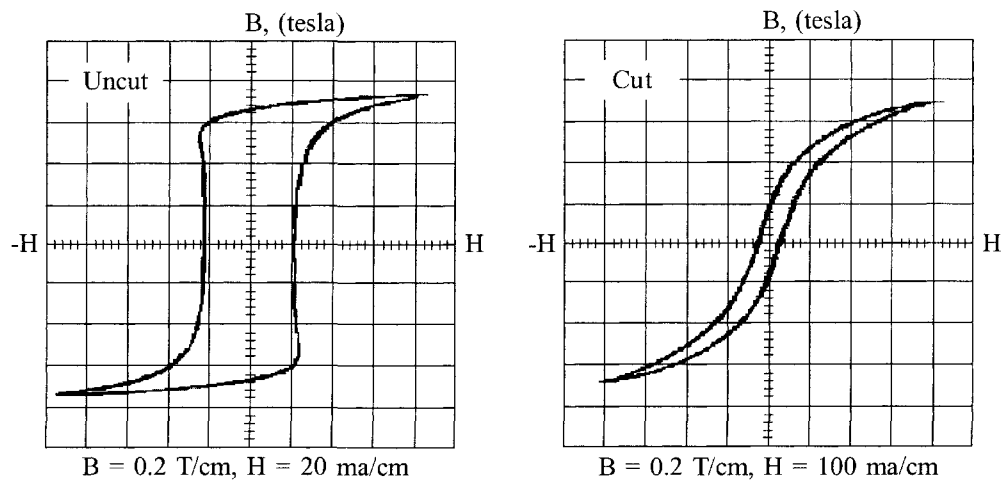


Figure 2-49. Square Permalloy (D) B-H Loop, Uncut and Cut with Minimum Gap.

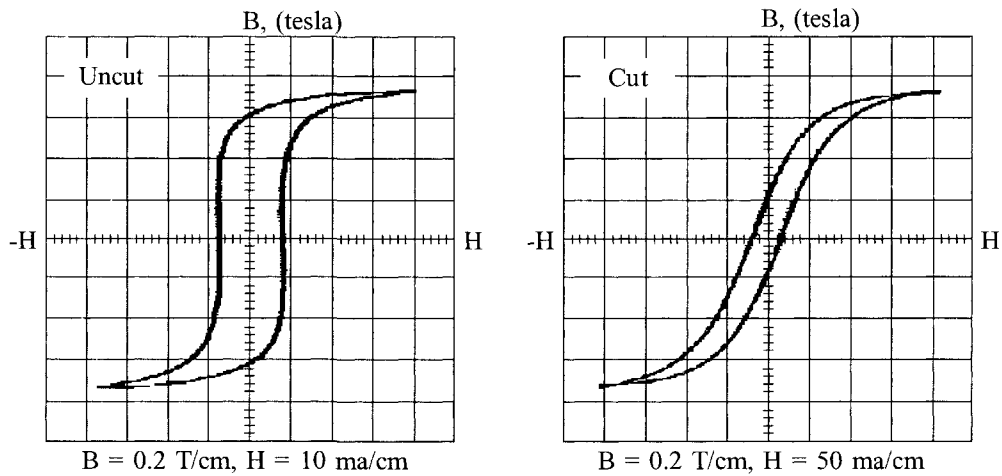


Figure 2-50. Supermalloy (F) B-H Loop, Uncut and Cut with Minimum Gap.

Table 2-18.

Comparing B_r/B_m on Uncut and Cut Cores.					
Core Number*	Trade Name	B_s Tesla	Turns N	Uncut B_r/B_m	Cut B_r/B_m
52029-2A	Orthonol	1.45	54	0.96	0.62
52029-2D	Sq. Permalloy	0.75	54	0.86	0.21
52029-2F	Superpermalloy	0.75	54	0.81	0.24
52029-2K	Magnesil	1.60	54	0.93	0.22

*Magnetics toroidal cores.

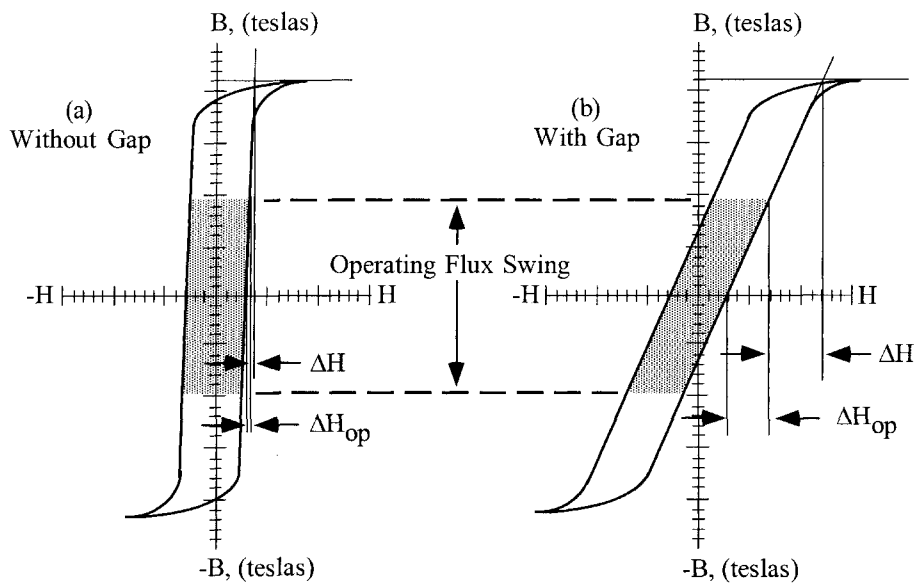


Figure 2-51. Defining ΔH_{op} and ΔH .

Table 2-19. Comparing ΔH and ΔH_{op} on Uncut and Cut Cores.

Comparing ΔH and ΔH_{op} on Uncut and Cut Cores.							
Material *Trade Name	B_m Tesla	B_{ac} Tesla	B_{dc} Tesla	Amp-turns/cm			
				Uncut		Cut	
				ΔH_{op}	ΔH	ΔH_{op}	ΔH
Orthonol	1.44	1.15	0.288	0.0125	0	0.895	0.178
Sq. Permalloy	0.73	0.58	0.146	0.0100	0.005	0.983	0.178
Supermalloy	0.63	0.58	0.136	0.0175	0.005	0.491	0.224
Magnesil	1.54	1.23	0.310	0.0750	0.025	7.150	1.780

*Magnetics Cores.

A direct comparison of cut and uncut cores was made electrically by means of two different test circuits. The magnetic material used in this branch of the test was Orthonol. The frequency was 2.4 kHz, and the flux density was 0.6 T. The first test circuit, shown in Figure 2-52, was a driven inverter operating into a 30-W load, with the power MOSFETs, operating into and out of saturation. Drive was applied continuously. S1 controls the supply voltage to Q1 and Q2.

With switch S1 closed, transistor Q1 was turned on and allowed to saturate. This applied voltage, $E-V_{DS(on)}$, across the transformer winding. Switch S1 was then opened. Then, the flux in transformer, T2, dropped to the residual flux density, B_r . Switch S1 was closed again. This was done several times in succession to catch the flux in an additive direction. Figures 2-53 and 2-54 show the inrush current measured at the center tap of T2.

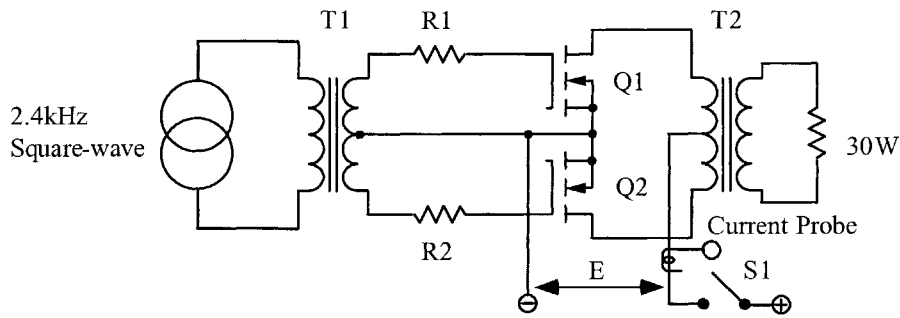


Figure 2-52. Inverter Inrush Current Test Fixture.

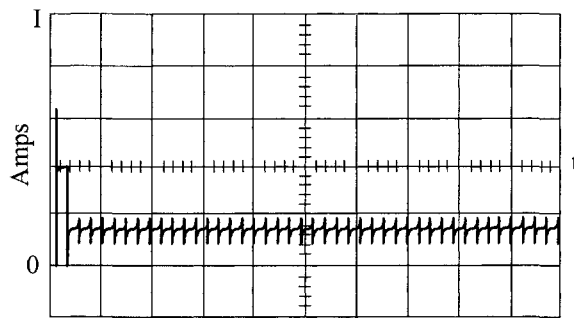


Figure 2-53. Typical Inrush Current of a Uncut Core in a Driven Inverter.

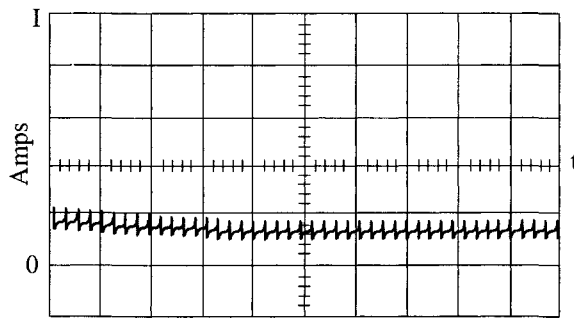


Figure 2-54. Resulting Inrush Current using a Cut Core.

It will be noted, in Figure 2-53, that the uncut core saturated, and the inrush current was limited only by circuit resistance and power, MOSFETs $R_{DS(on)}$. Figure 2-54 shows that saturation did not occur in the case of the cut core. Thus, the high inrush current and transistor stress were virtually eliminated.

The second test circuit arrangement is shown in Figure 2-55. The purpose of this test was to excite a transformer and measure the inrush current, using a current probe. A square wave power oscillator was used to excite transformer, T2. Switch, S1, was opened and closed several times to catch the flux in an additive direction. Figures 2-56 and 2-57 show inrush current for an uncut and cut core, respectively.

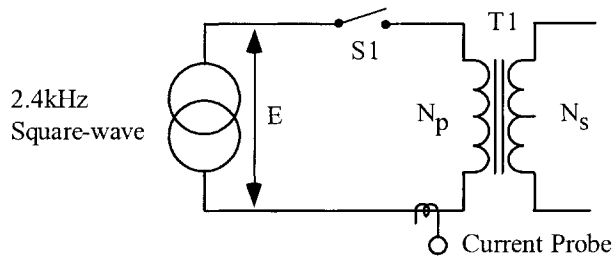


Figure 2-55. Transformer Rectifier Inrush Current Measurement.

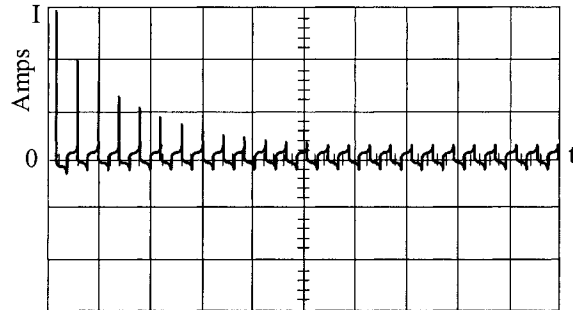


Figure 2-56. Inrush Current of a Transformer using a Uncut Core.

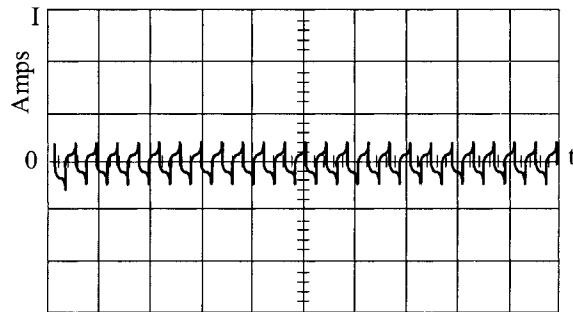


Figure 2-57. Inrush Current of a Transformer using a Cut Core.

A small amount of air gap, less than 25 μm , has a powerful effect on the demagnetizing force, but little effect on the core loss. This small air gap decreases the residual magnetism by “shearing over” the hysteresis loop, which eliminates the problem of the core tending to remain saturated.

A typical example of the merits of the cut core occurred in the checkout of a Mariner spacecraft. During the checkout of a prototype science package, a large (8 A, 200 s) turn-on transient was observed. The normal running current was 0.06 A, fused with a parallel-redundant 1/8-A fuse, as required by the Mariner Mars design philosophy. With the 8-A inrush current, the 1/8-A fuses were easily blown. This did not happen, on every turn-on, but only when the core would “latch up” in the wrong direction for turn-on. Upon inspection, the transformer turned out to be a 50-50 nickel-iron toroid. The design was changed from a toroidal core to a cut core with a 25 μm , air gap. The new design was completely successful in eliminating the 8-A turn-on transient.

Composite Core Configuration

A composite core configuration has been developed for transformers that combine the protective feature of a gapped core with the much lower magnetizing current requirement of an uncut core. The uncut core functions, under normal operating conditions, and the cut core takes over during abnormal conditions to prevent high switching transients and their potentially destructive effect on the transistors.

This configuration is a composite of cut and uncut cores assembled together concentrically, with the uncut core nested within the cut core. The uncut core has high permeability, and thus requires a very small magnetizing current. On the other hand, the cut core has a low permeability and thus requires a much higher magnetization current. The uncut core is designed to operate at a flux density that is sufficient for normal operation of the converter. The uncut core may saturate under the abnormal conditions previously described. The cut core then takes over and supports the applied voltage so that excessive current does not flow. In a sense, it acts like a ballast resistor in some circuits to limit current flow to a safe level.

Figures 2-58 and 2-59 show the magnetization curves for an uncut core and a composite core of the same material at the same flux density. The much lower, B_r characteristic of the composite compared to the uncut core is readily apparent.

The desired features of the composite core can be obtained more economically by using different materials for the cut and uncut portions of the core. It was found that when the design required high nickel (4/79), the cut portion could be low nickel, (50/50), and because low nickel has twice as high a flux density as high nickel, the core was made of 66% high nickel, and 33% low nickel.

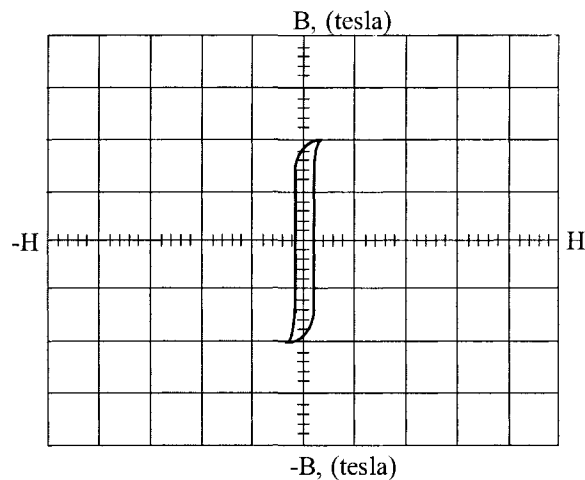


Figure 2-58. Uncut Core Excited at 0.2 T/cm.

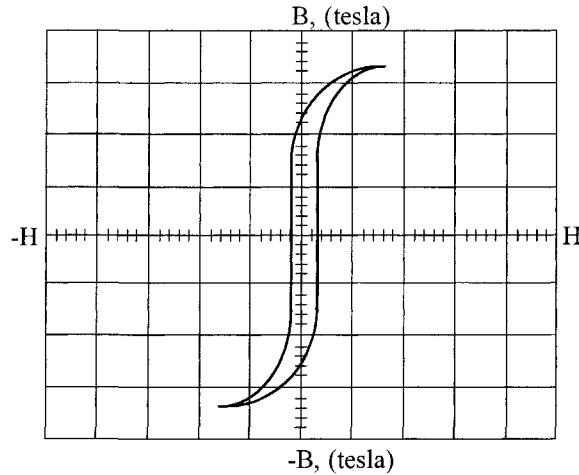


Figure 2-59. Both Cut and Uncut Cores Excited at 0.2 T/cm.

Figure 2-60 shows cut and uncut cores that have been impregnated to bond the ribbon layers together. The uncut core was first trimmed to fit within the inner diameter of the cut core by peeling off a wrap or two of the ribbon steel. The two cores are assembled into a composite core (Figure 2-61, on the right).

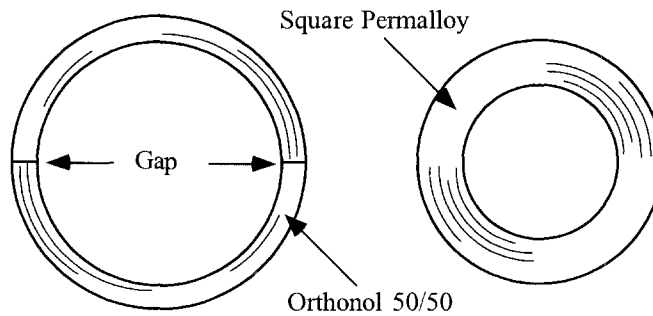


Figure 2-60. Composite Cores Ready for final Assembly.

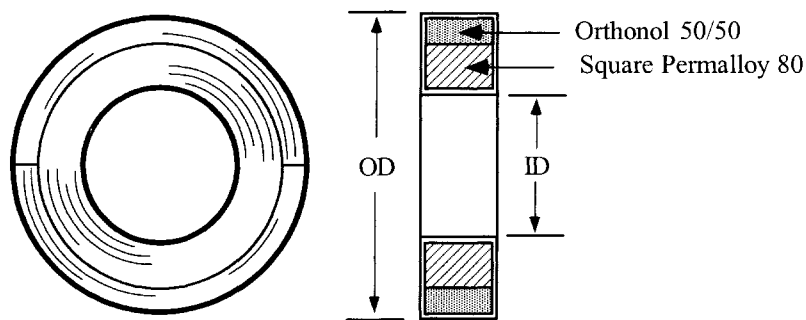


Figure 2-61. Composite Cores Assembled in Final Form.

To ensure uniform characteristics for gapped cores, a gap dimension of 50 μm is recommended, because variations produced by thermal cycling will not affect this gap greatly. In the composite core, the gap is obtained by inserting a sheet of paper Mylar or Kapton film material between the core ends during banding.

The same protective feature can be accomplished in transformers with laminated cores. When laminations are stacked by interleaving them one-by-one, the result will be a minimum air gap, as shown in Figure 2-62 by the squareness of the B-H loop. Shearing over of the B-H loop, or decreasing the residual flux, as shown in Figure 2-63, is accomplished by butt joining half the laminations in the core-cross section, which introduces a small, additional air gap.

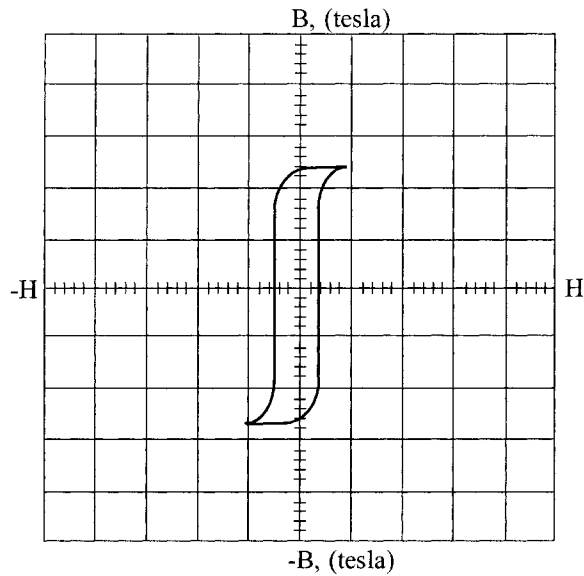


Figure 2-62. B-H Loop with Laminations Stacked 1x1 Interleaved.

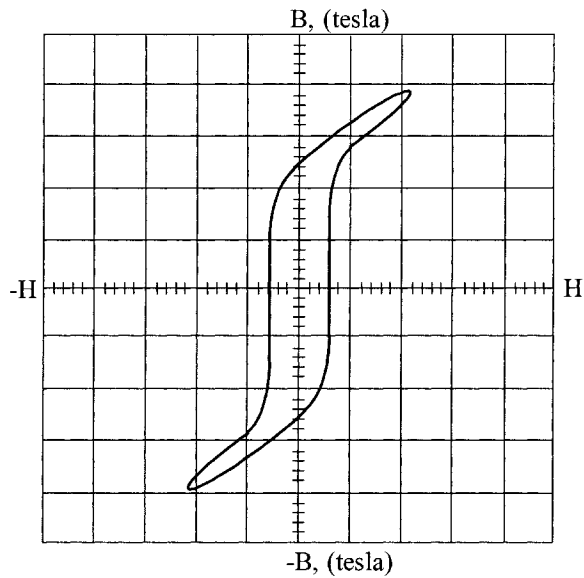


Figure 2-63. B-H Loop with Laminations Stack Half 1x1 and Half Butt Stack.

Table 2-20 is a compiling of composite cores manufactured by Magnetics Inc., alongside their standard dimensional equivalent cores. Also, included in Table 2-20, is the cores' area product, A_p , and the core geometry K_g , which is discussed in Chapter 7.

Table 2-20. Composite Core Listing Along with the Area Product and Core Geometry.

Magnetics Inc. Composite Cores			
Composite Number	Standard Core Number	A_p (cm^4)	K_g (cm^5)
01605-2D	52000	0.0728	0.00105
01754-2D	52002	0.1440	0.00171
01755-2D	52076	0.2850	0.00661
01609-D2	52061	0.3890	0.00744
01756-2D	52106	0.4390	0.00948
01606-2D	52094	0.6030	0.02210
01761-2D	52318	0.7790	0.02600
01757-2D	52029	1.0900	0.02560
01760-2D	52188	1.1520	0.05120
02153-2D	52181	1.2200	0.04070
01758-2D	52032	1.4550	0.04310
01607-2D	52026	2.1800	0.08740
01966-2D	52030	2.3370	0.06350
01759-2D	52038	2.9100	0.14000
01608-2D	52035	4.6760	0.20600
01623-2D	52425	5.2550	0.26200
01624-2D	52169	7.1300	0.41800
$A_c = 66\%$ Square Permalloy 4 / 79. $A_c = 33\%$ Orthonol 50 / 50. $l_g = 2$ mil Kapton.			

Summary

Low-loss tape-wound toroidal core materials, that have a very square hysteresis characteristic, (B-H loop), have been used extensively in the design of spacecraft transformers. Due to the squareness of the B-H loops of these materials, transformers designed with them tend to saturate quite easily. As a result, large voltage and current spikes, which cause undue stress on the electronic circuitry, can occur. Saturation occurs when there is any unbalance in the ac drive to the transformer, or when any dc excitation exists. Also, due to the square characteristic, a high residual flux state, (high B_r), may remain when excitation is removed. Reapplication of excitation in the same direction may cause deep saturation, and an extremely large current spike, limited only by source impedance and transformer winding resistance, can result. This can produce catastrophic failure.

With the introduction of a small, (less than 25 μm), air gap into the core, the problems described above can be avoided while retaining the low-loss properties of the materials. The air gap has the effect of "shearing over" the B-H loop of the material so that the residual flux state is low and the margin between operating,

flux density, and saturation, flux density is high. The air gap thus has a powerful demagnetizing effect upon the square loop materials. Properly designed transformers, using cut toroid or C core square-loop materials, will not saturate upon turn-on, and can tolerate a certain amount of unbalanced drive or dc excitation.

It must be emphasized, however, that because of the nature of the material and the small size of the gap, extreme care and control must be taken in performing the gapping operation. Otherwise, the desired shearing effect will not be achieved, and the low-loss properties will be lost. The cores must be very carefully cut, lapped, and etched to provide smooth, residue-free surfaces. Reassembly must be performed with equal care.

Chapter 3

Magnetic Cores

Table of Contents

1. Introduction	
2. Core Type and Shell Type Construction	
3. Types of Core Materials	
4. Eddy Currents and Insulation	
5. Laminations	
6. Annealing and Stress-Relief	
7. Stacking Laminations and Polarity	
8. Flux Crowding	
9. Exciting Current	
10. Tape Wound C, EE, and Toroidal Cores	
11. Tape Toroidal Cores	
12. Toroidal, Powder Core	
13. Stacking Factors	
14. Design and Dimensional Data for EI Laminations	
15. Design and Dimensional Data for UI Laminations	
16. Design and Dimensional Data for LL Laminations	
17. Design and Dimensional Data for DU Laminations	
18. Design and Dimensional Data for Three Phase Laminations	
19. Design and Dimensional Data for Tape Wound C Cores	
20. Dimensional Outline for Tape Wound EE Cores	
21. Design and Dimensional Data for Tape Wound Toroidal Cores	
22. Design and Dimensional Data for EE and EI Ferrite Cores	
23. Design and Dimensional Data for EE and EI Planar, Ferrite Cores	
24. Design and Dimensional Data for EC, Ferrite Cores.....	
25. Design and Dimensional Data for ETD, Ferrite Cores	
26. Design and Dimensional Data for ETD/(low profile), Ferrite Cores	
27. Design and Dimensional Data for ER, Ferrite Cores.....	
28. Design and Dimensional Data for EFD, Ferrite Cores	
29. Design and Dimensional Data for EPC, Ferrite Cores	
30. Design and Dimensional Data for PC, Ferrite Cores	
31. Design and Dimensional Data for EP, Ferrite Cores	
32. Design and Dimensional Data for PQ, Ferrite Cores.....	
33. Design and Dimensional Data for PQ/(low profile), Ferrite Cores	
34. Design and Dimensional Data for RM, Ferrite Cores	

35. Design and Dimensional Data for RM/(low profile), Ferrite Cores	
36. Design and Dimensional Data for DS, Ferrite Cores	
37. Design and Dimensional Data for UUR, Ferrite Cores	
38. Design and Dimensional Data for UUS, Ferrite Cores	
39. Design and Dimensional Data for Toroidal, Ferrite Cores	
40. Design and Dimensional Data for Toroidal, MPP Powder Cores	
41. Design and Dimensional Data for Toroidal, Iron Powder Cores	
42. Design and Dimensional Data for Toroidal, Sendust Powder Cores	
43. Design and Dimensional Data for Toroidal, High Flux Powder Cores	
44. Design and Dimensional Data for EE, Iron Powder Cores	
45. Design and Dimensional Data for EE, Sendust Powder Cores	
46. References	

Introduction

The key ingredient in a magnetic device is the magnetic field (flux) created when current is passed through a coiled wire. The ability to control (channel, predict, conduct), the magnetic field (flux) is critical to controlling the operation of the magnetic device.

The ability of a material to conduct magnetic flux is defined as permeability. A vacuum is defined as having a permeability of 1.0 and the permeability of all other materials is measured against this baseline. Most materials such as air, paper, and wood are poor conductors of magnetic flux, in that they have low permeability. If wire is wound on a dowel, it exhibits a magnetic field exactly, as shown in Figure 3-1. There are a few materials, such as iron, nickel, cobalt, and their alloys that have high permeabilities, sometimes ranging into the hundreds of thousands. These materials and their alloys are used as the base materials for all core materials.

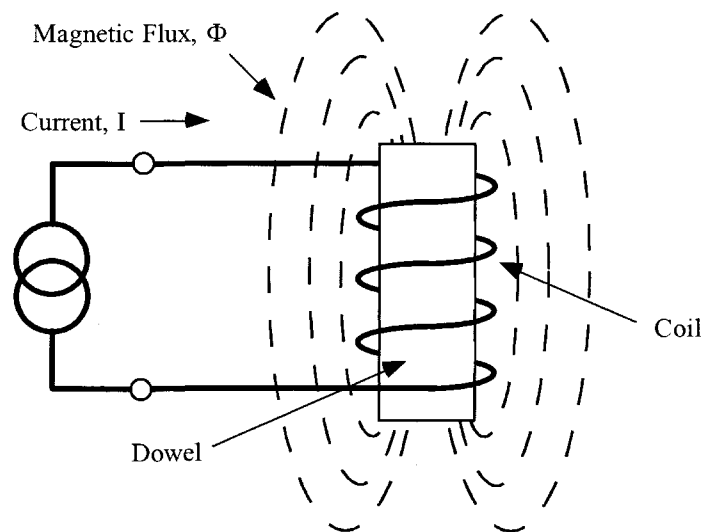


Figure 3-1. Air Core with an Intensified Magnetic Field.

The main purpose of the core is to contain the magnetic flux and create a well-defined, predictable path for the flux. This flux path, and the mean distance covered by the flux within the magnetic material, is defined as the Magnetic Path Length (MPL) (see Figure 3-2). The Magnetic Path Length and permeability are vital keys in predicting the operation characteristic of a magnetic device. Selection of a core material and geometry are usually based on a compromise between conflicting requirements, such as size, weight, temperature rise, flux density, core loss, and operating frequency.

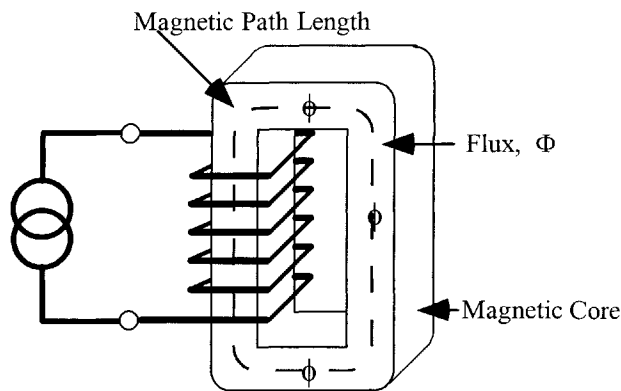


Figure 3-2. Magnetic Core Confines the Magnetic Field.

Core Type and Shell Type Construction

There are two types of construction for magnetic cores, core type and shell type. The shell type construction is shown in Figure 3-3, and the core type construction is shown in Figure 3-4. In the shell type, shown in Figure 3-3, the core surrounds the coil. Here the magnetic fields are around the outside of the coil. The advantage of this configuration is that it requires only one coil. In the core type of construction, shown in Figure 3-4, the coils are outside of the core. A good example of this is a toroid, where the coil is wound on the outside of a core.

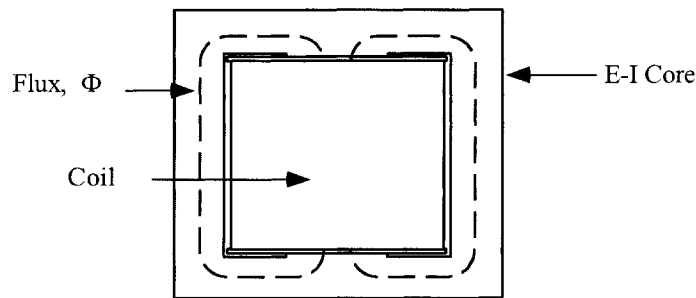


Figure 3-3. Shell Type Construction: the Core Surrounds the Coil.

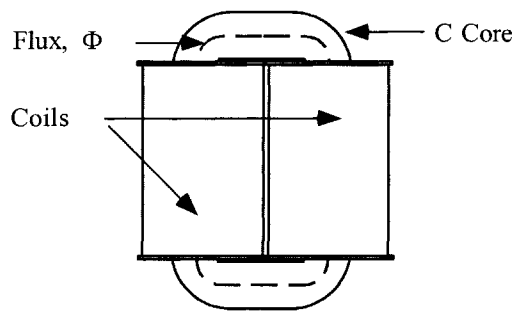


Figure 3-4. Core Type Construction the Coil Surrounds the Core.

Types of Core Materials

Magnetic cores are made of three basic materials. The first is bulk metal, the second is powdered materials, and the third is ferrite material.

The bulk metals are processed from the furnace into ingots. Then, the material is put into a process of hot and cold rolling. The rolling process produces a sheet of material with a thickness ranging from 0.004 to 0.031 inches that can be punched into laminations. It can be further rolled to thicknesses ranging from 0.002 to 0.000125 inches, then slit and wound into tape cores, such as C cores, E cores and toroids.

The powder cores, such as powder molypermalloy and powdered iron materials, are die-pressed into toroids, EE cores and slugs. Powder core processing starts at the ingot, then goes through various steps of grinding until the powder is the right consistency for the required performance. Normally, powder cores are not machined after processing.

Ferrites are ceramic materials of iron oxide, alloyed with oxides or carbonate of manganese, zinc, nickel, magnesium, or cobalt. Alloys are selected and mixed, based on the required permeability of the core. Then, these mixtures are molded into the desired shape with pressure of approximately 150-200 tons per square inch and fired at temperatures above 2000 degrees F. After the parts are made, they are usually tumbled to remove burrs and sharp edges, which are characteristic of this process. Ferrites can be machined to almost any shape to meet the engineer's needs.

Eddy Currents and Insulation

Transformers, operating at moderate frequency, require the reduction of eddy current losses in the magnetic material. To reduce the eddy current losses to a reasonable value requires electrical steel to have adequate resistivity. Also, it needs to be rolled to a specific thickness, and it needs effective electrical insulation or coating of the magnetic material.

If an alternating voltage is applied to the primary winding, as shown in Figure 3-5, it will induce an alternating flux in the core. The alternating flux will, in turn, induce a voltage on the secondary winding. This alternating flux also induces a small alternating voltage in the core material. These voltages produce currents called eddy currents, which are proportional to the voltage. The magnitude of these eddy currents is also limited by the resistivity of the material. The alternating flux is proportional to the applied voltage. Doubling the applied voltage will double the eddy currents. This will raise the core loss by a factor of four. Eddy currents not only flow in the lamination itself, but could flow within the core as a unit, if the lamination is not properly stamped, and if the lamination is not adequately insulated, as shown in Figure 3-6.

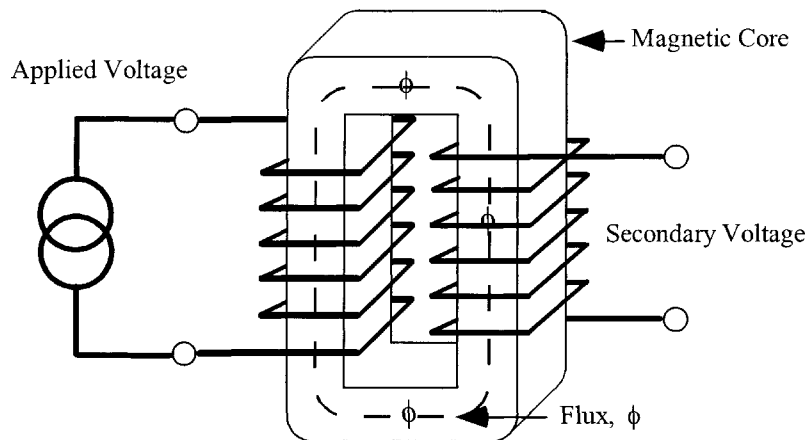


Figure 3-5. Applied Alternating Voltage Induces an Alternating Flux.

There are two eddy currents, as shown in Figure 3-6, i_a and i_b . The intralaminar eddy current, i_a , is governed by flux, per lamination and resistance of the lamination. It is, therefore, dependent on lamination width, thickness, and volume resistivity.

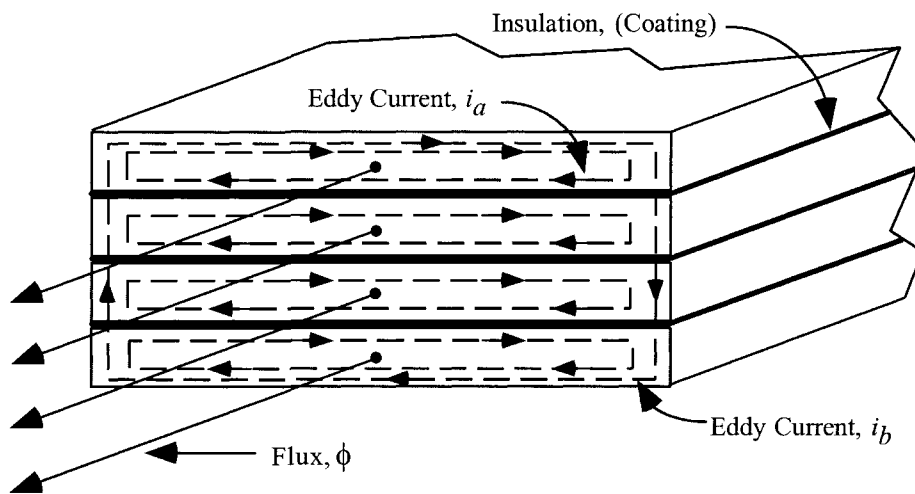


Figure 3-6. Insulation is Required Between Laminations to Reduce Eddy Currents.

The interlaminar eddy current, i_b , is governed by total flux and resistance of the core stack. It is primarily dependent upon stack width and height, the number of laminations, and the surface insulation resistance, per lamination.

The magnetic materials used for tape cores and laminations are coated with an insulating material. The insulating coating is applied to reduce eddy currents. The American Iron and Steel Institute (AISI) has set up insulation standards for transformer steels used in different applications. High permeability, nickel-iron cores are very strain sensitive. Manufacturers of these cores normally have their own proprietary, insulating material.

Laminations

Laminations are available in scores of different shapes and sizes. The punch press technology for fabricating laminations has been well-developed. Most lamination sizes have been around forever. The most commonly used laminations are the EI, EE, FF, UI, LL, and the DU, as shown in Figure 3-7. The laminations differ from each other by the location of the cut in the magnetic path length. This cut introduces an air gap, which results in the loss of permeability. To minimize the resulting air gap, the laminations are generally stacked in such a way the air gaps in each layer are staggered.

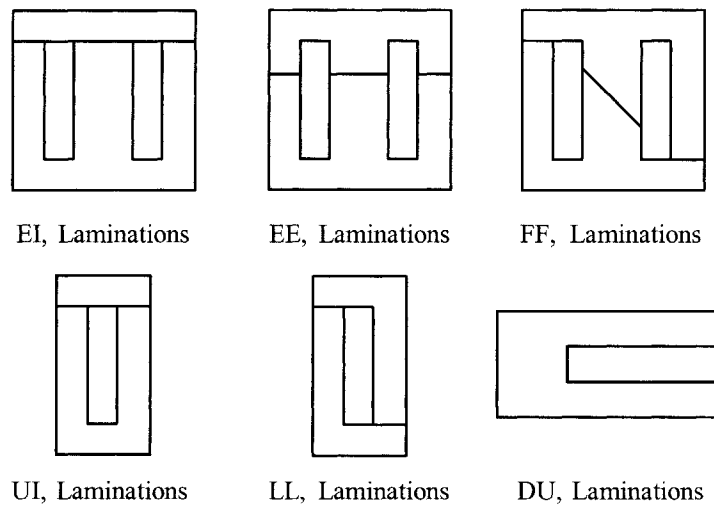


Figure 3-7. Commonly Used, Lamination Shapes.

There are bobbins and brackets for almost all standard stacking dimensions. Most of the EI lamination is the scrapless. The name, scrapless, is derived from shapes that are punched with minimum waste, as shown in Figure 3-8.

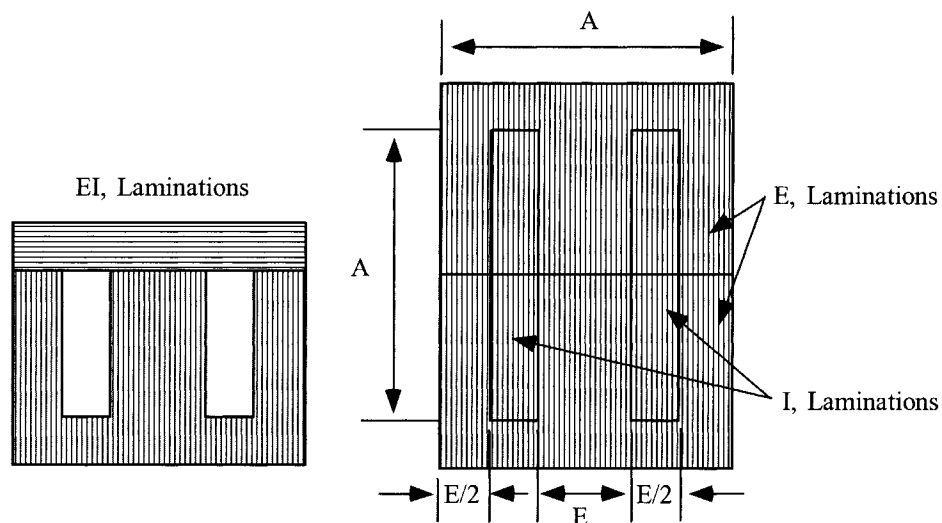


Figure 3-8. Typical, Scrapless EI Lamination.

Annealing and Stress-Relief

One of the most important parameters in transformer steels is permeability. Any stress or strain of the magnetic materials will have an impact on the permeability. The resulting stress could cause higher magnetizing current, or a lower inductance. When the transformer is being assembled (in the stacking process), and a lamination is bent (does not return to its original shape), that lamination has been stressed and should be replaced.

Some of the important magnetic properties are lost due to stress and strain after stamping, shearing and slitting. These properties that have been lost or seriously reduced can be restored to the magnetic materials by annealing. Basically, stress relief is accomplished by heating (annealing) the magnetic material to prescribed temperature, (depending on the material), followed by cooling to room temperature. The entire annealing process is a delicate operation. The annealing must be done under controlled conditions of time, temperature and the ambient atmosphere that will avoid, even minute, adverse changes in the chemistry of the steel.

Stacking Laminations and Polarity

The edges of the magnetic material that have been stamped, sheared, or slit, will have a burr, as shown in Figure 3-9. The quality of the equipment will keep the burr to a minimum. This burr now gives the lamination a polarity. When a transformer is being stacked, the lamination build is normally sized by dimensions, or it just fills the bobbin.

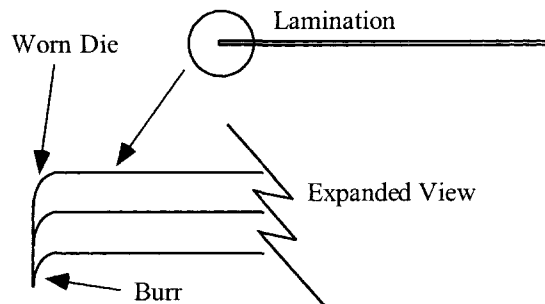


Figure 3-9. Expanded View, Showing Lamination Burr.

If the laminations are stacked correctly, all of the burred ends will be aligned. If the laminations are stacked randomly, such as the burr ends facing each other, then, the stacking factor would be affected. The stacking factor has a direct impact on the cross-section of the core. The end result would be less iron. This could lead to premature saturation, as an increase in the magnetizing current, or a loss of inductance.

There are several methods used in stacking transformer laminations. The most common technique used in stacking laminations is the alternate method. The alternate method is where one set of laminations, such as an E and an I, are assembled. Then, the laminations are reversed, as shown in Figure 3-10. This technique, used in stacking, provides the lowest air gap and the highest permeability. Another method for stacking

laminations is to interleave two-by-two, also shown in Figure 3-10. The second method of stacking would be in groups of two or more. This is done to cut assembly time. The loss in performance in stacking, other than one by one, is the increase in magnetizing current and a loss of permeability.

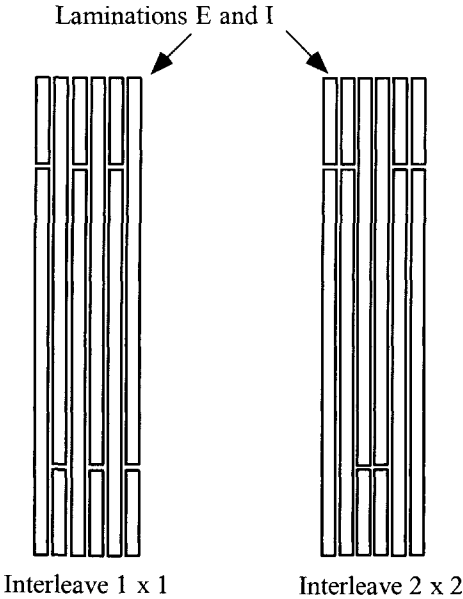


Figure 3-10. Methods for Stacking Laminations.

Flux Crowding

When laminations are stacked, as shown in Figure 3-11, there is flux crowding. This flux crowding is caused by the difference in spacing between the E, I, and the adjacent lamination. The adjacent lamination has a minimum air gap, which translates into a higher permeability.

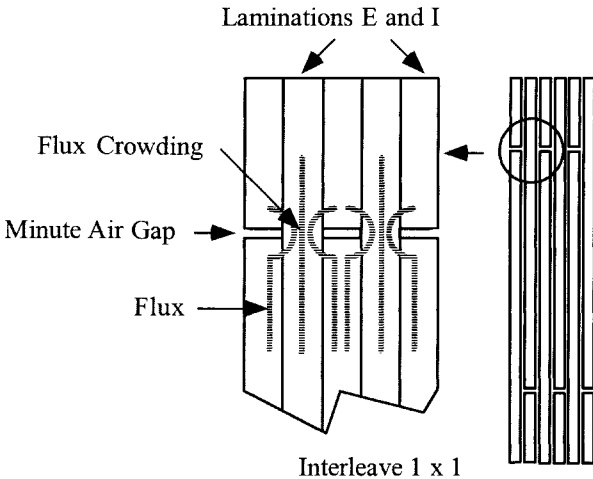


Figure 3-11. Flux Crowding, when Laminations are Interleaved.

Exciting Current

The flux will skirt the low permeability air gap and migrate into the adjacent lamination, causing flux crowding in that lamination. Eventually, this crowding will cause saturation in that portion of the lamination, and the excitation current will rise. After that portion of the lamination has saturated, the flux will migrate back to the lower permeability segment of the lamination from where it left. This effect can be easily viewed by observing the B-H loops at low and high flux densities, and comparing them with a toroidal core of the same material, with a minimum air gap, as shown in Figure 3-12. The B-H loop, along with the magnetizing current, I_m , of a toroidal core, is shown in Figure 3-12A. The toroidal core, with its inherent minimum air gap, will have almost a square of current. Using the same material in lamination form will exhibit a B-H loop, and a magnetizing current, I_m , similar to Figure 3-12B operating at low flux densities. Increasing the excitation will cause premature saturation of the lamination, as seen by the non-linear, exciting current, as shown in Figure 3-12C

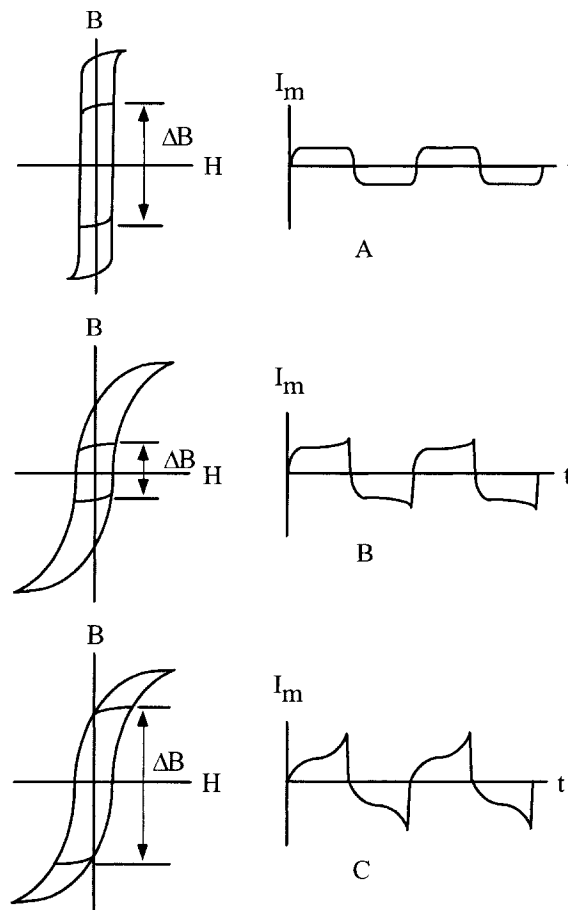


Figure 3-12. Comparing the Exciting Currents and Three B-H Loops.

Most finished transformers or inductors will have some sort of bracket, such as an L bracket, end bells, a channel bracket or maybe a bolt through the mounting holes to the chassis. When transformers are being assembled, there is a certain amount of attention that has to be used to get proper performance. The insulation material used to coat the lamination is normally very durable, but it can be scratched off and degrade the performance. When brackets are used in the transformer assembly, as shown in Figure 3-13, care must be taken on how the bolts and brackets are put together. The transformer assembly bolts, shown in Figure 3-13, should be the recommended size for the mounting hole and use all of the required hardware. This hardware should include the correct bolt size and length, and correct surface washer, lock washer and nut. Also, included in this hardware, should be fiber shoulder washers and proper sleeving to cover the bolt threads. If insulating hardware is not used, there is a good chance of a partial, shorted turn. The continuity for this partial turn can be created through the bolts and bracket, or the bolts, bracket, and the chassis. This partial shorted turn will downgrade the performance of the transformer.

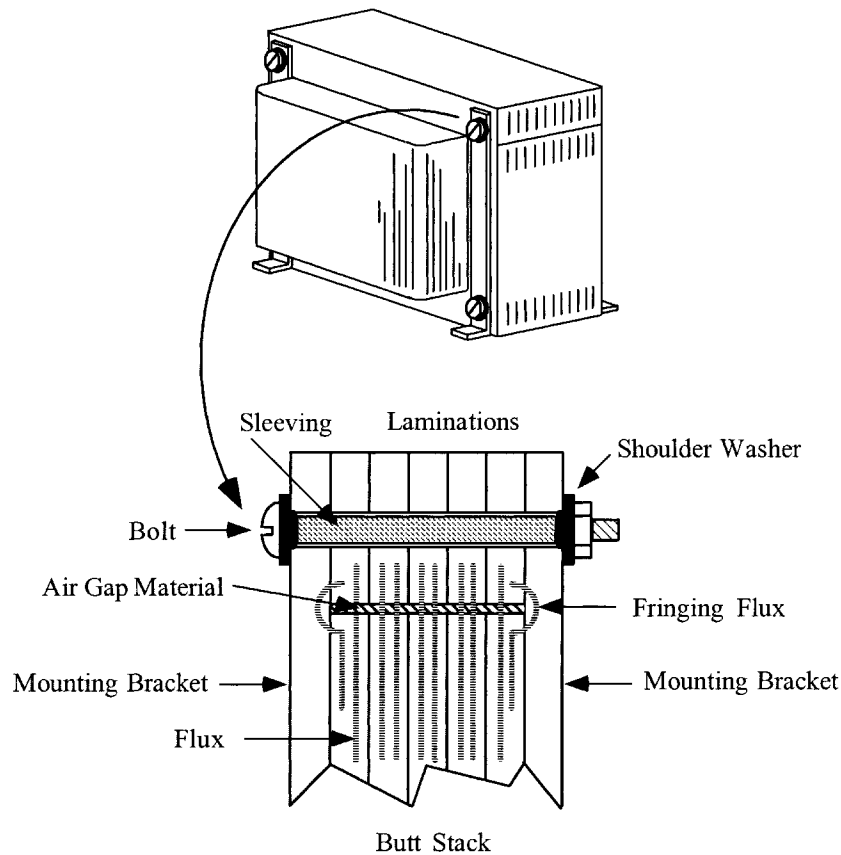


Figure 3-13. Lamination Mounting Hardware.

Tape Wound C, EE, and Toroidal Cores

Tape wound cores are constructed by winding around a mandrel, a magnetic material in the form of a preslit tape, as shown in Figure 3-14. This tape material comes in all of the iron alloys, plus the amorphous materials. The tape thickness varies from 0.0005 inch (0.0127 mm) to 0.012 inch (0.305 mm). The advantage of this type of construction is that the flux is parallel with the direction of rolling of the magnetic material. This provides the maximum utilization of flux with the minimum of magnetizing force. There are two disadvantages in this type of construction. When the core is cut in half, as shown in Figure 3-15, the mating surface has to be ground, lapped, and then, acid-etched. This is done to provide a smooth mating surface with the minimum of air gap and the maximum of permeability. The other disadvantage is when the cores are reassembled, the method used is normally done with a band and buckle, and this procedure requires a little skill to provide the right alignment and correct tension, as shown in Figure 3-16. The C cores are impregnated for strength, prior to being cut. The cut C core can be used in many configurations in the design of a magnetic component, as shown in Figure 3-17. The EE cores are constructed in the same way as C cores, but they have an additional overwind, as shown in Figure 3-18. The assembled three-phase transformer is shown in Figure 3-19.

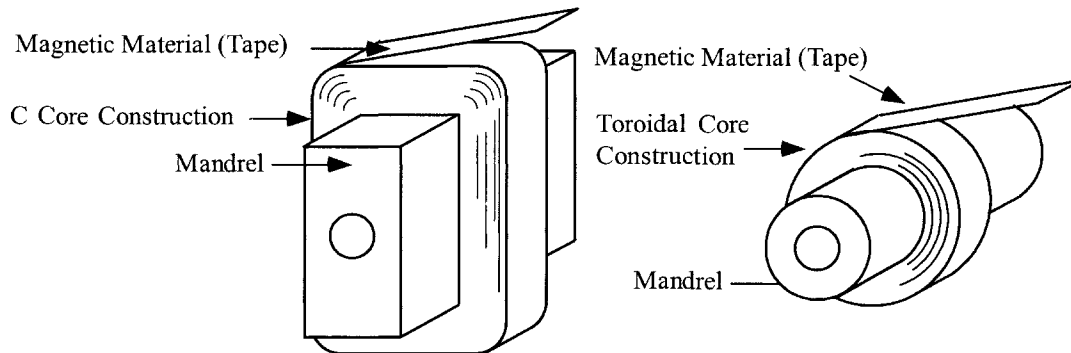


Figure 3-14. Tape Cores Being Wound on a Mandrel.

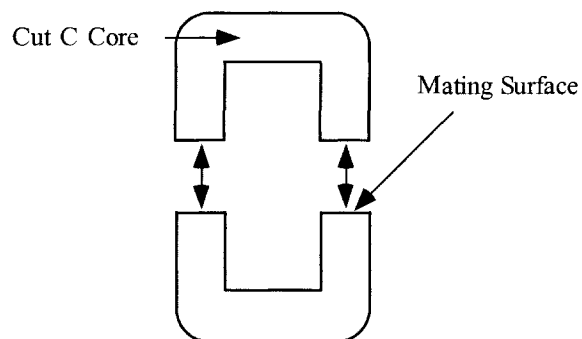


Figure 3-15. Two Halves of a Cut C Core.

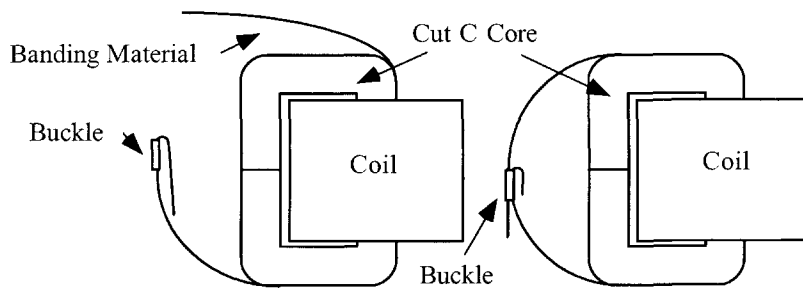


Figure 3-16. Banding the Cut C Core.

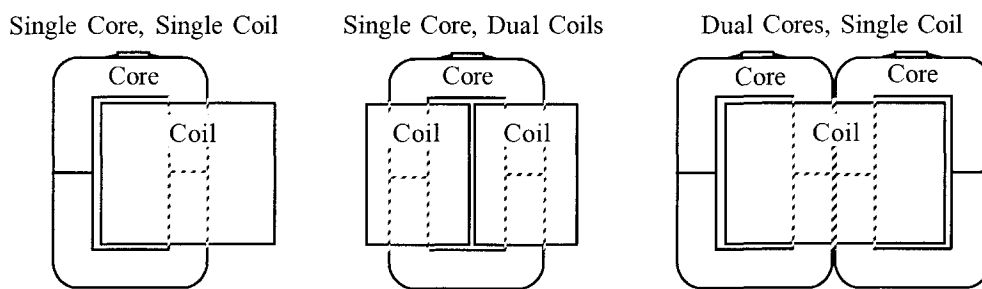


Figure 3-17. Three Different C Core Configurations.

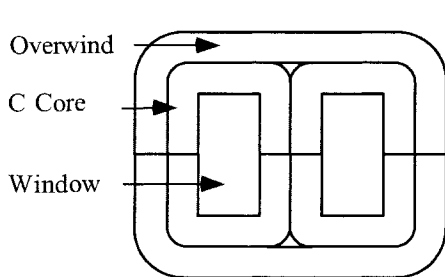


Figure 3-18. Three-Phase, Cut EE Core.

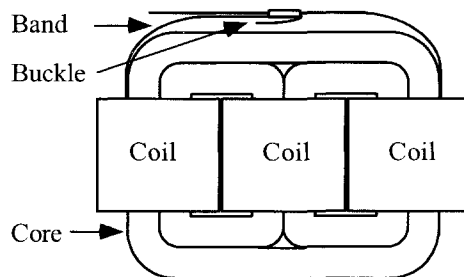


Figure 3-19. Typical, Assembled EE Cut Core.

Tape Toroidal Cores

Tape toroidal cores are constructed in the same way as tape C cores, by winding the magnetic material around a mandrel, in the form of a preslit tape. This tape material comes in all of the iron alloys, plus the amorphous materials. The tape thickness varies from 0.000125 inch (0.00318 mm) to 0.012 inch (0.305 mm). The tape toroid is normally offered in two configurations, cased and encapsulated, as shown in Figure 3-20. The cased toroid offers superior electrical properties and stress protection against winding. The encapsulated cores are used when not all of the fine magnetic properties are important to the design, such as in power transformers.

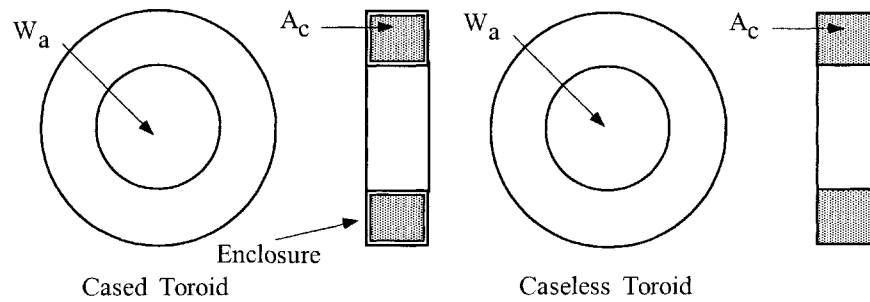


Figure 3-20. Outline of a Cased and a Caseless Toroidal Core.

Toroidal, Powder Core

Powder cores, as shown in Figure 3-21, are very unique. They give the engineer another tool to speed the initial design. Powder cores have a built-in air gap. They come in a variety of materials and are very stable with time and temperature. The cores are manufactured with good engineering aids. Manufacturers provide catalogs for their cores, listing not only the size, but also permeability and Millihenrys per 1000 turns. The data is presented to the engineer in such a way that it takes the minimum amount of time to have a design that will function.

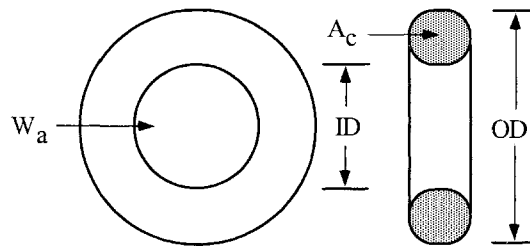


Figure 3-21. Outline of a Powder Toroidal Core.

Stacking Factors

The standard stacking factors for tape cores, wound cut cotes and laminations are shown in Table 3-1.

Table 3-1. Standard Stacking Factors.

Thickness mils	Tape Cores	Wound Cut Cores	Laminations		(S.F.) ²
			Butt Stack	Interleave 1x1	
0.125	0.250				0.062
0.250	0.375				0.141
0.500	0.500				0.250
1.000	0.750	0.830			0.562
2.000	0.850	0.890			0.722
4.000	0.900	0.900	0.900	0.800	0.810
6.000		0.900	0.900	0.850	0.810
12.000	0.940	0.950			0.884
14.000	0.940	0.950	0.950	0.900	0.902
18.000			0.950	0.900	0.810
25.000			0.950	0.920	0.846

Design and Dimensional Data for EI Laminations

Laminations are still one of the most widely-used cores in power conversion. The dimensional outline for EI laminations and an assembled transformer is shown in Figure 3-22. Dimensional data for EI laminations is given in Table 3-2; design data is given in Table 3-3.

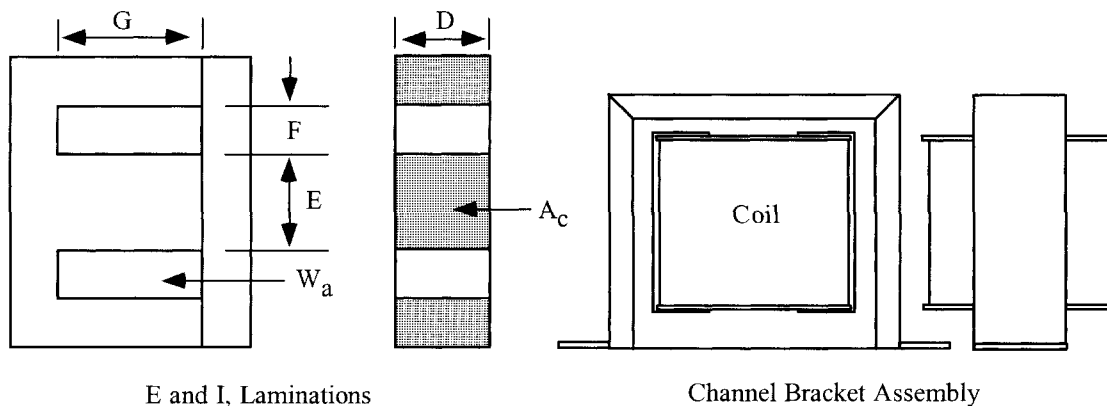


Figure 3-22. EI Lamination Outline.

Table 3-2. Dimensional Data for EI Laminations.

EI, Laminations, (Tempel) 14 mil									
Part No.	D cm	E cm	F cm	G cm	Part No.	D cm	E cm	F cm	G cm
EI-375	0.953	0.953	0.794	1.905	EI-112	2.857	2.857	1.429	4.286
EI-021	1.270	1.270	0.794	2.064	EI-125	3.175	3.175	1.588	4.763
EI-625	1.588	1.588	0.794	2.381	EI-138	3.493	3.493	1.746	5.239
EI-750	1.905	1.905	0.953	2.857	EI-150	3.810	3.810	1.905	5.715
EI-875	2.223	2.223	1.111	3.333	EI-175	4.445	4.445	2.223	6.668
EI-100	2.540	2.540	1.270	3.810	EI-225	5.715	5.715	2.858	8.573

Table 3-3. Design Data for 14 mil EI Laminations.

EI, Laminations, (Tempel) 14 mil											
Part No.	W _{tcu} grams	W _{tfe} grams	MLT cm	MPL cm	W _a		A _c cm ²	W _a cm ²	A _p cm ⁴	K _g cm ⁵	A _t cm ²
					A _c						
EI-375	36.1	47.2	6.7	7.3	1.754	0.862	1.512	1.303	0.067	46.2	
EI-021	47.6	94.3	8.2	8.3	1.075	1.523	1.638	2.510	0.188	62.1	
EI-625	63.5	170.0	9.5	9.5	0.418	2.394	1.890	4.525	0.459	83.2	
EI-750	108.8	296.0	11.2	11.4	0.790	3.448	2.723	9.384	1.153	120.0	
EI-875	171.0	457.0	13.0	13.3	0.789	4.693	3.705	17.384	2.513	163.0	
EI-100	254.0	676.0	14.8	15.2	0.790	6.129	4.839	29.656	4.927	212.9	
EI-112	360.0	976.0	16.5	17.2	0.789	7.757	6.124	47.504	8.920	269.4	
EI-125	492.0	1343.0	18.3	19.1	0.789	9.577	7.560	72.404	15.162	333.0	
EI-138	653.0	1786.0	20.1	21.0	0.789	11.588	9.148	106.006	24.492	403.0	
EI-150	853.0	2334.0	22.0	22.9	0.789	13.790	10.887	150.136	37.579	479.0	
EI-175	1348.0	3711.0	25.6	26.7	0.789	18.770	14.818	278.145	81.656	652.0	
EI-225	2844.0	7976.0	32.7	34.3	0.789	31.028	24.496	760.064	288.936	1078.0	

Design and Dimensional Data for UI Laminations

The dimensional outline for UI laminations and an assembled transformer is shown in Figure 3-23. Dimensional data for UI laminations is given in Table 3-4; design data is given in Table 3-5.

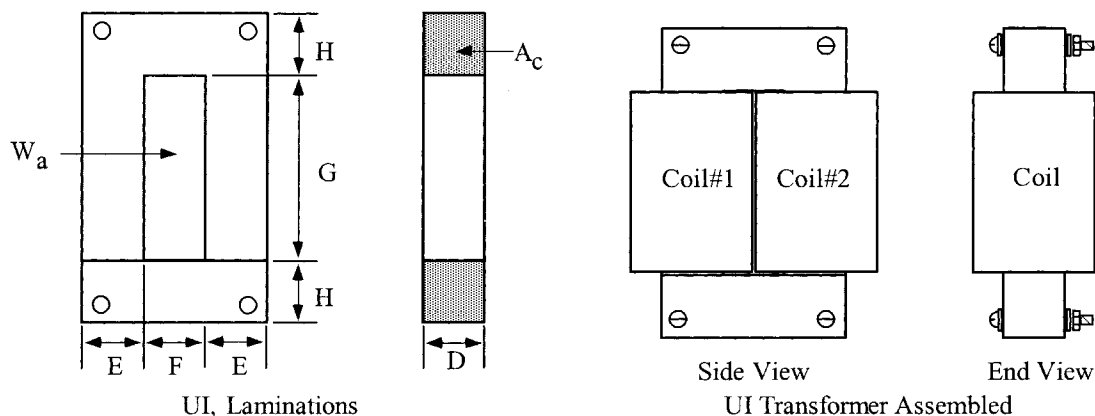


Figure 3-23. UI Lamination Outline.

Table 3-4. Dimensional Data for UI Laminations.

UI, Standard Laminations 14 mil											
Part No.	D cm	E cm	F cm	G cm	H cm	Part No.	D cm	E cm	F cm	G cm	H cm
50UI	1.270	1.270	1.270	3.810	1.270	125UI	3.175	3.175	3.175	9.525	3.175
60UI	1.429	1.429	2.223	5.398	1.429	150UI	3.810	3.810	3.810	11.430	3.810
75UI	1.905	1.905	1.905	5.715	1.905	180UI	4.572	4.572	4.572	11.430	4.572
100UI	2.540	2.540	2.540	7.620	2.540	240UI	6.096	6.096	6.096	15.240	6.096

Table 3-5. Design Data for 14 mil UI Laminations.

UI, Standard Laminations 14 mil											
Part No.	W _{tcu} grams	W _{tfe} grams	MLT cm	MPL cm	W _a		A _c cm ²	W _a cm ²	A _p cm ⁴	K _g cm ⁵	A _t cm ²
					W _a	A _c					
50UI	132	173	7.68	15.24	3.159	1.532	4.839	7.414	0.592	110	
60UI	418	300	9.81	18.10	6.187	1.939	11.996	23.263	1.839	209	
75UI	434	585	11.22	22.86	3.157	3.448	10.887	37.534	4.614	247	
100UI	1016	1384	14.76	30.48	3.158	6.129	19.355	118.626	19.709	439	
125UI	1967	2725	18.29	38.10	3.158	9.577	30.242	289.614	60.647	685	
150UI	3413	4702	22.04	45.72	3.158	13.790	43.548	600.544	150.318	987	
180UI	4884	7491	26.28	50.29	2.632	19.858	52.258	1037.740	313.636	1296	
240UI	11487	17692	34.77	67.06	2.632	35.303	92.903	3279.770	1331.997	2304	

Design and Dimensional Data for LL Laminations

The dimensional outline for LL laminations and an assembled transformer is shown in Figure 3-24. Dimensional data for LL laminations is given in Table 3-6; design data is given in Table 3-7.

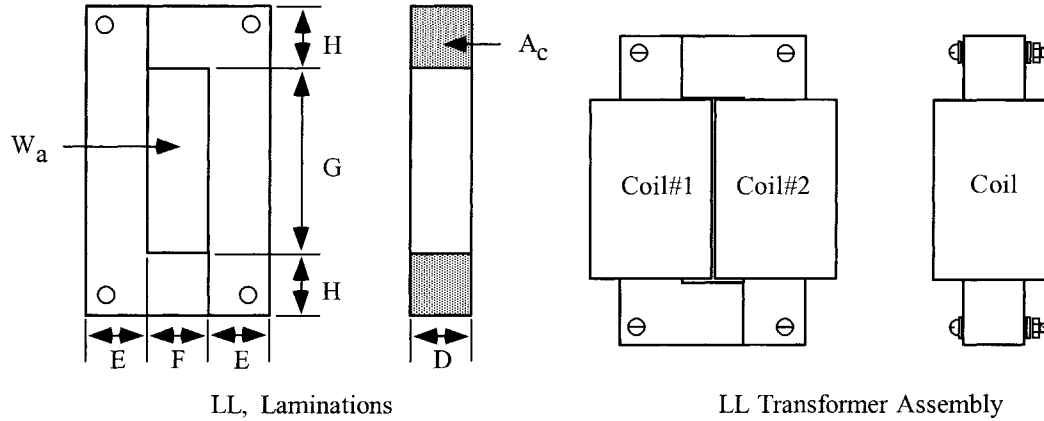


Figure 3-24. LL Lamination Outline.

Table 3-6. Dimensional Data for 14 mil LL Laminations.

LL, Standard Laminations 14 mil											
Part No.	D cm	E cm	F cm	G cm	H cm	Part Number	D cm	E cm	F cm	G cm	H cm
141L	0.635	0.635	1.270	2.858	0.635	104L	1.270	1.270	1.984	5.555	1.270
108L	1.031	1.031	0.874	3.334	1.111	105L	1.270	1.270	1.905	6.826	1.270
250L	1.031	1.031	0.874	5.239	1.111	102L	1.429	1.429	1.588	5.398	1.429
101L	1.111	1.111	1.588	2.858	1.111	106L	1.429	1.429	2.223	5.398	1.429
7L	1.270	1.270	1.270	3.810	1.270	107L	1.588	1.588	2.064	6.350	1.588
4L	1.270	1.270	1.905	3.810	1.270						

Table 3-7. Design Data for 14 mil LL Laminations.

LL, Standard Laminations 14 mil											
Part No.	W _{icu} grams	W _{tfc} grams	MLT cm	MPL cm	W _a		A _c cm ²	W _a cm ²	A _p cm ⁴	K _g cm ⁵	A _t cm ²
					A _c						
141L	63.8	31.3	4.9	10.8	9.473		0.383	3.629	1.390	0.043	55.2
108L	61.2	97.9	5.9	12.7	2.884		1.010	2.913	2.943	0.201	70.3
250L	96.1	127.1	5.9	16.5	4.532		1.010	4.577	4.624	0.316	92.0
101L	118.5	115.9	7.3	13.3	3.867		1.173	4.536	5.322	0.340	97.3
7L	132.2	173.9	7.7	15.2	3.159		1.532	4.839	7.414	0.592	109.7
4L	224.0	185.2	8.7	16.5	4.737		1.532	7.258	11.121	0.785	141.9
104L	344.9	228.0	8.8	20.2	7.193		1.532	11.020	16.885	1.176	180.2
105L	401.3	256.5	8.7	22.5	8.488		1.532	13.004	19.925	1.407	199.4
102L	268.6	284.1	8.8	19.7	4.419		1.939	8.569	16.617	1.462	167.6
106L	418.6	302.1	9.8	21.0	6.187		1.939	11.996	23.263	1.839	208.8
107L	475.2	409.5	10.2	23.2	5.474		2.394	13.105	31.375	2.946	235.8

Design and Dimensional Data for DU Laminations

The dimensional outline for DU laminations and an assembled transformer is shown in Figure 3-25. Dimensional data for DU laminations is given in Table 3-8; design data is given in Table 3-9.

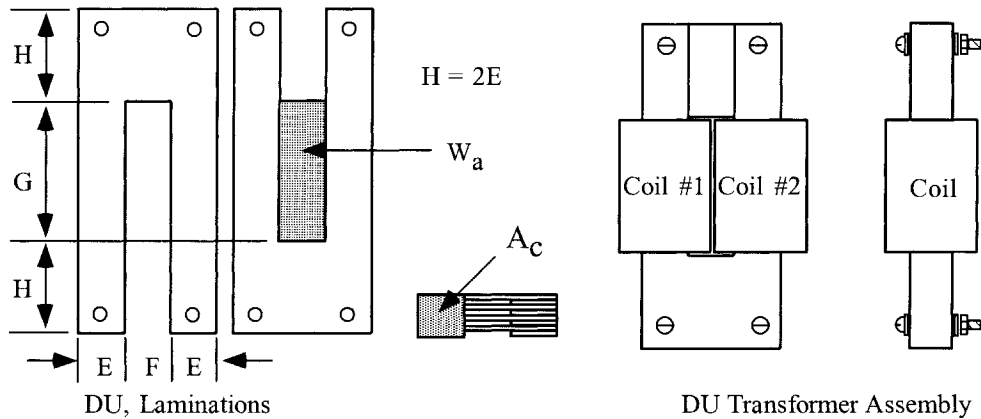


Figure 3-25. DU Lamination Outline.

Table 3-8. Dimensional Data for 14 mil DU Laminations.

DU, Standard Laminations 14 mil											
Part No.	D cm	E cm	F cm	G cm	H cm	Part No.	D cm	E cm	F cm	G cm	H cm
DU-63	0.159	0.159	0.318	0.794	0.318	DU-39	0.953	0.953	0.953	2.858	1.905
DU-124	0.318	0.318	0.476	1.191	0.635	DU-37	0.953	0.953	1.905	3.810	1.905
DU-18	0.476	0.476	0.635	1.588	0.953	DU-50	1.270	1.270	2.540	5.080	2.540
DU-26	0.635	0.635	0.635	1.905	1.270	DU-75	1.905	1.905	3.810	7.620	3.810
DU-25	0.635	0.635	0.953	2.064	1.270	DU-1125	2.858	2.858	5.715	11.430	5.715
DU-1	0.635	0.635	0.953	3.810	1.270	DU-125	3.175	3.175	5.080	10.160	6.350

Table 3-9. Design Data for 14 mil DU Laminations.

DU, Standard Laminations 14 mil											
Part No.	W _{teu} grams	W _{ife} grams	MLT cm	MPL cm	W _a		A _c cm ²	W _a cm ²	A _p cm ⁴	K _R cm ⁵	A _t cm ²
					A _c	A _c					
DU-63	1.4	0.6	1.5	3.2	10.500	0.024	0.252	0.006	0.00003	4.2	
DU-124	4.9	4.3	2.4	5.2	5.906	0.096	0.567	0.054	0.0009	11.8	
DU-18	11.9	13.5	3.3	7.3	4.688	0.215	1.008	0.217	0.0057	23.4	
DU-26	17.0	28.9	3.9	8.9	3.159	0.383	1.210	0.463	0.0180	33.9	
DU-25	31.1	30.4	4.4	9.9	5.133	0.383	1.966	0.753	0.0260	44.3	
DU-1	57.3	42.4	4.4	13.3	9.634	0.383	3.630	1.390	0.0479	60.9	
DU-39	55.3	104.5	5.7	13.3	3.158	0.862	2.722	2.346	0.1416	76.2	
DU-37	186.0	124.5	7.2	17.2	8.420	0.862	7.258	6.256	0.2992	134.3	
DU-50	443.9	287.8	9.7	22.8	8.422	1.532	12.903	19.771	1.2524	238.0	
DU-75	1467.0	985.2	14.2	34.3	8.420	3.448	29.032	100.091	9.7136	537.1	
DU-1125	4880.0	3246.0	21.0	51.4	8.421	7.757	65.322	506.709	74.8302	1208.0	
DU-125	3906.0	3966.0	21.3	41.4	5.389	9.577	51.610	494.275	88.9599	1147.0	

Design and Dimensional Data for Three Phase Laminations

The dimensional outline for 3Phase EI laminations and an assembled transformer is shown in Figure 3-26. Dimensional data for 3Phase EI laminations is given in Table 3-10; design data is given in Table 3-11.

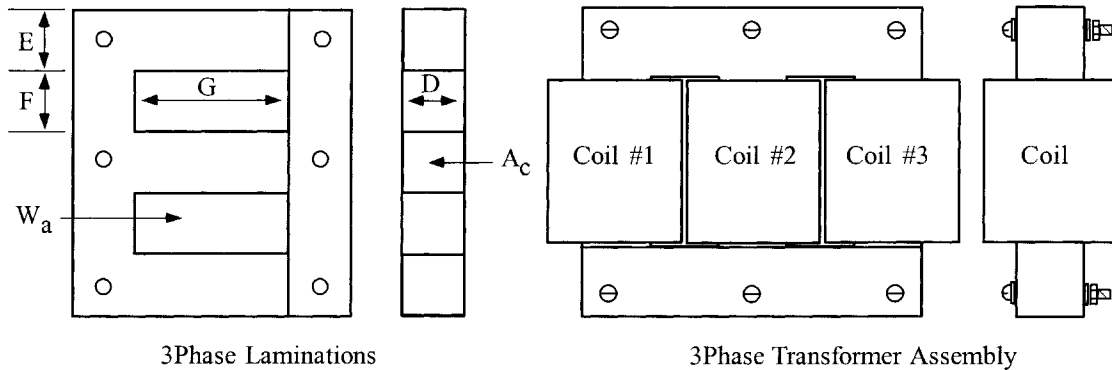


Figure 3-26. EI Three Phase Laminations Outline.

Table 3-10. Dimensional Data for 14 mil EI Three Phase Laminations.

3Phase, Standard Laminations, Thomas & Skinner 14 mil									
Part No.	D cm	E cm	F cm	G cm	Part No.	D cm	E cm	F cm	G cm
0.250EI	0.635	0.635	0.871	2.858	1.000EI	2.540	2.540	3.810	7.620
0.375EI	0.953	0.953	1.270	3.175	1.200EI	3.048	3.048	3.048	7.620
0.500EI	1.270	1.270	1.588	3.493	1.500EI	3.810	3.810	3.810	9.525
0.562EI	1.427	1.427	1.588	5.398	1.800EI	4.572	4.572	4.572	11.430
0.625EI	1.588	1.588	1.984	5.634	2.400EI	6.096	6.096	6.096	15.240
0.875EI	2.223	2.223	2.779	6.111	3.600EI	9.144	9.144	9.144	22.860

Table 3-11. Design Data for 14 mil EI Three Phase Laminations.

3Phase, Standard Laminations, Thomas & Skinner 14 mil									
Part No.	W _{tcu} grams	W _{tfe} grams	MLT cm	W _a	A _c cm ²	W _a cm ²	A _p cm ⁴	K _g cm ⁵	A _t cm ²
				2A _c					
0.250EI	57	54	4.3	3.251	0.383	2.49	1.43	0.051	53
0.375EI	134	154	6.2	2.339	0.862	4.03	5.21	0.289	102
0.500EI	242	324	8.2	1.810	1.532	5.54	12.74	0.955	159
0.562EI	403	421	8.8	2.213	1.936	8.57	24.88	2.187	207
0.625EI	600	706	10.1	2.334	2.394	11.18	40.13	3.816	275
0.875EI	1255	1743	13.9	1.809	4.693	16.98	119.53	16.187	487
1.000EI	2594	2751	16.7	2.368	6.129	29.03	266.91	39.067	730
1.200EI	2178	3546	17.6	1.316	8.826	23.23	307.48	61.727	725
1.500EI	4266	6957	22.0	1.316	13.790	36.29	750.68	187.898	1132
1.800EI	7326	12017	26.3	1.316	19.858	52.26	1556.61	470.453	1630
2.400EI	17230	28634	34.8	1.316	35.303	92.90	4919.66	1997.995	2899
3.600EI	58144	96805	52.2	1.316	79.432	209.03	24905.75	15174.600	6522

Design and Dimensional Data for Tape Wound C Cores

The dimensional outline for C cores is shown in Figure 3-27. Dimensional data for C cores is given in Table 3-12; design data is given in Table 3-13.

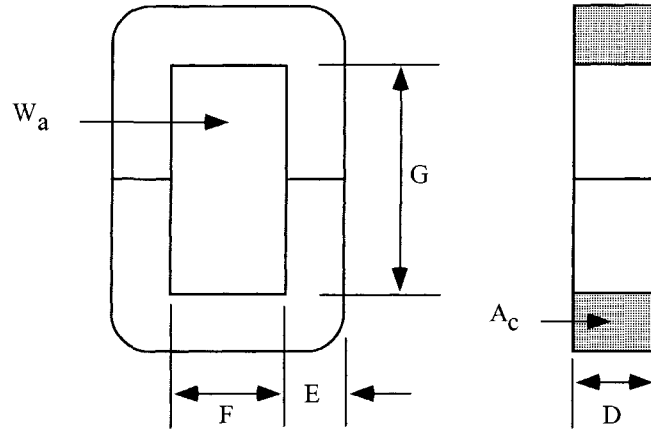


Figure 3-27. Tape C Core Dimensional Outline.

Table 3-12. Dimensional Data for Tape C Cores.

C Cores, Magnetic Metals, 2 mil									
Part No.	D cm	E cm	F cm	G cm	Part No.	D cm	E cm	F cm	G cm
ML-002	0.635	0.476	0.635	1.588	ML-014	1.270	1.270	1.270	3.969
ML-004	0.635	0.635	0.635	2.223	ML-016	1.905	1.270	1.270	3.969
ML-006	1.270	0.635	0.635	2.223	ML-018	1.270	1.111	1.588	3.969
ML-008	0.953	0.953	0.953	3.016	ML-020	2.540	1.588	1.588	3.969
ML-010	1.588	0.953	0.953	3.016	ML-022	2.540	1.588	1.588	4.921
ML-012	1.270	1.111	1.270	2.858	ML-024	2.450	1.588	1.905	5.874

Table 3-13. Design Data for Tape C Cores.

C Cores, Magnetic Metals, 2 mil										
Part No.	W _{tcu} grams	W _{tfe} grams	MLT cm	MPL cm	W _a	A _c cm ²	W _a cm ²	A _p cm ⁴	K _g cm ⁵	A _t cm ²
					A _c					
ML-002	13.0	13.0	3.6	6.4	3.747	0.269	1.008	0.271	0.0080	21.0
ML-004	19.8	22.6	3.9	8.3	3.933	0.359	1.412	0.507	0.0184	29.8
ML-006	27.2	45.2	5.4	8.3	1.967	0.718	1.412	1.013	0.0537	37.5
ML-008	58.4	72.5	5.7	11.8	3.556	0.808	2.874	2.323	0.1314	63.6
ML-010	73.5	120.8	7.2	11.8	2.134	1.347	2.874	3.871	0.2902	74.7
ML-012	95.1	121.7	7.4	12.7	2.891	1.256	3.630	4.558	0.3109	87.1
ML-014	137.7	170.4	7.7	15.6	3.513	1.435	5.041	7.236	0.5408	112.1
ML-016	160.5	255.6	9.0	15.6	2.341	2.153	5.041	10.854	1.0443	126.8
ML-018	176.2	149.1	7.9	15.6	5.019	1.256	6.303	7.915	0.5056	118.9
ML-020	254.5	478.4	11.4	17.5	1.756	3.590	6.303	22.626	2.8607	182.0
ML-022	315.6	530.5	11.4	19.4	2.177	3.590	7.815	28.053	3.5469	202.0
ML-024	471.7	600.1	11.9	21.9	3.117	3.590	11.190	40.170	4.8656	244.8

Dimensional Outline for Tape Wound EE Cores

The dimensional outline for EE cores is shown in Figure 3-28. Dimensional data for EE cores is given in Table 3-14; design data is given in Table 3-15.

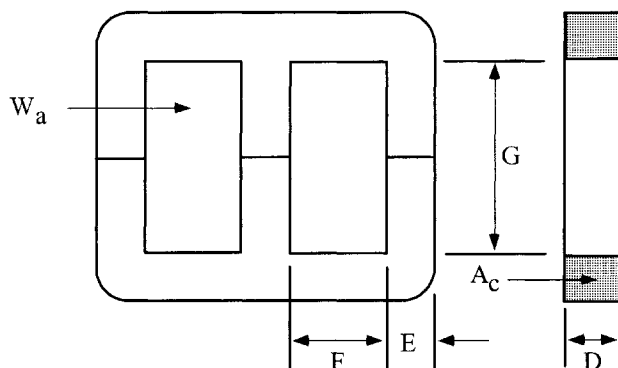


Figure 3-28. Tape EE Core Dimensional Outline.

Table 3-14. Dimensional Data for Tape EE Cores.

3Phase E Cores, National-Arnold Magnetics, 14 mil									
Part No.	D cm	E cm	F cm	G cm	Part No.	D cm	E cm	F cm	G cm
CTA-25	1.905	1.905	1.905	2.858	CTA-12	3.810	2.540	2.381	6.350
CTA-22	3.175	1.429	1.905	5.239	CTA-20	5.715	2.540	2.540	6.350
CTA-17	3.175	1.746	1.905	6.350	CTA-03	4.445	2.540	3.493	9.843
CTA-14	3.175	2.223	2.381	4.763	CTA-15	5.080	3.493	2.540	7.620

Table 3-15. Design Data for Tape EE Cores.

3Phase E Cores, National-Arnold Magnetics, 14 mil									
Part No.	W _{tcu} grams	W _{tfe} grams	MLT cm	W _a	A _c cm ²	W _a cm ²	A _p cm ⁴	K _g cm ⁵	A _t cm ²
				2A _c					
CTA-25	326	686	11.2	0.789	3.448	5.44	28.16	3.461	261
CTA-22	682	1073	12.8	1.158	4.310	9.98	64.53	8.686	324
CTA-17	867	1422	13.4	1.148	5.266	12.10	95.56	14.977	400
CTA-14	916	1803	15.1	0.846	6.705	11.34	114.06	20.203	468
CTA-12	1391	2899	17.3	0.822	9.194	15.12	208.50	44.438	613
CTA-20	1834	4420	21.3	0.585	13.790	16.13	333.64	86.347	737
CTA-03	3717	4597	20.3	1.602	10.730	34.38	553.15	117.079	993
CTA-15	2266	6544	22.0	0.574	16.860	19.35	489.40	150.340	956

Design and Dimensional Data for Tape Wound Toroidal Cores

The dimensional outline for tape wound Toroidal cores is shown in Figure 3-29. Dimensional data for cased tape wound Toroidal cores is given in Table 3-16; design data is given in Table 3-17.

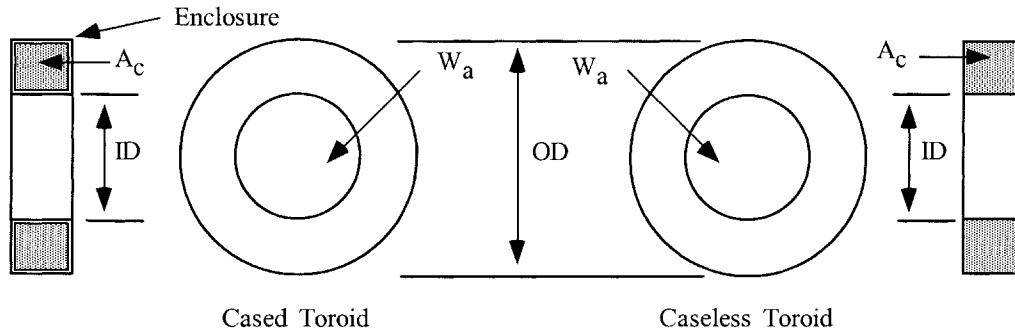


Figure 3-29. Tape Toroidal Core Dimensional Outline.

Table 3-16. Dimensional Data for Tape Toroidal Cores.

Toroidal Tape Cores, Magnetics 2 mil Iron Alloy (cased and coated)											
Part No.	OD cm	ID cm	HT cm	Part No.	OD cm	ID cm	HT cm	Part No.	OD cm	ID cm	HT cm
52402	1.346	0.724	0.610	52057	2.134	1.359	0.610	52061	2.781	1.664	0.927
52107	1.651	1.041	0.610	52000	2.134	1.041	0.610	52004	3.429	2.286	0.927
52153	1.499	0.724	0.610	52155	1.659	0.884	0.927	52076	2.794	1.334	0.762
52056	1.816	1.041	0.610	52176	2.134	1.041	0.927	52007	2.794	1.334	0.927

Table 3-17. Design Data for Tape Toroidal Cores.

Toroidal Tape Cores, Magnetics 2 mil Iron Alloy (cased)										
Part No.	W _{icu} grams	W _{tfe} grams	MLT cm	MPL cm	W _a	A _c	W _a	A _p	K _g	A _t
					A _c	cm ²	cm ²	cm ⁴	cm ⁵	cm ²
52402	2.84	0.50	2.16	3.25	18.727	0.022	0.412	0.00906	0.0000388	9.80
52107	6.76	0.70	2.30	4.24	38.682	0.022	0.851	0.01872	0.0000717	15.50
52153	3.20	1.10	2.20	3.49	9.581	0.043	0.412	0.01770	0.0001400	11.20
52056	7.40	1.50	2.40	4.49	19.791	0.043	0.851	0.03660	0.0002592	16.80
52057	13.80	1.80	2.70	5.48	33.744	0.043	1.451	0.06237	0.0003998	23.70
52000	8.10	3.30	2.70	4.99	9.895	0.086	0.851	0.07320	0.0009384	20.60
52155	6.10	2.60	2.80	3.99	7.140	0.086	0.614	0.05278	0.0006461	16.00
52176	9.70	6.50	3.20	4.99	4.977	0.171	0.851	0.14554	0.0031203	23.30
52061	28.70	9.10	3.70	6.98	12.719	0.171	2.175	0.37187	0.0068597	40.30
52004	61.70	11.70	4.20	8.97	24.000	0.171	4.104	0.70184	0.0113585	62.20
52076	17.20	9.50	3.50	6.48	7.244	0.193	1.398	0.26975	0.0060284	34.60
52007	18.50	12.70	3.70	6.48	5.440	0.257	1.398	0.35920	0.0099305	36.40

Design and Dimensional Data for EE Ferrite Cores

The dimensional outline for EE ferrite cores is shown in Figure 3-30. Dimensional data for EE ferrite cores is given in Table 3-18; design data is given in Table 3-19.

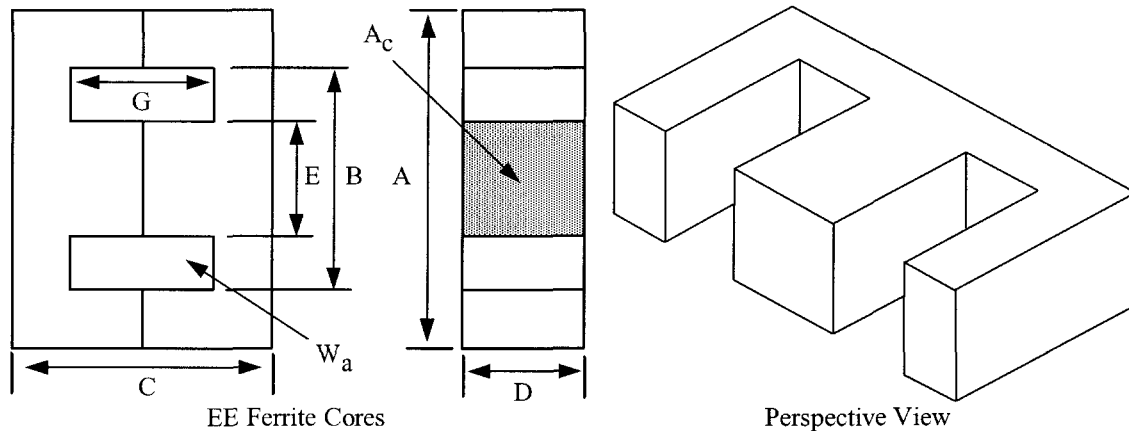


Figure 3-30. Dimension Outline for EE Ferrite Cores.

Table 3-18. Dimensional Data for EE Ferrite Cores.

EE, Ferrite Cores (Magnetics)													
Part No.	A cm	B cm	C cm	D cm	E cm	G cm	Part No.	A cm	B cm	C cm	D cm	E cm	G cm
EE-187	1.930	1.392	1.620	0.478	0.478	1.108	EE-21	4.087	2.832	3.300	1.252	1.252	2.080
EE-2425	2.515	1.880	1.906	0.653	0.610	1.250	EE-625	4.712	3.162	3.940	1.567	1.567	2.420
EE-375	3.454	2.527	2.820	0.935	0.932	1.930	EE-75	5.657	3.810	4.720	1.880	1.880	2.900

Table 3-19. Design Data for EE Ferrite Cores.

EE, Ferrite Cores (Magnetics)												
Part No.	W_{tcu} grams	W_{tfe} grams	MLT cm	MPL cm	W_a	A_c cm ²	W_a cm ²	A_p cm ⁴	K_g cm ⁵	A_t cm ²	*AL mh/1K	
					A_c							
EE-187	6.8	4.4	3.8	4.01	2.219	0.228	0.506	0.116	0.0028	14.4	500	
EE-2425	13.9	9.5	4.9	4.85	2.068	0.384	0.794	0.305	0.0095	23.5	767	
EE-375	36.4	33.0	6.6	6.94	1.875	0.821	1.539	1.264	0.0624	45.3	1167	
EE-21	47.3	57.0	8.1	7.75	1.103	1.490	1.643	2.448	0.1802	60.9	1967	
EE-625	64.4	103.0	9.4	8.90	0.808	2.390	1.930	4.616	0.4700	81.8	2767	
EE-75	111.1	179.0	11.2	10.70	0.826	3.390	2.799	9.487	1.1527	118.0	3467	

*This AL value has been normalized for a permeability of 1K. For a close approximation of AL for other values of permeability, multiply this AL value by the new permeability in kilo-perm. If the new permeability is 2500, then use 2.5.

Design and Dimensional Data for EE and EI Planar, Ferrite Cores

The dimensional outline for EE and EI planar ferrite cores is shown in Figure 3-31. Dimensional data for EE and EI planar ferrite cores is given in Table 3-20; design data is given in Table 3-21.

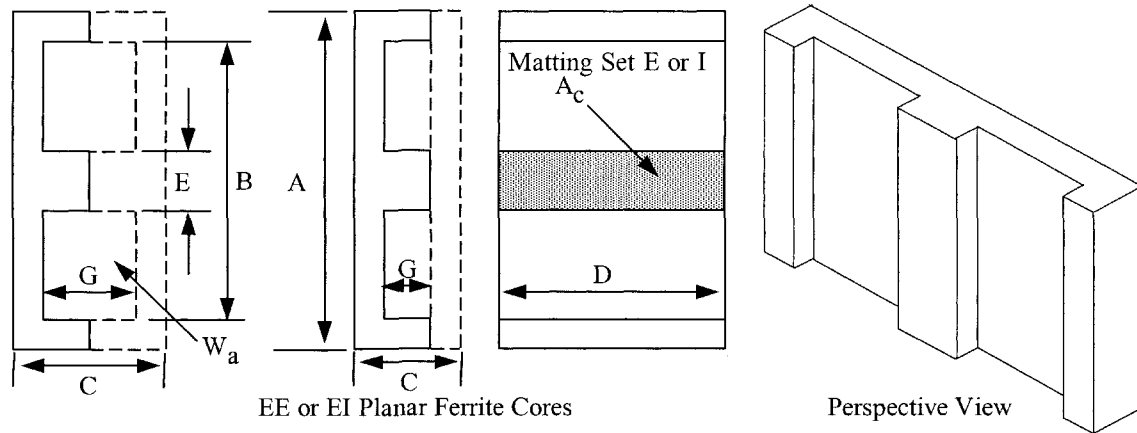


Figure 3-31. Dimension Outline for EE, EI Planar Ferrite Cores.

Table 3-20. Dimensional Data for EE, EI Planar Ferrite Cores.

EE&EI/LP, Ferrite Cores (Magnetics)													
Part No.	A cm	B cm	C cm	D cm	E cm	G cm	Part No.	A cm	B cm	C cm	D cm	E cm	G cm
EI-41805	1.800	1.370	0.638	1.000	0.398	0.188	EI-43208	3.175	2.490	0.953	2.032	0.635	0.305
EE-41805	1.800	1.370	0.796	1.000	0.398	0.376	EE-43208	3.175	2.490	1.270	2.032	0.635	0.610
EI-42216	2.160	1.610	0.867	1.590	0.508	0.297	EI-44310	4.318	3.440	1.395	2.790	0.813	0.533
EE-42216	2.160	1.610	1.144	1.590	0.508	0.610	EE-44310	4.318	3.440	1.906	2.790	0.813	1.066

Table 3-21. Design Data for EE, EI Planar Ferrite Cores.

EE&EI/LP, Ferrite Cores (Magnetics)												
Part No.	W _{tcu} grams	W _{tfc} grams	MLT cm	MPL cm	W _a		A _c cm ²	W _a cm ²	A _p cm ⁴	K _g cm ⁵	A _t cm ²	*AL mh/1K
					W _a	A _c						
EI-41805	1.5	4.1	4.7	2.03	0.2269	0.401	0.091	0.0366	0.00124	10.4	1737	
EE-41805	3.1	4.9	4.7	2.42	0.4564	0.401	0.183	0.0715	0.00248	11.6	1460	
EI-42216	3.8	10.4	6.5	2.58	0.2035	0.806	0.164	0.1319	0.00651	17.8	2592	
EE-42216	7.8	13.0	6.5	3.21	0.4169	0.806	0.336	0.2709	0.01337	20.5	2083	
EI-43208	8.9	22.0	8.9	3.54	0.224	1.290	0.289	0.3649	0.02126	33.4	3438	
EE-43208	17.8	26.0	8.9	4.17	0.4388	1.290	0.566	0.7299	0.04253	37.9	2915	
EI-44310	29.7	58.0	11.9	5.06	0.3084	2.270	0.700	1.5892	0.12085	65.4	4267	
EE-44310	59.4	70.8	11.9	6.15	0.6167	2.270	1.400	3.1784	0.24170	75.3	3483	

*This AL value has been normalized for a permeability of 1K. For a close approximation of AL for other values of permeability, multiply this AL value by the new permeability in kilo-perm. If the new permeability is 2500, then use 2.5.

Design and Dimensional Data for EC, Ferrite Cores

The dimensional outline for EC ferrite cores is shown in Figure 3-32. Dimensional data for EC ferrite cores is given in Table 3-22; design data is given in Table 3-23.

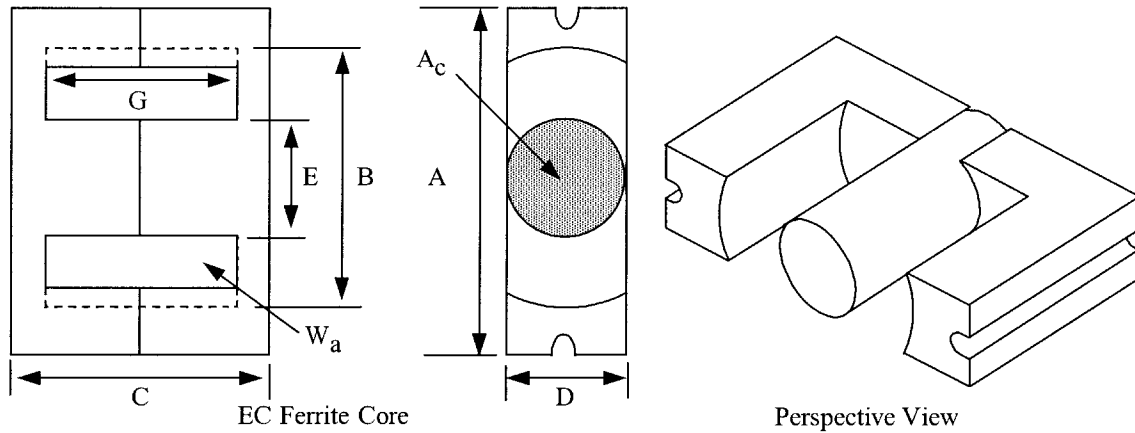


Figure 3-32. Dimension Outline for EC Ferrite Cores.

Table 3-22. Dimensional Data for EC Ferrite Cores.

EC, Ferrite Cores (Magnetics)						
Part No.	A cm	B cm	C cm	D cm	E cm	G cm
EC-35	3.450	2.270	3.460	0.950	0.950	2.380
EC-41	4.060	2.705	3.901	1.161	1.161	2.697
EC-52	5.220	3.302	4.841	1.340	1.340	3.099
EC-70	7.000	4.450	6.900	1.638	1.638	4.465

Table 3-23. Design Data for EC Ferrite Cores.

EC, Ferrite Cores (Magnetics)											
Part No.	W_{tcu} grams	W_{tfc} grams	MLT cm	MPL cm	W_a	A_c	W_a	A_p	K_g cm ⁵	A_t cm ²	*AL mh/1K
					A_c	cm ²	cm ²	cm ⁴			
EC-35	35.1	36.0	6.3	7.59	2.213	0.710	1.571	1.115	0.050	50.2	1000
EC-41	55.4	52.0	7.5	8.76	1.964	1.060	2.082	2.207	0.125	67.6	1233
EC-52	97.8	111.0	9.0	10.30	2.156	1.410	3.040	4.287	0.267	106.5	1680
EC-70	256.7	253.0	11.7	14.10	2.927	2.110	6.177	13.034	0.941	201.7	1920

*This AL value has been normalized for a permeability of 1K. For a close approximation of AL for other values of permeability, multiply this AL value by the new permeability in kilo-perm. If the new permeability is 2500, then use 2.5.

Design and Dimensional Data for ETD, Ferrite Cores

The dimensional outline for ETD ferrite cores is shown in Figure 3-33. Dimensional data for ETD ferrite cores is given in Table 3-24; design data is given in Table 3-25.

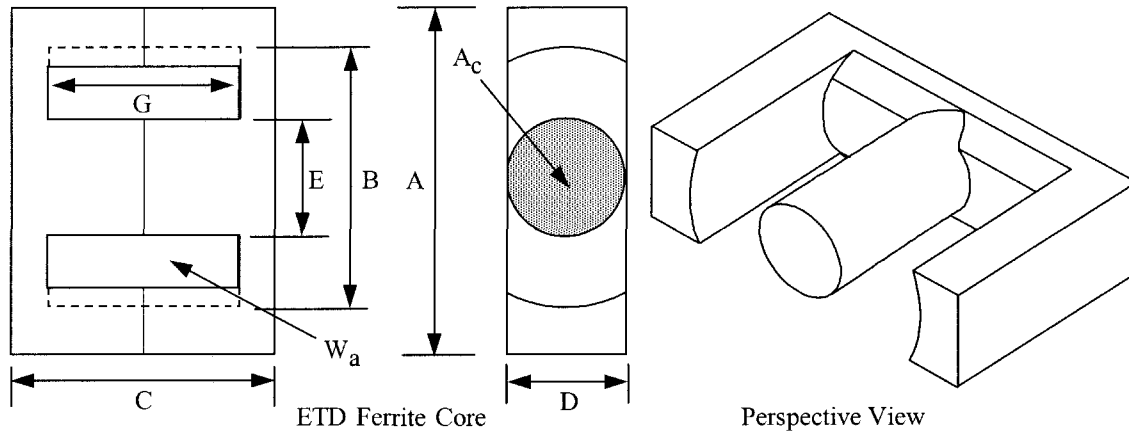


Figure 3-33. Dimension Outline for ETD Ferrite Cores.

Table 3-24. Dimensional Data for ETD Ferrite Cores.

ETD, Ferrite Cores (Ferrocube)													
Part No.	A cm	B cm	C cm	D cm	E cm	G cm	Part No.	A cm	B cm	C cm	D cm	E cm	G cm
ETD-29	3.060	2.270	3.160	0.980	0.980	2.200	ETD-49	4.980	3.610	4.940	1.670	1.670	3.540
ETD-34	3.500	2.560	3.460	1.110	1.110	2.360	ETD-54	5.450	4.120	5.520	1.890	1.890	4.040
ETD-39	4.000	2.930	3.960	1.280	1.280	2.840	ETD-59	5.980	4.470	6.200	2.165	2.165	4.500
ETD-44	4.500	3.250	4.460	1.520	1.520	3.220							

Table 3-25. Design Data for ETD Ferrite Cores.

ETD, Ferrite Cores (Ferrocube)												
Part No.	W _{tcu} grams	W _{tfc} grams	MLT cm	MPL cm	W _a	A _c cm ²	W _a cm ²	A _p cm ⁴	K _R cm ⁵	A _t cm ²	*AL mh/1K	
					A _c							
ETD-29	32.1	28.0	6.4	7.20	1.865	0.761	1.419	1.0800	0.0517	42.5	1000	
ETD-34	43.4	40.0	7.1	7.87	1.757	0.974	1.711	1.6665	0.0911	53.4	1182	
ETD-39	69.3	60.0	8.3	9.22	1.871	1.252	2.343	2.9330	0.1766	69.9	1318	
ETD-44	93.2	94.0	9.4	10.30	1.599	1.742	2.785	4.8520	0.3595	87.9	1682	
ETD-49	126.2	124.0	10.3	11.40	1.627	2.110	3.434	7.2453	0.5917	107.9	1909	
ETD-54	186.9	180.0	11.7	12.70	1.609	2.800	4.505	12.6129	1.2104	133.7	2273	
ETD-59	237.7	260.0	12.9	13.90	1.410	3.677	5.186	19.0698	2.1271	163.1	2727	

*This AL value has been normalized for a permeability of 1K. For a close approximation of AL for other values of permeability, multiply this AL value by the new permeability in kilo-perm. If the new permeability is 2500, then use 2.5.

Design and Dimensional Data for ETD/(low profile), Ferrite Cores

The dimensional outline for ETD/lp low profile ferrite cores is shown in Figure 3-34. Dimensional data for ETD/lp low profile ferrite cores is given in Table 3-26; design data is given in Table 3-27.

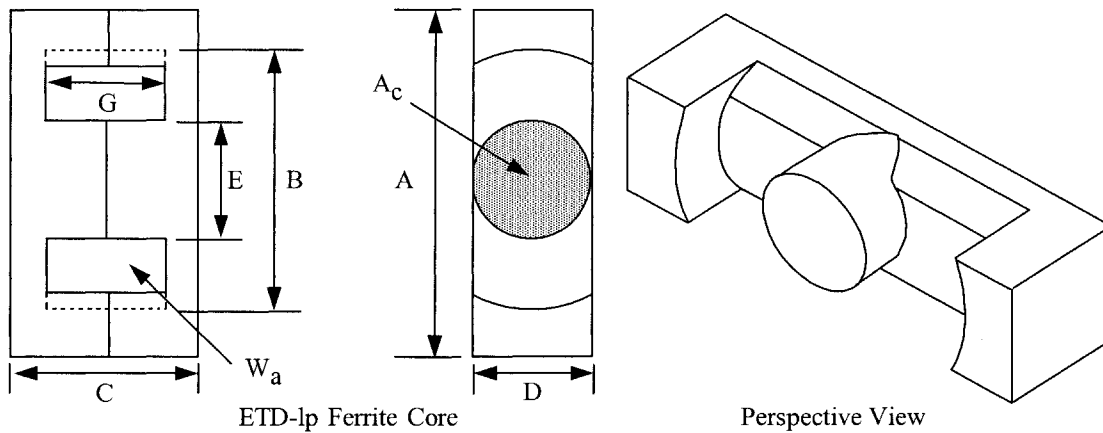


Figure 3-34. Dimension Outline for ETD/lp Ferrite Cores.

Table 3-26. Dimensional Data for ETD/lp Ferrite Cores.

ETD/lp, Ferrite Cores (TSC Ferrite International)						
Part No.	A cm	B cm	C cm	D cm	E cm	G cm
ETD34(lp)	3.421	2.631	1.804	1.080	1.080	0.762
ETD39(lp)	3.909	3.010	1.798	1.250	1.250	0.762
ETD44(lp)	4.399	3.330	1.920	1.481	1.481	0.762
ETD49(lp)	4.869	3.701	2.082	1.631	1.631	0.762

Table 3-27. Design Data for ETD/lp Ferrite Cores.

ETD/lp, Ferrite Cores (TSC Ferrite International)											
Part No.	W _{icu} grams	W _{tfe} grams	MLT cm	MPL cm	W _a	A _c cm ²	W _a cm ²	A _p cm ⁴	K _g cm ⁵	A _t cm ²	*AL mh/1K
					A _c						
ETD34(lp)	15.1	32.7	7.2	4.65	0.609	0.970	0.591	0.5732	0.0310	33.1	2382
ETD39(lp)	20.0	46.3	8.4	5.03	0.559	1.200	0.671	0.8047	0.0461	39.6	2838
ETD44(lp)	24.6	72.1	9.5	5.40	0.420	1.730	0.727	1.2583	0.0914	48.4	3659
ETD49(lp)	29.1	95.0	10.4	5.85	0.374	2.110	0.789	1.6641	0.1353	58.2	4120

*This AL value has been normalized for a permeability of 1K. For a close approximation of AL for other values of permeability, multiply this AL value by the new permeability in kilo-perm. If the new permeability is 2500, then use 2.5.

Design and Dimensional Data for ER, Ferrite Cores

Surface Mount Device, SMD

The dimensional outline for ER ferrite cores is shown in Figure 3-35. Dimensional data for ER ferrite cores is given in Table 3-28; design data is given in Table 3-29.

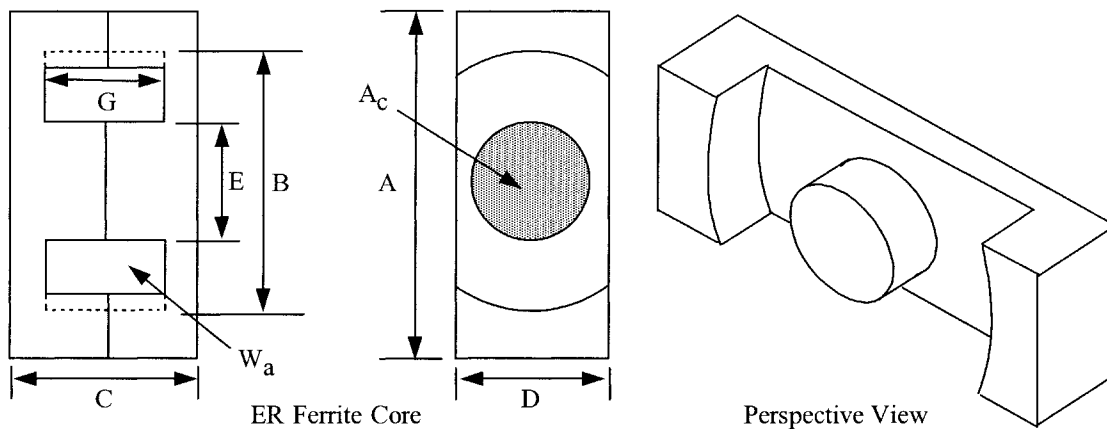


Figure 3-35. Dimension Outline for ER Ferrite Cores.

Table 3-28. Dimensional Data for ER Ferrite Cores.

ER, Ferrite Cores (Ferroxcube)													
Part No.	A cm	B cm	C cm	D cm	E cm	G cm	Part No.	A cm	B cm	C cm	D cm	E cm	G cm
ER 9.5	0.950	0.750	0.490	0.500	0.350	0.320	ER 42	4.200	3.005	4.480	1.560	1.550	3.090
ER 11	1.100	0.870	0.490	0.600	0.425	0.300	ER 48	4.800	3.800	4.220	2.100	1.800	2.940
ER 35	3.500	2.615	4.140	1.140	1.130	2.950	ER 54	5.350	4.065	3.660	1.795	1.790	2.220

Table 3-29. Design Data for ER Ferrite Cores.

ER, Ferrite Cores (Ferroxcube)											
Part No.	W _{tcu} grams	W _{tfe} grams	MLT cm	MPL cm	W _a	A _c cm ²	W _a cm ²	A _p cm ⁴	K _g cm ⁵	A _t cm ²	*AL mh/1K
					A _c						
ER 9.5	0.6	0.7	2.700	1.42	0.842	0.076	0.0640	0.00486	0.000054	3.0	435
ER 11	0.7	1.0	3.200	1.47	0.650	0.103	0.0670	0.00688	0.000090	3.7	609
ER 35	56.7	46.0	7.300	9.08	2.190	1.000	2.1900	2.19037	0.120340	62.4	1217
ER 42	72.9	96.0	9.100	9.88	1.189	1.890	2.2480	4.24867	0.352444	81.0	2000
ER 48	120.7	128.0	11.500	10.00	1.185	2.480	2.9400	7.29120	0.626245	100.1	2478
ER 54	101.9	122.0	11.400	9.18	1.052	2.400	2.5250	6.06060	0.512544	96.2	2652

*This AL value has been normalized for a permeability of 1K. For a close approximation of AL for other values of permeability, multiply this AL value by the new permeability in kilo-perm. If the new permeability is 2500, then use 2.5.

Design and Dimensional Data for EFD, Ferrite Cores

Surface Mount Device, SMD

The EFD cores, (**Economic Flat Design**), offer a significant advance in power transformer circuit miniaturization. The dimensional outline for EFD ferrite cores is shown in Figure 3-36. Dimensional data for EFD ferrite cores is given in Table 3-30; design data is given in Table 3-31.

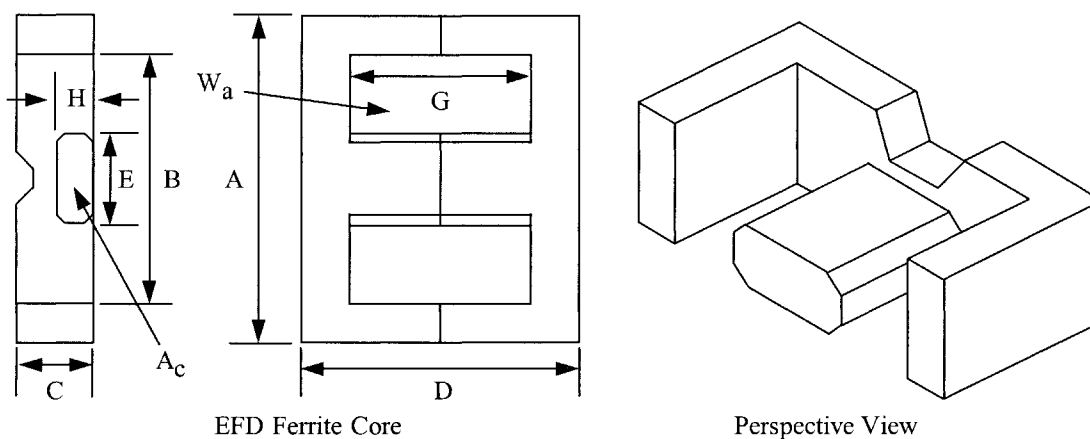


Figure 3-36. Dimension Outline for EFD Ferrite Cores.

Table 3-30. Dimensional Data for EFD Ferrite Cores.

EFD, Ferrite Cores (Ferroxcube)							
Part No.	A cm	B cm	C cm	D cm	E cm	G cm	H cm
EFD-10	1.050	0.765	0.270	1.040	0.455	0.750	0.145
EFD-15	1.500	1.100	0.465	1.500	0.530	1.100	0.240
EFD-20	2.000	1.540	0.665	2.000	0.890	1.540	0.360
EFD-25	2.500	1.870	0.910	2.500	1.140	1.860	0.520
EFD-30	3.000	2.240	0.910	3.000	1.460	2.240	0.490

Table 3-31. Design Data for EFD Ferrite Cores.

EFD, Ferrite Cores (Ferroxcube)											
Part No.	W_{icu} grams	W_{tfe} grams	MLT cm	MPL cm	W_a	A_c cm ²	W_a cm ²	A_p cm ⁴	K_g cm ⁵	A_t cm ²	*AL mh/1K
					A_c						
EFD-10	0.8	0.90	1.8	2.37	1.611	0.072	0.116	0.00837	0.00013	3.3	254
EFD-15	3.0	2.80	2.7	3.40	2.093	0.150	0.314	0.04703	0.00105	7.3	413
EFD-20	6.8	7.00	3.8	4.70	1.616	0.310	0.501	0.15516	0.00506	13.3	565
EFD-25	11.5	16.00	4.8	5.70	1.171	0.580	0.679	0.39376	0.01911	21.6	957
EFD-30	17.0	24.00	5.5	6.80	1.267	0.690	0.874	0.60278	0.03047	28.9	913

*This AL value has been normalized for a permeability of 1K. For a close approximation of AL for other values of permeability, multiply this AL value by the new permeability in kilo-perm. If the new permeability is 2500, then use 2.5.

Design and Dimensional Data for EPC, Ferrite Cores

Surface Mount Device, SMD

The dimensional outline for EPC ferrite cores is shown in Figure 3-37. Dimensional data for EPC ferrite cores is given in Table 3-32; design data is given in Table 3-33.

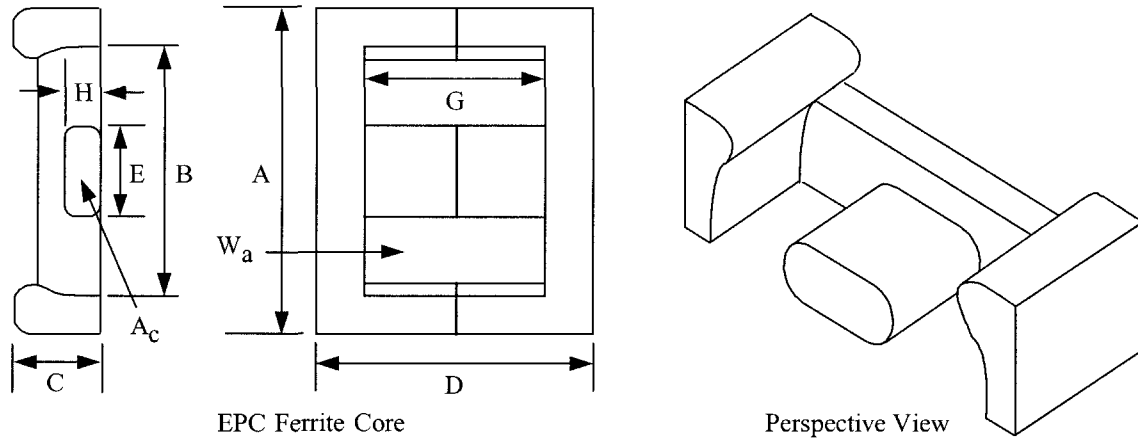


Figure 3-37. Dimension Outline for EPC Ferrite Cores.

Table 3-32. Dimensional Data for EPC Ferrite Cores.

EPC, Ferrite Cores (TDK)							
Part No.	A cm	B cm	C cm	D cm	E cm	G cm	H cm
EPC-10	1.020	0.760	0.340	0.810	0.500	0.530	0.190
EPC-13	1.325	1.050	0.460	1.320	0.560	0.900	0.205
EPC-17	1.760	1.430	0.600	1.710	0.770	1.210	0.280
EPC-19	1.910	1.580	0.600	1.950	0.850	1.450	0.250
EPC-25	2.510	2.040	0.800	2.500	1.150	1.800	0.400
EPC-27	2.710	2.160	0.800	3.200	1.300	2.400	0.400
EPC-30	3.010	2.360	0.800	3.500	1.500	2.600	0.400

Table 3-33. Design Data for EPC Ferrite Cores.

EPC, Ferrite Cores (TDK)												
Part No.	W_{icu} grams	W_{tfe} grams	MLT cm	MPL cm	W_a		A_c cm ²	W_a cm ²	A_p cm ⁴	K_g cm ⁵	A_t cm ²	*AL mh/1K
					A_c							
EPC-10	0.5	1.1	1.9	1.78	0.735	0.094	0.069	0.00647	0.000128	2.9	416	
EPC-13	2.0	2.1	2.5	3.06	1.768	0.125	0.221	0.02756	0.000549	5.9	363	
EPC-17	4.9	4.5	3.4	4.02	1.750	0.228	0.399	0.09104	0.002428	10.2	479	
EPC-19	6.9	5.3	3.7	4.61	2.330	0.227	0.529	0.12014	0.002981	12.1	392	
EPC-25	14.8	13.0	5.0	5.92	1.804	0.464	0.837	0.38837	0.014532	20.6	650	
EPC-27	18.8	18.0	5.1	7.31	1.890	0.546	1.032	0.56347	0.024036	26.8	642	
EPC-30	21.9	23.0	5.5	8.16	1.833	0.610	1.118	0.68198	0.030145	31.5	654	

*This AL value has been normalized for a permeability of 1K. For a close approximation of AL for other values of permeability, multiply this AL value by the new permeability in kilo-perm. If the new permeability is 2500, then use 2.5.

Design and Dimensional Data for PC, Ferrite Cores

The dimensional outline for PC ferrite pot cores is shown in Figure 3-38. Dimensional data for PC ferrite pot cores is given in Table 3-34; design data is given in Table 3-35.

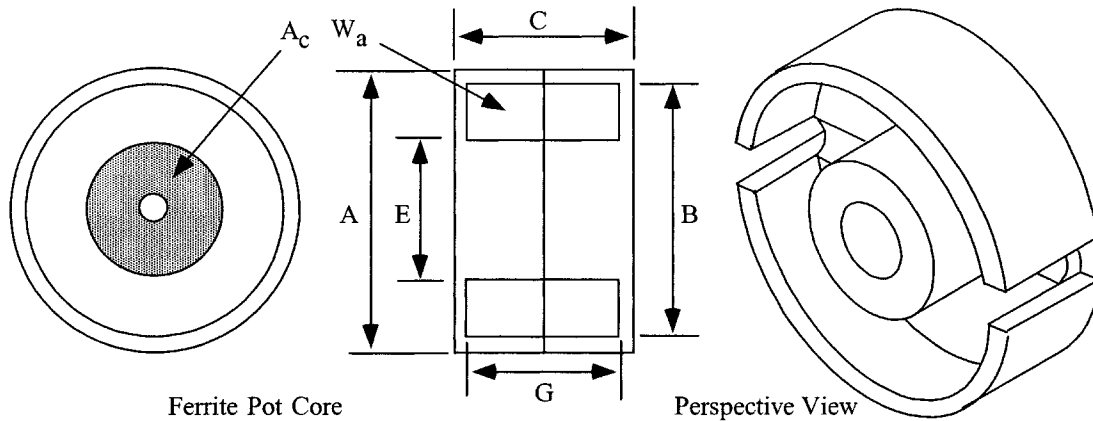


Figure 3-38. Dimension Outline for PC Ferrite Cores.

Table 3-34. Dimensional Data for PC Ferrite Cores.

PC, Ferrite Cores (Magnetics)											
Part No.	A cm	B cm	C cm	E cm	G cm	Part Number	A cm	B cm	C cm	E cm	G cm
PC-40905	0.914	0.749	0.526	0.388	0.361	PC-42616	2.550	2.121	1.610	1.148	1.102
PC-41408	1.400	1.160	0.848	0.599	0.559	PC-43019	3.000	2.500	1.880	1.350	1.300
PC-41811	1.800	1.498	1.067	0.759	0.720	PC-43622	3.560	2.990	2.200	1.610	1.460
PC-42213	2.160	1.790	1.340	0.940	0.920	PC-44229	4.240	3.560	2.960	1.770	2.040

Table 3-35. Design Data for PC Ferrite Cores.

PC, Ferrite Cores (Magnetics)											
Part No.	W _{tcu} grams	W _{tfe} grams	MLT cm	MPL cm	W _a	A _c	W _a	A _p	K _g	A _t	*AL
					A _c	cm ²	cm ²	cm ⁴	cm ⁵	cm ²	mh/1K
PC-40905	0.5	1.0	1.9	1.25	0.650	0.100	0.065	0.00652	0.000134	2.8	455
PC-41408	1.6	3.2	2.9	1.97	0.631	0.249	0.157	0.03904	0.001331	6.8	933
PC-41811	3.5	7.3	3.7	2.59	0.620	0.429	0.266	0.11413	0.005287	11.1	1333
PC-42213	6.2	13.0	4.4	3.12	0.612	0.639	0.391	0.24985	0.014360	16.4	1633
PC-42616	10.1	20.0	5.3	3.76	0.576	0.931	0.536	0.49913	0.035114	23.1	2116
PC-43019	16.7	34.0	6.3	4.50	0.550	1.360	0.748	0.97175	0.080408	31.9	2700
PC-43622	26.7	57.0	7.5	5.29	0.499	2.020	1.007	2.03495	0.220347	44.5	3400
PC-44229	55.9	104.0	8.6	6.85	0.686	2.660	1.826	4.85663	0.600289	67.7	4000

*This AL value has been normalized for a permeability of 1K. For a close approximation of AL for other values of permeability, multiply this AL value by the new permeability in kilo-perm. If the new permeability is 2500, then use 2.5.

Design and Dimensional Data for EP, Ferrite Cores

The EP ferrite cores are typically used in transformer applications. The shape of the assembly is almost cubical, allowing high package densities on the PCB. The dimensional outline for EP ferrite cores is shown in Figure 3-39. Dimensional data for EP ferrite cores is given in Table 3-36; design data is given in Table 3-37.

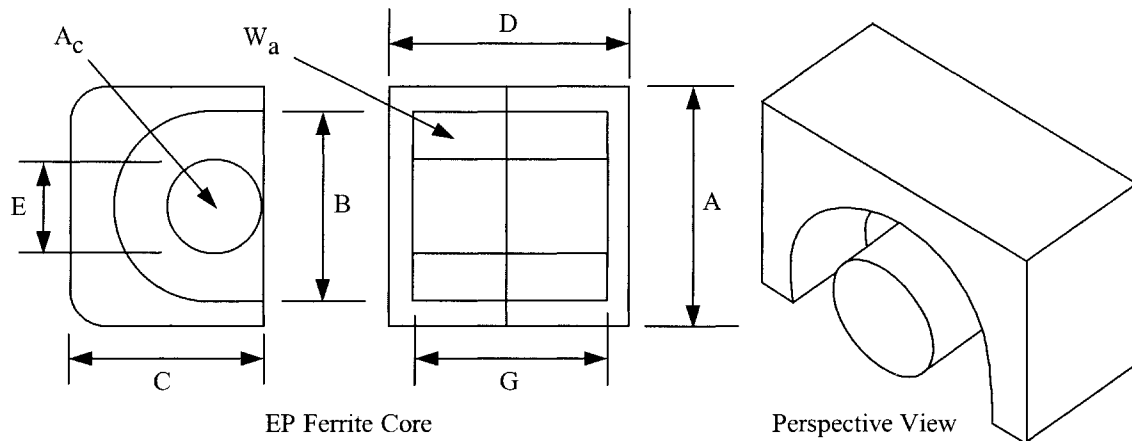


Figure 3-39. Dimension Outline for EP Ferrite Cores.

Table 3-36. Dimensional Data for EP Ferrite Cores.

EP, Ferrite Cores (Magnetics)						
Part No.	A cm	B cm	C cm	D cm	E cm	G cm
EP-07	0.920	0.720	0.635	0.740	0.340	0.500
EP-10	1.150	0.920	0.760	1.030	0.345	0.720
EP-13	1.250	0.972	0.880	1.290	0.452	0.899
EP-17	1.798	1.160	1.100	1.680	0.584	1.118
EP-20	2.400	1.610	1.495	2.139	0.899	1.397

Table 3-37. Design Data for EP Ferrite Cores.

EP, Ferrite Cores (Magnetics)											
Part No.	W_{tcu} grams	W_{tfe} grams	MLT cm	MPL cm	W_a	A_c cm ²	W_a cm ²	A_p cm ⁴	K_g cm ⁵	A_t cm ²	*AL mh/1K
					A_c						
EP-07	1.4	1.4	1.8	1.57	0.922	0.103	0.095	0.00979	0.00022	3.5	413
EP-10	1.6	2.8	2.1	1.92	1.832	0.113	0.207	0.02339	0.00049	5.7	400
EP-13	2.0	5.1	2.4	2.42	1.200	0.195	0.234	0.04558	0.00148	7.7	667
EP-17	11.6	11.6	2.9	2.85	0.950	0.339	0.322	0.10915	0.00510	13.7	1033
EP-20	7.4	27.6	4.2	3.98	0.637	0.780	0.497	0.38737	0.02892	23.8	1667

*This AL value has been normalized for a permeability of 1K. For a close approximation of AL for other values of permeability, multiply this AL value by the new permeability in kilo-perm. If the new permeability is 2500, then use 2.5.

Design and Dimensional Data for PQ, Ferrite Cores

The PQ ferrite cores, (Power Quality), feature round center legs with rather small cross-sections. The dimensional outline for PQ ferrite cores is shown in Figure 3-40. Dimensional data for PQ ferrite cores is given in Table 3-38; design data is given in Table 3-39.

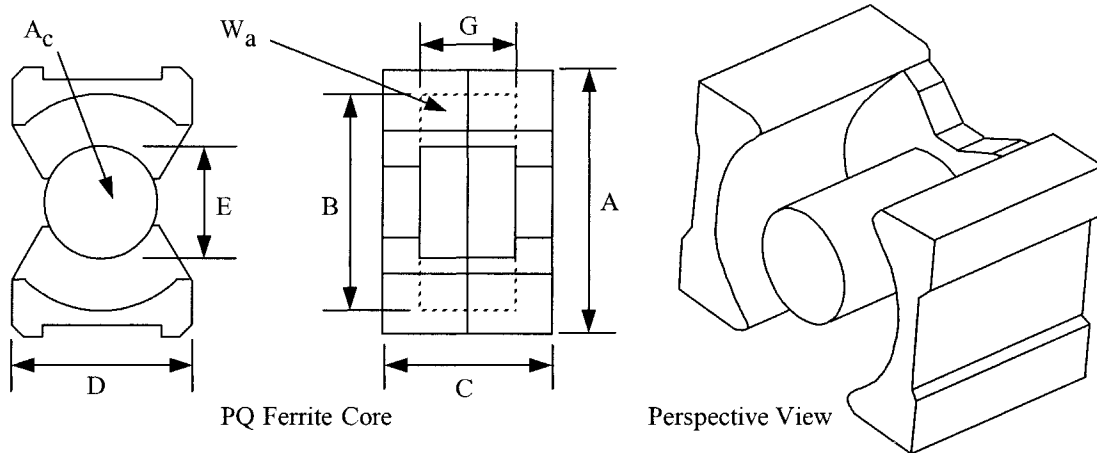


Figure 3-40. Dimension Outline for PQ Ferrite Cores.

Table 3-38. Dimensional Data for PQ Ferrite Cores.

PQ, Ferrite Cores (TDK)													
Part No.	A cm	B cm	C cm	D cm	E cm	G cm	Part No.	A cm	B cm	C cm	D cm	E cm	G cm
PQ20/16	2.050	1.800	1.620	1.400	0.880	1.030	PQ32/30	3.200	2.750	3.035	2.200	1.345	2.130
PQ20/20	2.050	1.800	2.020	1.400	0.880	1.430	PQ35/35	3.510	3.200	3.475	2.600	1.435	2.500
PQ26/20	2.650	2.250	2.015	1.900	1.200	1.150	PQ40/40	4.050	3.700	3.975	2.800	1.490	2.950
PQ26/25	2.650	2.250	2.475	1.900	1.200	1.610	PQ50/50	5.000	4.400	4.995	3.200	2.000	3.610
PQ32/20	3.200	2.750	2.055	2.200	1.345	1.150							

Table 3-39. Design Data for PQ Ferrite Cores.

PQ, Ferrite Cores (TDK)												
Part No.	W _{teu} grams	W _{tfe} grams	MLT cm	MPL cm	W _a	A _c	W _a cm ²	A _p cm ⁴	K _r cm ⁵	A _t cm ²	*AL mh/1K	
					A _c	cm ²						
PQ20/16	7.4	13.0	4.4	3.74	0.765	0.620	0.474	0.294	0.0167	16.9	1617	
PQ20/20	10.4	15.0	4.4	4.54	1.061	0.620	0.658	0.408	0.0227	19.7	1313	
PQ26/20	31.0	31.0	5.6	4.63	0.508	1.190	0.604	0.718	0.0613	28.4	2571	
PQ26/25	17.0	36.0	5.7	5.55	0.716	1.180	0.845	0.997	0.0832	32.6	2187	
PQ32/20	18.9	42.0	6.6	5.55	0.475	1.700	0.808	1.373	0.1417	36.3	3046	
PQ32/30	35.5	55.0	6.7	7.46	0.929	1.610	1.496	2.409	0.2326	46.9	2142	
PQ35/35	59.0	73.0	7.5	8.79	1.126	1.960	2.206	4.324	0.4510	60.7	2025	
PQ40/40	97.2	95.0	8.4	10.20	1.622	2.010	3.260	6.552	0.6280	77.1	1792	
PQ50/50	158.5	195.0	10.3	11.30	1.321	3.280	4.332	14.209	1.8120	113.9	2800	

*This AL value has been normalized for a permeability of 1K. For a close approximation of AL for other values of permeability, multiply this AL value by the new permeability in kilo-perm. If the new permeability is 2500, then use 2.5.

Design and Dimensional Data for PQ/(low profile), Ferrite Cores

The PQ/lp cores are a cut down version of the standard PQ cores. The PQ/lp cores have a substantially reduced total height. The dimensional outline for PQ ferrite cores is shown in Figure 3-41. Dimensional data for PQ ferrite cores is given in Table 3-40; design data is given in Table 3-41.

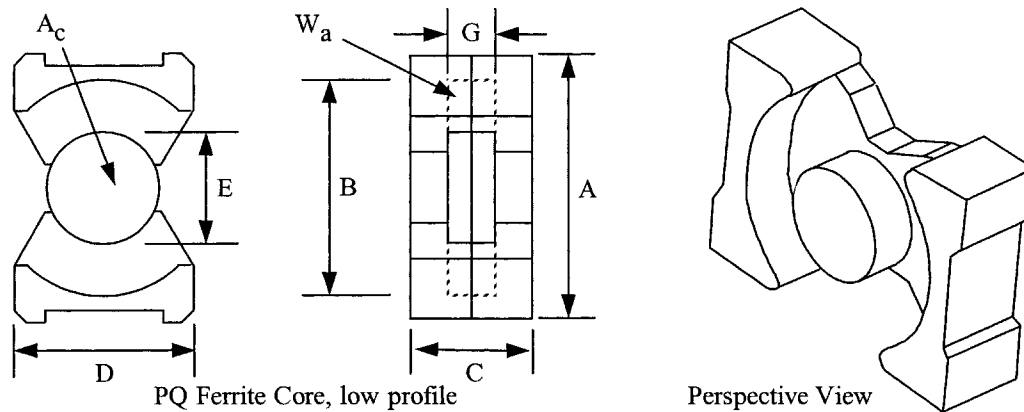


Figure 3-41. Dimension Outline for PQ/lp Ferrite Cores.

Table 3-40. Dimensional Data for PQ/lp Ferrite Cores.

PQ/lp, Ferrite Cores (Ferrite International)						
Part No.	A cm	B cm	C cm	D cm	E cm	G cm
PQ20-14-14lp	2.125	1.801	1.352	1.400	0.884	0.762
PQ26-16-14lp	2.724	2.250	1.630	1.900	1.199	0.762
PQ32-17-22lp	3.302	2.751	1.670	2.200	1.348	0.762
PQ35-17-26lp	3.612	3.200	1.738	2.601	1.435	0.762
PQ40-18-28lp	4.148	3.701	1.784	2.799	1.491	0.762

Table 3-41. Design Data for PQ/lp Ferrite Cores.

PQ/lp, Ferrite Cores (TSC Ferrite International)											
Part No.	W _{icu} grams	W _{ife} grams	MLT cm	MPL cm	W _a		W _a cm ²	A _p cm ⁴	K _g cm ⁵	A _t cm ²	*AL mh/1K
					A _c	A _c cm ²					
PQ20-14-14lp	5.4	12.5	4.4	3.2	0.563	0.620	0.349	0.217	0.0123	15.4	1948
PQ26-16-19lp	7.9	28.0	5.6	3.9	0.336	1.190	0.400	0.477	0.0407	25.4	3170
PQ32-17-22lp	12.5	39.4	6.6	4.8	0.315	1.700	0.535	0.909	0.0937	32.9	3659
PQ35-17-26lp	17.8	44.9	7.4	5.3	0.343	1.960	0.672	1.318	0.1389	40.4	3893
PQ40-18-28lp	24.9	63.5	8.3	5.8	0.419	2.010	0.842	1.692	0.1637	48.0	3850

*This AL value has been normalized for a permeability of 1K. For a close approximation of AL for other values of permeability, multiply this AL value by the new permeability in kilo-perm. If the new permeability is 2500, then use 2.5.

Design and Dimensional Data for RM, Ferrite Cores

The RM cores, (Rectangular Modular), were developed for high Printed Circuit Board, (PCB), packing densities. The dimensional outline for RM ferrite cores is shown in Figure 3-42. Dimensional data for RM ferrite cores is given in Table 3-42; design data is given in Table 3-43.

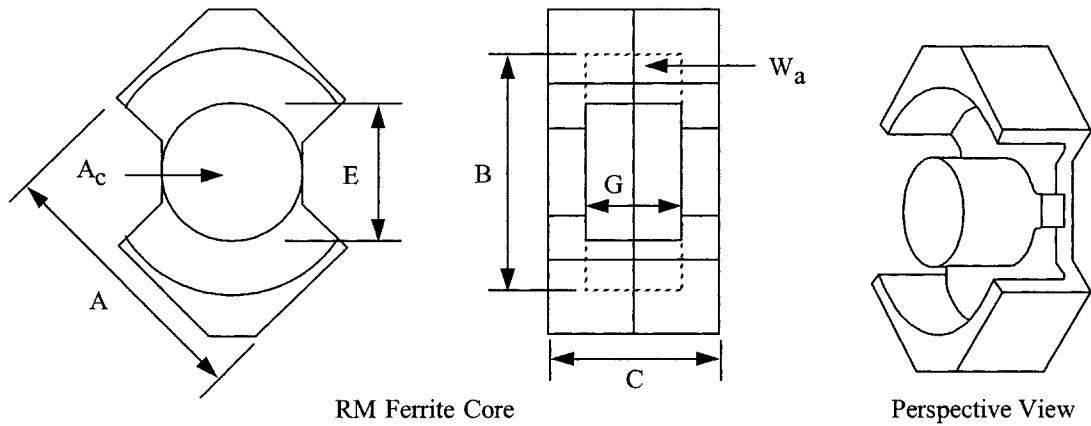


Figure 3-42. Dimension Outline for RM Ferrite Cores.

Table 3-42. Dimensional Data for RM Ferrite Cores.

RM, Ferrite Cores (TDK)											
Part No.	A cm	B cm	C cm	E cm	G cm	Part No.	A cm	B cm	C cm	E cm	G cm
RM-4	0.963	0.815	1.04	0.38	0.72	RM-10	2.415	2.165	1.86	1.07	1.27
RM-5	1.205	1.04	1.04	0.48	0.65	RM-12	2.925	2.55	2.35	1.26	1.71
RM-6	1.44	1.265	1.24	0.63	0.82	RM-14	3.42	2.95	2.88	1.47	2.11
RM-8	1.935	1.73	1.64	0.84	1.1						

Table 3-43. Design Data for RM Ferrite Cores.

RM, Ferrite Cores (TDK)												
Part No.	W _{tcu} grams	W _{tfe} grams	MLT cm	MPL cm	W _a		A _c cm ²	W _a cm ²	A _p cm ⁴	K _g cm ⁵	A _t cm ²	*AL mh/1K
					A _c	A _c						
RM-4	1.1	1.7	2.0	2.27	1.121	0.140	0.157	0.0219	0.0006	5.9	489	
RM-5	1.6	3.0	2.5	2.24	0.768	0.237	0.182	0.0431	0.0016	7.9	869	
RM-6	2.9	5.5	3.1	2.86	0.710	0.366	0.260	0.0953	0.0044	11.3	1130	
RM-8	7.3	13.0	4.2	3.80	0.766	0.640	0.490	0.3133	0.0191	20.2	1233	
RM-10	13.2	23.0	5.3	4.40	0.709	0.980	0.695	0.6814	0.0502	29.6	1833	
RM-12	24.4	42.0	6.2	5.69	0.788	1.400	1.103	1.5440	0.1389	44.6	2434	
RM-14	39.9	70.0	7.2	6.90	0.830	1.880	1.561	2.7790	0.2755	62.8	2869	

*This AL value has been normalized for a permeability of 1K. For a close approximation of AL for other values of permeability, multiply this AL value by the new permeability in kilo-perm. If the new permeability is 2500, then use 2.5.

Design and Dimensional Data for RM/(low profile), Ferrite Cores

Surface Mount Device, SMD

The RM/lp ferrite cores are a cut down version of the standard RM cores. The dimensional outline for RM/lp ferrite cores is shown in Figure 3-43. Dimensional data for RM/lp ferrite cores is given in Table 3-44; design data is given in Table 3-45.

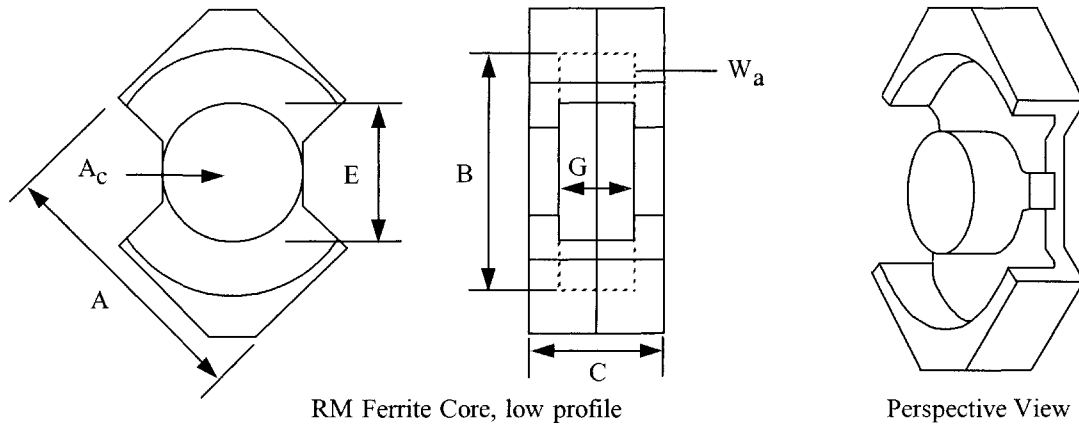


Figure 3-43. Dimension Outline for RM/lp Ferrite Cores.

Table 3-44. Dimensional Data for RM/lp Ferrite Cores.

RM/lp, Ferrite Cores (Ferroxcube)											
Part No.	A cm	B cm	C cm	E cm	G cm	Part No.	A cm	B cm	C cm	E cm	G cm
RM4/ILP	0.980	0.795	0.780	0.390	0.430	RM8/ILP	1.970	1.700	1.160	0.855	0.590
RM5/ILP	1.230	1.020	0.780	0.490	0.360	RM10/ILP	2.470	2.120	1.300	1.090	0.670
RM6S/LP	1.470	1.240	0.900	0.640	0.450	RM12/ILP	2.980	2.500	1.680	1.280	0.900
RM7/ILP	1.720	1.475	0.980	0.725	0.470	RM14/ILP	3.470	2.900	2.050	1.500	1.110

Table 3-45. Design Data for RM/lp Ferrite Cores.

RM/lp, Ferrite Cores (Ferroxcube)												
Part No.	W_{icu} grams	W_{ife} grams	MLT cm	MPL cm	W_a		A_c cm^2	W_a cm^2	A_p cm^4	K_g cm^5	A_t cm^2	AL mh/1K
					W_a	A_c						
RM4/ILP	0.6	1.5	2.0	1.73	0.770	0.113	0.087	0.00984	0.00022	5.0	609	
RM5/ILP	0.9	2.2	2.5	1.75	0.525	0.181	0.095	0.01727	0.00049	6.9	1022	
RM6S/LP	1.5	4.2	3.1	2.18	0.433	0.312	0.135	0.04212	0.00169	9.6	1380	
RM7/ILP	2.3	6.0	3.6	2.35	0.444	0.396	0.176	0.06979	0.00306	12.7	1587	
RM8/ILP	3.7	10.0	4.2	2.87	0.449	0.554	0.249	0.13810	0.00733	16.9	1783	
RM10/ILP	6.4	17.0	5.2	3.39	0.426	0.809	0.345	0.27915	0.01736	25.0	2435	
RM12/ILP	11.9	34.0	6.1	4.20	0.439	1.250	0.549	0.68625	0.05627	37.8	3087	
RM14/ILP	19.5	55.0	7.1	5.09	0.463	1.680	0.777	1.30536	0.12404	52.5	3652	

*This AL value has been normalized for a permeability of 1K. For a close approximation of AL for other values of permeability, multiply this AL value by the new permeability in kilo-perm. If the new permeability is 2500, then use 2.5.

Design and Dimensional Data for DS, Ferrite Cores

The DS ferrite cores are similar to standard Pot Cores. These cores have a large opening to bring out many strands of wire, which is convenient for high power and multiple outputs. The dimensional outline for DS ferrite cores is shown in Figure 3-44. Dimensional data for DS ferrite cores is given in Table 3-46; design data is given in Table 3-47.

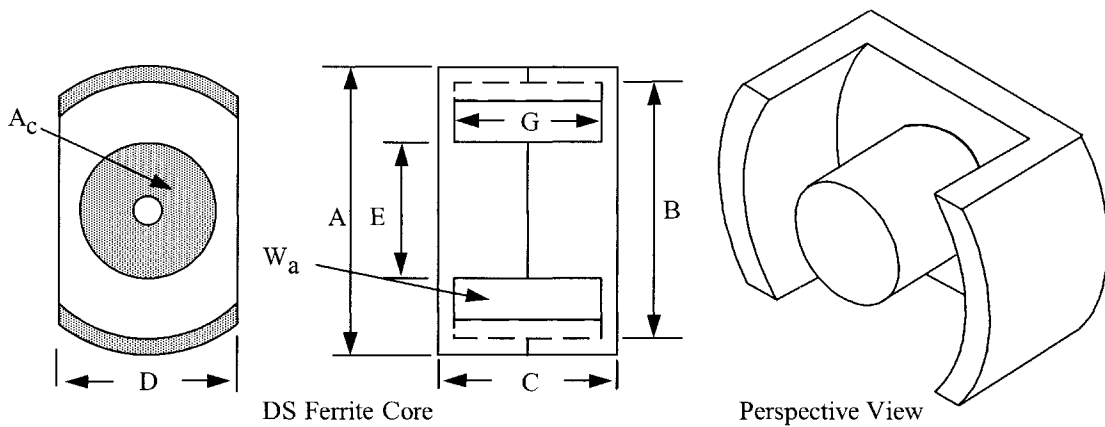


Figure 3-44. Dimension Outline for DS Ferrite Cores.

Table 3-46. Dimensional Data for DS Ferrite Cores.

DS, Ferrite Cores (Magnetics)						
Part No.	A cm	B cm	C cm	D cm	E cm	G cm
DS-42311	2.286	1.793	1.108	1.540	0.990	0.726
DS-42318	2.286	1.793	1.800	1.540	0.990	1.386
DS-42616	2.550	2.121	1.610	1.709	1.148	1.102
DS-43019	3.000	2.500	1.880	1.709	1.351	1.300
DS-43622	3.561	2.985	2.170	2.385	1.610	1.458
DS-44229	4.240	3.561	2.960	2.840	1.770	2.042

Table 3-47. Design Data for DS Ferrite Cores.

DS, Ferrite Cores (Magnetics)											
Part No.	W_{tcu} grams	W_{tfe} grams	MLT cm	MPL cm	W_a	A_c	W_a	A_p	K_g	A_t	*AL mh/1K
					A_c	cm ²	cm ²	cm ⁴	cm ⁵	cm ²	
DS-42311	4.7	10.0	4.5	2.68	0.770	0.378	0.291	0.110	0.00368	16.2	1487
DS-42318	9.1	13.0	4.6	3.99	1.366	0.407	0.556	0.227	0.00800	21.1	1267
DS-42616	10.1	15.0	5.3	3.89	0.855	0.627	0.536	0.336	0.01593	23.1	1667
DS-43019	16.7	22.0	6.3	4.62	0.778	0.960	0.747	0.717	0.04380	31.9	1933
DS-43622	26.6	37.0	7.5	5.28	0.802	1.250	1.002	1.253	0.08404	44.2	2333
DS-44229	56.0	78.0	8.6	7.17	1.028	1.780	1.829	3.255	0.26917	67.7	2800

*This AL value has been normalized for a permeability of 1K. For a close approximation of AL for other values of permeability, multiply this AL value by the new permeability in kilo-perm. If the new permeability is 2500, then use 2.5.

Design and Dimensional Data for UUR, Ferrite Cores

The UUR ferrite cores feature round legs with rather small cross sections. The round legs allow easy winding with either wire or foil. U cores are used for power, pulse and high-voltage transformers. The dimensional outline for UUR ferrite cores is shown in Figure 3-45. Dimensional data for UUR ferrite cores is given in Table 3-48; design data is given in Table 3-49.

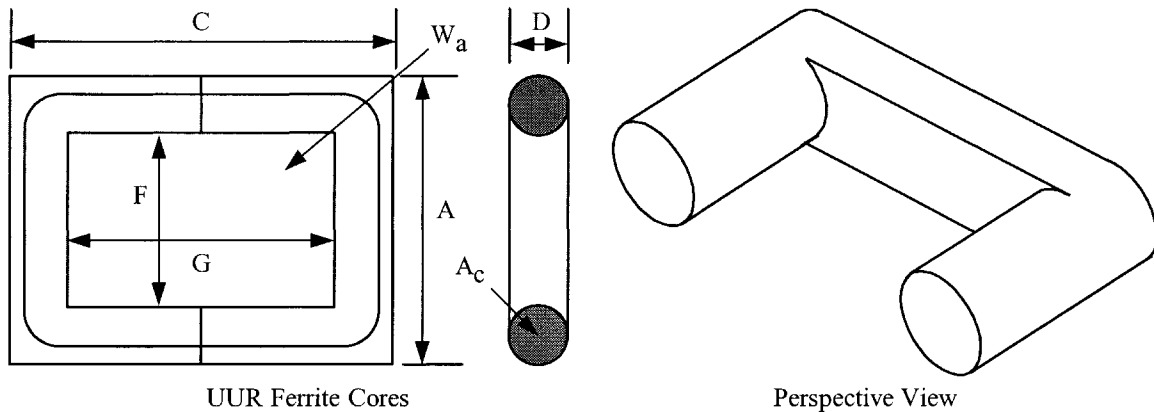


Figure 3-45. Dimension Outline for UUR Ferrite Cores.

Table 3-48. Dimensional Data for UUR Ferrite Cores.

UUR, Ferrite Cores (Magnetics)					
Part No.	A cm	C cm	D cm	F cm	G cm
UUR-44121	4.196	4.120	1.170	1.910	2.180
UUR-44119	4.196	4.180	1.170	1.910	2.680
UUR-44125	4.196	5.080	1.170	1.910	3.140
UUR-44130	4.196	6.100	1.170	1.910	4.160

Table 3-49. Design Data for UUR Ferrite Cores.

UUR, Ferrite Cores (Magnetics)												
Part No.	W _{tcu} grams	W _{tfc} grams	MLT cm	MPL cm	W _a		A _c cm ²	W _a cm ²	A _p cm ⁴	K _g cm ⁵	A _t cm ²	*AL mh/1K
					A _c	A _c						
UUR-44121	119.0	55.0	8.0	11.3	4.215	0.988	4.164	4.114	0.202	98.5	616	
UUR-44119	146.2	54.0	8.0	12.1	5.619	0.911	5.119	4.663	0.211	102.9	710	
UUR-44125	171.3	64.0	8.0	13.3	6.070	0.988	5.997	5.925	0.291	116.1	702	
UUR-44130	227.0	75.0	8.0	15.3	8.043	0.988	7.946	7.850	0.386	134.9	610	

*This AL value has been normalized for a permeability of 1K. For a close approximation of AL for other values of permeability, multiply this AL value by the new permeability in kilo-perm. If the new permeability is 2500, then use 2.5.

Design and Dimensional Data for UUS, Ferrite Cores

The UUS ferrite cores feature square or rectangular legs. U cores are used for power, pulse and high-voltage transformers. The dimensional outline for UUS ferrite cores is shown in Figure 3-46. Dimensional data for UUS ferrite cores is given in Table 3-50; design data is given in Table 3-51.

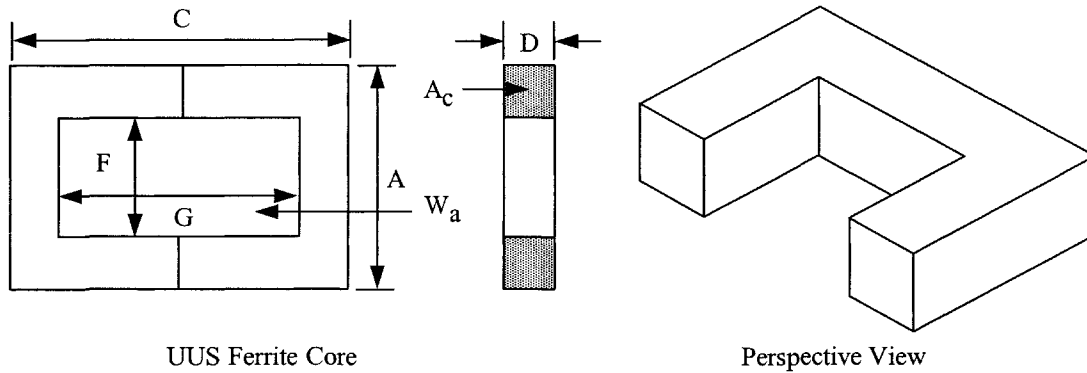


Figure 3-46. Dimension Outline for UUS Ferrite Cores.

Table 3-50. Dimensional Data for UUS Ferrite Cores.

UUS, Ferrite Cores (Ferroxcube)					
Part No.	A cm	C cm	D cm	F cm	G cm
U10-08-03	1.000	1.640	0.290	0.435	1.000
U20-16-07	2.080	3.120	0.750	0.640	1.660
U25-20-13	2.480	3.920	1.270	0.840	2.280
U30-25-16	3.130	5.060	1.600	1.050	2.980
U67-27-14	6.730	5.400	1.430	3.880	2.540
U93-76-16	9.300	15.200	1.600	3.620	9.600

Table 3-51. Design Data for UUS Ferrite Cores.

UUS, Ferrite Cores (Ferroxcube)												
Part No.	W _{tcu} grams	W _{tfe} grams	MLT cm	MPL cm	W _a		A _c cm ²	W _a cm ²	A _p cm ⁴	K _g cm ⁵	A _t cm ²	*AL mh/1K
					A _c	A _c						
U10-08-03	3.5	1.8	2.2	3.8	5.370	0.081	0.435	0.0352	0.000510	8.1	213	
U20-16-07	16.4	19.0	4.4	6.8	1.896	0.560	1.062	0.5949	0.030661	29.5	826	
U25-20-13	41.6	47.0	6.1	8.8	1.841	1.040	1.915	1.9920	0.135669	51.1	1261	
U30-25-16	83.9	86.0	7.5	11.1	1.943	1.610	3.129	5.0380	0.430427	82.5	1609	
U67-27-14	435.0	170.0	12.4	17.3	4.831	2.040	9.855	20.1050	1.321661	240.2	1652	
U93-76-16	1875.2	800.0	15.2	35.4	7.757	4.480	34.752	155.6890	18.386023	605.3	1478	

*This AL value has been normalized for a permeability of 1K. For a close approximation of AL for other values of permeability, multiply this AL value by the new permeability in kilo-perm. If the new permeability is 2500, then use 2.5.

Design and Dimensional Data for Toroidal, Ferrite Cores

The toroidal ferrite core has the best possible shape from the magnetic point of view. The magnetic flux path is completely enclosed within the magnetic structure. The toroidal structure fully exploits the capabilities of a ferrite material. The dimensional outline for toroidal ferrite cores is shown in Figure 3-47. Dimensional data for toroidal ferrite cores is given in Table 3-52; design data is given in Table 3-53.

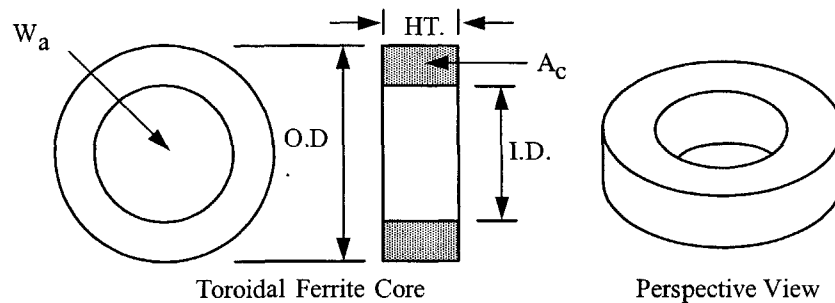


Figure 3-47. Dimension Outline for Toroidal Ferrite Cores.

Table 3-52. Dimensional Data for Toroidal Ferrite Cores.

Toroidal, Ferrite Z Coated Cores (Magnetics)							
Part No.	OD cm	ID cm	HT cm	Part No.	OD cm	ID cm	HT cm
TC-40907	1.016	0.495	0.768	TC-42206	2.286	1.295	0.691
TC-41005	1.016	0.411	0.529	TC-42908	2.990	1.811	0.806
TC-41206	1.334	0.452	0.691	TC-43806	3.925	1.790	0.691
TC-41306	1.334	0.729	0.691	TC-43610	3.689	2.212	1.065
TC-41605	1.664	0.812	0.521	TC-43813	3.925	1.790	1.334
TC-42106	2.134	1.193	0.691	TC-48613	8.738	5.389	1.334

Table 3-53. Design Data for Toroidal Ferrite Cores.

Toroidal, Ferrite Cores (Magnetics)												
Part No.	W _{icu} grams	W _{tfc} grams	MLT cm	MPL cm	W _a		A _c cm ²	W _a cm ²	A _p cm ⁴	K _r cm ⁵	A _t cm ²	*AL mh/IK
					A _c	A _c						
TC-41005	0.8	1.2	1.7	2.07	1.243	0.107	0.133	0.014196	0.000366	5.3	657	
TC-40907	1.4	1.6	2.0	2.27	1.422	0.135	0.192	0.025980	0.000687	6.6	752	
TC-41206	1.2	3.3	2.2	2.46	0.724	0.221	0.160	0.035462	0.001443	8.6	1130	
TC-41306	3.2	2.4	2.2	3.12	2.856	0.146	0.417	0.060939	0.001638	10.2	591	
TC-41605	4.0	2.8	2.2	3.68	3.386	0.153	0.518	0.079231	0.002240	12.8	548	
TC-42106	11.2	5.4	2.8	5.00	4.840	0.231	1.118	0.258216	0.008482	22.7	600	
TC-42206	13.7	6.4	2.9	5.42	5.268	0.250	1.317	0.329283	0.011221	25.8	600	
TC-42908	33.7	12.9	3.7	7.32	7.196	0.358	2.576	0.922167	0.035869	44.6	630	
TC-43806	38.0	29.4	4.2	8.97	4.006	0.628	2.516	1.580357	0.093505	61.2	878	
TC-43610	63.6	26.4	4.7	8.30	6.742	0.570	3.843	2.190456	0.107283	68.5	883	
TC-43813	47.2	51.7	5.3	8.30	2.188	1.150	2.516	2.893966	0.252394	71.0	1665	
TC-48613	740.1	203.0	9.1	21.50	12.197	1.870	22.809	42.652794	3.496437	348.0	1091	

*This AL value has been normalized for a permeability of 1K. For a close approximation of AL for other values of permeability, multiply this AL value by the new permeability in kilo-perm. If the new permeability is 2500, then use 2.5.

Design and Dimensional Data for Toroidal, MPP Powder Cores

The dimensional outline for MPP powder cores is shown in Figure 3-48. Dimensional data for MPP powder cores is given in Table 3-54; design data is given in Table 3-55. For more information, see Chapter 2.

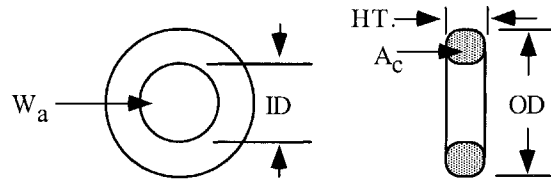


Figure 3-48. Dimension Outline for Toroidal MPP Powder Cores.

Table 3-54. Dimensional Data for Toroidal MPP Powder Cores.

MPP Powder Cores, Magnetics 60 mu (coated)											
Part No.	OD cm	ID cm	HT cm	Part No.	OD cm	ID cm	HT cm	Part No.	OD cm	ID cm	HT cm
55021	0.699	0.229	0.343	55381	1.803	0.902	0.711	55076	3.670	2.150	1.135
55281	1.029	0.427	0.381	55848	2.110	1.207	0.711	55083	4.080	2.330	1.537
55291	1.029	0.427	0.460	55059	2.360	1.334	0.838	55439	4.760	2.330	1.892
55041	1.080	0.457	0.460	55351	2.430	1.377	0.965	55090	4.760	2.790	1.613
55131	1.181	0.584	0.460	55894	2.770	1.410	1.194	55716	5.170	3.090	1.435
55051	1.346	0.699	0.551	55071	3.380	1.930	1.143	55110	5.800	3.470	1.486
55121	1.740	0.953	0.711	55586	3.520	2.260	0.978				

Table 3-55. Design Data for Toroidal MPP Powder Cores.

MPP Powder Cores, Magnetics 60 mu (coated)											
Part No.	W _{tcu} grams	W _{tfe} grams	MLT cm	MPL cm	W _a	A _c	W _a	A _p	K _g cm ⁵	A _t cm ²	AL mh/1K
					A _c	cm ²	cm ²	cm ⁴			
55021	0.10	0.553	1.10	1.36	0.723	0.047	0.034	0.001610	0.000027	2.30	24
55281	0.70	1.307	1.40	2.18	1.729	0.075	0.130	0.009757	0.000204	4.80	25
55291	0.70	1.645	1.60	2.18	1.376	0.095	0.130	0.012359	0.000301	5.10	32
55041	0.90	1.795	1.60	2.38	1.500	0.100	0.150	0.014998	0.000375	5.60	32
55131	1.50	1.993	1.70	2.69	2.759	0.091	0.250	0.022735	0.000492	6.90	26
55051	2.50	2.886	2.00	3.12	3.175	0.114	0.362	0.041279	0.000961	9.30	27
55121	6.10	6.373	2.50	4.11	3.563	0.192	0.684	0.131267	0.003985	16.00	35
55381	5.60	7.670	2.60	4.14	2.634	0.232	0.611	0.141747	0.005099	16.30	43
55848	11.10	8.836	2.80	5.09	4.898	0.226	1.107	0.250092	0.008001	22.70	32
55059	15.20	14.993	3.20	5.67	4.097	0.331	1.356	0.448857	0.018406	28.60	43
55351	17.90	18.706	3.50	5.88	3.727	0.388	1.446	0.561153	0.024969	31.40	51
55894	22.30	33.652	4.10	6.35	2.320	0.654	1.517	0.992423	0.062916	39.80	75
55071	46.20	44.086	4.50	8.15	4.263	0.672	2.865	1.925420	0.114179	58.30	61
55586	61.40	32.806	4.40	8.95	8.681	0.454	3.941	1.789128	0.074166	64.40	38
55076	60.20	48.692	4.80	8.98	5.255	0.678	3.563	2.415897	0.137877	68.00	56
55083	85.30	86.198	5.70	9.84	3.910	1.072	4.191	4.492709	0.336608	87.50	81
55439	101.90	170.140	6.80	10.74	2.106	1.990	4.191	8.340010	0.971244	112.60	135
55090	136.90	122.576	6.40	11.63	4.497	1.340	6.026	8.075211	0.677485	117.20	86
55716	169.30	132.540	6.40	12.73	5.917	1.251	7.402	9.260268	0.720435	133.10	73
55110	233.30	164.500	7.00	14.300	6.474	1.444	9.348	13.498792	1.111049	164.70	75

Design and Dimensional Data for Toroidal, Iron Powder Cores

The dimensional outline for Iron powder cores is shown in Figure 3-49. Dimensional data for Iron powder cores is given in Table 3-56; design data is given in Table 3-57. For more information, see Chapter 2.

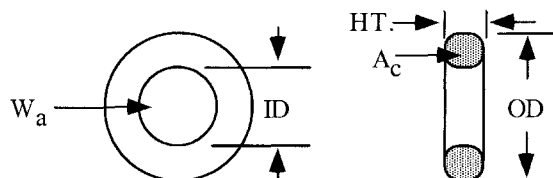


Figure 3-49. Dimension Outline for Toroidal Iron Powder Cores.

Table 3-56. Dimensional Data for Toroidal Iron Powder Cores.

Iron Powder Cores, Micrometals 75 mu (coated)											
Part No.	OD cm	ID cm	HT cm	Part No.	OD cm	ID cm	HT cm	Part No.	OD cm	ID cm	HT cm
T20-26	0.508	0.224	0.178	T50-26	1.270	0.770	0.483	T130-26	3.300	1.980	1.110
T25-26	0.648	0.305	0.244	T60-26	1.520	0.853	0.594	T132-26	3.300	1.780	1.110
T26-26	0.673	0.267	0.483	T68-26	1.750	0.940	0.483	T131-26	3.300	1.630	1.110
T30-26	0.780	0.384	0.325	T80-26	2.020	1.260	0.635	T141-26	3.590	2.240	1.050
T37-26	0.953	0.521	0.325	T94-26	2.390	1.420	0.792	T150-26	3.840	2.150	1.110
T38-26	0.953	0.445	0.483	T90-26	2.290	1.400	0.953	T175-26	4.450	2.720	1.650
T44-26	1.120	0.582	0.404	T106-26	2.690	1.450	1.110				

Table 3-57. Design Data for Toroidal Iron Powder Cores.

Iron Powder Cores, Micrometals 75 mu (coated)											
Part No.	W _{tcu} grams	W _{tfe} grams	MLT cm	MPL cm	W _a	A _c	W _a	A _p	K _g	A _t	AL
					A _c	cm ²	cm ²	cm ⁴	cm ⁵	cm ²	mh/1K
T20-26	0.10	0.19	0.70	1.15	1.713	0.023	0.039	0.000900	0.000010	1.2	18.5
T25-26	0.24	0.39	0.90	1.50	1.973	0.037	0.073	0.002700	0.000038	2.0	24.5
T26-26	0.26	0.93	1.30	1.47	0.644	0.090	0.058	0.005030	0.000130	2.6	57
T30-26	0.47	0.77	1.14	1.84	1.933	0.060	0.116	0.006940	0.000140	3.1	33.5
T37-26	0.97	1.04	1.28	2.31	3.328	0.064	0.213	0.013630	0.000270	4.5	28.5
T38-26	0.85	1.74	1.50	2.18	1.360	0.114	0.155	0.017700	0.000520	4.8	49
T44-26	1.46	1.86	1.50	2.68	2.687	0.099	0.266	0.026320	0.000670	6.2	37
T50-26	2.96	2.50	1.80	3.19	4.071	0.112	0.456	0.052120	0.001300	8.8	33
T60-26	4.40	4.89	2.20	3.74	3.053	0.187	0.571	0.106800	0.003680	12.2	50
T68-26	5.36	5.30	2.17	4.23	3.877	0.179	0.694	0.124150	0.004090	14.4	43.5
T80-26	11.66	8.31	2.63	5.14	5.394	0.231	1.246	0.287880	0.010100	21.4	46
T94-26	17.44	15.13	3.10	5.97	4.373	0.362	1.583	0.573000	0.026770	29.6	60
T90-26	18.37	15.98	3.40	5.78	3.894	0.395	1.538	0.607740	0.029600	29.4	70
T106-26	23.05	29.94	3.93	6.49	2.504	0.659	1.650	1.087660	0.072990	38.0	93
T130-26	48.33	40.46	4.40	8.28	4.408	0.698	3.077	2.148800	0.135810	56.9	81
T132-26	39.05	44.85	4.40	7.96	3.089	0.805	2.487	2.002190	0.145990	53.9	103
T131-26	32.75	47.83	4.40	7.72	2.357	0.885	2.086	1.845820	0.147960	51.7	116
T141-26	62.70	45.70	4.60	9.14	5.743	0.674	3.871	2.608887	0.154516	66.6	75
T150-26	62.55	58.24	4.85	9.38	4.091	0.887	3.629	3.218620	0.235550	71.6	96
T175-26	128.04	105.05	6.20	11.20	4.334	1.340	5.808	7.782300	0.672790	107.4	105

Design and Dimensional Data for Toroidal, Sendust Powder Cores

The dimensional outline for Sendust powder cores is shown in Figure 3-50. Dimensional data for Sendust powder cores is given in Table 3-58; design data is given in Table 3-59. For more information, see Chapter 2.

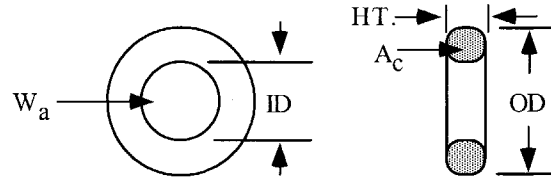


Figure 3-50. Dimension Outline for Toroidal Sendust Powder Cores.

Table 3-58. Dimensional Data for Toroidal Sendust Powder Cores.

Sendust Powder Cores, Magnetics 60 mu (coated)											
Part No.	OD cm	ID cm	HT cm	Part No.	OD cm	ID cm	HT cm	Part No.	OD cm	ID cm	HT cm
77021	0.699	0.229	0.343	77381	1.803	0.902	0.711	77076	3.670	2.150	1.135
77281	1.029	0.427	0.381	77848	2.110	1.207	0.711	77083	4.080	2.330	1.537
77291	1.029	0.427	0.460	77059	2.360	1.334	0.838	77439	4.760	2.330	1.892
77041	1.080	0.457	0.460	77351	2.430	1.377	0.965	77090	4.760	2.790	1.613
77131	1.181	0.584	0.460	77894	2.770	1.410	1.194	77716	5.170	3.090	1.435
77051	1.346	0.699	0.551	77071	3.380	1.930	1.143	77110	5.800	3.470	1.486
77121	1.740	0.953	0.711	77586	3.520	2.260	0.978				

Table 3-59. Design Data for Toroidal Sendust Powder Cores.

Sendust Powder Cores, Magnetics 60 mu (coated)											
Part No.	W _{tcu} grams	W _{tfe} grams	MLT cm	MPL cm	W _a	A _c	W _a	A _p	K _g cm ⁵	A _t cm ²	AL mh/1K
					A _c	cm ²	cm ²	cm ⁴			
77021	0.10	0.448	1.10	1.36	0.723	0.047	0.034	0.001610	0.000027	2.30	24
77281	0.70	1.148	1.40	2.18	1.729	0.075	0.130	0.009757	0.000204	4.80	25
77291	0.70	1.442	1.60	2.18	1.376	0.095	0.130	0.012359	0.000301	5.10	32
77041	0.90	1.666	1.60	2.38	1.500	0.100	0.150	0.014998	0.000375	5.60	32
77131	1.50	1.706	1.70	2.69	2.759	0.091	0.250	0.022735	0.000492	6.90	26
77051	2.50	2.490	2.00	3.12	3.175	0.114	0.362	0.041279	0.000961	9.30	27
77121	6.10	5.524	2.50	4.11	3.563	0.192	0.684	0.131267	0.003985	16.00	35
77381	5.60	6.723	2.60	4.14	2.634	0.232	0.611	0.141747	0.005099	16.30	43
77848	11.10	8.052	2.80	5.09	4.898	0.226	1.107	0.250092	0.008001	22.70	32
77059	15.20	13.137	3.20	5.67	4.097	0.331	1.356	0.448857	0.018406	28.60	43
77351	17.90	15.970	3.50	5.88	3.727	0.388	1.446	0.561153	0.024969	31.40	51
77894	22.30	29.070	4.10	6.35	2.320	0.654	1.517	0.992423	0.062916	39.80	75
77071	46.20	38.338	4.50	8.15	4.263	0.672	2.865	1.925420	0.114179	58.30	61
77586	61.40	28.443	4.40	8.95	8.681	0.454	3.941	1.789128	0.074166	64.40	38
77076	60.20	42.619	4.80	8.98	5.255	0.678	3.563	2.415897	0.137877	68.00	56
77083	85.30	73.839	5.70	9.84	3.910	1.072	4.191	4.492709	0.336608	87.50	81
77439	101.90	149.608	6.80	10.74	2.106	1.990	4.191	8.340010	0.971244	112.60	135
77090	136.90	109.089	6.40	11.63	4.497	1.340	6.026	8.075211	0.677485	117.20	86
77716	169.30	111.477	6.40	12.73	5.917	1.251	7.402	9.260268	0.720435	133.10	73
77110	233.30	144.544	7.00	14.300	6.474	1.444	9.348	13.498792	1.111049	164.70	75

Design and Dimensional Data for Toroidal, High Flux Powder Cores

The dimensional outline for High Flux powder cores is shown in Figure 3-51. Dimensional data for High Flux powder cores is given in Table 3-60; design data is given in Table 3-61. For more information, see Chapter 2.

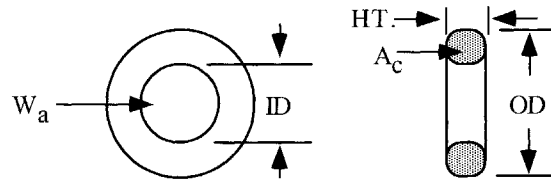


Figure 3-51. Dimension Outline for Toroidal High Flux Powder Cores.

Table 3-60. Dimensional Data for Toroidal High Flux Powder Cores.

High Flux Powder Cores, Magnetics 60 mu (coated)											
Part No.	OD cm	ID cm	HT cm	Part No.	OD cm	ID cm	HT cm	Part No.	OD cm	ID cm	HT cm
58021	0.699	0.229	0.343	58381	1.803	0.902	0.711	58076	3.670	2.150	1.135
58281	1.029	0.427	0.381	58848	2.110	1.207	0.711	58083	4.080	2.330	1.537
58291	1.029	0.427	0.460	58059	2.360	1.334	0.838	58439	4.760	2.330	1.892
58041	1.080	0.457	0.460	58351	2.430	1.377	0.965	58090	4.760	2.790	1.613
58131	1.181	0.584	0.460	58894	2.770	1.410	1.194	58716	5.170	3.090	1.435
58051	1.346	0.699	0.551	58071	3.380	1.930	1.143	58110	5.800	3.470	1.486
58121	1.740	0.953	0.711	58586	3.520	2.260	0.978				

Table 3-61. Design Data for Toroidal High Flux Powder Cores.

High Flux Powder Cores, Magnetics 60 mu (coated)											
Part No.	W _{icu} grams	W _{tfe} grams	MLT cm	MPL cm	W _a A _c	A _c cm ²	W _a cm ²	A _p cm ⁴	K _g cm ⁵	A _t cm ²	AL mh/IK
58021	0.10	0.504	1.10	1.36	0.723	0.047	0.034	0.001610	0.000027	2.30	24
58281	0.70	1.222	1.40	2.18	1.729	0.075	0.130	0.009757	0.000204	4.80	25
58291	0.70	1.598	1.60	2.18	1.376	0.095	0.130	0.012359	0.000301	5.10	32
58041	0.90	1.692	1.60	2.38	1.500	0.100	0.150	0.014998	0.000375	5.60	32
58131	1.50	1.880	1.70	2.69	2.759	0.091	0.250	0.022735	0.000492	6.90	26
58051	2.50	2.726	2.00	3.12	3.175	0.114	0.362	0.041279	0.000961	9.30	27
58121	6.10	6.016	2.50	4.11	3.563	0.192	0.684	0.131267	0.003985	16.00	35
58381	5.60	7.238	2.60	4.14	2.634	0.232	0.611	0.141747	0.005099	16.30	43
58848	11.10	8.366	2.80	5.09	4.898	0.226	1.107	0.250092	0.008001	22.70	32
58059	15.20	14.100	3.20	5.67	4.097	0.331	1.356	0.448857	0.018406	28.60	43
58351	17.90	17.672	3.50	5.88	3.727	0.388	1.446	0.561153	0.024969	31.40	51
58894	22.30	31.772	4.10	6.35	2.320	0.654	1.517	0.992423	0.062916	39.80	75
58071	46.20	41.548	4.50	8.15	4.263	0.672	2.865	1.925420	0.114179	58.30	61
58586	61.40	30.926	4.40	8.95	8.681	0.454	3.941	1.789128	0.074166	64.40	38
58076	60.20	45.966	4.80	8.98	5.255	0.678	3.563	2.415897	0.137877	68.00	56
58083	85.30	81.310	5.70	9.84	3.910	1.072	4.191	4.492709	0.336608	87.50	81
58439	101.90	160.740	6.80	10.74	2.106	1.990	4.191	8.340010	0.971244	112.60	135
58090	136.90	115.620	6.40	11.63	4.497	1.340	6.026	8.075211	0.677485	117.20	86
58716	169.30	125.020	6.40	12.73	5.917	1.251	7.402	9.260268	0.720435	133.10	73
58110	233.30	155.100	7.00	14.300	6.474	1.444	9.348	13.498792	1.111049	164.70	75

Design and Dimensional Data for EE, Iron Powder Cores

The dimensional outline for EE iron powder cores is shown in Figure 3-52. Dimensional data for EE iron powder cores is given in Table 3-62; design data is given in Table 3-63. For more information, see Chapter 2.

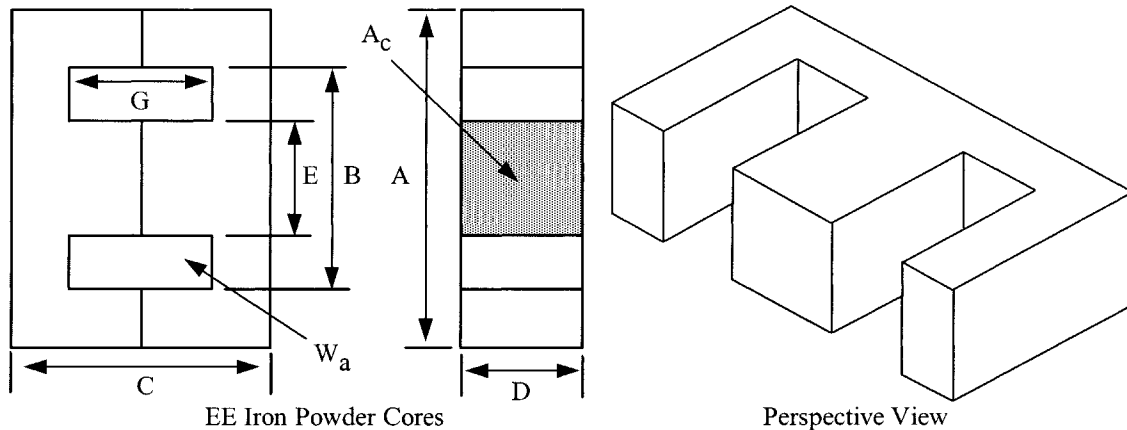


Figure 3-52. Dimension Outline for EE Iron Powder Cores.

Table 3-62. Dimensional Data for EE Iron Powder Cores.

EE, Iron Powder Cores (Micrometals) 75 mu Mix-26													
Part No.	A cm	B cm	C cm	D cm	E cm	G cm	Part No.	A cm	B cm	C cm	D cm	E cm	G cm
DIN-16-5	1.640	1.130	1.630	0.462	0.462	1.200	DIN-42-15	4.280	3.070	4.220	1.500	1.200	3.070
EI-187	1.910	1.430	1.610	0.475	0.475	1.160	DIN-42-20	4.280	3.070	4.220	2.000	1.200	3.070
EE-24-25	2.540	1.910	1.910	0.635	0.635	1.270	EI-625	4.740	3.180	3.940	1.570	1.570	2.420
EI-375	3.490	2.540	2.910	0.953	0.953	1.960	DIN-55-21	5.610	3.860	5.540	2.080	1.730	3.830
EI-21	4.130	2.860	3.410	1.270	1.270	2.140	EI-75	5.690	3.810	4.760	1.890	1.890	2.900

Table 3-63. Design Data for EE Iron Powder Cores.

EE, Iron Powder Cores (Micrometals) 75 mu Mix-26												
Part No.	W _{tcu} grams	W _{ife} grams	MLT cm	MPL cm	W _a		A _c cm ²	W _a cm ²	A _p cm ⁴	K _g cm ⁵	A _t cm ²	AL mh/1K
					W _a	A _c						
DIN-16-5	4.7	5.3	3.3	3.98	1.790	0.224	0.401	0.090	0.00243	11.5	58	
EI-187	7.5	5.5	3.8	4.10	2.451	0.226	0.554	0.125	0.00297	14.4	64	
EI-24-25	14.3	12.2	5.0	5.10	2.010	0.403	0.810	0.326	0.01062	23.5	92	
EI-375	37.1	40.1	6.7	7.40	1.714	0.907	1.555	1.411	0.07624	46.8	134	
EI-21	50.2	80.8	8.2	8.40	1.071	1.610	1.725	2.777	0.21852	63.3	210	
DIN-42-15	91.3	112.4	8.9	10.40	1.586	1.810	2.870	5.196	0.42050	84.4	195	
DIN-42-20	101.5	149.6	9.9	10.40	1.191	2.410	2.870	6.918	0.67054	92.9	232	
EI-625	65.2	141.1	9.4	9.5	0.785	2.480	1.948	4.831	0.50894	82.4	265	
DIN-55-21	167.9	283.7	11.6	13.2	1.133	3.600	4.079	14.684	1.82699	141.3	275	
EI-75	110.7	245.8	11.2	11.5	0.778	3.580	2.784	9.9667	1.27615	119.3	325	

Design and Dimensional Data for EE, Sendust Powder Cores

The dimensional outline for EE Sendust cores is shown in Figure 3-53. Dimensional data for EE Sendust powder cores is given in Table 3-64; design data is given in Table 3-65. For more information, see Chapter 2.

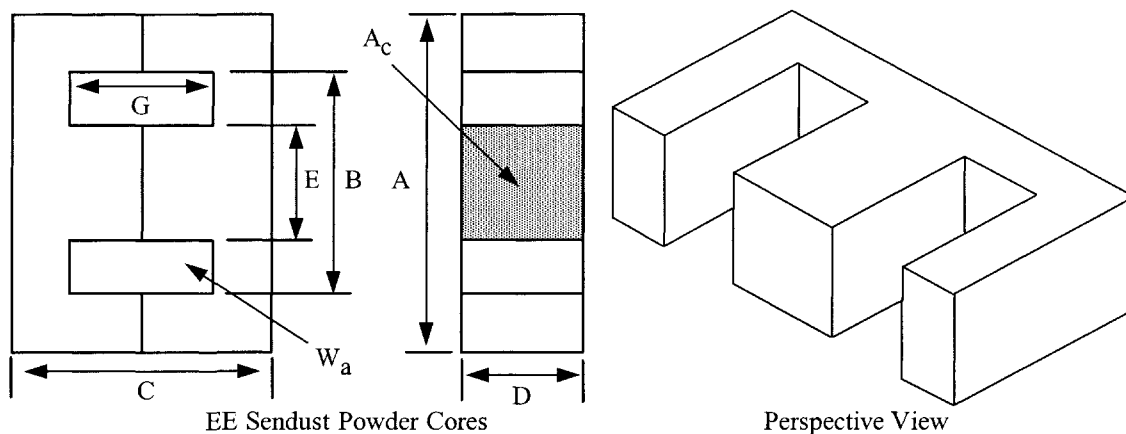


Figure 3-53. Dimension Outline for EE Sendust Powder Cores.

Table 3-64. Dimensional Data for EE Sendust Powder Cores.

EE, Sendust Powder Cores (Magnetics) 60 mu													
Part No.	A cm	B cm	C cm	D cm	E cm	G cm	Part No.	A cm	B cm	C cm	D cm	E cm	G cm
EI-187	1.910	1.430	1.610	0.475	0.475	1.160	DIN-42-15	4.280	3.070	4.220	1.500	1.200	3.070
EE-24-25	2.540	1.910	1.910	0.635	0.635	1.270	DIN-42-20	4.280	3.070	4.220	2.000	1.200	3.070
EI-375	3.490	2.540	2.910	0.953	0.953	1.960	DIN-55-21	5.610	3.860	5.540	2.080	1.730	3.830
EI-21	4.130	2.860	3.410	1.270	1.270	2.140							

Table 3-65. Design Data for EE Sendust Powder Cores.

EE, Sendust Powder Cores (Magnetics) 60 mu												
Part No.	W _{tcu} grams	W _{tfe} grams	MLT cm	MPL cm	W _a		A _c cm ²	W _a cm ²	A _p cm ⁴	K _μ cm ⁵	A _t cm ²	AL mh/K
					W _a	A _c						
EI-187	7.5	6.4	3.8	4.01	2.451	0.226	0.554	0.125	0.00297	14.4	48	
EI-24-25	14.3	13.1	5.0	4.85	2.010	0.403	0.810	0.326	0.01062	23.5	70	
EI-375	37.1	40.8	6.7	6.94	1.714	0.907	1.555	1.411	0.07624	46.8	102	
EI-21	50.2	82.6	8.2	7.75	1.071	1.610	1.725	2.777	0.21852	63.3	163	
DIN-42-15	91.3	126.0	8.9	9.84	1.586	1.810	2.870	5.196	0.42050	84.4	150	
DIN-42-20	101.5	163.0	9.9	9.84	1.191	2.410	2.870	6.918	0.67054	92.9	194	
DIN-55-21	167.9	302.0	11.6	12.3	1.133	3.600	4.079	14.684	1.82699	141.3	219	

References

Magnetics

Home Office and Factory

P.O. Box 11422

Pittsburgh, PA 15238-0422

1-800-245-3984

1-412-696-0333, Fax

www.mag-inc.com -----magnetics@spang.com

Micrometals

5615 E. La Palma Ave.

Anaheim, CA 92807

1-800-356-5977, USA

1-714-970-0400, Fax

www.micrometals.com

TSC International

39105 North Magnetics Blvd.

P.O. Box 399

Wadsworth, IL 60083-0399

1-847-249-4900

1-847-249-4988, Fax

www.tscinternational.com ---- sales@tscinternational.com

Magnetic Metals Corp.

2475 La Palma Ave.

Anaheim, CA 92801

1-800-331-0278, USA

1-714-828-4279, Fax

www.magmet.com

Thomas and Skinner, Inc.

1120 East 23rd Street

P.O. Box 150

Indianapolis, Indiana 46206

1-317-923-2501

1-317-923-5919, Fax

www.thomas-skinner.com

Tempel Steel Co.

5500 N. Wolcott

Chicago, Il 60640-1020

1-773-250-8000

1-773-250-8910, Fax

www.tempel.com

Chapter 4

Window Utilization, Magnet Wire, and Insulation

Table of Contents

1. Window Utilization Factor, K_u	
2. S_1 , Wire Insulation	
3. S_2 , Fill Factor	
4. S_3 , Effective Window	
5. S_4 , Insulation Factor	
6. Summary	
7. Window Utilization Factor, K_u for Bobbin Ferrites	
8. Circular mil and Square mil	
9. Magnet Wire	
10. Magnet Wire, Film Insulation	
11. Wire Table	
12. Solderable Insulation	
13. Bondable Magnet Wire	
14. Base Film Insulation	
15. Bonding Methods	
16. Miniature Square Magnet Wire	
17. Multistrand Wire and Skin Effect	
18. Reduce Skin Effect in Transformers	
19. Calculating Skin Effect in Inductors	
20. Multistrand Litz Wire.....	
21. Proximity Effect	
22. Proximity Effect in Transformers.....	
23. Multiple Layer High Frequency Transformer and High Loss.....	
24. Proximity Effect Using Dowell Curves	
25. Specialty Wire	
26. Triple Insulated Wire.....	
27. Triple Insulated Litz	
28. Polyfilar Magnetic Wire	
29. Standard Foils	
30. The Use of Foils	
31. Calculating, MLT.....	
32. Calculating, MLT (toroid).....	
33. Copper Resistance	
34. Copper Weight	
35. Electrical Insulating Materials	
36. References	

Window Utilization Factor, K_u

The window utilization factor is the amount of copper that appears in the window area of the transformer or inductor. The window utilization factor is influenced by five main factors:

1. Wire insulation, S_1 .
2. Wire lay fill factor, layer or random wound, S_2 .
3. Effective window area (or when using a toroid, the clearance hole for passage of the shuttle), S_3 .
4. Insulation required for multilayer windings, or between windings, S_4 .
5. Workmanship, (quality).

These factors, multiplied together, will give a normalized window utilization of $K_u = 0.4$, as shown in Figure 4-1.

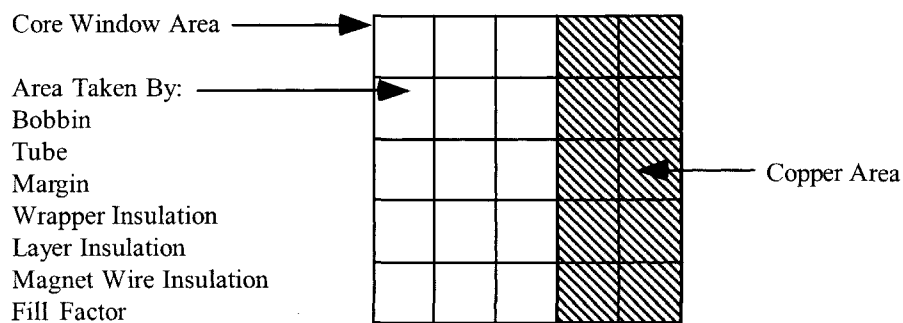


Figure 4-1. Window Area Occupied by Copper.

The window utilization factor, K_u , of the available core window is that space occupied by the winding (copper), and is calculated from areas S_1 , S_2 , S_3 , and S_4 :

$$K_u = S_1 S_2 S_3 S_4 \quad [4-1]$$

Where:

S_1 = conductor area/wire area

S_2 = wound area/usable window area

S_3 = usable window area/window area

S_4 = usable window area/usable window area + insulation

In which:

Conductor area, $A_{w(B)}$ = copper area.

Wire area, A_w = copper area + insulation area.

Wound area = number of turns x wire area of one turn.

Usable window area = available window area - residual area, that results from the particular winding technique used.

Window area = available window area.

Insulation area = area used for winding insulation.

S_1 , Wire Insulation

In the design of high-current or low-current transformers, the ratio of the conductor area to the total wire area can vary from 0.941 to 0.673, depending on the wire size. In Figure 4-2, the thickness of the insulation has been exaggerated to show how the insulation impacts the overall area of the wire.

It can be seen, in Figure 4-2, that, by using multi-strands of fine wire to reduce the skin effect, it will have a significant impact on the window utilization factor, K_u . S_1 is not only dependent upon wire size, but it is also dependent upon insulation coating. Table 4-1 shows the ratio of bare magnet wire to the magnet wire with insulation for single, heavy, triple, and quad insulation. When designing low-current transformers, it is advisable to re-evaluate S_1 because of the increased amount of insulating material.

$$S_1 = \frac{A_{w(B)}}{A_w} \quad [4-2]$$

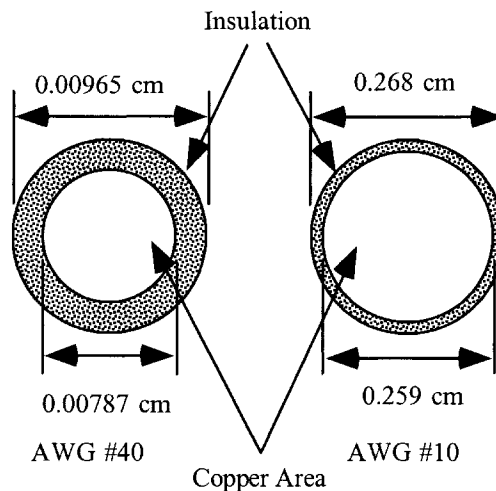


Figure 4-2. Comparing Insulation with Different Wire Gauges.

Table 4-1

Magnetic Wire Data (Nominal)					
Size AWG	Bare Area (cm ²)	Ratio Bare/Single	Ratio Bare/Heavy	Ratio Bare/Triple	Ratio Bare/Quad
10	0.1019	0.961	0.930	0.910	0.880
15	0.0571	0.939	0.899	0.867	0.826
20	0.0320	0.917	0.855	0.812	0.756
25	0.0179	0.878	0.793	0.733	0.662
30	0.0100	0.842	0.743	0.661	0.574
35	0.0056	0.815	0.698	0.588	0.502
40	0.0031	0.784	0.665	0.544	0.474

S₂, Fill Factor

S₂ is the fill factor, or the wire lay, for the usable window area. When winding a large number of turns tightly on a smooth surface, the winding length exceeds the calculated value from the wire diameter by 10 to 15%, depending on the wire gauge. See Figure 4-3. The wire lay is subjected to wire tension, and wire quality, such as continuous wire diameter and the winding technique depending on the skill of the operator. The wire lay factor relationship for various wire sizes for layer wound coils is shown in Table 4-2, and for random wound coils in Table 4-3. The Tables list the outside diameter for heavy film magnetic wire, 10 – 44 AWG.

Table 4-2

Wire Lay Factor For Layer Wound Coils			
AWG	Insulated Wire OD (inch)	Insulated Wire OD (cm)	Wire Lay Factor
10 to 25	0.1051 - 0.0199	0.2670 - 0.0505	0.90
26 to 30	0.0178 - 0.0116	0.0452 - 0.0294	0.89
31 to 35	0.0105 - 0.0067	0.0267 - 0.0170	0.88
36 to 38	0.0060 - 0.0049	0.0152 - 0.0124	0.87
39 to 40	0.0043 - 0.0038	0.0109 - 0.0096	0.86
41 to 44	0.0034 - 0.0025	0.00863 - 0.00635	0.85
Heavy film magnetic wire.			

Table 4-3

Wire Lay Factor For Random Wound Coils			
AWG	Insulated Wire OD (inch)	Insulated Wire OD (cm)	Wire Lay Factor
10 to 22	0.1051 - 0.0276	0.267 - 0.0701	0.90
23 to 39	0.0623 - 0.0109	0.0249 - 0.0043	0.85
40 to 44	0.0038 - 0.0025	0.0096 - 0.00635	0.75
Heavy film magnet wire.			

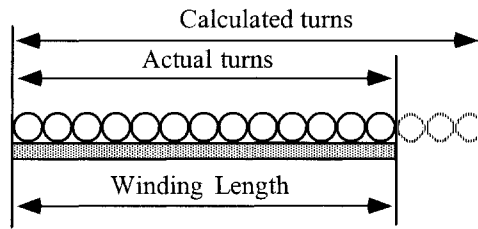


Figure 4-3. Capable Turns per Unit Length.

There are two ideal winding arrangements shown in Figure 4-4 and Figure 4-5. The square winding is shown in Figure 4-4 and the hexagonal winding is shown in Figure 4-5. The simplest form of winding is done by a coil being wound, turn-by-turn and layer-upon-layer, as shown in Figure 4-4. The square winding pattern has a theoretical fill factor of 0.785.

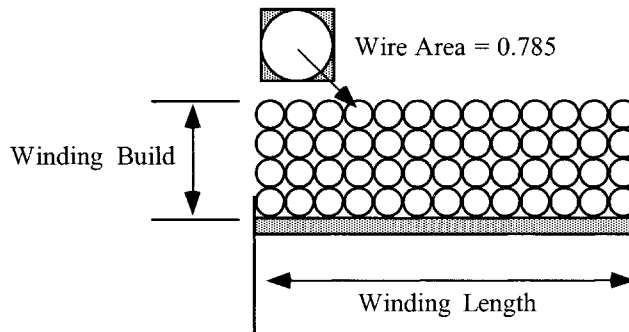


Figure 4-4. Theoretically, the Square Winding Pattern Fill Factor 0.785.

A seemingly, better fill factor can be achieved by using the hexagonal winding in Figure 4-5, compared to the square winding in Figure 4-4. In this type of winding, the individual wires do not lie exactly above each other, as in the square winding pattern. Instead, the wires lie in the grooves of the lower layer, as shown in Figure 4-5. This style of winding produces the tightest possible packing of the wire. The hexagonal style of winding will yield a theoretical fill factor of 0.907.

The fill factor, using the square winding pattern of 0.785, would be nearly impossible to achieve by hand winding without some layer insulation. Any layer insulation will reduce the fill factor even further. The fill factor, using the hexagonal winding pattern of 0.907, is just as hard to get. Hand winding, using the hexagonal technique, will result in the following: The first layer goes down with almost complete order. In the second layer, some disordering has occurred. With the third and fourth layer, disordering really sets in and the winding goes completely awry. This type of winding performs well with a small number of turns, but, with a large number of turns, it becomes randomly wound.

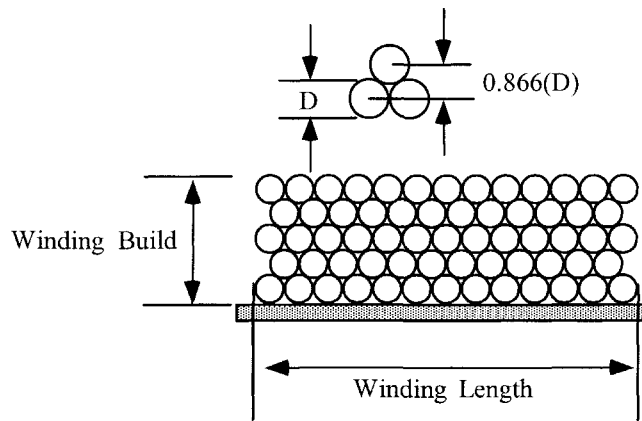


Figure 4-5. Theoretically, the Hexagonal Winding Pattern Fill Factor 0.907.

The ideal winding on a rectangular bobbin is shown in Figure 4-6. Then, when winding rectangular bobbins or tubes, the actual winding height in the region covered by the core will be greater than the calculated winding height or build due to the bowing of the windings. See Figure 4-7. The amount of bowing depends on the proportions of the winding and the height of the winding. Usually, the available winding build should be reduced by 15 to 20%, or $0.85x$ the winding build. When winding on a round bobbin or tube, this bowing effect is negligible.

The conclusion is, in comparing the square winding pattern used in the layer wound coil with its insulation with the hexagonal winding pattern and its awry winding pattern, both seem to have a fill factor of about 0.61. But there is always the hundred to one exception, such as, when a design happens to have the right bobbin, the right number of turns, and the right wire size. This normally only happens when the design is not critical.

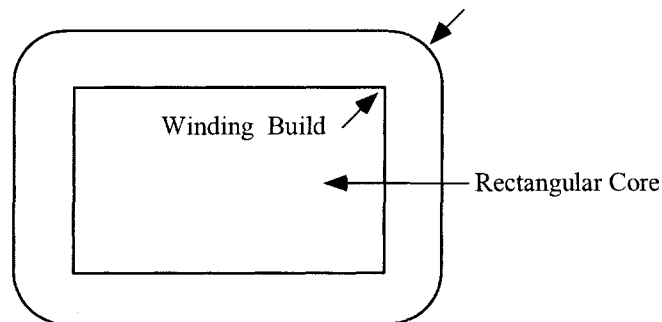


Figure 4-6. Ideal Winding on a Rectangular Bobbin.

To minimize this bowing effect and to insure a minimum build for either random or layer winding, the round bobbin, shown in Figure 4-8, will provide the most compact design. It can be seen, in Figure 4-8, that the round bobbin provides a uniform tension, all 360 degrees around the bobbin, for both layer and random windings. The other benefit, in using a round bobbin, is the reduction and minimizing of the leakage inductance caused from the bowing.

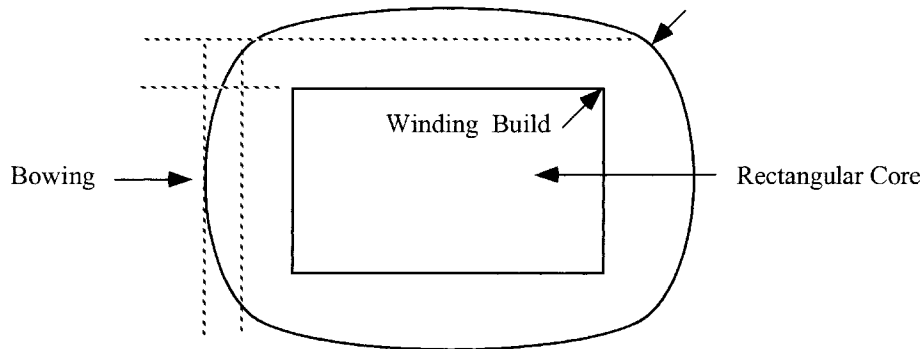


Figure 4-7. Bowing in Transformer Windings.

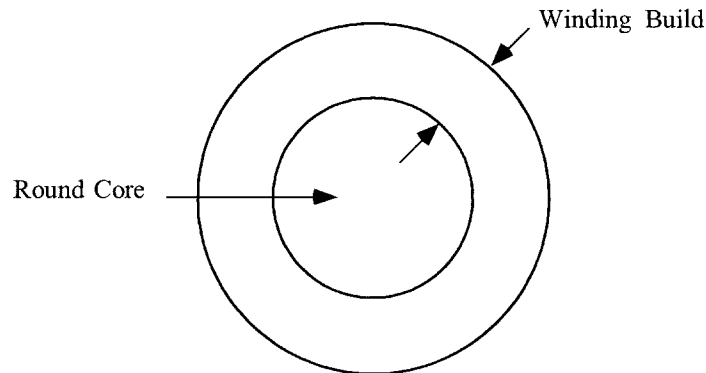


Figure 4-8. A Round Bobbin Insures Minimum Bowing.

S₃, Effective Window

The effective window, S_3 , defines how much of the available window space may actually be used for the winding. The winding area available to the designer depends on the bobbin or tube configuration. Designing a layer winding that uses a tube will require a margin, as shown in Figure 4-9. The margin dimensions will vary with wire size. See Table 4-4. It can be seen, in Figure 4-9 and Table 4-4, how the margin reduces the effective window area. When transformers are constructed, using the layer winding technique, there is an industry standard for layer insulation thickness. This thickness is based on the diameter of the wire, as shown in Table 4-5.

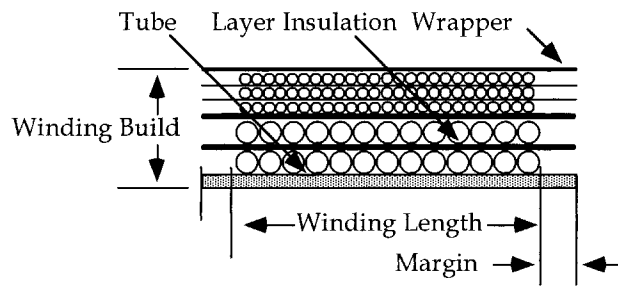


Figure 4-9. Transformer Windings with Margins.

Table 4-4

Winding Margins Versus AWG		
AWG	Margin	
	cm	inch
10-15	0.635	0.25
16-18	0.475	0.187
19-21	0.396	0.156
22-31	0.318	0.125
32-37	0.236	0.093
38-up	0.157	0.062

Table 4-5

Layer Insulation Thickness		
AWG	Insulation Thickness	
	cm	inch
10 - 16	0.02540	0.01000
17 - 19	0.01780	0.00700
20 - 21	0.01270	0.00500
22 - 23	0.00760	0.00300
24 - 27	0.00510	0.00200
28 - 33	0.00381	0.00150
34 - 41	0.00254	0.00100
42 - 46	0.00127	0.00050

A single bobbin design, as shown in Figure 4-10, offers an effective area, W_a , between 0.835 to 0.929 for laminations, and 0.55 to 0.75 for ferrites; a two bobbin configuration, as shown in Figure 4-11, offers an effective area, W_a , between 0.687 to 0.873 for the tape C cores.

The toroid is a little different. The term, S_3 , defines how much of the available window space can actually be used for the winding. In order to wind the toroidal core, there has to be room to allow free passage of the shuttle. If half of the inside diameter is set aside for the shuttle, then, there will be 75% of the window

area, (W_a), left for the design which is a good value for the effective window area factor, $S_3 = 0.75$, as shown in Figure 4-12. The toroid would fall into all of the above categories.

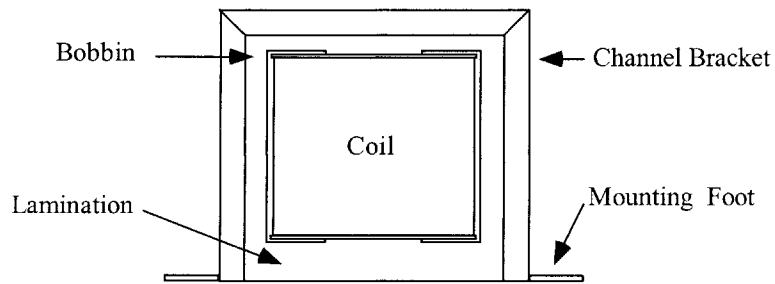


Figure 4-10. Transformer Construction with Single Bobbin.

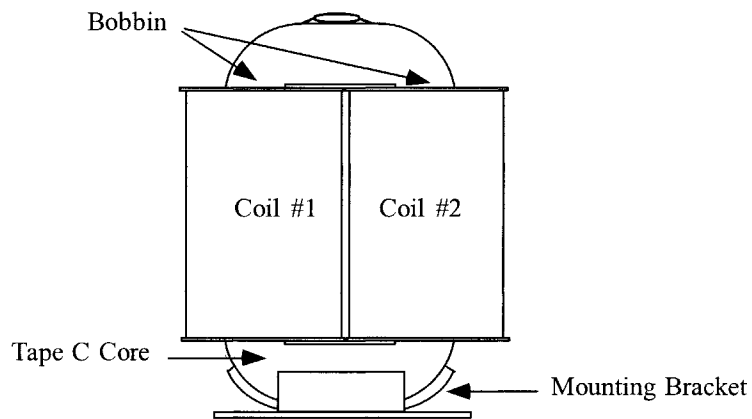
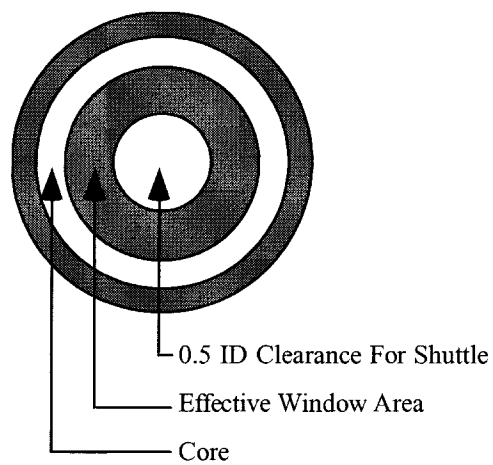


Figure 4-11. Transformer Construction with Dual Bobbins.



$$\text{Effective Window area } W_{a(\text{eff})} = (0.75)(\pi)(ID)^2/4$$

Figure 4-12. Effective Winding Area of a Toroidal Core.

S₄, Insulation Factor

The insulation factor, S₄, defines how much of the usable window space is actually being used for insulation. If the transformer has multiple secondaries with significant amounts of insulation, S₄ should be reduced by 5 to 10% for each additional secondary winding, partly because of the added space occupied by insulation and partly because of the poorer space factor.

The insulation factor, S₄, is not taken into account in Figure 4-12. The insulation factor, S₄, is to be 1.0. The window utilization factor, K_w, is highly influenced by insulation factor, S₄, because of the rapid buildup of insulation in the toroid, as shown in Figure 4-13.

In Figure 4-13, it can be seen that the insulation buildup is greater on the inside, than on the outside. For example, in Figure 4-13, if 1.27 cm (1/2") wide tape was used with an overlap of 0.32 cm (1/8") on the outside diameter, the overlap thickness would be four times the thickness of the tape. It should be noted that the amount of overlap depends greatly on the size of the toroid and the required tape. In the design of toroidal components, and using the 0.5 ID remaining for passage of the shuttle, there is normally enough room for the wrapper.

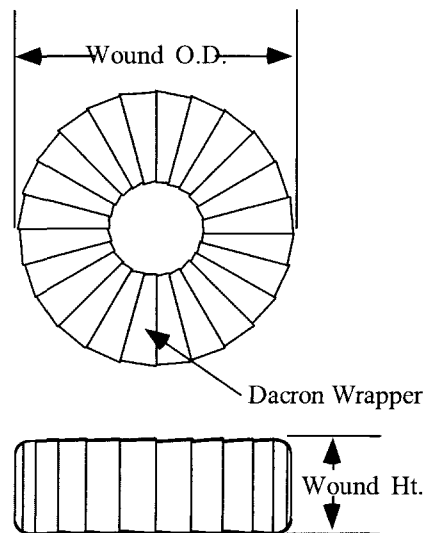


Figure 4-13. Wrapped Toroid.

Summary

The author hopes to have cleared up some of the mystery of how the window utilization factor, K_w, was derived and that the magic of 0.4 is now clear. All the different parts making up window utilization, have been explained, hopefully eliminating confusion and simplifying the complexity of the subject.

As stated at the beginning of this chapter, a good approximation for the window utilization factor is $K_u = 0.4$.

$$S_1 = \text{conductor area/wire area} = 0.855, \text{ #20 AWG}$$

$$S_2 = \text{wound area/usable window area} = 0.61$$

$$S_3 = \text{usable window area/window area} = 0.75$$

$$S_4 = \text{usable window area/usable window area} + \text{insulation} = 1$$

$$K_u = S_1 S_2 S_3 S_4$$

$$K_u = (0.855)(0.61)(0.75)(1.0) = 0.391 \approx 0.4 \quad [4-3]$$

Being a very conservative number, it can be used in most designs. It is an important factor in all designs of magnetic components.

Window Utilization Factor, K_u for Bobbin Ferrites

In high frequency power electronics, the majority of the designs will use some kind of bobbin ferrite. The main reasons for using ferrites is its high frequency performance and cost. The window utilization factor, K_u , for bobbin ferrites is not as high as it is for iron alloy materials, such as laminations and C cores. Design engineers, who have been using bobbin ferrite materials, know the drawback in the window utilization factor, K_u . Once this problem is understood, then, the problem should go away.

Ferrite materials are fired in kilns like ceramic pottery. There is a certain amount of shrinkage after firing, and the amount varies from one manufacturer's process to another. The amount of shrinkage could vary as much as 15 to 30%, as shown in Figure 4-14. The ferrite manufacturers try to keep a tight control on the amount of shrinkage, because these cores must meet a dimensional tolerance after firing. Even though the shrinkage is under tight control, the tolerances on the end product are much larger than the iron alloy, stamped laminations. The end result is the bobbin has to slip on and meet all of the minimum and maximum dimensional tolerances.

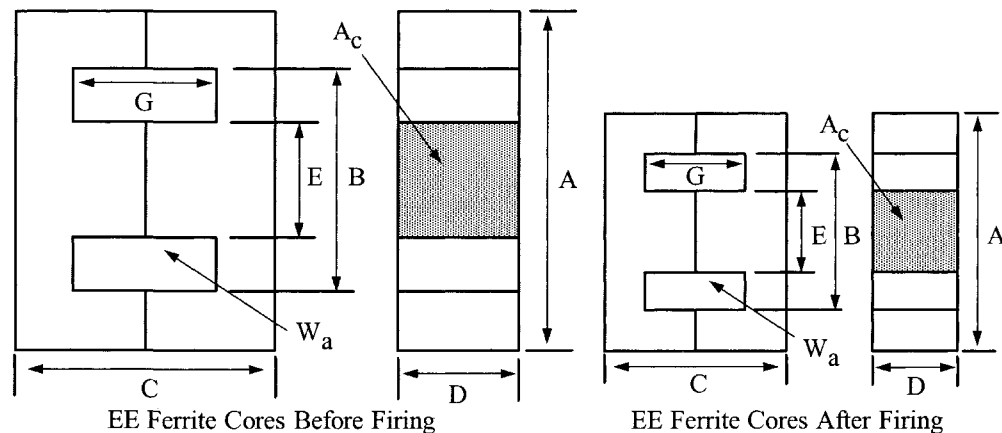


Figure 4-14. Ferrite EE Core Before and After Firing.

This dimensional tolerance has an impact on the winding area of the bobbin, clearly shown in Table 4-6. This smaller winding area reduces the power handling capability of the core. Operating at high frequency will also reduce the power handling capability of the core because of the skin effect. The skin effect requires the use of multistrands of fine wire in place of a large single strand. The selection of the correct wire size to minimize the skin effect at given frequency is shown in Equations [4-5] through [4-9]. Also shown is an example of the largest wire size that should be used when operating at 100kHz. Reevaluate the, K_u , Equation [4-3] so that it can operate at 100kHz, using a #26 wire, and using a cut ferrite core.

$$S_1 = \text{conductor area/wire area} = 0.79, \text{ #26 AWG}$$

$$S_2 = \text{wound area/usable window area} = 0.61$$

$$S_3 = \text{usable window area/window area} = 0.6$$

$$S_4 = \text{usable window area/usable window area} + \text{insulation} = 1$$

$$K_u = S_1 S_2 S_3 S_4$$

$$K_u = (0.79)(0.61)(0.6)(1.0) = 0.289 \quad [4-4]$$

Table 4-6. Effective Window Area.

Effective Window Area			
Core	Window cm ²	Bobbin cm ²	Ratio B/W
RM-6	0.260	0.150	0.577
RM-8	0.456	0.303	0.664
RM-12	1.103	0.730	0.662
PQ-20/16	0.474	0.256	0.540
PQ-26/25	0.845	0.502	0.594
PQ-35/35	2.206	1.590	0.721
EFD-10	0.116	0.042	0.362
EFD-15	0.314	0.148	0.471
EFD-25	0.679	0.402	0.592
EC-35	1.571	0.971	0.618
EC-41	2.082	1.375	0.660
EC-70	6.177	4.650	0.753
Laminations			
EI-187	0.529	0.368	0.696
EI-375	1.512	1.170	0.774
EI-21	1.638	1.240	0.757

Circular mil and Square mil

There are engineers that use circular mils (CM)/amp or square mils/amp. This is the reciprocal current density. The norm is to use amps/cm², which is a true current density. There have been some requests to define circular mils and square mils. First, let's define a mil, which is .001 inch. Figure 4-15 shows the area of a square mil, and the area of a circular mil.

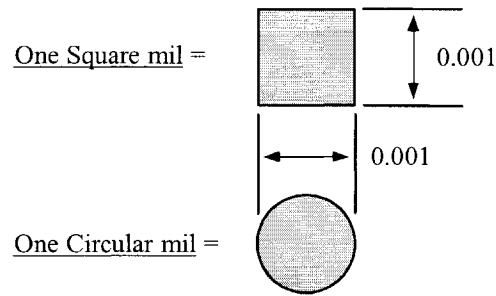


Figure 4-15. Comparing Circular-Mils and Square-Mils.

To convert Square mils to Circular mils , multiply by 1.2732.

To convert Circular mils to Square mils , multiply by 0.7854.

To convert Circular mils to Square centimeters , multiply by 5.066×10^{-6} .

To convert Square mils to Square centimeters , multiply by 6.45×10^{-6}

Note:

Designers have for many years used this rule of thumb:

$$500\text{CM}/\text{Amp} \approx 400\text{Amps}/\text{cm}^2$$

$$1000\text{CM}/\text{Amp} \approx 200\text{Amps}/\text{cm}^2$$

Magnet Wire

Standard magnet wire is available in three different materials, shown in Table 4-7. The most common is copper, but aluminum and silver are available. Aluminum magnet wire is one-third the weight of copper for the same size conductor and one-half the weight for the same conductivity. Aluminum magnet wire is a little more difficult to terminate, but it can be done. Silver magnet wire has the highest conductivity, easy to solder to, and weighs 20% more than copper.

Table 4-7

Magnet Wire Material Properties						
Material	Symbol	Density grams/cm ³	Resistivity μΩ/cm	Weight Factor	Resistance Factor	Temperature Coefficient
Copper	Cu	8.89	1.72	1	1	0.00393
Silver	Ag	10.49	1.59	1.18	0.95	0.00380
Aluminum	Al	2.703	2.83	0.3	1.64	0.00410

Magnet Wire, Film Insulation

It is the design engineer's responsibility to ensure that the selected magnet wire used in the design is compatible with the environmental and design specification. The environmental specification will set the ambient temperature. The maximum operating temperature of the magnet wire is obtained by summing the maximum ambient temperature, plus the temperature rise of the magnetic component. After the maximum temperature has been obtained, see Table 4-8 for the Temperature Class. The magnet wire insulation guide listing in Table 4-7, is only a partial list from NEMA, Standard MW 1000.

The maximum operating temperature is the "Achilles Heel" to the magnet wire. Standard magnet wire is rated by temperature. The range is from 105°C to 220°C, as shown in Table 4-8. The insulation film of the magnet wire is on the surface of the copper wire. This insulation film is the most vulnerable to thermal overloads, so the selection of the insulation film is very critical for long life. When magnet wire is subjected to thermal overloads, or a high ambient temperature above its rated temperature, the life of the magnet wire is greatly reduced, as shown in Figures 4-16 and 4-17. The engineer must be very careful of hot spots so as not to degrade the service life of the magnetic component.

Table 4-8

Magnet Wire Insulation Guide			
Temperature Class	Insulation Type	Dielectric Constant	NEMA Standard MW 1000
105°C	Polyurethane*	6.20	MW-2-C
105°C	Formvar	3.71	MW-15-C
130°C	Polyurethane-Nylon*	6.20	MW-28-C
155°C	Polyurethane-155	6.20	MW-79-C
180°C	Polyester Solderable*	3.95	MW-77-C
200°C	Polyester-amid-imide	4.55	MW-35-C
220°C	Polyimide (ML)	3.90	MW-16-C

*Solderable insulations.

Wire Table

Table 4-9 is the Wire Table for AWG, 10 to 44, heavy film wire. The bare wire areas are given in cm² in column 2, and the circular mils are given in column 3 for each wire size. The equivalent resistance in micro-ohms per centimeter ($\mu\Omega/\text{cm}$ or $10^{-6} \Omega/\text{cm}$) is given in column 4 for each wire size. Columns 5 through 13 relate to heavy, insulated film coating. The weight of the magnet wire is found in column 13, in grams, per centimeter.

Table 4-10 provides the maximum outside diameter for magnet wire with single, heavy, triple, and quad film insulation. The dimensional data is in centimeters and inches, for AWG 10 through 44.

Table 4-9

Wire Table												
AWG	Bare Area		Resistance $\mu\Omega/\text{cm}$ 20°C	Heavy Synthetics								
				Area		Diameter		Turns-Per		Turns-Per		Weight
	$\text{cm}^2(10^{-3})$	cir-mil	$\text{cm}^2(10^{-3})$	cir-mil	cm	Inch	cm	Inch	cm^2	Inch ²	gm/cm	
1	2	3	4	5	6	7	8	9	10	11	12	13
10	52.6100	10384.00	32.7	55.9000	11046.00	0.2670	0.105	3.9	10	11	69	0.46800
11	41.6800	8226.00	41.4	44.5000	8798.00	0.2380	0.094	4.4	11	13	90	0.37500
12	33.0800	6529.00	52.1	35.6400	7022.00	0.2130	0.084	4.9	12	17	108	0.29770
13	26.2600	5184.00	65.6	28.3600	5610.00	0.1900	0.075	5.5	13	21	136	0.23670
14	20.8200	4109.00	82.8	22.9500	4556.00	0.1710	0.068	6.0	15	26	169	0.18790
15	16.5100	3260.00	104.3	18.3700	3624.00	0.1530	0.060	6.8	17	33	211	0.14920
16	13.0700	2581.00	131.8	14.7300	2905.00	0.1370	0.054	7.3	19	41	263	0.11840
17	10.3900	2052.00	165.8	11.6800	2323.00	0.1220	0.048	8.2	21	51	331	0.09430
18	8.2280	1624.00	209.5	9.3260	1857.00	0.1090	0.043	9.1	23	64	415	0.07474
19	6.5310	1289.00	263.9	7.5390	1490.00	0.0980	0.039	10.2	26	80	515	0.05940
20	5.1880	1024.00	332.3	6.0650	1197.00	0.0879	0.035	11.4	29	99	638	0.04726
21	4.1160	812.30	418.9	4.8370	954.80	0.0785	0.031	12.8	32	124	800	0.03757
22	3.2430	640.10	531.4	3.8570	761.70	0.0701	0.028	14.3	36	156	1003	0.02965
23	2.5880	510.80	666.0	3.1350	620.00	0.0632	0.025	15.8	40	191	1234	0.02372
24	2.0470	404.00	842.1	2.5140	497.30	0.0566	0.022	17.6	45	239	1539	0.01884
25	1.6230	320.40	1062.0	2.0020	396.00	0.0505	0.020	19.8	50	300	1933	0.01498
26	1.2800	252.80	1345.0	1.6030	316.80	0.0452	0.018	22.1	56	374	2414	0.01185
27	1.0210	201.60	1687.0	1.3130	259.20	0.0409	0.016	24.4	62	457	2947	0.00945
28	0.8046	158.80	2142.0	1.0515	207.30	0.0366	0.014	27.3	69	571	3680	0.00747
29	0.6470	127.70	2664.0	0.8548	169.00	0.0330	0.013	30.3	77	702	4527	0.00602
30	0.5067	100.00	3402.0	0.6785	134.50	0.0294	0.012	33.9	86	884	5703	0.00472
31	0.4013	79.21	4294.0	0.5596	110.20	0.0267	0.011	37.5	95	1072	6914	0.00372
32	0.3242	64.00	5315.0	0.4559	90.25	0.0241	0.010	41.5	105	1316	8488	0.00305
33	0.2554	50.41	6748.0	0.3662	72.25	0.0216	0.009	46.3	118	1638	10565	0.00241
34	0.2011	39.69	8572.0	0.2863	56.25	0.0191	0.008	52.5	133	2095	13512	0.00189
35	0.1589	31.36	10849.0	0.2268	44.89	0.0170	0.007	58.8	149	2645	17060	0.00150
36	0.1266	25.00	13608.0	0.1813	36.00	0.0152	0.006	62.5	167	3309	21343	0.00119
37	0.1026	20.25	16801.0	0.1538	30.25	0.0140	0.006	71.6	182	3901	25161	0.00098
38	0.0811	16.00	21266.0	0.1207	24.01	0.0124	0.005	80.4	204	4971	32062	0.00077
39	0.0621	12.25	27775.0	0.0932	18.49	0.0109	0.004	91.6	233	6437	41518	0.00059
40	0.0487	9.61	35400.0	0.0723	14.44	0.0096	0.004	103.6	263	8298	53522	0.00046
41	0.0397	7.84	43405.0	0.0584	11.56	0.0086	0.003	115.7	294	10273	66260	0.00038
42	0.0317	6.25	54429.0	0.0456	9.00	0.0076	0.003	131.2	333	13163	84901	0.00030
43	0.0245	4.84	70308.0	0.0368	7.29	0.0069	0.003	145.8	370	16291	105076	0.00023
44	0.0202	4.00	85072.0	0.0316	6.25	0.0064	0.003	157.4	400	18957	122272	0.00020

Table 4-10

Dimensional Data for Film Insulated Magnetic Wire								
Wire Size AWG	Maximum Diameter							
	Single-Insulation		Heavy-Insulation		Triple-Insulation		Quad-Insulation	
	Inches	Centimeters	Inches	Centimeters	Inches	Centimeters	Inches	Centimeters
10	0.1054	0.2677	0.1071	0.2720	0.1084	0.2753	0.1106	0.2809
11	0.9410	2.3901	0.0957	0.2431	0.0969	0.2461	0.0991	0.2517
12	0.0840	0.2134	0.0855	0.2172	0.0867	0.2202	0.0888	0.2256
13	0.0750	0.1905	0.0765	0.1943	0.0776	0.1971	0.0796	0.2022
14	0.0670	0.1702	0.0684	0.1737	0.0695	0.1765	0.0715	0.1816
15	0.0599	0.1521	0.0613	0.1557	0.0624	0.1585	0.0644	0.1636
16	0.0534	0.1356	0.0548	0.1392	0.0558	0.1417	0.0577	0.1466
17	0.0478	0.1214	0.0492	0.1250	0.0502	0.1275	0.0520	0.1321
18	0.0426	0.1082	0.0440	0.1118	0.0450	0.1143	0.0468	0.1189
19	0.0382	0.0970	0.0395	0.1003	0.0404	0.1026	0.0422	0.1072
20	0.0341	0.0866	0.0353	0.0897	0.0362	0.0919	0.0379	0.0963
21	0.0306	0.0777	0.0317	0.0805	0.0326	0.0828	0.0342	0.0869
22	0.0273	0.0693	0.0284	0.0721	0.0292	0.0742	0.0308	0.0782
23	0.0244	0.0620	0.0255	0.0648	0.0263	0.0668	0.0279	0.0709
24	0.0218	0.0554	0.0229	0.0582	0.0237	0.0602	0.2520	0.6401
25	0.0195	0.0495	0.0206	0.0523	0.0214	0.0544	0.0228	0.0579
26	0.0174	0.0442	0.0185	0.0470	0.0192	0.0488	0.0206	0.0523
27	0.0156	0.0396	0.0165	0.0419	0.0172	0.0437	0.0185	0.0470
28	0.0139	0.0353	0.0148	0.0376	0.0155	0.0394	0.0166	0.0422
29	0.0126	0.0320	0.0134	0.0340	0.0141	0.0358	0.0152	0.0386
30	0.0112	0.0284	0.0120	0.0305	0.0127	0.0323	0.0137	0.0348
31	0.0100	0.0254	0.0108	0.0274	0.0115	0.0292	0.0124	0.0315
32	0.0091	0.0231	0.0098	0.0249	0.0105	0.0267	0.0113	0.0287
33	0.0081	0.0206	0.0088	0.0224	0.0095	0.0241	0.0102	0.0259
34	0.0072	0.0183	0.0078	0.0198	0.0084	0.0213	0.0091	0.0231
35	0.0064	0.0163	0.0070	0.0178	0.0076	0.0193	0.0082	0.0208
36	0.0058	0.0147	0.0063	0.0160	0.0069	0.0175	0.0074	0.0188
37	0.0052	0.0132	0.0057	0.0145	0.0062	0.0157	0.0067	0.0170
38	0.0047	0.0119	0.0051	0.0130	0.0056	0.0142	0.0060	0.0152
39	0.0041	0.0104	0.0045	0.0114	0.0050	0.0127	0.0053	0.0135
40	0.0037	0.0094	0.0040	0.0102	0.0044	0.0112	0.0047	0.0119
41	0.0033	0.0084	0.0036	0.0091	0.0040	0.0102	0.0043	0.0109
42	0.0030	0.0076	0.0032	0.0081	0.0037	0.0094	0.0038	0.0097
43	0.0026	0.0066	0.0029	0.0074	0.0033	0.0084	0.0035	0.0089
44	0.0024	0.0061	0.0027	0.0069	0.0030	0.0076	0.0032	0.0081

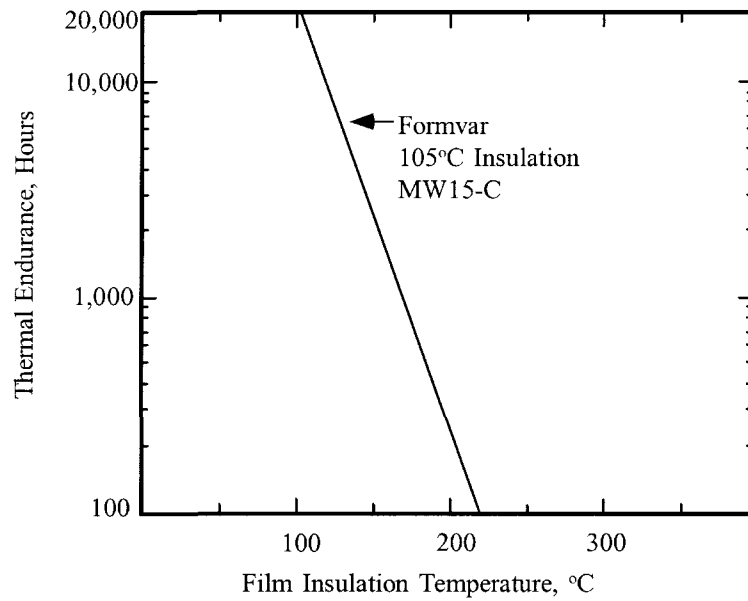


Figure 4-16. Thermal Endurance, for 105°C Formvar Insulation.

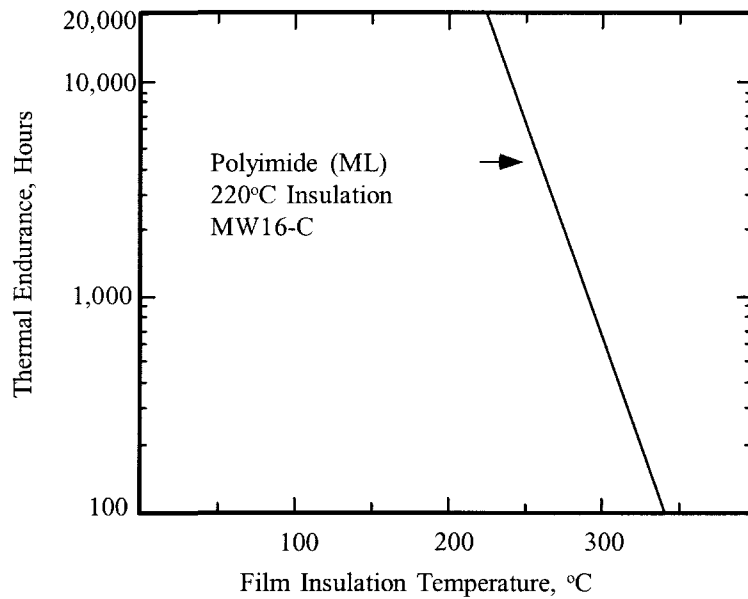


Figure 4-17. Thermal Endurance for 220°C Polyimide Insulation (ML).

Solderable Insulation

Solderable insulation is a special film insulation that is used on magnet wire in low cost, high volume applications. The magnet wire, with this solderable insulation, is wrapped around the terminal or pin, as shown in Figure 4-18. Then the terminal can be dip-soldered at the prescribed temperature without prior stripping. The ambient temperature range for this type of film insulation is 105°C to 180°C.

There are drawbacks in using some of the solderable insulation magnet wire. Prior to using, check your application with the wire manufacturer. Some solderable film insulation is not recommended where severe overloads may occur. Some solderable film insulations are susceptible to softening, due to prolonged exposure to strong solvents, such as alcohol, acetone, and methylethylketone.

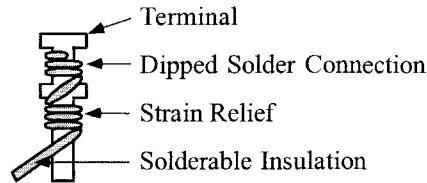


Figure 4-18. Solderable Insulation on a Dip Solder Terminal.

Bondable Magnet Wire

Bondable, magnet wires are a film-coated, copper or aluminum, with an additional coating of a thermoplastic adhesive. See Figure 4-19. They are used in applications where it is desirable to have the bonding agent, such as a solvent, which will hold the coil form until it is oven-baked. Most adhesive coatings can be softened with solvents or heat. If a coil is wound with an irregular shape, held in a form, and then raised to the appropriate temperature, the coil will retain its shape. Bondable magnet wires have applications such as armatures, field coils, and self-supporting coils.

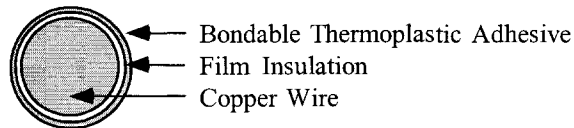


Figure 4-19. Typical Cross-Section of a Bondable Magnet Wire.

Base Film Insulation

All conventional film insulations may be adhesive-coated to achieve a bondable wire. However, care should be taken in selecting wires, which are insulated with high temperature films, since the adhesive coating may not withstand the equally high temperatures. See Table 4-11. The temperatures, in Table 4-11, are for reference only. It is wise to always check with the manufacturer for the latest in materials and application notes. The addition of the adhesive coating over the film insulation will result in an increase in the finished diameter, by the same magnitude, as if going from a single to a heavy insulation.

Table 4-11

Bondable Overcoats			
Type	Operating Temperature	Heat Activation Temperature	Solvents Activating Agents
Polyvinyl Butryal	105°C	120° - 140°C	Alcohol
Epoxy	130°C	130° - 150°C	Methylethylketone Acetone
Polyester	130°C	130° - 150°C	Methylethylketone
Nylon	155°C	180° - 220°C	None

Bonding Methods

Heat Bonding may be accomplished by the use of a temperature-controlled oven. Small components can use a controlled hot air blower to bond the wires. In either case, caution should be used when handling the coil while it is still hot, since deformation can take place.

Resistance Bonding is a method where a current is passed through the winding to achieve the desired bonding temperature. This method generates a very even, heat distribution resulting in a good bonding throughout the winding. Many coils can be resistance-bonded at the same time. The current required for one coil, will be the same current required when many are connected in series. Just solder the coils in series then adjust the applied voltage until the same current is reached.

Solvent Bonding is a method where the solvent activates the bonding material. This can be done, by passing the wire through a solvent-saturated felt pad or a light spray application. There are many activating solvents that can be used: denatured ethyl alcohol, isopropyl alcohol, methylethylketone and acetone. The solvents should always be checked on with the manufacturer for the latest in materials and application notes.

Miniature Square Magnet Wire

When product miniaturization calls for more copper in a given area, MWS Microsquare film, insulated magnet wire, allows the design of compact coils to deliver more power in less space. See Table 4-12. Microsquare magnet wire is available in both copper and aluminum. It is also available in a range of solderable and high temperature film insulation. A cross-section of a number 26, heavy build, microsquare magnet wire is shown in Figure 4-20.

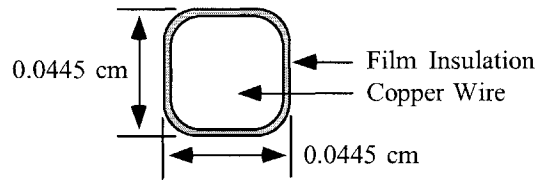


Figure 4-20. Cross-Section of a #26, Heavy, Microsquare Magnet Wire.

Table 4-12

Micro-Square Magnetic Wire (Nominal Dimension)								
Wire Size AWG	Bare Width cm	Bare Width Inch	Wire Area cm ²	Wire Area sq-mils	Copper Resistance Ω/cm	Aluminum Resistance Ω/cm	Single Width cm	Heavy Width cm
15	0.1450	0.0571	0.019614	3041	0.0000879	0.000144	0.1483	0.1514
16	0.1290	0.0508	0.015228	2361	0.0001132	0.000186	0.1323	0.1354
17	0.1151	0.0453	0.011816	1832	0.0001459	0.000239	0.1184	0.1212
18	0.1024	0.0403	0.009675	1500	0.0001782	0.000293	0.1054	0.1080
19	0.0912	0.0359	0.007514	1165	0.0002294	0.000377	0.0940	0.0968
20	0.0813	0.0320	0.006153	954	0.0002802	0.000460	0.0841	0.0866
21	0.0724	0.0285	0.004786	742	0.0003602	0.000591	0.0749	0.0772
22	0.0643	0.0253	0.003935	610	0.0004382	0.000719	0.0668	0.0688
23	0.0574	0.0226	0.003096	480	0.0005568	0.000914	0.0599	0.0620
24	0.0511	0.0201	0.002412	374	0.0007147	0.001173	0.0536	0.0556
25	0.0455	0.0179	0.002038	316	0.0008458	0.001388	0.0480	0.0498
26	0.0404	0.0159	0.001496	232	0.0011521	0.001891	0.0427	0.0445
27	0.0361	0.0142	0.001271	197	0.0013568	0.002227	0.0389	0.0409
28	0.0320	0.0126	0.001006	156	0.0017134	0.002813	0.0348	0.0366
29	0.0287	0.0113	0.000787	122	0.0021909	0.003596	0.0312	0.0330
30	0.0254	0.0100	0.000587	91	0.0029372	0.004822	0.0277	0.0295

Multistrand Wire and Skin Effect

Electronic equipment now operate at higher frequencies, and the predicted efficiency is altered, since the current carried by a conductor is distributed uniformly across the conductor, cross-section only, with direct current, and at low frequencies. The flux generated by the magnet wire is shown in Figure 4-21. There is a concentration of current near the wire surface at higher frequencies, which is termed the skin effect. This is the result of magnetic flux lines that generate eddy currents in the magnet wire, as shown in Figure 4-22.

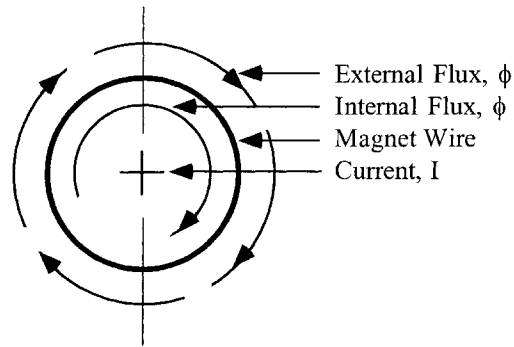


Figure 4-21. Flux Distribution in a Magnet Wire.

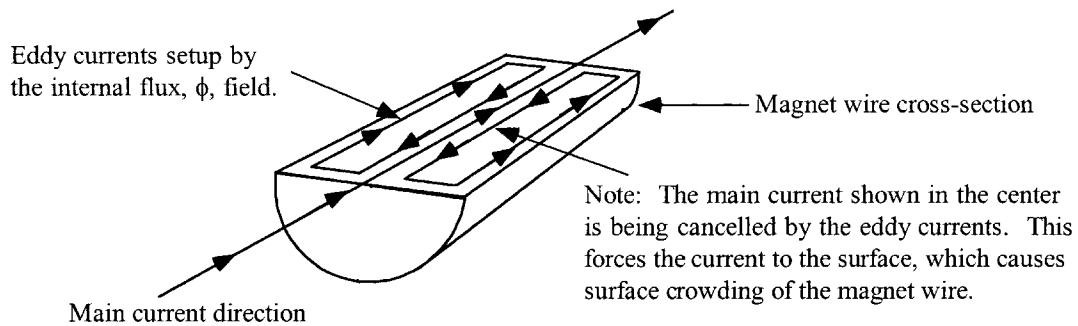


Figure 4-22. Eddy Currents Generated in a Magnet Wire.

Reduce Skin Effect in Transformers

Skin effect accounts for the fact that the ratio of effective alternating current resistance to direct current is greater than unity. The magnitude of this effect, at high frequency on conductivity, magnetic permeability, and inductance, is sufficient to require further evaluation of conductor size, during design. The skin depth is defined as the distance below the surface, where the current density has fallen to $1/e$ or 37 percent of its value at the surface.

$$\epsilon = \left(\frac{6.62}{\sqrt{f}} \right) K, \text{ [cm]} \quad [4-5]$$

ϵ , is the skin depth
 f , is frequency in hertz
 K , is equal to 1 for copper

When selecting the wire for high frequency, select a wire where the relationship between the ac resistance and the dc resistance is 1.

$$R_R = \frac{R_{ac}}{R_{dc}} = 1 \quad [4-6]$$

Using this approach, select the largest wire, operating at 100 kHz.

$$\epsilon = \left(\frac{6.62}{\sqrt{f}} \right) K, \text{ [cm]}$$

$$\epsilon = \left(\frac{6.62}{\sqrt{100,000}} \right) (1), \text{ [cm]} \quad [4-7]$$

$$\epsilon = 0.0209, \text{ [cm]}$$

The wire diameter is:

$$D_{AWG} = 2(\epsilon), \text{ [cm]}$$

$$D_{AWG} = 2(0.0209), \text{ [cm]} \quad [4-8]$$

$$D_{AWG} = 0.0418, \text{ [cm]}$$

The bare wire area $A_{w(B)}$ is:

$$A_{w(B)} = \frac{\pi D_{AWG}^2}{4}, \text{ [cm}^2\text{]}$$

$$A_{w(B)} = \frac{(3.14)(0.0418)^2}{4}, \text{ [cm}^2\text{]} \quad [4-9]$$

$$A_{w(B)} = 0.00137, \text{ [cm}^2\text{]}$$

The wire size closest to this area of 0.00137 is AWG #26 with 0.00128 cm². (See Table 4-9).

Calculating Skin Effect in Inductors

Inductors have skin effect problems just like transformers. The skin effect depends on the amount of ac current ΔI in the inductor. The high frequency inductor current has two components: the dc current, I_{dc} and the ac current, ΔI . The dc current travels in the center of the conductor, and the ac travels on the surface of the conductor, as shown in Figure 4-23.

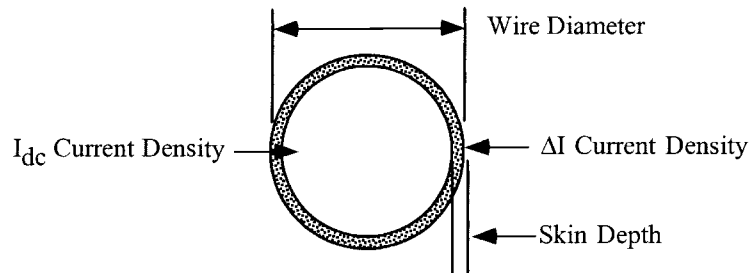


Figure 4-23. DC Inductor High Frequency Current Distribution.

The following procedure is used to calculate the high frequency current density, ΔI , while using Figure 4-23 as a reference.

The skin depth equation is:

$$\epsilon = \left(\frac{6.62}{\sqrt{f}} \right) K, \text{ [cm]} \quad [4-10]$$

Calculate the diameter of the copper conductor:

$$D_{AWG} = \sqrt{\frac{4(A_{w(B)})}{\pi}}, \text{ [cm]} \quad [4-11]$$

Subtract two times the skin depth, ϵ from the diameter, D_{AWG} .

$$D_n = D_{AWG} - 2\epsilon, \text{ [cm]} \quad [4-12]$$

Calculate the new wire area, A_n .

$$A_n = \frac{\pi(D_n)^2}{4}, \text{ [cm}^2\text{]} \quad [4-13]$$

The high frequency wire area, $A_{w(\Delta I)}$ is the difference between the wire area, $A_{w(B)}$ and the new area, A_n .

$$A_{w(\Delta I)} = A_{w(B)} - A_n, \text{ [cm}^2\text{]} \quad [4-14]$$

The ac current, ΔI in an inductor is a triangular waveform. The ΔI_{rms} current is:

$$\Delta I_{rms} = I_{pk} \sqrt{\frac{1}{3}}, \text{ [amps]} \quad [4-15]$$

Calculate the current density for the delta rms current, ΔI_{rms} .

$$J = \frac{\Delta I_{rms}}{A_{w(\Delta I)}}, \text{ [amps-per-cm}^2\text{]} \quad [4-16]$$

The delta rms current, ΔI_{rms} current density, J should be:

$$\Delta I_{rms} \text{ current density} \leq I_{dc} \text{ current density}$$

A graph of skin depth, as a function of frequency, is shown in Figure 4-24. The relationship of skin depth to AWG radius is shown in Figure 4-25, where $R_{ac}/R_{dc} = 1$ is plotted on a graph of AWG versus frequency.

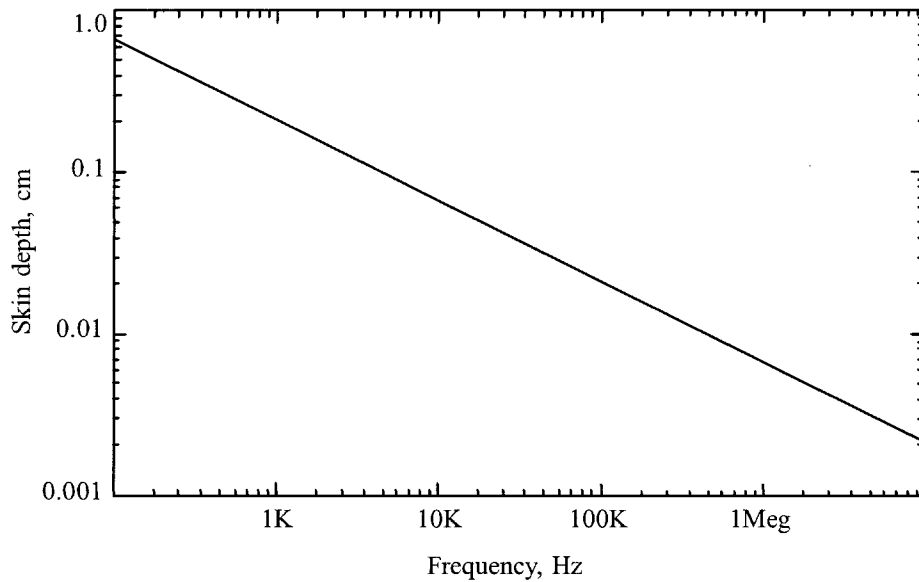


Figure 4-24. Skin Depth Versus Frequency.

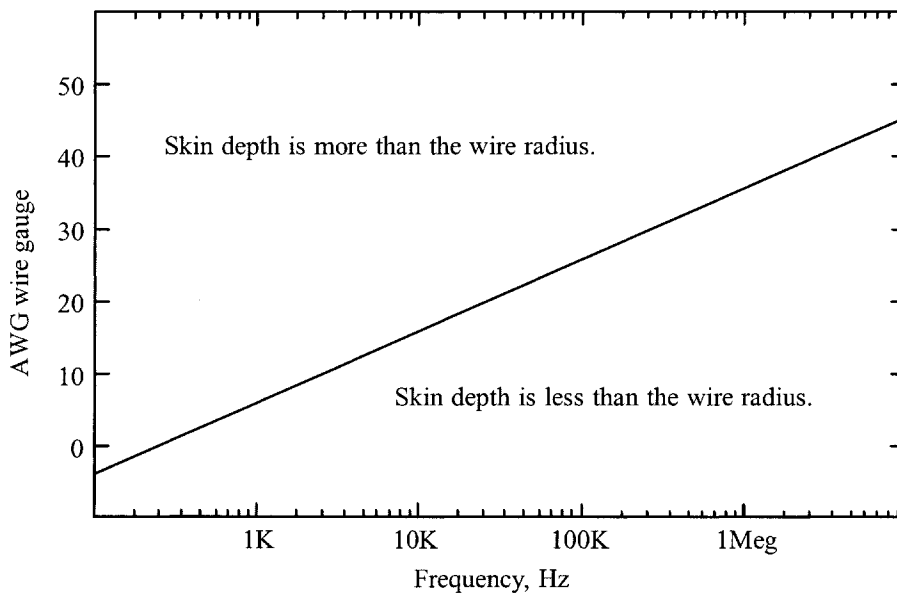


Figure 4-25. AWG Versus Frequency at Which Skin Depth Equals the Radius.

To illustrate how the AWG ac/dc resistance ratio changes with frequency, see Table 4-13. In Table 4-13, it can be seen that when a converter operates at 100 kHz, the largest wire that should be used is a number 26, with an ac/dc resistance ratio of 1.001.

Table 4-13

AWG ac/dc Resistance Ratio at Common Converter Frequencies									
AWG	D _(AWG) cm	25 kHz		50 kHz		100 kHz		200 kHz	
		ε cm	R _{ac}	ε cm	R _{ac}	ε cm	R _{ac}	ε cm	R _{ac}
			R _{dc}		R _{dc}		R _{dc}		R _{dc}
12	0.20309	0.041868	1.527	0.029606	2.007	0.020934	2.704	0.014802	3.699
14	0.16132	0.041868	1.300	0.029606	1.668	0.020934	2.214	0.014802	2.999
16	0.12814	0.041868	1.136	0.029606	1.407	0.020934	1.829	0.014802	2.447
18	0.10178	0.041868	1.032	0.029606	1.211	0.020934	1.530	0.014802	2.011
20	0.08085	0.041868	1.001	0.029606	1.077	0.020934	1.303	0.014802	1.672
22	0.06422	0.041868	1.000	0.029606	1.006	0.020934	1.137	0.014802	1.410
24	0.05101	0.041868	1.000	0.029606	1.000	0.020934	1.033	0.014802	1.214
26	0.04052	0.041868	1.000	0.029606	1.000	0.020934	1.001	0.014802	1.078
28	0.03219	0.041868	1.000	0.029606	1.000	0.020934	1.000	0.014802	1.006
30	0.02557	0.041868	1.000	0.029606	1.000	0.020934	1.000	0.014802	1.000

AWG Copper, skin depth is at 20°C.

Multistrand Litz Wire

The term litz wire is extracted from the German word, meaning woven wire. Litz wire is generally defined, as a wire constructed of individually, film insulated wires, braided together in a uniform pattern of twists and length of lay. This multistrand configuration minimizes the power losses, otherwise encountered, in a solid conductor, due to the skin effect. The minimum and maximum number of strand for standard litz wire is shown in Table 4-14. Magnet wire suppliers will supply larger, twisted magnet wire on request.

Table 4-14

Standard Litz Wire				
AWG	Minimum Strands	Approximate AWG	Maximum Strands	Approximate AWG
30	3	25	20	17.0
32	3	27	20	19.0
34	3	29	20	21.0
36	3	31	60	18.5
38	3	33	60	20.5
40	3	35	175	18.0
41	3	36	175	18.5
42	3	37	175	19.5
43	3	38	175	21.0
44	3	39	175	21.5
45	3	40	175	22.5
46	3	41	175	23.5
47	3	42	175	25.0
48	3	43	175	25.5

Proximity Effect

The operating frequency for power supplies is now in the range of 50 to 500 kHz. With it came along some new tasks for the engineer to address skin effect and proximity effect. They are quite similar in that they both generate eddy currents in the magnet wire. The eddy currents produced by these effects have the same solution, keeping the ratio of the ac resistance, R_{ac} , to the dc resistance, R_{dc} down:

$$R_R = \frac{R_{ac}}{R_{dc}} \quad [4-17]$$

The information provided here on proximity effect is taken from the five references provided at the end of this Chapter. The references are excellent, providing an in-depth analysis of the losses due to proximity effect, which is beyond the intent of this effort.

Proximity effect is caused by eddy currents induced in a wire due to the alternating magnetic field of other conductors in the vicinity. The flux generated by the magnet wire is shown in Figure 4-26. The eddy currents cause a distortion of the current density. This distortion is the result of magnetic flux lines that generate eddy currents in the magnet wire, therefore enhancing the main current, I , on one side and subtracting from the main current on the other, as shown in Figure 4-27. A magnet wire with its distorted current density is shown in Figure 4-28.

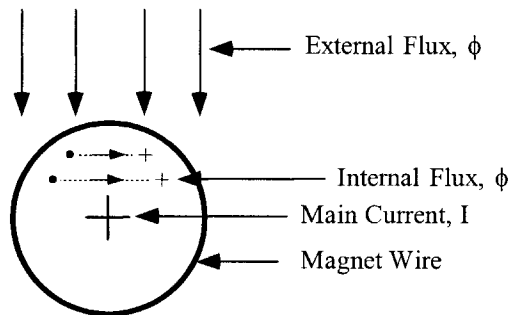


Figure 4-26. Flux Distribution in a Magnet Wire.

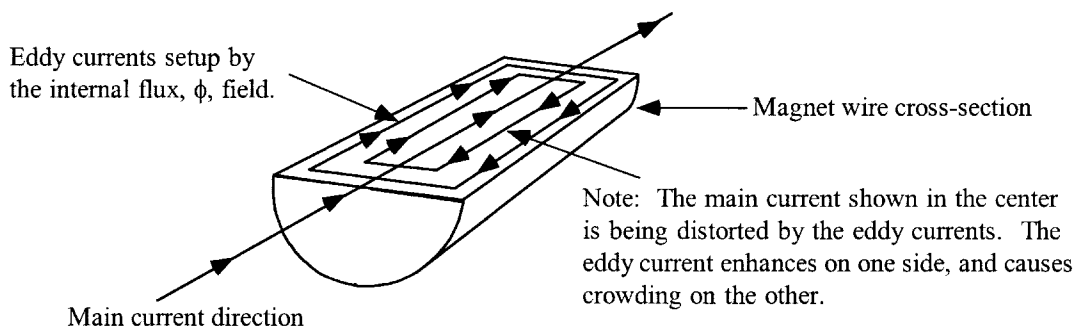


Figure 4-27. Eddy Currents Generated in a Magnet Wire.

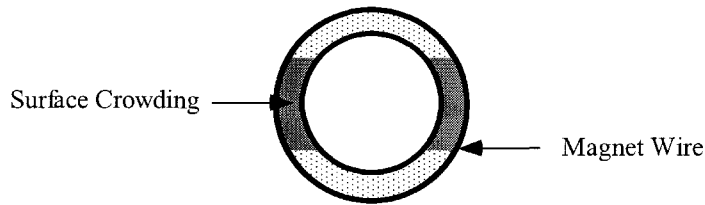


Figure 4-28. Magnet Wire, Showing Distorted Surface Crowding.

Proximity Effect in Transformers

Proximity effect has a minimum of impact on a transformer with a single layer secondary, as shown in Figure 4-29 along with its low frequency magneto-motive force (mmf) diagram. Keeping the proximity effect to a minimum requires the transformer to be designed with a minimum of layers. The selection of a core with a long narrow window will produce a design with a minimum of layers, in the same way as picking a core for a minimum of leakage inductance.

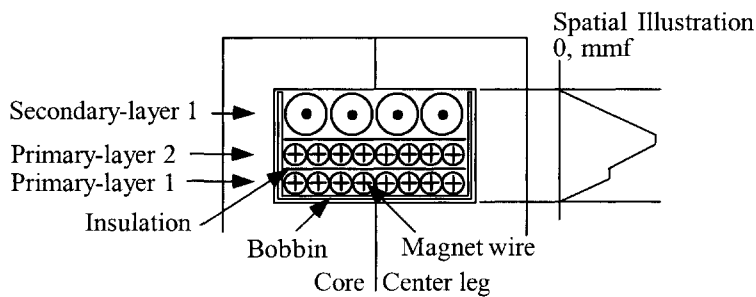


Figure 4-29. Simple Transformer Showing mmf.

Multiple Layer High Frequency Transformers and High Loss

The proximity effect is outlined for a transformer having a secondary with three layers, evenly spaced, as shown in Figure 4-30. A schematic diagram version of the transformer is shown in Figure 4-31, showing the different magneto-motive force ($\text{mmf} = F_m$) potentials. It is assumed that the high frequency penetration depth is 25%. The transformer has a 24 turn primary and a 24 turn secondary at 1 ampere. The transformer, A-T or magneto-motive force, (mmf) or F_m , is equal to 24.

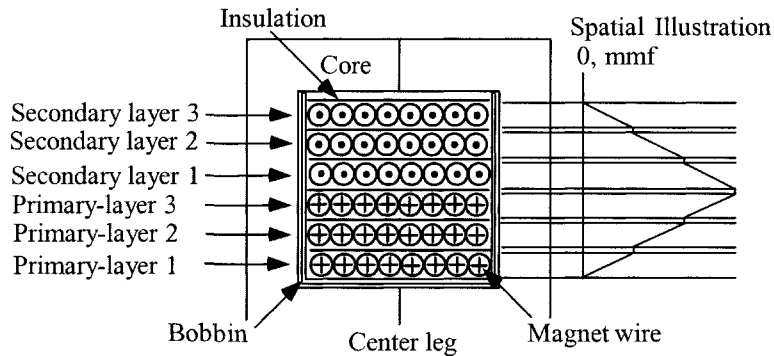


Figure 4-30. A Simple Transformer, Showing the Magneto-Motive Force, mmf.

$$F_m = NI, \quad [\text{magneto-motive force, mmf}]$$

$$\text{cgs, } F_m = 0.8NI, \quad [\text{magneto-motive force, mmf}] \quad [4-18]$$

The schematic diagram as shown in Figure 4-31, is used as a guide to show how the proximity effect impacts the layer wound transformers. The load current, I_o , equals 1 amp, and the secondary will have three identical layers, with each layer having eight turns. Due to the skin effect or penetration depth, each wire uses only 25% of the available area. Therefore, the current will be crowded into 25% of the available copper wire.

To the right of S3, the mmf is 0. At the left of S3, $F_m = 8 \text{ A-T}$.

1. The magnet field, ϕ_3 set up by the load current, I_o of 1 amp in layer S3 will generate a current, $1I_g$ in the winding layer, S2. It is in the opposite direction to the normal current flow and cancels the load current, I_o . The magneto-motive force, F_m , will generate 16 A-T or $I_c = 2$ amps to preserve the original load current, I_o , of 1 amp.
2. The magnet field, ϕ_2 set up by the load current, I_o , plus the difference between I_c and I_g in S2 will generate, $2I_g$, in the winding layer, S1. This is in the opposite direction to the normal current flow that cancels the load current, I_o , out. The magneto-motive force, F_m will generate, 24 A-T or $I_c = 3$ amps, to preserve the original load current, I_o , equals 1 amp.

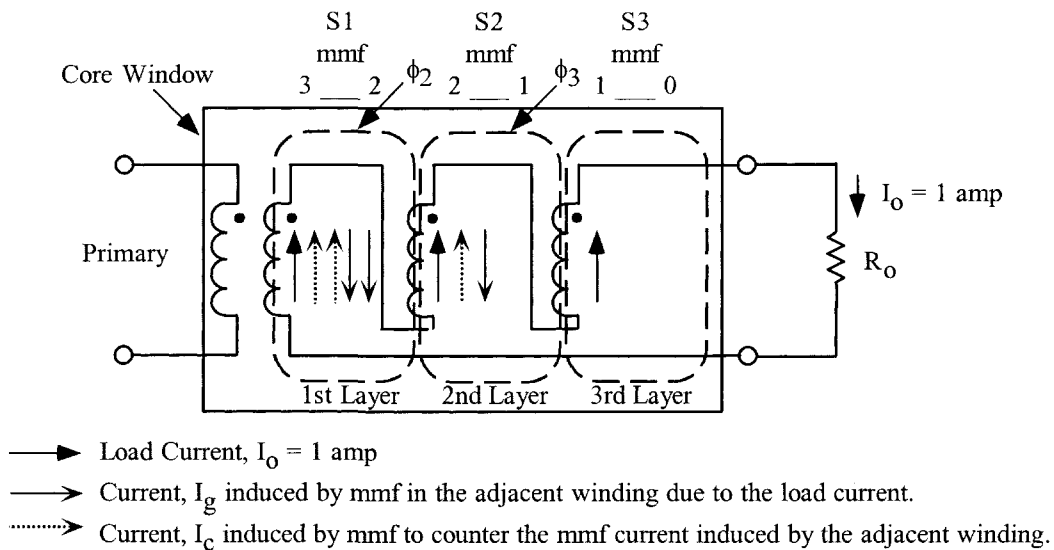


Figure 4-31. Transformer Schematic Diagram Showing mmf.

If the current in each layer is just the 1 amp, and limited in penetration, due to skin effect of only 25% of the conductor's thickness, the ac to dc resistance ratio, R_R , would be 4:1. The surface currents successive layers become much larger, as discussed above. The winding currents are tabulated in Table 4-15. The summation of the currents is given in Table 4-15. The current, I_g , is the adjacent winding induced current. The current, I_c , is the counter current induced by the magneto-motive force, mmf.

Table 4-15

Secondary Current Levels						
Winding	I_o	I_c	$I_o + I_c$	$I_o + I_c$	I_g	Total Wire Current
	amps	amps	amps	amps ²	amps	amps ²
S3	1	0	1	1	0	$(I_o + I_c)^2 = 1$
S2	1	1	2	4	1	$(I_o + I_c)^2 + (I_g)^2 = 5$
S1	1	2	3	9	2	$(I_o + I_c)^2 + (I_g)^2 = 13$

It can be seen, from the data in Table 4-15 that transformers with multiple layers operating at high frequency could be a real problem with proximity effect. The eddy current losses caused by the proximity effect go up exponentially as the number of layers. The selection of a core with a long winding length to a winding height ratio, will reduce the number of layers, as shown in Figure 4-32.

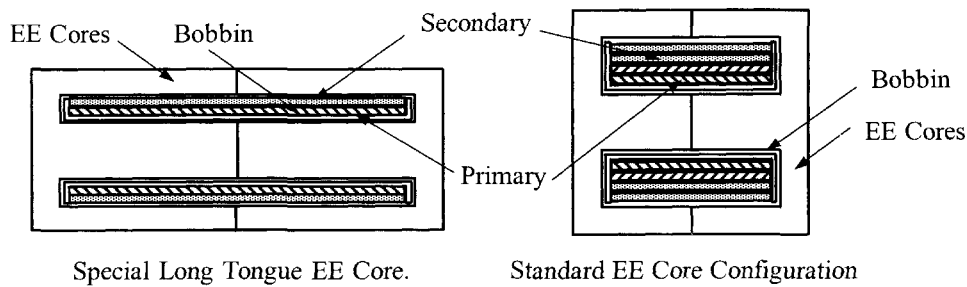


Figure 4-32. Comparing the Standard and the Special Long Tongue EE Cores.

Proximity Effect Using Dowell Curves

Dowell curves on proximity effect are shown in Figure 4-33. The vertical scale is, R_R , the ratio of R_{ac} to R_{dc} . The horizontal scale, K , is the ratio of the effective conductor height, or layer thickness, to the penetration depth, ϵ . On the right side of the curve it is labeled Number of Layers. These are segmented layers. Segmented layers are when the secondary is interleaved with the primary, then, each separation is a segment. The equation for K is:

$$K = \frac{h\sqrt{F_l}}{\epsilon} \quad [4-19]$$

$$h = 0.866D_{AWG}$$

Where:

$$F_l = \frac{ND_{AWG}}{l_w} \quad [4-20]$$

The variables in Equation 4-20 are described in Figure 4-34. It can be seen that if the number of turns, N , times the wire diameter, D_{AWG} are equal to the winding length, l_w , then, Equation 4-21 is simplified to:

$$K = \frac{h}{\varepsilon} \quad [4-21]$$

$$h = 0.866D_{AWG}$$

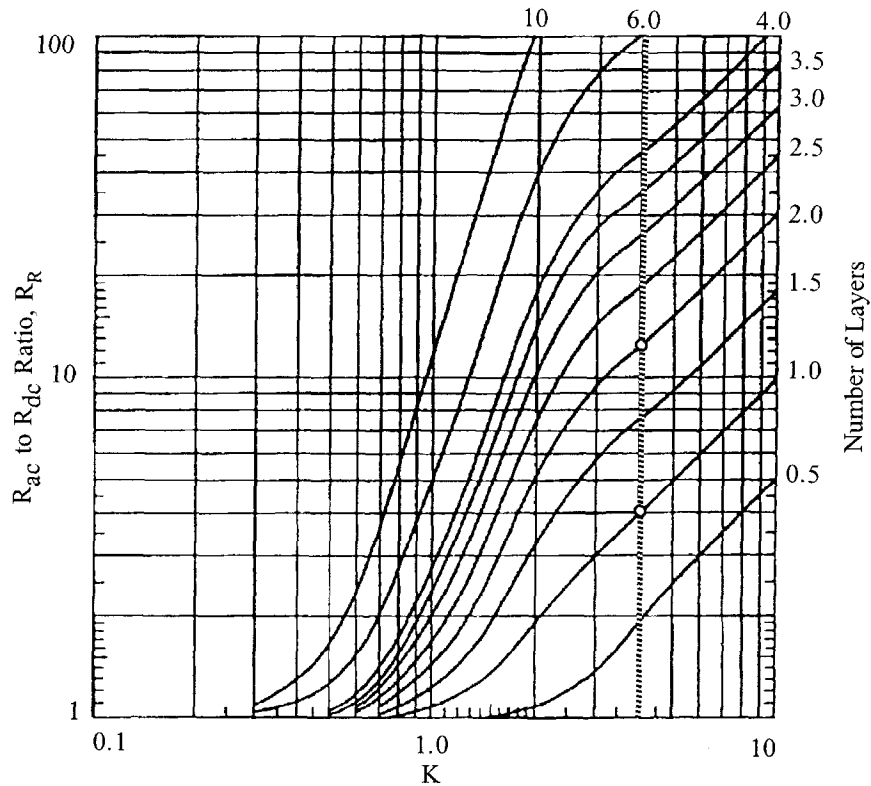


Figure 4-33. Ratio of ac/dc Resistance Due to Proximity Effect.

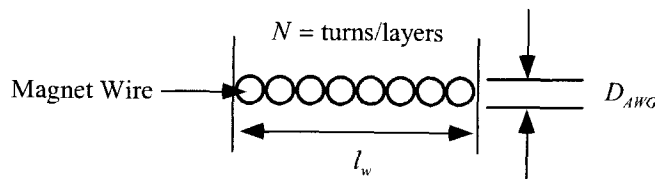


Figure 4-34. Winding Layer Parameters.

Using the Dowell curves as shown in Figure 4-33. Compare the loss ratio between the transformer in configuration A with two layers and transformer B that has the secondary interleaved with the primary, as shown in Figure 4-35. With a skin effect penetration depth of 25%, it will yield a, K , factor of 4. Both transformers, A and B, have the same A-T, but since the windings on transformer B are interleaved, it has only half the low frequency magneto-motive force (mmf).

There is a vertical dotted line shown in Figure 4-33, where $K = 4$. Follow the dotted line up to where it intersects 1 layer, then read the vertical column on the left, $R_R = 4$. Now follow the dotted line up to where it intersects 2 layer, then read the vertical column on the left, $R_R = 13$. Transformer B with its interleaved windings has a lower ac to dc resistance ratio, R_R , by a factor 3.25.

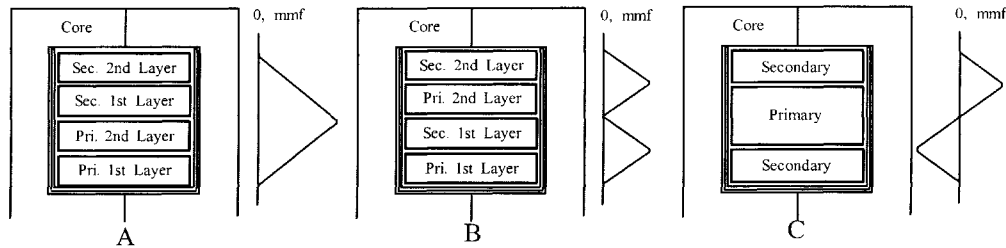


Figure 4-35. Transformers Wound with Different Primary and Secondary Configurations.

The proximity effect, with its exponentially losses tends to be the dominant conductor loss mechanism in high frequency magnetic components, particularly when windings are multi-layered.

Specialty Wire

There are a lot of new ideas out in the wire industry, if only the engineer had the time to evaluate these new concepts to build confidence and apply them.

Triple Insulated Wire

Transformers designed to meet the IEC/VDE safety specification requirements for creepage and clearance must adhere to one of the following specifications:

1. VDE0805
2. IEC950
3. EN60950
4. UL1950-3e
5. CSA 950-95

The engineer must be aware that one specification does not encompass all applications. For example, the IEC has specifications for office machines, data-processing equipment, electromedical equipment, appliances, and others.

Originally these IEC specifications were developed around linear 50 and 60 Hz transformers, and were not, always, conducive to optimal designs for high frequency, such as switching power transformers. The complexity of a standard, high frequency, switching type transformer, designed to the IEC/VDE safety specification, is shown in Figure 4-36. In any switching transformer, coupling has the highest priority because of the leakage flux.

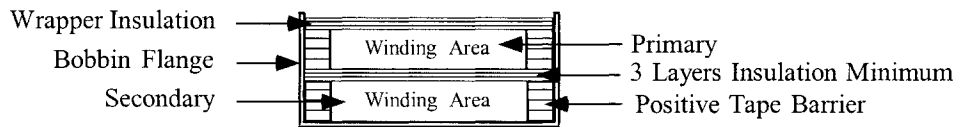


Figure 4-36. Bobbin Cross-Section Design to Meet IEC/VDE Specifications.

The triple, insulated wire was developed to meet the above specification and eliminate the need for three layers of insulating tape between primary and secondary. Also, the triple, insulated wire eliminates the need for the creepage margin, and now, the whole bobbin can be used for winding. This wire can also be used as hook-up wire, from the primary or secondary, to the circuits, without the use of sleeving or tubing.

The construction of the triple, insulated wire is shown in Figure 4-37. The temperature range for this type of wire is from 105°C to 180°C. The dimensions for triple, insulated wire are shown in Table 4-16, using a 0.002 inch coat per layer. Other thicknesses are available. The manufacturer, Rubadue Wire Company, is listed in the Reference section on page 4-41.

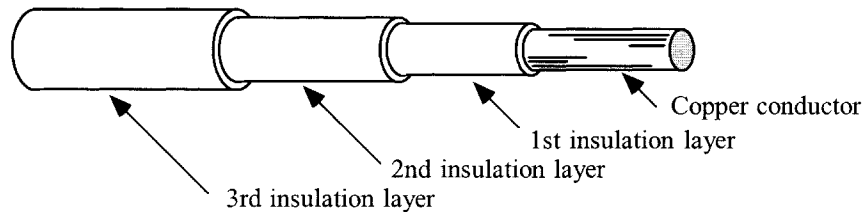


Figure 4-37. Triple, Insulated Wire Construction.

Triple Insulated Litz

High frequency litz wire, shown in Figure 4-38, is also available as a triple insulated wire from manufacturers. The insulation layers' thickness for litz wire comes in 0.002 and 0.003 inches.

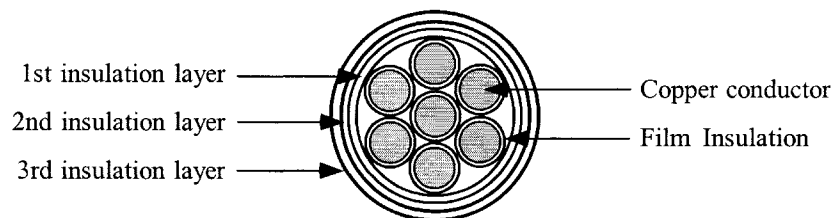


Figure 4-38. Triple, Insulated Litz Wire.

Table 4-16

Triple Insulated Wire (.002) Material						
AWG	Bare Wire				With Insulation	
	Area cm ² (10 ⁻³)	Diameter inch	Diameter mm	Resistance μΩ/cm	Diameter inch	Diameter mm
16	13.0700	0.0508	1.2903	132	0.0628	1.5951
18	8.2280	0.0403	1.0236	166	0.0523	1.3284
19	6.5310	0.0359	0.9119	264	0.0479	1.2167
20	5.1880	0.0320	0.8128	332	0.0440	1.1176
21	4.1160	0.0285	0.7239	419	0.0405	1.0287
22	3.2430	0.0253	0.6426	531	0.0373	0.9474
23	2.5880	0.0226	0.5740	666	0.0346	0.8788
24	2.0470	0.0201	0.5105	842	0.0321	0.8153
25	1.6230	0.0179	0.4547	1062	0.0299	0.7595
26	1.2800	0.0159	0.4039	1345	0.0279	0.7087
27	1.0210	0.0142	0.3607	1687	0.0262	0.6655
28	0.8046	0.0126	0.3200	2142	0.0246	0.6248
29	0.6470	0.0113	0.2870	2664	0.0233	0.5918
30	0.5067	0.0100	0.2540	3402	0.0220	0.5588
32	0.3242	0.0080	0.2032	5315	0.0200	0.5080
34	0.2011	0.0063	0.1600	8572	0.0183	0.4648
36	0.1266	0.0050	0.1270	13608	0.0170	0.4318
38	0.0811	0.0040	0.1016	21266	0.0160	0.4064

Polyfilar Magnetic Wire

Poly or multiple strands of magnet wire, bonded together, can be used in many high frequency transformer and inductor applications. Round polyfilar magnet wire is shown in Figure 4-39, and square polyfilar is shown in Figure 4-40. Both can be used in place of foil in some applications. Polyfilar magnet wire can be used as a foil type winding, such as a low voltage, high current, or even a Faraday shield. The polyfilar, magnet wire strip width can be easily increased or decreased by adding or removing wires to provide the proper strip width to fit a bobbin. It is relatively easy to wind. Polyfilar wire has complete insulation, and it does not have the sharp edge problem that could cut insulation in the way foil does. It is not recommended to wind a transformer with polyfilar magnet wire in order to have an exact center tap, unless it is just a few turns, because of the penalty in capacitance. If the use of polyfilar is necessary, then use a magnet wire with a film insulation that has a low dielectric constant. See Table 4-8.

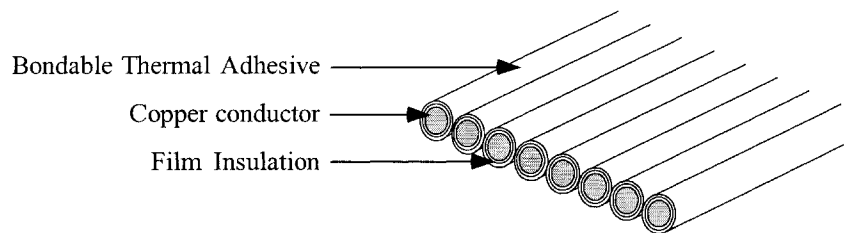


Figure 4-39. Polyfilar, Strip-Bonded, Round Magnet Wire.

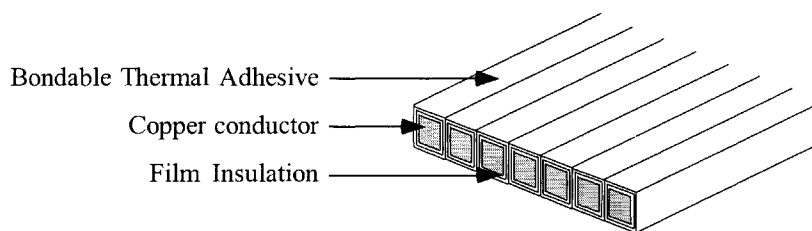


Figure 40. Polyfilar, Strip-Bonded, Square Magnet Wire.

Standard Foils

The biggest advantage for using foil over magnet wire is the fill factor. The design of a high current, high frequency, dc to dc converter is common place. The main reason for going to high frequency is the reduction in size. The power transformer is the largest component in the design. When designing high frequency transformers, the design equations relate to a very small transformer. When operating transformers at high frequencies, the skin effect becomes more and more dominate, and requires the use of smaller wire. If larger wire is required, because of the required current density, then, more parallel strands of wire will have to be used (litz wire). The use of small wire has a large effect on the fill factor.

When using foil, the gain in the fill factor is the biggest improvement over litz. To make a comparison, a litz design is shown in Figure 4-41, and a foil design is shown in Figure 4-42. In the litz design, there is a percentage of the winding area which cannot be used for the conductors. This lost area is made up of voids, space between the wires, and the insulation film on the wire. The foil wound coil, shown in Figure 4-42, can be designed to make optimum use of the available winding area. Each turn of the foil can extend, within limits, edge-to-edge of the bobbin or tube. The insulation required between layers is at a minimum, as long as the foil has been rolled to remove the sharp burr as shown in Figure 4-46.

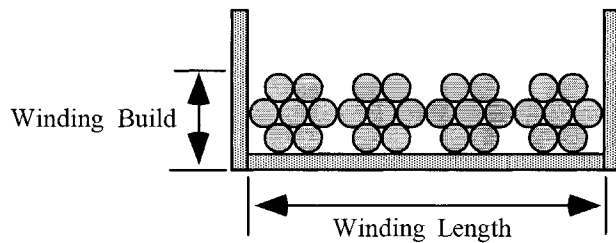


Figure 4-41. Layer Winding, Using Litz Magnet Wire.

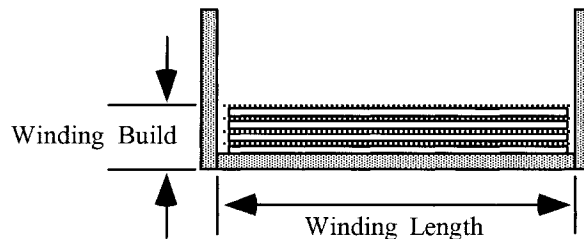


Figure 4-42. Layer Winding, Using Foil with Insulation.

The Use of Foils

Designing transformers and inductors, with foil, is a very laborious task, especially if the engineer only does it now and then. A monumental job, in itself, is finding out where to get the materials. Foil has its advantages, mainly, in high current, high frequency, and a high density environment.

The window utilization factor, K_u , can be greater than 0.6, under the right conditions, without a lot of force. The standard foil materials used, by transformer engineers, are copper and aluminum. The engineer has a good selection of standard thicknesses as shown:

1.0 mil, 1.4 mil, 2.0 mil, 5.0 mil, and 10 mil

The engineer will find other thicknesses available, but standard thicknesses should be considered first. Be careful of using a nonstandard thickness. What you might be using could be from an overrun, and could create problems for you. Foil comes in standard widths, in inches, as shown:

0.25, 0.375, 0.50, 0.625, 0.75, 1.0, 1.25, 1.50, 2.00, 2.50, 3.00, 4.00 (inches)

Standard widths are the widths that are most readily available. There are also different styles of pre-fab foils, as shown in Figures 4-43, 4-44, and 4-45.

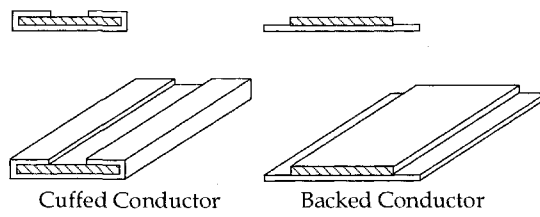


Figure 4-43. Pre-fab Foils.

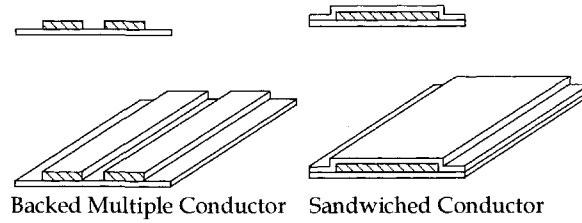


Figure 4-44. Pre-fab Foils.

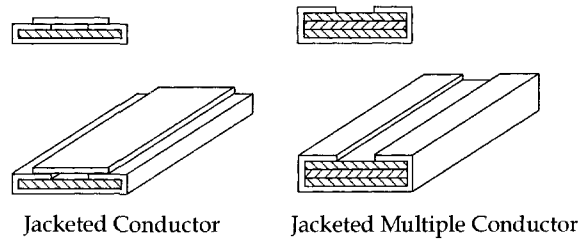


Figure 4-45. Pre-fab Foils.

Although special slitting is done all the time, there is normally a minimum buy. When slitting is done, special care must be attended to, with the sharp edges, as shown in Figure 4-46. The cut edge should be rolled after slitting it, at least two times, to remove the sharp burrs that could cut through the insulation. Therefore it is wise not to use insulation between layers of less than 1 mil.

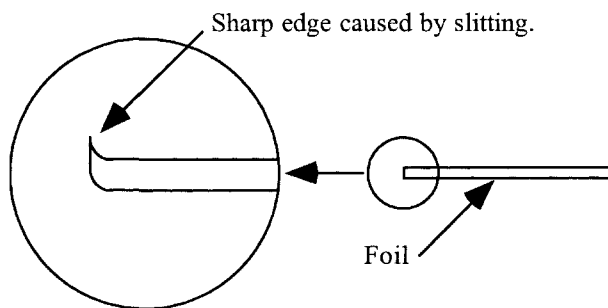


Figure 4-46. Foil with Sharp Edge Burrs after Slitting.

When winding transformers or inductors with foil, special care must be taken with lead finishing. One of the biggest problems about using foil is solder wicking. This wicking will puncture the insulation, resulting in a shorted turn. The normal insulation used for foil is very thin. Winding with foil, the coil is still subjected to bowing, only more so, as shown in Figure 4-7.

Foil used for winding transformers and inductors should be dead soft. There is another shortcoming about using foil, and that is, the inherent capacitance build-up, as shown in Figure 4-47.

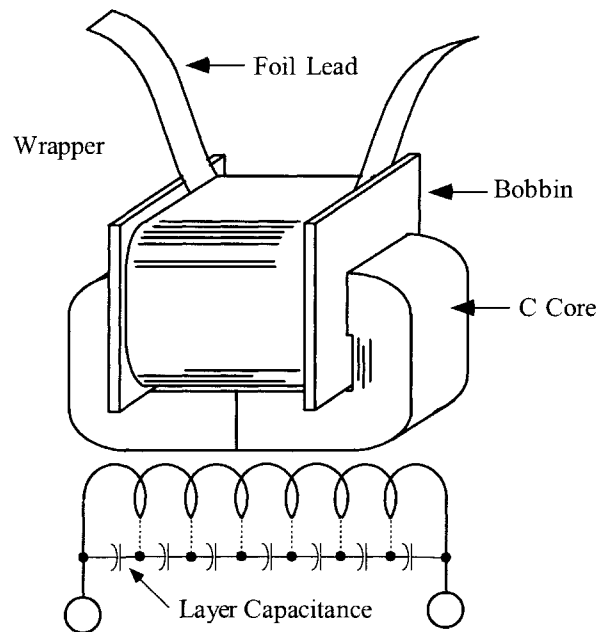


Figure 4-47. Foil Capacitance Equation.

The capacitance build-up is expressed:

$$C = 0.0885 \left(\frac{K(N-1)(MLT)(G)}{d} \right), \quad [pfd] \quad [4-22]$$

K = Dielectric Constant

MLT = Mean Length Turn

N = Number of Turns

G = Foil Width, cm

d = Layer Insulation Thickness, cm

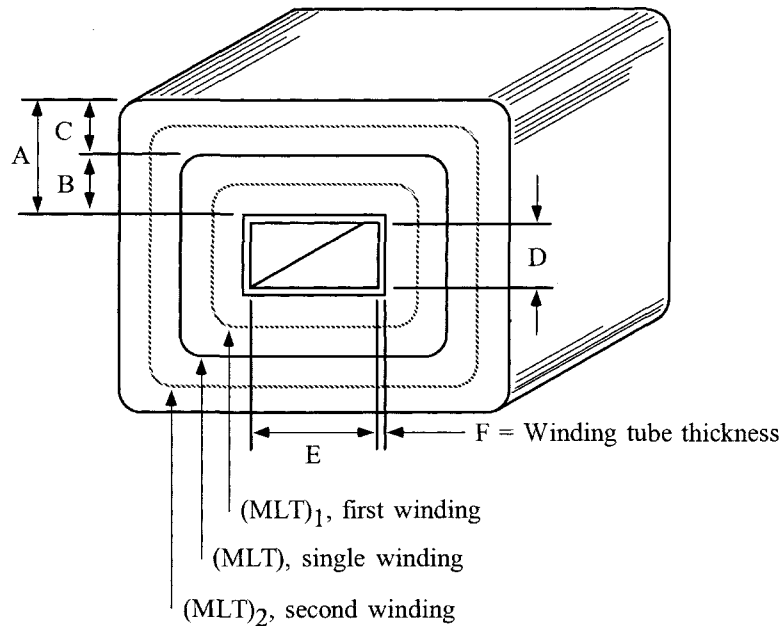
The dielectric constant K for different materials can be found in Table 4-17.

Table 4-17

Dielectric Constants	
Material	K
Kapton	3.2-3.5
Mylar	3-3.5
Kraft Paper	1.5-3.0
Fish Paper	1.5-3.0
Nomex	1.6-2.9

Calculating, MLT

The Mean Length Turn, (MLT), is required to calculate the winding resistance and weight for any given winding. The winding dimensions, relating to the Mean Length Turn, (MLT) for a tube or bobbin coil, are shown in Figure 4-48.



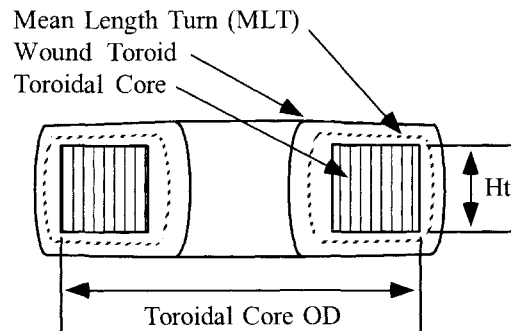
$$\begin{aligned}
 \text{MLT} &= 2(D + 2F) + 2(E + 2F) + \pi A, \quad \text{single winding} \\
 \text{MLT}_1 &= 2(D + 2F) + 2(E + 2F) + \pi B, \quad \text{first winding} \\
 \text{MLT}_2 &= 2(D + 2F) + 2(E + 2F) + \pi(2B + C), \quad \text{second winding}
 \end{aligned}
 \tag{4-23}$$

Figure 4-48. Dimensions, Relating to the Winding Mean Length Turn, (MLT).

Calculating, MLT (toroid)

It is very difficult to calculate the Mean Length Turn (MLT) for a toroidal core that would satisfy all conditions. There are just too many ways to wind a toroid. If the toroid were designed to be wound by machine, then that would require a special clearance for a wire shuttle. If the toroid were designed to be

hand-wound, the wound inside diameter would be different. The fabrication of a toroidal design is weighted heavily on the skill of the winder. A good approximation for a toroidal core, Mean Length Turn (MLT), is shown in Figure 4-49.



$$MLT = 0.8(OD + 2(Ht)), \text{ approximation [4-24]}$$

Figure 4-49. Toroidal Mean Length Turn (MLT), is an Approximation.

Copper Resistance

The dc resistance calculation of a winding requires knowing the total length, l , of the conductor, the cross-sectional area, A_w , of the conductor, and the resistivity, ρ , of the conductor material. The value for the resistivity, ρ , in $\mu\Omega$ per cm for three different conductor materials can be found in Table 4-7.

$$R_{dc} = \left(\frac{\rho l}{A_w} \right), \text{ } [\Omega] \text{ [4-20]}$$

Copper Weight

The weight calculation of a winding requires knowing the total length, l , of the conductor, the cross-sectional area, A_w , of the conductor, and the density, λ , of the conductor material. The value for the density, λ , in grams per cm^3 for three different conductor materials, can be found in Table 4-7.

$$W_t = \lambda l A_w, \text{ [grams] [4-21]}$$

Electrical Insulating Materials

The reliability and life span of a magnetic component depends on the stress level put upon the insulating materials. If the design or workmanship is not incorporated, then, insulation will not help you.

References

1. P.L. Dowell, "Effects of Eddy Currents in Transformer Windings," Proceedings IEE (UK), Vol. 113, No.8, August 1966, pp 1387-1394.
2. B. Carsten, "High Frequency Conductor Losses in Switch Mode Magnetics," High Frequency Power Converter Conference, 1986, pp 155-176.
3. L. Dixon, Eddy Current Losses in Transformer Windings and Circuit Wiring, Unitrode Corp. Power Supply Seminar Handbook, Unitrode Corp., Watertown MA, 1988.
4. E. Snelling, Soft Ferrites, pp 341-348, Iliffe, London, 1969.
5. A.I. Pressman, Switching Power Supply Design, pp 298-317, McGraw-Hill, Inc., New York 1991.
6. E.C. Snelling, Soft Ferrites, CRC Press, Iliffe Books Ltd., 42 Russell Square, London, W.C.I, 1969.
7. Werner Osterland, "The Influence of Wire Characteristics on the Winding Factor and Winding Method," WIRE, Coburg, Germany. Issue 97, October 1968.
8. H.A. George, "Orthocyclic Winding of Magnet Wire Without Interleaving Materials," Insulation/Circuits, August 1976.
9. MWS Wire Industries, "Wire Catalog," Revised June, 1992, 31200 Cedar Valley Drive, Westlake Village, CA 91362.
10. Alpha-Core Inc. (Special Foils), 915 Pembroke Street, Bridgeport, CT 06608 Phone: (203) 335 6805.
11. Industrial Dielectrics West, Inc., (Special Foils), 455 East 9th Street, San Bernardino, CA 92410 Phone: (909) 381 4734.
12. Rubadue Wire Company, Inc., (Triple Insulated Wire), 5150 E. LaPalma Avenue, Suite 108, Anaheim Hills, CA 92807 Phone: (714) 693 5512, Email: www.rubaduewire.com.

Chapter 5

Transformer Design Trade-Offs

Table of Contents

1. Introduction	5-3
2. The Design Problem Generally	5-3
3. Power Handling Ability	5-4
4. Relationship, A_p , to Transformer Power Handling Capability	5-4
5. Relationship, K_g , to Transformer Regulation and Power Handling Capability	5-5
6. Transformer Area Product, A_p	5-6
7. Transformer Volume and the Area Product, A_p	5-6
8. Transformer Weight and the Area Product, A_p	5-9
9. Transformer Surface Area and the Area Product, A_p	5-11
10. Transformer Current Density, J , and the Area Product, A_p	5-14
11. Transformer Core Geometry, K_g , and the Area Product, A_p	5-17
12. Weight Versus Transformer Regulation	5-20
13. References	5-20

Introduction

The conversion process in power electronics requires the use of transformer components that are frequently the heaviest and bulkiest item in the conversion circuit. They also have a significant effect upon the overall performance and efficiency of the system. Accordingly, the design of such transformers has an important influence on the overall system weight, power conversion efficiency, and cost. Because of the interdependence and interaction of these parameters, judicious trade-offs are necessary to achieve design optimization.

The Design Problem Generally

The designer is faced with a set of constraints that must be observed in the design on any transformer. One of these constraints is the output power, P_o (operating voltage multiplied by maximum current demand) in that the secondary winding must be capable of delivering to the load within specified regulation limits. Another constraint relates to minimum efficiency of operation, which is dependent upon the maximum power loss that can be allowed in the transformer. Still another constraint defines the maximum permissible temperature rise for the transformer when it is used in a specified temperature environment.

One of the basic steps in transformer design is the selection of proper core material. Magnetic materials used to design low and high frequency transformers are shown in Table 5-1. Each one of these materials has its own optimum point in the cost, size, frequency and efficiency spectrum. The designer should be aware of the cost difference between silicon-iron, nickel-iron, amorphous and ferrite materials. Other constraints relate to volume occupied by the transformer and, particularly in aerospace applications, weight minimization is an important goal. Finally, cost effectiveness is always an important consideration.

Depending upon the application, some of these constraints will dominate. Parameters affecting others may then be traded off, as necessary, to achieve the most desirable design. It is not possible to optimize all parameters in a single design because of their interaction and interdependence. For example, if volume and weight are of great significance, reductions in both can often be affected, by operating the transformer at a higher frequency, but with the penalty being in efficiency. When, the frequency cannot be increased, reduction in weight and volume may still be possible by selecting a more efficient core material, but with the penalty of increased cost. Thus, judicious trade-offs must be affected to achieve the design goals.

Transformer designers have used various approaches in arriving at suitable designs. For example, in many cases, a rule of thumb is used for dealing with current density. Typically, an assumption is made that a good working level is 200 amps-per-cm² (1000 circular mils-per-ampere). This rule of thumb will work in many instances, but the wire size needed to meet this requirement may produce a heavier and bulkier transformer than desired or required. The information presented in this Chapter makes it possible to avoid the assumption use of this and other rules of thumb, and to develop a more economical design with great accuracy.

Table 5-1. Magnetic Materials and Their Characteristics

Magnetic Core Material Characteristics					
Material Name	Initial Permeability μ_i	Flux Density Tesla B_s	Curie Temperature °C	dc, Coercive Force, Hc Oersteds	Operating Frequency f
Iron Alloys					
Magnesil	1.5 K	1.5-1.8	750	0.4-0.6	< 2kHz
Supermendur*	0.8 K	1.9-2.2	940	0.15-0.35	< 1kHz
Orthonol	2 K	1.42-1.58	500	0.1-0.2	< 2kHz
Sq. Permalloy	12 K-100 K	0.66-0.82	460	0.02-0.04	< 25kHz
Supermalloy	10 K-50 K	0.65-0.82	460	0.003-0.008	< 25kHz
Amorphous					
2605-SC	3K	1.5-1.6	370	0.03-0.08	< 250kHz
2714A	20K	0.5-0.58	> 200	0.008-0.02	< 250kHz
Vitro perm 500	30K	1.0-1.2	> 200	< 0.05	< 250kHz
Ferrite					
MnZn	0.75-15K	0.3-0.5	100-300	0.04-0.25	< 2MHz
NiZn	15-1500	0.3-0.5	150-450	0.3-0.5	< 100MHz
* Field Anneal.					

Power Handling Ability

For years, manufacturers have assigned numeric codes to their cores to indicate their power-handling ability. This method assigns to each core a number called the area product, A_p . That is the product of the window area, W_a , and the core cross-section, A_c . The core suppliers use these numbers to summarize dimensional and electrical properties in their catalogs. They are available for laminations, C cores, ferrite cores, powder cores, and toroidal tape wound cores.

Relationship, A_p , to Transformer Power Handling Capability

Transformers

According to the newly developed approach, the power handling capability of a core is related to its area product, A_p , by an equation, which may be stated as:

$$A_p = \frac{P_t (10^4)}{K_f K_u B_m J f}, \quad [\text{cm}^4] \quad [5-1]$$

Where:

K_f = waveform coefficient

4.0 square wave

4.44 sine wave

From the above, it can be seen that factors such as flux density, frequency of operation, and window utilization factor K_u , define the maximum space which may be occupied by the copper in the window.

Relationship, K_g , to Transformer Regulation and Power Handling Capability

Although most transformers are designed for a given temperature rise, they can also be designed for a given regulation. The regulation and power-handling ability of a core is related to two constants:

$$\alpha = \frac{P_t}{2K_g K_e}, \quad [\%] \quad [5-2]$$

$$\alpha = \text{Regulation } (\%) \quad [5-3]$$

The constant, K_g , (See Chapter 7) is determined by the core geometry, which may be related by the following equations:

$$K_g = \frac{W_a A_c^2 K_u}{\text{MLT}}, \quad [\text{cm}^5] \quad [5-4]$$

The constant, K_e , is determined by the magnetic and electric operating conditions, which may be related by the following equation:

$$K_e = 0.145 K_f^2 f^2 B_m^2 (10^{-4}) \quad [5-5]$$

Where:

K_f = waveform coefficient

4.0 square wave

4.44 sine wave

From the above, it can be seen that factors such as flux density, frequency of operation, and waveform coefficient, have an influence on the transformer size. Because of their significance, the area product, A_p , and the core geometry, K_g , are treated extensively in this handbook. A great deal of other information is also presented for the convenience of the designer. Much of the information is in tabular form to assist designers in making the trade-offs best suited for the particular application, in a minimum amount of time.

Transformer Area Product, A_p

The author has developed additional relationships between, A_p , numbers and current density, J , for given regulation and temperature rise. The area product, A_p , is a length dimension to the fourth power, (l^4), as shown in Figure 5-1.

$$\begin{aligned} W_a &= FG, \quad [\text{cm}^2] \\ A_c &= DE, \quad [\text{cm}^2] \quad [5-6] \\ A_p &= W_a A_c, \quad [\text{cm}^4] \end{aligned}$$

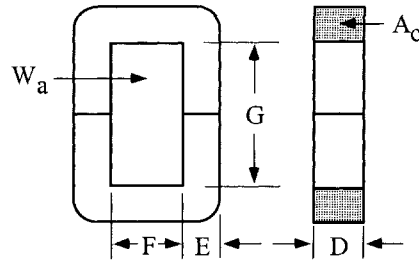


Figure 5-1. C Core Outline Showing the Window Area, W_a and Iron Area, A_c .

It should be noted. The constants for tape-wound cores, such as: K_{vol} , K_w , K_s , K_j and K_p will have a tendency to jump around and not be consistent. This inconsistency has to do with the core being in a housing, without true proportions.

Transformer Volume and the Area Product, A_p

The volume of a transformer can be related to the area product, A_p of a transformer, treating the volume, as shown in Figures 5-2 to 5-4, as a solid quantity without any subtraction for the core window. The relationship is derived according to the following reasoning: Volume varies in accordance with the cube of any linear dimension, (l), whereas area product, A_p , varies as the fourth power:

$$\text{Volume} = K_1 l^3, \quad [\text{cm}^3] \quad [5-7]$$

$$A_p = K_2 l^4, \quad [\text{cm}^4] \quad [5-8]$$

$$l^4 = \frac{A_p}{K_2} \quad [5-9]$$

$$l = \left(\frac{A_p}{K_2} \right)^{(0.25)} \quad [5-10]$$

$$l^3 = \left[\left(\frac{A_p}{K_2} \right)^{0.25} \right]^3 = \left(\frac{A_p}{K_2} \right)^{0.75} \quad [5-11]$$

$$\text{Volume} = K_1 \left(\frac{A_p}{K_2} \right)^{0.75} \quad [5-12]$$

$$K_{vol} = \frac{K_1}{K_2^{(0.75)}} \quad [5-13]$$

The volume-area product, A_p , relationship is therefore:

$$\text{Volume} = K_{vol} A_p^{(0.75)}, \quad [\text{cm}^3] \quad [5-14]$$

in which, K_{vol} , is a constant related to core configuration whose values are given in Table 5-2. These values were obtained by averaging the values from the data taken from Tables 3-1 through Tables 3-64 in Chapter 3.

Table 5-2. Volume-Area Product Relationship.

Volume-Area Product Relationship	
Core Type	K_{vol}
Pot Core	14.5
Powder Core	13.1
Laminations	19.7
C Core	17.9
Single-coil C Core	25.6
Tape-wound Core	25.0

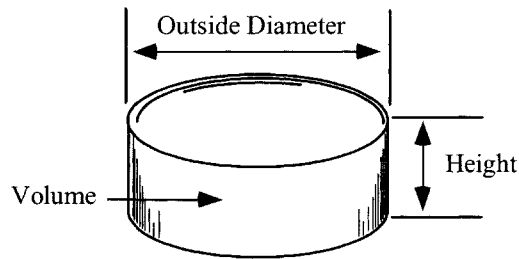


Figure 5-2. Toroidal Transformer Outline, Showing the Volume.

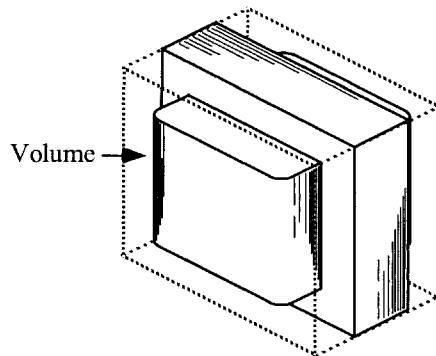


Figure 5-3. EI Core Transformer Outline, Showing the Volume.

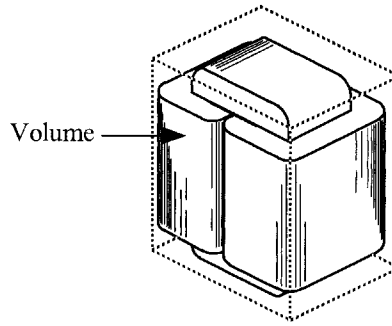


Figure 5-4. C Core Transformer Outline, Showing the Volume.

The relationship between volume and area product, A_p , for various core types is graphed in Figures 5-5 through 5-7. The data for these Figures has been taken from Tables in Chapter 3.

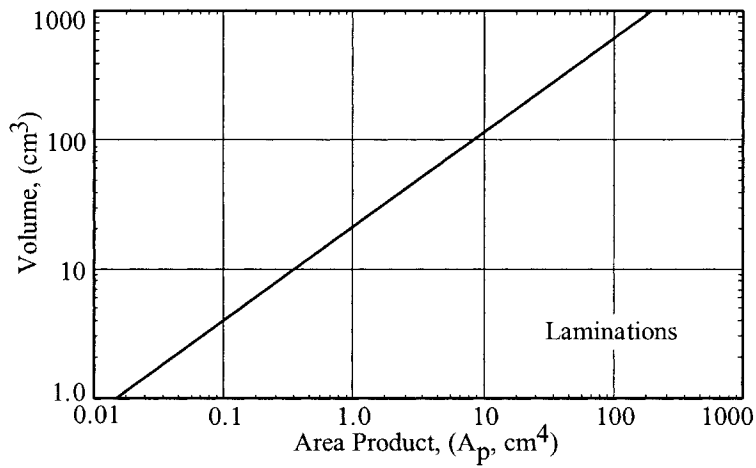


Figure 5-5. Volume Versus Area Product, A_p for EI Laminations.

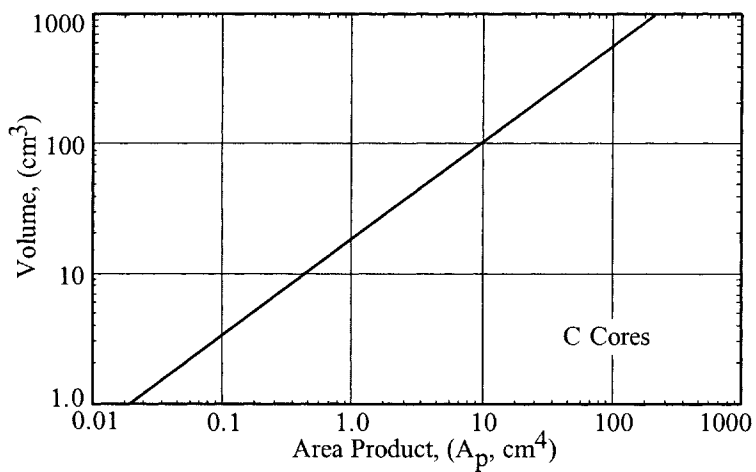


Figure 5-6. Volume Versus Area Product, A_p for C Cores.

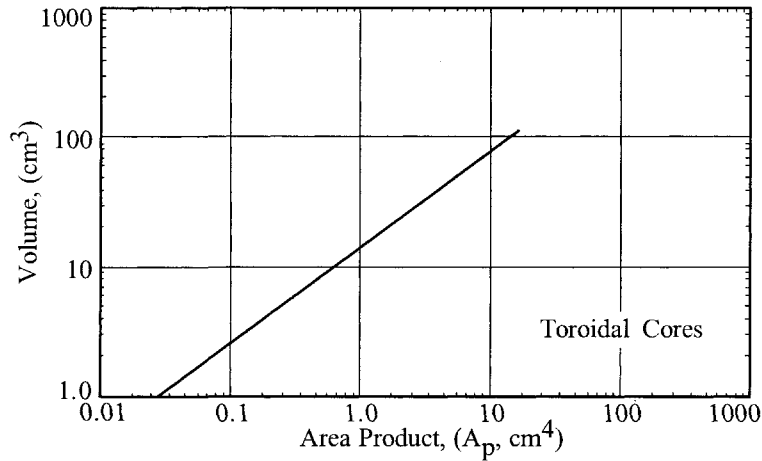


Figure 5-7. Volume Versus Area Product, A_p , for Toroidal MPP Cores.

Transformer Weight and the Area Product, A_p

The total weight of a transformer can also be related to the area product, A_p , of a transformer. The relationship is derived according to the following reasoning: weight, W_t , varies, in accordance with the cube of any linear dimension l , whereas area product, A_p , varies, as the fourth power:

$$W_t = K_3 l^3, \quad [\text{grams}] \quad [5-15]$$

$$A_p = K_2 l^4, \quad [\text{cm}^4] \quad [5-16]$$

$$l^4 = \frac{A_p}{K_2} \quad [5-17]$$

$$l^4 = \left(\frac{A_p}{K_2} \right)^{(0.25)} \quad [5-18]$$

$$l^3 = \left[\left(\frac{A_p}{K_2} \right)^{(0.25)} \right]^3 = \left(\frac{A_p}{K_2} \right)^{0.75} \quad [5-19]$$

$$W_t = K_3 \left(\frac{A_p}{K_2} \right)^{0.75} \quad [5-20]$$

$$K_w = \frac{K_3}{K_2^{(0.75)}} \quad [5-21]$$

The weight-area product, A_p , relationship is therefore:

$$W_t = K_w A_p^{(0.75)} \quad [5-22]$$

in which, K_w , is a constant related to core configuration, whose values are given in Table 5-3, These values were obtained by averaging the values from the data taken from Tables 3-1 through Tables 3-64 in Chapter 3.

Table 5-3. Weight-Area Product Relationship.

Weight-Area Product Relationship	
Core Type	K_w
Pot Core	48.0
Powder Core	58.8
Laminations	68.2
C Core	66.6
Single-coil C Core	76.6
Tape-wound Core	82.3

The relationship between weight and area product, A_p , for various core types is graphed in Figures 5-8 through 5-10. The data for Figures 5-8 through 5-10 has been taken from Tables in Chapter 3.

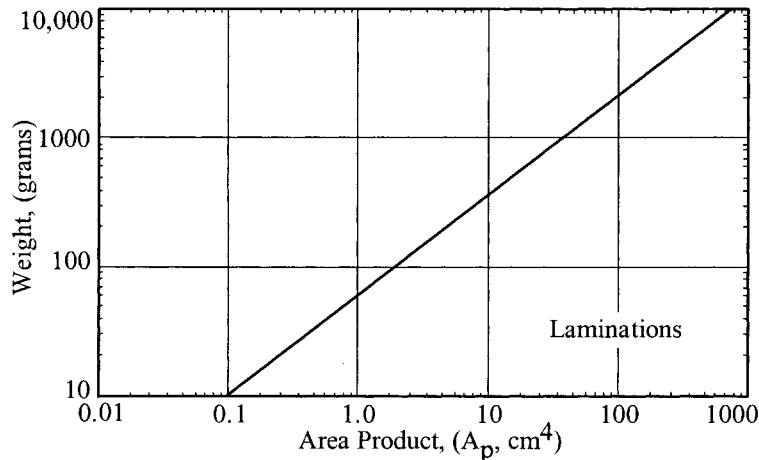


Figure 5-8. Total Weight Versus Area Product, A_p , for EI Laminations.

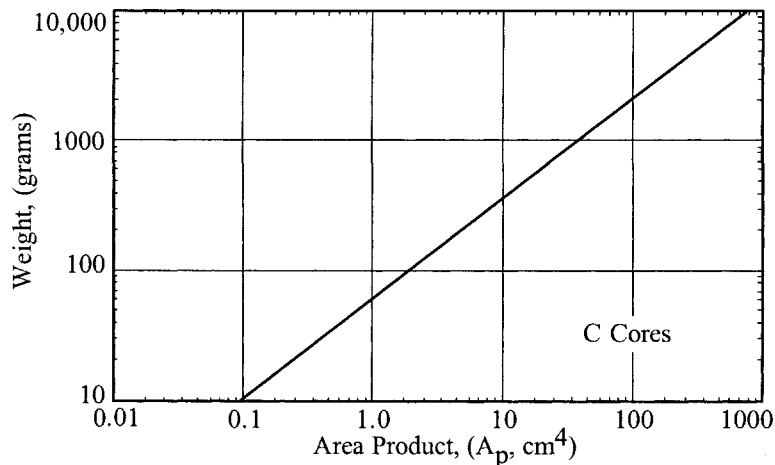


Figure 5-9. Total Weight Versus Area Product, A_p , for C Cores.

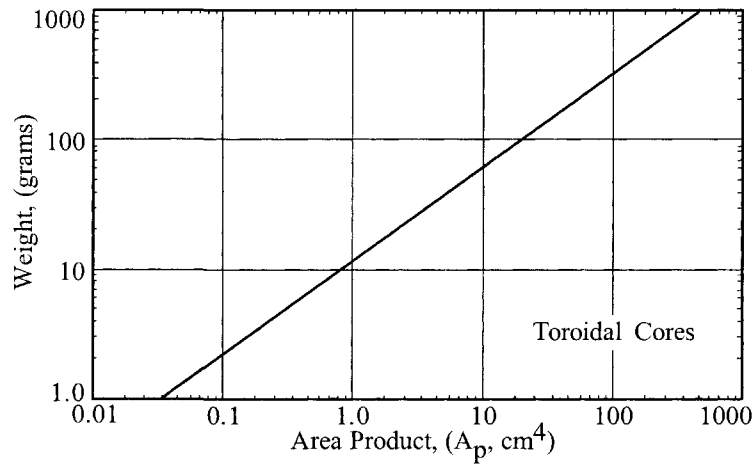


Figure 5-10. Total Weight Versus Area Product, A_p , for Toroidal MPP Cores.

Transformer Surface Area and the Area Product, A_p

The surface area of a transformer can be related to the area product, A_p , of a transformer, treating the surface area, as shown in Figure 5-11 through 5-13. The relationship is derived in accordance with the following reasoning: the surface area varies with the square of any linear dimension (l), whereas the area product, A_p , varies as the fourth power.

$$A_s = K_4 l^2, \quad [\text{cm}^2] \quad [5-23]$$

$$A_p = K_2 l^4, \quad [\text{cm}^4] \quad [5-24]$$

$$l^4 = \frac{A_p}{K_2} \quad [5-25]$$

$$l = \left(\frac{A_p}{K_2} \right)^{(0.25)} \quad [5-26]$$

$$l^2 = \left[\left(\frac{A_p}{K_2} \right)^{(0.25)} \right]^2 = \left(\frac{A_p}{K_2} \right)^{0.5} \quad [5-27]$$

$$A_s = K_4 \left(\frac{A_p}{K_2} \right)^{0.5} \quad [5-28]$$

$$K_s = \frac{K_4}{K_2^{(0.5)}} \quad [5-29]$$

The relationship between surface area, A_t and area product, A_p can be expressed as:

$$A_t = K_s A_p^{(0.5)} \quad [5-30]$$

in which, K_s , is a constant related to core configuration, whose values are given in Table 5-4. These values were obtained by averaging the values from the data taken from Tables 3-1 through Tables 3-64 in Chapter 3.

Table 5-4. Surface Area-Area Product Relationship.

Surface Area-Area Product Relationship	
Core Type	K_s
Pot Core	33.8
Powder Core	32.5
Laminations	41.3
C Core	39.2
Single-coil C Core	44.5
Tape-wound Core	50.9

The surface area for toroidal type transformers is calculated, as shown below.

$$\text{Top and Bottom Surface} = 2 \left(\frac{\pi(OD)^2}{4} \right), \quad [\text{cm}^2]$$

$$\text{Periphery Surface} = (\pi(OD))(\text{Height}), \quad [\text{cm}^2] \quad [5-31]$$

$$A_t = \frac{\pi(OD)^2}{2} + (\pi(OD))(\text{Height}), \quad [\text{cm}^2]$$

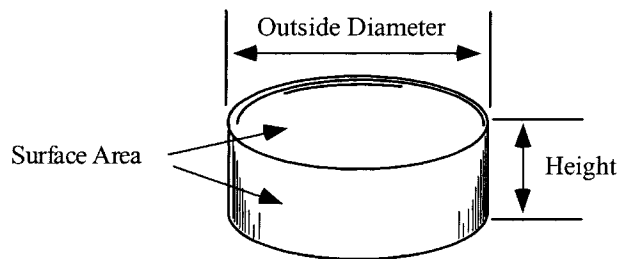


Figure 5-11. Toroidal Transformer Outline Showing the Surface Area.

The surface areas for C cores, Laminations and similar configurations are calculated as shown below. There is a small amount of area that is deducted because the sides and the ends are not a complete square.

$$\text{End} = (\text{Height})(\text{Length}), \quad [\text{cm}^2]$$

$$\text{Top} = (\text{Length})(\text{Width}), \quad [\text{cm}^2]$$

$$\text{Side} = (\text{Height})(\text{Width}), \quad [\text{cm}^2]$$

$$\text{Surface Area} = 2(\text{End}) + 2(\text{Top}) + 2(\text{Side}), \quad [\text{cm}^2]$$

[5-32]

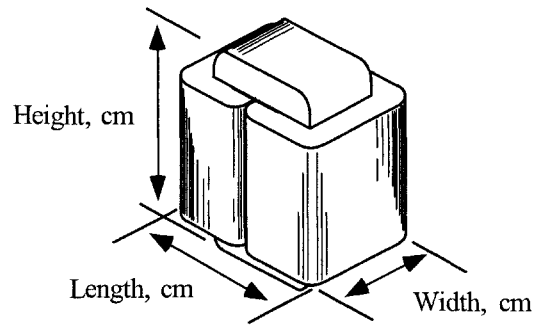


Figure 5-12. C Core Transformer Outline, Showing the Surface Area.

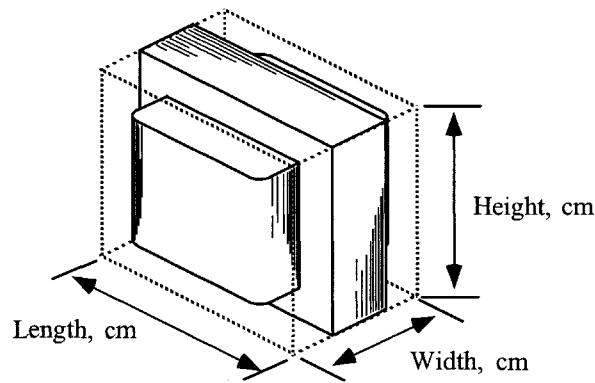


Figure 5-13. Typical EE or EI Transformer Outline, Showing the Surface Area.

The relationship between surface area and area product, A_p , for various core types is graphed in Figures 5-14 through 5-16. The data for these Figures has been taken from Tables in Chapter 3.

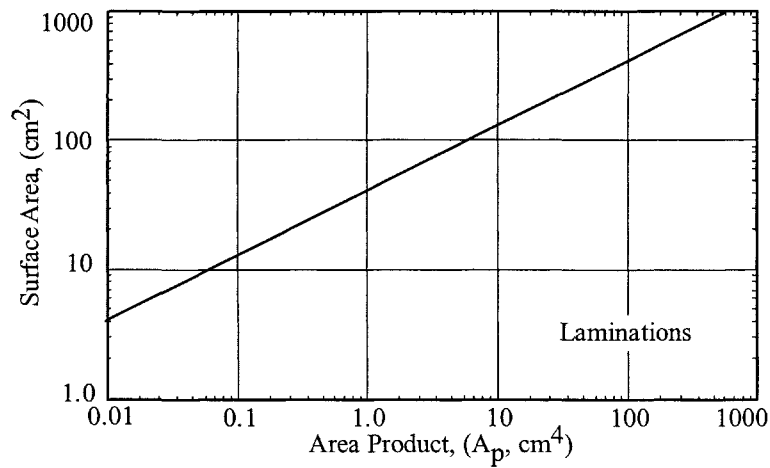


Figure 5-14. Surface Area, A_t , Versus Area Product, A_p , for EI Laminations.

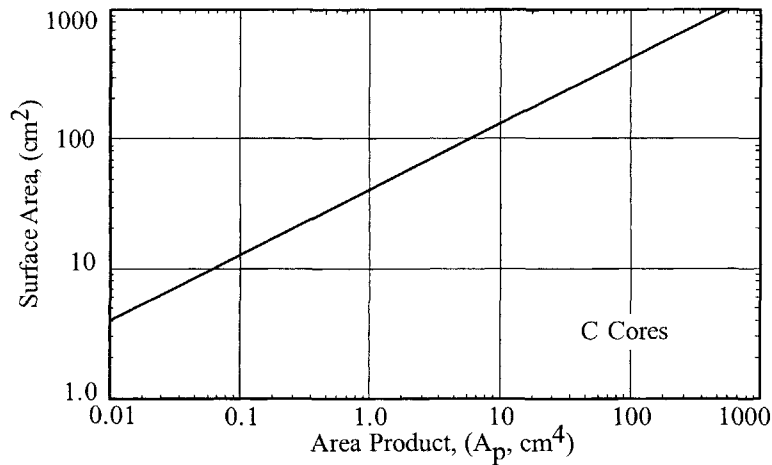


Figure 5-15. Surface Area, A_t , Versus Area Product, A_p , for C Cores.

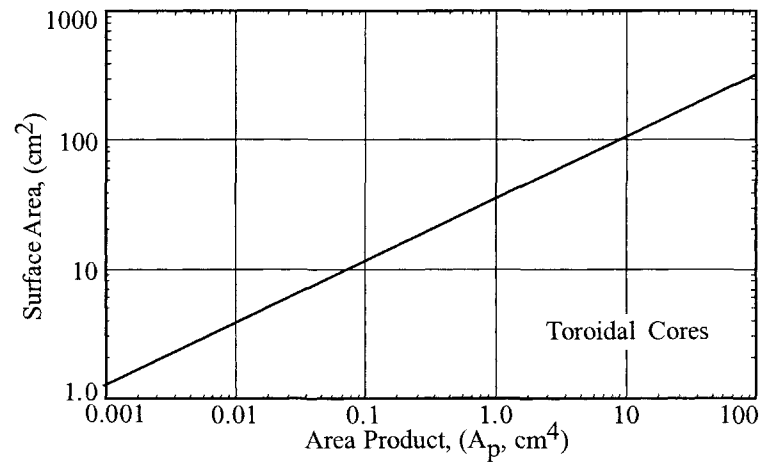


Figure 5-16. Surface Area, A_t , Versus Area Product, A_p , for Toroidal MPP Cores.

Transformer Current Density, J , and the Area Product, A_p

The current density, J , of a transformer can be related to the area product, A_p , of a transformer for a given temperature rise. The relationship can be derived as follows:

$$A_t = K_s A_p^{(0.5)}, \quad [\text{cm}^2] \quad [5-33]$$

$$P_{cu} = I^2 R, \quad [\text{watts}] \quad [5-34]$$

$$I = A_w J, \quad [\text{amps}] \quad [5-35]$$

Therefore,

$$P_{cu} = A_w^2 J^2 R \quad [5-36]$$

And since,

$$R = \frac{\text{MLT}}{A_w} N \rho, \quad [\text{ohms}] \quad [5-37]$$

We have:

$$P_{cu} = A_w^2 J^2 \frac{MLT}{A_w} N \rho \quad [5-38]$$

$$P_{cu} = A_w J^2 (MLT) N \rho \quad [5-39]$$

Since MLT has a dimension of length,

$$MLT = K_5 A_p^{(0.25)} \quad [5-40]$$

$$P_{cu} = A_w J^2 (K_5 A_p^{(0.25)}) N \rho \quad [5-41]$$

$$A_w N = K_3 W_a = K_6 A_p^{(0.5)} \quad [5-42]$$

$$P_{cu} = (K_6 A_p^{(0.5)}) (K_5 A_p^{(0.25)}) J^2 \rho \quad [5-43]$$

Let:

$$K_7 = K_6 K_5 \rho \quad [5-44]$$

Then assuming the core loss is the same as the copper loss for optimized transformer operation: (See Chapter 6),

$$P_{cu} = K_7 A_p^{(0.75)} J^2 = P_{fe} \quad [5-45]$$

$$P_\Sigma = P_{cu} + P_{fe} \quad [5-46]$$

$$\Delta T = K_8 \frac{P_\Sigma}{A_r} \quad [5-47]$$

$$\Delta T = \frac{2K_8 K_7 J^2 A_p^{(0.75)}}{K_5 A_p^{(0.5)}} \quad [5-48]$$

To simplify, let:

$$K_9 = \frac{2K_8 K_7}{K_5} \quad [5-49]$$

Then,

$$\Delta T = K_9 J^2 A_p^{(0.25)} \quad [5-50]$$

$$J^2 = \frac{\Delta T}{K_9 A_p^{(0.25)}} \quad [5-51]$$

Then, letting:

$$K_{10} = \frac{\Delta T}{K_9} \quad [5-52]$$

We have:

$$J^2 = K_{10} A_p^{(0.25)} \quad [5-53]$$

The relationship between current density, J , and area product, A_p , can, therefore, be expressed as:

$$J = K_j A_p^{(0.125)} \quad [5-54]$$

The constant, K_j , is related to the core configuration, whose values are given in Table 5-5. These values have been derived by averaging the values from the data taken from Tables 3-1 through Tables 3-64 in Chapter 3.

Table 5-5. Constant, K_j , for Temperature Increase of 25°C and 50°C.

Temperature Constant, K_j		
Core Type	$K_j (\Delta 25^\circ)$	$K_j (\Delta 50^\circ)$
Pot Core	433	632
Powder Core	403	590
Laminations	366	534
C Core	322	468
Single-coil C Core	395	569
Tape-wound Core	250	365

The relationship between current density, J , and area product, A_p , for temperature increases of 25°C and 50°C is graphed in Figures 5-17 through 5-19 from data calculated of Tables 3-1 through 3-64 in Chapter 3.

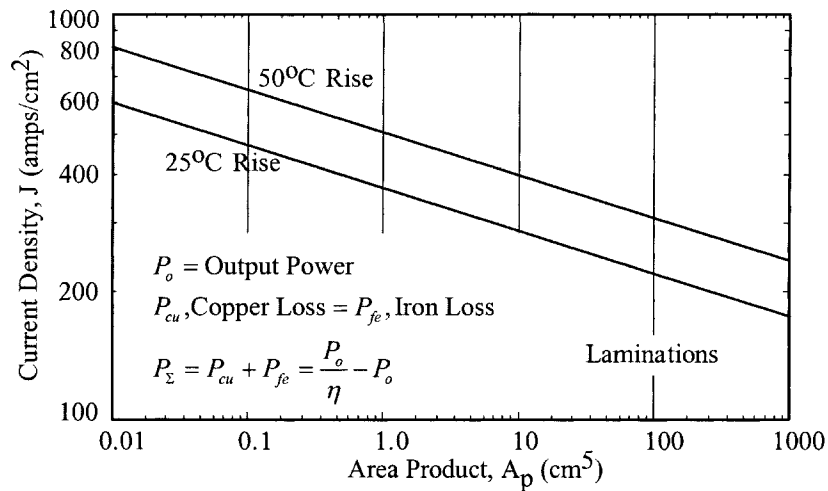


Figure 5-17. Current Density, J , Versus Area Product, A_p , for EI Laminations.

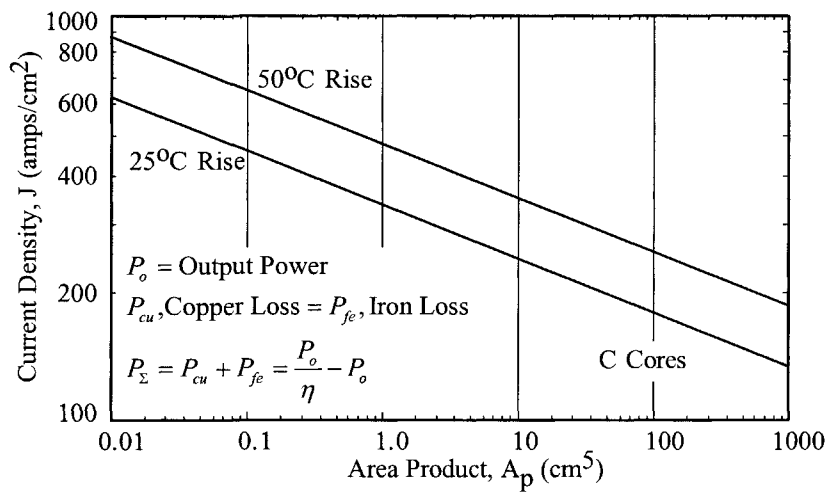


Figure 5-18. Current Density, J , Versus Area Product, A_p , for C Cores.

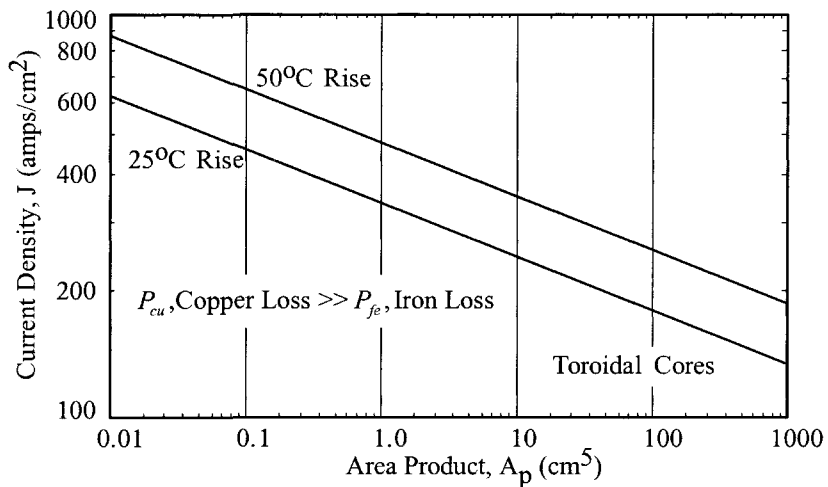


Figure 5-19. Current Density, J , Versus Area Product, A_p , for MPP Cores.

Transformer Core Geometry, K_g , and the Area Product, A_p

The core geometry, K_g , of a transformer can be related to the area product, A_p . The relationship is according to the following: the core geometry, K_g , varies in accordance with the fifth power of any linear dimension, (1), whereas area product, A_p , varies as the fourth power.

$$K_g = \frac{W_a A_c^2 K_u}{MLT}, \quad [\text{cm}^5] \quad [5-55]$$

$$K_g = K_{10} l^5 \quad [5-56]$$

$$A_p = K_2 I^4 \quad [5-57]$$

From Equation 5-56,

$$I = \left(\frac{K_g}{K_{10}} \right)^{(0.2)} \quad [5-58]$$

Then,

$$I^4 = \left[\left(\frac{K_g}{K_{10}} \right)^{(0.2)} \right]^4 = \left(\frac{K_g}{K_{10}} \right)^{(0.8)} \quad [5-59]$$

Substituting Equation 5-59 into Equation 5-57,

$$A_p = K_2 \left(\frac{K_g}{K_{10}} \right)^{(0.8)} \quad [5-60]$$

Let:

$$K_p = \frac{K_2}{K_{10}^{(0.8)}} \quad [5-61]$$

Then,

$$A_p = K_p K_g^{(0.8)} \quad [5-62]$$

The constant, K_p , is related to the core configuration, whose values are given in Table 5-6. These values have been derived by averaging the values from the data taken from Tables 3-1 through Tables 3-64 in Chapter 3.

Table 5-6. Configuration Constant, K_p , for Area Product, A_p , and Core geometry, K_g .

Constant, K_p	
Core Type	K_p
Pot Core	8.9
Powder Core	11.8
Laminations	8.3
C Core	12.5
Tape-wound Core	14.0

The relationship between area product, A_p , and core geometry, K_g , is graphed in Figures 5-20 through 5-22, from the data taken from Tables 3-1 through Tables 3-64 in Chapter 3.

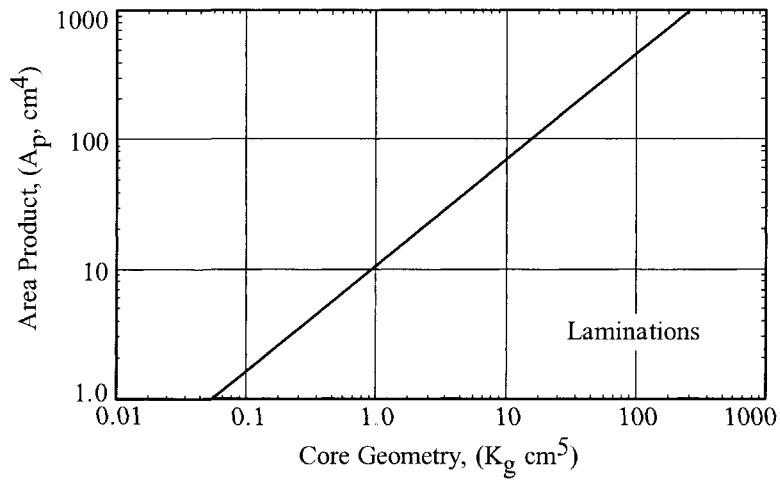


Figure 5-20. Area Product, A_p , Versus Core Geometry, K_g , for EI Laminations.

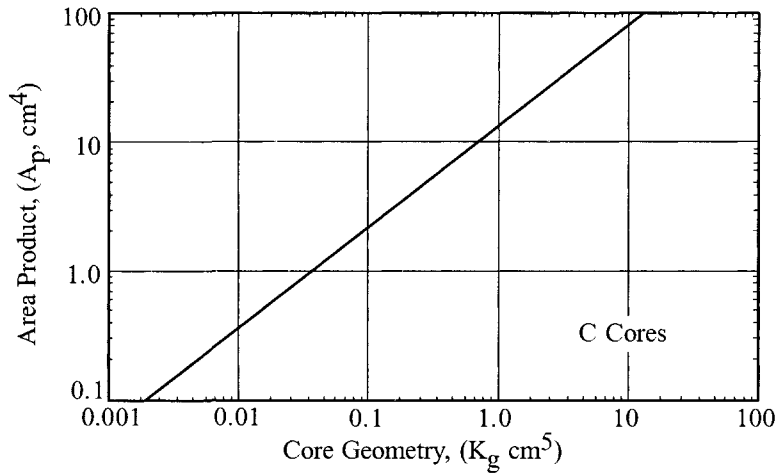


Figure 5-21. Area Product, A_p , Versus Core Geometry, K_g , for C Cores.

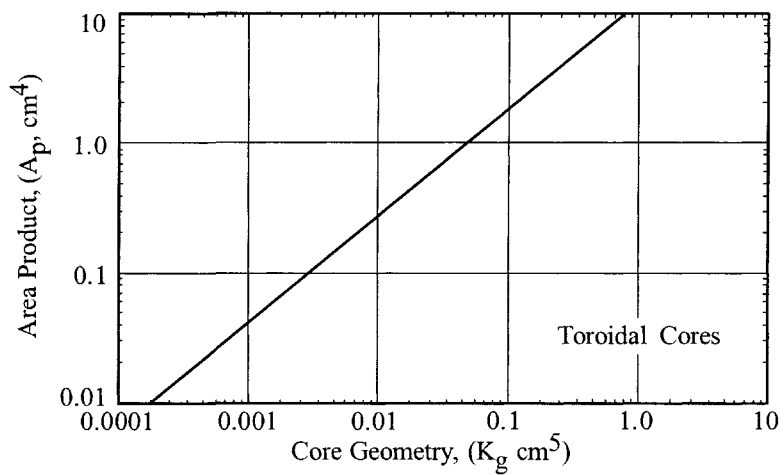


Figure 5-22. Area Product, A_p , Versus Core Geometry, K_g , for MPP Powder Cores.

Weight Versus Transformer Regulation

There are many design tasks where the transformer weight is very important in meeting the design specification. The engineer will raise the operating frequency in order to reduce the size and weight. The magnetic materials will be reviewed for performance at the operating frequency and at minimum and maximum temperatures. When the idealized magnetic material has been found and the weight of the transformer is still too high, then the only solution is to change the regulation. The regulation of a transformer versus the weight is shown in Figure 5-23. There are times when the engineer would like to know what the weight impact would be, if the regulation were to be increased or decreased.

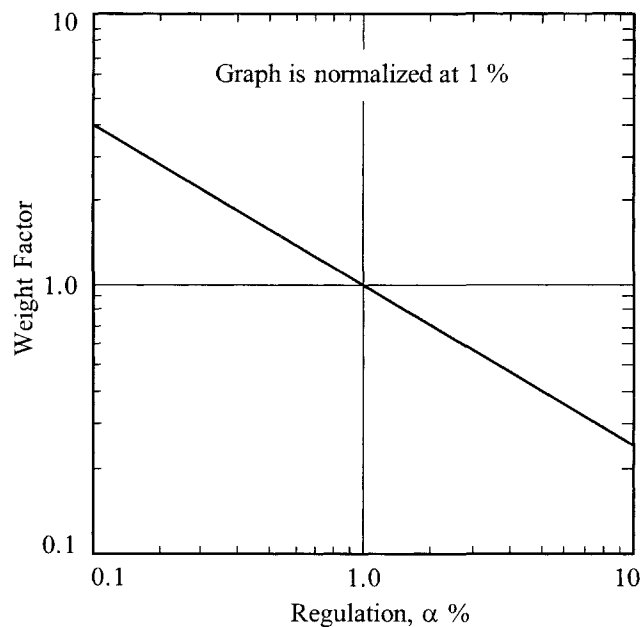


Figure 5-23. Weight Versus Regulation.

References

1. C. McLyman, Transformer Design Tradeoffs, Technical Memorandum 33-767 Rev. 1, Jet Propulsion Laboratory, Pasadena, CA.
2. W. J. Muldoon, High Frequency Transformer Optimization, HAC Trade Study Report 2228/1130, May, 1970
3. R. G. Klimo, A. B. Larson, and J. E. Murray, Optimization Study of High Power Static Inverters and Converters, Quarterly report No. 2 NASA-CR-54021, April 20, 1964, Contract NAS 3-2785.

4. F. F. Judd and D. R. Kessler, Design Optimization of Power Transformers, Bell Laboratories, Whippany, New Jersey IEEE Applied Magnetics Workshop, June 5-6, 1975

Chapter 6

Transformer-Inductor Efficiency, Regulation, and Temperature Rise

Table of Contents

1. Introduction	
2. Transformer Efficiency	
3. Maximum Efficiency	
4. Transformer Dissipation, by Radiation and Convection	
5. Temperature Rise Versus Surface Area, A_t , Dissipation	
6. Surface Area, A_t , Required for Heat Dissipation	
7. Required Surface Area, A_t	
8. Regulation as a Function of Efficiency	
9. References	

Introduction

Transformer efficiency, regulation, and temperature rise are all interrelated. Not all of the input power to the transformer is delivered to the load. The difference between input power and output power is converted into heat. This power loss can be broken down into two components: core loss, P_{fe} , and copper loss, P_{cu} . The core loss is a fixed loss, and the copper loss is a variable loss that is related to the current demand of the load. The copper loss increases by the square of the current and also is termed a quadratic loss. Maximum efficiency is achieved when the fixed loss is equal to the quadratic loss at rated load. Transformer regulation, α , is the copper loss, P_{cu} , divided by the output power, P_o .

$$\alpha = \frac{P_{cu}}{P_o} (100), \quad [\%] \quad [6-1]$$

Transformer Efficiency

The efficiency of a transformer is a good way to measure the effectiveness of the design. Efficiency is defined as the ratio of the output power, P_o , to the input power, P_{in} . The difference between, P_o , and, P_{in} , is due to losses. The total power loss, P_{Σ} , in the transformer is determined by the fixed losses in the core and the quadratic losses in the windings or copper. Thus,

$$P_{\Sigma} = P_{fe} + P_{cu}, \quad [\text{watts}] \quad [6-2]$$

Where, P_{fe} is the core loss, and P_{cu} is the copper loss.

Maximum Efficiency

Maximum efficiency is achieved when the fixed loss is made equal to the quadratic loss, as shown by Equation 6-12. A graph of transformer loss versus output load current is shown in Figure 6-1.

The copper loss increases as the square of the output power, P_o , multiplied by a constant, K_c :

$$P_{cu} = K_c P_o^2 \quad [6-3]$$

Which may be rewritten as:

$$P_{\Sigma} = P_{fe} + K_c P_o^2 \quad [6-4]$$

Since:

$$P_{in} = P_o + P_{\Sigma} \quad [6-5]$$

The efficiency can be expressed as:

$$\eta = \frac{P_o}{P_o + P_{\Sigma}} \quad [6-6]$$

Then, substituting Equation 6-4 into 6-6 gives:

$$\eta = \frac{P_o}{P_o + P_{fe} + KP_o^2} = \frac{P_o}{P_{fe} + P_o + KP_o^2} \quad [6-7]$$

And, differentiating with respect to P_o :

$$\frac{d\eta}{dP_o} = \frac{P_{fe} + P_o + KP_o^2 - P_o(1 + 2KP_o)}{(P_{fe} + P_o + KP_o^2)^2} \quad [6-8]$$

Then, to solve for the maximum, equate Equation 6-8 to 0.

$$\frac{P_{fe} + P_o + KP_o^2 - P_o(1 + 2KP_o)}{(P_{fe} + P_o + KP_o^2)^2} = 0 \quad [6-9]$$

$$-P_o(1 + 2KP_o) + (P_{fe} + P_o + KP_o^2) = 0 \quad [6-10]$$

$$-P_o - 2KP_o^2 + P_{fe} + P_o + KP_o^2 = 0 \quad [6-11]$$

Therefore,

$$P_{fe} = KP_o^2 = P_{cu} \quad [6-12]$$

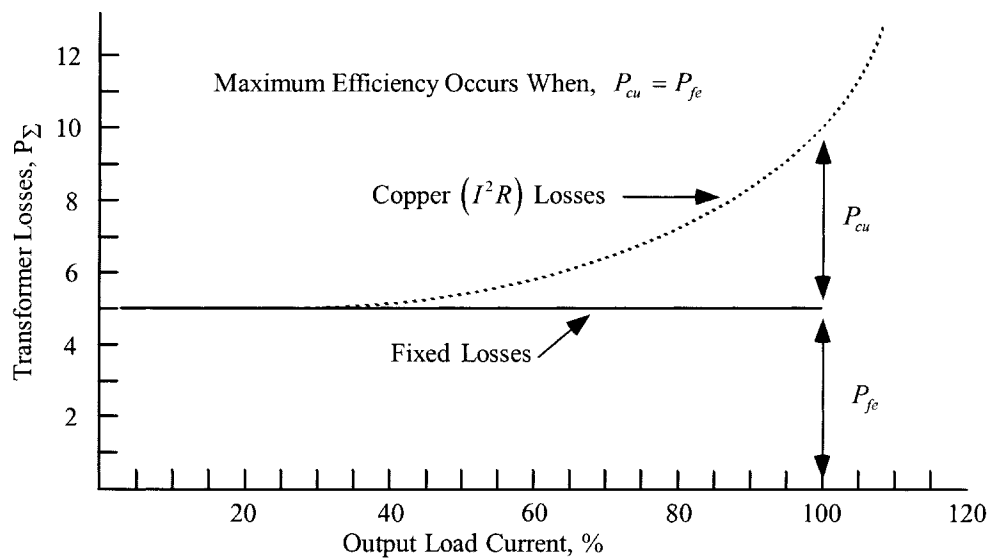


Figure 6-1. Transformer Losses Versus Output Load Current.

Transformer Dissipation, by Radiation and Convection

Temperature rise in a transformer winding cannot be predicted with complete precision, despite the fact that many techniques are described in the literature for its calculation. One reasonable accurate method for open core and winding construction is based upon the assumption that core and winding losses may be lumped together as:

$$P_{\Sigma} = P_{cu} + P_{fe}, \quad [\text{watts}] \quad [6-13]$$

And the assumption is made that thermal energy is dissipated uniformly throughout the surface area of the core and winding assembly.

Transfer of heat by thermal radiation occurs when a body is raised to a temperature above its surroundings and emits radiant energy in the form of waves. In accordance with Stefan-Boltzmann Law, (Ref. 1) this transfer of heat may be expressed as:

$$W_r = K_r \varepsilon (T_2^4 - T_1^4) \quad [6-14]$$

Where:

W_r , is watts per square centimeter of surface

$$K_r = 5.70(10^{-12}) W / (cm^2 / K^4)$$

ε , is the emissivity factor

T_2 , is the hot body temperature, K (kelvin)

T_1 , is the ambient or surrounding temperature, K (kelvin)

Transfer of heat by convection occurs when a body is hotter than the surrounding medium, which is usually air. The layer of air in contact with the hot body that is heated by conduction expands and rises, taking the absorbed heat with it. The next layer, being colder, replaces the risen layer and, in turn, on being heated, also rises. This transfer continues as long as the air, or other medium surrounding the body, is at a lower temperature. The transfer of heat by convection is stated mathematically as:

$$W_c = K_c F \theta^{(n)} \sqrt{P} \quad [6-15]$$

Where:

W_c , is the watts loss per square centimeter

$$K_c = 2.17(10^{-4})$$

F , is the air friction factor (unity for a vertical surface)

θ , is the temperature rise, $^{\circ}C$

P , is the relative barometric pressure (unity at sea level)

η , is the exponential value, which ranges from 1.0 to 1.25,

depending on the shape and position of the surface being cooled

The total heat dissipated from a plane vertical surface is expressed by Equations 6-13 and 6-15:

$$W = 5.70(10^{-12}) \varepsilon (T_2^4 - T_1^4) + 1.4(10^{-3}) F \theta^{(1.25)} \sqrt{P} \quad [6-16]$$

Temperature Rise Versus Surface Area, A_s , Dissipation

The temperature rise that can be expected for various levels of power loss is shown in the monograph of Figure 6-2. It is based on Equation 6-16, relying on data obtained from Blume (1938) (Ref. 1) for heat transfer affected by the combination of 55% radiation and 45% convection, from a surface having an emissivity of 0.95, in an ambient temperature of 25°C, at sea level. Power loss (heat dissipation) is expressed in watts per square centimeter of the total surface area. Heat dissipation, by convection from the upper side of a horizontal flat surface, is on the order of 15-20% more than from vertical surface. Heat dissipation, from the underside of a horizontal flat surface, depends upon area and conductivity.

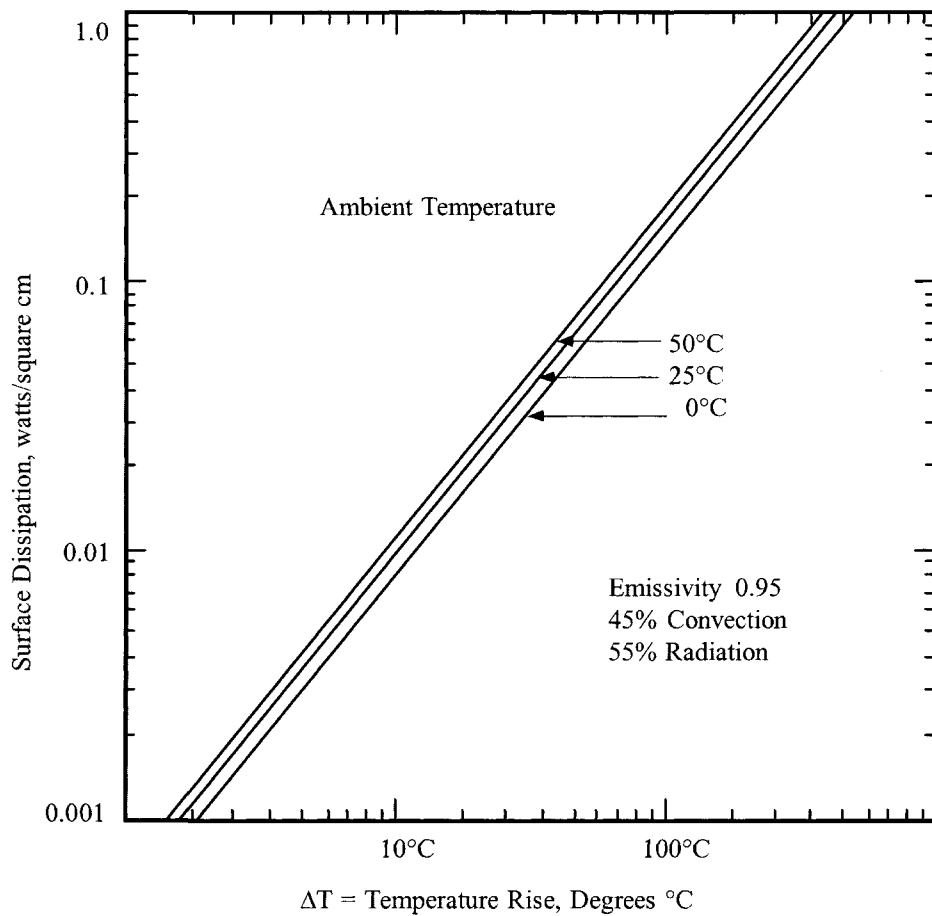


Figure 6-2. Temperature Rise Versus Surface Dissipation.

(Adapted from L. F. Blume, Transformers Engineering, Wiley, New York, 1938, Figure 7.)

Surface Area, A_t , Required for Heat Dissipation

The effective surface area, A_t , required to dissipate heat, (expressed as watts dissipated per unit area), is:

$$A_t = \frac{P_\Sigma}{\psi}, \quad [\text{cm}^2] \quad [6-17]$$

In which ψ is the power density or the average power dissipated per unit area from the surface of the transformer and, P_Σ , is the total power lost or dissipated.

The surface area, A_t , of a transformer can be related to the area product, A_p , of a transformer. The straight-line logarithmic relationship, shown in Figure 6-3, has been plotted from the data in Chapter 3. The derivation for the surface area, A_t , and the area product, A_p , is in Chapter 5.

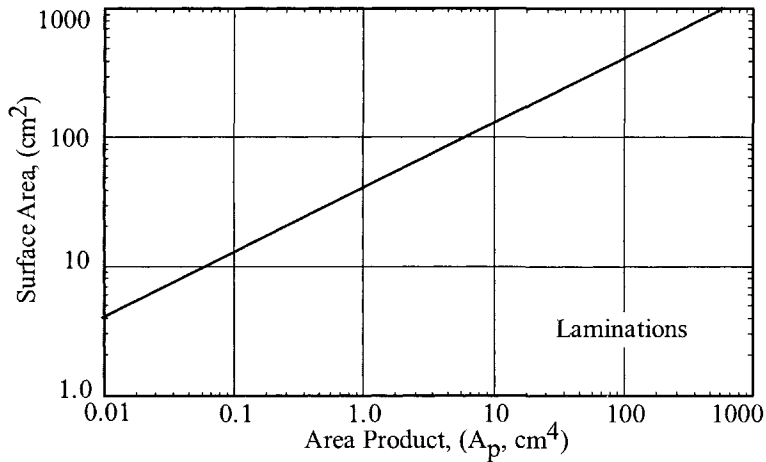


Figure 6-3. Surface Area, A_t Versus Area Product, A_p .

From this surface area, A_t , the following relationship evolves:

$$A_t = K_s (A_p)^{(0.5)} = \frac{P_\Sigma}{\psi}, \quad [\text{cm}^2] \quad [6-18]$$

And from Figure 6-3:

$$\psi = 0.03, \quad [\text{watts-per-cm}^2 \text{ at } 25^\circ\text{C}]$$

$$\psi = 0.07, \quad [\text{watts-per-cm}^2 \text{ at } 50^\circ\text{C}]$$

The temperature rise, T_r , equation in $^\circ\text{C}$ is:

$$T_r = 450(\psi)^{(0.826)}, \quad [^\circ\text{C}] \quad [6-19]$$

Required Surface Area, A_t

There are two common allowable temperature rises for transformers above the ambient temperature. These temperatures are shown in Figure 6-4. The surface area, A_t , required for a 25°C and 50°C rise above the ambient temperature for the total watts, dissipated. The presented data is used as a basis for determining the needed transformer surface area, A_t , in cm^2 .

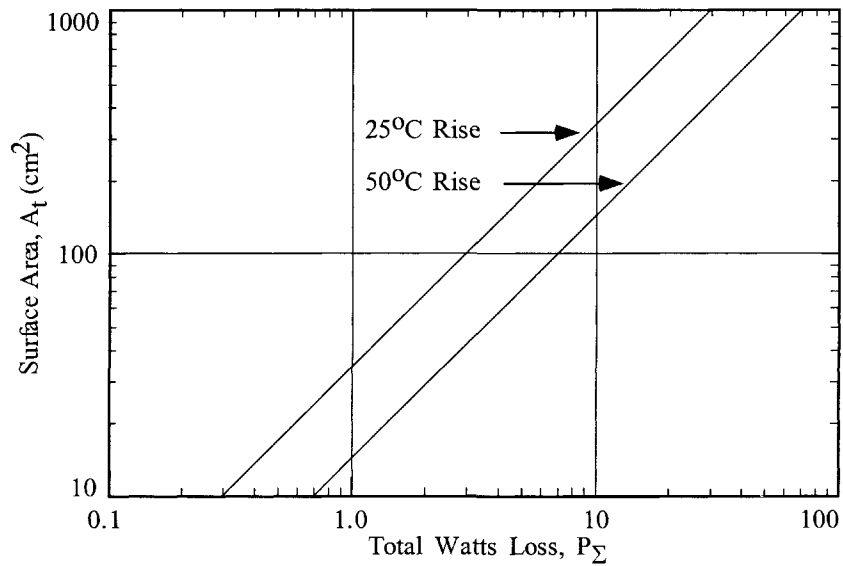


Figure 6-4. Surface Area, A_t Versus total Watts Loss for Temperature increases of 25°C and 50°C.

If the transformer is said to be homogeneous, and the thermal energy is dissipated uniformly throughout the surface area of the core and winding assembly, then Figure 6-5 will give a good approximation for the required time constant for a transformer to reach 63% of the final temperature. The temperature rise of a typical transformer is shown in Figure 6-6.

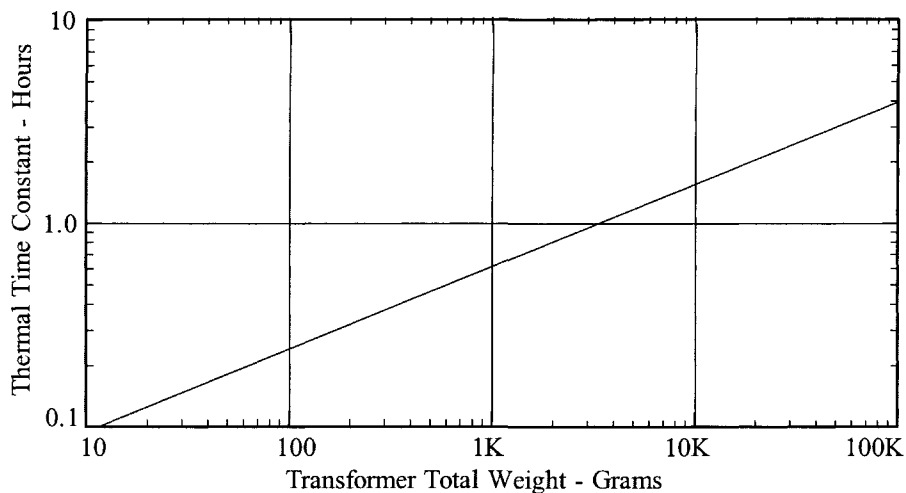


Figure 6-5. Time Required to Reach 63% of Final Temperature.

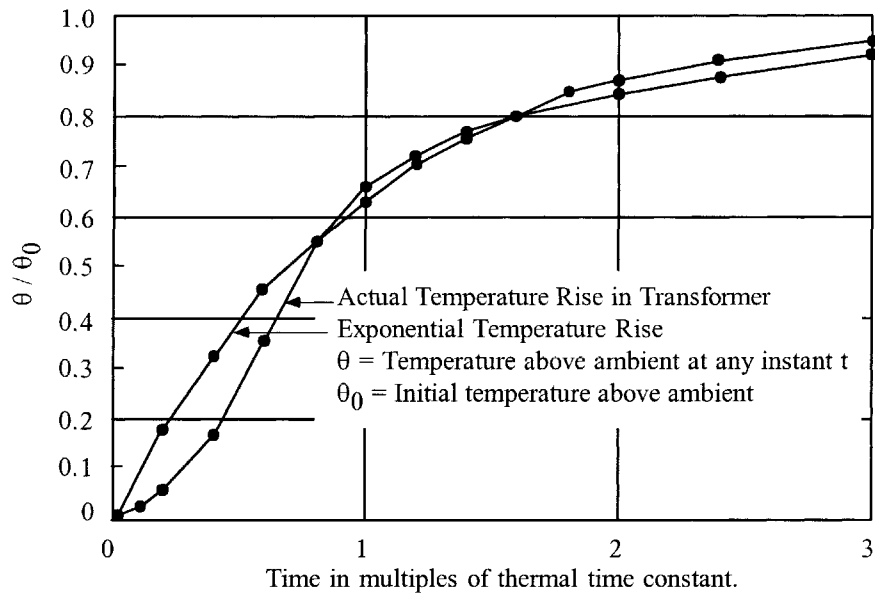


Figure 6-6. Transformer Temperature Rise Time.

Regulation as a Function of Efficiency

The minimum size of a transformer is usually determined either by a temperature rise limit, or by allowable voltage regulation, assuming that size and weight are to be minimized. Figure 6-7 shows a circuit diagram of a transformer with one secondary. Note that α = regulation (%).

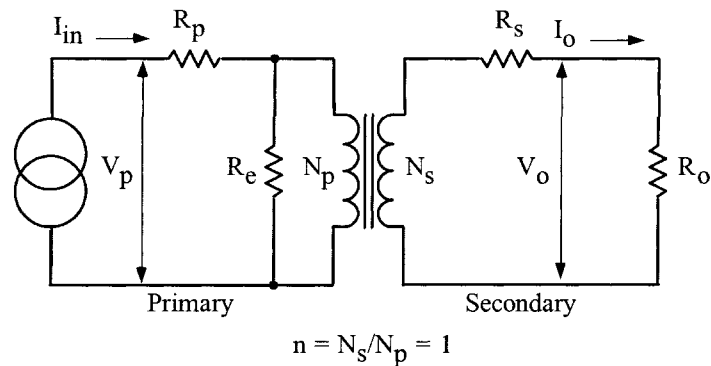


Figure 6-7. Transformer Circuit Diagram.

The assumption is that distributed capacitance in the secondary can be neglected because the frequency and secondary voltage are not excessively high. Also, the winding geometry is designed to limit the leakage inductance to a level, low enough, to be neglected, under most operating conditions. The transformer window allocation is shown in Figure 6-8.

$$\frac{W_a}{2} = \text{Primary} = \text{Secondary} \quad [6-20]$$

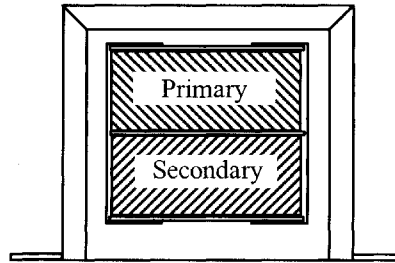


Figure 6-8. Transformer Window Allocation.

Transformer voltage regulation can now be expressed as:

$$\alpha = \frac{V_o(\text{N.L.}) - V_o(\text{F.L.})}{V_o(\text{F.L.})} (100), \quad [\%] \quad [6-21]$$

in which, $V_o(\text{N.L.})$, is the no load voltage and, $V_o(\text{F.L.})$, is the full load voltage. For the sake of simplicity, assume the transformer, in Figure 6-5, is an isolation transformer, with a 1:1 turns ratio, and the core impedance, R_c , is infinite.

If the transformer has a 1:1 turns ratio, and the core impedance is infinite, then:

$$I_{in} = I_o, \quad [\text{amps}]$$

$$R_p = R_s, \quad [\text{ohms}] \quad [6-22]$$

With equal window areas allocated for the primary and secondary windings, and using the same current density, J :

$$\Delta V_p = I_{in} R_p = \Delta V_s = I_o R_s, \quad [\text{volts}] \quad [6-23]$$

Then Regulation is:

$$\alpha = \frac{\Delta V_p}{V_p} (100) + \frac{\Delta V_s}{V_s} (100), \quad [\%] \quad [6-24]$$

Multiply the equation by currents, I :

$$\alpha = \frac{\Delta V_p I_{in}}{V_p I_{in}} (100) + \frac{\Delta V_s I_o}{V_s I_o} (100), \quad [\%] \quad [6-25]$$

Primary copper loss is:

$$P_p = \Delta V_p I_{in}, \text{ [watts]} \quad [6-26]$$

Secondary copper loss is:

$$P_s = \Delta V_s I_o, \text{ [watts]} \quad [6-27]$$

Total copper loss is:

$$P_{cu} = P_p + P_s, \text{ [watts]} \quad [6-28]$$

Then, the regulation equation can be rewritten to:

$$\alpha = \frac{P_{cu}}{P_o} (100), \text{ [%]} \quad [6-29]$$

References

1. Blume, L.F., *Transformer Engineering*, John Wiley & Sons Inc. New York, N.Y. 1938. Pages 272-282.
2. Terman, F.E., *Radio Engineers Handbook*, McGraw-Hill Book Co., Inc., New York, N.Y., 1943. Pages 28-37.

Chapter 7

Power Transformer Design

Table of Contents

1. Introduction	
2. The Design Problem Generally	
3. Power-Handling Ability	
4. Output Power, P_o , Versus Apparent Power, P_t , Capability	
5. Transformers with Multiple Outputs	
6. Regulation	
7. Relationship, K_g , to Power Transformer Regulation Capability	
8. Relationship, A_p , to Transformer Power Handling Capability	
9. Different Cores Same Area Product	
10. 250 Watt Isolation Transformer Design, Using the Core Geometry, K_g , Approach	
11. 38 Watt 100kHz Transformer Design, Using the Core Geometry, K_g , Approach	

Introduction

The conversion process in power electronics requires the use of transformers and components that are frequently the heaviest and bulkiest item in the conversion circuit. They also have a significant effect upon the overall performance and efficiency of the system. Accordingly, the design of such transformers has an important influence on the overall system weight, power conversion efficiency and cost. Because of the interdependence and interaction of parameters, judicious tradeoffs are necessary to achieve design optimization.

The Design Problem Generally

The designer is faced with a set of constraints that must be observed in the design on any transformer. One of these constraints is the output power, P_o , (operating voltage multiplied by maximum current demand). The secondary winding must be capable of delivering to the load within specified regulation limits. Another constraint relates to the minimum efficiency of operation, which is dependent upon the maximum power loss that can be allowed in the transformer. Still another defines the maximum permissible temperature rise for the transformer when it is used in a specified temperature environment.

One of the basic steps in transformer design is the selection of proper core material. Magnetic materials used to design low and high frequency transformers are shown in Table 7-1. Each one of these materials has its own optimum point in the cost, size, frequency and efficiency spectrum. The designer should be aware of the cost difference between silicon-iron, nickel-iron, amorphous and ferrite materials. Other constraints relate to the volume occupied by the transformer and, particularly in aerospace applications, the weight, since weight minimization is an important goal in today's electronics. Finally, cost effectiveness is always an important consideration.

Depending upon the application, certain ones of these constraints will dominate. Parameters affecting others may then be traded off as necessary to achieve the most desirable design. It is not possible to optimize all parameters in a single design because of their interaction and interdependence. For example, if volume and weight are of great significance, reductions in both can often be affected, by operating the transformer at a higher frequency, but, at a penalty in efficiency. When the frequency cannot be increased, reduction in weight and volume may still be possible by selecting a more efficient core material, but, at the penalty of increased cost. Thus, judicious trade-offs must be affected to achieve the design goals.

Transformer designers have used various approaches in arriving at suitable designs. For example, in many cases, a rule of thumb is used for dealing with current density. Typically, an assumption is made that a good working level is 200 amps-per-cm² (1000 circular mils-per-ampere). This will work in many

Table 7-1 Magnetic Materials

Magnetic Material Properties				
Material Name	Trade Name Composition	Initial Permeability μ_i	Flux Density Tesla B_s	Typical Operating Frequency
Silicon	3-97 SiFe	1500	1.5-1.8	50-2k
Orthonol	50-50 NiFe	2000	1.42-1.58	50-2k
Permalloy	80-20 NiFe	25000	0.66-0.82	1k-25k
Amorphous	2605SC	1500	1.5-1.6	250k
Amorphous	2714A	20,000	0.5-6.5	250k
Amorphous	Nanocrystalline	30,000	1.0-1.2	250k
Ferrite	MnZn	0.75-15k	0.3-0.5	10k-2M
Ferrite	NiZn	0.20-1.5k	0.3-0.4	0.2M-100M

instances, but the wire size needed to meet this requirement may produce a heavier and bulkier transformer than desired or required. The information presented in this volume makes it possible to avoid the use of this assumption and other rules of thumb, and to develop a more economical design with great accuracy.

Power-Handling Ability

For years manufacturers have assigned numeric codes to their cores; these codes represent the power-handling ability. This method assigns to each core a number that is the product of its window area, W_a , and core cross-section area, A_c , and is called the area product, A_p .

These numbers are used by core suppliers to summarize dimensional and electrical properties in their catalogs. They are available for laminations, C-cores, pot cores, powder cores, ferrite toroids, and toroidal tape-wound cores.

The regulation and power-handling ability of a core is related to the core geometry, K_g . Every core has its own inherent, K_g . The core geometry is relatively new, and magnetic core manufacturers do not list this coefficient.

Because of their significance, the area product, A_p , and core geometry, K_g , are treated extensively in this book. A great deal of other information is also presented for the convenience of the designer. Much of the material is in tabular form to assist the designer in making trade-offs, best-suited for his particular application in a minimum amount of time.

These relationships can now be used as new tools to simplify and standardize the process of transformer design. They make it possible to design transformers of lighter weight and smaller volume, or to optimize efficiency, without going through a cut-and-try, design procedure. While developed especially for aerospace applications, the information has wider utility, and can be used for the design of non-aerospace, as well.

Output Power, P_o , Versus Apparent Power, P_t , Capability

Output power, P_o , is of the greatest interest to the user. To the transformer designer, the apparent power, P_t , which is associated with the geometry of the transformer, is of greater importance. Assume, for the sake of simplicity, that the core of an isolation transformer has only two windings in the window area, a primary and a secondary. Also, assume that the window area, W_a , is divided up in proportion to the power-handling capability of the windings, using equal current density. The primary winding handles, P_{in} , and the secondary handles, P_o , to the load. Since the power transformer has to be designed to accommodate the primary, P_{in} , and P_o , then,

By definition:

$$\begin{aligned} P_t &= P_{in} + P_o, \quad [\text{watts}] \\ P_{in} &= \frac{P_o}{\eta}, \quad [\text{watts}] \end{aligned} \quad [7-1]$$

The primary turns can be expressed using Faraday's Law:

$$N_p = \frac{V_p (10^4)}{A_c B_{ac} f K_f}, \quad [\text{turns}] \quad [7-2]$$

The winding area of a transformer is fully utilized when:

$$K_u W_a = N_p A_{wp} + N_s A_{ws} \quad [7-3]$$

By definition the wire area is:

$$A_w = \frac{I}{J}, \quad [\text{cm}^2] \quad [7-4]$$

Rearranging the equation shows:

$$K_u W_a = N_p \left(\frac{I_p}{J} \right) + N_s \left(\frac{I_s}{J} \right) \quad [7-5]$$

Now, substitute in Faraday's Equation:

$$K_u W_a = \frac{V_p (10^4)}{A_c B_{ac} f K_f} \left(\frac{I_p}{J} \right) + \frac{V_s (10^4)}{A_c B_{ac} f K_f} \left(\frac{I_s}{J} \right) \quad [7-6]$$

Rearranging shows:

$$W_a A_c = \frac{[(V_p I_p) + (V_s I_s)] (10^4)}{B_{ac} f J K_f K_u}, \quad [\text{cm}^4] \quad [7-7]$$

The output power, P_o , is:

$$P_o = V_s I_s, \quad [\text{watts}] \quad [7-8]$$

The input power, P_{in} , is:

$$P_{in} = V_p I_p, \quad [\text{watts}] \quad [7-9]$$

Then:

$$P_t = P_{in} + P_o, \quad [\text{watts}] \quad [7-10]$$

Substitute in, P_t :

$$W_a A_c = \frac{P_t (10^4)}{B_{ac} f J K_f K_u}, \quad [\text{cm}^4] \quad [7-11]$$

By definition, A_p , equals:

$$A_p = W_a A_c, \quad [\text{cm}^4] \quad [7-12]$$

Then:

$$A_p = \frac{P_t (10^4)}{B_{ac} f J K_f K_u}, \quad [\text{cm}^4] \quad [7-13]$$

The designer must be concerned with the apparent power, P_t , and power handling capability of the transformer core and windings. P_t may vary by a factor, ranging from 2 to 2.828 times the input power, P_{in} , depending upon the type of circuit in which the transformer is used. If the current in the rectifier transformer becomes interrupted, its effective RMS value changes. Thus, transformer size is not only determined by the load demand, but also, by application, because of the different copper losses incurred, due to the current waveform.

For example, for a load of one watt, compare the power handling capabilities required for each winding, (neglecting transformer and diode losses, so that $P_{in} = P_o$) for the full-wave bridge circuit of Figure 7-1, the full-wave center-tapped secondary circuit of Figure 7-2, and the push-pull, center-tapped full-wave circuit in Figure 7-3, where all the windings have the same number of turns, (N).

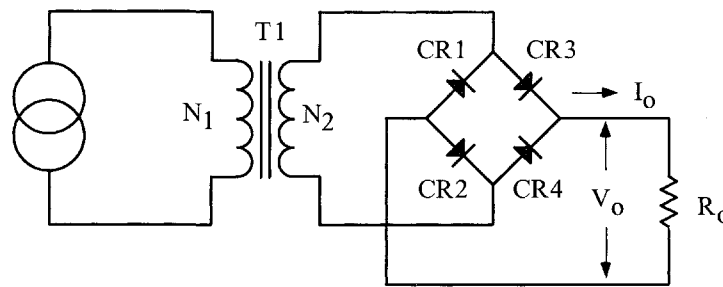


Figure 7-1. Full-Wave Bridge Secondary.

The total apparent power, P_t , for the circuit shown in Figure 7-1 is 2 watts.

This is shown in the following equation:

$$P_t = P_{in} + P_o, \text{ [watts]} \quad [7-14]$$

$$P_t = 2P_{in}, \text{ [watts]} \quad [7-15]$$

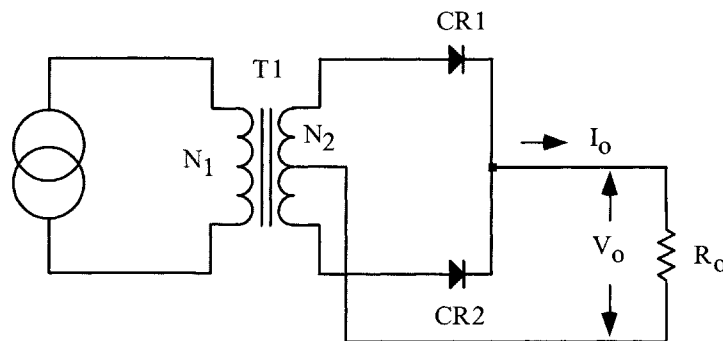


Figure 7-2. Full-Wave, Center-Tapped Secondary.

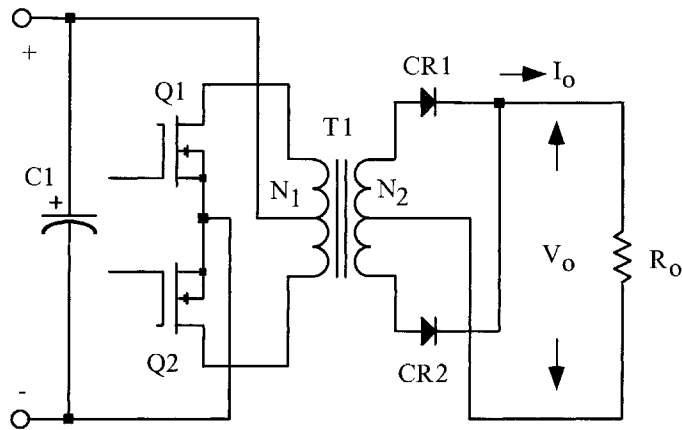


Figure 7-3. Push-Pull Primary, Full-Wave, Center-Tapped Secondary.

The total power, P_t , for the circuit shown in Figure 7-2, increased 20.7%, due to the distorted wave form of the interrupted current flowing in the secondary winding. This is shown in the following equation:

$$P_t = P_{in} + P_o \sqrt{2}, \quad [\text{watts}] \quad [7-16]$$

$$P_t = P_{in} (1 + \sqrt{2}), \quad [\text{watts}] \quad [7-17]$$

The total power, P_t , for the circuit is shown in Figure 7-3, which is typical of a dc to dc converter. It increases to 2.828 times, P_{in} , because of the interrupted current flowing in both the primary and secondary windings.

$$P_t = P_{in} \sqrt{2} + P_o \sqrt{2}, \quad [\text{watts}] \quad [7-18]$$

$$P_t = 2P_{in} \sqrt{2}, \quad [\text{watts}] \quad [7-19]$$

Transformers with Multiple Outputs

This example shows how the apparent power, P_o , changes with a multiple output transformers.

Output	Circuit
5 V @ 10A	center-tapped $V_d = \text{diode drop} = 1 \text{ V}$
15 V @ 1A	full-wave bridge $V_d = \text{diode drop} = 2 \text{ V}$
Efficiency = 0.95	

The output power seen by the transformer in Figure 7-4 is:

$$\begin{aligned}
 P_{o1} &= (V_{o1} + V_d)(I_{o1}), \text{ [watts]} \\
 P_{o1} &= (5+1)(10), \text{ [watts]} \\
 P_{o1} &= 60, \text{ [watts]} \qquad [7-20]
 \end{aligned}$$

And:

$$\begin{aligned}
 P_{o2} &= (V_{o2} + V_d)(I_{o2}), \text{ [watts]} \\
 P_{o2} &= (15+2)(1.0), \text{ [watts]} \\
 P_{o2} &= 17, \text{ [watts]} \qquad [7-21]
 \end{aligned}$$

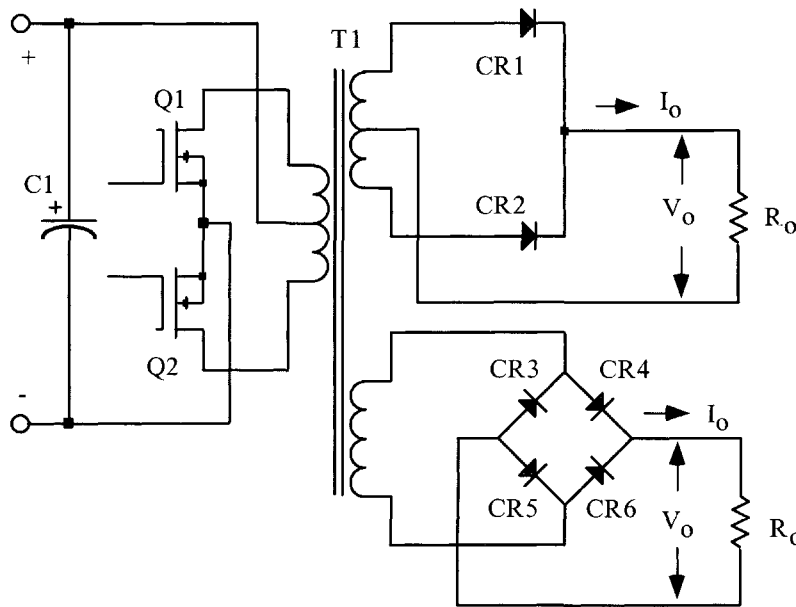


Figure 7-4. Multiple Output Converter.

Because of the different winding configurations, the apparent power, P_t , the transformer outputs will have to be summed to reflect this. When a winding has a center-tap and produces a discontinuous current, then, the power in that winding, be it primary or secondary, has to be multiplied by the factor, U . The factor, U , corrects for the rms current in that winding. If the winding has a center-tap, then the factor, U , is equal to 1.41. If not, the factor, U , is equal to 1.

For an example, summing up the output power of a multiple output transformer, would be:

$$P_{\Sigma} = P_{o1}(U) + P_{o2}(U) + P_n(U) + \dots \qquad [7-22]$$

Then:

$$\begin{aligned}
 P_{\Sigma} &= P_{o1}(U) + P_{o2}(U), \quad [\text{watts}] \\
 P_{\Sigma} &= 60(1.41) + 17(1), \quad [\text{watts}] \\
 P_{\Sigma} &= 101.6, \quad [\text{watts}] \quad [7-23]
 \end{aligned}$$

After the secondary has been totaled, then the primary power can be calculated.

$$\begin{aligned}
 P_{in} &= \frac{P_{o1} + P_{o2}}{\eta}, \quad [\text{watts}] \\
 P_{in} &= \frac{(60) + (17)}{(0.95)}, \quad [\text{watts}] \\
 P_{in} &= 81, \quad [\text{watts}] \quad [7-24]
 \end{aligned}$$

Then, the apparent power, P_t , equals:

$$\begin{aligned}
 P_t &= P_{in}(U) + P_{\Sigma}, \quad [\text{watts}] \\
 P_t &= (81)(1.41) + (101.6), \quad [\text{watts}] \\
 P_t &= 215.8, \quad [\text{watts}] \quad [7-25]
 \end{aligned}$$

Regulation

The minimum size of a transformer is usually determined either by a temperature rise limit, or by allowable voltage regulation, assuming that size and weight are to be minimized. Figure 7-5 shows a circuit diagram of a transformer with one secondary.

Note that α = regulation (%).

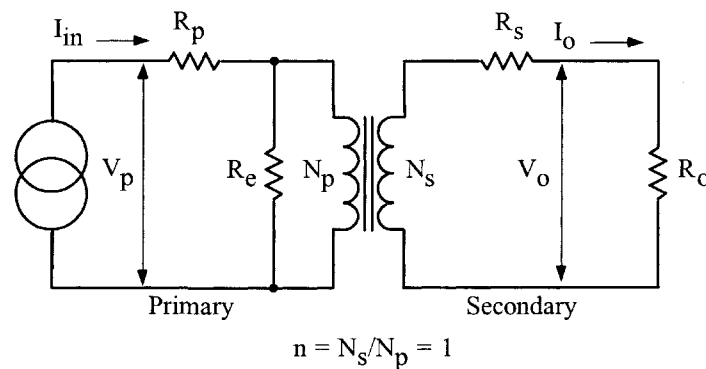


Figure 7-5. Transformer Circuit Diagram.

The assumption is that distributed capacitance in the secondary can be neglected because the frequency and secondary voltage are not excessively high. Also, the winding geometry is designed to limit the leakage inductance to a level, low enough, to be neglected under most operating conditions.

Transformer voltage regulation can now be expressed as:

$$\alpha = \frac{V_o(\text{N.L.}) - V_o(\text{F.L.})}{V_o(\text{F.L.})}(100), \quad [\%] \quad [7-26]$$

in which, $V_o(\text{N.L.})$, is the no load voltage and, $V_o(\text{F.L.})$, is the full load voltage. For the sake of simplicity, assume the transformer in Figure 7-5, is an isolation transformer, with a 1:1 turns ratio, and the core impedance, R_c , is infinite.

If the transformer has a 1:1 turns ratio, and the core impedance is infinite, then:

$$I_{in} = I_o, \quad [\text{amps}]$$

$$R_p = R_s, \quad [\text{ohms}] \quad [7-27]$$

With equal window areas allocated for the primary and secondary windings, and using the same current density, J :

$$\Delta V_p = I_{in} R_p = \Delta V_s = I_o R_s, \quad [\text{volts}] \quad [7-28]$$

Regulation is then:

$$\alpha = \frac{\Delta V_p}{V_p}(100) + \frac{\Delta V_s}{V_s}(100), \quad [\%] \quad [7-29]$$

Multiply the equation by currents, I :

$$\alpha = \frac{\Delta V_p I_{in}}{V_p I_{in}}(100) + \frac{\Delta V_s I_o}{V_s I_o}(100), \quad [\%] \quad [7-30]$$

Primary copper loss is:

$$P_p = \Delta V_p I_{in}, \quad [\text{watts}] \quad [7-31]$$

Secondary copper loss is:

$$P_s = \Delta V_s I_o, \quad [\text{watts}] \quad [7-32]$$

Total copper loss is:

$$P_{cu} = P_p + P_s, \text{ [watts]} \quad [7-33]$$

Then, the regulation equation can be rewritten to:

$$\alpha = \frac{P_{cu}}{P_o}(100), \text{ [%]} \quad [7-34]$$

Regulation can be expressed as the power lost in the copper. A transformer, with an output power of 100 watts and a regulation of 2%, will have a 2 watt loss in the copper:

$$P_{cu} = \frac{P_o \alpha}{100}, \text{ [watts]} \quad [7-35]$$

$$P_{cu} = \frac{(100)(2)}{100}, \text{ [watts]} \quad [7-36]$$

$$P_{cu} = 2, \text{ [watts]} \quad [7-37]$$

Relationship, K_g , to Power Transformer Regulation Capability

Although most transformers are designed for a given temperature rise, they can also be designed for a given regulation. The regulation and power-handling ability of a core is related to two constants:

$$\alpha = \frac{P_t}{2K_g K_e}, \text{ [%]} \quad [7-38]$$

$$\alpha = \text{Regulation (\%)} \quad [7-39]$$

The constant, K_g , is determined by the core geometry, which may be related by the following equations:

$$K_g = \frac{W_a A_c^2 K_u}{MLT}, \text{ [cm}^5\text{]} \quad [7-40]$$

The constant, K_e , is determined by the magnetic and electric operating conditions, which may be related by the following equation:

$$K_e = 0.145 K_f^2 f^2 B_m^2 (10^{-4}) \quad [7-41]$$

Where:

K_f = waveform coefficient

4.0 square wave

4.44 sine wave

From the above, it can be seen that factors such as flux density, frequency of operation, and the waveform coefficient have an influence on the transformer size.

Relationship, A_p , to Transformer Power Handling Capability

Transformers

According to the newly developed approach, the power handling capability of a core is related to its area product, A_p , by an equation which may be stated as:

$$A_p = \frac{P_t (10^4)}{K_f K_u B_m J f}, \quad [\text{cm}^4] \quad [7-42]$$

Where:

K_f = waveform coefficient

4.0 square wave

4.44 sine wave

From the above, it can be seen that factors such as flux density, frequency of operation, and the window utilization factor, K_u , define the maximum space which may be occupied by the copper in the window.

Different Cores Same Area Product

The area product, A_p , of a core is the product of the available window area, W_a , of the core in square centimeters, (cm^2), multiplied by the effective, cross-sectional area, A_c , in square centimeters, (cm^2), which may be stated as:

$$A_p = W_a A_c, \quad [\text{cm}^4] \quad [7-43]$$

Figures 7-6 through Figure 7-9 show, in outline form, three transformer core types that are typical of those shown in the catalogs of suppliers.

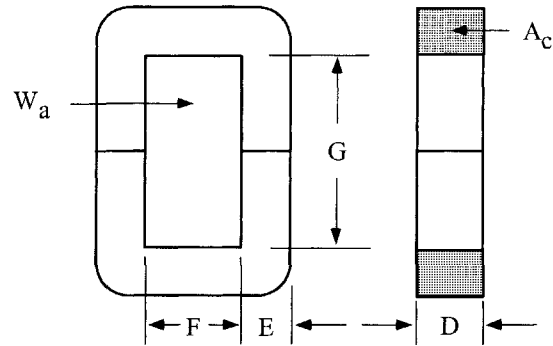


Figure 7-6. Dimensional Outline of a C Core.

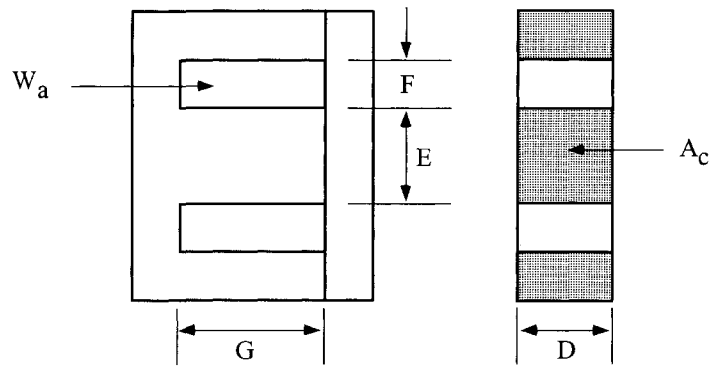


Figure 7-7. Dimensional Outline of a EI Lamination.

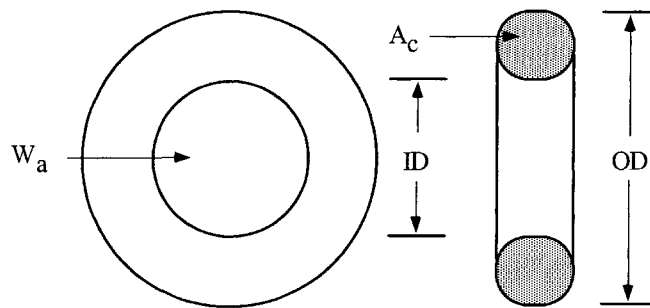


Figure 7-8. Dimensional Outline of a Toroidal Core.

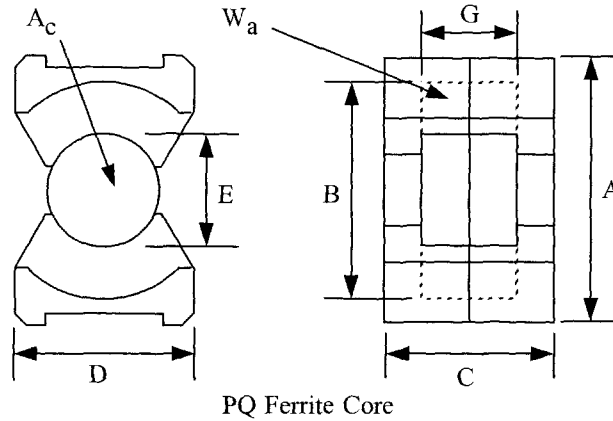


Figure 7-9. Dimensional Outline of a PQ Ferrite Core.

250 Watt Isolation Transformer Design, Using the Core Geometry, K_g , Approach

The following information is the Design specification for a 250 watt isolation transformer, operating at 47 Hz, using the, K_g , core geometry approach. For a typical design example, assume with the following specification:

1. Input voltage, V_{in} = 115 volts
2. Output voltage, V_o = 115 volts
3. Output current, I_o = 2.17 amps
4. Output power, P_o = 250 watts
5. Frequency, f = 47Hz
6. Efficiency, η = 95%
7. Regulation, α = 5 %
8. Operating flux density, B_{ac} = 1.6 tesla
9. Core Material = Silicon M6X
10. Window utilization, K_u = 0.4
11. Temperature rise goal, T_r = 30°C

Step No. 1 Calculate the transformer apparent power, P_t ,

$$P_t = P_o \left(\frac{1}{\eta} + 1 \right), \text{ [watts]}$$

$$P_t = 250 \left(\frac{1}{0.95} + 1 \right), \text{ [watts]}$$

$$P_t = 513, \text{ [watts]}$$

Step No. 2 Calculate the electrical conditions, K_e .

$$K_e = 0.145(K_f)^2(f)^2(B_m)^2(10^{-4})$$

$$K_f = 4.44, \text{ [sine wave]}$$

$$K_e = 0.145(4.44)^2(47)^2(1.6)^2(10^{-4})$$

$$K_e = 1.62$$

Step No. 3 Calculate the core geometry, K_g .

$$K_g = \frac{P_r}{2K_e\alpha}, \text{ [cm}^5\text{]}$$

$$K_g = \frac{(513)}{2(1.62)(5)}, \text{ [cm}^5\text{]}$$

$$K_g = 31.7, \text{ [cm}^5\text{]}$$

Step No. 4 Select a lamination from Chapter 3, comparable in core geometry, K_g .

Lamination number	EI-150
Manufacturer	Thomas and Skinner
Magnetic path length, MPL.....	22.9 cm
Core weight, W_{tfe}	2.334 kilograms
Copper weight, W_{tcu}	853 grams
Mean length turn, MLT	22 cm
Iron area, A_c	13.8 cm ²
Window area, W_a	10.89 cm ²
Area product, A_p	150 cm ⁴
Core geometry, K_g	37.6 cm ⁵
Surface area, A_t	479 cm ²

Step No. 5 Calculate the number of primary turns, N_p using Faraday's Law.

$$N_p = \frac{V_{in}(10^4)}{K_f B_{ac} f A_c}, \text{ [turns]}$$

$$N_p = \frac{(115)(10^4)}{(4.44)(1.6)(47)(13.8)}, \text{ [turns]}$$

$$N_p = 250, \text{ [turns]}$$

Step No. 6 Calculate the current density, J .

$$J = \frac{P_i(10^4)}{K_f K_a B_{ac} f A_p}, \quad [\text{amps/cm}^2]$$
$$J = \frac{513(10^4)}{(4.44)(0.4)(1.6)(47)(150)}, \quad [\text{amps/cm}^2]$$
$$J = 256, \quad [\text{amps/cm}^2]$$

Step No. 7 Calculate the input current, I_{in} .

$$I_{in} = \frac{P_o}{V_{in} \eta}, \quad [\text{amps}]$$
$$I_{in} = \frac{250}{(115)(0.95)}, \quad [\text{amps}]$$
$$I_{in} = 2.28, \quad [\text{amps}]$$

Step No. 8 Calculate the primary bare wire area, $A_{wp(B)}$.

$$A_{wp(B)} = \frac{I_{in}}{J}, \quad [\text{cm}^2]$$
$$A_{wp(B)} = \frac{(2.28)}{256}, \quad [\text{cm}^2]$$
$$A_{wp(B)} = 0.0089, \quad [\text{cm}^2]$$

Step No. 9 Select the wire from the Wire Table, in Chapter 4.

$$AWG = \#18$$
$$A_{wp(B)} = 0.00822, \quad [\text{cm}^2]$$
$$A_{wp} = 0.00933, \quad [\text{cm}^2]$$
$$\left(\frac{\mu\Omega}{\text{cm}}\right) = 209, \quad [\text{micro-ohm/cm}]$$

Step No. 10 Calculate the primary resistance, R_p .

$$R_p = \text{MLT}(N_p) \left(\frac{\mu\Omega}{\text{cm}}\right) (10^{-6}), \quad [\text{ohms}]$$
$$R_p = (22)(250)(209)(10^{-6}), \quad [\text{ohms}]$$
$$R_p = 1.15, \quad [\text{ohms}]$$

Step No. 11 Calculate the primary copper loss, P_p .

$$P_p = I_p^2 R_p, \text{ [watts]}$$

$$P_p = (2.28)^2 (1.15), \text{ [watts]}$$

$$P_p = 5.98, \text{ [watts]}$$

Step No. 12 Calculate the secondary turns, N_s .

$$N_s = \frac{N_p V_s}{V_{in}} \left(1 + \frac{\alpha}{100} \right), \text{ [turns]}$$

$$N_s = \frac{(250)(115)}{(115)} \left(1 + \frac{5}{100} \right), \text{ [turns]}$$

$$N_s = 262.5 \text{ use } 263, \text{ [turns]}$$

Step No. 13 Calculate the secondary bare wire area, $A_{ws(B)}$.

$$A_{ws(B)} = \frac{I_o}{J}, \text{ [cm}^2\text{]}$$

$$A_{ws(B)} = \frac{(2.17)}{256}, \text{ [cm}^2\text{]}$$

$$A_{ws(B)} = 0.00804, \text{ [cm}^2\text{]}$$

Step No. 14 Select the wire from the Wire Table, in Chapter 4.

$$AWG = \#18$$

$$A_{wp(B)} = 0.00822, \text{ [cm}^2\text{]}$$

$$A_{wp} = 0.00933, \text{ [cm}^2\text{]}$$

$$\left(\frac{\mu\Omega}{\text{cm}} \right) = 209, \text{ [micro-ohm/cm]}$$

Step No. 15 Calculate the secondary winding resistance, R_s .

$$R_s = \text{MLT}(N_s) \left(\frac{\mu\Omega}{\text{cm}} \right) (10^{-6}), \text{ [ohms]}$$

$$R_s = (22)(263)(209)(10^{-6}), \text{ [ohms]}$$

$$R_s = 1.21, \text{ [ohms]}$$

Step No. 16 Calculate the secondary copper loss, P_s .

$$P_s = I_o^2 R_s, \text{ [watts]}$$

$$P_s = (2.17)^2 (1.21), \text{ [watts]}$$

$$P_s = 5.70, \text{ [watts]}$$

Step No. 17 Calculate the total primary and secondary copper loss, P_{cu} .

$$\begin{aligned}P_{cu} &= P_p + P_s, \text{ [watts]} \\P_{cu} &= 5.98 + 5.7, \text{ [watts]} \\P_{cu} &= 11.68, \text{ [watts]}\end{aligned}$$

Step No. 18 Calculate the transformer regulation, α .

$$\begin{aligned}\alpha &= \frac{P_{cu}}{P_o}(100), \text{ [%]} \\ \alpha &= \frac{(11.68)}{(250)}(100), \text{ [%]} \\ \alpha &= 4.67, \text{ [%]}\end{aligned}$$

Step No. 19 Calculate the watts per kilogram, W/K. Use the equation for this material in Chapter 2.

$$\begin{aligned}W / K &= 0.000557(f)^{1.68}(B_{ac})^{1.86} \\ W / K &= 0.000557(47)^{1.51}(1.6)^{1.86} \\ W / K &= 0.860\end{aligned}$$

Step No. 20 Calculate the core loss, P_{fe} .

$$\begin{aligned}P_{fe} &= (W / K)(W_{fe})(10^{-3}), \text{ [watts]} \\ P_{fe} &= (0.860)(2.33), \text{ [watts]} \\ P_{fe} &= 2.00, \text{ [watts]}\end{aligned}$$

Step No. 21 Calculate the total loss, P_{Σ} .

$$\begin{aligned}P_{\Sigma} &= P_{cu} + P_{fe}, \text{ [watts]} \\ P_{\Sigma} &= (11.68) + (2.00), \text{ [watts]} \\ P_{\Sigma} &= 13.68, \text{ [watts]}\end{aligned}$$

Step No. 22 Calculate the watts per unit area, ψ .

$$\begin{aligned}\psi &= \frac{P_{\Sigma}}{A_t}, \text{ [watts/cm}^2\text{]} \\ \psi &= \frac{(13.68)}{(479)}, \text{ [watts/cm}^2\text{]} \\ \psi &= 0.0286, \text{ [watts/cm}^2\text{]}\end{aligned}$$

Step No. 23 Calculate the temperature rise, T_r .

$$T_r = 450(\psi)^{(0.826)}, \text{ [}^\circ\text{C]}$$

$$T_r = 450(0.0286)^{(0.826)}, \text{ [}^\circ\text{C]}$$

$$T_r = 23.9, \text{ [}^\circ\text{C]}$$

Step No. 24 Calculate the total window utilization, K_u .

$$K_u = K_{up} + K_{us}$$

$$K_{us} = \frac{N_s A_{ws(B)}}{W_a}$$

$$K_{us} = \frac{(263)(0.00822)}{(10.89)} = 0.199$$

$$K_{up} = \frac{N_p A_{wp(B)}}{W_a}$$

$$K_{up} = \frac{(250)(0.00822)}{(10.89)} = 0.189$$

$$K_u = (0.189) + (0.199)$$

$$K_u = 0.388$$

38 Watt 100kHz Transformer Design, Using the Core Geometry, K_g , Approach

The following information is the design specification for a 38 watt push-pull transformer, operating at 100kHz, using the K_g core geometry approach. For a typical design example, assume a push-pull, full-wave, center-tapped circuit, as shown in Figure 7-4, with the following specification:

1. Input voltage, $V_{(min)}$ = 24 volts
2. Output voltage #1, $V_{(o1)}$ = 5.0 volts
3. Output current #1, $I_{(o1)}$ = 4.0 amps
4. Output voltage #2, $V_{(o2)}$ = 12.0 volts
5. Output current #2, $I_{(o2)}$ = 1.0 amps
6. Frequency, f = 100kHz
7. Efficiency, η = 98%
8. Regulation, α = 0.5%
9. Diode voltage drop, V_d = 1.0 volt
10. Operating flux density, B_{ac} = 0.05 tesla
11. Core Material = ferrite
12. Window utilization, K_u = 0.4
13. Temperature rise goal, T_r = 30°C
14. Notes:

Using a center-tapped winding, $U = 1.41$

Using a single winding, $U = 1.0$

At this point, select a wire so that the relationship between the ac resistance and the dc resistance is 1:

$$\frac{R_{ac}}{R_{dc}} = 1$$

The skin depth, ϵ , in centimeters, is:

$$\epsilon = \frac{6.62}{\sqrt{f}}, \quad [\text{cm}]$$

$$\epsilon = \frac{6.62}{\sqrt{100,000}}, \quad [\text{cm}]$$

$$\epsilon = 0.0209, \quad [\text{cm}]$$

Then, the wire diameter, D_{AWG} , is:

$$D_{AWG} = 2(\varepsilon), \text{ [cm]}$$

$$D_{AWG} = 2(0.0209), \text{ [cm]}$$

$$D_{AWG} = 0.0418, \text{ [cm]}$$

Then, the bare wire area, A_w , is:

$$A_w = \frac{\pi(D_{AWG})^2}{4}, \text{ [cm}^2\text{]}$$

$$A_w = \frac{(3.1416)(0.0418)^2}{4}, \text{ [cm}^2\text{]}$$

$$A_w = 0.00137, \text{ [cm}^2\text{]}$$

From the Wire Table 4-9 in Chapter 4, number 27 has a bare wire area of 0.001021 centimeters. This will be the minimum wire size used in this design. If the design requires more wire area to meet the specification, then the design will use a multifilar of #26. Listed Below are #27 and #28, just in case #26 requires too much rounding off.

Wire AWG	Bare Area	Area Ins.	Bare/Ins.	$\mu\Omega/\text{cm}$
#26	0.001280	0.001603	0.798	1345
#27	0.001021	0.001313	0.778	1687
#28	0.0008046	0.0010515	0.765	2142

Step No. 1 Calculate the transformer output power, P_o .

$$P_o = P_{o1} + P_{o2}, \text{ [watts]}$$

$$P_{o1} = I_{o1}(V_{o1} + V_d), \text{ [watts]}$$

$$P_{o1} = 4(5 + 1), \text{ [watts]}$$

$$P_{o1} = 24, \text{ [watts]}$$

$$P_{o2} = I_{o2}(V_{o2} + V_d), \text{ [watts]}$$

$$P_{o2} = 1(12 + 2), \text{ [watts]}$$

$$P_{o2} = 14, \text{ [watts]}$$

$$P_o = (24 + 14), \text{ [watts]}$$

$$P_o = 38, \text{ [watts]}$$

Step No. 2 Calculate the total secondary apparent power, P_{ts} .

$$P_{ts} = P_{iso1} + P_{iso2}, \text{ [watts]}$$

$$P_{iso1} = P_{o1}(U), \text{ [watts]}$$

$$P_{iso1} = 24(1.41), \text{ [watts]}$$

$$P_{iso1} = 33.8, \text{ [watts]}$$

$$P_{iso2} = P_{o2}(U), \text{ [watts]}$$

$$P_{iso2} = 14(1), \text{ [watts]}$$

$$P_{iso2} = 14, \text{ [watts]}$$

$$P_{ts} = (33.8 + 14), \text{ [watts]}$$

$$P_{ts} = 47.8, \text{ [watts]}$$

Step No. 3 Calculate the total apparent power, P_t .

$$P_{in} = \left(\frac{P_o}{\eta} \right), \text{ [watts]}$$

$$P_{ip} = P_{in} P_a, \text{ [watts]}$$

$$P_t = P_{ip} + P_{ts}, \text{ [watts]}$$

$$P_t = \left(\frac{38}{0.98} \right)(1.41) + 47.8, \text{ [watts]}$$

$$P_t = 102.5, \text{ [watts]}$$

Step No. 4 Calculate the electrical conditions, K_e .

$$K_e = 0.145 (K_f)^2 (f)^2 (B_m)^2 (10^{-4})$$

$$K_f = 4.0, \text{ [square wave]}$$

$$K_e = 0.145 (4.0)^2 (100000)^2 (0.05)^2 (10^{-4})$$

$$K_e = 5800$$

Step No. 5 Calculate the core geometry, K_g .

$$K_g = \frac{P_t}{2 K_e \alpha}, \text{ [cm}^5\text{]}$$

$$K_g = \frac{(102.5)}{2(5800)0.5}, \text{ [cm}^5\text{]}$$

$$K_g = 0.0177, \text{ [cm}^5\text{]}$$

When operating at high frequencies, the engineer has to review the window utilization factor, K_u , in Chapter 4. When using a small bobbin ferrites, use the ratio of the bobbin winding area to the core window area is only about 0.6. Operating at 100kHz and having to use a #26 wire, because of the skin effect, the ratio of the bare copper area to the total area is 0.78. Therefore, the overall window utilization, K_u , is reduced. To return the design back to the norm, the core geometry, K_g , is to be multiplied by 1.35, and then, the current density, J , is calculated, using a window utilization factor of 0.29.

$$K_g = 0.0177 (1.35), \quad [\text{cm}^5]$$

$$K_g = 0.0239, \quad [\text{cm}^5]$$

Step No. 6 Select a PQ core from Chapter 3, comparable in core geometry K_g .

Core number	PQ-2020
Manufacturer	TDK
Magnetic material	PC44
Magnetic path length , MPL.....	4.5 cm
Window height, G	1.43 cm
Core weight, W_{tfe}	15 grams
Copper weight, W_{tcu}	10.4 grams
Mean length turn, MLT	4.4 cm
Iron area, A_c	0.62 cm ²
Window area, W_a	0.658 cm ²
Area product, A_p	0.408 cm ⁴
Core geometry, K_g	0.0227 cm ⁵
Surface area, A_t	19.7 cm ²
Millihenrys per 1000 turns, AL	3020

Step No. 7 Calculate the number of primary turns, N_p , using Faraday's Law.

$$N_p = \frac{V_p (10^4)}{K_f B_{ac} f A_c}, \quad [\text{turns}]$$

$$N_p = \frac{(24)(10^4)}{(4.0)(0.05)(100000)(0.62)}, \quad [\text{turns}]$$

$$N_p = 19, \quad [\text{turns}]$$

Step No. 8 Calculate the current density, J, using a window utilization, $K_u = 0.29$.

$$J = \frac{P_t (10^4)}{K_f K_u B_{acf} A_p}, \quad [\text{amps} / \text{cm}^2]$$

$$J = \frac{102.5 (10^4)}{(4.0)(0.29)(0.05)(100000)(0.408)}, \quad [\text{amps} / \text{cm}^2]$$

$$J = 433, \quad [\text{amps} / \text{cm}^2]$$

Step No. 9 Calculate the input current, I_{in} .

$$I_{in} = \frac{P_o}{V_{in} \eta}, \quad [\text{amps}]$$

$$I_{in} = \frac{38}{(24)(0.98)}, \quad [\text{amps}]$$

$$I_{in} = 1.61, \quad [\text{amps}]$$

Step No. 10 Calculate the primary bare wire area, $A_{wp(B)}$.

$$A_{wp(B)} = \frac{I_{in} \sqrt{D_{max}}}{J}, \quad [\text{cm}^2]$$

$$A_{wp(B)} = \frac{(1.61)(0.707)}{433}, \quad [\text{cm}^2]$$

$$A_{wp(B)} = 0.00263, \quad [\text{cm}^2]$$

Step No. 11 Calculate the required number of primary strands, S_{np} .

$$S_{np} = \frac{A_{wp(B)}}{\# 26}$$

$$S_{np} = \frac{0.00263}{0.00128}$$

$$S_{np} = 2.05 \text{ use } 2$$

Step No. 12 Calculate the primary new $\mu\Omega$ per centimeter.

$$(\text{new}) \mu\Omega / \text{cm} = \frac{\mu\Omega / \text{cm}}{S_{np}}$$

$$(\text{new}) \mu\Omega / \text{cm} = \frac{1345}{2}$$

$$(\text{new}) \mu\Omega / \text{cm} = 673$$

Step No. 13 Calculate the primary resistance, R_p .

$$R_p = \text{MLT} (N_p) \left(\frac{\mu\Omega}{\text{cm}} \right) (10^{-6}) \quad [\text{ohms}]$$

$$R_p = (4.4)(19)(673)(10^{-6}) \quad [\text{ohms}]$$

$$R_p = 0.0563, \quad [\text{ohms}]$$

Step No. 14 Calculate the primary copper loss, P_p .

$$P_p = I_p^2 R_p, \quad [\text{watts}]$$

$$P_p = (1.61)^2 (0.0563), \quad [\text{watts}]$$

$$P_p = 0.146, \quad [\text{watts}]$$

Step No. 15 Calculate the secondary turns, N_{s1} .

$$N_{s1} = \frac{N_p V_{s1}}{V_{in}} \left(1 + \frac{\alpha}{100} \right), \quad [\text{turns}]$$

$$V_{s1} = V_o + V_d, \quad [\text{volts}]$$

$$V_{s1} = 5 + 1, \quad [\text{volts}]$$

$$V_{s1} = 6, \quad [\text{volts}]$$

$$N_{s1} = \frac{(19)(6)}{(24)} \left(1 + \frac{0.5}{100} \right), \quad [\text{turns}]$$

$$N_{s1} = 4.77 \text{ use } 5, \quad [\text{turns}]$$

Step No. 16 Calculate the secondary turns, N_{s2} .

$$N_{s2} = \frac{N_p V_{s2}}{V_{in}} \left(1 + \frac{\alpha}{100} \right), \quad [\text{turns}]$$

$$V_{s2} = V_o + 2V_d, \quad [\text{volts}]$$

$$V_{s2} = 12 + 2, \quad [\text{volts}]$$

$$V_{s2} = 14, \quad [\text{volts}]$$

$$N_{s2} = \frac{(19)(14)}{(24)} \left(1 + \frac{0.5}{100} \right), \quad [\text{turns}]$$

$$N_{s2} = 11.1 \text{ use } 11, \quad [\text{turns}]$$

Step No. 17 Calculate the secondary bare wire area, A_{ws1} .

$$A_{ws1} = \frac{I_o \sqrt{D_{\max}}}{J}, \quad [\text{cm}^2]$$

$$A_{ws1} = \frac{(4)(0.707)}{433}, \quad [\text{cm}^2]$$

$$A_{ws1} = 0.00653, \quad [\text{cm}^2]$$

Step No. 18 Calculate the required number of secondary strands, S_{ns1} .

$$S_{ns1} = \frac{A_{ws1}(B)}{\#26}$$

$$S_{ns1} = \frac{0.00653}{0.00128}$$

$$S_{ns1} = 5.1 \text{ use } 5$$

Step No. 19 Calculate the secondary, S_1 new $\mu\Omega$ per centimeter.

$$(\text{new}) \mu\Omega / \text{cm} = \frac{\mu\Omega / \text{cm}}{S_{ns1}}$$

$$(\text{new}) \mu\Omega / \text{cm} = \frac{1345}{5}$$

$$(\text{new}) \mu\Omega / \text{cm} = 269$$

Step No. 20 Calculate the secondary S_1 resistance, R_{s1} .

$$R_{s1} = \text{MLT}(N_{s1}) \left(\frac{\mu\Omega}{\text{cm}} \right) (10^{-6}), \quad [\text{ohms}]$$

$$R_{s1} = (4.4)(5)(269)(10^{-6}), \quad [\text{ohms}]$$

$$R_{s1} = 0.0059, \quad [\text{ohms}]$$

Step No. 21 Calculate the secondary copper loss, P_{s1} .

$$P_{s1} = I_{s1}^2 R_{s1}, \quad [\text{watts}]$$

$$P_{s1} = (4.0)^2 (0.0059), \quad [\text{watts}]$$

$$P_{s1} = 0.0944, \quad [\text{watts}]$$

Step No. 22 Calculate the secondary bare wire area, A_{ws2} .

$$A_{ws2} = \frac{I_2}{J}, \quad [\text{cm}^2]$$

$$A_{ws2} = \frac{(1)}{433}, \quad [\text{cm}^2]$$

$$A_{ws2} = 0.00231, \quad [\text{cm}^2]$$

Step No. 23 Calculate the required number of secondary strands, S_{ns2} .

$$S_{ns2} = \frac{A_{ws2}(B)}{\#26}$$

$$S_{ns2} = \frac{0.00231}{0.00128}$$

$$S_{ns2} = 1.8 \text{ use } 2$$

Step No. 24 Calculate the secondary, S_2 new $\mu\Omega$ per centimeter.

$$(\text{new}) \mu\Omega / \text{cm} = \frac{\mu\Omega / \text{cm}}{S_{ns2}}$$

$$(\text{new}) \mu\Omega / \text{cm} = \frac{1345}{2}$$

$$(\text{new}) \mu\Omega / \text{cm} = 673$$

Step No. 25 Calculate the secondary, S_2 resistance, R_{s2} .

$$R_{s2} = \text{MLT} (N_{s1}) \left(\frac{\mu\Omega}{\text{cm}} \right) (10^{-6}) \quad [\text{ohms}]$$

$$R_{s2} = (4.4)(11)(673)(10^{-6}) \quad [\text{ohms}]$$

$$R_{s2} = 0.0326, \quad [\text{ohms}]$$

Step No. 26 Calculate the secondary, S_2 copper loss, P_{s2} .

$$P_{s2} = I_{s2}^2 R_{s2}, \quad [\text{watts}]$$

$$P_{s2} = (1.0)^2 (0.0326), \quad [\text{watts}]$$

$$P_{s2} = 0.0326, \quad [\text{watts}]$$

Step No. 27 Calculate the total secondary copper loss, P_s .

$$P_s = P_{s1} + P_{s2}, \quad [\text{watts}]$$

$$P_s = 0.0944 + 0.0326, \quad [\text{watts}]$$

$$P_s = 0.127, \quad [\text{watts}]$$

Step No. 28 Calculate the total primary and secondary copper loss, P_{cu} .

$$P_{cu} = P_p + P_s, \quad [\text{watts}]$$

$$P_{cu} = 0.146 + 0.127, \quad [\text{watts}]$$

$$P_{cu} = 0.273, \quad [\text{watts}]$$

Step No. 29 Calculate the transformer regulation, α .

$$\alpha = \frac{P_{cu}}{P_o} (100), \quad [\%]$$

$$\alpha = \frac{(0.273)}{(38)} (100), \quad [\%]$$

$$\alpha = 0.718, \quad [\%]$$

Step No. 30 Calculate the milliwatts per gram, mW/g . Use the equation for this material in Chapter 2.

$$mW / g = 0.000318 (f)^{1.51} (B_{ac})^{2.747}$$

$$mW / g = 0.000318 (100000)^{1.51} (0.05)^{2.747}$$

$$mW / g = 3.01$$

Step No. 31 Calculate the core loss, P_{fe} .

$$P_{fe} = (mW / g) (W_{fe}) (10^{-3}) \quad [\text{watts}]$$

$$P_{fe} = (3.01) (15) (10^{-3}) \quad [\text{watts}]$$

$$P_{fe} = 0.045, \quad [\text{watts}]$$

Step No. 32 Calculate the total loss, P_Σ .

$$P_\Sigma = P_{cu} + P_{fe}, \quad [\text{watts}]$$

$$P_\Sigma = (0.273) + (0.045), \quad [\text{watts}]$$

$$P_\Sigma = 0.318, \quad [\text{watts}]$$

Step No. 33 Calculate the watts per unit area, ψ .

$$\psi = \frac{P_{\Sigma}}{A_t}, \quad [\text{watts} / \text{cm}^2]$$

$$\psi = \frac{(0.318)}{(19.7)}, \quad [\text{watts} / \text{cm}^2]$$

$$\psi = 0.0161, \quad [\text{watts} / \text{cm}^2]$$

Step No. 34 Calculate the temperature rise, T_r .

$$T_r = 450 (\psi)^{(0.826)}, \quad [^{\circ}\text{C}]$$

$$T_r = 450 (0.0161)^{(0.826)}, \quad [^{\circ}\text{C}]$$

$$T_r = 14.9, \quad [^{\circ}\text{C}]$$

Step No. 35 Calculate the total window utilization, K_u .

$$K_u = K_{up} + K_{us}$$

$$K_{us} = K_{us1} + K_{us2}$$

$$K_{us1} = \frac{N_{s1} S_{n1} A_{ws1(B)}}{W_a}$$

$$K_{us1} = \frac{(10)(5)(0.00128)}{(0.658)} = 0.0973$$

$$K_{us2} = \frac{(11)(2)(0.00128)}{(0.658)} = 0.0428$$

$$K_{up} = \frac{N_p S_{np} A_{wp(B)}}{W_a}$$

$$K_{up} = \frac{(38)(2)(0.00128)}{(0.658)} = 0.148$$

$$K_u = (0.148) + (0.0973 + 0.0428)$$

$$K_u = 0.288$$

Chapter 8

DC Inductor Design Using Gapped Cores

Table of Contents

1. Introduction	
2. Critical Inductance for Sine Wave Rectification	
3. Critical Inductance for Buck Type Converters	
4. Core Materials, Used in PWM Converters	
5. Fundamental Considerations	
6. Fringing Flux	
7. Inductors	
8. Relationship of, A_p , to Inductor's Energy-Handling Capability	
9. Relationship of, K_g , to Inductor's Energy-Handling Capability	
10. Gapped Inductor Design Example Using the Core Geometry, K_g , Approach.....	
11. Gapped Inductor Design Example Using the Area Product, A_p , Approach	

Introduction

Designers have used various approaches in arriving at suitable inductor designs. For example, in many cases, a rule of thumb used for dealing with current density is that a good working level is 200 amps-per-cm² (1000 Cir-Mils-per-amp). This rule is satisfactory in many instances; however, the wire size used to meet this requirement may produce a heavier and bulkier inductor than desired or required. The information presented herein will make it possible to avoid the use of this and other rules of thumb and to develop an economical and a better design.

Critical Inductance for Sine Wave Rectification

The LC filter is the basic method of reducing ripple levels. The two basic rectifier circuits are the full-wave center-tap as shown in Figure 8-1 and the full-wave bridge, as shown in Figure 8-2. To achieve normal inductor operation, it is necessary that there be a continuous flow of current through the input inductor, L1.

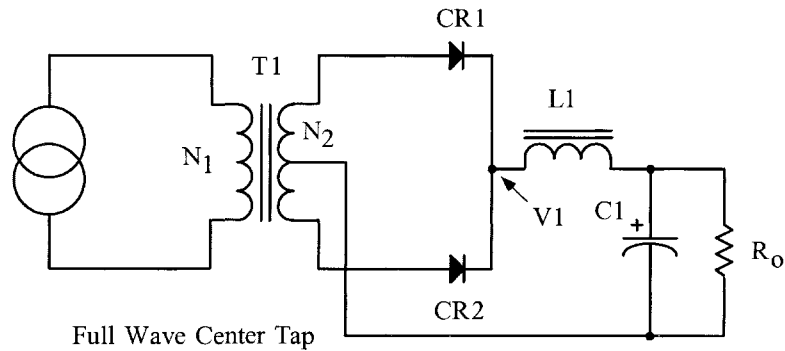


Figure 8-1. Full-Wave Center Tap with an LC filter.

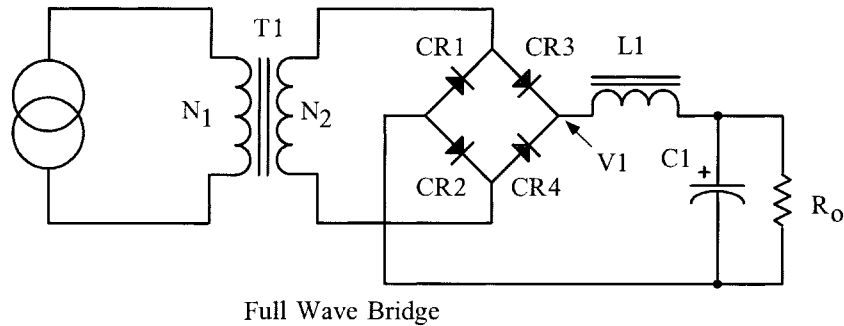


Figure 8-2. Full-Wave Bridge with an LC filter.

The value for minimum inductance called critical inductance, $L_{(crit)}$ is:

$$L_{(crit)} = \frac{R_{o(max)}}{3\omega}, \quad [\text{henrys}] \quad [8-1]$$

Where:

$$\omega = 2\pi f$$

$$f = \text{line frequency}$$

The higher the load resistance, R_o , (i.e., the lower the dc load current), the more difficult it is to maintain a continuous flow of current. The filter inductor operates in the following manner: When R_o approaches infinity, under an unloaded condition, (no bleeder resistor), $I_o = 0$, the filter capacitor will charge to V_{1pk} , the peak voltage. Therefore, the output voltage will be equal to the peak value of the input voltage, as shown in Figure 8-3.

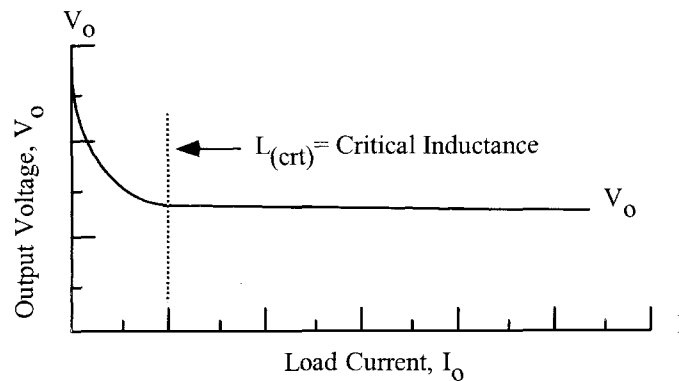


Figure 8-3. Critical Inductance Point.

The ripple reduction from a single stage LC filter can be calculated, using Equation 8-2 and Figure 8-4.

$$V_{r(pk)} = V_{in(pk)} \left(\frac{1}{(2\pi f)^2 L1C1} \right), \quad [\text{volts-peak}] \quad [8-2]$$

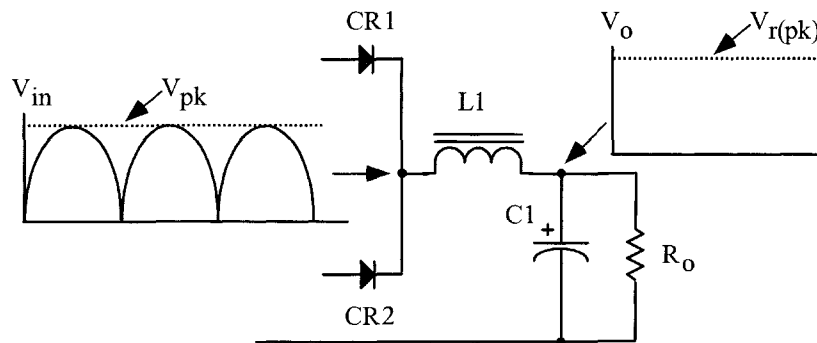


Figure 8-4. LC Filter Ripple Reduction.

Critical Inductance for Buck Type Converters

The buck type converter schematic is shown in Figure 8-5, and the buck type dc-to-dc converter is shown in Figure 8.6. The buck regulator filter circuit shown in Figure 8-5 has three current probes. These current probes monitor the three basic currents in a switch mode, buck output filter. Current probe A monitors the power MOSFET, Q1, switching current. Current probe B monitors the commutating current through CR1. Current probe C monitors the current through the output inductor, L1.

The typical filter waveforms of the buck converter are shown in Figure 8-7. The waveforms are shown with the converter operating at a 0.5 duty ratio. The applied voltage, V1 to the filter, is shown in Figure 8-7A. The power MOSFET, Q1, current is shown in Figure 8-7B. The commutating current flowing through CR1 is shown in Figure 8-7C. The commutating current is the result of Q1 being turned off, and the field in L1 collapsing, producing the commutating current. The current flowing through L1 is shown in Figure 8-7D. The current flowing through L1 is the sum of the currents in Figure 8-7B and 8-7C.

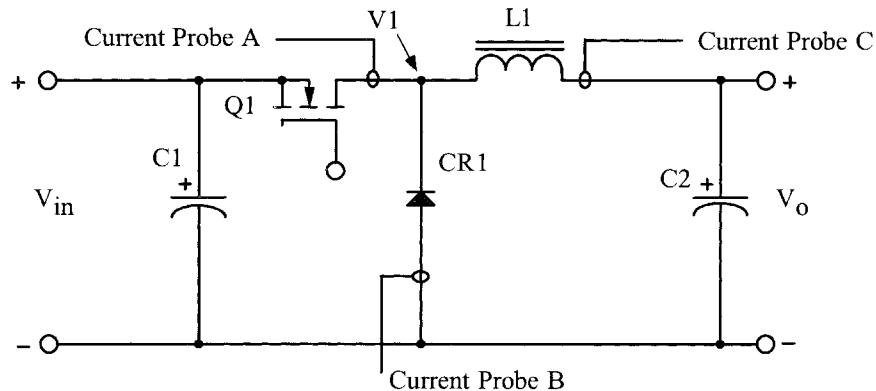


Figure 8-5. Buck Regulator Converter.

The critical inductance current is shown in Figure 8-8, 8-B and is realized in Equation 8-3. The critical inductance current is when the ratio of the delta current to the output load current is equal to $2 = \Delta I / I_o$. If the output load current is allowed to go beyond this point, the current will become discontinuous, as shown in Figure 8-8, 8-D. The applied voltage, V1, will have ringing at the level of the output voltage, as shown in Figure 8-8, 8-C. When the current in the output inductor becomes discontinuous, as shown in Figure 8-8, 8-D, the response time for a step load becomes very poor.

When designing multiple output converters similar to Figure 8-6, the slaved outputs should never have the current in the inductor go discontinuous or to zero. If the current goes to zero, a slaved output voltage will rise to the value of V1. If the current is allowed to go to zero, then, there is no potential difference between the input and output voltage of the filter. Then the output voltage will rise to equal the peak input voltage.

$$L_{(critical)} = \frac{V_o T (1 - D_{(min)})}{2 I_{o(min)}}, \text{ [henrys] [8-3]}$$

$$D_{(min)} = \frac{V_o}{(\eta V_{in(max)})} \text{ [8-4]}$$

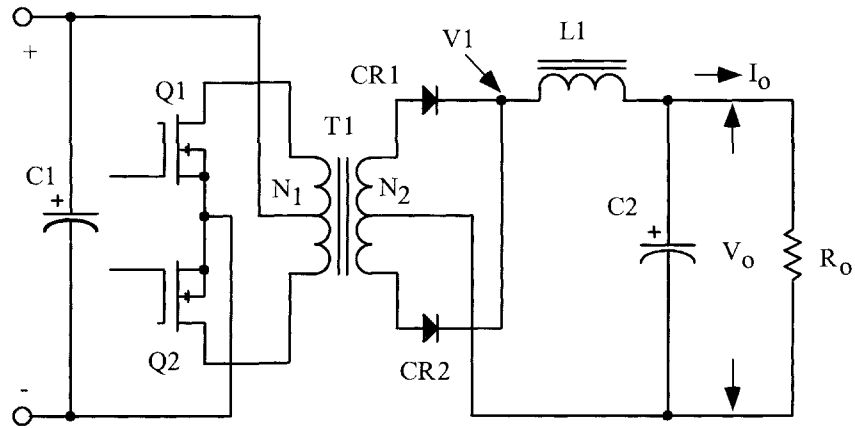


Figure 8-6. Push-Pull Buck Type Converter.

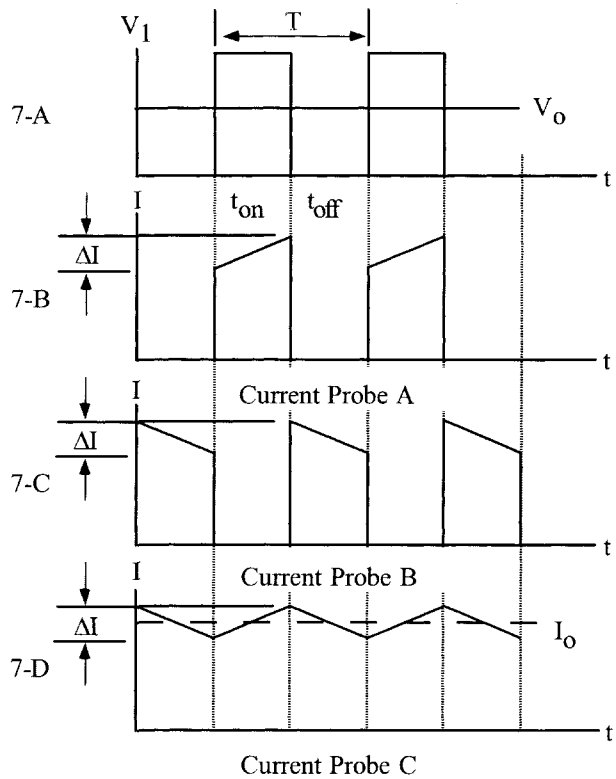


Figure 8-7. Typical Buck Converter Waveforms, Operating at a 0.5 Duty Ratio.

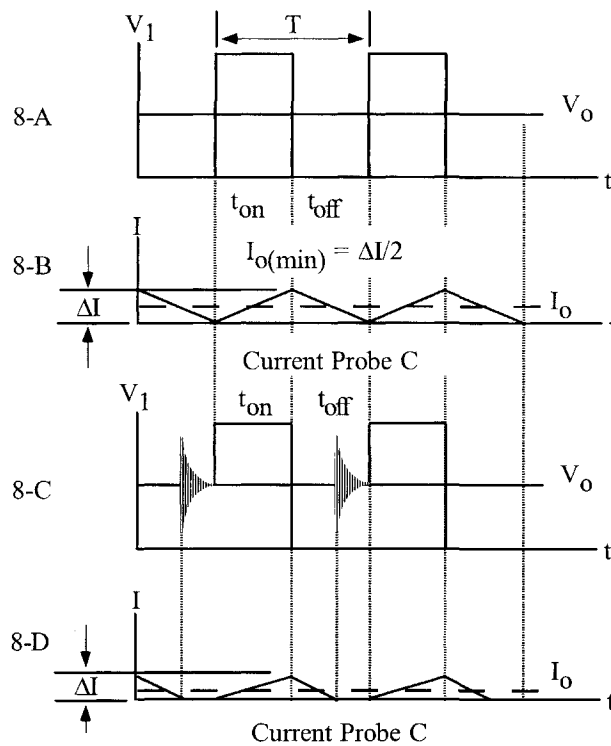


Figure 8-8. Buck Converter, Output Filter Inductor Goes from Critical to Discontinuous Operation.

Core Materials, Used in PWM Converters

Designers have routinely tended to specify Molypermalloy powder materials for filter inductors used in high-frequency, power converters and pulse-width-modulators (PWM) switched regulators, because of the availability of manufacturers' literature containing tables, graphs, and examples that simplify the design task. Use of these cores may result in an inductor design not optimized for size and weight. For example, as shown in Figure 8-9, Molypermalloy powder cores, operating with a dc bias of $0.3T$, have only about 80% of the original inductance, with very rapid falloff at higher flux densities. When size is of greatest concern then, magnetic materials with high flux saturation, B_s , would be first choice. Materials, such as silicon or some amorphous materials, have approximately four times the useful flux density compared to Molypermalloy powder cores. Iron alloys retain 90% of their original inductance at greater than $1.2T$. Iron alloys, when designed correctly and used in the right application, will perform well at frequencies up to 100kHz. When operating above 100kHz, then the only material is ferrite. Ferrite materials have a negative temperature coefficient regarding flux density. The operating temperature and temperature rise should be used to calculate the maximum flux density.

To get optimum performance, together with size, the engineer must evaluate the materials for both, B_s , and B_{ac} . See Table 8-1. The operating dc flux has only to do with I^2R losses, (copper). The ac flux, B_{ac} , has to do with core loss. This loss depends directly on the material. There are many factors that impact a design: cost, size, temperature rise and material availability.

There are significant advantages to be gained by the use of iron alloys and ferrites in the design of power inductors, despite certain disadvantages, such as the need for banding and gapping materials, banding tools, mounting brackets, and winding mandrels.

Iron alloys and ferrites provide greater flexibility in the design of high frequency power inductors, because the air gap can be adjusted to any desired length, and because the relative permeability is high, even at high, dc flux density.

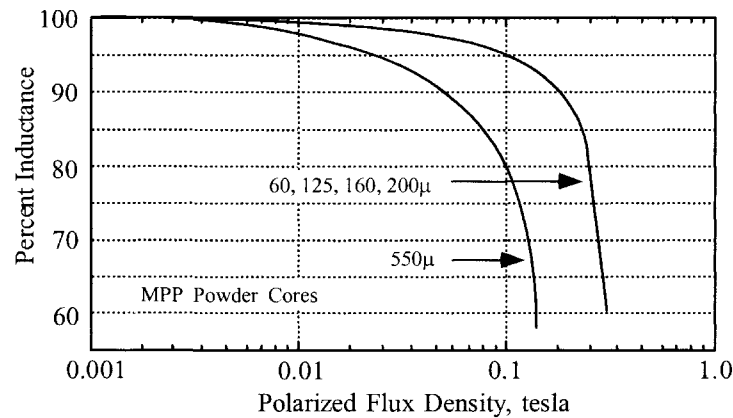


Figure 8-9. Inductance Versus dc Bias.

Table 8-1. Magnetic Material Properties

Magnetic Material Properties					
Material Name	Composition	Initial Permeability μ_i	Flux Density Tesla B_s	Curie Temp. °C	Density grams/cm ³ δ
Silicon	3-97 SiFe	1500	1.5-1.8	750	7.63
Orthonol	50-50 NiFe	2000	1.42-1.58	500	8.24
Permalloy	80-20 NiFe	25000	0.66-0.82	460	8.73
Amorphous	81-3.5 FeSi	1500	1.5-1.6	370	7.32
Amorphous	66-4 CoFe	800	0.57	250	7.59
Amorphous(μ)	73-15 FeSi	30000	1.0-1.2	460	7.73
Ferrite	MnZn	2500	0.5	>230	4.8

Fundamental Considerations

The design of a linear reactor depends upon four related factors:

1. Desired inductance, L
2. Direct current, I_{dc}
3. Alternating current, ΔI
4. Power loss and temperature, T_r

With these requirements established, the designer must determine the maximum values for, B_{dc} , and, B_{ac} , that will not produce magnetic saturation. The designer must make trade-offs that will yield the highest inductance for a given volume. It should be remembered the peak operating flux, B_{pk} , depends upon, B_{dc} + B_{ac} , in the manner in Figure 8-10.

$$B_{pk} = B_{dc} + \frac{B_{ac}}{2}, \quad [\text{tesla}] \quad [8-5]$$

$$B_{dc} = \frac{0.4\pi N I_{dc} (10^{-4})}{l_g + \left(\frac{MPL}{\mu_m}\right)}, \quad [\text{tesla}] \quad [8-6]$$

$$B_{ac} = \frac{0.4\pi N \left(\frac{\Delta I}{2}\right) (10^{-4})}{l_g + \left(\frac{MPL}{\mu_m}\right)}, \quad [\text{tesla}] \quad [8-7]$$

$$B_{pk} = \frac{0.4\pi N \left(I_{dc} + \frac{\Delta I}{2}\right) (10^{-4})}{l_g + \left(\frac{MPL}{\mu_m}\right)}, \quad [\text{tesla}] \quad [8-8]$$

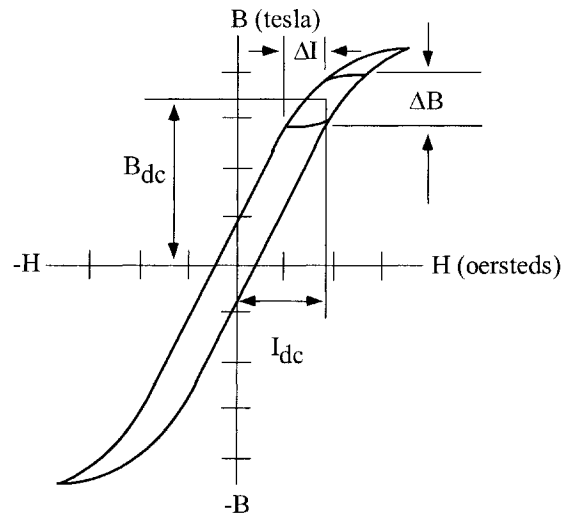


Figure 8-10. Inductor Flux Density Versus $I_{dc} + \Delta I$ Current.

The inductance of an iron-core inductor carrying direct current and having an air gap may be expressed as:

$$L = \frac{0.4\pi N^2 A_c (10^{-8})}{l_g + \left(\frac{MPL}{\mu_m}\right)}, \text{ [henrys] [8-9]}$$

This equation shows that inductance is dependent on the effective length of the magnetic path, which is the sum of the air gap length, l_g , and the ratio of the core mean length to the material permeability, MPL/μ_m . When the core air gap, l_g , is large compared to the ratio, MPL/μ_m , because of material permeability, μ_m , variations in μ_m do not substantially affect the total effective magnetic path length or the inductance. Then the inductance Equation [8-9] reduces to:

$$L = \frac{0.4\pi N^2 A_c (10^{-8})}{l_g}, \text{ [henrys] [8-10]}$$

Final determination of the air gap size requires consideration of the effect of fringing flux, which is a function of gap dimension, the shape of the pole faces, and the shape, size, and location of the winding. Its net effect is to shorten the air gap. Because of the fringing flux it is wise to lower the initial operating flux density, 10 to 20%.

Fringing Flux

Fringing flux decreases the total reluctance of the magnetic path and therefore, increases the inductance by a factor, F , to a value greater than that calculated from Equation 8-10. Fringing flux is a larger percentage of the total for the larger gaps.

The fringing factor is:

$$F = 1 + \frac{l_g}{\sqrt{A_c}} \ln \left(\frac{2G}{l_g} \right) \quad [8-11]$$

Where G is the winding length, defined in Chapter 3. This equation is valid for laminations, C cores and cut ferrites. Equation [8-11] is plotted in Figure 8-11.

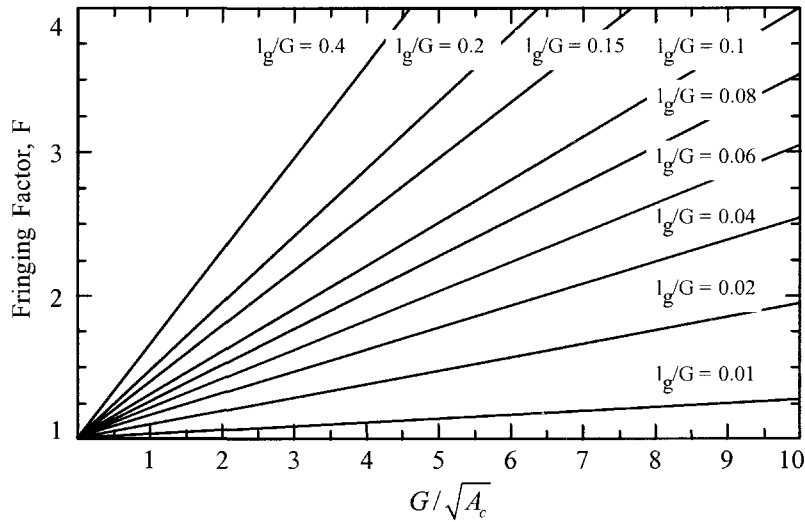


Figure 8-11. Increase of Inductance with Fringing Flux at the Gap.

As the air gap increases, the flux across the gap fringes more and more. Some of the fringing flux strikes the core, perpendicular to the strip or tape, and sets up eddy currents, which cause additional losses in the core. If the gap dimension gets too large, the fringing flux will strike the copper winding and produce eddy currents, generating heat, just like an induction heater. The fringing flux will jump the gap and produce eddy currents, in both the core and winding, as shown in Figure 8-12.

The inductance, L computed in Equation [8-10], does not include the effect of the fringing flux. The value of inductance, L' corrected for fringing flux is:

$$L' = \frac{0.4\pi N^2 F A_c (10^{-8})}{l_g}, \quad [\text{henrys}] \quad [8-12]$$

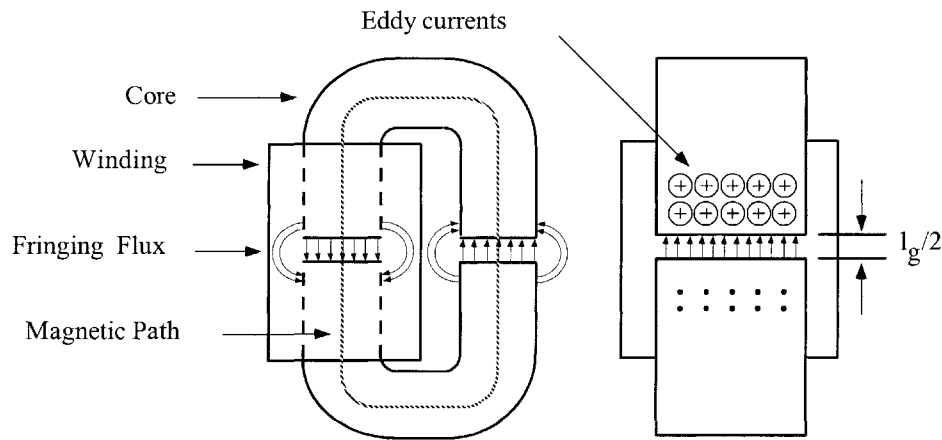


Figure 8-12. Fringing Flux Around the Gap of an Inductor.

The effective permeability may be calculated from the following equation:

$$\mu_e = \frac{\mu_m}{1 + \left(\frac{l_g}{MPL}\right)\mu_m} \quad [8-13]$$

Where, μ_m , is the material permeability.

Inductors

Inductors that carry direct current are used frequently in a wide variety of ground, air, and space applications. Selection of the best magnetic core for an inductor frequently involves a trial-and-error type of calculation.

The author has developed a simplified method of designing optimum, dc carrying inductors with gapped cores. This method allows the engineer to select the proper core that will provide correct copper loss, and make allowances for fringing flux, without relying on trial-and-error and the use of the cumbersome Hanna's curves.

Rather than discuss the various methods used by transformer designers, the author believes it is more useful to consider typical design problems, and to work out solutions using the approach based upon newly formulated relationships. Two gapped core designs will be compared. To compare their merits, the first design example will use the core geometry, K_g , and the second design will use the area product, A_p .

Inductors, designed in this handbook, are banded together with phosphor bronze banding material, or held together with aluminum brackets. The use of steel banding material; or brackets that bridge the gap are not recommended, because the use of steel across the gap is called shorting the gap. When the gap is shorted, the inductance will increase from the calculated value.

Relationship of, A_p , to Inductor's Energy-Handling Capability

The energy-handling capability of a core is related to its area product, A_p , by the equation:

$$A_p = \frac{2(\text{Energy})(10^4)}{B_m J K_u}, \quad [\text{cm}^4] \quad [8-14]$$

Where: Energy is in watt-seconds.

B_m is the flux density, tesla.

J is the current density, amps-per-cm².

K_u is the window utilization factor. (See Chapter 4)

From the above, it can be seen that factors such as flux density, B_m , window utilization factor, K_u , (which defines the maximum space that may be used by the copper in the window), and the current density, J , which controls the copper loss, all impact the area product, A_p . The energy-handling capability of a core is derived from:

$$\text{Energy} = \frac{LI^2}{2}, \quad [\text{watt-seconds}] \quad [8-15]$$

Relationship of, K_g , to Inductor's Energy-Handling Capability

Inductors, like transformers, are designed for a given temperature rise. They can also be designed for a given regulation. The regulation and energy handling ability of a core is related to two constants:

$$\alpha = \frac{(\text{Energy})^2}{K_g K_e}, \quad [\%] \quad [8-16]$$

Where, α , is the regulation, %:

The constant, K_g , is determined by the core geometry:

$$K_g = \frac{W_a A_c^2 K_u}{MLT}, \quad [\text{cm}^5] \quad [8-17]$$

The constant, K_e , is determined by the magnetic and electrical operating conditions:

$$K_e = 0.145 P_o B_{pk}^2 (10^{-4}) \quad [8-18]$$

The peak operating flux density, B_{pk} , is:

$$B_{pk} = B_{dc} + \frac{B_{ac}}{2}, \quad [\text{tesla}] \quad [8-19]$$

From the above, it can be seen that the flux density, B_{pk} , is the predominant factor governing size.

The output power, P_o , is defined in Figure 8-13.

$$P_{o(L1)} = V_{(01)} I_{(01)} \quad P_{o(L2)} = V_{(02)} I_{(02)} \quad [8-20]$$

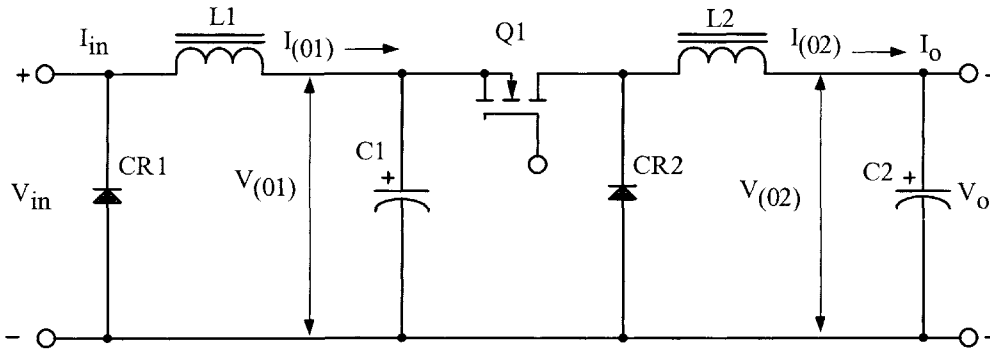


Figure 8-13. Defining the Inductor Output Power.

Gapped Inductor Design Example Using the Core Geometry, K_g , Approach

Step No. 1 Design a linear dc inductor with the following specifications.

1. Inductance, L = 0.0025 henrys
2. dc current, I_o = 1.5 amps
3. ac current, ΔI = 0.2 amps
4. Output power, P_o = 100 watts
5. Regulation, α = 1.0 %
6. Ripple Frequency = 200 kHz
7. Operating flux density, B_m = 0.22 tesla
8. Core Material = ferrite
9. Window utilization, K_u = 0.4
10. Temperature rise goal, T_r = 25°C

Step No. 2 Calculate the peak current, I_{pk} .

$$I_{pk} = I_o + \frac{\Delta I}{2}, \quad [\text{amps}]$$

$$I_{pk} = (1.5) + \frac{(0.2)}{2}, \quad [\text{amps}]$$

$$I_{pk} = 1.6, \quad [\text{amps}]$$

Step No. 3 Calculate the energy-handling capability.

$$\text{Energy} = \frac{LI_{pk}^2}{2}, \quad [\text{watt-seconds}]$$

$$\text{Energy} = \frac{(0.0025)(1.6)^2}{2}, \quad [\text{watt-seconds}]$$

$$\text{Energy} = 0.0032, \quad [\text{watt-seconds}]$$

Step No. 4 Calculate the electrical conditions coefficient, K_e .

$$K_e = 0.145 P_o B_m^2 (10^{-4})$$

$$K_e = 0.145(100)(0.22)^2 (10^{-4})$$

$$K_e = 0.0000702$$

Step No. 5 Calculate the core geometry coefficient, K_g .

$$K_g = \frac{(\text{Energy})^2}{K_e \alpha}, \quad [\text{cm}^5]$$

$$K_g = \frac{(0.0032)^2}{(0.0000702)(1.0)}, \quad [\text{cm}^5]$$

$$K_g = 0.146, \quad [\text{cm}^5]$$

Step No. 6 Select an ETD ferrite core from Chapter 3. The data listed is the closest core to the calculated core geometry, K_g .

- | | |
|------------------------------------|-------------------------|
| 1. Core Number | = ETD-39 |
| 2. Magnetic Path Length, MPL | = 9.22 cm |
| 3. Core Weight, W_{ife} | = 60 grams |
| 4. Mean Length Turn, MLT | = 8.3 cm |
| 5. Iron Area, A_c | = 1.252 cm ² |
| 6. Window Area, W_a | = 2.34 cm ² |
| 7. Area Product, A_p | = 2.93 cm ⁴ |
| 8. Core Geometry, K_g | = 0.177 cm ⁵ |
| 9. Surface Area, A_t | = 69.9 cm ² |
| 10. Material, P | = 2500 μ |
| 11. Millihenrys-per-1k, AL | = 3295 mh |
| 12. Winding Length, G | = 2.84 cm |

Step No. 7 Calculate the current density, J , using the area product equation, A_p .

$$J = \frac{2(\text{Energy})(10^4)}{B_m A_p K_u}, \quad [\text{amps-per-cm}^2]$$
$$J = \frac{2(0.0032)(10^4)}{(0.22)(2.93)(0.4)}, \quad [\text{amps-per-cm}^2]$$
$$J = 248, \quad [\text{amps-per-cm}^2]$$

Step No. 8 Calculate the rms current, I_{rms} .

$$I_{rms} = \sqrt{I_o^2 + \Delta I^2}, \quad [\text{amps}]$$
$$I_{rms} = \sqrt{(1.5)^2 + (0.2)^2}, \quad [\text{amps}]$$
$$I_{rms} = 1.51, \quad [\text{amps}]$$

Step No. 9 Calculate the required bare wire area, $A_{w(B)}$.

$$A_{W(B)} = \frac{I_{rms}}{J}, \quad [\text{cm}^2]$$
$$A_{W(B)} = \frac{(1.51)}{(248)}, \quad [\text{cm}^2]$$
$$A_{W(B)} = 0.00609, \quad [\text{cm}^2]$$

Step No. 10 Select a wire from the Wire Table in Chapter 4. If the area is not within 10%, take the next smallest size. Also, record the micro-ohms per centimeter.

$$\text{AWG} = \#19$$
$$\text{Bare, } A_{W(B)} = 0.00653, \quad [\text{cm}^2]$$
$$\text{Insulated, } A_w = 0.00754, \quad [\text{cm}^2]$$
$$\left(\frac{\mu\Omega}{\text{cm}} \right) = 264, \quad [\text{micro-ohm/cm}]$$

Step No. 11 Calculate the effective window area, $W_{a(\text{eff})}$. Using the window area found in Step 6. A typical value for, S_3 , is 0.75, as shown in Chapter 4.

$$W_{a(\text{eff})} = W_a S_3, \quad [\text{cm}^2]$$
$$W_{a(\text{eff})} = (2.34)(0.75), \quad [\text{cm}^2]$$
$$W_{a(\text{eff})} = 1.76, \quad [\text{cm}^2]$$

Step No. 12 Calculate the number turns possible, N, using the insulated wire area, A_w , found in Step 10. A typical value for, S_2 , is 0.6, as shown in Chapter 4.

$$N = \frac{W_{a(eff)} S_2}{A_w}, \quad [\text{turns}]$$

$$N = \frac{(1.76)(0.60)}{(0.00754)}, \quad [\text{turns}]$$

$$N = 140, \quad [\text{turns}]$$

Step No. 13 Calculate the required gap, l_g .

$$l_g = \frac{0.4\pi N^2 A_c (10^{-8})}{L} - \left(\frac{\text{MPL}}{\mu_m} \right), \quad [\text{cm}]$$

$$l_g = \frac{(1.26)(140)^2 (1.25)(10^{-8})}{(0.0025)} - \left(\frac{9.22}{2500} \right), \quad [\text{cm}]$$

$$l_g = 0.120, \quad [\text{cm}]$$

Step No. 14 Calculate the equivalent gap in mils.

$$\text{mils} = \text{cm}(393.7)$$

$$\text{mils} = (0.120)(393.7)$$

$$\text{mils} = 47.2 \text{ use } 50$$

Step No. 15 Calculate the fringing flux factor, F.

$$F = 1 + \frac{l_g}{\sqrt{A_c}} \ln \left(\frac{2G}{l_g} \right)$$

$$F = 1 + \frac{(0.120)}{\sqrt{1.25}} \ln \left(\frac{2(2.84)}{0.120} \right)$$

$$F = 1.41$$

Step No. 16 Calculate the new number of turns, N_n , by inserting the fringing flux, F.

$$N_n = \sqrt{\frac{l_g L}{0.4\pi A_c F (10^{-8})}}, \quad [\text{turns}]$$

$$N_n = \sqrt{\frac{(0.120)(0.0025)}{(1.26)(1.25)(1.41)(10^{-8})}}, \quad [\text{turns}]$$

$$N_n = 116, \quad [\text{turns}]$$

Step No. 17 Calculate the winding resistance, R_L . Use the MLT from Step 6 and the micro-ohm per centimeter from Step 10.

$$R_L = (\text{MLT})(N_n) \left(\frac{\mu\Omega}{\text{cm}} \right) (10^{-6}), \text{ [ohms]}$$

$$R_L = (8.3)(116)(264)(10^{-6}), \text{ [ohms]}$$

$$R_L = 0.254, \text{ [ohms]}$$

Step No. 18 Calculate the copper loss, P_{cu} .

$$P_{cu} = I_{rms}^2 R_L, \text{ [watts]}$$

$$P_{cu} = (1.51)^2 (0.254), \text{ [watts]}$$

$$P_{cu} = 0.579, \text{ [watts]}$$

Step No. 19 Calculate the regulation, α .

$$\alpha = \frac{P_{cu}}{P_o} (100), \text{ [%]}$$

$$\alpha = \frac{(0.579)}{(100)} (100), \text{ [%]}$$

$$\alpha = 0.579, \text{ [%]}$$

Step No. 20 Calculate the ac flux density, B_{ac} .

$$B_{ac} = \frac{0.4\pi N_n F \left(\frac{\Delta I}{2} \right) (10^{-4})}{l_g + \left(\frac{\text{MPL}}{\mu_m} \right)}, \text{ [tesla]}$$

$$B_{ac} = \frac{(1.26)(116)(1.41) \left(\frac{0.2}{2} \right) (10^{-4})}{(0.120) + \left(\frac{9.22}{2500} \right)}, \text{ [tesla]}$$

$$B_{ac} = 0.0167, \text{ [tesla]}$$

Step No. 21 Calculate the watts per kilogram for ferrite, P , material in Chapter 2. Watts per kilogram can be written in milliwatts per gram.

$$\text{mW/g} = k f^{(m)} B_{ac}^{(n)}$$

$$\text{mW/g} = (0.00004855)(200000)^{(1.63)} (0.0167)^{(2.62)}$$

$$\text{mW/g} = 0.468$$

Step No. 22 Calculate the core loss, P_{fe} .

$$P_{fe} = (\text{mW/g})(W_{fe})(10^{-3}), \text{ [watts]}$$

$$P_{fe} = (0.468)(60)(10^{-3}), \text{ [watts]}$$

$$P_{fe} = 0.0281, \text{ [watts]}$$

Step No. 23 Calculate the total loss, copper plus iron, P_{Σ} .

$$P_{\Sigma} = P_{fe} + P_{cu}, \text{ [watts]}$$

$$P_{\Sigma} = (0.0281) + (0.579), \text{ [watts]}$$

$$P_{\Sigma} = 0.607, \text{ [watts]}$$

Step No. 24 Calculate the watt density, ψ . The surface area, A_t , can be found in Step 6.

$$\psi = \frac{P_{\Sigma}}{A_t}, \text{ [watts/cm}^2\text{]}$$

$$\psi = \frac{(0.607)}{(69.9)}, \text{ [watts/cm}^2\text{]}$$

$$\psi = 0.00868, \text{ [watts/cm}^2\text{]}$$

Step No. 25 Calculate the temperature rise, T_r .

$$T_r = 450(\psi)^{(0.826)}, \text{ [}^{\circ}\text{C]}$$

$$T_r = 450(0.00868)^{(0.826)}, \text{ [}^{\circ}\text{C]}$$

$$T_r = 8.92, \text{ [}^{\circ}\text{C]}$$

Step No. 26 Calculate the peak flux density, B_{pk} .

$$B_{pk} = \frac{0.4\pi N_n F \left(I_{dc} + \frac{\Delta I}{2} \right) (10^{-4})}{l_g + \left(\frac{\text{MPL}}{\mu_m} \right)}, \text{ [tesla]}$$

$$B_{pk} = \frac{(1.26)(116)(1.41)(1.6)(10^{-4})}{(0.127) + \left(\frac{9.22}{2500} \right)}, \text{ [tesla]}$$

$$B_{pk} = 0.252, \text{ [tesla]}$$

Note:

The big advantage in using the core geometry design procedure is that the wire current density is calculated. When using the area product design procedure, the current density is an estimate, at best. In this next design the same current density will be used as in the core geometry design.

Gapped Inductor Design Example Using the Area Product, A_p , Approach

Step No. 1 Design a linear dc inductor with the following specifications:

- 1. Inductance, L = 0.0025 henrys
- 2. dc current, I_o = 1.5 amps
- 3. ac current, ΔI = 0.2 amps
- 4. Output power, P_o = 100 watts
- 5. Current Density, J = 250 amps-per-cm²
- 6. Ripple Frequency = 200 kHz
- 7. Operating flux density, B_m = 0.22 tesla
- 8. Core Material = ferrite
- 9. Window utilization, K_u = 0.4
- 10. Temperature rise goal, T_r = 25°C

Step No. 2 Calculate the peak current, I_{pk} .

$$I_{pk} = I_o + \frac{\Delta I}{2}, \text{ [amps]}$$

$$I_{pk} = (1.5) + \frac{(0.2)}{2}, \text{ [amps]}$$

$$I_{pk} = 1.6, \text{ [amps]}$$

Step No. 3 Calculate the energy-handling capability.

$$\text{Energy} = \frac{LI_{pk}^2}{2}, \text{ [watt-seconds]}$$

$$\text{Energy} = \frac{(0.0025)(1.6)^2}{2}, \text{ [watt-seconds]}$$

$$\text{Energy} = 0.0032, \text{ [watt-seconds]}$$

Step No. 4 Calculate the area product, A_p .

$$A_p = \frac{2(\text{Energy})(10^4)}{B_m J K_u}, \quad [\text{cm}^4]$$

$$A_p = \frac{2(0.0032)(10^4)}{(0.22)(248)(0.4)}, \quad [\text{cm}^4]$$

$$A_p = 2.93, \quad [\text{cm}^4]$$

Step No. 5 Select an ETD ferrite core from Chapter 3. The data listed is the closest core to the calculated area product, A_p .

- | | |
|------------------------------------|-------------------------|
| 1. Core Number | = ETD-39 |
| 2. Magnetic Path Length, MPL | = 9.22 cm |
| 3. Core Weight, W_{tfe} | = 60 grams |
| 4. Mean Length Turn, MLT | = 8.3 cm |
| 5. Iron Area, A_c | = 1.252 cm ² |
| 6. Window Area, W_a | = 2.34 cm ² |
| 7. Area Product, A_p | = 2.93 cm ⁴ |
| 8. Core Geometry, K_g | = 0.177 cm ⁵ |
| 9. Surface Area, A_t | = 69.9 cm ² |
| 10. Material, P | = 2500μ |
| 11. Millihenrys-per-1k, A L | = 3295 mh |
| 12. Winding Length, G | = 2.84 cm |

Step No. 6 Calculate the rms current, I_{rms} .

$$I_{rms} = \sqrt{I_o^2 + \Delta I^2}, \quad [\text{amps}]$$

$$I_{rms} = \sqrt{(1.5)^2 + (0.2)^2}, \quad [\text{amps}]$$

$$I_{rms} = 1.51, \quad [\text{amps}]$$

Step No. 7 Calculate the required bare wire area, $A_{w(B)}$.

$$A_{w(B)} = \frac{I_{rms}}{J}, \quad [\text{cm}^2]$$

$$A_{w(B)} = \frac{(1.51)}{(248)}, \quad [\text{cm}^2]$$

$$A_{w(B)} = 0.00609, \quad [\text{cm}^2]$$

Step No. 8 Select a wire from the Wire Table in Chapter 4. If the area is not within 10%, take the next smallest size. Also, record micro-ohms per centimeter.

$$\text{AWG} = \#19$$

$$\text{Bare, } A_{w(b)} = 0.00653, \text{ [cm}^2\text{]}$$

$$\text{Insulated, } A_w = 0.00754, \text{ [cm}^2\text{]}$$

$$\left(\frac{\mu\Omega}{\text{cm}}\right) = 264, \text{ [micro-ohm/cm]}$$

Step No. 9 Calculate the effective window area, $W_{a(\text{eff})}$. Use the window area found in Step 6. A typical value for, S_3 , is 0.75, as shown in Chapter 4.

$$W_{a(\text{eff})} = W_a S_3, \text{ [cm}^2\text{]}$$

$$W_{a(\text{eff})} = (2.34)(0.75), \text{ [cm}^2\text{]}$$

$$W_{a(\text{eff})} = 1.76, \text{ [cm}^2\text{]}$$

Step No. 10 Calculate the number turns possible, N , using the insulated wire area, A_w found in Step 8. A typical value for, S_2 , is 0.6, as shown in Chapter 4.

$$N = \frac{W_{a(\text{eff})} S_2}{A_w}, \text{ [turns]}$$

$$N = \frac{(1.76)(0.60)}{(0.00754)}, \text{ [turns]}$$

$$N = 140, \text{ [turns]}$$

Step No. 11 Calculate the required gap, l_g .

$$l_g = \frac{0.4\pi N^2 A_c (10^{-8})}{L} - \left(\frac{\text{MPL}}{\mu_m}\right), \text{ [cm]}$$

$$l_g = \frac{(1.26)(140)^2 (1.25)(10^{-8})}{(0.0025)} - \left(\frac{9.22}{2500}\right), \text{ [cm]}$$

$$l_g = 0.120, \text{ [cm]}$$

Step No. 12 Calculate the equivalent gap in mils.

$$\text{mils} = \text{cm}(393.7)$$

$$\text{mils} = (0.120)(393.7)$$

$$\text{mils} = 47.2 \text{ use } 50$$

Step No. 13 Calculate the fringing flux factor, F.

$$F = 1 + \frac{l_g}{\sqrt{A_c}} \ln \left(\frac{2G}{l_g} \right)$$
$$F = 1 + \frac{(0.120)}{\sqrt{1.25}} \ln \left(\frac{2(2.84)}{0.120} \right)$$
$$F = 1.41$$

Step No. 14 Calculate the new number of turns, N_n , by inserting the fringing flux, F.

$$N_n = \sqrt{\frac{l_g L}{0.4\pi A_c F (10^{-8})}}, \text{ [turns]}$$
$$N_n = \sqrt{\frac{(0.120)(0.0025)}{(1.26)(1.25)(1.41)(10^{-8})}}, \text{ [turns]}$$
$$N_n = 116, \text{ [turns]}$$

Step No. 15 Calculate the winding resistance, R_L . Use the MLT, from Step 5, and the micro-ohm per centimeter, from Step 10.

$$R_L = (\text{MLT})(N_n) \left(\frac{\mu\Omega}{\text{cm}} \right) (10^{-6}), \text{ [ohms]}$$
$$R_L = (8.3)(116)(264)(10^{-6}), \text{ [ohms]}$$
$$R_L = 0.254, \text{ [ohms]}$$

Step No. 16 Calculate the copper loss, P_{cu} .

$$P_{cu} = I_{rms}^2 R_L, \text{ [watts]}$$
$$P_{cu} = (1.51)^2 (0.254), \text{ [watts]}$$
$$P_{cu} = 0.579, \text{ [watts]}$$

Step No. 17 Calculate the regulation, α .

$$\alpha = \frac{P_{cu}}{P_o} (100), \text{ [%]}$$
$$\alpha = \frac{(0.579)}{(100)} (100), \text{ [%]}$$
$$\alpha = 0.579, \text{ [%]}$$

Step No. 18 Calculate the ac flux density, B_{ac} .

$$B_{ac} = \frac{0.4\pi N_n F \left(\frac{\Delta l}{2}\right) (10^{-4})}{l_g + \left(\frac{MPL}{\mu_m}\right)}, \quad [\text{tesla}]$$

$$B_{ac} = \frac{(1.26)(116)(1.41) \left(\frac{0.2}{2}\right) (10^{-4})}{(0.120) + \left(\frac{9.22}{2500}\right)}, \quad [\text{tesla}]$$

$$B_{ac} = 0.0167, \quad [\text{tesla}]$$

Step No. 19 Calculate the watts per kilogram for ferrite, P , material in Chapter 2. Watts per kilogram can be written in milliwatts per gram.

$$\text{mW/g} = k f^{(m)} B_{ac}^{(n)}$$

$$\text{mW/g} = (0.00004855)(200000)^{(1.63)} (0.0167)^{(2.62)}$$

$$\text{mW/g} = 0.468$$

Step No. 20 Calculate the core loss, P_{fe} .

$$P_{fe} = (\text{mW/g})(W_{fe})(10^{-3}), \quad [\text{watts}]$$

$$P_{fe} = (0.468)(60)(10^{-3}), \quad [\text{watts}]$$

$$P_{fe} = 0.0281, \quad [\text{watts}]$$

Step No. 21 Calculate the total loss copper plus iron, P_{Σ} .

$$P_{\Sigma} = P_{fe} + P_{cu}, \quad [\text{watts}]$$

$$P_{\Sigma} = (0.0281) + (0.579), \quad [\text{watts}]$$

$$P_{\Sigma} = 0.607, \quad [\text{watts}]$$

Step No. 22 Calculate the watt density, ψ . The surface area, A_i , can be found in Step 5.

$$\psi = \frac{P_{\Sigma}}{A_i}, \quad [\text{watts/cm}^2]$$

$$\psi = \frac{(0.607)}{(69.9)}, \quad [\text{watts/cm}^2]$$

$$\psi = 0.00868, \quad [\text{watts/cm}^2]$$

Step No. 23 Calculate the temperature rise, T_r .

$$T_r = 450(\psi)^{(0.826)}, \quad [^{\circ}\text{C}]$$

$$T_r = 450(0.00868)^{(0.826)}, \quad [^{\circ}\text{C}]$$

$$T_r = 8.92, \quad [^{\circ}\text{C}]$$

Step No. 24 Calculate the peak flux density, B_{pk} .

$$B_{pk} = \frac{0.4\pi N_n F \left(I_{dc} + \frac{\Delta I}{2} \right) (10^{-4})}{l_g + \left(\frac{\text{MPL}}{\mu_m} \right)}, \quad [\text{tesla}]$$

$$B_{pk} = \frac{(1.26)(116)(1.41)(1.6)(10^{-4})}{(0.127) + \left(\frac{9.22}{2500} \right)}, \quad [\text{tesla}]$$

$$B_{pk} = 0.252, \quad [\text{tesla}]$$

Step No. 25 Calculate the effective permeability, μ_e . Knowing the effective permeability, the ETD-39 ferrite core can be ordered with a built in gap.

$$\mu_e = \frac{\mu_m}{1 + \left(\frac{l_g}{\text{MPL}} \right) \mu_m}$$

$$\mu_e = \frac{(2500)}{1 + \left(\frac{(0.120)}{9.22} \right) (2500)}$$

$$\mu_e = 74.5 \quad \text{use } 75$$

Step No. 26 Calculate the window utilization, K_u .

$$K_u = \frac{N_n A_w(B)}{W_a}$$

$$K_u = \frac{(116)(0.00653)}{(2.34)}$$

$$K_u = 0.324$$

Chapter 9

DC Inductor Design Using Powder Cores

Table of Contents

1. Introduction	
2. Molybdenum Permalloy Powder Cores (MPP)	
3. High Flux Powder Cores (HF)	
4. Sendust Powder Cores (Magnetics Kool M μ)	
5. Iron Powder Cores	
6. Inductors	
7. Relationship of, A_p , to Inductor's Energy-Handling Capability	
8. Relationship of, K_g , to Inductor's Energy-Handling Capability	
9. Fundamental Considerations	
10. Toroidal Powder Core Design Using the Core Geometry, K_g , Approach	
11. Toroidal Powder Core Inductor Design, Using the Area Product, A_p , Approach.....	

Introduction

Powder cores are manufactured from very fine particles of magnetic materials. The powder is coated with an inert insulation to minimize eddy current losses and to introduce a distributed air gap into the core structure. The insulated powder is then compacted into toroidal and EE cores. The magnetic flux in a toroidal powder core can be contained inside the core more readily than in a lamination or C core, as the winding covers the core along the entire magnetic path length. The design of an inductor also frequently involves consideration of the effect of its magnetic field on devices near where it is placed. This is especially true in the design of high-current inductors for converters and switching regulators used in spacecraft.

Toroidal powder cores are widely used in high-reliability military and space applications because of their good stability over wide temperature ranges, and their ability to withstand high levels of shock, vibration, and nuclear radiation without degradation. Other applications for these cores are:

1. Stable, high-Q filters operating in the frequency range of 1kHz to 1 MHz.
2. Loading coils used to cancel out the distributed capacitance in telephone cables.
3. Pulse transformers.
4. Differential mode EMI noise filters.
5. Flyback transformers.
6. Energy storage, or output inductors, in circuits with large amounts of dc current flowing.

Molybdenum Permalloy Powder Cores (MPP)

Molybdenum Permalloy Powder Cores (MPP) are manufactured from very fine particles of an 81% nickel, 17% iron, and a 2% molybdenum alloy. The insulated powder is then compacted into EE and toroidal cores. The toroidal cores range in size from 0.1 inch (0.254 cm) to 5 inches (12.7 cm) in the outside diameter. MPP cores are available in permeabilities ranging from 14 up to 550. See Table 9-1

High Flux Powder Cores (HF)

High Flux Powder Cores (HF) are manufactured from very fine particles of a 50% nickel, and 50% iron. The insulated powder is then compacted into EE and toroidal cores. The toroidal cores range in size from 0.25 inch (0.635 cm) to 3 inches (7.62 cm) in the outside diameter. HF cores are available in permeabilities ranging from 14 up to 160. See Table 9-1.

Sendust Powder Cores (Magnetics Kool M μ)

Sendust powder cores are manufactured from very fine particles of an 85% iron, 9% silicon, and 6% aluminum. The insulated powder is then compacted into EE and toroidal cores. The toroidal cores range in size from 0.14 inch (0.35 cm) to 3 inches (7.62 cm) in the outside diameter. Sendust cores are available in permeabilities ranging from 26 up to 125. See Table 9-1

Iron Powder Cores

The low cost iron powder cores are typically used in today's low and high frequency power switching conversion applications for differential-mode, input and output, power inductors. The distributed air gap characteristic of iron powder produces a core with permeability ranging from 10 to 100. This feature, in conjunction with the inherent high saturation point of iron, makes it very difficult to saturate. While iron powder cores may be limited in their use because of low permeability or rather high core loss at high frequency, they have become a very popular choice in either EE or toroidal as a core material for high-volume commercial applications. They are popular due to their low cost compared with other core materials. The toroidal cores range in size from 0.3 inch (0.76 cm) to 6.5 inches (16.5 cm) in the outside diameter. See Table 9-1

Table 9-1. Standard Powder Core Permeability

Standard Powder Core Permeabilities				
Powder Material	MPP	High Flux	Sendust (Kool M μ)	Iron Powder
Initial Permeability, μ_i				
10				X
14	X	X		
26	X	X	X	
35				X
55				X
60	X	X	X	X
75			X	X
90			X	
100				X
125	X	X	X	
147	X	X		
160	X	X		
173	X			
200	X			
300	X			
550	X			

Inductors

Inductors that carry direct current are used frequently in a wide variety of ground, air, and space applications. Selection of the best magnetic core for an inductor frequently involves a trial-and-error type of calculation.

The design of an inductor also frequently involves consideration of the effect of its magnetic field on other devices in the immediate vicinity. This is especially true in the design of high-current inductors for converters and switching regulators used in spacecraft, which may also employ sensitive magnetic field detectors. For this type of design problem, frequently it is imperative that a toroidal core be used. The magnetic flux in a powder core can be contained inside the core more readily than in a lamination or C core, as the winding covers the core along the entire magnetic path length. The author has developed a simplified method of designing optimum dc carrying inductors with powder cores. This method allows the correct core permeability to be determined without relying on the trial and error method.

Relationship of, A_p , to Inductor's Energy-Handling Capability

The energy-handling capability of a core is related to its area product, A_p , by the equation:

$$A_p = \frac{2(\text{Energy})(10^4)}{B_m J K_u}, \quad [\text{cm}^4] \quad [9-1]$$

Where: Energy is in watt-seconds.

B_m is the flux density, tesla.

J is the current density, amps-per-cm².

K_u is the window utilization factor. (See Chapter 4)

From the above factors, such as flux density, B_m , window utilization factor, K_u , (which defines the maximum space that may be used by the copper in the window), and the current density, J , which controls the copper loss can be seen. The energy-handling capability of a core is derived from:

$$\text{Energy} = \frac{LI^2}{2}, \quad [\text{watt-seconds}] \quad [9-2]$$

Relationship of, K_g , to Inductor's Energy-Handling Capability

Inductors, like transformers, are designed for a given temperature rise. They can also be designed for a given regulation. The regulation and energy handling ability of a core is related to two constants:

$$\alpha = \frac{(\text{Energy})^2}{K_g K_e}, \quad [\%] \quad [9-3]$$

Where α is the regulation, %.

The constant, K_g , is determined by the core geometry:

$$K_g = \frac{W_a A_c^2 K_u}{MLT}, \quad [\text{cm}^5] \quad [9-4]$$

The constant, K_e , is determined by the magnetic and electrical operating conditions:

$$K_e = 0.145 P_o B_m^2 (10^{-4}) \quad [9-5]$$

The output power, P_o , is defined in Figure 9-1.

$$P_{o(L1)} = V_{(01)} I_{(01)} \quad P_{o(L2)} = V_{(02)} I_{(02)} \quad [9-6]$$

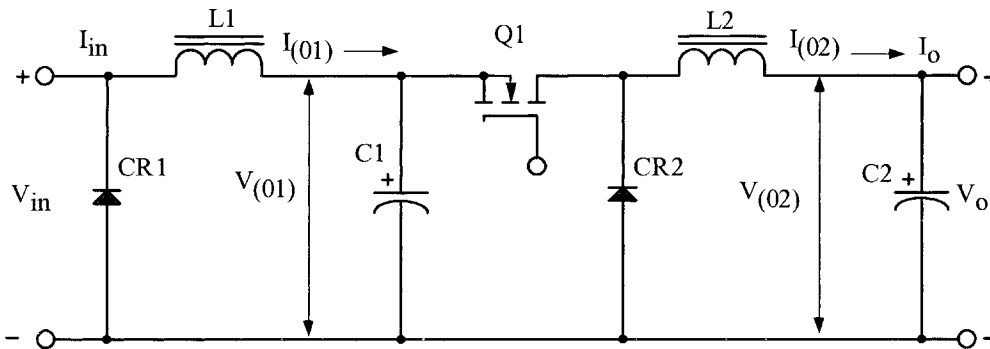


Figure 9-1. Defining the Inductor Output Power.

The operating flux density, B_m , is:

$$B_m = B_{dc} + \frac{B_{ac}}{2}, \quad [\text{tesla}] \quad [9-7]$$

From the above, it can be seen that the flux density, B_m , is the predominant factor in governing size.

Fundamental Considerations

The design of a linear reactor depends upon four related factors:

1. Desired inductance, L .
2. Direct current, I_{dc} .
3. Alternating current, ΔI .
4. Power loss and temperature, T_r .

With these requirements established, the designer must determine the maximum values for, B_{dc} , and B_{ac} , that will not produce magnetic saturation and must make trade-offs that will yield the highest inductance for a given volume. The core permeability chosen dictates the maximum dc flux density that can be tolerated for a given design.

If an inductance is to be constant with the increasing direct current, there must be a negligible drop in inductance over the operating current range. The maximum H (magnetizing force) then is an indication of a core's capability, as shown in Figure 9-2.

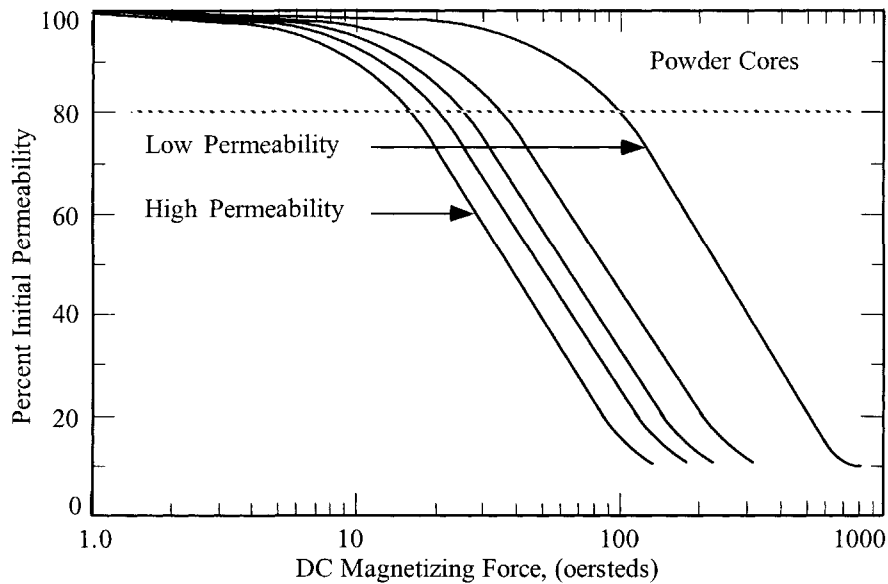


Figure 9-2. Typical Permeability Versus dc Bias Curves for Powder Cores.

Most manufacturers give the dc magnetizing force, H in oersteds:

$$H = \frac{0.4\pi NI}{MPL}, \text{ [oersteds]} \quad [9-8]$$

Some engineers prefer amp-turns:

$$NI = 0.8H(MPL), \text{ [amp-turns]} \quad [9-9]$$

Inductance decreases with increasing flux density, B, and magnetizing force, H, for various materials of different values of permeability. The selection of the correct permeability for a given design is made using Equation [9-10].

$$\mu_{\Delta} = \frac{B_m (MPL)(10^4)}{0.4\pi W_a J K_u} \quad [9-10]$$

It should be remembered the maximum flux, B_m , depends upon, $B_{dc} + B_{ac}$, in the manner in Figure 9-3.

$$B_m = B_{dc} + \frac{B_{ac}}{2}, \text{ [tesla]} \quad [9-11]$$

$$B_{dc} = \frac{0.4\pi N I_{dc} \mu (10^{-4})}{MPL}, \text{ [tesla] [9-12]}$$

$$B_{ac} = \frac{0.4\pi N \left(\frac{\Delta I}{2}\right) \mu (10^{-4})}{MPL}, \text{ [tesla] [9-13]}$$

$$B_{pk} = \frac{0.4\pi N \left(I_{dc} + \frac{\Delta I}{2}\right) \mu (10^{-4})}{MPL}, \text{ [tesla] [9-14]}$$

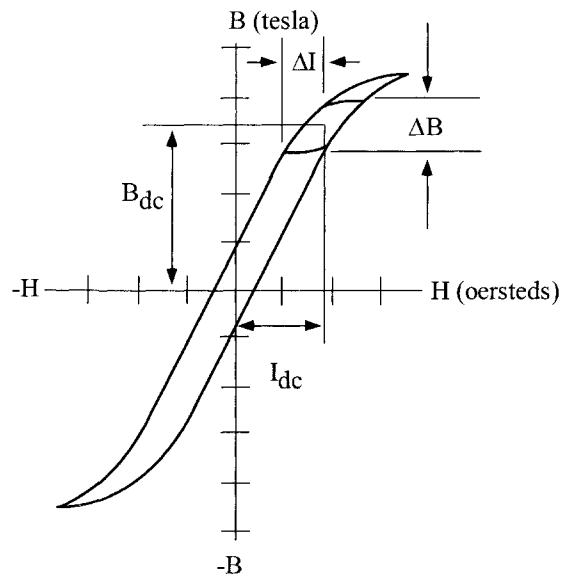


Figure 9-3. Inductor Flux Density Versus $I_{dc} + \Delta I$ Current.

The flux density for the initial design for Molypermalloy powder cores should be limited to 0.3T maximum for, $B_{dc} + B_{ac}$, as shown in Figure 9-4.

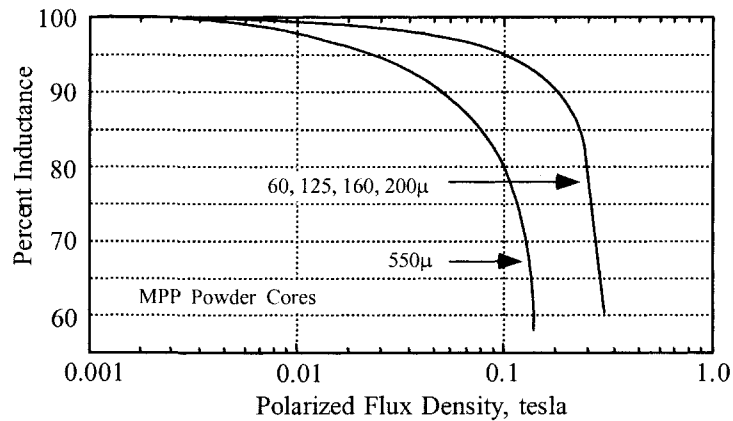


Figure 9-4. Inductance Versus dc Bias.

Toroidal Powder Core Design Using the Core Geometry, K_g , Approach

This design procedure will work with all powder cores.

Step No. 1 Design a linear dc inductor with the following specifications.

1. Inductance, L = 0.0025 henrys
2. dc current, I_o = 1.5 amps
3. ac current, ΔI = 0.2 amps
4. Output power, P_o = 100 watts
5. Regulation, α = 1.0 %
6. Ripple Frequency = 20 kHz
7. Operating flux density, B_m = 0.3 tesla
8. Core Material = MPP
9. Window utilization, K_u = 0.4
10. Temperature rise goal, T_r = 25°C

Step No. 2 Calculate the peak current, I_{pk} .

$$I_{pk} = I_o + \frac{\Delta I}{2}, \text{ [amps]}$$

$$I_{pk} = (1.5) + \frac{(0.2)}{2}, \text{ [amps]}$$

$$I_{pk} = 1.6, \text{ [amps]}$$

Step No. 3 Calculate the energy-handling capability.

$$\text{Energy} = \frac{LI_{pk}^2}{2}, \text{ [watt-seconds]}$$

$$\text{Energy} = \frac{(0.0025)(1.6)^2}{2}, \text{ [watt-seconds]}$$

$$\text{Energy} = 0.0032, \text{ [watt-seconds]}$$

Step No. 4 Calculate the electrical conditions coefficient, K_e .

$$K_e = 0.145 P_o B_m^2 (10^{-4})$$

$$K_e = 0.145(100)(0.3)^2 (10^{-4})$$

$$K_e = 0.0001305$$

Step No. 5 Calculate the core geometry coefficient, K_g .

$$K_g = \frac{(\text{Energy})^2}{K_e \alpha}, \quad [\text{cm}^5]$$

$$K_g = \frac{(0.0032)^2}{(0.0001305)(1.0)}, \quad [\text{cm}^5]$$

$$K_g = 0.0785, \quad [\text{cm}^5]$$

Step No. 6 Select a MPP powder core from Chapter 3. The data listed is the closest core to the calculated core geometry, K_g .

1. Core Number	= 55586
2. Magnetic Path Length, MPL	= 8.95 cm
3. Core Weight, W_{ife}	= 34.9 grams
4. Mean Length Turn, MLT	= 4.40 cm
5. Iron Area, A_c	= 0.454 cm ²
6. Window Area, W_a	= 3.94 cm ²
7. Area Product, A_p	= 1.79 cm ⁴
8. Core Geometry, K_g	= 0.0742 cm ⁵
9. Surface Area, A_t	= 64.4 cm ²
10. Permeability, μ	= 60
11. Millihenrys-per-1k, A L	= 38 mh

Step No. 7 Calculate the current density, J , using the area product Equation, A_p .

$$J = \frac{2(\text{Energy})(10^4)}{B_m A_p K_u}, \quad [\text{amps-per-cm}^2]$$

$$J = \frac{2(0.0032)(10^4)}{(0.3)(1.79)(0.4)}, \quad [\text{amps-per-cm}^2]$$

$$J = 298, \quad [\text{amps-per-cm}^2]$$

Step No. 8 Calculate the rms current, I_{rms} .

$$I_{\text{rms}} = \sqrt{I_o^2 + \Delta I^2}, \quad [\text{amps}]$$

$$I_{\text{rms}} = \sqrt{(1.5)^2 + (0.2)^2}, \quad [\text{amps}]$$

$$I_{\text{rms}} = 1.51, \quad [\text{amps}]$$

Step No. 9 Calculate the required bare wire area, $A_{w(B)}$.

$$A_{w(B)} = \frac{I_{rms}}{J}, \quad [\text{cm}^2]$$

$$A_{w(B)} = \frac{(1.51)}{(298)}, \quad [\text{cm}^2]$$

$$A_{w(B)} = 0.00507, \quad [\text{cm}^2]$$

Step No. 10 Select a wire from the Wire Table in Chapter 4. If the area is not within 10%, take the next smallest size. Also, record micro-ohms per centimeter.

$$\text{AWG} = \#20$$

$$\text{Bare, } A_{w(B)} = 0.00519, \quad [\text{cm}^2]$$

$$\text{Insulated, } A_w = 0.00606, \quad [\text{cm}^2]$$

$$\left(\frac{\mu\Omega}{\text{cm}} \right) = 332, \quad [\text{micro-ohm/cm}]$$

Step No. 11 Calculate the effective window area, $W_{a(\text{eff})}$. Use the window area found in Step 6. A typical value for, S_3 , is 0.75, as shown in Chapter 4.

$$W_{a(\text{eff})} = W_a S_3, \quad [\text{cm}^2]$$

$$W_{a(\text{eff})} = (3.94)(0.75), \quad [\text{cm}^2]$$

$$W_{a(\text{eff})} = 2.96, \quad [\text{cm}^2]$$

Step No. 12 Calculate the number turns possible for, N . Use the insulated wire area, A_w , found in Step 10. A typical value for, S_2 , is 0.6, as shown in Chapter 4.

$$N = \frac{W_{a(\text{eff})} S_2}{A_w}, \quad [\text{turns}]$$

$$N = \frac{(2.96)(0.60)}{(0.00606)}, \quad [\text{turns}]$$

$$N = 293, \quad [\text{turns}]$$

Step No. 13 Calculate the required core permeability, μ .

$$\mu_\Delta = \frac{B_m (\text{MPL})(10^4)}{0.4\pi W_a J K_u}$$

$$\mu_\Delta = \frac{(0.30)(8.95)(10^4)}{(1.26)(3.94)(298)(0.4)}$$

$$\mu_\Delta = 45.4$$

Note:

The permeability of 45.4 is close enough to use a 60 μ core. Also note that there are other permeabilities available, See Table 9-1. Because of size, Chapter 3 has listed only 60 μ Tables for MPP, High Flux, Sendust and a 75 μ Table for Iron powder. For cores with other than 60 μ , use the manufacturer's catalog.

Step No. 14 Calculate the number of turns, N_L , required.

$$N_L = 1000 \sqrt{\frac{L}{L_{(1000)}}}, \text{ [turns]}$$

$$N_L = 1000 \sqrt{\left(\frac{2.5}{38}\right)}, \text{ [turns]}$$

$$N_L = 256, \text{ [turns]}$$

Step No. 15 Calculate the winding resistance, R_L . Use the MLT from Step 6 and the micro-ohm per centimeter from Step 10.

$$R_L = (\text{MLT})(N_L) \left(\frac{\mu\Omega}{\text{cm}}\right) (10^{-6}), \text{ [ohms]}$$

$$R_L = (4.4)(256)(332)(10^{-6}), \text{ [ohms]}$$

$$R_L = 0.374, \text{ [ohms]}$$

Step No. 16 Calculate the copper loss, P_{cu} .

$$P_{cu} = I_{rms}^2 R_L, \text{ [watts]}$$

$$P_{cu} = (1.51)^2 (0.374), \text{ [watts]}$$

$$P_{cu} = 0.853, \text{ [watts]}$$

Step No. 17 Calculate the regulation, α .

$$\alpha = \frac{P_{cu}}{P_o} (100), \text{ [%]}$$

$$\alpha = \frac{(0.853)}{(100)} (100), \text{ [%]}$$

$$\alpha = 0.853, \text{ [%]}$$

Step No. 18 Calculate the ac flux density, B_{ac} .

$$B_{ac} = \frac{0.4\pi N_L \left(\frac{\Delta I}{2}\right) \mu (10^{-4})}{MPL}, \text{ [tesla]}$$

$$B_{ac} = \frac{(1.25)(256) \left(\frac{0.2}{2}\right) (60)(10^{-4})}{(8.95)}, \text{ [tesla]}$$

$$B_{ac} = 0.0215, \text{ [tesla]}$$

Step No. 19 Calculate the watts per kilogram for the appropriate MPP powder core material in Chapter 2. Watts per kilogram can be written in milliwatts per gram.

$$\text{mW/g} = k f^{(m)} B_{ac}^{(n)}$$

$$\text{mW/g} = (0.00551)(20000)^{(1.23)} (0.0215)^{(2.12)}$$

$$\text{mW/g} = 0.313$$

Step No. 20 Calculate the core loss, P_{fe} .

$$P_{fe} = (\text{mW/g})(W_{fe})(10^{-3}), \text{ [watts]}$$

$$P_{fe} = (0.313)(34.9)(10^{-3}), \text{ [watts]}$$

$$P_{fe} = 0.011, \text{ [watts]}$$

Step No. 21 Calculate the total loss copper plus iron, P_{Σ} .

$$P_{\Sigma} = P_{fe} + P_{cu}, \text{ [watts]}$$

$$P_{\Sigma} = (0.011) + (0.853), \text{ [watts]}$$

$$P_{\Sigma} = 0.864, \text{ [watts]}$$

Step No. 22 Calculate the watt density, ψ . The surface area, A_t can be found in Step 6.

$$\psi = \frac{P_{\Sigma}}{A_t}, \text{ [watts/cm}^2\text{]}$$

$$\psi = \frac{(0.864)}{(64.4)}, \text{ [watts/cm}^2\text{]}$$

$$\psi = 0.0134, \text{ [watts/cm}^2\text{]}$$

Step No. 23 Calculate the temperature rise, T_r .

$$T_r = 450(\psi)^{(0.826)}, \text{ [}^\circ\text{C]}$$

$$T_r = 450(0.0134)^{(0.826)}, \text{ [}^\circ\text{C]}$$

$$T_r = 12.8, \text{ [}^\circ\text{C]}$$

Step No. 24 Calculate the dc magnetizing force, H .

$$H = \frac{0.4\pi N_L I_{pk}}{\text{MPL}}, \text{ [oersteds]}$$

$$H = \frac{(1.26)(256)(1.6)}{(8.95)}, \text{ [oersteds]}$$

$$H = 57.7, \text{ [oersteds]}$$

Step No. 25 Calculate the window utilization, K_u .

$$K_u = \frac{N_{L(new)} A_{w(B)\#20}}{W_a}$$

$$K_u = \frac{((256)(0.00519))}{(3.94)}$$

$$K_u = 0.337$$

Note:

The big advantage in using the core geometry design procedure is that the current density is calculated. Using the area product design procedure, the current density is an estimate at best. In this next design the same current density will be used as in core geometry.

Toroidal Powder Core Inductor Design, Using the Area Product, A_p , Approach

Step No. 1 Design a linear dc inductor with the following specifications.

1. Inductance, L = 0.0025 henrys
2. dc current, I_o = 1.5 amps
3. ac current, ΔI = 0.2 amps
4. Output power, P_o = 100 watts
5. Current Density, J = 300 amps-per-cm²
6. Ripple Frequency = 20 kHz
7. Operating flux density, B_m = 0.3 tesla
8. Core Material = MPP
9. Window utilization, K_u = 0.4
10. Temperature rise goal, T_r = 25^oC

Step No. 2 Calculate the peak current, I_{pk} .

$$I_{pk} = I_o + \frac{\Delta I}{2}, \text{ [amps]}$$

$$I_{pk} = (1.5) + \frac{(0.2)}{2}, \text{ [amps]}$$

$$I_{pk} = 1.6, \text{ [amps]}$$

Step No. 3 Calculate the energy-handling capability.

$$\text{Energy} = \frac{LI_{pk}^2}{2}, \text{ [watt-seconds]}$$

$$\text{Energy} = \frac{(0.0025)(1.6)^2}{2}, \text{ [watt-seconds]}$$

$$\text{Energy} = 0.0032, \text{ [watt-seconds]}$$

Step No. 4 Calculate the area product, A_p .

$$A_p = \frac{2(\text{Energy})(10^4)}{B_m J K_u}, \text{ [cm}^4\text{]}$$

$$A_p = \frac{2(0.0032)(10^4)}{(0.3)(300)(0.4)}, \text{ [cm}^4\text{]}$$

$$A_p = 1.78, \text{ [cm}^4\text{]}$$

Step No. 5 Select a MPP powder core from Chapter 3. The data listed is the closest core to the calculated core geometry, K_g .

- | | |
|------------------------------------|--------------------------|
| 1. Core Number | = 55586 |
| 2. Magnetic Path Length, MPL | = 8.95 cm |
| 3. Core Weight, W_{ife} | = 34.9 grams |
| 4. Mean Length Turn, MLT | = 4.40 cm |
| 5. Iron Area, A_c | = 0.454 cm ² |
| 6. Window Area, W_a | = 3.94 cm ² |
| 7. Area Product, A_p | = 1.79 cm ⁴ |
| 8. Core Geometry, K_g | = 0.0742 cm ⁵ |
| 9. Surface Area, A_s | = 64.4 cm ² |
| 10. Permeability, μ | = 60 |
| 11. Millihenrys-per-1k, A L | = 38 mh |

Step No. 6 Calculate the rms current, I_{rms} .

$$I_{rms} = \sqrt{I_o^2 + \Delta I^2}, \text{ [amps]}$$

$$I_{rms} = \sqrt{(1.5)^2 + (0.2)^2}, \text{ [amps]}$$

$$I_{rms} = 1.51, \text{ [amps]}$$

Step No. 7 Calculate the required bare wire area, $A_{w(B)}$.

$$A_{w(B)} = \frac{I_{rms}}{J}, \text{ [cm}^2\text{]}$$

$$A_{w(B)} = \frac{(1.51)}{(298)}, \text{ [cm}^2\text{]}$$

$$A_{w(B)} = 0.00507, \text{ [cm}^2\text{]}$$

Step No. 8 Select a wire from the Wire Table in Chapter 4. If the area is not within 10%, take the next smallest size. Also, record the micro-ohms per centimeter.

$$\text{AWG} = \#20$$

$$\text{Bare, } A_{w(B)} = 0.00519, \text{ [cm}^2\text{]}$$

$$\text{Insulated, } A_w = 0.00606, \text{ [cm}^2\text{]}$$

$$\left(\frac{\mu\Omega}{\text{cm}}\right) = 332, \text{ [micro-ohm/cm]}$$

Step No. 9 Calculate the effective window area, $W_{a(\text{eff})}$. Use the window area found in Step 5. A typical value for, S_3 is 0.75 as shown in Chapter 4.

$$W_{a(\text{eff})} = W_a S_3, \text{ [cm}^2\text{]}$$

$$W_{a(\text{eff})} = (3.94)(0.75), \text{ [cm}^2\text{]}$$

$$W_{a(\text{eff})} = 2.96, \text{ [cm}^2\text{]}$$

Step No. 10 Calculate the number turns possible, N . Use the insulated wire area, A_w found in Step 8. A typical value for, S_2 , is 0.6, as shown in Chapter 4.

$$N = \frac{W_{a(\text{eff})} S_2}{A_w}, \text{ [turns]}$$

$$N = \frac{(2.96)(0.60)}{(0.00606)}, \text{ [turns]}$$

$$N = 293, \text{ [turns]}$$

Step No. 11 Calculate the required core permeability, μ .

$$\mu_{\Delta} = \frac{B_m (\text{MPL})(10^4)}{0.4\pi W_a J K_u}$$
$$\mu_{\Delta} = \frac{(0.30)(8.95)(10^4)}{(1.26)(3.94)(298)(0.4)}$$
$$\mu_{\Delta} = 45.4$$

Note:

The permeability of 45.4 is close enough to use a 60 μ core. Also note there are other permeabilities available, See Table 9-1. Because of size, Chapter 3 has listed only 60 μ tables for MPP, High Flux, Sendust and 75 μ table for Iron powder. For cores with other than 60 μ , use the manufacturer's catalog.

Step No. 12 Calculate the number of turns, N_L , required.

$$N_L = 1000 \sqrt{\frac{L}{L_{(1000)}}}, \text{ [turns]}$$
$$N_L = 1000 \sqrt{\left(\frac{2.5}{38}\right)}, \text{ [turns]}$$
$$N_L = 256, \text{ [turns]}$$

Step No. 13 Calculate the winding resistance, R_L . Use the MLT from Step 6 and the micro-ohm per centimeter from Step 10.

$$R_L = (\text{MLT})(N_L)\left(\frac{\mu\Omega}{\text{cm}}\right)(10^{-6}), \text{ [ohms]}$$
$$R_L = (4.4)(256)(332)(10^{-6}), \text{ [ohms]}$$
$$R_L = 0.374, \text{ [ohms]}$$

Step No. 14 Calculate the copper loss, P_{cu} .

$$P_{cu} = I_{rms}^2 R_L, \text{ [watts]}$$
$$P_{cu} = (1.51)^2 (0.374), \text{ [watts]}$$
$$P_{cu} = 0.853, \text{ [watts]}$$

Step No. 15 Calculate the ac flux density, B_{ac} .

$$B_{ac} = \frac{0.4\pi N_L \left(\frac{\Delta I}{2}\right) \mu (10^{-4})}{MPL}, \text{ [tesla]}$$

$$B_{ac} = \frac{(1.25)(256) \left(\frac{0.2}{2}\right) (60) (10^{-4})}{(8.95)}, \text{ [tesla]}$$

$$B_{ac} = 0.0215, \text{ [tesla]}$$

Step No. 16 Calculate the watts per kilogram for the appropriate MPP powder core material in Chapter 2. Watts per kilogram can be written in milliwatts per gram.

$$\text{mW/g} = k f^{(m)} B_{ac}^{(n)}$$

$$\text{mW/g} = (0.00551)(20000)^{(1.23)} (0.0215)^{(2.12)}$$

$$\text{mW/g} = 0.313$$

Step No. 17 Calculate the core loss, P_{fe} .

$$P_{fe} = (\text{mW/g})(W_{fe})(10^{-3}), \text{ [watts]}$$

$$P_{fe} = (0.313)(34.9)(10^{-3}), \text{ [watts]}$$

$$P_{fe} = 0.011, \text{ [watts]}$$

Step No. 18 Calculate the total copper loss plus iron, P_{Σ} .

$$P_{\Sigma} = P_{fe} + P_{cu}, \text{ [watts]}$$

$$P_{\Sigma} = (0.011) + (0.853), \text{ [watts]}$$

$$P_{\Sigma} = 0.864, \text{ [watts]}$$

Step No. 19 Calculate the watt density, ψ . The surface area, A_i can be found in Step 5.

$$\psi = \frac{P_{\Sigma}}{A_i}, \text{ [watts/cm}^2\text{]}$$

$$\psi = \frac{(0.864)}{(64.4)}, \text{ [watts/cm}^2\text{]}$$

$$\psi = 0.0134, \text{ [watts/cm}^2\text{]}$$

Step No. 20 Calculate the temperature rise, T_r .

$$T_r = 450(\psi)^{(0.826)}, \text{ [}^\circ\text{C]}$$

$$T_r = 450(0.0134)^{(0.826)}, \text{ [}^\circ\text{C]}$$

$$T_r = 12.8, \text{ [}^\circ\text{C]}$$

Step No. 21 Calculate the dc magnetizing force, H .

$$H = \frac{0.4\pi N_L I_{pk}}{\text{MPL}}, \text{ [oersteds]}$$

$$H = \frac{(1.26)(256)(1.6)}{(8.95)}, \text{ [oersteds]}$$

$$H = 57.7, \text{ [oersteds]}$$

Step No. 22 Calculate the window utilization, K_u .

$$K_u = \frac{N_{L(\text{new})} A_{w(B)\#20}}{W_a}$$

$$K_u = \frac{((256)(0.00519))}{(3.94)}$$

$$K_u = 0.337$$

Chapter 10

AC Inductor Design

Table of Contents

1. Introduction.....	
2. Requirements.....	
3. Relationship of, A_p , to the Inductor Volt-Amp Capability	
4. Relationship of, K_g , to the Inductor Volt-Amp Capability	
5. Fundamental Considerations	
6. Fringing Flux	
7. AC Inductor Design Example	
8. Reference	

Introduction

The design of an ac inductor is quite similar to that of a transformer. If there is no dc flux in the core, the design calculations are straightforward. The apparent power, P_t , of an inductor is the VA of the inductor; that is, the product of the excitation voltage and the current through the inductor.

$$P_t = VA, \text{ [watts]} \quad [10-1]$$

Requirements

The design of the ac inductor requires the calculation of the volt-amp (VA) capability. In some applications the inductance is specified, and in others, the current is specified. If the inductance is specified, then, the current has to be calculated. If the current is specified, then the inductance has to be calculated. A series, ac inductor, L1, being used in a Ferroresonant Voltage Stabilizer is shown in Figure 10-1.

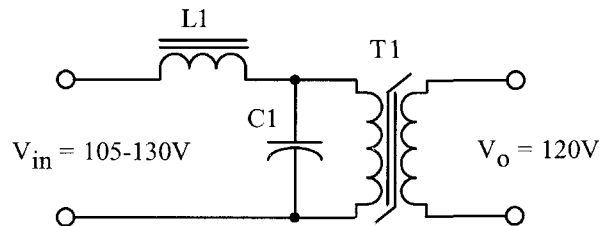


Figure 10-1. Series ac Inductor, L1, as used in a Ferroresonant Voltage Stabilizer.

Relationship of, A_p , to the Inductor Volt-Amp Capability

The volt-amp capability of a core is related to its area product, A_p , by the equation that may be stated as follows:

$$A_p = \frac{VA(10^4)}{K_f K_u B_{ac} f J}, \text{ [cm}^4\text{]} \quad [10-2]$$

Where:

K_f = wave form factor.

K_u = window utilization factor.

B_{ac} = operating flux density, T, tesla

f = operating frequency, Hz

J = current density, amps/cm²

From the above, it can be seen that factors such as flux density, B_{ac} , the window utilization factor, K_u , (which defines the maximum space occupied by the copper in the window), and the current density, J , all have an influence on the inductor area product, A_p .

Relationship, K_g , to the Inductor Volt-Amp Capability

Although most inductors are designed for a given temperature rise, they can also be designed for a given regulation. The regulation and volt-amp ability of a core is related to two constants:

$$\alpha = \frac{VA}{K_g K_e}, \quad [\%] \quad [10-3]$$

$$\alpha = \text{Regulation } (\%) \quad [10-4]$$

The constant, K_g , is determined by the core geometry, which may be related by the following equations:

$$K_g = \frac{W_a A_c^2 K_u}{MLT}, \quad [\text{cm}^5] \quad [10-5]$$

The constant, K_e , is determined by the magnetic and electric operating conditions, which may be related by the following equation:

$$K_e = 0.145 K_f^2 f^2 B_m^2 (10^{-4}) \quad [10-6]$$

Where:

K_f = waveform coefficient

4.0 square wave

4.44 sine wave

From the above, it can be seen that factors such as flux density, frequency of operation, and the waveform coefficient have an influence on the transformer size.

Fundamental Considerations

The design of a linear ac inductor depends upon five related factors:

1. Desired inductance
2. Applied voltage, (across inductor)
3. Frequency
4. Operating Flux density
5. Temperature Rise

With these requirements established, the designer must determine the maximum values for, B_{ac} , which will not produce magnetic saturation, and make trade-offs that will yield the highest inductance for a given volume. The core material selected determines the maximum flux density that can be tolerated for a given design. Magnetic materials and their operating flux levels are given in Chapter 2.

The ac inductor like a transformer, must support the applied voltage, V_{ac} . The number of turns is calculated from Faraday's Law, which states:

$$N = \frac{V_{ac}(10^4)}{K_f B_{ac} f A_c}, \quad [\text{turns}] \quad [10-7]$$

The inductance of an iron-core inductor, with an air gap, may be expressed as:

$$L = \frac{0.4\pi N^2 A_c (10^{-8})}{l_g + \left(\frac{\text{MPL}}{\mu_m}\right)}, \quad [\text{henrys}] \quad [10-8]$$

Inductance is seen to be inversely dependent on the effective Magnetic Path Length, MPL, which is the sum of the air gap length, l_g , and the ratio of the Magnetic Path Length, MPL, to material permeability, μ_m .

When the core air gap, l_g , is larger compared to the ratio, MPL/μ_m , because of the high material permeability, μ_m , variations in, μ_m , do not substantially affect the total effective Magnetic Path Length, MPL, or the inductance, L. The inductance equation then reduces to:

$$L = \frac{0.4\pi N^2 A_c (10^{-8})}{l_g}, \quad [\text{henrys}] \quad [10-9]$$

Rearranging the equation to solve for the gap:

$$l_g = \frac{0.4\pi N^2 A_c (10^{-8})}{L}, \quad [\text{cm}] \quad [10-10]$$

Fringing Flux

Final determination of the air gap requires consideration of the effect of fringing flux, which is a function of gap dimension, the shape of the pole faces, and the shape, size, and location of the winding, as shown in Figure 10-2 and Figure 10-3. Its net effect is to make the effective air gap less than its physical dimension.

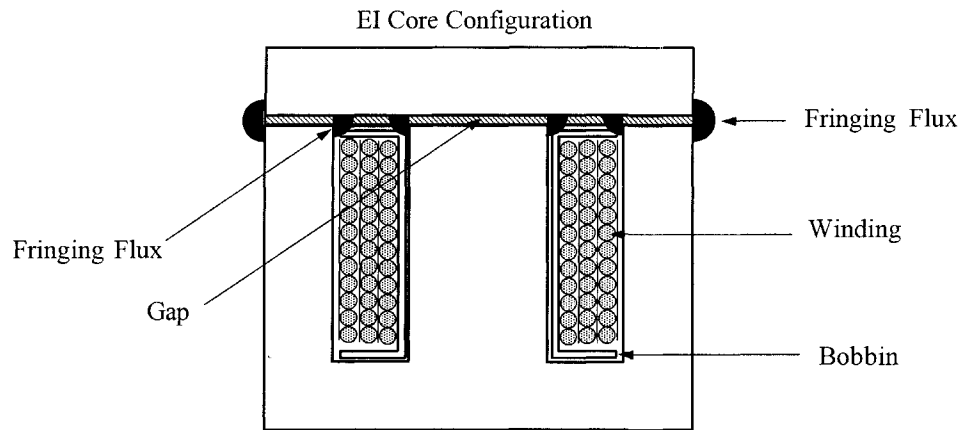


Figure 10-2. Fringing Flux Location on an EI Core Configuration.

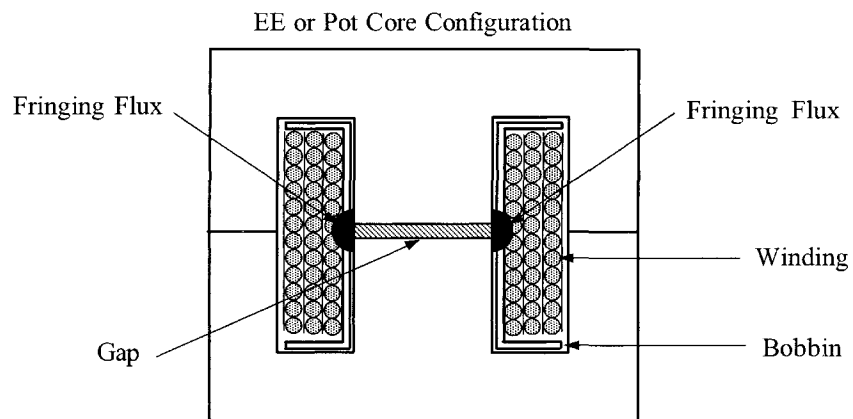


Figure 10-3. Fringing Flux Location on an EE or Pot Core Configuration.

Fringing flux decreases the total reluctance of the magnetic path, and therefore increases the inductance by a factor, F , to a value greater than that calculated from Equation [10-9]. Fringing flux is a larger percentage of the total for larger gaps. The fringing flux factor is:

$$F = \left(1 + \frac{l_g}{\sqrt{A_c}} \ln \left(\frac{2G}{l_g} \right) \right) \quad [10-11]$$

Where G is a dimension, (winding length), defined in Chapter 3. Equation [10-11] is valid for cut C cores, laminations and cut ferrite cores.

The inductance, L , computed in Equation [10-9] does not include the effect of fringing flux. The value of inductance, L' , in Equation [10-12] does correct for fringing flux:

$$L' = \frac{0.4\pi N^2 A_c F (10^{-8})}{l_g}, \quad [\text{henrys}] \quad [10-12]$$

Now that the fringing flux, F , has been calculated, it is necessary to recalculate the number of turns using the fringing flux, Factor F .

$$N_{(new)} = \sqrt{\frac{L l_g}{0.4\pi A_c F (10^{-8})}}, \quad [\text{turns}] \quad [10-13]$$

After the new turns, $N_{(new)}$, have been calculated, then, use Equation [10-13] with the new turns, $N_{(new)}$, and solve for B_{ac} . This check will provide the operating flux density, in order to calculate the core loss, P_{fe} , and will also provide a check on core saturation margin.

$$B_{ac} = \frac{V_{ac} (10^4)}{K_f N_{(new)} f A_c}, \quad [\text{tesla}] \quad [10-14]$$

The losses in an ac inductor are made up of three components:

1. Copper loss, P_{cu}
2. Iron loss, P_{fe}
3. Gap loss, P_g

The copper loss, P_{cu} , is I^2R and is straightforward, if the skin effect is minimal. The iron loss, P_{fe} , is calculated from core manufacturers' data. Gap loss, P_g , is independent of core material strip thickness and permeability. Maximum efficiency is reached in an inductor, as in a transformer, when the copper loss, P_{cu} , and the iron loss, P_{fe} , are equal, but only when the gap of the core is zero. The gap loss does not occur in the air gap, itself, but is caused by magnetic flux, fringing around the gap, and reentering the core in a direction of high loss. As the air gap increases, the flux across the gap fringes more and more, and some of the fringing flux strikes the core, perpendicular to the laminations, and sets up eddy currents which cause additional losses called gap loss, P_g . Also distribution of the fringing flux is affected by other aspects of the core geometry, the proximity of the coils turns to the core, and whether there are turns on both legs. (See Table 10-1). Accurate prediction of the gap loss depends on the amount of fringing flux. (See the Reference at the end of this Chapter)

$$P_g = K_i E l_g f B_{ac}^2, \quad [\text{watt}] \quad [10-15]$$

Where, E (as defined in Chapter 3) is the strip or tongue width, in cm.

Table 10-1. Gap Loss Coefficient

Configuration	K_i
Two-coil C core	0.0388
Single-coil C core	0.0775
Lamination	0.1550

When designing inductors where there is a choice of cores, always pick the core with the smallest ratio:

$$\frac{W_a}{A_c} = [\text{smallest ratio}] \quad [10-16]$$

Comparing two cores with identical area products, A_p , for the same design specification, the core with a minimum of window area will generate a minimum of fringing flux. If there is a design change and it requires the use of the next larger core, it would be far more beneficial to double up on the core being used, than to pick a larger core, as shown in Figure 10-4.

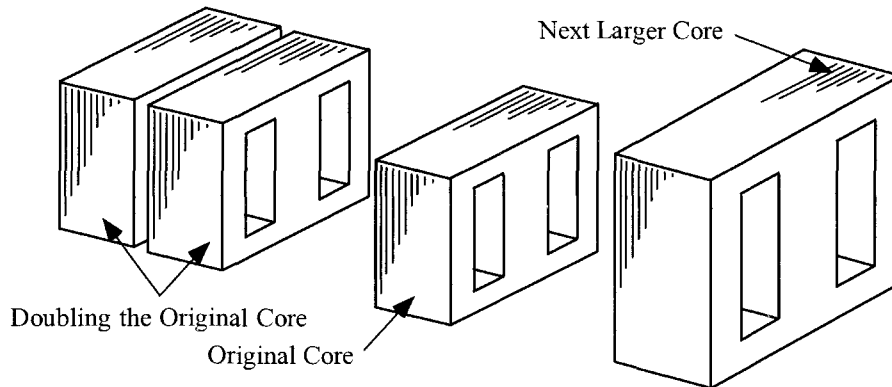


Figure 10-4. Comparing Core Configurations.

For example, if the next larger core was selected, normally all of the core proportions will increase. This means, the window, W_a , and the iron cross-section, A_c , would have both increased. (A larger core should not be used as the fringing flux would also increase.) If you want to keep the fringing flux to a minimum, then double up on the original core. Therefore the iron area, A_c , would double, but the window area, W_a , will remain the same. This will reduce the, W_a/A_c , ratio, as shown in Equation 10-16. With an increase in iron cross-section, A_c , the turns would have to decrease for the same window area, W_a . With a decrease in turns, the gap would also decrease, resulting in less fringing flux.

When designing a transformer, the engineer will push the flux density as far he can without saturating the core. That cannot be done with an ac inductor because you must leave a margin for the fringing flux factor. One of the biggest problems in designing ac inductors is keeping the gap to a minimum. This problem becomes acute when designing high frequency ac inductors. The problem in designing high frequency inductors is the required turns to support the applied voltage, then gapping to provide the proper inductance. This problem is minimized when using powder cores if the right permeability can be found.

AC Inductor Design Example

Step No. 1 Design a linear ac inductor with the following specifications.

1. Applied voltage, V_L = 120 volts
2. Line current, I_L = 1.0 amps
3. Line frequency = 60 hertz.
4. Current density, J = 300 amp/cm²
5. Efficiency goal, $\eta(100)$ = 90%
6. Magnetic material = Silicon
7. Magnetic material permeability, μ_m = 1500
8. Flux density, B_{ac} = 1.4 tesla
9. Window utilization, K_u = 0.4
10. Waveform factor, K_f = 4.44
11. Temperature rise goal, T_r = 50°C

Step No. 2 Calculate the apparent power, P_t or VA of the inductor, L.

$$VA = V_L I_L, \text{ [watts]}$$

$$VA = (120)(1.0), \text{ [watts]}$$

$$VA = 120, \text{ [watts]}$$

Step No. 3 Calculate the area product, A_p .

$$A_p = \frac{VA(10^4)}{K_f K_u f B_{ac} J}, \text{ [cm}^4\text{]}$$

$$A_p = \frac{(120)(10^4)}{(4.44)(0.4)(60)(1.4)(300)}, \text{ [cm}^4\text{]}$$

$$A_p = 26.8, \text{ [cm}^4\text{]}$$

Step No. 4 Select an EI lamination from Chapter 3. The closest lamination to the calculated area product, A_p , is the EI-100.

1. Core Number = EI-100
2. Magnetic Path Length, MPL = 15.2 cm
3. Core Weight, W_{tfe} = 676 grams
4. Mean Length Turn, MLT = 14.8 cm
5. Iron Area, A_c = 6.13 cm²
6. Window Area, W_a = 4.84 cm²
7. Area Product, A_p = 29.7 cm⁴

8. Core Geometry, K_g = 4.93 cm⁵
 9. Surface Area, A_t = 213 cm²
 10. Winding length, G = 3.81 cm
 11. Lamination tongue, E = 2.54 cm

Step No. 5 Calculate the number of inductor turns, N_L .

$$N_L = \frac{V_L (10^4)}{K_f B_{ac} f A_c}, \text{ [turns]}$$

$$N_L = \frac{(120)(10^4)}{(4.44)(1.4)(60)(6.13)}, \text{ [turns]}$$

$$N_L = 525, \text{ [turns]}$$

Step No. 6 Calculate the inductive reactance, X_L .

$$X_L = \frac{V_L}{I_L}, \text{ [ohms]}$$

$$X_L = \frac{(120)}{(1.0)}, \text{ [ohms]}$$

$$X_L = 120, \text{ [ohms]}$$

Step No. 7 Calculate the required inductance, L .

$$L = \frac{X_L}{2\pi f}, \text{ [henrys]}$$

$$L = \frac{120}{2(3.14)(60)}, \text{ [henrys]}$$

$$L = 0.318, \text{ [henrys]}$$

Step No. 8 Calculate the required gap, L_g .

$$l_g = \left(\frac{0.4\pi N_L^2 A_c (10^{-8})}{L} \right) - \left(\frac{MPL}{\mu_m} \right), \text{ [cm]}$$

$$l_g = \left(\frac{(1.26)(525)^2 (6.13)(10^{-8})}{0.318} \right) - \left(\frac{15.2}{1500} \right), \text{ [cm]}$$

$$l_g = 0.0568, \text{ [cm]} \text{ or } l_g = 22.4, \text{ [mils]: This would be in 10 mils each leg.}$$

Step No. 9 Calculate the fringing flux, F.

$$F = \left(1 + \frac{l_g}{\sqrt{A_c}} \ln \frac{2(G)}{l_g} \right)$$

$$F = \left(1 + \frac{0.0568}{\sqrt{6.13}} \ln \frac{2(3.81)}{0.0568} \right)$$

$$F = 1.112$$

Step No. 10 Using the fringing flux, recalculate the series inductor turns, $N_{L(new)}$.

$$N_{L(new)} = \sqrt{\frac{l_g L}{0.4\pi A_c F (10^{-8})}}, \text{ [turns]}$$

$$N_{L(new)} = \sqrt{\frac{(0.0568)(0.318)}{(1.26)(6.13)(1.112)(10^{-8})}}, \text{ [turns]}$$

$$N_{L(new)} = 459, \text{ [turns]}$$

Step No. 11 Using the new turns, recalculate the flux density, B_{ac} .

$$B_{ac} = \frac{V_L (10^4)}{K_f N_{L(new)} A_c f}, \text{ [tesla]}$$

$$B_{ac} = \frac{(120)(10^4)}{(4.44)(459)(6.13)(60)}, \text{ [tesla]}$$

$$B_{ac} = 1.6, \text{ [tesla]}$$

Step No. 12 Calculate the inductor bare wire area, $A_{wL(B)}$.

$$A_{wL(B)} = \frac{I_L}{J}, \text{ [cm}^2\text{]}$$

$$A_{wL(B)} = \frac{(1.0)}{(300)}, \text{ [cm}^2\text{]}$$

$$A_{wL(B)} = 0.00333, \text{ [cm}^2\text{]}$$

Step No. 13 Select a wire from the Wire Table in Chapter 4.

$$AWG = \#22$$

$$A_{w(B)} = 0.00324, \text{ [cm}^2\text{]}$$

$$\left(\frac{\mu\Omega}{\text{cm}} \right) = 531, \text{ [micro-ohm/cm]}$$

Step No. 14 Calculate the inductor winding resistance, R_L . Use the MLT from the core data found in Step 4 and the micro-ohm per centimeter found in Step 13.

$$R_L = (\text{MLT})(N_s) \left(\frac{\mu\Omega}{\text{cm}} \right) (10^{-6}), \quad [\text{ohms}]$$

$$R_L = (14.8)(459)(531)(10^{-6}), \quad [\text{ohms}]$$

$$R_L = 3.61, \quad [\text{ohms}]$$

Step No. 15 Calculate the inductor winding copper loss, P_L .

$$P_L = (I_L)^2 R_L, \quad [\text{watts}]$$

$$P_L = (1.0)^2 (3.61), \quad [\text{watts}]$$

$$P_L = 3.61, \quad [\text{watts}]$$

Step No. 16 Calculate the watts-per-kilograms, W/K , for the appropriate core material. See Chapter 2.

$$W/K = 0.000557 f^{(1.68)} B_s^{(1.86)}, \quad [\text{watts-per-kilogram}]$$

$$W/K = 0.000557 (60)^{(1.68)} (1.6)^{(1.86)}, \quad [\text{watts-per-kilogram}]$$

$$W/K = 1.30, \quad [\text{watts-per-kilogram}]$$

Step No. 17 Calculate the core loss in watts, P_{fe} .

$$P_{fe} = (W/K) W_{fe}, \quad [\text{watts}]$$

$$P_{fe} = (1.30)(0.676), \quad [\text{watts}]$$

$$P_{fe} = 0.878, \quad [\text{watts}]$$

Step No. 18 Calculate the gap loss, P_g .

$$P_g = K_i E l_g f B_{ac}^2, \quad [\text{watts}]$$

$$P_g = (0.155)(2.54)(0.0568)(60)(1.6)^2, \quad [\text{watts}]$$

$$P_g = 3.43, \quad [\text{watts}]$$

Step No. 19 Calculate the total inductor losses, P_Σ .

$$P_\Sigma = P_{cu} + P_{fe} + P_g, \quad [\text{watts}]$$

$$P_\Sigma = (3.61) + (0.878) + (3.43), \quad [\text{watts}]$$

$$P_\Sigma = 7.92, \quad [\text{watts}]$$

Step No. 20 Calculate the inductor surface area watt density, ψ .

$$\psi = \frac{P_{\Sigma}}{A_t}, \text{ [watts-per-cm}^2\text{]}$$

$$\psi = \frac{(7.92)}{(213)}, \text{ [watts-per-cm}^2\text{]}$$

$$\psi = 0.0372, \text{ [watts-per-cm}^2\text{]}$$

Step No. 21 Calculate the temperature rise, T_r .

$$T_r = 450(\psi)^{(0.826)}, \text{ [}^{\circ}\text{C]}$$

$$T_r = 450(0.0372)^{(0.826)}, \text{ [}^{\circ}\text{C]}$$

$$T_r = 29.7, \text{ [}^{\circ}\text{C]}$$

Step No. 22 Calculate the window utilization, K_u .

$$K_u = \frac{N_{L(new)} A_{w(B) \#22}}{W_a}$$

$$K_u = \frac{((459)(0.00324))}{(4.84)}$$

$$K_u = 0.307$$

Reference

1. Ruben, L., and Stephens, D. Gap Loss in Current-Limiting Transformer. Electromechanical Design, April 1973, pp. 24-126.

Chapter 11

Constant Voltage Transformer (CVT)

Table of Contents

1. Introduction	
2. Constant-Voltage Transformer, Regulating Characteristics	
3. Electrical Parameters of a CVT Line Regulator	
4. Constant-Voltage Transformer, Design Equations	
5. Constant-Voltage Transformer, Design Example	
6. Series AC Inductor, Design Example	
7. References	

Introduction

The constant-voltage transformer (CVT) has a wide application, particularly where reliability and inherent regulating ability against line voltage changes are of prime importance. The output of a constant-voltage transformer is essentially a square wave, which is desirable for rectifier output applications while, also having good circuit characteristics. The main disadvantage to a constant-voltage transformer is efficiency and regulation for frequency and load. The equations presented here for designing a constant-voltage transformers at line frequency have been used at 400 Hz on aircraft, and as high as 20 kHz.

Constant-Voltage Transformer, Regulating Characteristics

The basic two-component (CVT) Ferroresonant regulator is shown in Figure 11-1. The inductor, L1, is a linear inductor and is in series with C1 across the input line. The voltage across capacitor, C1, would be considerably greater than the line voltage, because of the resonant condition between L1 and C1.

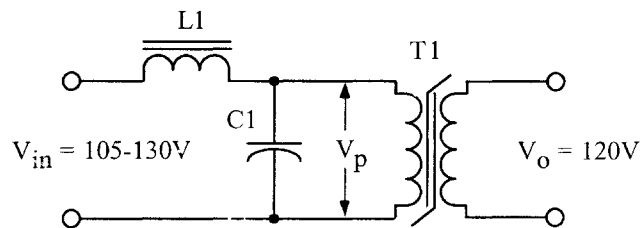


Figure 11-1. Two Component Ferroresonant Voltage Stabilizer.

The voltage, V_p , can be limited to a predetermined amplitude by using a self-saturating transformer, T1, which has high impedance, until a certain level of flux density is reached. At that flux density, the transformer saturates and becomes a low-impedance path, which prevents further voltage buildup across the capacitor. This limiting action produces a voltage waveform that has a fairly flat top characteristic as shown in Figure 11-2 on each half-cycle.

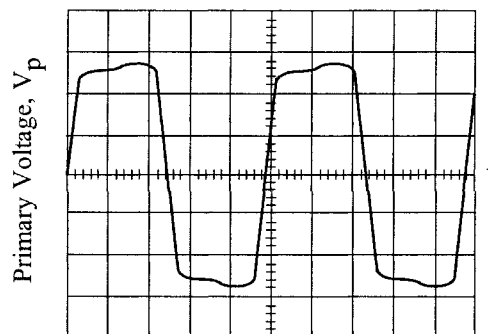


Figure 11-2. Primary Voltage Waveform of a Constant Voltage Transformer.

Electrical Parameters of a CVT Line Regulator

When the constant voltage transformer is operating as a line regulator, the output voltage will vary as a function of the input voltage, as shown in Figure 11-3. The magnetic material used to design transformer, T1, has an impact on line regulation. Transformers designed with a square B-H loop will result in better line regulation. If the output of the line regulator is subjected to a load power factor (lagging) with less than unity, the output will change, as shown in Figure 11-4.

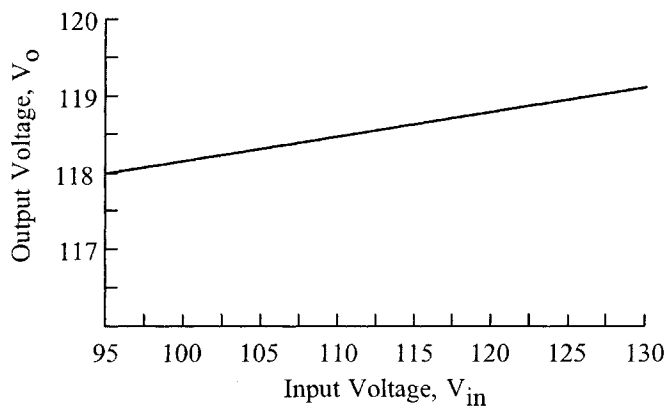


Figure 11-3. Output Voltage Variation, as a Function of Input Voltage.

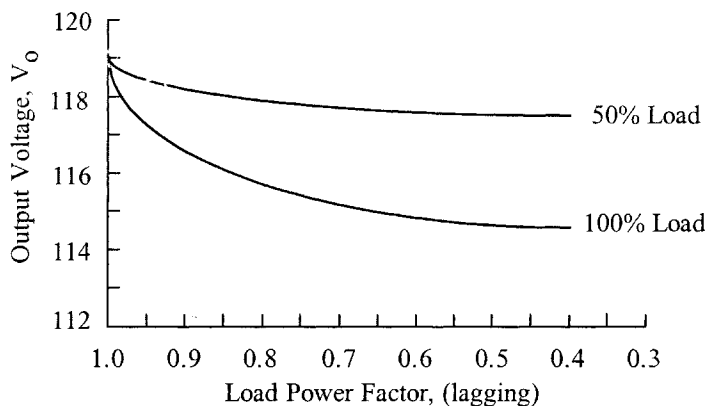


Figure 11-4. Output Voltage Variation, as a Function of Load Power Factor.

If the constant voltage transformer is subjected to a line voltage frequency change the output voltage will vary, as shown in Figure 11-5. The regulation of a constant-voltage transformer can be designed to be better than a few percent. Capability for handling a short circuit is an inherent feature of a constant-voltage transformer. The short-circuit current is limited and set by the series inductance, L . The regulation characteristics at various lines and loads are shown in Figure 11-6. It should be noted that a dead short, corresponding to zero output voltage, does not greatly increase the load current; whereas for most transformers, this dead short would be destructive.

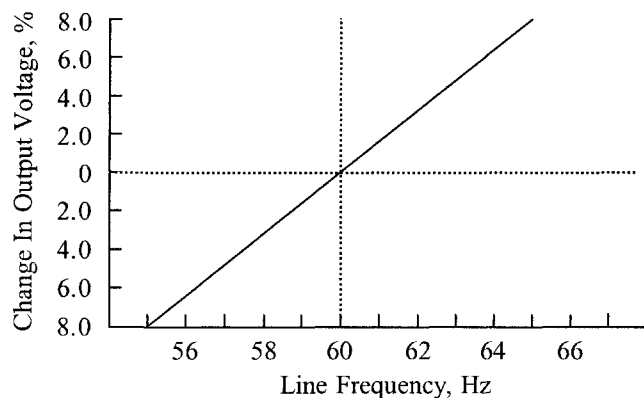


Figure 11-5. Output Voltage Variation, as a Function of Line Frequency Change.

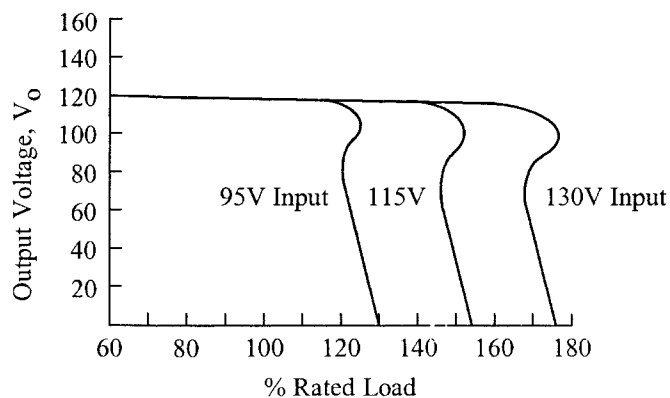


Figure 11-6. Output Voltage Variation, as a Function of Output Voltage vs. Load.

Constant-Voltage Transformer, Design Equations

Proper operation and power capacity of a constant-voltage transformer (CVT) depends on components, L1 and C1, as shown in Figure 11-7. Experience has shown that the, LC, relationship is:

$$LC\omega^2 = 1.5 \quad [11-1]$$

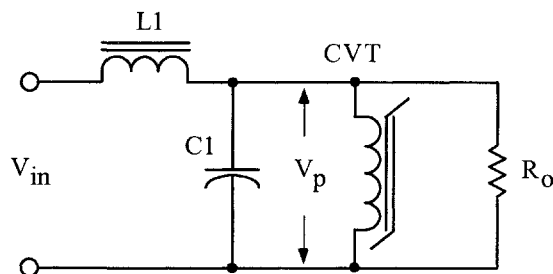


Figure 11-7. Basic, Constant Voltage Transformer Circuit.

The inductance can be expressed as:

$$L = \frac{R_{o(R)}}{2\omega}, \text{ [henrys] [11-2]}$$

The capacitance can be expressed as:

$$C = \frac{1}{0.33\omega R_{o(R)}}, \text{ [farads] [11-3]}$$

Referring to Figure 11-7, assume there is a sinusoidal input voltage, an ideal input inductor, L1, and a series capacitor, C1. All voltage and currents are rms values. V_{in} is the voltage value just before the circuit starts to regulate at full load; $R_{o(R)}$, is the reflected resistance back to the primary, including efficiency; η is the efficiency, and, P_o , is the output power.

$$P_o = \frac{V_s^2}{R_o}, \text{ [watts] [11-4]}$$

$$R_{o(R)} = \frac{(V_p)^2 \eta}{P_o}, \text{ [ohms] [11-5]}$$

It is common practice for the output to be isolated from the input and to connect C1 to a step-up winding on the constant-voltage transformer (CVT). In order to use smaller capacitor values, a step-up winding must be added, as shown in Figure 11-8. The penalty for using a smaller capacitor requires the use of a step-up winding. This step-up winding increases the VA or size of the transformer. This can be seen in Equation 11-6. The energy in a capacitor is:

$$\text{Energy} = \frac{CV^2}{2}, \text{ [watt-seconds] [11-6]}$$

$$C = \frac{2(\text{Energy})}{V^2}, \text{ [farads]}$$

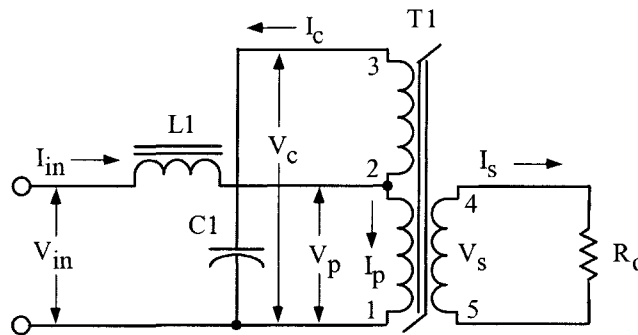


Figure 11-8. CVT, with a Capacitor Step-up Winding.

The secondary current, I_s , can be expressed as:

$$I_s = \frac{P_o}{V_s}, \quad [\text{amps}] \quad [11-7]$$

With the step-up winding, the primary current, I_p , is related to the secondary current by the following Equation [Ref. 3]:

$$I_p = \frac{I_s (V_{s(4-5)})}{\eta (V_{p(1-2)})} \left(1 + \sqrt{\frac{V_{p(1-2)}}{V_{c(1-3)}}} \right), \quad [\text{amps}] \quad [11-8]$$

The current, I_c , through the capacitor, is increased by, K_c , because of the effective higher frequency. Due to the quasi-voltage waveform as shown in Figure 11-2, the equivalent ac impedance of the resonant capacitor is reduced to some value lower than its normal sine wave value. This is due to an increase in odd harmonics.

$$I_c = K_c V_c \omega C, \quad [\text{amps}] \quad [11-9]$$

Where, K_c , can vary from 1.0 to 1.5.

Empirically, it has been shown that for good performance the primary operating voltage should be:

$$V_p = V_{in} (0.95), \quad [\text{volts}] \quad [11-10]$$

When the resonating capacitor is connected across a step-up winding, as is Figure 11-8, both the value of the capacitor and the volume can be reduced. C_n , is the new capacitance value, and, V_n , is the new voltage across the capacitor.

$$C_n V_n^2 = C_{(1-2)} V_{(1-2)}^2$$

The apparent power, P_t , is the sum of each winding, VA:

$$P_t = (VA_{(1-2)}) + (VA_{(2-3)}) + (VA_{(4-5)}), \quad [\text{watts}] \quad [11-11]$$

The line voltage regulation of a constant-voltage transformer is:

$$\Delta V_p = 4.44 \Delta B_s A_c f N_p (10^4), \quad [\text{volts}] \quad [11-12]$$

The output voltage regulation of a constant-voltage transformer, for a change in line voltage, is a function of the squareness of the B-H loop, as shown in Figure 11-9. The saturation flux density, B_s , is dependent on the annealing process of the magnetic material. It seems that each manufacturer has his own annealing process, which has an impact on the saturation flux density, B_s .

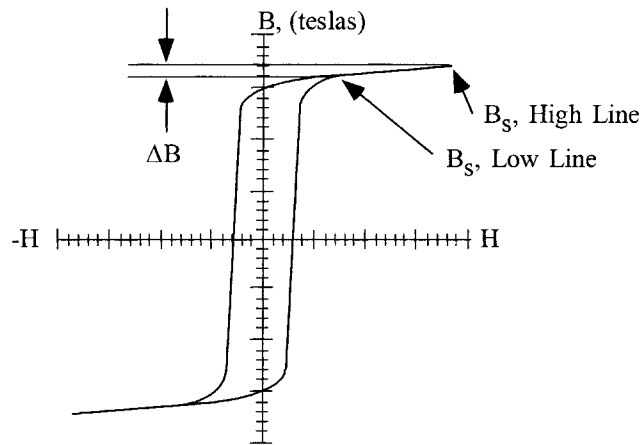


Figure 11-9. B-H Loop of a CVT at High and Low Line.

Constant-Voltage Transformer, Design Example

Design a constant-voltage line regulator (CVT) with the following specifications.

1. Input voltage = 105-129 volts
2. Line frequency = 60 hertz.
3. Output voltage, V_s = 120 volts
4. Output VA = 250 watts.
5. Transformer current density, J = 300 amps/cm²
6. Capacitor voltage, V_c = 440 volts
7. Capacitor coefficient, K_c = 1.5
8. Efficiency goal, $\eta(100)$ = 85%
9. Magnetic Material = Silicon
10. Saturating flux density, B_s = 1.95 tesla
11. Window utilization, K_u = 0.4
12. Temperature rise goal, T_r = 50°C

Step No. 1 Calculate the primary voltage, V_p .

$$V_p = V_{in(\min)} (0.95), \text{ [volts]}$$

$$V_p = (105)(0.95), \text{ [volts]}$$

$$V_p = 99.75, \text{ [volts]}$$

Step No. 2 Calculate the reflected resistance, $R_{o(R)}$ back to the primary, including efficiency η .

$$R_{o(R)} = \frac{(V_p)^2 \eta}{P_o}, \text{ [ohms]}$$

$$R_{o(R)} = \frac{(99.75)^2 (0.85)}{250}, \text{ [ohms]}$$

$$R_{o(R)} = 33.8, \text{ [ohms]}$$

Step No. 3 Calculate the required capacitance, C1.

$$C = \frac{1}{0.33\omega R_{o(R)}}, \text{ [farads]}$$

$$C = \frac{1}{0.33(377)(33.8)}, \text{ [farads]}$$

$$C = 238(10^{-6}), \text{ [farads]}$$

Step No. 4 Calculate the new capacitance value, using the higher voltage, V_c .

$$C_{(1-3)} = \frac{C_{(1-2)} (V_{(1-2)})^2}{(V_{(1-3)})^2}, \text{ [farads]}$$

$$C_{(1-3)} = \frac{(238(10^{-6}))(99.75)^2}{(440)^2}, \text{ [farads]}$$

$$C_{(1-3)} = 12.3(10^{-6}), \text{ [farads]}$$

A standard motor run capacitor is a 12.5 $\mu\text{f}/440\text{v}$.

Step No. 5 Calculate the capacitor current, I_c .

$$I_c = 1.5V_c \omega C, \text{ [amps]}$$

$$I_c = 1.5(440)(377)(12.5(10^{-6})), \text{ [amps]}$$

$$I_c = 3.11, \text{ [amps]}$$

Step No. 6 Calculate the secondary current, I_s .

$$I_s = \frac{P_o}{V_s}, \text{ [amps]}$$

$$I_s = \frac{250}{120}, \text{ [amps]}$$

$$I_s = 2.08, \text{ [amps]}$$

Step No. 7 Calculate the primary current, I_p .

$$I_p = \frac{I_s (V_{s(4-5)})}{\eta (V_{p(1-2)})} \left(1 + \sqrt{\frac{V_{p(1-2)}}{V_{c(1-3)}}} \right), \text{ [amps]}$$

$$I_p = \frac{2.08(120)}{(0.85)(99.75)} \left(1 + \sqrt{\frac{99.75}{440}} \right), \text{ [amps]}$$

$$I_p = 4.35, \text{ [amps]}$$

Step No. 8 Calculate the apparent power P_t .

$$P_t = (VA_{(1-2)}) + (VA_{(2-3)}) + (VA_{(4-5)}), \text{ [watts]}$$

$$VA_{(1-2)} = V_p I_p = (99.75)(4.35) = 434, \text{ [watts]}$$

$$VA_{(2-3)} = (V_c - V_p) I_c = (340)(3.11) = 1057, \text{ [watts]}$$

$$VA_{(4-5)} = V_s I_s = (120)(2.08) = 250, \text{ [watts]}$$

$$P_t = (434) + (1057) + (250), \text{ [watts]}$$

$$P_t = 1741, \text{ [watts]}$$

Step No. 9 Calculate the area product, A_p .

$$A_p = \frac{P_t (10^4)}{K_f K_u f B_s J}, \text{ [cm}^4\text{]}$$

$$A_p = \frac{(1742)(10^4)}{(4.44)(0.4)(60)(1.95)(300)}, \text{ [cm}^4\text{]}$$

$$A_p = 279, \text{ [cm}^4\text{]}$$

Step No. 10 Select an EI lamination from Chapter Three. The closest lamination to the calculated area product, A_p , is the EI-175.

1. Core Number = EI-175
2. Magnetic Path Length, MPL = 26.7 cm
3. Core Weight, W_{ife} = 3.71 kilograms
4. Mean Length Turn, MLT = 25.6 cm
5. Iron Area, A_c = 18.8 cm²
6. Window Area, W_a = 14.8 cm²
7. Area Product, A_p = 278 cm⁴
8. Core Geometry, K_g = 81.7 cm⁵
9. Surface Area, A_t = 652 cm²

Step No. 11 Calculate the number of primary turns, N_p .

$$N_p = \frac{V_p (10^4)}{K_f B_s f A_c}, \text{ [turns]}$$
$$N_p = \frac{(99.75)(10^4)}{(4.44)(1.95)(60)(18.8)}, \text{ [turns]}$$
$$N_p = 102, \text{ [turns]}$$

Step No. 12 Calculate the primary bare wire area, $A_{wp(B)}$.

$$A_{wp(B)} = \frac{I_p}{J}, \text{ [cm}^2\text{]}$$
$$A_{wp(B)} = \frac{(4.35)}{(300)}, \text{ [cm}^2\text{]}$$
$$A_{wp(B)} = 0.0145, \text{ [cm}^2\text{]}$$

Step No. 13 Select a wire from the Wire Table in Chapter 4.

$$AWG = \#16$$
$$A_{w(B)} = 0.0131, \text{ [cm}^2\text{]}$$
$$\left(\frac{\mu\Omega}{\text{cm}}\right) = 132, \text{ [micro-ohm/cm]}$$

Step No. 14 Calculate the primary resistance, R_p . Use the MLT from the core data and the micro-ohm per centimeter found in Step 13.

$$R_p = (\text{MLT})(N_p)\left(\frac{\mu\Omega}{\text{cm}}\right)(10^{-6}), \text{ [ohms]}$$
$$R_p = (25.6)(102)(132)(10^{-6}), \text{ [ohms]}$$
$$R_p = 0.345, \text{ [ohms]}$$

Step No. 15 Calculate the primary copper loss, P_p .

$$P_p = (I_p)^2 R_p, \text{ [watts]}$$
$$P_p = (4.35)^2 (0.345), \text{ [watts]}$$
$$P_p = 6.53, \text{ [watts]}$$

Step No. 16 Calculate the required turns for the step-up capacitor winding, N_c .

$$N_c = \frac{N_p (V_c - V_p)}{V_p}, \quad [\text{turns}]$$
$$N_c = \frac{(102)(440 - 99.75)}{99.75}, \quad [\text{turns}]$$
$$N_c = 348, \quad [\text{turns}]$$

Step No. 17 Calculate the capacitor step-up winding bare wire area, $A_{wc(B)}$.

$$A_{wc(B)} = \frac{I_c}{J}, \quad [\text{cm}^2]$$
$$A_{wc(B)} = \frac{(3.11)}{(300)}, \quad [\text{cm}^2]$$
$$A_{wc(B)} = 0.0104, \quad [\text{cm}^2]$$

Step No. 18 Select a wire from the Wire Table in Chapter 4.

$$AWG = \#17$$
$$A_{w(B)} = 0.0104, \quad [\text{cm}^2]$$
$$\left(\frac{\mu\Omega}{\text{cm}} \right) = 166, \quad [\text{micro-ohm/cm}]$$

Step No. 19 Calculate the capacitor winding resistance, R_c . Use the MLT from the core data and the micro-ohm per centimeter found in Step 18.

$$R_c = (\text{MLT})(N_c) \left(\frac{\mu\Omega}{\text{cm}} \right) (10^{-6}), \quad [\text{ohms}]$$
$$R_c = (25.6)(348)(166)(10^{-6}), \quad [\text{ohms}]$$
$$R_c = 1.48, \quad [\text{ohms}]$$

Step No. 20 Calculate the capacitor step-up winding copper loss, P_c .

$$P_c = (I_c)^2 R_c, \quad [\text{watts}]$$
$$P_c = (3.11)^2 (1.48), \quad [\text{watts}]$$
$$P_c = 14.3, \quad [\text{watts}]$$

Step No. 21 Calculate the turns for the secondary, N_s .

$$N_s = \frac{N_p V_s}{V_p}, \text{ [turns]}$$

$$N_s = \frac{(102)(120)}{99.75}, \text{ [turns]}$$

$$N_s = 123, \text{ [turns]}$$

Step No. 22 Calculate the secondary bare wire area, $A_{ws(B)}$.

$$A_{ws(B)} = \frac{I_s}{J}, \text{ [cm}^2\text{]}$$

$$A_{ws(B)} = \frac{(2.08)}{(300)}, \text{ [cm}^2\text{]}$$

$$A_{ws(B)} = 0.00693, \text{ [cm}^2\text{]}$$

Step No. 23 Select a wire from the Wire Table in Chapter 4.

$$AWG = \#19$$

$$A_{w(B)} = 0.00653, \text{ [cm}^2\text{]}$$

$$\left(\frac{\mu\Omega}{\text{cm}}\right) = 264, \text{ [micro-ohm/cm]}$$

Step No. 24 Calculate the secondary winding resistance, R_s . Use the MLT from the core data and the micro-ohm per centimeter found in Step 23.

$$R_s = (\text{MLT})(N_s)\left(\frac{\mu\Omega}{\text{cm}}\right)(10^{-6}), \text{ [ohms]}$$

$$R_s = (25.6)(123)(264)(10^{-6}), \text{ [ohms]}$$

$$R_s = 0.831, \text{ [ohms]}$$

Step No. 25 Calculate the secondary winding copper loss, P_s .

$$P_s = (I_s)^2 R_s, \text{ [watts]}$$

$$P_s = (2.08)^2 (0.831), \text{ [watts]}$$

$$P_s = 3.59, \text{ [watts]}$$

Step No. 26 Calculate the total copper loss, P_{cu} .

$$P_{cu} = P_p + P_s + P_c, \quad [\text{watts}]$$

$$P_{cu} = (6.53) + (3.59) + (14.3), \quad [\text{watts}]$$

$$P_{cu} = 24.4, \quad [\text{watts}]$$

Step No. 27 Calculate the watts-per-kilogram, W/K , for the appropriate core material. See Chapter 2.

$$W / K = 0.000557 f^{(1.68)} B_s^{(1.86)}, \quad [\text{watts-per-kilogram}]$$

$$W / K = 0.000557 (60)^{(1.68)} (1.95)^{(1.86)}, \quad [\text{watts-per-kilogram}]$$

$$W / K = 1.87, \quad [\text{watts-per-kilogram}]$$

Step No. 28 Calculate the core loss in watts, P_{fe} .

$$P_{fe} = (W / K) W_{fe}, \quad [\text{watts}]$$

$$P_{fe} = (1.87)(3.71), \quad [\text{watts}]$$

$$P_{fe} = 6.94, \quad [\text{watts}]$$

Step No. 29 Calculate the total losses, P_{Σ} .

$$P_{\Sigma} = P_{cu} + P_{fe}, \quad [\text{watts}]$$

$$P_{\Sigma} = (24.4) + (6.94), \quad [\text{watts}]$$

$$P_{\Sigma} = 31.34, \quad [\text{watts}]$$

Step No. 30 Calculate the transformer surface watt density, ψ .

$$\psi = \frac{P_{\Sigma}}{A_t}, \quad [\text{watts-per-cm}^2]$$

$$\psi = \frac{(31.34)}{(652)}, \quad [\text{watts-per-cm}^2]$$

$$\psi = 0.0481, \quad [\text{watts-per-cm}^2]$$

Step No. 31 Calculate the temperature rise, T_r .

$$T_r = 450(\psi)^{(0.826)}, \quad [^{\circ}\text{C}]$$

$$T_r = 450(0.0481)^{(0.826)}, \quad [^{\circ}\text{C}]$$

$$T_r = 36.7, \quad [^{\circ}\text{C}]$$

Step No. 32 Calculate the transformer efficiency, η .

$$\eta = \frac{P_o}{(P_o + P_\Sigma)}(100), \quad [\%]$$

$$\eta = \frac{(250)}{(250 + 31.3)}(100), \quad [\%]$$

$$\eta = 88.9, \quad [\%]$$

Step No. 33 Calculate the window utilization, K_u .

$$K_u = \frac{N_p A_{wp(B)\#16} + N_c A_{wc(B)\#17} + N_s A_{ws(B)\#19}}{W_a}$$

$$K_u = \frac{((102)(0.0131)) + ((348)(0.0104)) + ((123)(0.00653))}{(14.6)}$$

$$K_u = 0.394$$

Series AC Inductor, Design Example

(Also See Chapter 9)

Step No. 33 Design a series, linear ac inductor with the following specifications:

1. Applied voltage = 129 volts
2. Line frequency = 60 hertz
3. Current density, J = 300 amp/cm²
4. Efficiency goal, $\eta(100)$ = 85%
5. Magnetic material = Silicon
6. Magnetic material permeability, μ_m = 1500
7. Flux density, B_{ac} = 1.4 tesla
8. Window utilization, K_u = 0.4
9. Waveform factor, K_f = 4.44
10. Temperature rise goal, T_r = 50°C

Step No. 34 Calculate the required series inductance, L1. See Figure 11-8.

$$L1 = \frac{R_{o(R)}}{2\omega}, \quad [\text{henrys}]$$

$$L1 = \frac{(33.8)}{2(377)}, \quad [\text{henrys}]$$

$$L1 = 0.0448, \quad [\text{henrys}]$$

Step No. 35 Calculate the inductor reactance, X_L .

$$X_L = 2\pi f L1, \text{ [ohms]}$$

$$X_L = (6.28)(60)(0.0448), \text{ [ohms]}$$

$$X_L = 16.9, \text{ [ohms]}$$

Step No. 36 Calculate the short-circuit current, I_L .

$$I_L = \frac{V_{in(max)}}{X_L}, \text{ [amps]}$$

$$I_L = \frac{(129)}{(16.9)}, \text{ [amps]}$$

$$I_L = 7.63, \text{ [amps]}$$

Step No. 37 Calculate the apparent power, P_i or VA, of the input series inductor, L1. Use the high line voltage of 129 volts and the normal running current, I_p , from Step 7.

$$VA = V_{in(max)} I_{L(n)}, \text{ [watts]}$$

$$VA = (129)(4.35), \text{ [watts]}$$

$$VA = 561, \text{ [watts]}$$

Step No. 38 Calculate the area product, A_p .

$$A_p = \frac{VA(10^4)}{K_f K_u f B_{uc} J}, \text{ [cm}^4\text{]}$$

$$A_p = \frac{(561)(10^4)}{(4.44)(0.4)(60)(1.4)(300)}, \text{ [cm}^4\text{]}$$

$$A_p = 125, \text{ [cm}^4\text{]}$$

Step No. 39 Select an EI lamination from Chapter Three with the closest calculated area product, A_p .

- | | |
|------------------------------------|------------------------|
| 1. Core Number | = EI-138 |
| 2. Magnetic Path Length, MPL | = 21 cm |
| 3. Core Weight, W_{fe} | = 1.79 kilograms |
| 4. Mean Length Turn, MLT | = 20.1 cm |
| 5. Iron Area, A_c | = 11.6 cm ² |
| 6. Window Area, W_a | = 9.15 cm ² |
| 7. Area Product, A_p | = 106 cm ⁴ |
| 8. Core Geometry, K_g | = 24.5 cm ⁵ |
| 9. Surface Area, A_t | = 403 cm ² |
| 10. Winding length, G | = 5.24 cm |
| 11. Lamination tongue, E | = 3.49 cm |

Step No. 40 Calculate the number of inductor turns, N_L .

$$N_L = \frac{V_{in(max)}(10^4)}{K_f B_{ac} f A_c}, \text{ [turns]}$$

$$N_L = \frac{(129)(10^4)}{(4.44)(1.4)(60)(11.6)}, \text{ [turns]}$$

$$N_L = 298, \text{ [turns]}$$

Step No. 41 Calculate the required gap, L_g .

$$l_g = \left(\frac{0.4\pi N_L^2 A_c (10^{-8})}{L} \right) - \left(\frac{MPL}{\mu_m} \right), \text{ [cm]}$$

$$l_g = \left(\frac{(1.26)(298)^2 (11.6)(10^{-8})}{0.0448} \right) - \left(\frac{21}{1500} \right), \text{ [cm]}$$

$$l_g = 0.276, \text{ [cm]} \text{ or } l_g = 0.109, \text{ [mils]: This would be 50mils in each leg.}$$

Step No. 42 Calculate the fringing flux, F .

$$F = \left(1 + \frac{l_g}{\sqrt{A_c}} \ln \frac{2(G)}{l_g} \right)$$

$$F = \left(1 + \frac{0.276}{\sqrt{11.6}} \ln \frac{2(5.24)}{0.276} \right)$$

$$F = 1.29$$

Step No. 43 Using the fringing flux, recalculate the series inductor turns, $N_{L(new)}$.

$$N_{L(new)} = \sqrt{\frac{l_g L}{0.4\pi A_c F (10^{-8})}}, \text{ [turns]}$$

$$N_{L(new)} = \sqrt{\frac{(0.276)(0.0448)}{(1.26)(11.6)(1.29)(10^{-8})}}, \text{ [turns]}$$

$$N_{L(new)} = 256, \text{ [turns]}$$

Step No. 44 Using the new turns, recalculate the flux density, B_{ac} .

$$B_{ac} = \frac{V_{in(max)}(10^4)}{K_f N_{L(new)} A_c f}, \text{ [tesla]}$$

$$B_{ac} = \frac{(129)(10^4)}{(4.44)(256)(11.6)(60)}, \text{ [tesla]}$$

$$B_{ac} = 1.63, \text{ [tesla]}$$

Step No. 45 Calculate the inductor bare wire area, $A_{wL(B)}$.

$$A_{wL(B)} = \frac{I_{L(n)}}{J}, \quad [\text{cm}^2]$$
$$A_{wL(B)} = \frac{(4.35)}{(300)}, \quad [\text{cm}^2]$$
$$A_{wL(B)} = 0.0145, \quad [\text{cm}^2]$$

Step No. 46 Select a wire from the Wire Table in Chapter 4.

$$AWG = \#16$$
$$A_{w(B)} = 0.01307, \quad [\text{cm}^2]$$
$$\left(\frac{\mu\Omega}{\text{cm}}\right) = 132, \quad [\text{micro-ohm/cm}]$$

Step No. 47 Calculate the inductor winding resistance, R_L . Use the MLT from the core data and the micro-ohm per centimeter found in Step 38.

$$R_L = (\text{MLT})(N_s) \left(\frac{\mu\Omega}{\text{cm}}\right) (10^{-6}), \quad [\text{ohms}]$$
$$R_L = (20.1)(256)(132)(10^{-6}), \quad [\text{ohms}]$$
$$R_L = 0.679, \quad [\text{ohms}]$$

Step No. 48 Calculate the inductor winding copper loss, P_L .

$$P_L = (I_L)^2 R_L, \quad [\text{watts}]$$
$$P_L = (4.35)^2 (0.679), \quad [\text{watts}]$$
$$P_L = 12.8, \quad [\text{watts}]$$

Step No. 49 Calculate the watts-per-kilogram, W/K , for the appropriate core material. See Chapter 2.

$$W/K = 0.000557 f^{(1.68)} B_s^{(1.86)}, \quad [\text{watts-per-kilogram}]$$
$$W/K = 0.000557 (60)^{(1.68)} (1.63)^{(1.86)}, \quad [\text{watts-per-kilogram}]$$
$$W/K = 1.34, \quad [\text{watts-per-kilogram}]$$

Step No. 50 Calculate the core loss in watts, P_{fe} .

$$P_{fe} = (W / K)W_{fe}, \text{ [watts]}$$

$$P_{fe} = (1.34)(1.79), \text{ [watts]}$$

$$P_{fe} = 2.4, \text{ [watts]}$$

Step No. 51 Calculate the gap loss, P_g .

$$P_g = K_i E l_g f B_{ac}^2, \text{ [watts]}$$

$$P_g = (0.155)(3.49)(0.276)(60)(1.63)^2, \text{ [watts]}$$

$$P_g = 23.8, \text{ [watts]}$$

Step No. 52 Calculate the total losses, P_Σ .

$$P_\Sigma = P_{cu} + P_{fe} + P_g, \text{ [watts]}$$

$$P_\Sigma = (12.8) + (2.4) + (23.8), \text{ [watts]}$$

$$P_\Sigma = 39, \text{ [watts]}$$

Step No. 53 Calculate the inductor surface area watt density, ψ .

$$\psi = \frac{P_\Sigma}{A_l}, \text{ [watts-per-cm}^2\text{]}$$

$$\psi = \frac{(39)}{(403)}, \text{ [watts-per-cm}^2\text{]}$$

$$\psi = 0.0968, \text{ [watts-per-cm}^2\text{]}$$

Step No. 54 Calculate the temperature rise, T_r .

$$T_r = 450(\psi)^{(0.826)}, \text{ [}^\circ\text{C]}$$

$$T_r = 450(0.0968)^{(0.826)}, \text{ [}^\circ\text{C]}$$

$$T_r = 65, \text{ [}^\circ\text{C]}$$

Step No. 55 Calculate the window utilization, K_u .

$$K_u = \frac{N_{L(new)} A_{w(\beta)\#16}}{W_a}$$

$$K_u = \frac{((256)(0.0131))}{(9.15)}$$

$$K_u = 0.367$$

References

1. Ruben, L., and Stephens, D. Gap Loss in Current-Limiting Transformer. *Electromechanical Design*, April 1973, pp. 24-126.
2. H. P. Hart and R. J. Kakalec, "The Derivation and Application of Design Equations for Ferroresonant Voltage Regulators and Regulated Rectifiers," *IEEE Trans. Magnetics*, vol. Mag-7, No.1, March 1971, pp 205-211.
3. I. B. Friedman, "The Analysis and Design of Constant Voltage Regulators," *IRE Trans. Component Parts*, vol. CP-3, March 1956, pp.11-14.
4. S. Lendena, "Design of a Magnetic Voltage Stabilizer." *Electronics Technology*, May 1961, pp. 154-155.

Chapter 12

Three-Phase Transformer Design

Table of Contents

1.	Introduction
2.	Primary Circuit
3.	Comparing Transformer, Physical Size
4.	Phase Current, Line Current, and Voltage in a Delta System
5.	Phase Voltage, Line Voltage, and Current in a Wye System
6.	Comparing Multiphase and Single-Phase Power
7.	Multiphase Rectifier Circuits
8.	Area Product, A_p , and Core Geometry, K_g , for Three-Phase Transformers
9.	Output Power Versus Apparent, P_t , Capability
10.	Relationship, K_g , to Power Transformer Regulation Capability
11.	Relationship, A_p , to Transformer Power Handling Capability
12.	Three-Phase Transformer, Design Example

Introduction

Three-phase power is used almost exclusively for generation, transmission, and distribution, as well as for all industrial uses. It is also used on aircraft, both commercial and military. It has many advantages over single-phase power. The transformer can be made smaller and lighter for the same power handling capability, because the copper and iron are used more effectively. In circuitry, for conversion from ac to dc, the output contains a much lower ripple amplitude, and a higher frequency component, which is 3 times and 6 times the line frequency, and which, in turn, requires less filtering.

Primary Circuit

The two most commonly used primary circuits for three-phase transformers are the Star, or Y connection, as shown in Figure 12-1, and the other being known as the Delta (Δ) connection, as shown in Figure 12-2. The design requirement for each particular job dictates which method of connection will be used.

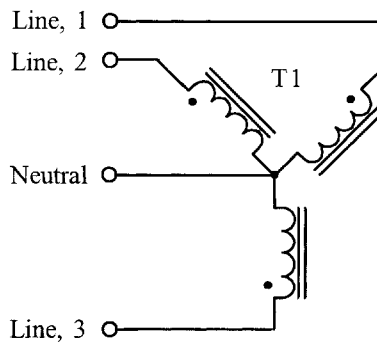


Figure 12-1. Three-Phase Transformer, Connected in Star.

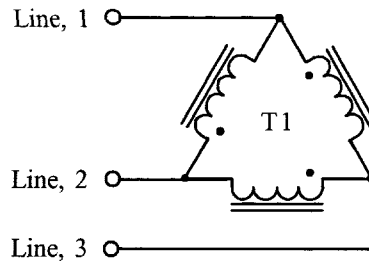


Figure 12-2. Three-Phase Transformer, Connected in Delta.

Comparing Transformer, Physical Size

The schematic diagram in Figure 12-3, shows the connection of three single-phase transformers: (a) Operating from a three-phase power source and a single three-phase transformer; and (b) Operating from a three-phase power source connected in a delta-delta configuration. The single three-phase transformer, T4, would be lighter and smaller than a bank of three single-phase transformers of the same total rating. Since the windings of the three-phase transformer are placed on a common magnetic core, rather than on three independent cores, the consolidation results in an appreciable saving in the copper, the core, and the insulating materials.

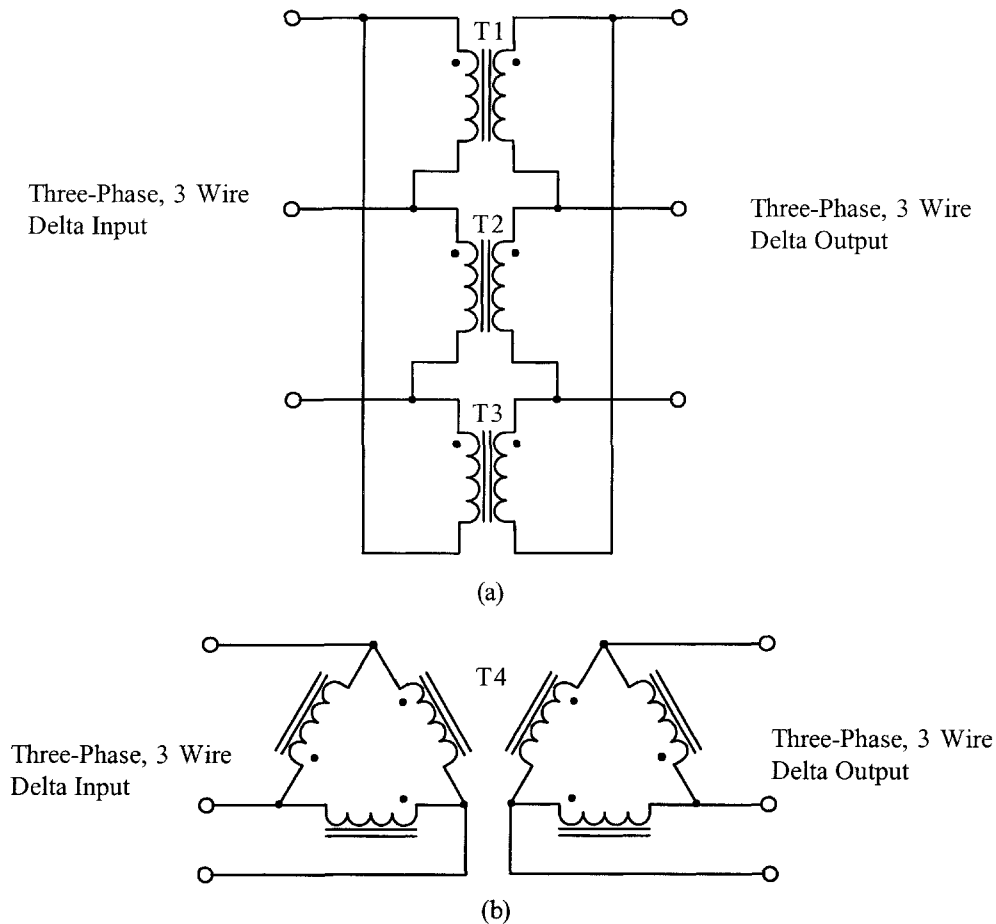


Figure 12-3. Comparing Three Single-Phase Transformers Connected in Three-Phase Delta.

A cutaway view of a single-phase transformer, showing the window area and iron area of two types of core configuration, is shown in Figure 12-4 and Figure 12-5. The EI lamination, shown in Figure 12-4, is known as a shell type, because it looks like the core surrounds the coil. The C core, shown in Figure 12-5, is known as a core type, because it looks like the coil surrounds the core.

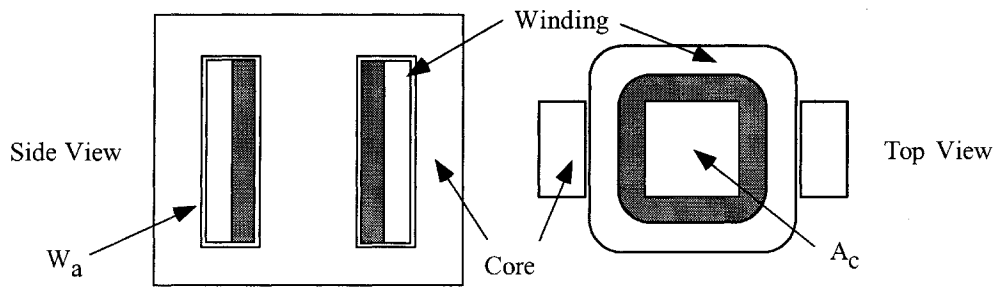


Figure 12-4. Illustrating a Shell Type Transformer.

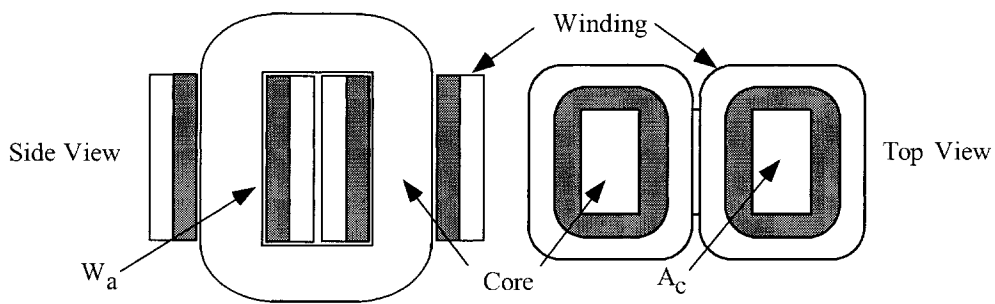


Figure 12-5. Illustrating a Core Type Transformer.

Cutaway views of a three-phase transformer are shown in Figure 12-6. These cross-sectional views show the window and iron areas. The three-legged core is designed to take advantage of the fact that, with balanced voltages impressed, the flux in each phase leg, adds up to zero. Therefore, no return leg is needed under normal conditions. When the transformer is subjected to unbalanced loads, or unbalanced line voltages, it may be best to use three single-phase transformers, because of the high-circulating currents.

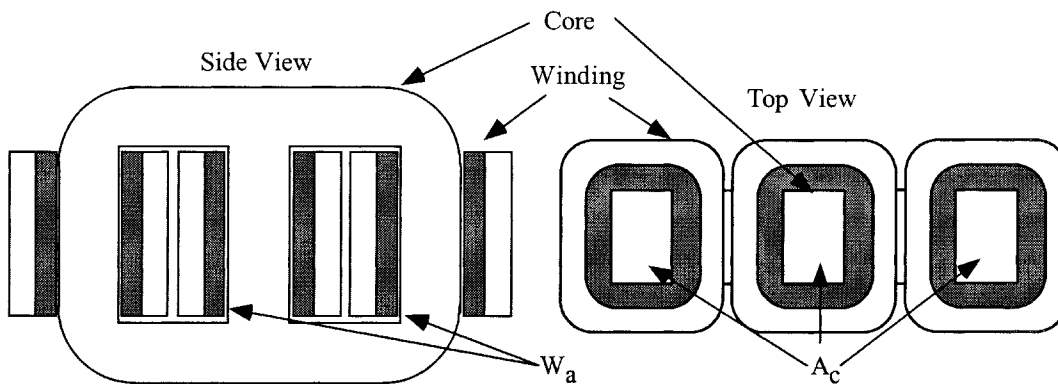


Figure 12-6. Cutaway View of a Three-Phase Transformer.

Phase Current, Line Current, and Voltage in a Delta System

In a Three-Phase Delta Circuit, such as the one shown in Figure 12-7, the line voltage and line current are commonly called phase voltage and phase current. The line voltage, $E_{(Line)}$, will be the same as the actual winding voltage of the transformer. However, the line current, $I_{(Line)}$, is equal to the phase current, $I_{(Phase)}$, times the square root of 3.

$$I_{(line)} = I_{(phase)}\sqrt{3}, \text{ [amps] [12-1]}$$

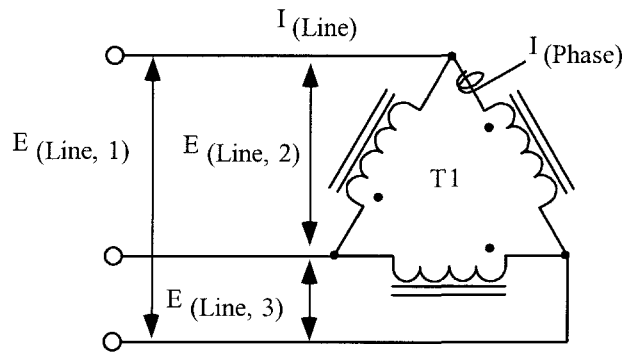


Figure 12-7. Voltage and Current Relationship of a Three-Phase Delta Circuit.

Phase Voltage, Line Voltage, and Current in a Wye System

The relationship between the Line voltage, and Line current, and the winding, or Phase voltage and Phase current, in a Three-Phase Wye Circuit can be seen in Figure 12-8. In a Wye System, the voltage between any two wires in the line will always be the square root of three times the phase voltage, $E_{(Phase)}$, between the neutral, and any one of the lines.

$$E_{(phase)} = \frac{E_{(line)}}{\sqrt{3}}, \text{ [volts] [12-2]}$$

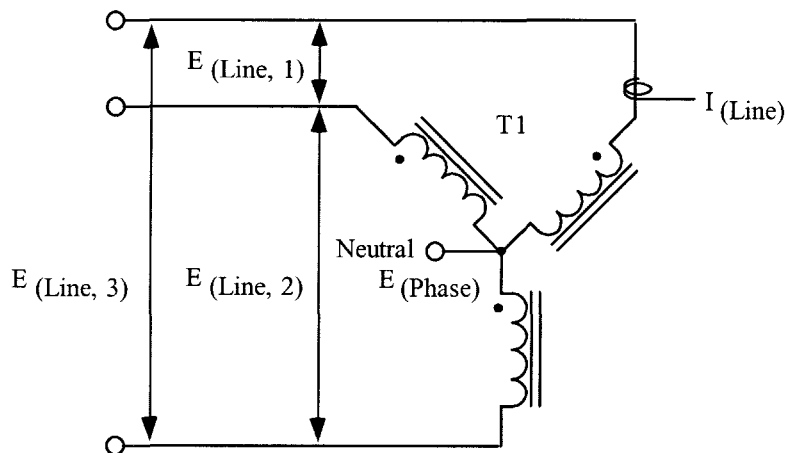


Figure 12-8. Voltage and Current Relationship for a Three-Phase Wye Circuit.

Comparing Multiphase and Single-Phase Power

Three-phase power distribution has a significant advantage over the single-phase. Most high power equipment and industrial complexes will use three-phase power. One of the biggest advantages in using three-phase power distribution has to do with smaller magnetic components handling the same power as single-phase. This can be seen in aircraft, and shipboard equipment, as well as fixed ground installations. One of the basic reasons for selecting three-phase is the transformer size. Another reason is, if dc is a requirement, the capacitor and inductor filtering components are both smaller. The odd shape of a three-phase transformer could be troublesome, as well as keeping balanced loads to minimize circulating currents.

The single-phase, full wave bridge circuit is shown in Figure 12-9. The ripple voltage frequency is always twice the line frequency. Only 50% of the total current flows through each rectifier. The three-phase, Delta full wave bridge circuit is shown in Figure 12-10. The ripple voltage frequency is always 6 times the line frequency. Only 33% of the total current flows through each rectifier. Looking at the ripple in Figure 12-10, it is obvious the LC components will be smaller.

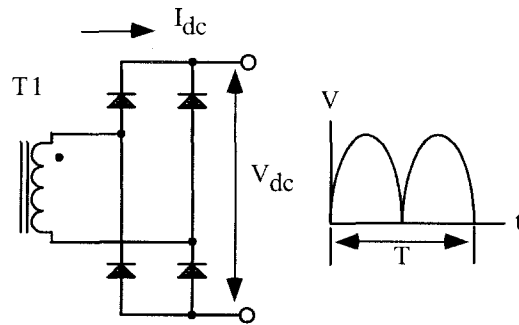


Figure 12-9. Single-Phase Full Wave Bridge.

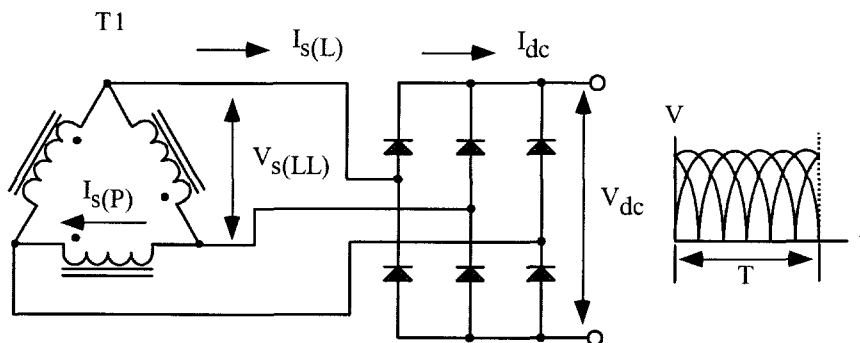


Figure 12-10. Three-Phase, "Delta" Full Wave Bridge.

Multiphase Rectifier Circuits

Table 12-1 lists voltage and current ratios for the circuits, shown in Figures 12-11 through Figures 12-14 for inductive output filters. These ratios apply for sinusoidal ac input voltages. Values shown do not take into consideration voltage drops which occur in the power transformer or rectifier diodes.

Table 12-1. Three-Phase Voltage and Current Ratios for Rectifier Circuits.

Three Phase Rectifier Circuit Data			
Delta-Delta Full Wave, Figure 12-11			
Item	Factor		
Primary VA	1.050	x	dc watts output
Secondary V/ leg	0.740	x	average dc output voltage
Secondary I/leg	0.471	x	average dc output current
Secondary VA	1.050	x	dc watts output
Ripple Voltage %	4.200		
Ripple Frequency	6f		
Delta-Wye Full Wave, Figure 12-12			
Item	Factor		
Primary VA	1.050	x	dc watts output
Secondary Line to Line	0.740	x	average dc output voltage
Secondary V/ leg	0.428 to Neutral	x	average dc output voltage
Secondary I/leg	0.817	x	average dc output current
Secondary VA	1.050	x	dc watts output
Ripple Voltage %	4.200		
Ripple Frequency	6f		
Delta-Wye Half Wave, Figure 12-13			
Item	Factor		
Primary VA	1.210	x	dc watts output
Secondary Line to Line	0.740	x	average dc output voltage
Secondary V/ leg	0.855 to Neutral	x	average dc output voltage
Secondary I/leg	0.577	x	average dc output current
Secondary VA	1.480	x	dc watts output
Ripple Voltage %	18.000		
Ripple Frequency	3f		
Delta-Wye 6 Phase Half Wave, Figure 12-14			
Item	Factor		
Primary VA	1.280	x	dc watts output
Secondary Line to Line	1.480	x	average dc output voltage
Secondary V/ leg	0.740 to Neutral	x	average dc output voltage
Secondary I/leg	0.408	x	average dc output current
Secondary VA	1.810	x	dc watts output
Ripple Voltage %	4.200		
Ripple Frequency	6f		
Root mean square values to the average dc.			
Sine-wave , infinite inductance, no transformer or rectifier losses.			

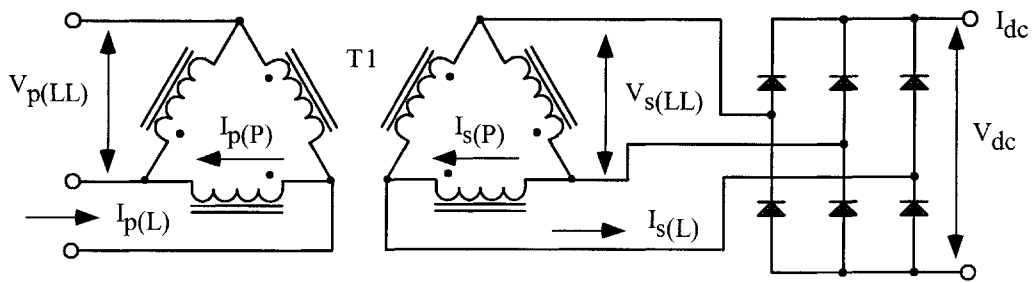


Figure 12-11. Three-Phase, "Delta-Delta" Full Wave Bridge.

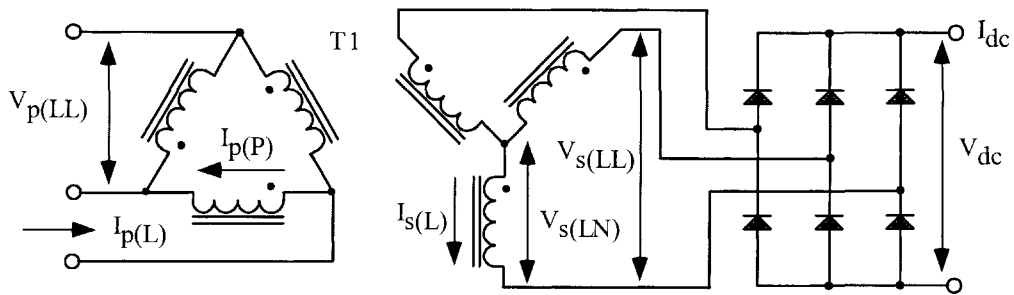


Figure 12-12. Three-Phase, "Delta-Wye" Full Wave Circuit.

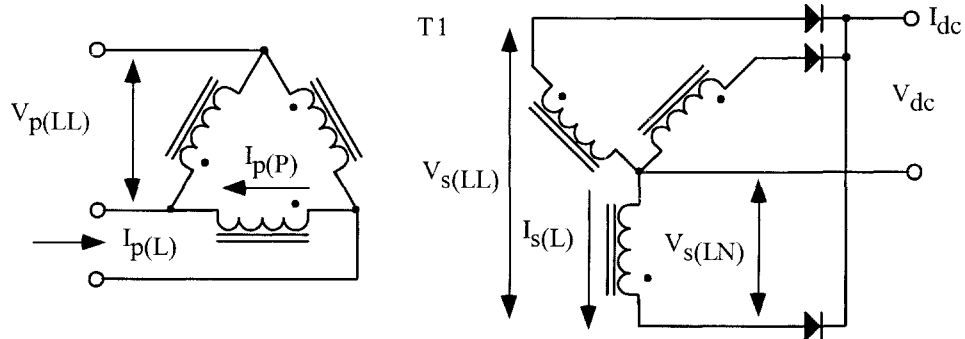


Figure 12-13. Three-Phase, "Delta-Wye" Half Wave Bridge.

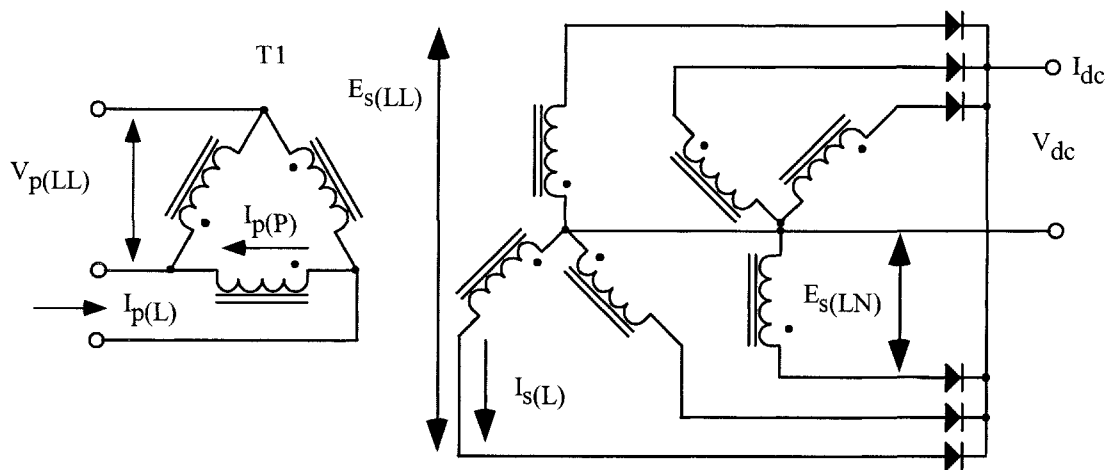


Figure 12-14. Three-Phase, "Delta-Wye" Six Phase Star.

Area Product, A_p , and Core Geometry, K_g , for Three-Phase Transformers

The area product, A_p , of a three-phase core is defined differently than that for a single-phase core. The window area, W_a , and iron area, A_c , for a single-phase transformer is shown in Figure 12-4 and 12-5. The window area, W_a , and iron area, A_c , for a three-phase transformer is shown in Figure 12-6. The area product, A_p , of a core is the product of the available window area, W_a , of the core in square centimeters (cm^2) multiplied by the effective, cross-section area, A_c , in square centimeters (cm^2), which may be stated as:

$$\text{Single-phase: } A_p = W_a A_c, \quad [\text{cm}^4] \quad [12-3]$$

This is alright for a single-phase transformer. For three-phase transformers, because there are basically two windows area, W_a , and three iron areas A_c , the window utilization is different, and the area product, A_p , changes to:

$$\text{Three-phase: } A_p = 3 \left(\frac{W_a}{2} A_c \right), \quad [\text{cm}^4] \quad [12-4]$$

This reduces to:

$$A_p = 1.5(W_a A_c), \quad [\text{cm}^4] \quad [12-5]$$

It is basically the same thing for the core geometry, K_g , for a single-phase transformer and the core geometry, K_g , for a three-phase transformer. The core geometry, K_g , for a single-phase transformer is:

$$\text{Single-phase: } K_g = \left(\frac{W_a A_c^2 K_u}{\text{MLT}} \right), \quad [\text{cm}^5] \quad [12-6]$$

In the three-phase transformer, core geometry, K_g , is:

$$\text{Three-phase: } K_g = 3 \left(\left(\frac{W_a}{2} \right) \frac{A_c^2 K_u}{\text{MLT}} \right), \quad [\text{cm}^5] \quad [12-7]$$

This reduces to:

$$K_g = 1.5 \left(\frac{W_a A_c^2 K_u}{\text{MLT}} \right), \quad [\text{cm}^5] \quad [12-8]$$

Output Power Versus Apparent Power, P_t , Capability

The apparent power, P_t , is described in detail in Chapter 7. The apparent power, P_t , of a transformer is the combined power of the primary and secondary windings which handle, P_{in} and P_o , to the load, respectively. Since the power transformer has to be designed to accommodate the primary, P_{in} , and the secondary, P_o :

$$P_t = P_{in} + P_o, \quad [\text{watts}] \quad [12-9]$$

$$P_{in} = \frac{P_o}{\eta}, \quad [\text{watts}] \quad [12-10]$$

Substituting:

$$P_t = \frac{P_o}{\eta} + P_o, \quad [\text{watts}] \quad [12-11]$$

$$P_t = P_o \left(\frac{1}{\eta} + 1 \right), \quad [\text{watts}] \quad [12-12]$$

The designer must be concerned with the apparent power handling capability, P_t , of the transformer core and winding. The apparent power, P_t , varies with the type of circuit in which the transformer is used. If the current in the rectifier is interrupted, its effective rms value changes. Transformer size is thus determined, not only by the load demand, but also by current wave shape. An example of the primary and secondary, VA, will be done to compare the power-handling capability required by each three-phase rectifier circuit in Table 12-1 and Figures 12-11 through 12-14. This comparison will negate transformer and diode losses so that $P_{in} = P_o$ ($\eta = 1$) for all three-phase rectifier circuits.

1. Delta-Delta, Full Wave, Figure 12-11.

$$P_t = P_o \left(\frac{P_{VA}}{\eta} + S_{VA} \right), \quad [\text{watts}]$$

$$P_t = P_o \left(\frac{1.05}{1} + 1.05 \right), \quad [\text{watts}] \quad [12-13]$$

$$P_t = P_o (2.1), \quad [\text{watts}]$$

2. Delta-Wye, Full Wave, Figure 12-12.

$$P_t = P_o \left(\frac{P_{VA}}{\eta} + S_{VA} \right), \quad [\text{watts}]$$

$$P_t = P_o \left(\frac{1.05}{1} + 1.05 \right), \quad [\text{watts}] \quad [12-14]$$

$$P_t = P_o (2.1), \quad [\text{watts}]$$

3. Delta-Wye, Half Wave, Figure 12-13.

$$P_t = P_o \left(\frac{P_{VA}}{\eta} + S_{VA} \right), \text{ [watts]}$$

$$P_t = P_o \left(\frac{1.21}{1} + 1.48 \right), \text{ [watts] [12-15]}$$

$$P_t = P_o (2.69), \text{ [watts]}$$

4. Delta-Wye, 6 Phase Half Wave, Figure 12-14.

$$P_t = P_o \left(\frac{P_{VA}}{\eta} + S_{VA} \right), \text{ [watts]}$$

$$P_t = P_o \left(\frac{1.28}{1} + 1.81 \right), \text{ [watts] [12-16]}$$

$$P_t = P_o (3.09), \text{ [watts]}$$

Relationship, K_g , to Power Transformer Regulation Capability

Although most transformers are designed for a given temperature rise, they can also be designed for a given regulation. The regulation and power-handling ability of a core are related to two constants:

$$\alpha = \frac{P_t}{2K_g K_e}, \text{ [%] [12-17]}$$

$$\alpha = \text{Regulation (\%)} \text{ [12-18]}$$

The constant, K_g , is determined by the core geometry, which may be related by the following equations:

$$K_g = 1.5 \left(\frac{W_a A_c^2 K_u}{\text{MLT}} \right) = \frac{P_t}{2K_e \alpha}, \text{ [cm}^5 \text{] [12-19]}$$

The constant, K_e , is determined by the magnetic and electric operating conditions, which may be related by the following equation:

$$K_e = 2.86 f^2 B^2 (10^{-4}) \text{ [12-20]}$$

From the above, it can be seen that factors such as flux density, frequency of operation, and waveform coefficient, have an influence on the transformer size.

Relationship, A_p , to Transformer Power Handling Capability

According to the newly developed approach, the power handling capability of a core is related to its area product, A_p , by an equation which may be stated as:

$$A_p = \frac{P_t (10^4)}{K_f K_u B_m J f}, \quad [\text{cm}^4] \quad [12-21]$$

$$A_p = 1.5(W_a A_c) = \frac{P_t (10^4)}{K_f K_u B_m J f}, \quad [\text{cm}^4] \quad [12-22]$$

Where:

K_f = waveform coefficient

K_f = 4.0 square wave

K_f = 4.44 sine wave

From the above, it can be seen that factors such as flux density, frequency of operation, and window utilization factor, K_u , define the maximum space, which may be occupied by the copper in the window.

Three-Phase Transformer, Design Example

The following information is the Design specification for a three-phase, isolation transformer, using the, K_g , core geometry approach.

Design specification:

- | | | |
|-----|--|---------------|
| 1. | Input voltage, V_{in} | 208 V, 3 Wire |
| 2. | Output voltage, V_o | 28 V |
| 3. | Output Current, I_o | 10 amps |
| 4. | Output Circuit | Full Bridge |
| 5. | Input / Output | Delta / Delta |
| 6. | Frequency, Three Phase, f | 60 hertz |
| 7. | Efficiency, $\eta(100)$ | 95 % |
| 8. | Regulation, α | 5 % |
| 9. | Flux Density, B_{ac} | 1.4 tesla |
| 10. | Magnetic Material | Silicon M6X |
| 11. | Window Utilization $K_u = (K_{up} + K_{us})$ | 0.4 |
| 12. | Diode Drop, V_d | 1.0 volt |

Step No. 1 Calculate the apparent power, P_t .

$$P_t = P_o \left(\frac{1.05}{\eta} + 1.05 \right), \text{ [watts]}$$

$$P_o = I_o (V_o + 2V_d) = (10)(30) = 300, \text{ [watts]}$$

$$P_t = 300 \left(\frac{1.05}{0.95} + 1.05 \right), \text{ [watts]}$$

$$P_t = 647, \text{ [watts]}$$

Step No. 2 Calculate the electrical conditions, K_e .

$$K_e = 2.86 f^2 B^2 (10^{-4})$$

$$K_e = 2.86(60)^2(1.4)^2(10^{-4})$$

$$K_e = 2.02$$

Step No. 3 Calculate the core geometry, K_g .

$$K_g = \frac{P_t}{2K_e \alpha}, \text{ [cm}^5\text{]}$$

$$K_g = \frac{647}{2(2.02)(5)}, \text{ [cm}^5\text{]}$$

$$K_g = 32, \text{ [cm}^5\text{]}$$

Step No. 4 This data is taken from Chapter 3. The section is on, EI, Three-Phase Laminations.

Core number	100EI-3P
Iron weight, W_{ife}	2.751 kilograms
Mean length turn, MLT	16.7 cm
Iron area, A_c	6.129 cm ²
Window area, W_a	29.0 cm ²
Area product, A_p	267cm ⁴
Core geometry, K_g	39 cm ⁵
Surface area, A_t	730 cm ²

Step No. 5 Calculate the number of primary turns, N_p , using Faraday's Law.

$$N_p = \frac{V_{p(\text{Line})}(10^4)}{4.44 B_{ac} A_c f}, \text{ [turns]}$$

$$N_p = \frac{208(10^4)}{4.44(1.4)(6.129)(60)}, \text{ [turns]}$$

$$N_p = 910, \text{ [turns]}$$

Step No. 6 Calculate the primary line current, $I_{p(Line)}$.

$$I_{p(Line)} = \frac{P_o}{3V_{p(Line)}\eta}, \text{ [amps]}$$

$$I_{p(Line)} = \frac{300}{3(208)(0.95)}, \text{ [amps]}$$

$$I_{p(Line)} = 0.506, \text{ [amps]}$$

Step No. 7 Calculate the primary phase current, $I_{p(phase)}$.

$$I_{p(Phase)} = \frac{I_{p(Line)}}{\sqrt{3}}, \text{ [amps]}$$

$$I_{p(Phase)} = \frac{0.506}{1.73}, \text{ [amps]}$$

$$I_{p(Phase)} = 0.292, \text{ [amps]}$$

Step No. 8 Calculate the primary bare wire area, $A_{wp(B)}$. The window area available for the primary is, $W_a / 4$. The primary window utilization, $K_{up} = 0.2$.

$$A_{wp(B)} = \left(\frac{K_{u(p)} W_a}{4N_p} \right), \text{ [cm}^2\text{]}$$

$$A_{wp(B)} = \left(\frac{(0.2)(29.0)}{4(910)} \right), \text{ [cm}^2\text{]}$$

$$A_{wp(B)} = 0.00159, \text{ [cm}^2\text{]}$$

Step No. 9 The selection of the wire would be from the Wire Table in Chapter 4.

AWG #25

$$A_{w(B)} = 0.001623, \text{ [cm}^2\text{]}$$

$$A_{w(Ins)} = 0.002002, \text{ [cm}^2\text{]}$$

$$\frac{\mu\Omega}{\text{cm}} = 1062$$

Step No. 10 Calculate the primary winding resistance. Use the MLT, from Step 4, and the micro-ohm, per centimeter, found in Step 9.

$$R_p = \text{MLT}(N_p) \left(\frac{\mu\Omega}{\text{cm}} \right) (10^{-6}), \text{ [ohms]}$$

$$R_p = (16.7)(910)(1062)(10^{-6}), \text{ [ohms]}$$

$$R_p = 16.1, \text{ [ohms]}$$

Step No. 11 Calculate the total primary copper loss, P_p .

$$P_p = 3(I_{p(\text{phase})})^2 R_p, \text{ [watts]}$$

$$P_p = 3(0.292)^2 (16.1), \text{ [watts]}$$

$$P_p = 4.12, \text{ [watts]}$$

Step No. 12 Calculate the secondary turns, N_s .

$$N_s = \frac{N_p V_s}{V_p} \left(1 + \frac{\alpha}{100}\right), \text{ [turns]}$$

$$V_s = (0.740)(V_o + 2V_d) = (0.740)(28 + 2) = 22.2$$

$$N_s = \frac{(910)(22.2)}{(208)} \left(1 + \frac{5}{100}\right), \text{ [turns]}$$

$$N_s = 102, \text{ [turns]}$$

Step No. 13 Calculate the secondary bare wire area, $A_{ws(B)}$.

$$A_{ws(B)} = \left(\frac{K_{u(s)} W_a}{4N_s}\right), \text{ [cm}^2\text{]}$$

$$A_{ws(B)} = \left(\frac{(0.2)(29.0)}{4(102)}\right), \text{ [cm}^2\text{]}$$

$$A_{ws(B)} = 0.0142, \text{ [cm}^2\text{]}$$

Step No. 14 The selection of the wire will be from the Wire Table in Chapter 4.

AWG #16

$$A_{w(B)} = 0.01307, \text{ [cm}^2\text{]}$$

$$A_{w(Ins)} = 0.01473, \text{ [cm}^2\text{]}$$

$$\frac{\mu\Omega}{\text{cm}} = 132$$

Step No. 15 Calculate the secondary winding resistance, R_s . Use the MLT, from Step 4, and the micro-ohm per centimeter, found in Step 14.

$$R_s = \text{MLT}(N_s) \left(\frac{\mu\Omega}{\text{cm}}\right) (10^{-6}), \text{ [ohms]}$$

$$R_s = (16.7)(102)(132)(10^{-6}), \text{ [ohms]}$$

$$R_s = 0.225, \text{ [ohms]}$$

Step No. 16 Calculate the secondary line current, $I_{s(line)}$.

$$I_{s(line)} = (0.471) I_o, \text{ [amps]}$$

$$I_{s(line)} = (0.471)(10), \text{ [amps]}$$

$$I_{s(line)} = 4.71, \text{ [amps]}$$

Step No. 17 Calculate the secondary phase current, $I_{s(phase)}$.

$$I_{s(phase)} = \frac{I_{s(line)}}{\sqrt{3}}, \text{ [amps]}$$

$$I_{s(phase)} = \frac{4.71}{1.73}, \text{ [amps]}$$

$$I_{s(phase)} = 2.72, \text{ [amps]}$$

Step No. 18 Calculate the total secondary copper loss, P_s .

$$P_s = 3(I_{s(phase)})^2 R_s, \text{ [watts]}$$

$$P_s = 3(2.72)^2 (0.225), \text{ [watts]}$$

$$P_s = 4.99, \text{ [watts]}$$

Step No. 19 Calculate the transformer regulation, α .

$$\alpha = \frac{P_{cu}}{P_o}(100), \text{ [%]}$$

$$P_{cu} = P_p + P_s, \text{ [watts]}$$

$$P_{cu} = 4.12 + 4.99, \text{ [watts]}$$

$$P_{cu} = 9.11, \text{ [watts]}$$

$$\alpha = \left(\frac{9.11}{300}\right)(100), \text{ [%]}$$

$$\alpha = 3.03, \text{ [%]}$$

Step No. 20 Calculate the watts per kilogram.

$$\text{Watts/kilogram} = K f^{(m)} B_{ac}^{(n)}$$

$$\text{Watts/kilogram} = 0.000557(60)^{(1.68)} (1.40)^{(1.86)}$$

$$\text{Watts/kilogram} = 1.01$$

Step No. 21 Calculate the core loss, P_{fe} . Core weight, W_{tfe} , is found in Step 4.

$$P_{fe} = \text{Watts/Kilogram}(W_{tfe}), \text{ [watts]}$$

$$P_{fe} = 1.01(2.751), \text{ [watts]}$$

$$P_{fe} = 2.78, \text{ [watts]}$$

Step No. 22 Summarize the total transformer losses, P_{Σ} .

$$P_{\Sigma} = P_p + P_s + P_{fe}, \text{ [watts]}$$

$$P_{\Sigma} = 4.12 + 4.99 + 2.78, \text{ [watts]}$$

$$P_{\Sigma} = 11.89, \text{ [watts]}$$

Step No. 23 Calculate the transformer efficiency, η .

$$\eta = \frac{P_o}{P_o + P_{\Sigma}}(100), \text{ [%]}$$

$$\eta = \frac{300}{300 + 11.89}(100), \text{ [%]}$$

$$\eta = 96.2, \text{ [%]}$$

Step No. 24 Calculate the watts per unit area, ψ . The surface area, A_t , is found in Step 4.

$$\psi = \frac{P_{\Sigma}}{A_t}, \text{ [watts per cm}^2\text{]}$$

$$\psi = \frac{(11.89)}{(730)}, \text{ [watts per cm}^2\text{]}$$

$$\psi = 0.0163, \text{ [watts per cm}^2\text{]}$$

Step No. 25 Calculate the temperature rise, T_r . The watts per unit area ψ is found in Step 24.

$$T_r = 450(\psi)^{0.826}, \text{ [}^{\circ}\text{C]}$$

$$T_r = 450(0.0163)^{0.826}, \text{ [}^{\circ}\text{C]}$$

$$T_r = 15, \text{ [}^{\circ}\text{C]}$$

Step No. 26 Calculate the total window utilization, K_u . The window area is found in Step 4.

$$K_u = K_{up} + K_{us}$$

$$K_u = \frac{4N_p A_{wp(B)(25)}}{W_a} + \frac{4N_s A_{ws(B)(16)}}{W_a}$$

$$K_u = \frac{4(910)(0.001623)}{29} + \frac{4(102)(0.01307)}{29}$$

$$K_u = (0.204) + (0.184)$$

$$K_u = 0.388$$

Chapter 13

Flyback Converter, Transformer Design

The author would like to thank **Dr. V. Vorperian**, Senior Engineer, Power and Sensor Electronics Group, Jet Propulsion Laboratory (JPL), **Richard Ozenbaugh** of Linear Magnetics and **Kit Sum**, Senior Consultant, for their help with the Flyback design equations.

Table of Contents

1. Introduction	
2. Energy Transfer	
3. Discontinuous Current Mode	
4. Continuous Current Mode	
5. Continuous and Discontinuous Boundary	
6. The Buck Converter	
7. Discontinuous Current Buck Converter Design Equations	
8. Continuous Current Buck Converter Design Equations	
9. The Boost Converter	
10. Discontinuous Current Boost Converter Design Equations	
11. Continuous Current Boost Converter Design Equations	
12. The Inverting Buck-Boost Converter	
13. Discontinuous Current Inverting, Buck-Boost Design Equations	
14. Continuous Current Inverting, Buck-Boost Design Equations	
15. The Isolated Buck-Boost Converter	
16. Discontinuous Current Isolated, Buck-Boost Design Equations	
17. Continuous Current Isolated, Buck-Boost Design Equations	
18. Design Example, Buck-Boost Isolated Converter Discontinuous Current	
19. Design Example, Boost Converter, Discontinuous Current	
20. Designing Boost Inductors for Power Factor Correction (PFC).....	
21. Standard Boost Flyback Converter	
22. Boost PFC Converter	
23. Design Example, (PFC) Boost Converter, Continuous Current	
24. References	

Introduction

The principle behind Flyback converters is based on the storage of energy in the inductor during the charging, or the “on period,” t_{on} , and the discharge of the energy to the load during the “off period,” t_{off} . There are four basic types that are the most common, energy storage, inductor type converter circuits.

1. Step down, or buck converter.
2. Step up, or boost converter.
3. Inverting, buck-boost converter.
4. Isolated, buck-boost converter.

Energy Transfer

Two distinct modes of operation are possible for the Flyback switching converters, shown in Figure 13-1:

Discontinuous Mode All energy stored in the inductor is transferred to an output capacitor and load circuit before another charging period occurs. This topology results in a smaller inductor size, but puts a larger stress on the capacitor and switching device.

Continuous Mode Energy stored in the inductor is not completely transferred to the output capacitor and load circuit before another charging period occurs.

The total period is:

$$T = \frac{1}{f} \quad [13-1]$$

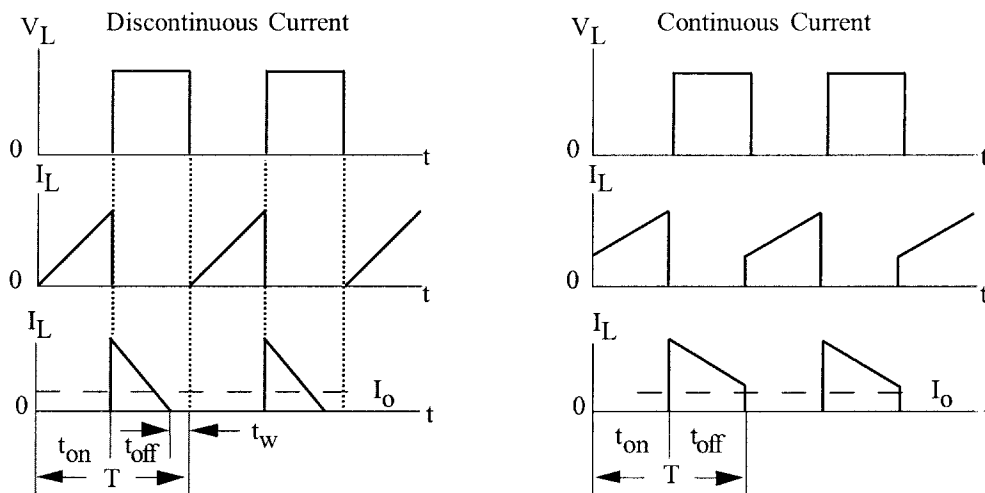


Figure 13-1. Comparing Discontinuous and Continuous Current Waveforms.

Discontinuous Current Mode

In the Discontinuous Mode, a smaller inductance is required, but the penalty results in higher peak currents in the switching transistor. As a consequence, the winding losses are increased because of the higher rms values, due to the higher peak currents. This also results, in a higher ripple current and ripple voltage in the input and output capacitor, and gives added stress to the switching transistor. The advantage of this circuit, other than having a smaller inductor, is that when the switching device is turned on, the initial current is zero. This means the output diode has completely recovered, and the switching device does not momentarily turn on into a short. This diode recovery reduces the EMI radiation. The discontinuous mode converter does not exhibit the right half plane zero. Without the right half plane zero, the loop is easy to stabilize.

Continuous Current Mode

In the Continuous Mode, a larger inductor is required; this results in a lower peak current at the end of the cycle than in a discontinuous system of equivalent output power. The Continuous Mode demands a high current flowing through the switch during turn-on, and can lead to high switch dissipation. The continuous mode converter does exhibit the right half-plane zero. With the right half-plane zero, the loop becomes very difficult to stabilize for a wide range of input voltage. The relationship between the B-H loops for continuous and discontinuous operation is shown in Figure 13-2.

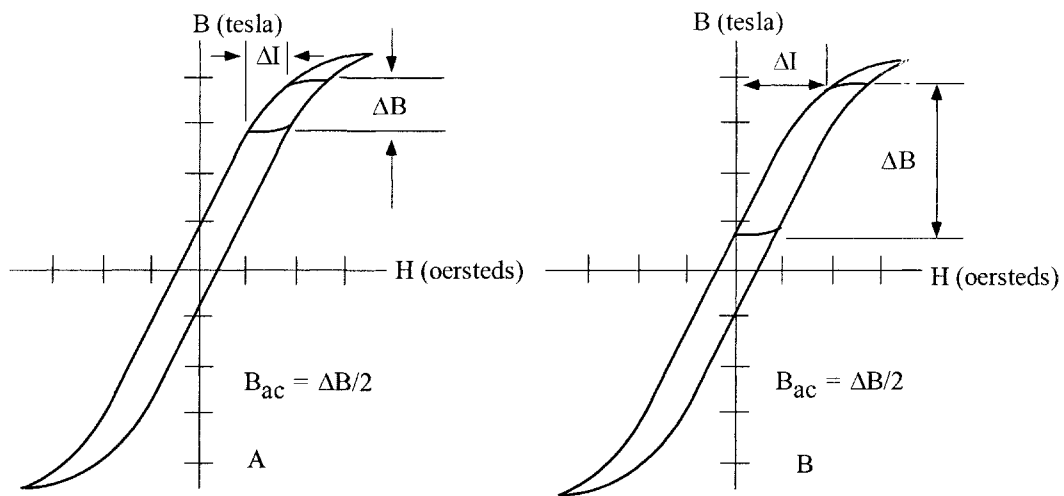


Figure 13-2. Continuous (A) and Discontinuous (B), B-H Loops, Showing ΔB and ΔI .

Continuous and Discontinuous Boundary

When the load current increases, the control circuit causes the transistor to increase the “on time,” t_{on} . The peak current in the inductor will increase, resulting in a steady reduction in the dwell time, t_w . When the load current increases to a critical level, t_w becomes zero, and the discontinuous boundary is reached. If the

load current is further increased, the inductor current will no longer discharge to zero on every cycle, and continuous current operation results.

The Buck Converter

The Buck Converter is shown in Figure 13-3. The output voltage of this converter is always less than the input voltage. In the buck circuit, the transistor switch, Q1, is placed in series with the dc input voltage. The transistor, Q1, interrupts the dc input voltage, providing a variable-width pulse, (duty ratio), to a simple averaging, LC, filter. When the transistor switch, Q1, is closed, the dc input voltage is applied across the output filter inductor, L1, and the current flows through the inductor to the load. When the switch is open, the energy, stored in the field of the inductor, L1, maintains the current through the load. The discontinuous voltage and current waveforms are shown in Figure 13-4, and the continuous waveforms in Figure 13-5.

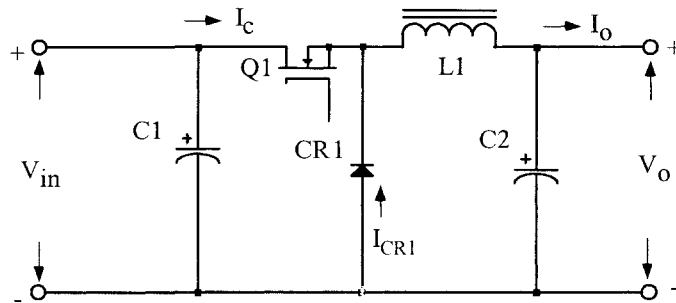


Figure 13-3. Schematic of a Buck Switching Converter.

Discontinuous Current Buck Converter Design Equations

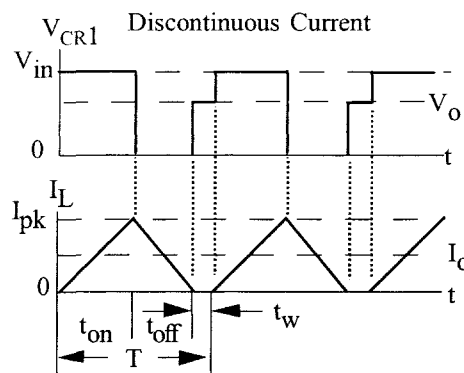


Figure 13-4. Discontinuous, Current Buck Converter Waveforms.

Inductance, L:

$$L_{\max} = \frac{(V_o + V_d)T(1 - D_{\max} - D_w)}{2I_{o(\max)}}, \quad [\text{henrys}] \quad [13-2]$$

Maximum duty ratio:

$$D_{(max)} = \frac{V_o (1 - D_w)}{(\eta V_{in(min)})} \quad [13-3]$$

Maximum on time:

$$t_{on(max)} = T D_{max} \quad [13-4]$$

Maximum off time:

$$t_{off(max)} = T(1 - D_{min}) \quad [13-5]$$

The inductor peak current, $I_{(pk)}$:

$$I_{(pk)} = \frac{2I_{o(max)}}{(1 - D_w)} \quad [13-6]$$

Continuous Current Buck Converter Design Equations

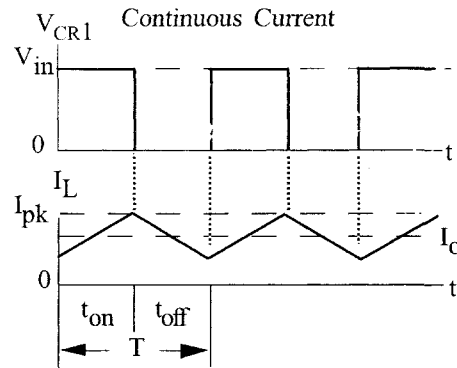


Figure 13-5. Continuous Current Buck Converter Waveforms.

Inductance, L:

$$L = \frac{V_o T (1 - D_{min})}{2I_{o(min)}}, \quad [\text{henrys}] \quad [13-7]$$

Maximum duty ratio:

$$D_{(max)} = \frac{V_o}{(\eta V_{in(min)})} \quad [13-8]$$

Minimum duty ratio:

$$D_{(\min)} = \frac{V_o}{(\eta V_{in(\max)})} \quad [13-9]$$

Maximum on time:

$$t_{on(\max)} = TD_{\max} \quad [13-10]$$

Maximum off time:

$$t_{off(\max)} = T(1 - D_{\max}) \quad [13-11]$$

The inductor delta current, ΔI :

$$\Delta I = \frac{(TV_{in(\max)}D_{(\min)})(1 - D_{(\min)})}{L} \quad [13-12]$$

The inductor peak current, $I_{(pk)}$:

$$I_{(pk)} = I_{o(\max)} + \frac{\Delta I}{2} \quad [13-13]$$

The Boost Converter

The Boost Converter is shown in Figure 13-6. The output voltage of this converter is always greater than the input voltage. The boost converter stores energy in the inductor, L1, and then, delivers the stored energy along with the energy from the dc source to the load. When the transistor switch, Q1, is closed, current flows through inductor, L1, and the transistor switch, Q1, charging inductor, L1, but does not deliver any current to the load. When the switch is open, the voltage across the load equals the dc input voltage plus the energy stored in inductor, L1. The energy is stored in, L1, then discharges, delivering current to the load. The discontinuous voltage and current waveforms are shown in Figure 13-7, and the continuous waveforms in Figure 13-8.

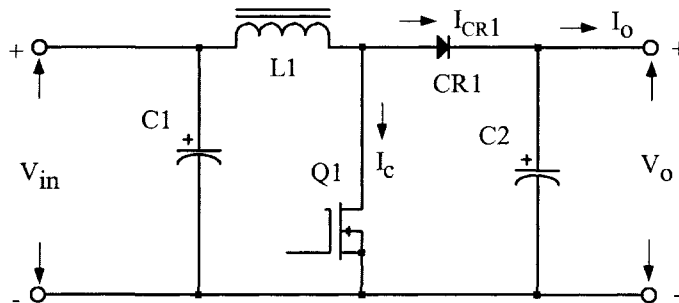


Figure 13-6. Schematic of a Boost Switching Converter.

Discontinuous Current Boost Converter Design Equations

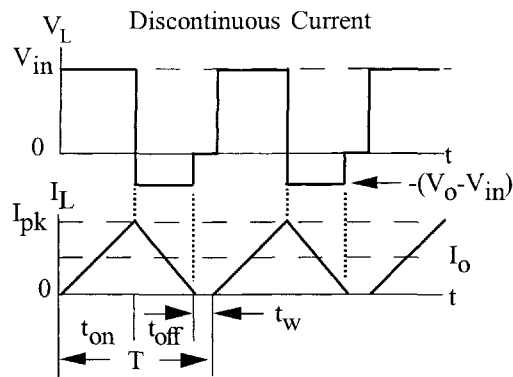


Figure 13-7. Discontinuous, Current Boost Converter Waveforms.

Inductance, L:

$$L_{\max} = \frac{(V_o + V_d) T D_{(\max)} (1 - D_{\max} - D_w)^2}{2I_{o(\max)}}, \text{ [henrys]} \quad [13-14]$$

Maximum duty ratio:

$$D_{(\max)} = (1 - D_w) \left(\frac{V_o - V_{in(\min)} + V_d}{V_o} \right) \quad [13-15]$$

Minimum duty ratio:

$$D_{(\min)} = (1 - D_w) \left(\frac{V_o - V_{in(\max)} + V_d}{V_o} \right) \quad [13-16]$$

Maximum on time:

$$t_{on(\max)} = T D_{\max} \quad [13-17]$$

Maximum off time:

$$t_{off(\max)} = T(1 - D_{\min}) \quad [13-18]$$

The inductor peak current, $I_{(pk)}$:

$$I_{(pk)} = \frac{2P_{o(\max)}}{\eta(V_o D_{(\min)})} \quad [13-19]$$

Continuous Current Boost Converter Design Equations

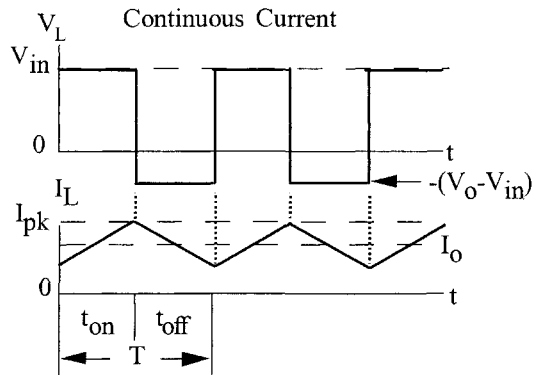


Figure 13-8. Continuous, Current Boost Converter Waveforms.

Inductance, L:

$$L = \frac{(V_o + V_d) T D_{(\min)} (1 - D_{\min})^2}{2 I_{o(\min)}}, \quad [\text{henrys}] \quad [13-20]$$

Maximum duty ratio:

$$D_{(\max)} = 1 - \left(\frac{V_{in(\min)} \eta}{V_o} \right) \quad [13-21]$$

Minimum duty ratio:

$$D_{(\min)} = 1 - \left(\frac{V_{in(\max)} \eta}{V_o} \right) \quad [13-22]$$

Maximum on time:

$$t_{on(\max)} = T D_{\max} \quad [13-23]$$

Maximum off time:

$$t_{off(\max)} = T(1 - D_{\min}) \quad [13-24]$$

The inductor delta current, ΔI :

$$\Delta I = \frac{(T V_{in(\max)} D_{(\min)})}{L} \quad [13-25]$$

The inductor peak current, $I_{(pk)}$:

$$I_{(pk)} = \left(\frac{I_{o(max)}}{1 - D_{(max)}} \right) + \left(\frac{\Delta I}{2} \right) \quad [13-26]$$

The Inverting Buck-Boost Converter

The inverting buck-boost converter is shown in Figure 13-9. It is a variation of the boost circuit. The inverting converter delivers only the energy stored by the inductor, L1, to the load. The output voltage of the inverting converter can be greater, or less than, the input voltage. When the transistor switch, Q1, is closed, the inductor is storing energy, but no current is delivered to the load because diode, CR1, is back-biased. When the transistor switch, Q1, is open, the blocking diode is forward-biased and the energy stored in inductor, L1, is transferred to the load. The discontinuous voltage and current waveforms are shown in Figure 13-10 and the continuous waveforms in Figure 13-11.

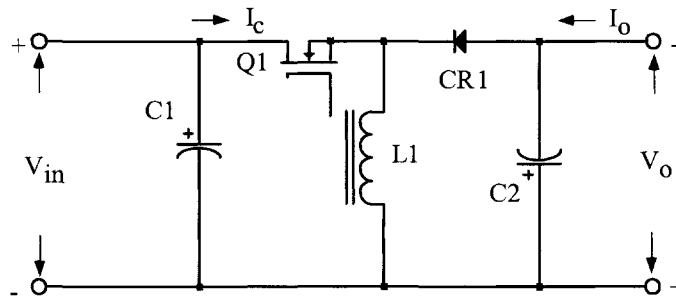


Figure 13-9. Schematic of an Inverting Buck-Boost Switching Converter.

Discontinuous Current Inverting, Buck-Boost Design Equations

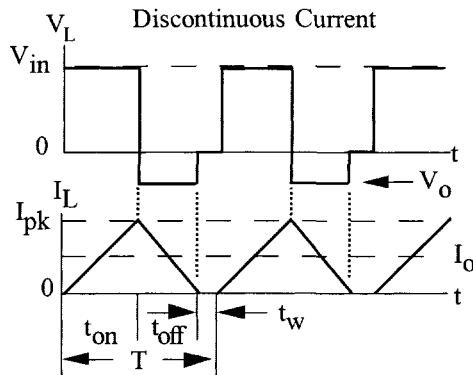


Figure 13-10. Discontinuous, Current Inverting, Buck-Boost Converter Waveforms.

Inductance, L:

$$L_{\max} = \frac{(V_o + V_d)T(1 - D_{\max} - D_w)^2}{2I_{o(\max)}}, \text{ [henrys] [13-27]}$$

Maximum duty ratio:

$$D_{\max} = \frac{(V_o + V_d)(1 - D_w)}{(V_o + V_d + V_{in(\min)})} \text{ [13-28]}$$

Minimum duty ratio:

$$D_{\min} = \frac{(V_o + V_d)(1 - D_w)}{V_o + V_d + V_{in(\max)}} \text{ [13-29]}$$

Maximum on time:

$$t_{on(\max)} = TD_{\max} \text{ [13-30]}$$

Maximum off time:

$$t_{off(\max)} = T(1 - D_{\min} - D_w) \text{ [13-31]}$$

The inductor peak current, $I_{(pk)}$:

$$I_{(pk)} = \frac{2P_{o(\max)}}{(D_{\max})V_{in(\min)}\eta} \text{ [13-32]}$$

Continuous Current Inverting, Buck-Boost Design Equations

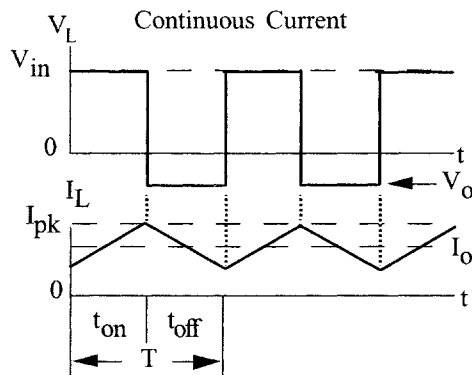


Figure 13-11. Continuous, Current Inverting, Buck-Boost Converter Waveforms.

Inductance, L:

$$L = \frac{(V_o + V_d)T(1 - D_{\min})^2}{2I_{o(\min)}}, \text{ [henrys]} \quad [13-33]$$

Maximum duty ratio:

$$D_{\max} = \frac{V_o}{V_o + (\eta V_{in(\min)})} \quad [13-34]$$

Minimum duty ratio:

$$D_{\min} = \frac{V_o}{V_o + (\eta V_{in(\max)})} \quad [13-35]$$

Maximum on time:

$$t_{on(\max)} = TD_{\max} \quad [13-36]$$

Maximum off time:

$$t_{off(\max)} = T(1 - D_{\min}) \quad [13-37]$$

The inductor delta current, ΔI :

$$\Delta I = \frac{(TV_{in(\max)}D_{(\min)})}{L} \quad [13-38]$$

The inductor peak current, $I_{(pk)}$:

$$I_{(pk)} = \left(\frac{I_{o(\max)}}{1 - D_{\max}} \right) + \left(\frac{\Delta I}{2} \right) \quad [13-39]$$

The Isolated Buck-Boost Converter

The Isolated Buck-Boost Converter is shown in Figure 13-12. This converter can provide line isolation, and also has the capability of multiple outputs, which require only a diode and a capacitor; the filter inductor is built-in. The isolated buck-boost converter is quite popular in low power applications because of simplicity and low cost. This converter does not lend itself to the VDE specification because of the required voltage insulation between primary and secondary. Care must be taken because this leakage inductance could generate high voltage spikes on the primary. The discontinuous voltage and current waveforms are shown in Figure 13-13, and the continuous waveforms in Figure 13-14.

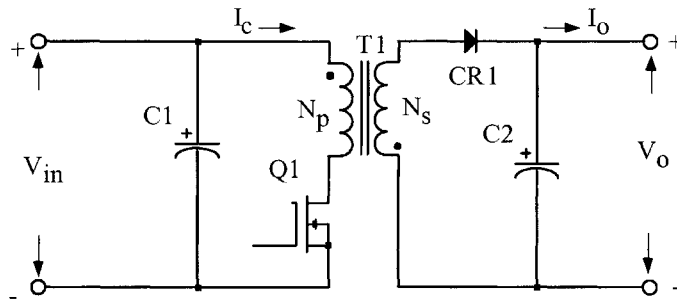


Figure 13-12. Schematic of an Isolated, Buck-Boost Switching Converter.

Discontinuous Current Isolated, Buck-Boost Design Equations

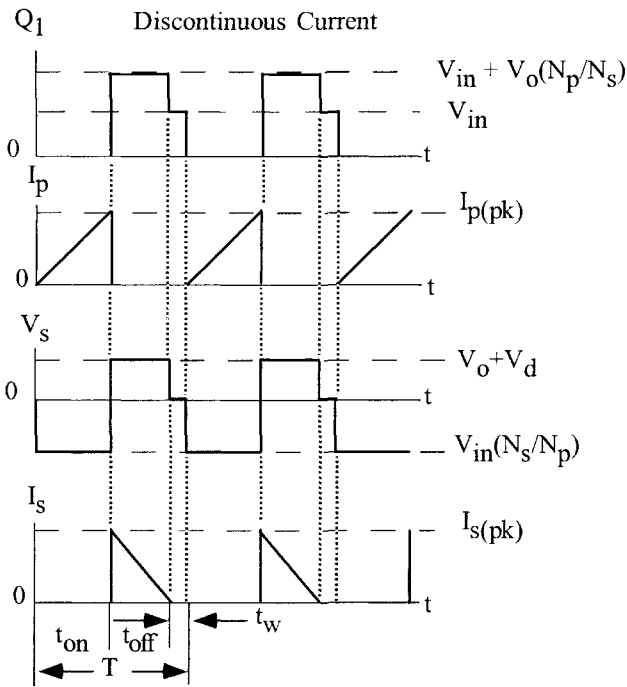


Figure 13-13. Discontinuous Current, Isolated, Buck-Boost Converter Waveforms.

Primary inductance, $L_{p(max)}$:

$$L_{p(max)} = \frac{(R_{in(equiv)})T(D_{max})^2}{2}, \text{ [henrys] [13-40]}$$

Maximum on time:

$$t_{on(max)} = TD_{max} \text{ [13-41]}$$

Maximum off time:

$$t_{off(max)} = T(1 - D_{min} - D_w) \quad [13-42]$$

Total output power:

$$P_{o(max)} = I_{o1(max)}(V_{o1} + V_d) + I_{o2(max)}(V_{o2} + V_d) + \dots \quad [13-43]$$

Maximum input power:

$$P_{in(max)} = \frac{P_{o(max)}}{\eta} \quad [13-44]$$

Equivalent input resistance:

$$R_{in(equiv)} = \frac{(V_{in(min)})^2}{P_{in(max)}} \quad [13-45]$$

The primary peak current, $I_{p(pk)}$:

$$I_{p(pk)} = \frac{2P_{in(max)}T}{T_{on(max)}V_{in(min)}} \quad [13-46]$$

Continuous Current Isolated, Buck-Boost Design Equations

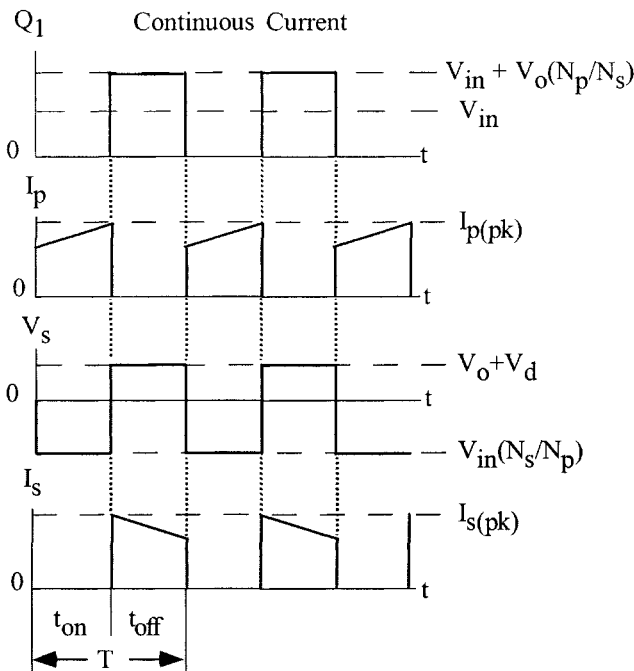


Figure 13-14. Continuous Current, Buck-Boost Converter Waveforms.

Inductance, L:

$$L = \frac{(V_{in(max)} D_{(min)})^2 T}{2P_{in(min)}}, \quad [\text{henrys}] \quad [13-47]$$

Minimum duty ratio:

$$D_{min} = \left(\frac{V_{in(min)}}{V_{in(max)}} \right) D_{(max)} \quad [13-48]$$

Maximum on time:

$$t_{on(max)} = T D_{max} \quad [13-49]$$

Maximum off time:

$$t_{off(max)} = T(1 - D_{min}) \quad [13-50]$$

Minimum output power:

$$P_{o(min)} = I_{o1(min)}(V_{o1} + V_d) + I_{o2(min)}(V_{o2} + V_d) + \dots \quad [13-51]$$

Minimum input power:

$$P_{in(min)} = \frac{P_{o(min)}}{\eta} \quad [13-52]$$

The inductor delta current, ΔI :

$$\Delta I = \frac{(TV_{in(min)} D_{(max)})}{L} \quad [13-53]$$

The inductor peak current, $I_{(pk)}$:

$$I_{(pk)} = \left(\frac{I_{in(max)}}{D_{max}} \right) + \left(\frac{\Delta I}{2} \right) \quad [13-54]$$

Design Example, Buck-Boost Isolated Converter Discontinuous Current

1. Input voltage nominal, V_{in} = 28 volts
2. Input voltage minimum, $V_{in(min)}$ = 24 volts
3. Input voltage maximum, $V_{in(max)}$ = 32 volts
4. Output voltage, V_{o1} = 5 volts
5. Output current, I_{o1} = 2 amps
6. Output voltage, V_{o2} = 12 volts
7. Output current, I_{o2} = 0.5 amps
8. *Window utilization, K_u = 0.29
9. Frequency, f = 100 kHz
10. Converter efficiency, η = 90%
11. Maximum duty ratio, $D_{(max)}$ = 0.5
12. Dwell time duty ratio, $D_{(w)}$ = 0.1
13. Regulation, α = 1.0%
14. Operating flux density, B_m = 0.25 tesla
15. Diode voltage, V_d = 1.0 volt

*When operating at high frequencies, the engineer has to review the window utilization factor, K_u . When using a small bobbin ferrite, the ratio of the bobbin winding area to the core window area is only about 0.6. Operating at 100kHz and having to use a #26 wire, because of the skin effect, the ratio of the bare copper area is 0.78. Therefore, the overall window utilization, K_u , is reduced. The core geometries, K_g , in Chapter 3 have been calculated with a window utilization, K_u , of 0.4. To return the design back to the norm, the core geometry, K_g is to be multiplied by 1.35, and then, the current density, J , is calculated, using a window utilization factor of 0.29. See Chapter 4.

Skin Effect

The skin effect on an inductor is the same as a transformer. In the normal dc inductor, the ac current (ac flux), is much lower, and does not require the use of the same, maximum wire size. This is not the case in the discontinuous, current type, flyback converter, where all of the flux is ac and without dc. In the discontinuous, flyback design, the skin effect has to be treated just like a high frequency transformer.

There are times when the larger wire is just too difficult to wind. Large wire is not only hard to handle, but it does not give the proper lay. It is easier to wind with bi-filar or quad-filar wire, with the equivalent cross-section.

Select a wire so that the relationship between the ac resistance and the dc resistance is 1:

$$\frac{R_{ac}}{R_{dc}} = 1 \quad [13-55]$$

The skin depth in centimeters is:

$$\varepsilon = \frac{6.62}{\sqrt{f}}, \text{ [cm]}$$

$$\varepsilon = \frac{6.62}{\sqrt{100,000}}, \text{ [cm]}$$

$$\varepsilon = 0.0209, \text{ [cm]}$$

Then, the wire diameter is:

$$\text{Wire Diameter} = 2(\varepsilon), \text{ [cm]}$$

$$\text{Wire Diameter} = 2(0.0209), \text{ [cm]}$$

$$\text{Wire Diameter} = 0.0418, \text{ [cm]}$$

Then, the bare wire area A_w is:

$$A_w = \frac{\pi D^2}{4}, \text{ [cm}^2\text{]}$$

$$A_w = \frac{(3.1416)(0.0418)^2}{4}, \text{ [cm}^2\text{]}$$

$$A_w = 0.00137, \text{ [cm}^2\text{]}$$

From the Wire Table in Chapter 4, Number 26 has a bare wire area of 0.00128 centimeters. This will be the minimum wire size used in this design. If the design requires more wire area to meet the specification, then, the design will use a multifilar of #26. Listed Below are #27 and #28, just in case #26 requires too much rounding off.

Wire AWG	Bare Area	Area Ins.	Bare/Ins.	$\mu\Omega/\text{cm}$
#26	0.001280	0.001603	0.798	1345
#27	0.001021	0.001313	0.778	1687
#28	0.0008046	0.0010515	0.765	2142

Step No. 1 Calculate the total period, T.

$$T = \frac{1}{f} \text{ [seconds]}$$

$$T = \frac{1}{100000} \text{ [seconds]}$$

$$T = 10 \text{ [}\mu\text{sec]}$$

Step No. 2 Calculate the maximum transistor on time, t_{on} .

$$t_{on} = TD_{\max} \text{ [}\mu\text{sec]}$$

$$t_{on} = (10 \times 10^{-6})(0.5) \text{ [}\mu\text{sec]}$$

$$t_{on} = 5.0 \text{ [}\mu\text{sec]}$$

Step No. 3 Calculate the secondary load power, P_{o1} .

$$P_{o1} = I_{o1}(V_{o1} + V_d) \quad [\text{watts}]$$

$$P_{o1} = (2)(5+1) \quad [\text{watts}]$$

$$P_{o1} = 12 \quad [\text{watts}]$$

Step No. 4 Calculate the secondary load power, P_{o2} .

$$P_{o2} = I_{o2}(V_{o2} + V_d) \quad [\text{watts}]$$

$$P_{o2} = (0.5)(12+1) \quad [\text{watts}]$$

$$P_{o2} = 6.5 \quad [\text{watts}]$$

Step No. 5 Calculate the total secondary load power, $P_{o(\max)}$.

$$P_{o(\max)} = P_{o1} + P_{o2} \quad [\text{watts}]$$

$$P_{o(\max)} = 12 + 6.5 \quad [\text{watts}]$$

$$P_{o(\max)} = 18.5 \quad [\text{watts}]$$

Step No. 6 Calculate the maximum input current, $I_{in(\max)}$.

$$I_{in(\max)} = \frac{P_{o(\max)}}{V_{in(\min)}\eta} \quad [\text{amps}]$$

$$I_{in(\max)} = \frac{18.5}{(24)(0.9)} \quad [\text{amps}]$$

$$I_{in(\max)} = 0.856 \quad [\text{amps}]$$

Step No. 7 Calculate the primary peak current, $I_{p(pk)}$.

$$I_{p(pk)} = \frac{2 P_{o(\max)} T}{\eta V_{in(\min)} t_{on(\max)}} \quad [\text{amps peak}]$$

$$I_{p(pk)} = \frac{2(18.5)(10 \times 10^{-6})}{(0.9)(24)(5 \times 10^{-6})} \quad [\text{amps peak}]$$

$$I_{p(pk)} = 3.43 \quad [\text{amps peak}]$$

Step No. 8 Calculate the primary rms current, $I_{p(rms)}$.

$$I_{p(rms)} = I_{p(pk)} \sqrt{\frac{t_{on}}{3T}} \quad [\text{amps}]$$

$$I_{p(rms)} = 3.43 \sqrt{\frac{5}{3(10)}} \quad [\text{amps}]$$

$$I_{p(rms)} = 1.40 \quad [\text{amps}]$$

Step No. 9 Calculate the maximum input power, $P_{in(max)}$.

$$P_{in(max)} = \frac{P_o(max)}{\eta} \quad [\text{watts}]$$

$$P_{in(max)} = \frac{18.5}{0.9} \quad [\text{watts}]$$

$$P_{in(max)} = 20.6 \quad [\text{watts}]$$

Step No. 10 Calculate the equivalent input resistance, $R_{in(equiv)}$.

$$R_{in(equiv)} = \frac{(V_{in(min)})^2}{P_{in(max)}}, \quad [\text{ohms}]$$

$$R_{in(equiv)} = \frac{(24)^2}{20.6}, \quad [\text{ohms}]$$

$$R_{in(equiv)} = 28, \quad [\text{ohms}]$$

Step No. 11 Calculate the required primary inductance, L .

$$L = \frac{(R_{in(equiv)})T(D_{max})^2}{2} \quad [\text{henry}]$$

$$L = \frac{(28)(10 \times 10^{-6})(0.5)^2}{2} \quad [\text{henry}]$$

$$L = 35 \quad [\mu\text{h}]$$

Step No. 12 Calculate the energy-handling capability in watt-seconds, w-s.

$$\text{Energy} = \frac{L I_{p(pk)}^2}{2} \quad [\text{w-s}]$$

$$\text{Energy} = \frac{(35 \times 10^{-6})(3.43)^2}{2} \quad [\text{w-s}]$$

$$\text{Energy} = 0.000206 \quad [\text{w-s}]$$

Step No. 13 Calculate the electrical conditions, K_e .

$$K_e = 0.145 P_o B_m^2 \times 10^{-4}$$

$$K_e = (0.145)(18.5)(0.25)^2 \times 10^{-4}$$

$$K_e = 0.0000168$$

Step No. 14 Calculate the core geometry, K_g . See the design specification, window utilization factor, K_u .

$$K_g = \frac{(\text{Energy})^2}{K_e \alpha} \quad [\text{cm}^5]$$

$$K_g = \frac{(0.000206)^2}{(16.8(10^{-6}))(1.0)} \quad [\text{cm}^5]$$

$$K_g = 0.00253 \quad [\text{cm}^5]$$

$$K_g = 0.00253(1.35), \quad [\text{cm}^5]$$

$$K_g = 0.00342, \quad [\text{cm}^5]$$

Step No. 15 Select, from Chapter 3, an EFD core comparable in core geometry, K_g .

Core number.....	EFD-20
Manufacturer.....	Philips
Material	3C85
Magnetic path length, MPL.....	= 4.7 cm
Core weight, W_{tfe}	= 7.0 grams
Copper weight, W_{tcu}	= 6.8 grams
Mean length turn, MLT.....	= 3.80 cm
Iron area, A_c	= 0.31 cm^2
Window Area, W_a	= 0.501 cm^2
Area Product, A_p	= 0.155 cm^4
Core geometry, K_g	= 0.00506 cm^5
Surface area, A_t	= 13.3 cm^2
Core Permeability	= 2500
Winding Length, G	= 1.54 cm

Step No. 16 Calculate the current density, J , using a window utilization, $K_u = 0.29$.

$$J = \frac{2(\text{Energy})(10^4)}{B_m A_p K_u}, \quad [\text{amps}/\text{cm}^2]$$

$$J = \frac{2(0.000206)(10^4)}{(0.25)(0.155)(0.29)}, \quad [\text{amps}/\text{cm}^2]$$

$$J = 367, \quad [\text{amps}/\text{cm}^2]$$

Step No. 17 Calculate the primary wire area, $A_{pw(B)}$.

$$A_{pw(B)} = \frac{I_{prms}}{J} \quad [\text{cm}^2]$$

$$A_{pw(B)} = \frac{1.4}{367} \quad [\text{cm}^2]$$

$$A_{pw(B)} = 0.00381 \quad [\text{cm}^2]$$

Step No. 18 Calculate the required number of primary strands, S_{np} .

$$S_{np} = \frac{A_{wp(B)}}{\#26 \text{ (bare area)}}$$

$$S_{np} = \frac{(0.00381)}{(0.00128)}$$

$$S_{np} = 2.97 \text{ use } 3$$

Step No. 19 Calculate the number of primary turns, N_p . Half of the available window is primary, $W_{ap}/2$. Using the number of strands, S_{np} , and the area for #26.

$$W_{ap} = \frac{W_a}{2} = \frac{0.501}{2} = 0.250, \quad [\text{cm}^2]$$

$$N_p = \frac{K_u W_{ap}}{3(\#26 \text{ (Bare Area)})}, \quad [\text{turns}]$$

$$N_p = \frac{(0.29)(0.25)}{3(0.00128)}, \quad [\text{turns}]$$

$$N_p = 18.9 \text{ use } 19, \quad [\text{turns}]$$

Step No. 20 Calculate the required gap, l_g .

$$l_g = \frac{0.4\pi N^2 A_c (10^{-8})}{L} - \left(\frac{\text{MPL}}{\mu_m} \right), \quad [\text{cm}]$$

$$l_g = \frac{(1.26)(19)^2 (0.31)(10^{-8})}{(0.000035)} - \left(\frac{4.7}{2500} \right), \quad [\text{cm}]$$

$$l_g = 0.0384, \quad [\text{cm}]$$

Step No. 21 Calculate the equivalent gap in mils.

$$\text{mils} = \text{cm}(393.7)$$

$$\text{mils} = (0.0384)(393.7)$$

$$\text{mils} = 15$$

Step No. 22 Calculate the fringing flux factor, F.

$$F = 1 + \frac{l_g}{\sqrt{A_c}} \ln \left(\frac{2G}{l_g} \right)$$

$$F = 1 + \frac{(0.0384)}{\sqrt{0.31}} \ln \left(\frac{2(1.54)}{0.0384} \right)$$

$$F = 1.30$$

Step No. 23 Calculate the new number of turns, N_{np} , by inserting the fringing flux, F.

$$N_{np} = \sqrt{\frac{l_g L}{0.4\pi A_c F (10^{-8})}}, \quad [\text{turns}]$$

$$N_{np} = \sqrt{\frac{(0.0384)(0.000035)}{(1.26)(0.31)(1.3)(10^{-8})}}, \quad [\text{turns}]$$

$$N_{np} = 16, \quad [\text{turns}]$$

Step No. 24 Calculate the peak flux density, B_{pk} .

$$B_{pk} = \frac{0.4\pi N_{np} F (I_{p(pk)}) (10^{-4})}{l_g + \left(\frac{\text{MPL}}{\mu_m} \right)}, \quad [\text{tesla}]$$

$$B_{pk} = \frac{(1.26)(16)(1.3)(3.43)(10^{-4})}{(0.0384) + \left(\frac{4.7}{2500} \right)}, \quad [\text{tesla}]$$

$$B_{pk} = 0.223, \quad [\text{tesla}]$$

Step No. 25 Calculate the primary, the new $\mu\Omega/\text{cm}$.

$$(\text{new}) \mu\Omega / \text{cm} = \frac{\mu\Omega / \text{cm}}{S_{np}}$$

$$(\text{new}) \mu\Omega / \text{cm} = \frac{1345}{3}$$

$$(\text{new}) \mu\Omega / \text{cm} = 448$$

Step No. 26 Calculate the primary winding resistance, R_p .

$$R_p = MLT (N_{np}) \left(\frac{\mu\Omega}{\text{cm}} \right) \times 10^{-6} \quad [\text{ohms}]$$

$$R_p = (3.8)(16)(448) \times 10^{-6} \quad [\text{ohms}]$$

$$R_p = 0.0272 \quad [\text{ohms}]$$

Step No. 27 Calculate the primary copper loss, P_p .

$$P_p = I_p^2 R_p \quad [\text{watts}]$$

$$P_p = (1.4)^2 (.0272) \quad [\text{watts}]$$

$$P_p = 0.0533 \quad [\text{watts}]$$

Step No. 28 Calculate the secondary turns, N_{s1} .

$$N_{s1} = \frac{N_{np} (V_{o1} + V_d)(1 - D_{\max} - D_w)}{(V_p D_{\max})} \quad [\text{turns}]$$

$$N_{s1} = \frac{16(5+1)(1-0.5-0.1)}{(24)(0.5)} \quad [\text{turns}]$$

$$N_{s1} = 3.2 \text{ use } 3 \quad [\text{turns}]$$

Step No. 29 Calculate the secondary peak current, $I_{s1(pk)}$.

$$I_{s1(pk)} = \frac{2I_{o1}}{(1 - D_{\max} - D_w)} \quad [\text{amps}]$$

$$I_{s1(pk)} = \frac{2(2.0)}{(1-0.5-0.1)} \quad [\text{amps}]$$

$$I_{s1(pk)} = 10 \quad [\text{amps}]$$

Step No. 30 Calculate the secondary rms current, $I_{s(rms)}$.

$$I_{s1(rms)} = I_{s1(pk)} \sqrt{\frac{(1 - D_{\max} - D_w)}{3}} \quad [\text{amps}]$$

$$I_{s1(rms)} = (10) \sqrt{\frac{(1-0.5-0.1)}{3}} \quad [\text{amps}]$$

$$I_{s1(rms)} = 3.65 \quad [\text{amps}]$$

Step No. 31 Calculate the secondary wire area, $A_{sw1(B)}$.

$$A_{sw1(B)} = \frac{I_{s1(rms)}}{J} \quad [\text{cm}^2]$$

$$A_{sw1(B)} = \frac{3.65}{367} \quad [\text{cm}^2]$$

$$A_{sw1(B)} = 0.00995 \quad [\text{cm}^2]$$

Step No. 32 Calculate the required number of secondary strands, S_{ns1} .

$$S_{ns1} = \frac{A_{swl(B)}}{\text{wire}_A}$$

$$S_{ns1} = \frac{(0.00995)}{(0.00128)}$$

$$S_{ns1} = 7.8 \text{ use } 8$$

Step No. 33 Calculate the, S_1 secondary, $\mu\Omega/cm$.

$$(S_1)\mu\Omega/cm = \frac{\mu\Omega/cm}{S_{ns1}}$$

$$(S_1)\mu\Omega/cm = \frac{1345}{8}$$

$$(S_1)\mu\Omega/cm = 168$$

Step No. 34 Calculate the winding resistance, R_{s1} .

$$R_{s1} = MLT(N_{s1})\left(\frac{\mu\Omega}{cm}\right) \times 10^{-6} \text{ [ohms]}$$

$$R_{s1} = 3.8(3)(168) \times 10^{-6} \text{ [ohms]}$$

$$R_{s1} = 0.00192 \text{ [ohms]}$$

Step No. 35 Calculate the secondary copper loss, P_{s1} .

$$P_{s1} = I_{s1}^2 R_{s1} \text{ [watts]}$$

$$P_{s1} = (3.65)^2 (0.00192) \text{ [watts]}$$

$$P_{s1} = 0.0256 \text{ [watts]}$$

Step No. 36 Calculate the secondary turns, N_{s2} .

$$N_{s2} = \frac{N_{np}(V_{o2} + V_d)(1 - D_{\max} - D_w)}{(V_p D_{\max})} \text{ [turns]}$$

$$N_{s2} = \frac{16(12+1)(1-0.5-0.1)}{(24)(0.5)} \text{ [turns]}$$

$$N_{s2} = 6.9 \text{ use } 7 \text{ [turns]}$$

Step No. 37 Calculate the secondary peak current, $I_{s2(pk)}$.

$$I_{s2(pk)} = \frac{2I_{o2}}{(1 - D_{\max} - D_w)} \text{ [amps]}$$

$$I_{s2(pk)} = \frac{2(0.5)}{(1-0.5-0.1)} \text{ [amps]}$$

$$I_{s2(pk)} = 2.5 \text{ [amps]}$$

Step No. 38 Calculate the secondary rms current, $I_{s2(rms)}$.

$$I_{s2(rms)} = I_{s2(pk)} \sqrt{\frac{(1 - D_{\max} - D_w)}{3}} \quad [\text{amps}]$$

$$I_{s2(rms)} = (2.5) \sqrt{\frac{(1 - 0.5 - 0.1)}{3}} \quad [\text{amps}]$$

$$I_{s2(rms)} = 0.913 \quad [\text{amps}]$$

Step No. 39 Calculate the secondary wire area, $A_{sw2(B)}$.

$$A_{sw2(B)} = \frac{I_{s2(rms)}}{J} \quad [\text{cm}^2]$$

$$A_{sw2(B)} = \frac{0.913}{367} \quad [\text{cm}^2]$$

$$A_{sw2(B)} = 0.00249 \quad [\text{cm}^2]$$

Step No. 40 Calculate the required number of secondary strands, S_{ns2} .

$$S_{ns2} = \frac{A_{sw2(B)}}{\text{wire}_A}$$

$$S_{ns2} = \frac{(0.00249)}{(0.00128)}$$

$$S_{ns2} = 1.95 \quad \text{use } 2$$

Step No. 41 Calculate the, S_2 secondary, $\mu\Omega/\text{cm}$.

$$(S_2) \mu\Omega / \text{cm} = \frac{\mu\Omega / \text{cm}}{S_{ns2}}$$

$$(S_2) \mu\Omega / \text{cm} = \frac{1345}{2}$$

$$(S_2) \mu\Omega / \text{cm} = 672$$

Step No. 42 Calculate the winding resistance, R_{s2} .

$$R_{s2} = MLT(N_{s2}) \left(\frac{\mu\Omega}{\text{cm}} \right) \times 10^{-6} \quad [\text{ohms}]$$

$$R_{s2} = 3.8(7)(672) \times 10^{-6} \quad [\text{ohms}]$$

$$R_{s2} = 0.0179 \quad [\text{ohms}]$$

Step No. 43 Calculate the secondary copper loss, P_{s2} .

$$P_{s2} = I_{s2}^2 R_{s2} \quad [\text{watts}]$$

$$P_{s2} = (0.913)^2 (.0179) \quad [\text{watts}]$$

$$P_{s2} = 0.0149 \quad [\text{watts}]$$

Step No. 44 Calculate the window utilization, K_u .

$$\begin{aligned} [\text{turns}] &= (N_p S_{np}) \quad [\text{primary}] \\ [\text{turns}] &= (16)(3)=48 \quad [\text{primary}] \\ [\text{turns}] &= (N_{s1} S_{ns1}) \quad [\text{secondary}] \\ [\text{turns}] &= (3)(8)=24 \quad [\text{secondary}] \\ [\text{turns}] &= (N_{s2} S_{ns2}) \quad [\text{secondary}] \\ [\text{turns}] &= (7)(2)=14 \quad [\text{secondary}] \\ N_t &= 86 \text{ turns} \#26 \\ K_u &= \frac{N_t A_w}{W_a} = \frac{(86)(0.00128)}{(0.501)} \\ K_u &= 0.220 \end{aligned}$$

Step No. 45 Calculate the total copper loss, P_{cu} .

$$\begin{aligned} P_{cu} &= P_p + P_{s1} + P_{s2} \quad [\text{watts}] \\ P_{cu} &= (0.0533) + (0.0256) + (0.0149) \quad [\text{watts}] \\ P_{cu} &= 0.0938 \quad [\text{watts}] \end{aligned}$$

Step No. 46 Calculate the regulation, α , for this design.

$$\begin{aligned} \alpha &= \frac{P_{cu}}{P_o} \times 100 \quad [\%] \\ \alpha &= \frac{(0.0938)}{(18.5)} \times 100 \quad [\%] \\ \alpha &= 0.507 \quad [\%] \end{aligned}$$

Step No. 47 Calculate the ac flux density, B_{ac} .

$$\begin{aligned} B_{ac} &= \frac{0.4\pi N_{np} F \left(\frac{I_p(pk)}{2} \right) (10^{-4})}{l_g + \left(\frac{MPL}{\mu_m} \right)}, \quad [\text{tesla}] \\ B_{ac} &= \frac{(1.26)(16)(1.3)(1.72)(10^{-4})}{(0.0384) + \left(\frac{4.7}{2500} \right)}, \quad [\text{tesla}] \\ B_{ac} &= 0.111, \quad [\text{tesla}] \end{aligned}$$

Step No. 48 Calculate the watts per kilogram, WK.

$$\begin{aligned} WK &= 4.855(10^{-5})(f)^{(1.63)}(B_{ac})^{(2.62)} \quad [\text{watts/kilogram}] \\ WK &= 4.855(10^{-5})(100000)^{(1.63)}(0.111)^{(2.62)} \quad [\text{watts/kilogram}] \\ WK &= 21.6 \quad [\text{watts/kilogram}] \text{ or } [\text{milliwatts/gram}] \end{aligned}$$

Step No. 49 Calculate the core loss, P_{fe} .

$$P_{fe} = \left(\frac{\text{milliwatts}}{\text{gram}} \right) W_{ffe} \times 10^{-3} \quad [\text{watts}]$$

$$P_{fe} = (21.6)(7) \times 10^{-3} \quad [\text{watts}]$$

$$P_{fe} = 0.151 \quad [\text{watts}]$$

Step No. 50 Calculate the total loss, core P_{fe} and copper P_{cu} , in watts, P_{Σ} .

$$P_{\Sigma} = P_{fe} + P_{cu} \quad [\text{watts}]$$

$$P_{\Sigma} = (0.151) + (0.0938) \quad [\text{watts}]$$

$$P_{\Sigma} = 0.245 \quad [\text{watts}]$$

Step No. 51 Calculate the watt density, ψ .

$$\psi = \frac{P_{\Sigma}}{A_t} \quad [\text{watts/cm}^2]$$

$$\psi = \frac{0.245}{13.3} \quad [\text{watts/cm}^2]$$

$$\psi = 0.0184 \quad [\text{watts/cm}^2]$$

Step No. 52 Calculate the temperature rise, T_r , in, $^{\circ}\text{C}$.

$$T_r = 450(\psi)^{(0.826)} \quad [^{\circ}\text{C}]$$

$$T_r = 450(0.0184)^{(0.826)} \quad [^{\circ}\text{C}]$$

$$T_r = 16.6 \quad [^{\circ}\text{C}]$$

Design Example, Boost Converter, Discontinuous Current

1. Input voltage nominal, V_{in} = 28 volts
2. Input voltage minimum, $V_{in(min)}$ = 26 volts
3. Input voltage maximum, $V_{in(max)}$ = 32 volts
4. Output voltage, V_{o1} = 50 volts
5. Output current, I_{o1} = 1 amps
6. *Window utilization, K_u = 0.29
7. Frequency, f = 100 kHz
8. Converter efficiency, η = 92 %
9. Dwell time duty ratio, $D_{(w)}$ = 0.1
10. Regulation, α = 1.0%
11. Operating flux density, B_m = 0.25 tesla
12. Diode voltage, V_d = 1.0 volts

*When operating at high frequencies, the engineer has to review the window utilization factor, K_u . When using a small bobbin ferrite, the ratio of the bobbin winding area to the core window area is only about 0.6. Operating at 100kHz and having to use a #26 wire, because of the skin effect, the ratio of the bare copper area is 0.78. Therefore, the overall window utilization, K_u , is reduced. The core geometries, K_g , in Chapter 3 have been calculated with a window utilization, K_u , of 0.4. To return the design back to the norm, the core geometry, K_g is to be multiplied by 1.35, and then, the current density, J , is calculated, using a window utilization factor of 0.29. See Chapter 4.

Skin Effect

The skin effect on an inductor is the same as a transformer. In the normal dc inductor, the ac current, (ac flux), is much lower and does not require the use of the same maximum wire size. This is not the case in the discontinuous, current type, flyback converter, where all of the flux is ac and without dc. In the discontinuous, flyback design, the skin effect has to be treated just like a high frequency transformer.

There are times when the larger wire is just too difficult to wind. Large wire is not only hard to handle, but it does not give the proper lay. It is easier to wind with bi-filar or quad-filar, wire with the equivalent cross-section.

At this point, select a wire so that the relationship between the ac resistance and the dc resistance is 1:

$$\frac{R_{ac}}{R_{dc}} = 1$$

The skin depth in centimeters is:

$$\varepsilon = \frac{6.62}{\sqrt{f}}, \text{ [cm]}$$

$$\varepsilon = \frac{6.62}{\sqrt{100,000}}, \text{ [cm]}$$

$$\varepsilon = 0.0209, \text{ [cm]}$$

Then, the wire diameter is:

$$\text{Wire Diameter} = 2(\varepsilon), \text{ [cm]}$$

$$\text{Wire Diameter} = 2(0.0209), \text{ [cm]}$$

$$\text{Wire Diameter} = 0.0418, \text{ [cm]}$$

Then, the bare wire area A_w is:

$$A_w = \frac{\pi D^2}{4}, \text{ [cm}^2\text{]}$$

$$A_w = \frac{(3.1416)(0.0418)^2}{4}, \text{ [cm}^2\text{]}$$

$$A_w = 0.00137, \text{ [cm}^2\text{]}$$

From the Wire Table in Chapter 4, Number 26 has a bare wire area of 0.001028 centimeters. This will be the minimum wire size used in this design. If the design requires more wire area to meet the specification, then, the design will use a multifilar of #26. Listed Below are #27 and #28, just in case #26 requires too much rounding off.

Wire AWG	Bare Area	Area Ins.	Bare/Ins.	$\mu\Omega/\text{cm}$
#26	0.001280	0.001603	0.798	1345
#27	0.001021	0.001313	0.778	1687
#28	0.0008046	0.0010515	0.765	2142

Step No. 1 Calculate the total period, T.

$$T = \frac{1}{f}, \text{ [seconds]}$$

$$T = \frac{1}{100,000}, \text{ [seconds]}$$

$$T = 10, \text{ [}\mu\text{sec]}$$

Step No. 2 Calculate the maximum output power, P_o .

$$P_o = (V_o + V_d)(I_o), \quad [\text{watts}]$$

$$P_o = (50 + 1.0)(1.0), \quad [\text{watts}]$$

$$P_o = 51, \quad [\text{watts}]$$

Step No. 3 Calculate the maximum input current, $I_{in(max)}$.

$$I_{in(max)} = \frac{P_o}{V_{in(min)}\eta}, \quad [\text{amps}]$$

$$I_{in(max)} = \frac{(51)}{(26)(0.92)}, \quad [\text{amps}]$$

$$I_{in(max)} = 2.13, \quad [\text{amps}]$$

Step No. 4 Calculate the maximum duty ratio, $D_{(max)}$.

$$D_{(max)} = (1 - D_w) \left(\frac{V_o - V_{in(min)} + V_d}{V_o} \right)$$

$$D_{(max)} = (1 - 0.1) \left(\frac{(50) - (26) + (1.0)}{50} \right)$$

$$D_{(max)} = 0.45$$

Step No. 5 Calculate the minimum duty ratio, $D_{(min)}$.

$$D_{(min)} = (1 - D_w) \left(\frac{V_o - V_{in(max)} + V_d}{V_o} \right)$$

$$D_{(min)} = (1 - 0.1) \left(\frac{(50) - (32) + (1.0)}{50} \right)$$

$$D_{(min)} = 0.342$$

Step No. 6 Calculate the required inductance, L .

$$L_{max} = \frac{(V_o + V_d)TD_{(max)}(1 - D_{max} - D_w)^2}{2I_{o(max)}}, \quad [\text{henrys}]$$

$$L_{max} = \frac{(50 + 1.0)(10(10^{-6}))(0.45)(1 - 0.45 - 0.1)^2}{2(1.0)}, \quad [\text{henrys}]$$

$$L = 23.2 \text{ use } 23, \quad [\mu\text{h}]$$

Step No. 7 Calculate the peak current, I_{pk} . In a discontinuous current boost the peak current is, $I_{(pk)} = \Delta I$.

$$I_{(pk)} = \frac{2P_{o(max)}}{\eta(V_o D_{(min)})}, \quad [\text{amps}]$$

$$I_{(pk)} = \frac{2(51)}{(0.92)((50)(0.342))}, \quad [\text{amps}]$$

$$I_{(pk)} = 6.48, \quad [\text{amps}]$$

Step No. 8 Calculate the rms current, $I_{(rms)}$.

$$I_{(rms)} = I_{pk} \sqrt{\frac{TD_{(max)}}{3T}}, \quad [\text{amps}]$$

$$I_{(rms)} = (6.48) \sqrt{\frac{(10 \times 10^{-6})(0.45)}{3(10 \times 10^{-6})}}, \quad [\text{amps}]$$

$$I_{(rms)} = 2.51, \quad [\text{amps}]$$

Step No. 9 Calculate the total energy-handling capability in watt-seconds, w-s.

$$\text{Energy} = \frac{L I_{pk}^2}{2}, \quad [\text{w-s}]$$

$$\text{Energy} = \frac{(23 \times 10^{-6})(6.48)^2}{2}, \quad [\text{w-s}]$$

$$\text{Energy} = 0.000483, \quad [\text{w-s}]$$

Step No. 10 Calculate the electrical conditions, K_e .

$$K_e = 0.145 P_o B_m^2 (10^{-4})$$

$$K_e = 0.145 (51) (0.25)^2 (10^{-4})$$

$$K_e = 0.0000462$$

Step No. 11 Calculate the core geometry, K_g .

$$K_g = \frac{(\text{Energy})^2}{K_e \alpha}, \quad [\text{cm}^5]$$

$$K_g = \frac{(0.000483)^2}{(0.0000462)(1.0)}, \quad [\text{cm}^5]$$

$$K_g = 0.00505, \quad [\text{cm}^5]$$

$$K_g = 0.00505 (1.35), \quad [\text{cm}^5]$$

$$K_g = 0.00682, \quad [\text{cm}^5]$$

Step No. 12 From Chapter 3, select a core that is comparable in core geometry, K_g .

Core number	RM-6
Manufacturer	TDK
Magnetic path length, MPL	= 2.86 cm
Core weight, W_{tfe}	= 5.5 grams
Copper weight, W_{tCu}	= 2.9 grams
Mean length turn, MLT	= 3.1 cm
Iron area, A_c	= 0.366 cm ²
Window Area, W_a	= 0.260 cm ²
Area Product, A_p	= 0.0953 cm ⁴
Core geometry, K_g	= 0.0044 cm ⁵
Surface area, A_t	= 11.3 cm ²
Permeability, μ_m	= 2500
Winding Length, G	= 0.82

Step No. 13 Calculate the current density, J , using a window utilization, $K_u = 0.29$.

$$J = \frac{2(\text{Energy})(10^4)}{B_m A_p K_u}, \quad [\text{amps/cm}^2]$$

$$J = \frac{2(0.000483)(10^4)}{(0.25)(0.0953)(0.29)}, \quad [\text{amps/cm}^2]$$

$$J = 1398, \quad [\text{amps/cm}^2]$$

Step No. 14 Calculate the wire area, $A_{w(B)}$.

$$A_{w(B)} = \frac{I_{rms}}{J} \quad [\text{cm}^2]$$

$$A_{w(B)} = \frac{2.51}{1398} \quad [\text{cm}^2]$$

$$A_{w(B)} = 0.00179 \quad [\text{cm}^2]$$

Step No. 15 Calculate the required number of strands, S_n .

$$S_n = \frac{A_{w(B)}}{\#26 \text{ (bare area)}}$$

$$S_n = \frac{(0.00180)}{(0.00128)}$$

$$S_n = 1.41 \text{ use } 2$$

Step No. 16 Calculate the number of turns, N , using the number of strands, S_n , and the area for #26.

$$N = \frac{K_u W_a}{S_n \#26}, \text{ [turns]}$$

$$N = \frac{(0.29)(0.26)}{2(0.00128)}, \text{ [turns]}$$

$$N = 29.5 \text{ use } 30, \text{ [turns]}$$

Step No. 17 Calculate the required gap, l_g .

$$l_g = \frac{0.4\pi N^2 A_c (10^{-8})}{L} - \left(\frac{\text{MPL}}{\mu_m} \right), \text{ [cm]}$$

$$l_g = \frac{(1.26)(30)^2 (0.366)(10^{-8})}{(0.000023)} - \left(\frac{2.86}{2500} \right), \text{ [cm]}$$

$$l_g = 0.179, \text{ [cm]}$$

Step No. 19 Calculate the equivalent gap in mils.

$$\text{mils} = \text{cm}(393.7)$$

$$\text{mils} = (0.179)(393.7)$$

$$\text{mils} = 70$$

Step No. 20 Calculate the fringing flux factor, F .

$$F = 1 + \frac{l_g}{\sqrt{A_c}} \ln \left(\frac{2G}{l_g} \right)$$

$$F = 1 + \frac{(0.179)}{\sqrt{0.366}} \ln \left(\frac{2(0.82)}{0.179} \right)$$

$$F = 1.66$$

Step No. 21 Calculate the new number of turns, N_n , by inserting the fringing flux, F .

$$N_{np} = \sqrt{\frac{l_g L}{0.4\pi A_c F (10^{-8})}}, \text{ [turns]}$$

$$N_{np} = \sqrt{\frac{(0.179)(0.000023)}{(1.26)(0.366)(1.66)(10^{-8})}}, \text{ [turns]}$$

$$N_{np} = 23, \text{ [turns]}$$

Step No. 22 Calculate the peak flux density, B_{pk} .

$$B_{pk} = \frac{0.4\pi N_n F(I_{(pk)}) (10^{-4})}{l_g + \left(\frac{MPL}{\mu_m}\right)}, \quad [\text{tesla}]$$

$$B_{pk} = \frac{(1.26)(23)(1.66)(6.48)(10^{-4})}{(0.179) + \left(\frac{2.86}{2500}\right)}, \quad [\text{tesla}]$$

$$B_{pk} = 0.177, \quad [\text{tesla}]$$

Step No. 23 Calculate the new, $\mu\Omega/\text{cm}$.

$$(\text{new})\mu\Omega/\text{cm} = \frac{\mu\Omega/\text{cm}}{S_n}$$

$$(\text{new})\mu\Omega/\text{cm} = \frac{1345}{2}$$

$$(\text{new})\mu\Omega/\text{cm} = 673$$

Step No. 24 Calculate the primary winding resistance, R .

$$R = MLT(N_n) \left(\frac{\mu\Omega}{\text{cm}}\right) \times 10^{-6} \quad [\text{ohms}]$$

$$R = (3.1)(23)(673) \times 10^{-6} \quad [\text{ohms}]$$

$$R = 0.0480 \quad [\text{ohms}]$$

Step No. 25 Calculate the copper loss, P_{cu} .

$$P_{cu} = I_{rms}^2 R \quad [\text{watts}]$$

$$P_{cu} = (2.51)^2 (.0480) \quad [\text{watts}]$$

$$P_{cu} = 0.302 \quad [\text{watts}]$$

Step No. 26 Calculate the regulation, α , for this design.

$$\alpha = \frac{P_{cu}}{P_o} \times 100, \quad [\%]$$

$$\alpha = \frac{(0.302)}{(50)} \times 100, \quad [\%]$$

$$\alpha = 0.604, \quad [\%]$$

Step No. 27 Calculate the ac flux density in tesla, B_{ac} .

$$B_{ac} = \frac{0.4\pi N_n F \left(\frac{\Delta I}{2} \right) (10^{-4})}{l_g + \left(\frac{MPL}{\mu_m} \right)}, \text{ [tesla]}$$

$$B_{ac} = \frac{(1.26)(23)(1.66)(3.24)(10^{-4})}{(0.179) + \left(\frac{2.86}{2500} \right)}, \text{ [tesla]}$$

$$B_{ac} = 0.0869, \text{ [tesla]}$$

Step No. 28 Calculate the watts per kilogram, WK.

$$WK = 4.855(10^{-5})(f)^{(1.63)}(B_{ac})^{(2.62)}, \text{ [watts/kilogram]}$$

$$WK = 4.855(10^{-5})(100000)^{(1.63)}(0.0869)^{(2.62)}, \text{ [watts/kilogram]}$$

$$WK = 11.39, \text{ [watts/kilogram] or [milliwatts/gram]}$$

Step No. 29 Calculate the core loss, P_{fe} .

$$P_{fe} = \left(\frac{\text{milliwatts}}{\text{gram}} \right) W_{fe} \times 10^{-3}, \text{ [watts]}$$

$$P_{fe} = (11.39)(5.5) \times 10^{-3}, \text{ [watts]}$$

$$P_{fe} = 0.0626, \text{ [watts]}$$

Step No. 30 Calculate the total loss, P_{Σ} , core, P_{fe} , and copper, P_{cu} .

$$P_{\Sigma} = P_{fe} + P_{cu}, \text{ [watts]}$$

$$P_{\Sigma} = (0.0626) + (0.302), \text{ [watts]}$$

$$P_{\Sigma} = 0.365, \text{ [watts]}$$

Step No. 31 Calculate the watt density, ψ .

$$\psi = \frac{P_{\Sigma}}{A_t}, \text{ [watts/cm}^2\text{]}$$

$$\psi = \frac{0.365}{11.3}, \text{ [watts/cm}^2\text{]}$$

$$\psi = 0.0323, \text{ [watts/cm}^2\text{]}$$

Step No. 32 Calculate the temperature rise, T_r in, °C.

$$T_r = 450(\psi)^{(0.826)}, \text{ [}^{\circ}\text{C]}$$

$$T_r = 450(0.0323)^{(0.826)}, \text{ [}^{\circ}\text{C]}$$

$$T_r = 26.4, \text{ [}^{\circ}\text{C]}$$

Designing Boost Inductors for Power Factor Correction (PFC)

Historically, the standard power supplies designed for electronic equipment have had a notoriously poor power factor in the area of (0.5-0.6), and a correspondingly, high, harmonic current content. This design approach utilizes a simple rectifier capacitor input filter that results in large current pulses drawn from the line, that cause distorting of the line voltage and create large amounts of EMI and noise.

The regulating bodies, IEC in Europe and IEEE in the United States, have been working to develop a standard for limiting harmonic current, in off-line equipment. The German standardization bodies have established IEC 1000-2, and it is generally accepted as the standard for limiting harmonic currents in off-line equipment.

Many new electronic products are required to have a near unity power factor and a distortion free, current input waveform. The conventional ac-dc converters usually employ a full wave, rectifier-bridge, with a simple filter to draw power from the ac line. The typical, rectifier capacitor, input bridge filter and associated waveforms, as shown in Figure 13-15, are no longer good enough.

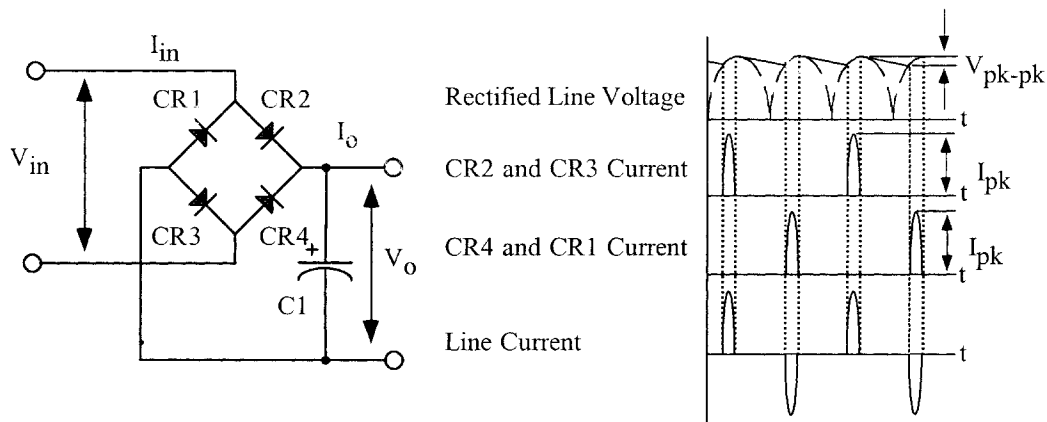


Figure 13-15. Typical, Capacitor Input Bridge Rectifier Filter.

The line current waveform for equipment that utilizes off-line rectifier capacitor input filter, is shown in Figure 13-15. The line current is supplied in narrow pulses. Consequently, the power factor is poor (0.5 – 0.6), due to a high harmonic distortion of the current waveform. The power supply can be designed with a power factor approaching unity, by the addition of an input inductor, as shown in Figure 13-16. The reasons why the input inductors are not designed into power supplies is very simple: cost, weight and bulk. The inductance equation for, L1, is shown below.

$$L1 = \frac{V_o}{3\omega I_{o(min)}}, \text{ [henrys] [13-56]}$$

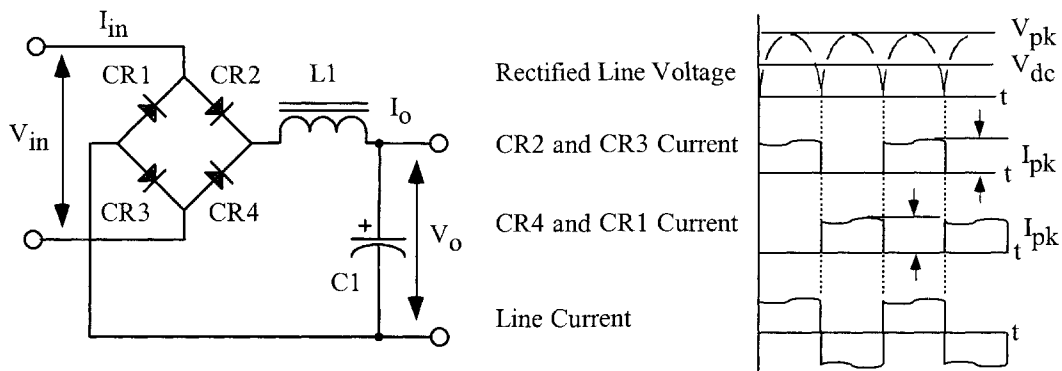


Figure 13-16. A Typical, Inductor Input Bridge Rectifier Filter.

Standard Boost Flyback Converter

The standard dc-to-dc boost flyback converter is shown in Figure 13-6, along with the voltage and current waveforms, shown in Figure 13-7 and 13-8. The boost converter has become the choice of many engineers as the power stage in the active power factor corrector design. The basic circuit can be operated in either the continuous or discontinuous mode.

Boost PFC Converter

The boost power factor correction converter is shown in Figure 13-17. The boost converter is the most popular of the power factor pre-regulators. The boost converter can operate in two modes, continuous and discontinuous. The current through the inductor, $L1$, is shown in Figure 13-18, for both continuous and discontinuous operation. After examining the schematic, the advantages and disadvantages of the boost converter can readily be seen. The disadvantage is the high output voltage to the load circuit and current limit cannot be implemented. The advantage is that the circuit requires a minimum of parts and the gate drive to, $Q1$, is referenced to ground.

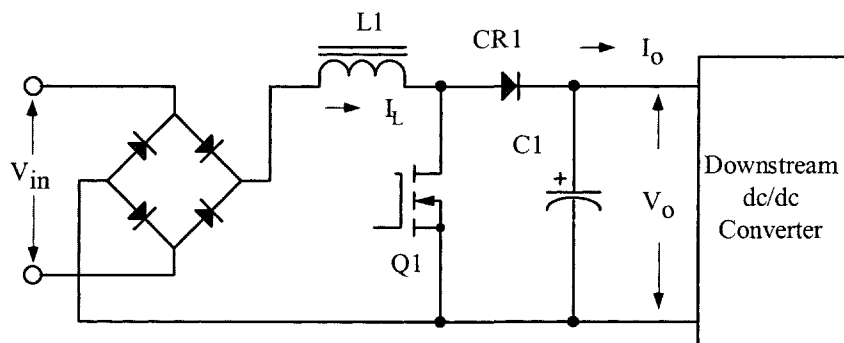


Figure 13-17. Boost PFC Converter.

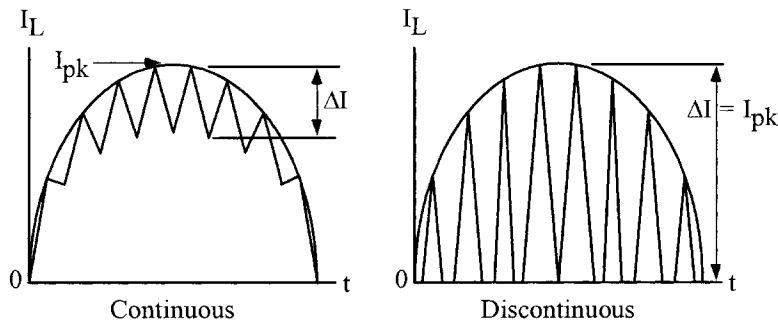


Figure 13-18. Current Through Inductor L1.

Design Example, (PFC) Boost Converter, Continuous Current

The following pages describe a step-by-step procedure for designing a continuous current boost inductor for a Power Factor Correction (PFC) converter, as shown in Figure 13-17, with the following specifications:

1. Output power, P_o = 250 watts
2. Input voltage range, V_{in} = 90 – 270 volts
3. Line frequency, $f_{(line)}$ = 47 – 65 Hz
4. Output voltage, V_o = 400 volts
5. Switching frequency, f = 100kHz
6. Inductor ripple current, ΔI = 20% of I_{pk}
7. Magnetic core = ETD
8. Magnetic material = R
9. Converter efficiency, η = 95%
10. Inductor regulation, α = 1%
11. *Window utilization, K_u = 0.29
12. Operating Flux, B_m = 0.25 tesla

*When operating at high frequencies, the engineer has to review the window utilization factor, K_u . When using a small bobbin ferrite, the ratio of the bobbin winding area to the core window area is only about 0.6. Operating at 100kHz and having to use a #26 wire, because of the skin effect, the ratio of the bare copper area is 0.78. Therefore, the overall window utilization, K_u , is reduced. The core geometries, K_g , in Chapter 3 have been calculated with a window utilization, K_u , of 0.4. To return the design back to the norm, the core geometry, K_g , is to be multiplied by 1.35, and then, the current density, J , is calculated, using a window utilization factor of 0.29. See Chapter 4.

Skin Effect

The skin effect on an inductor is the same as a transformer. In the normal dc inductor, the ac current (ac flux), is much lower, and does not require the use of the same, maximum wire size. This is not the case in the discontinuous, current type, flyback converter, where all of the flux is ac and no dc. In the discontinuous, flyback design, the skin effect has to be treated just like a high frequency transformer.

There are times when the larger wire is just too difficult to wind. Large wire is not only hard to handle, but it does not give the proper lay. It is easier to wind with bi-filar or quad-filar wire, with the equivalent cross-section.

Select a wire so that the relationship between the ac resistance and the dc resistance is 1:

$$\frac{R_{ac}}{R_{dc}} = 1$$

The skin depth in centimeters is:

$$\varepsilon = \frac{6.62}{\sqrt{f}}, \quad [\text{cm}]$$

$$\varepsilon = \frac{6.62}{\sqrt{100,000}}, \quad [\text{cm}]$$

$$\varepsilon = 0.0209, \quad [\text{cm}]$$

Then, the wire diameter is:

$$\text{Wire Diameter} = 2(\varepsilon), \quad [\text{cm}]$$

$$\text{Wire Diameter} = 2(0.0209), \quad [\text{cm}]$$

$$\text{Wire Diameter} = 0.0418, \quad [\text{cm}]$$

Then, the bare wire area, A_w , is:

$$A_w = \frac{\pi D^2}{4}, \quad [\text{cm}^2]$$

$$A_w = \frac{(3.1416)(0.0418)^2}{4}, \quad [\text{cm}^2]$$

$$A_w = 0.00137, \quad [\text{cm}^2]$$

From the Wire Table in Chapter 4, Number 26 has a bare wire area of 0.00128 centimeters. This will be the minimum wire size used in this design. If the design requires more wire area to meet the specification, then, the design will use a multifilar of #26.

Wire AWG	Bare Area	Area Ins.	Bare/Ins.	$\mu\Omega/\text{cm}$
#26	0.001280	0.001603	0.798	1345

Step No. 1 Calculate the input power, P_{in} .

$$P_{in} = \frac{P_o}{\eta}, \text{ [watts]}$$

$$P_{in} = \frac{250}{0.95}, \text{ [watts]}$$

$$P_{in} = 263, \text{ [watts]}$$

Step No. 2 Calculate the peak input current, I_{pk} .

$$I_{pk} = \frac{P_{in}\sqrt{2}}{V_{in(\min)}}, \text{ [amps]}$$

$$I_{pk} = \frac{(263)(1.41)}{90}, \text{ [amps]}$$

$$I_{pk} = 4.12, \text{ [amps]}$$

Step No. 3 Calculate the input ripple current, ΔI .

$$\Delta I = 0.2I_{pk}, \text{ [amps]}$$

$$\Delta I = 0.2(4.12), \text{ [amps]}$$

$$\Delta I = 0.824, \text{ [amps]}$$

Step No. 4 Calculate the maximum duty ratio, $D_{(\max)}$.

$$D_{(\max)} = \frac{(V_o - (V_{in(\min)}\sqrt{2}))}{V_o}$$

$$D_{(\max)} = \frac{(400 - (90\sqrt{2}))}{400}$$

$$D_{(\max)} = 0.683$$

Step No. 5 Calculate the required boost inductance, L .

$$L = \frac{(V_{in(\min)}\sqrt{2})D_{(\max)}}{\Delta I f}, \text{ [henrys]}$$

$$L = \frac{(126.9)(0.683)}{(0.824)(100000)}, \text{ [henrys]}$$

$$L = 0.00105, \text{ [henrys]}$$

Step No. 6 Calculate the Energy required, Eng .

$$Eng = \frac{LI_{pk}^2}{2}, \text{ [watt-seconds]}$$

$$Eng = \frac{(0.00105)(4.12)^2}{2}, \text{ [watt-seconds]}$$

$$Eng = 0.00891, \text{ [watt-seconds]}$$

Step No. 7 Calculate the electrical coefficient, K_e .

$$K_e = 0.145 P_o B_m^2 (10^{-4})$$

$$K_e = 0.145 (250) (0.25)^2 (10^{-4})$$

$$K_e = 0.000227$$

Step No. 8 Calculate the core geometry coefficient, K_g .

$$K_g = \frac{(\text{Eng})^2}{K_e \alpha}, \quad [\text{cm}^5]$$

$$K_g = \frac{(0.00891)^2}{(0.000227)(1)}, \quad [\text{cm}^5]$$

$$K_g = 0.35, \quad [\text{cm}^5]$$

$$K_g = 0.35(1.35), \quad [\text{cm}^5] \text{ Corrected}$$

$$K_g = 0.47, \quad [\text{cm}^5]$$

Step No. 9 From Chapter 3, select an ETD ferrite core, comparable in core geometry, K_g .

Core number	= ETD-44
Manufacturer	= Ferroxcube
Magnetic path length, MPL	= 10.3 cm
Core weight, W_{tfe}	= 93.2 grams
Copper weight, W_{tcu}	= 94 grams
Mean length turn, MLT	= 9.4 cm
Iron area, A_c	= 1.74 cm ²
Window Area, W_a	= 2.79 cm ²
Area Product, A_p	= 4.85 cm ⁴
Core geometry, K_g	= 0.360 cm ⁵
Surface area, A_t	= 87.9 cm ²
Permeability, μ_m	= 2000
Millihenrys per 1000 turns, AL	= 3365
Winding Length, G	= 3.22

Step No. 10 Calculate the current density, J .

$$J = \frac{2(\text{Eng})(10^4)}{B_m A_p K_u}, \quad [\text{amps/cm}^2]$$

$$J = \frac{2(0.00891)(10^4)}{(0.25)(4.85)(0.29)}, \quad [\text{amps/cm}^2]$$

$$J = 507, \quad [\text{amps/cm}^2]$$

Step No. 11 Calculate the rms current, I_{rms} .

$$I_{rms} = \frac{I_{pk}}{\sqrt{2}}, \text{ [amps]}$$

$$I_{rms} = \frac{4.12}{\sqrt{2}}, \text{ [amps]}$$

$$I_{rms} = 2.91, \text{ [amps]}$$

Step No. 12 Calculate the required bare wire area, $A_{w(B)}$.

$$A_{w(B)} = \frac{I_{rms}}{J}, \text{ [cm}^2\text{]}$$

$$A_{w(B)} = \frac{2.91}{507}, \text{ [cm}^2\text{]}$$

$$A_{w(B)} = 0.00574, \text{ [cm}^2\text{]}$$

Step No. 13 Calculate the required number of strands, S_n .

$$S_n = \frac{A_{w(B)}}{\#26(\text{bare area})}, \text{ [cm}^2\text{]}$$

$$S_n = \frac{(0.00574)}{(0.00128)}, \text{ [cm}^2\text{]}$$

$$S_n = 4.48 \text{ use } 5, \text{ [cm}^2\text{]}$$

Step No. 14 Calculate the required number of turns, N , using the number of strands, S_n , and the area for #26.

$$N = \frac{W_a K_u}{S_n \#26}, \text{ [turns]}$$

$$N = \frac{(2.79)(0.29)}{5(0.00128)}, \text{ [turns]}$$

$$N = 126, \text{ [turns]}$$

Step No. 15 Calculate the required gap, l_g .

$$l_g = \left(\frac{0.4\pi N^2 A_c (10^{-8})}{L} \right), \text{ [cm]}$$

$$l_g = \left(\frac{(1.257)(126)^2 (1.74)(10^{-8})}{0.00105} \right), \text{ [cm]}$$

$$l_g = 0.331, \text{ [cm]}$$

Change the gap to mils: $0.331 \times 393.7 = 130$ mils center or 65 mils per each outer leg.

Step No. 16 Calculate the fringing flux factor, F.

$$F = \left(1 + \left(\frac{l_g}{\sqrt{A_c}} \right) \ln \left(\frac{2G}{l_g} \right) \right)$$

$$F = \left(1 + \left(\frac{0.331}{1.32} \right) \ln \left(\frac{6.44}{0.331} \right) \right)$$

$$F = 1.74$$

Step No. 17 Calculate the new turns using the fringing flux.

$$N = \sqrt{\frac{l_g L}{0.4\pi A_c F (10^{-8})}}, \text{ [turns]}$$

$$N = \sqrt{\frac{(0.331)(0.00105)}{(1.257)(1.74)(1.74)(10^{-8})}}, \text{ [turns]}$$

$$N = 96, \text{ [turns]}$$

Step No. 18 Calculate the peak flux, B_{pk}.

$$B_{pk} = F \left(\frac{0.4\pi N I_{pk} (10^{-4})}{l_g} \right), \text{ [tesla]}$$

$$B_{pk} = 1.74 \left(\frac{(1.257)(96)(4.12)(10^{-4})}{0.331} \right), \text{ [tesla]}$$

$$B_{pk} = 0.261, \text{ [tesla]}$$

Step No. 19 Calculate the new, μΩ/cm.

$$(\text{new}) \mu\Omega / \text{cm} = \frac{\mu\Omega / \text{cm}}{S_n}$$

$$(\text{new}) \mu\Omega / \text{cm} = \frac{1345}{5}$$

$$(\text{new}) \mu\Omega / \text{cm} = 269$$

Step No. 20 Calculate the winding resistance, R.

$$R = (\text{MLT}) N \left(\frac{\mu\Omega}{\text{cm}} \right) (10^{-6}), \text{ [ohms]}$$

$$R = (9.4)(96)(269)(10^{-6}), \text{ [ohms]}$$

$$R = 0.243, \text{ [ohms]}$$

Step No. 21 Calculate the winding copper loss, P_{cu} .

$$P_{cu} = I_{rms}^2 R, \text{ [watts]}$$

$$P_{cu} = (2.91)^2 (0.243), \text{ [watts]}$$

$$P_{cu} = 2.06, \text{ [watts]}$$

Step No. 22 Calculate the regulation, α .

$$\alpha = \frac{P_{cu}}{P_o} 100, \text{ [%]}$$

$$\alpha = \frac{(2.06)}{(250)} 100, \text{ [%]}$$

$$\alpha = 0.824, \text{ [%]}$$

Step No. 23 Calculate the ac flux density, B_{ac} .

$$B_{ac} = \frac{0.4\pi N \left(\frac{\Delta I}{2} \right) (10^{-4})}{l_g}, \text{ [tesla]}$$

$$B_{ac} = \frac{(1.257)(96)(0.412)(10^{-4})}{0.331}, \text{ [tesla]}$$

$$B_{ac} = 0.0150, \text{ [tesla]}$$

Step No. 24 Calculate the watts per kilogram, W/K , using R material in Chapter 2.

$$W / K = 4.316(10^{-5})(f)^{1.64}(B_{ac})^{2.68}, \text{ [watts per kilogram]}$$

$$W / K = 4.316(10^{-5})(100000)^{1.64}(0.0150)^{2.68}, \text{ [watts per kilogram]}$$

$$W / K = 0.0885, \text{ [watts per kilogram]}$$

Step No. 25 Calculate the core loss, P_{fe} .

$$P_{fe} = W_{fe} (10^{-3})(W / K), \text{ [watts]}$$

$$P_{fe} = (93.2)(10^{-3})(0.0885), \text{ [watts]}$$

$$P_{fe} = 0.0082, \text{ [watts]}$$

Step No. 26 Calculate the total loss core loss, P_{fe} and copper loss, P_{cu} .

$$P = P_{cu} + P_{fe}, \text{ [watts]}$$

$$P = (2.03) + (0.0082), \text{ [watts]}$$

$$P = 2.04, \text{ [watts]}$$

Step No. 27 Calculate the watt density, ψ .

$$\psi = \frac{P}{A_r}, \text{ [watts per cm}^2\text{]}$$

$$\psi = \frac{2.04}{87.9}, \text{ [watts per cm}^2\text{]}$$

$$\psi = 0.023, \text{ [watts per cm}^2\text{]}$$

Step No. 28 Calculate the temperature rise, T_r .

$$T_r = 450(\psi)^{0.826}, \text{ [}^\circ\text{C]}$$

$$T_r = 450(0.023)^{0.826}, \text{ [}^\circ\text{C]}$$

$$T_r = 19.9, \text{ [}^\circ\text{C]}$$

Step No. 29 Calculate the window utilization, K_u .

$$K_u = \frac{NS_n A_{w(B)}}{W_u}$$

$$K_u = \frac{(95)(5)(0.00128)}{(2.79)}$$

$$K_u = 0.218$$

References

1. Unitode Application Note U-132, Power Factor Correction Using The UC3852 Controller on-time zero current Switching Technique.
2. Unitode Application Note U-134, UC3854 Controlled Power Factor Correction Circuit Design
3. AlliedSignal Application Guide: Power Factor Correction Inductor Design for Switch Mode Power Supplies using Powerlite C Cores.
4. PCIM August 1990, Active Power Factor Correction Using a Flyback Topology, James LoCascio and Mehmet Nalbant/ Micor Linear Corporation.
5. Silicon General Application SG3561A Power Factor Controller.
6. SGS Thomson Application Note AN628/0593 Designing a High Power Factor Pre-regulator with the L4981 Continuous Current.
7. IEEE, A Comparison Between Hysteretic and Fixed Frequency Boost Converter Used for Power Factor Correction, James J. Spanger Motorola and Anup K. Behera Illinois Institute Technology.

Chapter 14

Forward Converter, Transformer Design, and Output Inductor Design

The author would like to thank the late **Dr. J. K. Watson**, Professor of Electrical Engineering at the University of Florida for his help with the Forward Converter design equations.

Table of Contents

1. Introduction	
2. Circuit Operation	
3. Comparing the Dynamic B-H Loops	
4. Forward Converter Waveforms	
5. Transformer Design Using the Core Geometry, K_g , Approach	
6. Forward Converter Output Inductor Design	
7. Output Inductor Design Using the Core Geometry, K_g , Approach	

Introduction

When speaking of a forward converter, the circuit that comes to mind is the single-ended, forward converter circuit, as shown in Figure 14-1. This single-ended, forward converter was developed about 1974 and has become one of the most popular and widely-used topology for powers under 200 W. The single-ended, forward converter gets its name from a family of converters. A description of a forward converter is that when current is flowing in the primary, there is current flowing in the secondary, and in the load. The push-pull converter, full-bridge converter, and half-bridge converter are all, basically, forward converters. The voltage stress on the single-forward converter is the same as it is on the push-pull converter, $2V_{in}$. This circuit's main advantage, that is so appealing to engineers is its simplicity and parts' count.

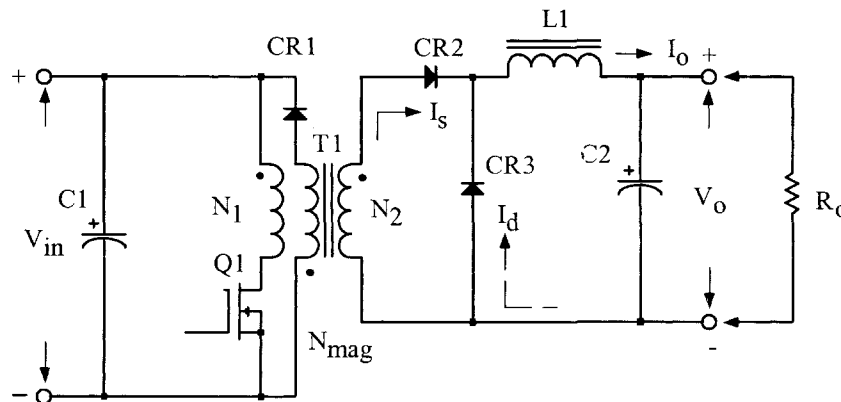


Figure 14-1. Schematic of a Single-Ended Forward Converter.

Circuit Operation

The basic circuit operation of this single-ended, forward converter is as follows: When the drive is applied to, Q1, the secondary current, I_s , will flow through, CR2, and, L1, and into the load. This process is due to transformer action, (T1). At the same time, the magnetizing current begins to build up in the transformer primary. When the base drive to, Q1, is removed, then, Q1, turns off the magnetizing current that has built up in the primary. The magnetizing current continues to flow through the demagnetizing winding, N_{mag} and CR1. The demagnetizing winding, N_{mag} , has the same number of turns as the primary winding. So, when the magnetizing field collapses, when Q1 is turned off, diode CR1 is clamped to the same voltage as the applied voltage during the t_{on} time. This means the transistor on time, t_{on} , divided by the total time, T, must not exceed 0.5 or 50%. Otherwise, the forward volt-seconds will exceed the reset volt-second

capability and the transformer will saturate. To ensure smooth transfer of the magnetizing current, the primary and demagnetizing winding must be tightly coupled (bifilar). In a push-pull converter, the reset of the core occurs naturally on each alternate half cycle.

Comparing the Dynamic B-H Loops

One of the main reasons for engineers to use the single-ended, forward converter circuit is the problem they have with the push-pull converter core-saturating. The core saturation can be due to an imbalance of the primary or secondary. The dynamic BH loops for the single-ended, forward converter and the push-pull converter are shown in Figure 14-2.

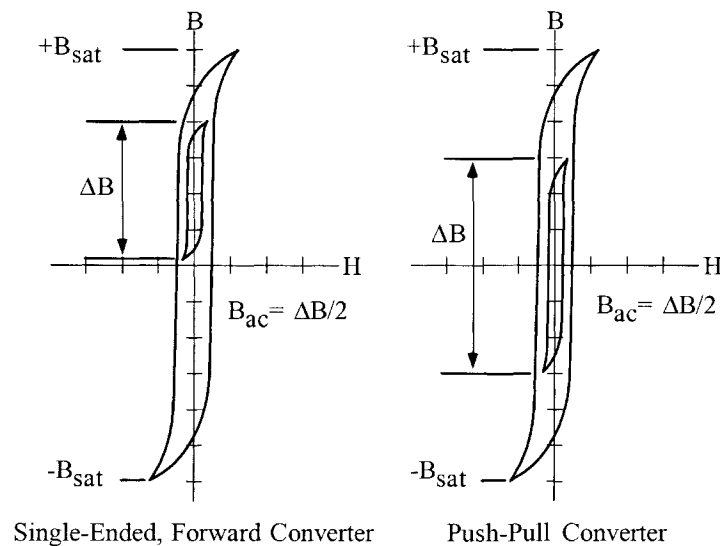


Figure 14-2. The dynamic BH loop comparison.

The average input current for the single-ended, forward converter is about the same as the push-pull converter, but the peak current is always greater than twice the average current. Operating the single-ended, forward converter at low input voltages, the high peak currents could be a component problem. The input filter and output filter for the single-ended, forward converter are always larger than the push-pull converter, because it is operating at the fundamental frequency.

The waveforms shown in Figure 14-3 are typical waveforms of the single-ended forward converter. The collector current, I_c , is shown in Figure (14-3-A), and the magnetizing current, I_m , is shown in Figure (14-3-B). The inductor, L1, current, I_L , made up from the rectifier, CR2, and the commutating rectifier, CR3, are shown in Figure (14-3-C). The collector voltage, V_c , is shown in Figure (14-3-D).

Forward Converter Waveforms

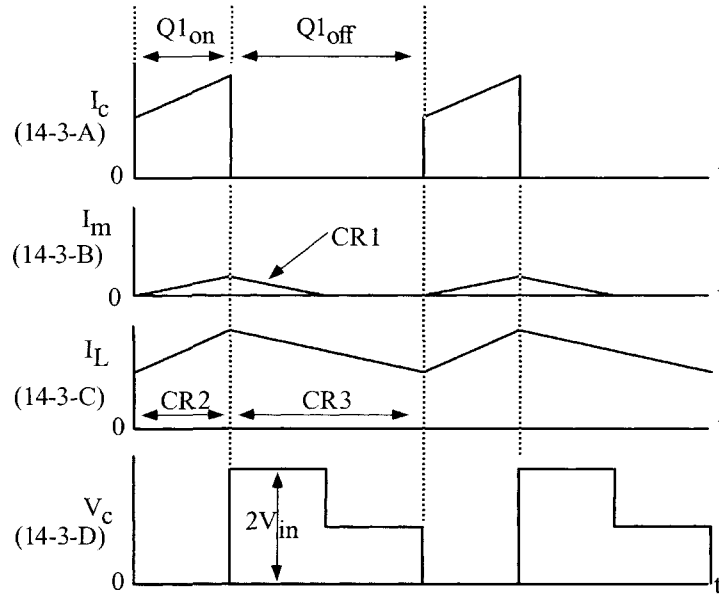


Figure 14-3. Typical Single-Ended Forward Converter Waveforms.

Another version of the classic, forward converter is the double-ended, forward converter, shown in Figure 14-4. The double-ended, forward converter has two transistors rather than one, compared to the single-ended, forward converter, shown in Figure 14-1. The double-ended forward converter is more complicated than the single-ended forward converter because one of the transistors is on the high side of the input voltage, but it has some significant advantages. The series switching transistors are subjected to only the input voltage, (V_{in}), rather than twice the input voltage, ($2V_{in}$). It also removes the need for a demagnetizing winding. The demagnetizing current now flows through the primary, through, CR1, and CR2, and back to the source, as shown in Figure 14-5. This demagnetizing path also provides a path for the energy stored in the leakage inductance. The resulting spiking voltage, caused from the leakage inductance, is now clamped to the input voltage, plus the two diode drops ($V_{in} + 2V_d$).

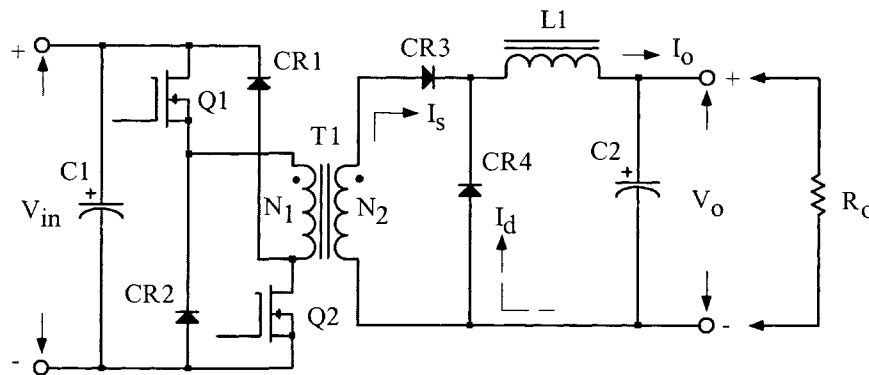


Figure 14-4. Schematic of a Double-Ended Forward Converter.

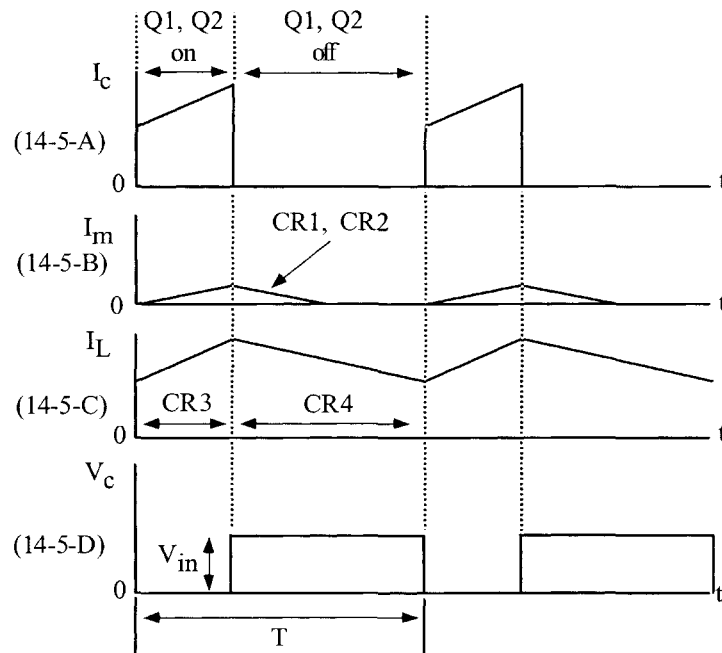


Figure 14-5. Typical Double-Ended Forward, Converter Waveforms.

Note:

The design equations are from communication and work with the late Dr. J. K. Watson, Professor of Electrical Engineering at the University of Florida.

Electrical coefficient is:

$$K_e = 0.145 f^2 \Delta B^2 (10^{-4}) \quad [14-1]$$

Core geometry is:

$$K_g = \frac{P_{in} D_{(max)}}{\alpha K_e}, \quad [cm^5] \quad [14-2]$$

Current density is:

$$J = \frac{2 P_{in} \sqrt{D_{(max)}} (10^4)}{f \Delta B A_c W_a K_u}, \quad [amps \text{ per } cm^2] \quad [14-3]$$

Primary current is:

$$I_p = \frac{P_{in}}{V_{in(min)} \sqrt{D_{(max)}}}, \quad [amps] \quad [14-4]$$

Transformer Design Using the Core Geometry, K_g , Approach

The following information is the Design specification for a 30 watts, single-ended transformer, operating at 100kHz, using the, K_g , core geometry approach. For a typical design example, assume a single-ended converter circuit, as shown in Figure 14-1, with the following specification:

1. Input voltage, $V_{(min)}$ = 22 volts
2. Input voltage, $V_{(nom)}$ = 28 volts
3. Input voltage, $V_{(max)}$ = 35 volts
4. Output voltage, V_o = 5.0 volts
5. Output current, I_o = 5.0 amps
6. Frequency, f = 100kHz
7. Efficiency, η = 98%
8. Regulation, α = 0.5%
9. Diode voltage drop, V_d = 1.0 volt
10. Operating flux density, ΔB , ($B_{ac} = \Delta B/2$) = 0.1 tesla
11. Core Material = ferrite
12. Window utilization, K_u = 0.3
13. Temperature rise goal, T_r = 30°C
14. Maximum duty ratio, D_{max} = 0.5
15. Notes:
 - Demag turns ratio, N_{mag}/N_p = 1
 - Demag power, P_{mag} = (0.1) P_o

Select a wire so that the relationship between the ac resistance and the dc resistance is 1:

$$\frac{R_{ac}}{R_{dc}} = 1$$

The skin depth in centimeters is:

$$\epsilon = \frac{6.62}{\sqrt{f}}, \quad [\text{cm}]$$

$$\epsilon = \frac{6.62}{\sqrt{100,000}}, \quad [\text{cm}]$$

$$\epsilon = 0.0209, \quad [\text{cm}]$$

Then, the wire diameter is:

$$\text{Wire Diameter} = 2(\varepsilon), \text{ [cm]}$$

$$\text{Wire Diameter} = 2(0.0209), \text{ [cm]}$$

$$\text{Wire Diameter} = 0.0418, \text{ [cm]}$$

Then, the bare wire area, A_w , is:

$$A_w = \frac{\pi D^2}{4}, \text{ [cm}^2\text{]}$$

$$A_w = \frac{(3.1416)(0.0418)^2}{4}, \text{ [cm}^2\text{]}$$

$$A_w = 0.00137, \text{ [cm}^2\text{]}$$

From the Wire Table, in Chapter 4, Number 26 has a bare wire area of 0.001280 centimeters. This will be the minimum wire size used in this design. If the design requires more wire area to meet the specification, then, the design will use a multifilar of #26. Listed Below are #27 and #28, just in case #26 requires too much rounding off.

Wire AWG	Bare Area	Area Ins.	Bare/Ins.	$\mu\Omega/\text{cm}$
#26	0.001280	0.001603	0.798	1345
#27	0.001021	0.001313	0.778	1687
#28	0.0008046	0.0010515	0.765	2142

Step No. 1 Calculate the transformer output power, P_o .

$$P_o = I_o(V_o + V_d), \text{ [watts]}$$

$$P_o = 5(5 + 1), \text{ [watts]}$$

$$P_o = 30, \text{ [watts]}$$

Step No. 2 Calculate the input power, P_{in} .

$$P_{in} = \frac{P_o(1.1)}{\eta}, \text{ [watts]}$$

$$P_{in} = \frac{30(1.1)}{(0.98)}, \text{ [watts]}$$

$$P_{in} = 33.67, \text{ [watts]}$$

Step No. 3 Calculate the electrical coefficient, K_e .

$$K_e = 0.145 f^2 \Delta B^2 (10^{-4})$$

$$K_e = 0.145 (100,000)^2 (0.1)^2 (10^{-4})$$

$$K_e = 1450$$

Step No. 4 Calculate the core geometry, K_g .

$$K_g = \frac{P_{in} D_{max}}{\alpha K_e}, \quad [\text{cm}^5]$$

$$K_g = \frac{(33.67)(0.5)}{(0.5)(1450)}, \quad [\text{cm}^5]$$

$$K_g = 0.0232, \quad [\text{cm}^5]$$

When operating at high frequencies, the engineer has to review the window utilization factor, K_u . When using small bobbin ferrites, the ratio of the bobbin winding area to the core window area is only about 0.6. Operating at 100kHz and having to use a #26 wire, because of the skin effect, the ratio of the bare copper area to the total area is 0.78. Therefore, the overall window utilization, K_u , is reduced. To return the design back to the norm, the core geometry, K_g , is to be multiplied by 1.35, and then, the current density, J , is calculated, using a window utilization factor of 0.29.

$$K_g = 0.0232 (1.35), \quad [\text{cm}^5]$$

$$K_g = 0.0313, \quad [\text{cm}^5]$$

Step No. 5 Select a EPC core from Chapter 3, comparable in core geometry K_g .

Core number	EPC-30
Manufacturer	TDK
Magnetic material	PC44
Magnetic path length , MPL.....	8.2 cm
Window height, G	2.6 cm
Core weight, W_{tfe}	23 grams
Copper weight, W_{tcu}	22 grams
Mean length turn, MLT	5.5 cm
Iron area, A_c	0.61 cm ²
Window area, W_a	1.118 cm ²
Area product, A_p	0.682 cm ⁴
Core geometry, K_g	0.0301 cm ⁵
Surface area, A_t	31.5 cm ²
Millihenrys per 1000 turns, AL	1570

Step No. 6 Calculate the number of primary turns, N_p .

$$N_p = \frac{V_{in(\min)} D_{(\max)} (10^4)}{f A_c \Delta B}, \quad [\text{turns}]$$

$$N_p = \frac{(22)(0.5)(10^4)}{(100,000)(0.61)(0.1)}, \quad [\text{turns}]$$

$$N_p = 18.0, \quad [\text{turns}]$$

Step No. 7 Calculate the current density, J , using a window utilization, $K_u = 0.29$.

$$J = \frac{2P_{in} \sqrt{D_{(\max)}} (10^4)}{f A_c \Delta B W_a K_u}, \quad [\text{amps} / \text{cm}^2]$$

$$J = \frac{2(33.67)(0.707)(10^4)}{(100,000)(0.61)(0.1)(1.118)(0.29)}, \quad [\text{amps} / \text{cm}^2]$$

$$J = 241, \quad [\text{amps} / \text{cm}^2]$$

Step No. 8 Calculate the primary rms current, I_p .

$$I_p = \frac{P_{in}}{V_{in(\min)} \sqrt{D_{(\max)}}}, \quad [\text{amps}]$$

$$I_p = \frac{(33.67)}{(22)(0.707)}, \quad [\text{amps}]$$

$$I_p = 2.16, \quad [\text{amps}]$$

Step No. 9 Calculate the primary bare wire area, $A_{wp(B)}$.

$$A_{wp(B)} = \frac{I_p}{J}, \quad [\text{cm}^2]$$

$$A_{wp(B)} = \frac{2.16}{241}, \quad [\text{cm}^2]$$

$$A_{wp(B)} = 0.00896, \quad [\text{cm}^2]$$

Step No. 10 Calculate the required number of primary strands, NS_p .

$$NS_p = \frac{A_{wp(B)}}{\#26}$$

$$NS_p = \frac{0.00896}{0.00128}$$

$$NS_p = 7$$

Step No. 11 Calculate the primary new $\mu\Omega$ per centimeter.

$$(\text{new}) \mu\Omega / \text{cm} = \frac{\mu\Omega / \text{cm}}{NS_p}$$

$$(\text{new}) \mu\Omega / \text{cm} = \frac{1345}{7}$$

$$(\text{new}) \mu\Omega / \text{cm} = 192$$

Step No. 12 Calculate the primary resistance, R_p .

$$R_p = \text{MLT} (N_p) \left(\frac{\mu\Omega}{\text{cm}} \right) (10^{-6}) \quad [\text{ohms}]$$

$$R_p = (5.5)(18)(192)(10^{-6}) \quad [\text{ohms}]$$

$$R_p = 0.0190, \quad [\text{ohms}]$$

Step No. 13 Calculate the primary copper loss, P_p .

$$P_p = I_p^2 R_p, \quad [\text{watts}]$$

$$P_p = (2.16)^2 (0.019), \quad [\text{watts}]$$

$$P_p = 0.0886, \quad [\text{watts}]$$

Step No. 14 Calculate the secondary turns, N_s .

$$N_s = \frac{N_p (V_o + V_d)}{D_{(\max)} V_{in(\min)}} \left(1 + \frac{\alpha}{100} \right), \quad [\text{turns}]$$

$$N_s = \frac{(18)(5+1)}{(0.5)(22)} \left(1 + \frac{0.5}{100} \right), \quad [\text{turns}]$$

$$N_s = 9.87 \text{ use } 10, \quad [\text{turns}]$$

Step No. 15 Calculate the secondary rms current, I_s .

$$I_s = \frac{I_o}{\sqrt{2}}, \quad [\text{amps}]$$

$$I_s = \frac{5}{1.41}, \quad [\text{amps}]$$

$$I_s = 3.55, \quad [\text{amps}]$$

Step No. 16 Calculate the secondary bare wire area, $A_{ws(B)}$.

$$A_{ws(B)} = \frac{I_s}{J}, \quad [\text{cm}^2]$$

$$A_{ws(B)} = \frac{3.55}{241}, \quad [\text{cm}^2]$$

$$A_{ws(B)} = 0.0147, \quad [\text{cm}^2]$$

Step No. 17 Calculate the required number of secondary strands, NS_s .

$$NS_s = \frac{A_{ws(B)}}{\#26}$$

$$NS_s = \frac{0.0147}{0.00128}$$

$$NS_s = 11.48 \text{ use } 11$$

Step No. 18 Calculate the secondary, new $\mu\Omega$ per centimeter.

$$(\text{new}) \mu\Omega / \text{cm} = \frac{\mu\Omega / \text{cm}}{NS_s}$$

$$(\text{new}) \mu\Omega / \text{cm} = \frac{1345}{11}$$

$$(\text{new}) \mu\Omega / \text{cm} = 122$$

Step No. 19 Calculate the secondary winding resistance, R_s .

$$R_s = \text{MLT} (N_s) \left(\frac{\mu\Omega}{\text{cm}} \right) (10^{-6}) \quad [\text{ohms}]$$

$$R_s = (5.5)(10)(122)(10^{-6}) \quad [\text{ohms}]$$

$$R_s = 0.00671, \quad [\text{ohms}]$$

Step No. 20 Calculate the secondary copper loss, P_s .

$$P_s = I_s^2 R_s, \quad [\text{watts}]$$

$$P_s = (3.55)^2 (0.00671), \quad [\text{watts}]$$

$$P_s = 0.0846, \quad [\text{watts}]$$

Step No. 21 Calculate the total primary and secondary copper loss, P_{cu} .

$$P_{cu} = P_p + P_s, \quad [\text{watts}]$$

$$P_{cu} = 0.0886 + 0.0846, \quad [\text{watts}]$$

$$P_{cu} = 0.173, \quad [\text{watts}]$$

Step No. 22 Calculate the transformer regulation, α .

$$\alpha = \frac{P_{cu}}{P_o} (100), \quad [\%]$$

$$\alpha = \frac{(0.173)}{(30)} (100), \quad [\%]$$

$$\alpha = 0.576, \quad [\%]$$

Step No. 23 Calculate the demag winding inductance, L_{demag} .

$$L_{demag} = L_{1000} N_{demag}^2 (10^{-6}) \quad [\text{mh}]$$

$$L_{demag} = (1570)(18)^2 (10^{-6}) \quad [\text{mh}]$$

$$L_{demag} = 0.509, \quad [\text{mh}]$$

Step No. 24 Calculate the time of, Δt . See Figure 14-6.

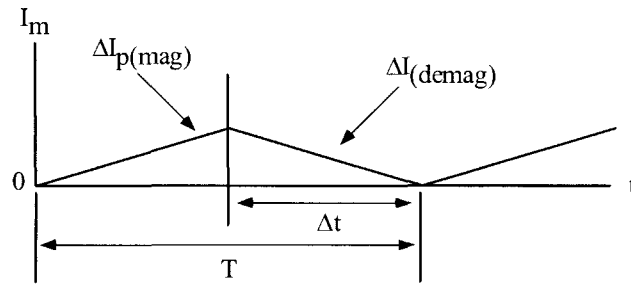


Figure 14-6. Magnetizing Current Waveform.

$$\Delta t = T D_{(\max)}, \quad [\text{seconds}]$$

$$T = \frac{1}{f}, \quad [\text{seconds}]$$

$$T = \frac{1}{100,000}, \quad [\text{seconds}]$$

$$T = 10(10^{-6}) \quad [\text{seconds}]$$

$$\Delta t = (10(10^{-6}))(0.5), \quad [\text{seconds}]$$

$$\Delta t = 5(10^{-6}) \quad [\text{seconds}]$$

Step No. 25 Calculate the demag, winding delta current, ΔI_{demag} .

$$\Delta I_{demag} = \frac{V_{in} \Delta t}{L_{demag}}, \text{ [amps]}$$

$$\Delta I_{demag} = \frac{(22)(5(10^{-6}))}{(509(10^{-6}))}, \text{ [amps]}$$

$$\Delta I_{demag} = 0.217, \text{ [amps]}$$

Step No. 26 Calculate the demag, winding rms current, I_{demag} . This is the rms equation for a saw tooth current.

$$I_{demag} = \Delta I \sqrt{\frac{D_{(max)}}{3}}, \text{ [amps]}$$

$$I_{demag} = (0.217)(0.408), \text{ [amps]}$$

$$I_{demag} = 0.089, \text{ [amps]}$$

Step No. 27 Calculate the required demag, wire area, $A_{w(demag)}$.

$$A_{w(demag)} = \frac{I_{demag}}{J}, \text{ [cm}^2\text{]}$$

$$A_{w(demag)} = \frac{0.089}{241}, \text{ [cm}^2\text{]}$$

$$A_{w(demag)} = 0.000369, \approx \#31 \text{ use a } \#26$$

Step No. 28 Calculate the window utilization, K_u .

$$K_u = \frac{N A_{w(B)(\#26)}}{W_a}$$

$$N = (N_p NS_p) + (N_s NS_s) + (N_{demag} NS_{demag})$$

$$N = (18)(7) + (10)(11) + (18)(1)$$

$$N = 254$$

$$K_u = \frac{(254)(0.00128)}{1.118}$$

$$K_u = 0.291$$

Step No. 29 Calculate the milliwatts per gram, mW/g.

$$\begin{aligned} \text{mW/g} &= 0.000318(f)^{1.51}(B_{ac})^{2.747} \\ \text{mW/g} &= 0.000318(100000)^{1.51}(0.05)^{2.747} \\ \text{mW/g} &= 3.01 \end{aligned}$$

Step No. 30 Calculate the core loss, P_{fe} .

$$\begin{aligned} P_{fe} &= (mW / g)(W_{tfe})(10^{-3}) \quad [\text{watts}] \\ P_{fe} &= (3.01)(23)(10^{-3}) \quad [\text{watts}] \\ P_{fe} &= 0.069, \quad [\text{watts}] \end{aligned}$$

Step No. 31 Calculate the total loss, P_{Σ} .

$$\begin{aligned} P_{\Sigma} &= P_{cu} + P_{fe}, \quad [\text{watts}] \\ P_{\Sigma} &= (0.173) + (0.069), \quad [\text{watts}] \\ P_{\Sigma} &= 0.242, \quad [\text{watts}] \end{aligned}$$

Step No. 32 Calculate the watts per unit area, ψ .

$$\begin{aligned} \psi &= \frac{P_{\Sigma}}{A_t}, \quad [\text{watts} / \text{cm}^2] \\ \psi &= \frac{(0.242)}{(31.5)}, \quad [\text{watts} / \text{cm}^2] \\ \psi &= 0.0077, \quad [\text{watts} / \text{cm}^2] \end{aligned}$$

Step No. 33 Calculate the temperature rise, T_r .

$$\begin{aligned} T_r &= 450(\psi)^{(0.826)}, \quad [^{\circ}\text{C}] \\ T_r &= 450(0.0077)^{(0.826)}, \quad [^{\circ}\text{C}] \\ T_r &= 8.08, \quad [^{\circ}\text{C}] \end{aligned}$$

Forward Converter Output Inductor Design

Part 2 is designing the output inductor, L1, as shown in Figure 14-7. The output filter inductor for switch-mode power supplies, (SMPS), probably has been designed more times than any other single component. Presented here is a straight-forward approach for selecting the core and the proper wire size to meet the specification.

The losses in the magnetic material will increase significantly when the converter is operating at a higher frequency. However, the core loss in the output inductor of a switching regulator is much lower compared to the core loss in the main converter transformer. The core loss in the output inductor is caused by the change in current or ΔI , which induces a change in flux, as shown in Figure 14-7.

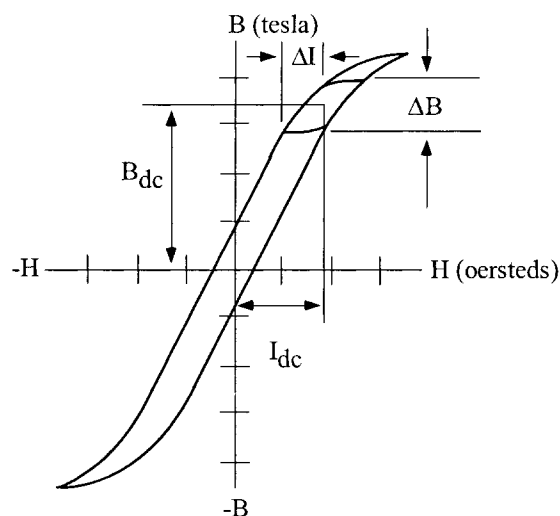


Figure 14-7. Typical output inductor BH Loop.

The single-ended, forward converter schematic is shown in Figure 14-8. This topology is appealing to engineers for its simplicity and parts' count. The output filter circuit, shown in Figure 14-8, has three current probes. These current probes monitor the three basic currents in a switch mode, converter output filter. Current probe A monitors the transformer's secondary current. Current probe B monitors the commutating current through CR3. Current probe C monitors the current through the output inductor, L1.

The typical secondary and filter waveforms of the forward converter are shown in Figure 14-8. The waveforms are shown with the converter operating at a 0.5 duty ratio. The applied voltage, V_1 , to the filter, is shown in Figure (14-9-A). The transformer's secondary current is shown in Figure (14-9-B). The commutating current flowing through, CR3, is shown in Figure (14-9-C). The commutating current is the result of Q1 being turned off, and the field in, L1, collapsing, producing the commutating current. The current flowing through L1 is shown in Figure (14-9-D). The current flowing through L1 is the sum of the currents in Figure (14-9-B) and (14-9-C).

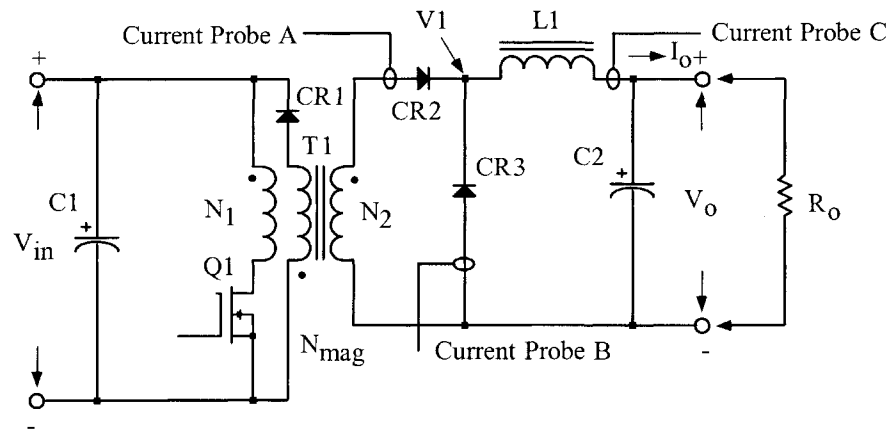


Figure 14-8. Typical single-ended, forward converter.

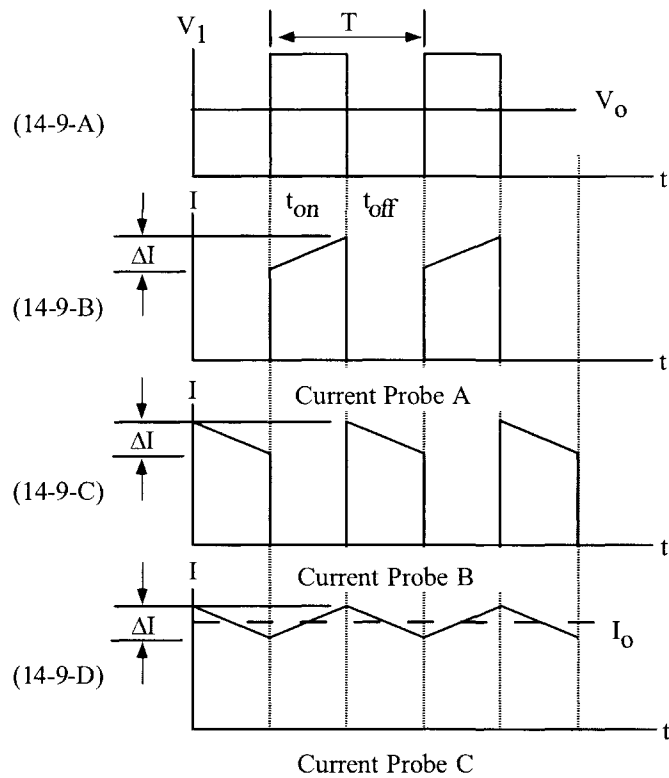


Figure 14-9. Typical forward converter waveforms, operating at a 0.5 duty ratio.

The critical inductance current is shown in Figure (14-10-B). The critical inductance current is when the ratio of the delta current to the output load current is equal to $2 = \Delta I / I_o$. If the output load current is allowed to go beyond this point, the current will become discontinuous, as shown in Figure (14-10-D). The applied voltage, V_1 , will have ringing at the level of the output voltage, as shown in Figure (14-10-C). When the current in the output inductor becomes discontinuous, as shown in Figure (14-10-D), the response time for a step load becomes very poor.

When designing multiple output converters, the slaved outputs should never have the current in the inductor go discontinuous or to zero. If the current goes to zero, a slaved output voltage will rise to the value of V_1 . If the current is allowed to go to zero, then, there is not any potential difference between the input and output voltage of the filter. Then the output voltage will rise to equal the peak input voltage.

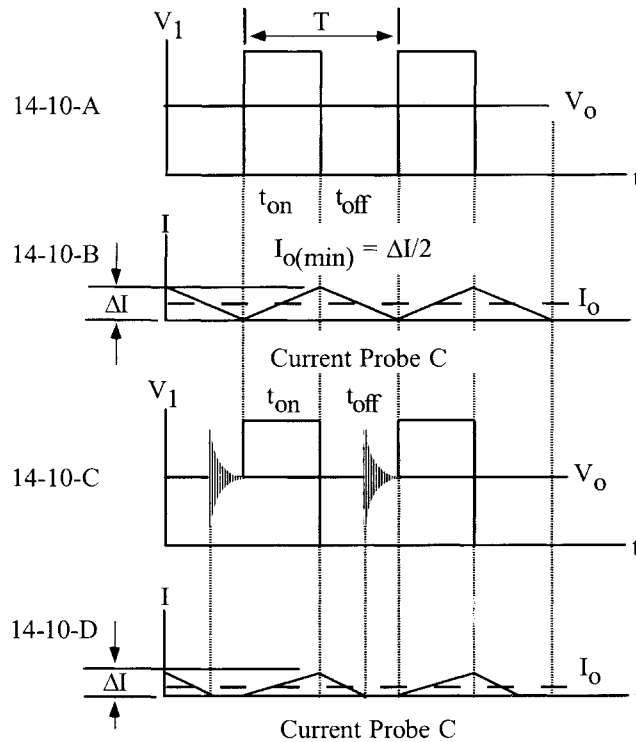


Figure 14-10. Forward converter; output filter inductor goes from critical to discontinuous operation.

Output Inductor Design Using the Core Geometry, K_g , Approach

The following information is the design specification for a forward converter, 30 watt output filter design, operating at 100kHz, using the K_g core geometry approach. For a typical design example, assume an output filter circuit, as shown in Figure 14-1, with the following specifications:

1. Frequency, f = 100kHz
2. Output voltage, V_o = 5 volts
3. Output current, $I_{o(max)}$ = 5.0 amps
4. Output current, $I_{o(max)}$ = 0.5 amps
5. Delta current, ΔI = 1.0 amps
6. Input voltage, $V_{1(max)}$ = 19 volts
7. Input voltage, $V_{1(min)}$ = 12 volts
8. Regulation, α = 1.0%

9. Output power $(V_o + V_d) (I_{o(max)})$, P_o = 30 watts
10. Operating flux density, B_{pk} = 0.3 tesla
11. Window utilization, K_u = 0.4
12. Diode voltage drop, V_d = 1.0 volt

This design procedure will work equally well with all of the various powder cores. Care must be taken regarding maximum flux density with different materials and core loss.

The skin effect on an inductor is the same as a transformer. The main difference is that the ac flux is much lower and does not require the use of the same maximum wire size. The ac flux is caused by the delta current, ΔI , and is normally only a fraction of the dc flux. In this design the ac current and the dc current will be treated the same.

At this point, select a wire so that the relationship between the ac resistance and the dc resistance is 1:

$$\frac{R_{ac}}{R_{dc}} = 1$$

The skin depth, ϵ , in centimeters, is:

$$\epsilon = \frac{6.62}{\sqrt{f}}, \quad [\text{cm}]$$

$$\epsilon = \frac{6.62}{\sqrt{100,000}}, \quad [\text{cm}]$$

$$\epsilon = 0.0209, \quad [\text{cm}]$$

Then, the wire diameter, D_w , is:

$$D_w = 2(\epsilon), \quad [\text{cm}]$$

$$D_w = 2(0.0209), \quad [\text{cm}]$$

$$D_w = 0.0418, \quad [\text{cm}]$$

Then, the bare wire area, A_w , is:

$$A_w = \frac{\pi(D_w)^2}{4}, \quad [\text{cm}^2]$$

$$A_w = \frac{(3.1416)(0.0418)^2}{4}, \quad [\text{cm}^2]$$

$$A_w = 0.00137, \quad [\text{cm}^2]$$

From the Wire Table in Chapter 4, Number 27 has a bare wire area of 0.001021 centimeters. This will be the minimum wire size used in this design. If the design requires more wire area to meet the specification, then the design will use a multifilar of #26. Listed Below are #27 and #28, just, in case #26 requires too much rounding off.

Wire AWG	Bare Area	Area Ins.	Bare/Ins.	$\mu\Omega/\text{cm}$
#26	0.001280	0.001603	0.798	1345
#27	0.001021	0.001313	0.778	1687
#28	0.0008046	0.0010515	0.765	2142

Step No. 1 Calculate the total period, T.

$$T = \frac{1}{f}, \text{ [seconds]}$$

$$T = \frac{1}{100,000}, \text{ [seconds]}$$

$$T = 10, \text{ [\mu sec]}$$

Step No. 2 Calculate the minimum duty ratio, D_{\min} .

$$D_{\min} = \frac{V_o}{V_{1\max}}$$

$$D_{\min} = \frac{5}{19}$$

$$D_{\min} = 0.263$$

Step No. 3 Calculate the required inductance, L.

$$L = \frac{T(V_o + V_d)(1 - D_{\min})}{\Delta I}, \text{ [henrys]}$$

$$L = \frac{(10 \times 10^{-6})(5.0 + 1.0)(1 - 0.263)}{(1.0)}, \text{ [henrys]}$$

$$L = 44.2, \text{ [\mu h]}$$

Step No. 4 Calculate the peak current, I_{pk} .

$$I_{pk} = I_{o(\max)} + \left(\frac{\Delta I}{2}\right), \text{ [amps]}$$

$$I_{pk} = (5.0) + \left(\frac{1.0}{2}\right), \text{ [amps]}$$

$$I_{pk} = 5.5, \text{ [amps]}$$

Step No. 5 Calculate the energy-handling capability in, watt-seconds.

$$\text{Energy} = \frac{LI_{pk}^2}{2}, \text{ [watt-seconds]}$$

$$\text{Energy} = \frac{(44.2 \times 10^{-6})(5.5)^2}{2}, \text{ [watt-seconds]}$$

$$\text{Energy} = 0.000668, \text{ [watt-seconds]}$$

Step No. 6 Calculate the electrical conditions, K_e .

$$K_e = 0.145 P_o B_m^2 \times 10^{-4}$$

$$K_e = (0.145)(30)(0.3)^2 \times 10^{-4}$$

$$K_e = 0.0000392$$

Step No. 7 Calculate the core geometry, K_g .

$$K_g = \frac{(\text{Energy})^2}{K_e \alpha} \text{ [cm}^5\text{]}$$

$$K_g = \frac{(0.000668)^2}{(0.0000392)(1.0)} \text{ [cm}^5\text{]}$$

$$K_g = 0.01138 \text{ [cm}^5\text{]}$$

Step No. 8 Select, from Chapter 4, a MPP powder core, comparable in core geometry, K_g .

Core number	MP-55059-A2
Manufacturer	Magnetics
Magnetic path length, MPL	= 5.7 cm
Core weight, W_{tfe}	= 16.0 grams
Copper weight, W_{tcu}	= 15.2 grams
Mean length turn, MLT	= 3.2 cm
Iron area, A_c	= 0.331 cm ²
Window Area, W_a	= 1.356 cm ²
Area Product, A_p	= 0.449 cm ⁴
Core geometry, K_g	= 0.0184 cm ⁵
Surface area, A_t	= 28.6 cm ²
Permeability, μ	= 60
Millihenrys per 1000 turns, AL.....	= 43

Step No. 9 Calculate the number of turns, N.

$$N = 1000 \sqrt{\frac{L_{(new)}}{L_{(1000)}}}, \quad [\text{turns}]$$

$$N = 1000 \sqrt{\frac{0.0442}{43}}, \quad [\text{turns}]$$

$$N = 32, \quad [\text{turns}]$$

Step No. 10 Calculate the rms current, I_{rms} .

$$I_{rms} = \sqrt{I_{o(max)}^2 + \Delta I^2}, \quad [\text{amps}]$$

$$I_{rms} = \sqrt{(5.0)^2 + (1.0)^2}, \quad [\text{amps}]$$

$$I_{rms} = 5.1, \quad [\text{amps}]$$

Step No. 11 Calculate the current density, J, using a window utilization, $K_u = 0.4$.

$$J = \frac{NI}{W_a K_u}, \quad [\text{amps-per-cm}^2]$$

$$J = \frac{(32)(5.1)}{(1.36)(0.4)}, \quad [\text{amps-per-cm}^2]$$

$$J = 300, \quad [\text{amps-per-cm}^2]$$

Step No. 12 Calculate the required permeability, $\Delta\mu$.

$$\Delta\mu = \frac{B_{pk} (\text{MPL})(10^4)}{0.4\pi W_a J K_u}, \quad [\text{perm}]$$

$$\Delta\mu = \frac{(0.3)(5.7)(10^4)}{(1.26)(1.36)(300)(0.4)}, \quad [\text{perm}]$$

$$\Delta\mu = 83.1, \quad \text{use } 60 \quad [\text{perm}]$$

Step No. 13 Calculate the peak flux density, B_{pk} .

$$B_{pk} = \frac{0.4\pi NI_{pk} \mu_r (10^{-4})}{(\text{MPL})}, \quad [\text{tesla}]$$

$$B_{pk} = \frac{(1.26)(32)(5.1)(60)(10^{-4})}{(5.7)}, \quad [\text{tesla}]$$

$$B_{pk} = 0.233, \quad [\text{tesla}]$$

Step No. 14 Calculate the required bare wire area, $A_{w(B)}$.

$$A_{w(B)} = \frac{I_{rms}}{J}, \quad [\text{cm}^2]$$

$$A_{w(B)} = \frac{5.1}{300}, \quad [\text{cm}^2]$$

$$A_{w(B)} = 0.017, \quad [\text{cm}^2]$$

Step No. 15 Calculate the required number of strands, S_n .

$$S_n = \frac{A_{w(B)}}{\#26}, \quad [\text{strands}]$$

$$S_n = \frac{0.017}{0.00128}, \quad [\text{strands}]$$

$$S_n = 13, \quad [\text{strands}]$$

Step No. 16 Calculate the new, $\mu\Omega$, per centimeter.

$$(\text{new}) \mu\Omega / \text{cm} = \frac{\mu\Omega / \text{cm}}{S_n}$$

$$(\text{new}) \mu\Omega / \text{cm} = \frac{1345}{13}$$

$$(\text{new}) \mu\Omega / \text{cm} = 103$$

Step No. 17 Calculate the winding resistance, R .

$$R = (\text{MLT})N \left(\frac{\mu\Omega}{\text{cm}} \right) (10^{-6}), \quad [\text{ohms}]$$

$$R = (3.2)(32)(103)(10^{-6}), \quad [\text{ohms}]$$

$$R = 0.0105, \quad [\text{ohms}]$$

Step No. 18 Calculate the winding copper loss, P_{cu} .

$$P_{cu} = I_{rms}^2 R, \quad [\text{watts}]$$

$$P_{cu} = (5.1)^2 (0.0105), \quad [\text{watts}]$$

$$P_{cu} = 0.273, \quad [\text{watts}]$$

Step No. 19 Calculate the magnetizing force in oersteds, H .

$$H = \frac{0.4\pi NI_{pk}}{\text{MPL}}, \quad [\text{oersteds}]$$

$$H = \frac{(1.26)(32)(5.5)}{5.7}, \quad [\text{oersteds}]$$

$$H = 38.9, \quad [\text{oersteds}]$$

Step No. 20 Calculate the ac flux density in tesla, B_{ac} .

$$B_{ac} = \frac{0.4\pi N \left(\frac{\Delta I}{2} \right) \mu_r (10^{-4})}{MPL}, \quad [\text{tesla}]$$

$$B_{ac} = \frac{(1.26)(32)(0.5)(60)(10^{-4})}{(5.7)}, \quad [\text{tesla}]$$

$$B_{ac} = 0.0212, \quad [\text{tesla}]$$

Step No. 21 Calculate the regulation, α , for this design.

$$\alpha = \frac{P_{cu}}{P_o}(100), \quad [\%]$$

$$\alpha = \frac{(0.273)}{(30)}(100), \quad [\%]$$

$$\alpha = 0.91, \quad [\%]$$

Step No. 22 Calculate the watts per kilogram, WK, using MPP 60 perm powder cores coefficients, shown in Chapter 2.

$$WK = 0.551(10^{-2})f^{(1.23)}B_{ac}^{(2.12)}, \quad [\text{watts-per-kilogram}]$$

$$WK = 0.551(10^{-2})(100000)^{(1.23)}(0.0212)^{(2.12)}, \quad [\text{watts-per-kilogram}]$$

$$WK = 2.203, \quad [\text{watts-per-kilogram}]$$

Step No. 23 Calculate the core loss, P_{fe} .

$$P_{fe} = \left(\frac{\text{milliwatts}}{\text{gram}} \right) W_{fe} (10^{-3}), \quad [\text{watts}]$$

$$P_{fe} = (2.203)(16)(10^{-3}), \quad [\text{watts}]$$

$$P_{fe} = 0.0352, \quad [\text{watts}]$$

Step No. 24 Calculate the total loss, P_{Σ} , core, P_{fe} , and copper, P_{cu} , in watts.

$$P_{\Sigma} = P_{fe} + P_{cu}, \quad [\text{watts}]$$

$$P_{\Sigma} = (0.0352) + (0.273), \quad [\text{watts}]$$

$$P_{\Sigma} = 0.308, \quad [\text{watts}]$$

Step No. 25 Calculate the watt density, ψ .

$$\psi = \frac{P_s}{A_t}, \text{ [watts-per-cm}^2\text{]}$$

$$\psi = \frac{(0.308)}{(28.6)}, \text{ [watts-per-cm}^2\text{]}$$

$$\psi = 0.0108, \text{ [watts-per-cm}^2\text{]}$$

Step No. 26 Calculate the temperature rise, in $^{\circ}\text{C}$.

$$T_r = 450(\psi)^{(0.826)}, \text{ [}^{\circ}\text{C]}$$

$$T_r = 450(0.0108)^{(0.826)}, \text{ [}^{\circ}\text{C]}$$

$$T_r = 10.7, \text{ [}^{\circ}\text{C]}$$

Step No. 27 Calculate the window utilization, K_u .

$$K_u = \frac{NS_n A_{w(B)}}{W_a}$$

$$K_u = \frac{(32)(13)(0.00128)}{(1.356)}$$

$$K_u = 0.393$$

Chapter 15

Input Filter Design

Table of Contents

1. Introduction.....	
2. Capacitor	
3. Inductor	
4. Oscillation	
5. Applying Power	
6. Resonant Charge	
7. Input Filter Inductor Design Procedure	
8. Input Filter Design Specification	
9. References	

Introduction

Today, almost all modern equipment uses some sort of power conditioning. There are a lot of different circuit topologies used. When you get to the bottom line, all power conditioning requires some kind of an input filter. The input LC filter has become very critical in its design and must be designed not only for EMI, but also for system stability, and for the amount of ac ripple current drawn from the source.

The input voltage supplied to the equipment is also supplied to other users. For this reason, there is a specification requirement regarding the amount of ripple current seen at the source, as shown in Figure 15-1. Ripple currents generated by the user induce a ripple voltage, V_z , across the source impedance. This ripple voltage could impede the performance of other equipment connected to the same bus.

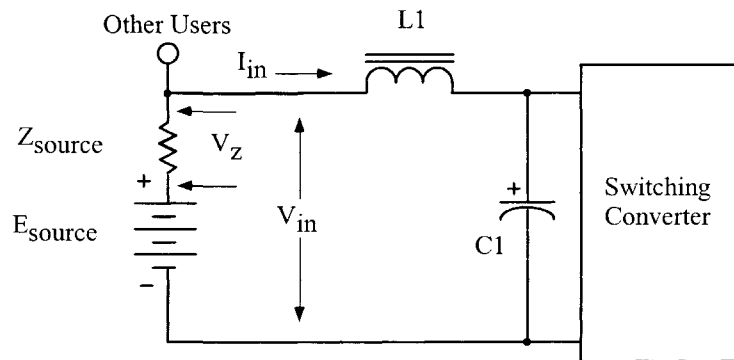


Figure 15-1. Simple, LC, Input Filter.

Capacitor

Switching regulators have required the engineer to put a significantly more analytical effort into the design of the input filter. The current pulse, induced by the switching regulator, has had the most impact on the input capacitor. These current pulses required the use of high quality capacitors with low ESR. The waveforms, induced by the switching regulator, are shown in Figure 15-2. In the input inductor, $L1$, peak-peak ripple current is I_L . In the capacitor, $C1$, peak-peak, ripple current is I_C . In the capacitor, $C1$, peak-peak, ripple voltage is, ΔV_C . The equivalent circuit for the capacitor is shown in Figure 15-3. The voltage, ΔV_C , developed across the capacitor, is the sum of two components, the equivalent series resistance, (ESR), and the reactance of the capacitor.

The voltage developed across the equivalent series resistance, (ESR), is:

$$V_{CR} = I_C (\text{ESR}), \text{ [volts] [15-1]}$$

The voltage developed across the capacitance is:

$$\Delta V_{CC} = I_C \left(\frac{(t_{on})(t_{off})}{(C1)(T)} \right), \text{ [volts] [15-2]}$$

The sum of the two voltages, ΔV_{CR} and ΔV_{CC} , is:

$$\Delta V_C = \Delta V_{CR} + \Delta V_{CC}, \text{ [volts] [15-3]}$$

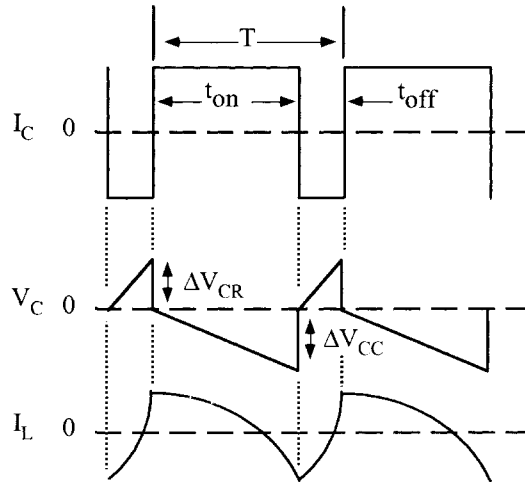


Figure 15-2. Typical Voltage, Current Waveforms.

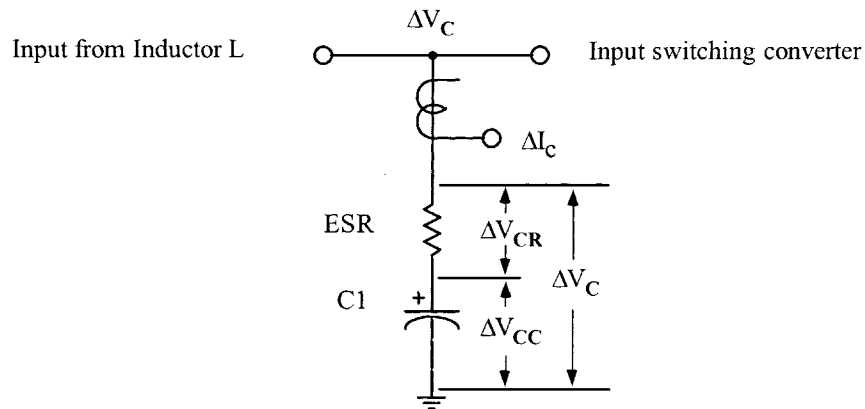


Figure 15-3. Capacitor, Individual Ripple, Components.

Inductor

The input filter inductor is basically a straight-forward design. There are four parameters required to achieve a good design: (1) required inductance, (2) dc current, (3) dc resistance, and (4) temperature rise. The requirement for the input inductor is to provide a low ac ripple current to the source. The low ac ripple current in the inductor produces an ac flux at a magnitude of about 0.025 tesla. This resulting low ac flux will keep the core loss to a minimum. The input inductor losses will normally be 80 to 90% copper. A high flux magnetic material is ideally suited in this application. Operating with a high dc flux and a low ac flux, silicon, with its high flux density of 1.6 teslas, will produce the smallest size, as shown in Table 15-1.

Table 15-1. Most Commonly Used Input Filter Material.

Magnetic Material Properties		
Material	Operating Flux, B, tesla	Permeability μ_i
Silicon	1.5-1.8	1.5K
Permalloy Powder	0.3	14-550
Iron Power	1.2-1.4	35-90
Ferrite	0.3	1K-15K

Oscillation

The input filter can affect the stability of the associated switching converter. The stability problem results from an interaction between the output impedance of the input filter and the input impedance of the switching converter. Oscillation occurs when the combined positive resistance of the LC filter, and power source exceed the negative dynamic resistance of the regulator's dc input. To prevent oscillation, the capacitor's ESR, and the inductor's resistance must provide sufficient damping. Oscillation will not occur when:

$$\left(\frac{\eta (V_{in})^2}{P_o} \right) > \left(\frac{L}{C + (R_L + R_s)(ESR)} \right) \left(\frac{R_L + R_s}{(R_L + R_s) + (ESR)} \right) \quad [15-4]$$

Where η is the switching converter efficiency, $V_{in(max)}$ is the input voltage; P_o is the output power in watts, L is the input inductor in henrys; where, C , is the filter capacitor in farads, R_L is inductor series resistance in ohms; R_s is the source resistance in ohms, and R_d (ESR), is the equivalent series resistance in ohms. If additional damping is required, it can be done, by increasing the R_d (ESR), and/or R_L . See Figure 15-4. The series resistance, R_d , lowers the Q of the filter and kills the potential Oscillation.

Applying Power

The inrush current has always been a problem with this simple LC input filter. When a step input is applied, such as a relay or switch S1 as shown in Figure 15-5, there is always a high inrush current.

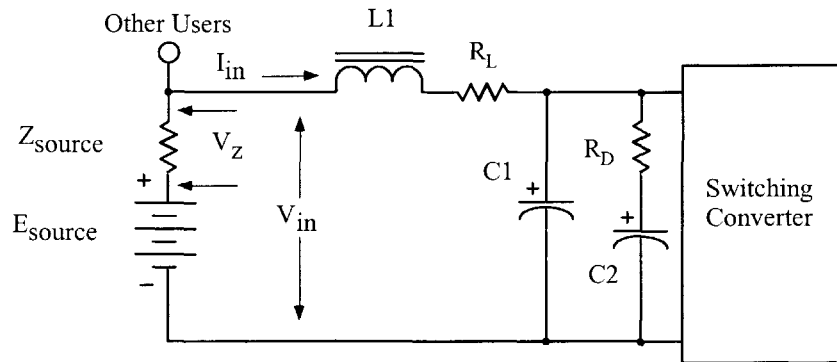


Figure 15-4. Input Filter, with Additional Damping.

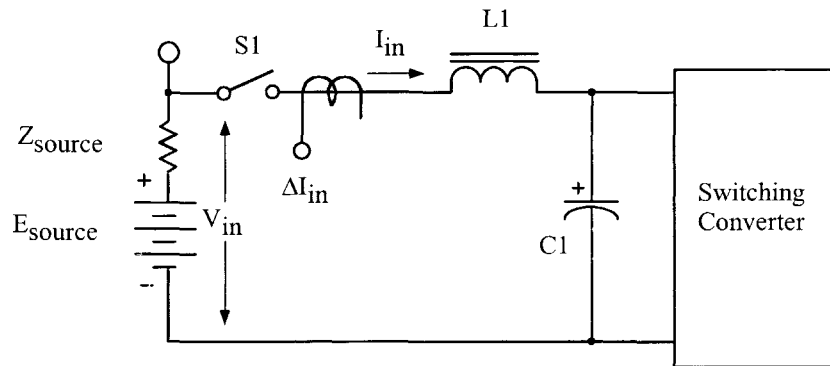


Figure 15-5. Input Filter Inrush Current Measurement.

When S1 is closed, the full input voltage, V_{in} , is applied directly across the input inductor, L1, because C1 is discharged. The applied input voltage, V_{in} , (volt-seconds), to the input inductor, L1, and the dc current, (amp-turns), flowing through it is enough to saturate the core. The inductor, L1, is normally designed, using the upper limits of the flux density for minimum size. There are two types of core configurations commonly used for input inductor design: powder cores and gapped cores. Some engineers prefer to design around powder cores because they are simple and less hassle, while others design using gapped cores. It is strictly a game of trade-offs. Tests were performed using three different core materials: (1) powder core, (2) ferrite core, and (3) iron alloy. All three materials were designed to have the same inductance and the same dc resistance. The three-inductor designs were tested to compare the inrush current under the same conditions. The inrush current, ΔI , for all three materials is shown in Figure 15-6, using the test circuit, shown in Figure 15-5.

As, shown in Figure 15-6, the inrush current for all three test inductors has about the same general shape and amplitude. The changes in permeability, with dc bias, for both gapped and powder cores are shown in Figure 15-7. Gapped cores have a definitely sharper knee while the powder cores roll off more gradually. The advantage in using a gapped core over the powder core is the ability to use the full flux capacity of the core up to the knee, before the permeability starts to droop.

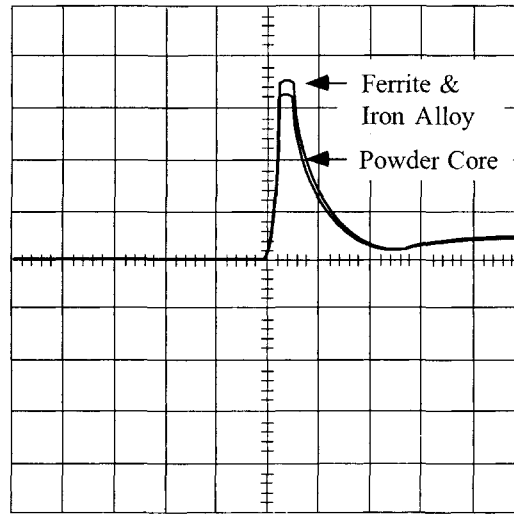


Figure 15-6. Typical, Inrush Current for a Simple Input.

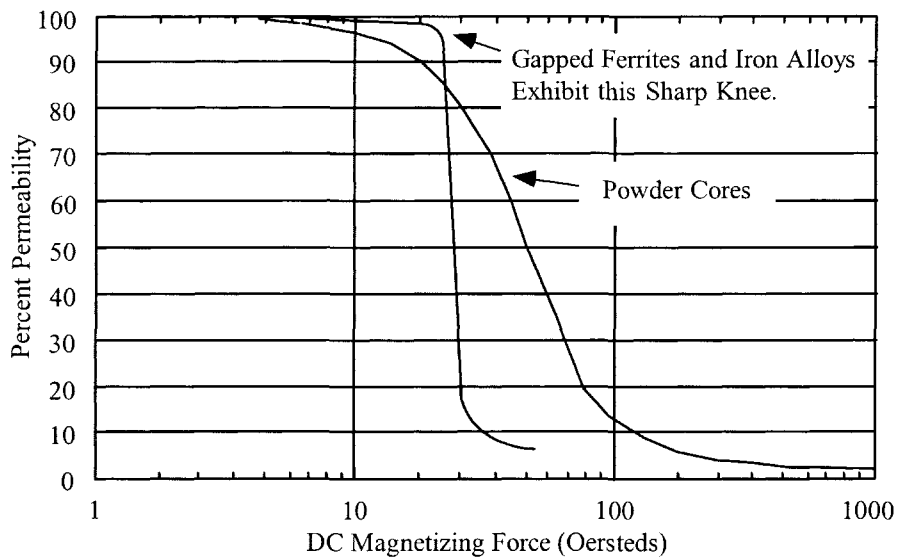


Figure 15-7. Comparing Gapped and Powder Cores, Permeability Change with DC Bias.

Resonant Charge

Most all types of electronic equipment are energized by either a switch or relay. This type of turn-on goes for spacecraft, aircraft, computer, medical equipment, and automobiles. There are some power sources that require some type of current limiting that does not follow the general rule. If the input voltage is applied via a switch or relay to an input filter, as shown in Figure 15-8, a resonant charge condition will develop with L1 and C1. The resulting resonant charge with L1 and C1 could put a potential on C1 that could be as much as twice the applied input voltage, as shown in Figure 15-9. The voltage rating of C1 must be high enough to sustain this peak voltage without damage. The oscillating voltage is applied to the switching converter.

A simple way to dampen this oscillation is to place one or two diodes across the input choke, as shown in Figure 15-10. The reason for two diodes is the ripple voltage, V_c , might be greater than the threshold voltage of the diode. As the voltage across C1 rises above the input voltage, V_{in} , due to the oscillation diodes, CR1 and CR2 will become forward-biased, clamping the voltage across C1 to two diode drops above the input voltage, V_{in} , as shown in Figure 15-11.

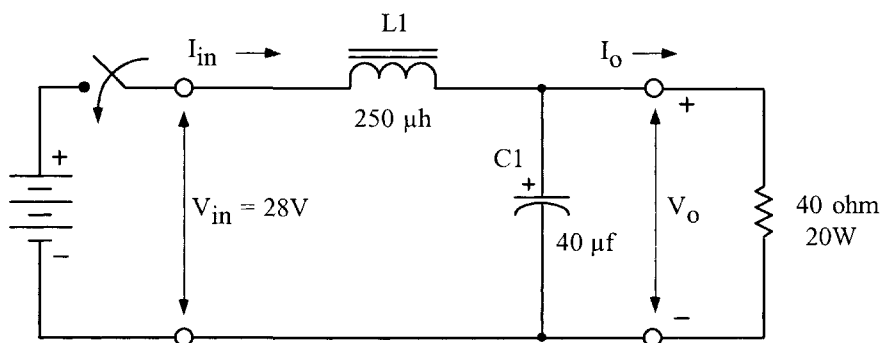


Figure 15-8. Typical, Simple LC, Input Filter.

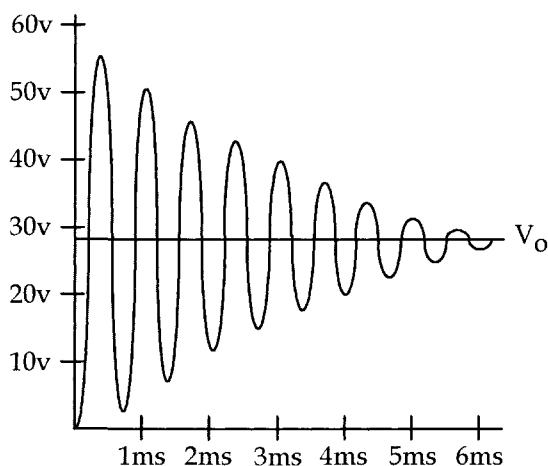


Figure 15-9. Resonating Voltage, across Capacitor, C1.

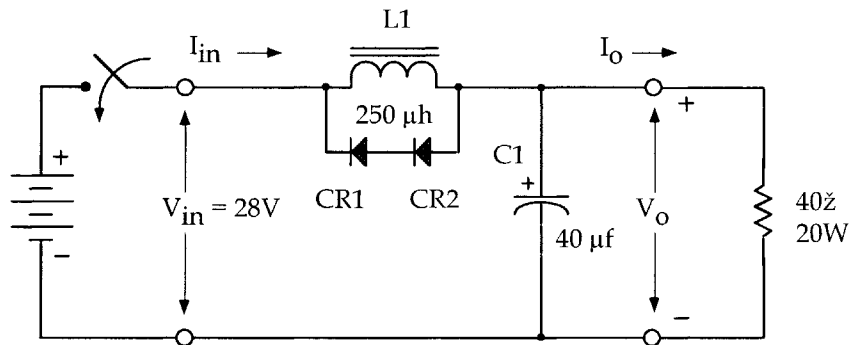


Figure 15-10. Input Inductor with Clamp Diodes.

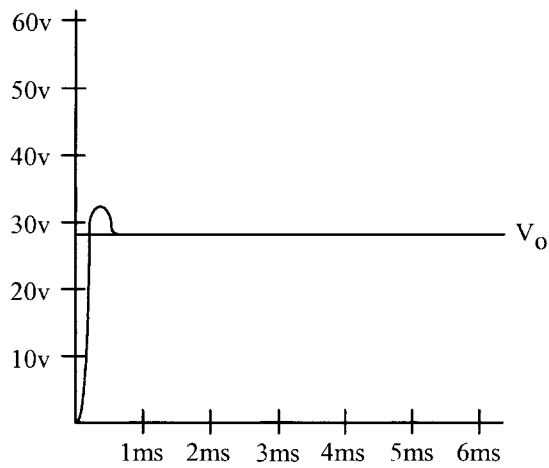


Figure 15-11. DC Voltage Across C1, with the Clamp Diodes.

Input Filter Inductor Design Procedure

The input filter inductor, L1, for this design is shown in Figure 15-12.

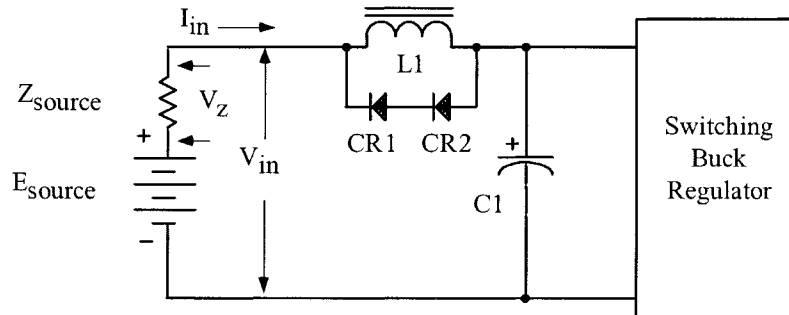


Figure 15-12. Input Filter Circuit.

The ac voltages and currents associated with the input capacitor, C1, are shown in Figure 15-13.

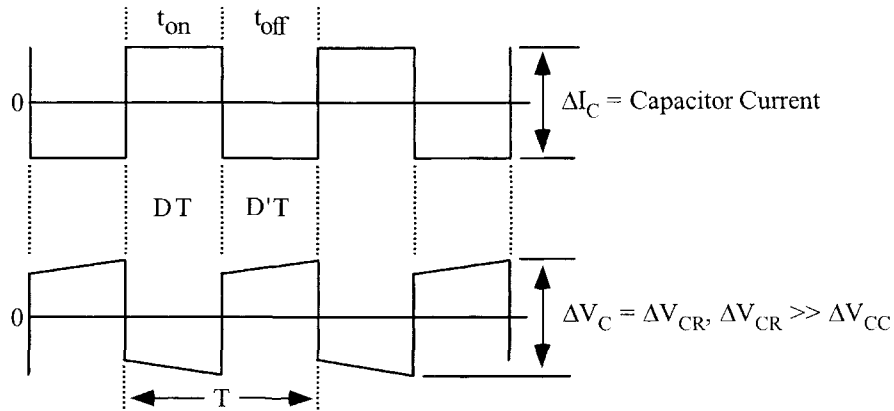


Figure 15-13. Input Capacitor Voltage and Current Ripple.

The ac voltages and currents impressed on the input capacitor, C1, are defined in Figure 15-14.

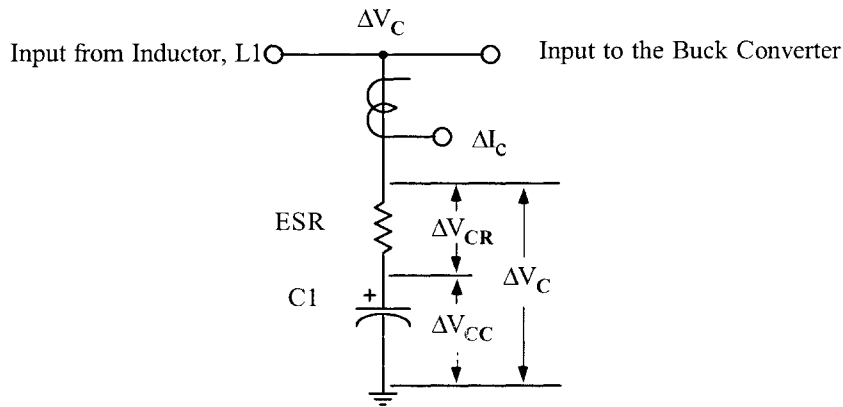


Figure 15-14. Defining the Input Capacitor Voltage and Current Ripple.

The components of the inductor current, due to, ΔV_{CR} and ΔV_{CC} , are:

ΔV_{CR} = Peak to Peak component due to capacitor, ESR.

ΔV_{CC} = Peak to Peak component due to capacitor.

ΔI_{LR} = Component of the inductor ripple current developed by ΔV_{CR} .

ΔI_{LC} = Component of the inductor ripple current developed by ΔV_{CC} .

$$\Delta I_{LR} = \left(\frac{\Delta V_{CR}}{L} \right) (DD'T), \quad [\text{amps}] \quad [15-5]$$

$$\Delta I_{LC} = \left(\frac{\Delta V_{CC}}{2L} \right) \left(\frac{T}{4} \right), \quad [\text{amps}]$$

It will be considered that, ΔI_{LR} , dominates because of the capacitor, ESR, so:

$$\Delta I_{LR} = \left(\frac{\Delta V_{CR}}{L} \right) (DD'T), \quad [\text{amps}] \quad [15-6]$$

Input Filter Design Specification

1. Peak-Peak ripple voltage, ΔV_{cr} = 0.5 volts
2. Peak-Peak ripple current to the source, ΔI_L = 0.010 amps
3. Period, T = 10 μ sec
4. *Converter on-time duty cycle, $D = t_{on}/T$ = 0.5
5. *Converter off-time duty cycle, $D' = t_{off}/T$ = 0.5
6. Regulation, α = 0.5%
7. Output power drawn from the filter network, P_o = 50 watts
8. Maximum current to the load, ΔI_c = 4 amps
9. Average input current, $I_{in} = I_{av} = \Delta I_c D$ = 2 amps
10. The ripple frequency, f = 100kHz
11. The core RM ferrite, gapped, B_{max} = 0.25 tesla

* The worse case time domain is where D and D' = 0.5

Step No. 1 Calculate the required inductance, L.

$$L = \frac{\Delta V_{CR}}{\Delta I_L} (DD'T), \text{ [henrys]}$$

$$L = \frac{0.5}{0.01} (0.5)(0.5)(10(10^{-6})), \text{ [henrys]}$$

$$L = 0.000125, \text{ [henrys]}$$

Step No. 2 Calculate the energy-handling capability.

$$\text{Energy} = \frac{L(I_{av})^2}{2}, \text{ [watt-second]}$$

$$\text{Energy} = \frac{125(10^{-6})(2.0)^2}{2}, \text{ [watt-second]}$$

$$\text{Energy} = 0.000250, \text{ [watt-second]}$$

Step No. 3 Calculate the electrical coefficient, K_e .

$$K_e = 0.145 P_o B_m^2 (10^{-4})$$

$$K_e = 0.145(50)(0.25)^2 (10^{-4})$$

$$K_e = 0.0000453$$

Step No. 4 Calculate the core geometry, K_g .

$$K_g = \frac{(\text{Energy})^2}{K_e \alpha}, \quad [\text{cm}^5]$$

$$K_g = \frac{(0.00025)^2}{(0.0000453)(0.5)}, \quad [\text{cm}^5]$$

$$K_g = 0.00275, \quad [\text{cm}^5]$$

Step No. 5 Select the comparable core geometry from the RM ferrite cores.

1. Core part number = RM-6
2. Core geometry, K_g = 0.0044 cm^5
3. Core cross-section, A_c = 0.366 cm^2
4. Window area, W_a = 0.260 cm^2
5. Area product, A_p = 0.0953 cm^4
6. Mean length turn, MLT = 3.1 cm
7. Magnetic path length, MPL = 2.86 cm
8. Core weight, W_{ife} = 5.5 grams
9. Surface area, A_t = 11.3 cm^2
10. Winding Length, G = 0.82 cm
11. Permeability, μ_m = 2500

Step No. 6 Calculate the current density, J , using the area product equation, A_p .

$$J = \frac{2(\text{Energy})(10^4)}{B_m A_p K_u}, \quad [\text{amps-per-cm}^2]$$

$$J = \frac{2(0.00025)(10^4)}{(0.25)(0.0953)(0.4)}, \quad [\text{amps-per-cm}^2]$$

$$J = 525, \quad [\text{amps-per-cm}^2]$$

Step No. 7 Calculate the required bare wire area, $A_{w(B)}$.

$$A_{w(B)} = \frac{I_{\text{avg}}}{J}, \quad [\text{cm}^2]$$

$$A_{w(B)} = \frac{(2.0)}{(525)}, \quad [\text{cm}^2]$$

$$A_{w(B)} = 0.00381, \quad [\text{cm}^2]$$

Step No. 8 Select a wire from the Wire Table in Chapter 4. If the area is not within 10%, take the next smallest size. Also record micro-ohms per centimeter.

$$\text{AWG} = \#21$$

$$\text{Bare, } A_{W(B)} = 0.00411, \text{ [cm}^2\text{]}$$

$$\text{Insulated, } A_W = 0.00484, \text{ [cm}^2\text{]}$$

$$\left(\frac{\mu\Omega}{\text{cm}} \right) = 419, \text{ [micro-ohm/cm]}$$

Step No. 9 Calculate the effective window area, $W_{a(\text{eff})}$. Use the window area found in Step 5. A typical value for, S_3 is 0.75, as shown in Chapter 4.

$$W_{a(\text{eff})} = W_a S_3, \text{ [cm}^2\text{]}$$

$$W_{a(\text{eff})} = (0.260)(0.75), \text{ [cm}^2\text{]}$$

$$W_{a(\text{eff})} = 0.195, \text{ [cm}^2\text{]}$$

Step No. 10 Calculate the number turns possible, N . Use the insulated wire area, A_w , found in Step 8. A typical value for, S_2 , is 0.6, as shown in Chapter 4.

$$N = \frac{W_{a(\text{eff})} S_2}{A_w}, \text{ [turns]}$$

$$N = \frac{(0.195)(0.60)}{(0.00484)}, \text{ [turns]}$$

$$N = 24, \text{ [turns]}$$

Step No. 11 Calculate the required gap, l_g .

$$l_g = \frac{0.4\pi N^2 A_c (10^{-8})}{L} - \left(\frac{\text{MPL}}{\mu_m} \right), \text{ [cm]}$$

$$l_g = \frac{(1.26)(24)^2 (0.366)(10^{-8})}{(0.000125)} - \left(\frac{2.86}{2500} \right), \text{ [cm]}$$

$$l_g = 0.0201, \text{ [cm]}$$

Step No. 12 Calculate the equivalent gap in mils.

$$\text{mils} = \text{cm}(393.7)$$

$$\text{mils} = (0.0197)(393.7)$$

$$\text{mils} = 7.91 \text{ use } 8$$

Step No. 13 Calculate the fringing flux factor, F .

$$F = 1 + \frac{l_g}{\sqrt{A_c}} \ln\left(\frac{2G}{l_g}\right)$$

$$F = 1 + \frac{(0.0201)}{\sqrt{0.366}} \ln\left(\frac{2(0.82)}{0.0201}\right)$$

$$F = 1.146$$

Step No. 14 Calculate the new number of turns, N_n , by inserting the fringing flux, F .

$$N_n = \sqrt{\frac{l_g L}{0.4\pi A_c F (10^{-8})}}, \quad [\text{turns}]$$

$$N_n = \sqrt{\frac{(0.0201)(0.000125)}{(1.26)(0.366)(1.146)(10^{-8})}}, \quad [\text{turns}]$$

$$N_n = 22, \quad [\text{turns}]$$

Step No. 15 Calculate the winding resistance, R_L . Use the, MLT, from Step 5 and the micro-ohm per centimeter, from Step 8.

$$R_L = (\text{MLT})(N_n)\left(\frac{\mu\Omega}{\text{cm}}\right)(10^{-6}), \quad [\text{ohms}]$$

$$R_L = (3.1)(22)(419)(10^{-6}), \quad [\text{ohms}]$$

$$R_L = 0.0286, \quad [\text{ohms}]$$

Step No. 16 Calculate the copper loss, P_{cu} .

$$P_{cu} = I_{avg}^2 R_L, \quad [\text{watts}]$$

$$P_{cu} = (2.0)^2 (0.0286), \quad [\text{watts}]$$

$$P_{cu} = 0.114, \quad [\text{watts}]$$

Step No. 17 Calculate the regulation, α .

$$\alpha = \frac{P_{cu}}{P_o}(100), \quad [\%]$$

$$\alpha = \frac{(0.114)}{(50)}(100), \quad [\%]$$

$$\alpha = 0.228, \quad [\%]$$

Step No. 18 Calculate the ac flux density, B_{ac} .

$$B_{ac} = \frac{0.4\pi N_n F \left(\frac{\Delta I}{2}\right) (10^{-4})}{l_g + \left(\frac{MPL}{\mu_m}\right)}, \quad [\text{tesla}]$$

$$B_{ac} = \frac{(1.26)(22)(1.14) \left(\frac{0.01}{2}\right) (10^{-4})}{(0.0197) + \left(\frac{2.86}{2500}\right)}, \quad [\text{tesla}]$$

$$B_{ac} = 0.000758, \quad [\text{tesla}]$$

Step No. 19 Calculate the watts-per-kilogram, for ferrite, P, material in Chapter 2. Watts per kilogram can be written in milliwatts-per-gram.

$$\text{mW/g} = k f^{(m)} B_{ac}^{(n)}$$

$$\text{mW/g} = (0.00198)(100000)^{(1.36)} (0.000758)^{(2.86)}$$

$$\text{mW/g} = 0.0000149$$

Step No. 20 Calculate the core loss, P_{fe} .

$$P_{fe} = (\text{mW/g})(W_{fe})(10^{-3}), \quad [\text{watts}]$$

$$P_{fe} = (0.0000149)(5.5)(10^{-3}), \quad [\text{watts}]$$

$$P_{fe} = 0.082(10^{-6}), \quad [\text{watts}]$$

Step No. 21 Calculate the total loss copper plus iron, P_{Σ} .

$$P_{\Sigma} = P_{fe} + P_{cu}, \quad [\text{watts}]$$

$$P_{\Sigma} = (0.000) + (0.114), \quad [\text{watts}]$$

$$P_{\Sigma} = 0.114, \quad [\text{watts}]$$

Step No. 22 Calculate the watt density, ψ . The surface area, A_t , can be found in Step 5.

$$\psi = \frac{P_{\Sigma}}{A_t}, \quad [\text{watts/cm}^2]$$

$$\psi = \frac{(0.114)}{(11.3)}, \quad [\text{watts/cm}^2]$$

$$\psi = 0.010, \quad [\text{watts/cm}^2]$$

Step No. 23 Calculate the temperature rise, T_r .

$$T_r = 450(\psi)^{(0.826)}, \quad [^{\circ}\text{C}]$$

$$T_r = 450(0.010)^{(0.826)}, \quad [^{\circ}\text{C}]$$

$$T_r = 10.0, \quad [^{\circ}\text{C}]$$

Step No. 24 Calculate the peak flux density, B_{pk} .

$$B_{pk} = \frac{0.4\pi N_n F \left(I_{dc} + \frac{\Delta I}{2} \right) (10^{-4})}{I_g + \left(\frac{\text{MPL}}{\mu_m} \right)}, \quad [\text{tesla}]$$

$$B_{pk} = \frac{(1.26)(22)(1.14)(2.005)(10^{-4})}{(0.0197) + \left(\frac{2.86}{2500} \right)}, \quad [\text{tesla}]$$

$$B_{pk} = 0.304, \quad [\text{tesla}]$$

Step No. 25 Calculate the window utilization, K_u .

$$K_u = \frac{A_{v(B)} N_n}{W_u}$$

$$K_u = \frac{(0.00411)(22)}{(0.260)}$$

$$K_u = 0.348$$

References

1. T. K. Phelps and W. S. Tate, "Optimizing Passive Input Filter Design," (no source).
2. David Silber, "Simplifying the Switching Regulator Input Filter," *Solid-State Power Conversion*, May/June 1975.
3. Dan Sheehan, "Designing a Regulator's LC Input Filter: 'Ripple' Method Prevents Oscillation Woes," *Electronic Design* 16, August 2, 1979.

Note:

I would like to thank Jerry Fridenberg, for modeling the circuits in Figure 15-8 and 15-10, on his SPICE program. The modeling results are shown in Figures 15-9 and 15-11.

Chapter 16

Current Transformer Design

Table of Contents

1. Introduction	
2. Analysis of the Input Current Component	
3. Unique to a Current Transformer	
4. Current Transformer Circuit Applications	
5. Current Transformer Design Example	
6. Design Performance	

Introduction

Current transformers are used to measure, or monitor, the current in the lead of an ac power circuit. They are very useful in high-power circuits, where the current is large, i.e., higher than the ratings of so-called self-contained current meters. Other applications relate to overcurrent and undercurrent relaying for power circuit protection, such as, in the power lead of an inverter or converter. Multiturn secondaries then provide a reduced current for detecting overcurrent, undercurrent, peak current, and average current, as shown in Figure 16-1.

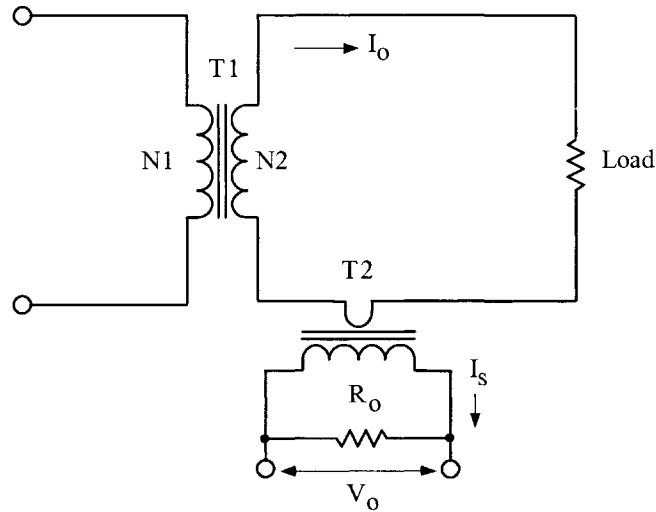


Figure 16-1. Simple, Secondary AC Current Monitor.

In current transformer designs, the core characteristics must be carefully selected because excitation current, I_m , essentially subtracts from the metered current and effects the true ratio and phase angle of the output current.

The simplified equivalent circuit of a current transformer, as shown in Figure 16-2, represents the important elements of a current transformer, where the ratio of primary to secondary turns is:

$$n = \frac{N_s}{N_p}, \text{ [turns ratio] [16-1]}$$

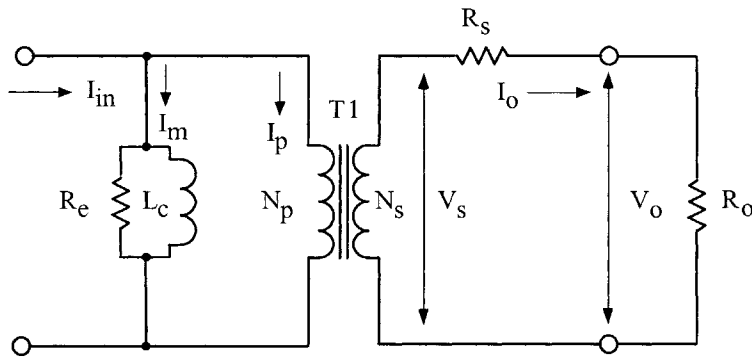


Figure 16-2. Simplified, Equivalent Circuit for a Current Transformer.

Analysis of the Input Current Component

A better understanding of the current transformer behavior may be achieved by considering the applied input current to the primary winding, in terms of various components. Only the ampere-turn component, $I_m N_p$, drives the magnetic flux around the core. The ampere-turn, $I_m N_p$, provides the core loss. The secondary ampere-turns, $I_s N_s$, balance the remainder of the primary ampere-turns.

The exciting current, I_m , in Figure 16-2, determines the maximum accuracy that can be achieved with a current transformer. Exciting current, I_m , may be defined as the portion of the primary current that satisfies the hysteresis and eddy current losses of the core. If the values of L_c and R_e , in Figure 16-2, are too low because the permeability of the core material is low and the core loss is high, only a part of the current, (I_p/n) , will flow in the output load resistor, R_o . The relationship of the exciting current, I_m , to the load current, I_o , is shown in Figure 16-3.

The exciting current is equal to:

$$I_m = \frac{H(\text{MPL})}{0.4\pi N}, \text{ [amps]} \quad [16-2]$$

where H is the magnetizing force and material dependent, and MPL is the Magnetic Path Length.

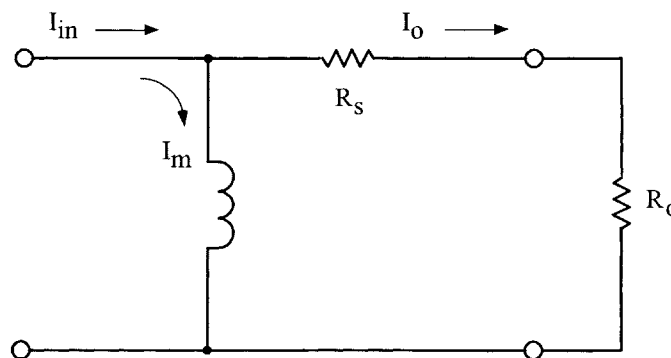


Figure 16-3. Input Current-Output Current Relationship.

The input current is comprised of two components: exciting current, I_m , and the load current, I_o .

$$I_{in}^2 = I_m^2 + I_o^2, \text{ [amps]} \quad [16-3]$$

Then:

$$I_m^2 = I_{in}^2 - I_o^2, \text{ [amps]} \quad [16-4]$$

$$I_m = I_{in} \left[1 - \left(\frac{I_o}{I_{in}} \right)^2 \right]^{1/2}, \text{ [amps]} \quad [16-5]$$

The above equation has shown graphically in Figure 16-4, that the higher the exciting current, I_m or core loss, the larger the error. The magnetizing impedance, R_e , determines accuracy, because it shunts part of the input current, I_{in} , away from the primary and thus, produces an error, as shown in Figure 16-4. Core material with the lowest value of H achieves the highest accuracy.

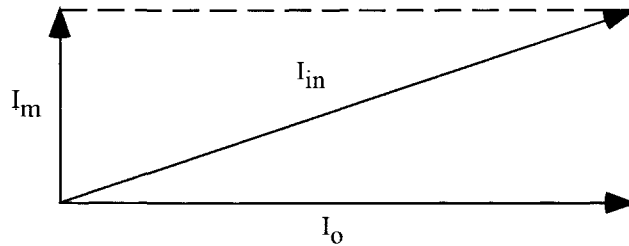


Figure 16-4. Input Current I_{in} Phase Relationship Diagram.

Unique to a Current Transformer

The current transformer function is different than that of a voltage transformer. A current transformer operates with a set primary current and will try to output a constant current to the load, independent of the load. The current transformer will operate into either a short circuit or a resistive load until the voltage induced is enough to saturate the core or cause voltage breakdown. For this reason a current transformer should never operate into an open circuit, as a voltage transformer should never operate into a short circuit. The primary current of a current transformer is not dependent of the secondary load current. The current is really injected into the primary by an external load current, I_m . If the load current, I_o , on the current transformer is removed from the secondary winding, while the external load current, I_m , is still applied, the flux in the core will rise to a high level, because there is not an opposing current in the secondary winding to prevent this. A very high voltage will appear across the secondary. A current transformer, like any other transformer, must satisfy the amp-turn equation:

$$\frac{I_p}{I_s} = \frac{N_s}{N_p} \quad [16-6]$$

The secondary load, R_o , secondary winding resistance, R_s , and secondary load current, I_o , determine the induced voltage of the current transformer.

$$V_s = I_o (R_s + R_o), \text{ [volts] [16-7]}$$

If the secondary is designed for dc, then the diode drop must be taken into account.

$$V_s = I_o (R_s + R_o) + V_d, \text{ [volts] [16-8]}$$

Simple form:

$$V_s = V_o + V_d, \text{ [volts] [16-9]}$$

The current ratio will set the turns ratio. The secondary, R_o load will determine the secondary voltage, V_s . The engineer would use Equation 16-10, to select the required core cross-section, A_c . It is now up to the engineer to pick a core material that would provide the highest permeability at the operating flux density, B_{ac} .

$$A_c = \frac{I_{in} (R_s + R_o) (10^4)}{K_f B_{ac} f N_s}, \text{ [cm}^2\text{] [16-10]}$$

The design requirements would dictate choosing a core material and operating flux density, B_{ac} , that would result in values of, L_c and R_e , as shown in Figure 16-2, values which would be large enough to reduce the current flowing in these elements to satisfy the ratio and phase requirements.

The inductance is calculated from the equation:

$$L_c = \frac{0.4\pi N_p^2 A_c \Delta\mu (10^{-8})}{MPL}, \text{ [henrys] [16-11]}$$

R_e is the equivalent core loss, (shunt), resistance. The current is, in phase, with the voltage.

$$R_e = \frac{V_s / n}{P_{fe}}, \text{ [ohms] [16-12]}$$

Where:

$$\frac{R_e}{n^2} \square R_s + R_o \text{ [16-13]}$$

And:

$$\frac{2\pi f L_c}{n^2} \square R_s + R_o \text{ [16-14]}$$

Then:

$$I_p = n I_s \text{ [16-15]}$$

Or:

$$I_p N_p = I_s N_s \quad [16-16]$$

Except for relatively low-accuracy industrial types, current transformers are wound on toroidal cores, which virtually eliminate errors due to leakage inductance. Some errors may be compensated for by adjusting the number of secondary turns.

Current Transformer Circuit Applications

Typical current transformer applications are shown in Figures 16-5 through 16-8.

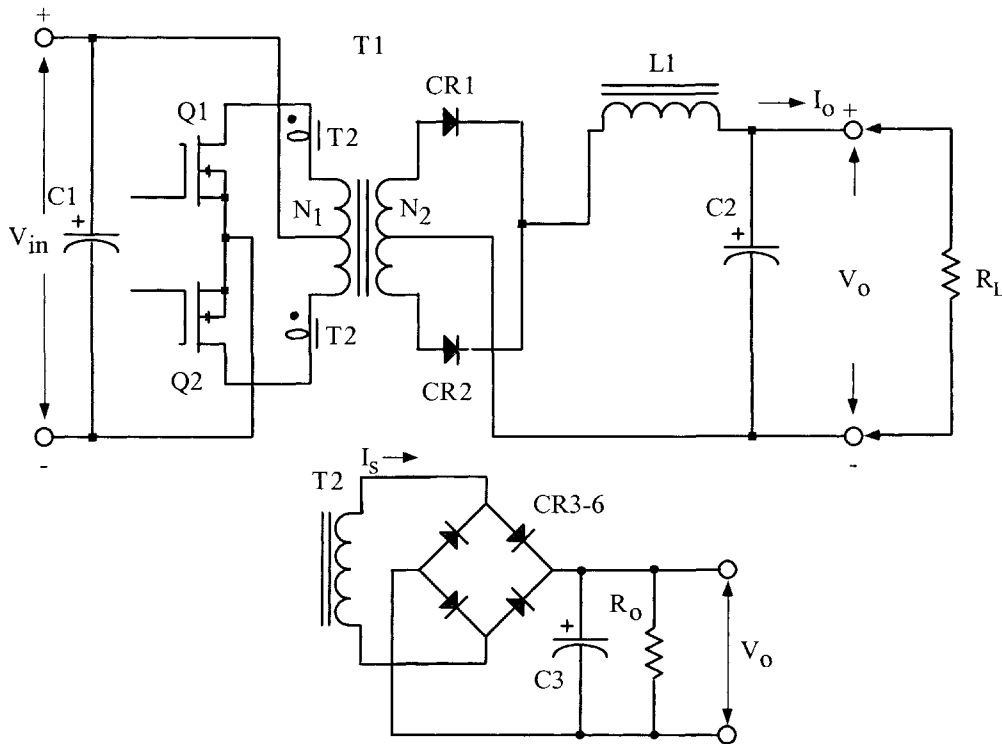


Figure 16-5. Current Transformer, T2, used to Monitor, Q1 and Q2, Drain Current.

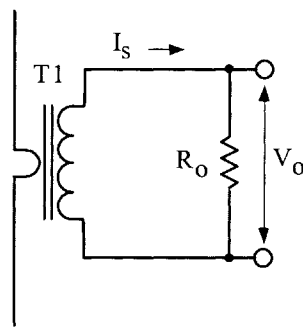


Figure 16-6. Current Transformer, T1, used to Monitor Line Current.

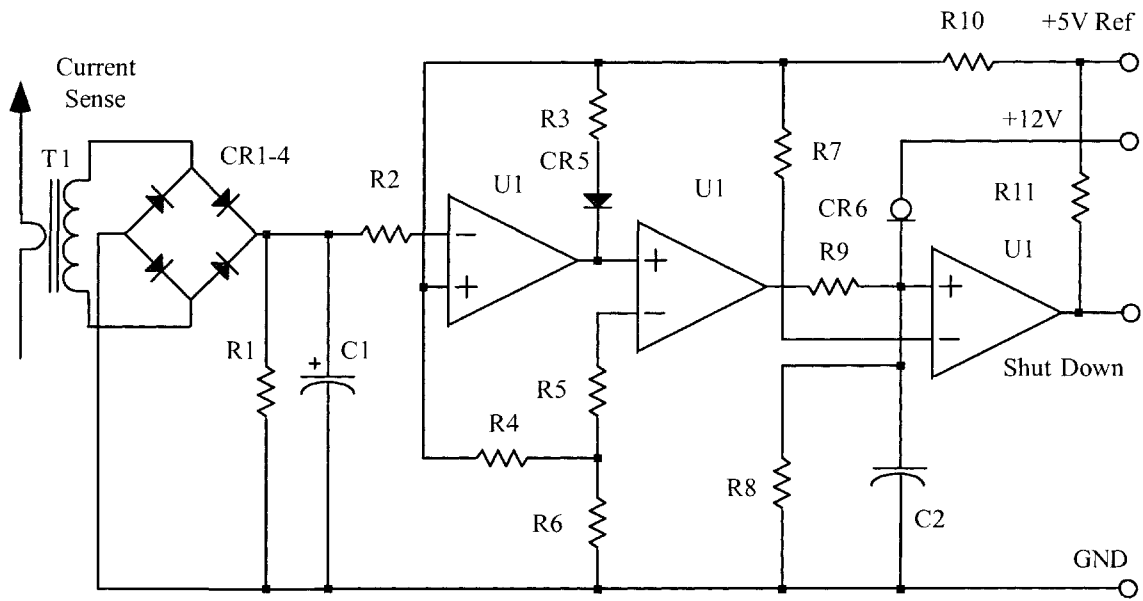


Figure 16-7. Current Transformer, T1, is used as a Level Detector.

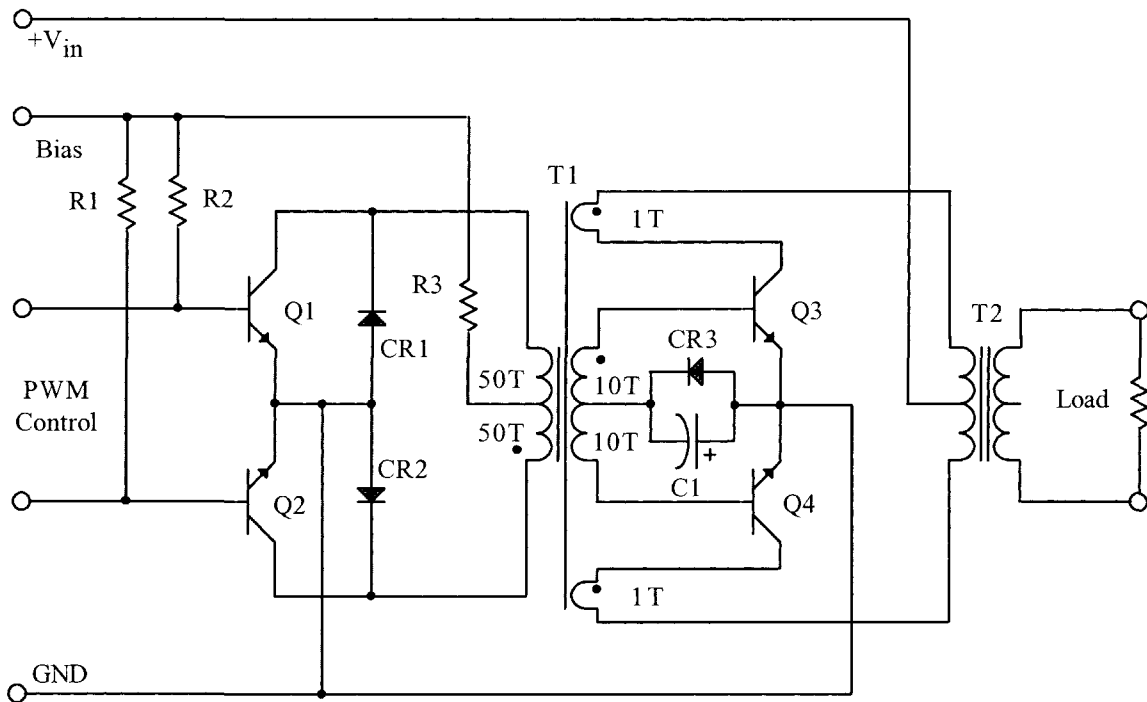


Figure 16-8. Current Transformer, T1, is used for regenerative drive.

Current Transformer Design Example

The following information is the design specification for a current transformer, as shown in Figure 16-9.

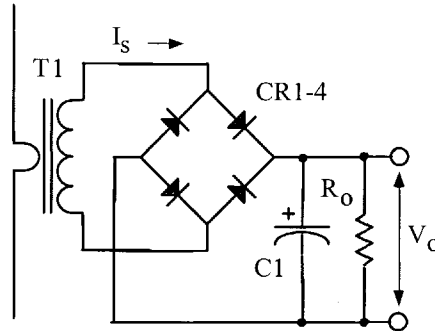


Figure 16-9. Current Monitoring Transformer with dc Output.

1. Primary	1 turn
2. Input current, I_{in}	0 – 5 amps
3. Output voltage, V_o	0 – 5 volts
4. Output load resistance, R_o	500 ohms
5. Operating frequency, f (square wave)	2500 hertz
6. Operating flux density, B_{ac}	0.2 tesla
7. Core loss less than	3% (error)
8. Diode drop, V_d	1 volt
9. Magnetic material	Supermalloy 2 mil
10. Waveform factor, K_f	4.0

Step 1. Calculate the secondary current, I_s .

$$I_s = \frac{V_o}{R_o}, \text{ [amps]}$$

$$I_s = \frac{5.0}{500}, \text{ [amps]}$$

$$I_s = 0.01, \text{ [amps]}$$

Step 2. Calculate the secondary turns, N_s .

$$N_s = \frac{I_p N_p}{I_s}, \text{ [turns]}$$

$$N_s = \frac{(5.0)(1.0)}{(0.01)}, \text{ [turns]}$$

$$N_s = 500, \text{ [turns]}$$

Step 3. Calculate the secondary voltage, V_s .

$$V_s = V_o + 2V_d, \text{ [volts]}$$

$$V_s = 5.0 + 2(1.0), \text{ [volts]}$$

$$V_s = 7.0, \text{ [volts]}$$

Step 4. Calculate the required core iron cross-section, A_c , using Faraday's Equation.

$$A_c = \frac{V_s (10^4)}{(K_f) B_{ac} f N_s}, \text{ [cm}^2\text{]}$$

$$A_c = \frac{(7.0)(10^4)}{(4.0)(0.2)(2500)(500)}, \text{ [cm}^2\text{]}$$

$$A_c = 0.070, \text{ [cm}^2\text{]}$$

Step 5. Select a 2mil tape, toroidal core from Chapter 3 with an iron cross-section, A_c , closest to the value calculated.

Core number	52000
Manufacturer	Magnetics
Magnetic material	2mil Silcon
Magnetic path length, MPL.....	4.99 cm
Core weight, W_{rfe}	3.3 grams
Copper weight, W_{tcu}	8.1 grams
Mean length turn, MLT	2.7 cm
Iron area, A_c	0.086 cm ²
Window area, W_a	0.851 cm ²
Area product, A_p	0.0732 cm ⁴
Core geometry, K_g	0.000938 cm ⁵
Surface area, A_t	20.6 cm ²

Step 6. Calculate the effective window area, $W_{a(\text{eff})}$. A typical value for, S_3 , is 0.75, as shown in Chapter 4.

$$W_{a(\text{eff})} = W_a S_3, \text{ [cm}^2\text{]}$$

$$W_{a(\text{eff})} = (0.851)(0.75), \text{ [cm}^2\text{]}$$

$$W_{a(\text{eff})} = 0.638, \text{ [cm}^2\text{]}$$

Step 7. Calculate the secondary window area, $W_{a(sec)}$.

$$W_{a(sec)} = \frac{W_{a(eff)}}{2}, \quad [\text{cm}^2]$$

$$W_{a(sec)} = \frac{0.638}{2}, \quad [\text{cm}^2]$$

$$W_{a(sec)} = 0.319, \quad [\text{cm}^2]$$

Step 8. Calculate the wire area, A_w , with insulation, using a fill factor, S_2 of 0.6.

$$A_w = \frac{W_{a(sec)} S_2}{N_s}, \quad [\text{cm}^2]$$

$$A_w = \frac{(0.319)(0.6)}{(500)}, \quad [\text{cm}^2]$$

$$A_w = 0.000383, \quad [\text{cm}^2]$$

Step 9. Select a wire area, A_w , with insulation from Wire Table in Chapter 4 for an equivalent AWG wire size. The rule is that when the calculated wire area does not fall within 10% of those listed, in Wire Table, then, the next smaller size should be selected.

AWG No. 33

$$A_w = 0.0003662, \quad [\text{cm}^2]$$

Step 10. Calculate the secondary winding resistance, R_s using the Wire Table in Chapter 4, for $\mu\Omega/\text{cm}$; and Step 5 for the MLT.

$$R_s = \text{MLT} (N_s) \left(\frac{\mu\Omega}{\text{cm}} \right) (10^{-6}), \quad [\text{ohms}]$$

$$R_s = (2.7)(500)(6748)(10^{-6}), \quad [\text{ohms}]$$

$$R_s = 9.11, \quad [\text{ohms}]$$

Step 11. Calculate the secondary output power, P_o .

$$P_o = I_s (V_o + 2V_d), \quad [\text{watts}]$$

$$P_o = (0.01)(5.0 + 2(1.0)), \quad [\text{watts}]$$

$$P_o = 0.070, \quad [\text{watts}]$$

Step 12. Calculate the acceptable core loss, P_{fe} .

$$P_{fe} = P_o \left(\frac{\text{core loss \%}}{100} \right), \text{ [watts]}$$

$$P_{fe} = (0.07) \left(\frac{3}{100} \right), \text{ [watts]}$$

$$P_{fe} = 0.0021, \text{ [watts]}$$

Step 13. Calculate the effective core weight, $W_{fe(eff)}$. Select the core weight correction factor, K_w , in Chapter 2, for Supermalloy.

$$W_{fe(eff)} = W_{fe} K_w, \text{ [grams]}$$

$$W_{fe(eff)} = (3.3)(1.148), \text{ [grams]}$$

$$W_{fe(eff)} = 3.79, \text{ [grams]}$$

Step 14. Calculate the allowable core loss, P_{fe} , in milliwatts per gram, mW/g.

$$\text{mW/g} = \frac{P_{fe}}{W_{fe}} (10^3), \text{ [milliwatts per gram]}$$

$$\text{mW/g} = \frac{(0.0021)}{(3.79)} (10^3), \text{ [milliwatts per gram]}$$

$$\text{mW/g} = 0.554, \text{ [milliwatts per gram]}$$

Step 15. Calculate the new flux density using the new core iron, cross-section, A_c .

$$B_{ac} = \frac{V_s (10^4)}{(K_f) A_c f N_s}, \text{ [tesla]}$$

$$B_{ac} = \frac{(7.0)(10^4)}{(4.0)(0.086)(2500)(500)}, \text{ [tesla]}$$

$$B_{ac} = 0.162, \text{ [tesla]}$$

Step 16. Calculate the core loss, P_{fe} , in milliwatts per gram, mW/g.

$$\text{mW/g} = 0.000179 (f)^{(1.48)} (B_{ac})^{(2.15)}, \text{ [milliwatts per gram]}$$

$$\text{mW/g} = 0.000179 (2500)^{(1.48)} (0.162)^{(2.15)}, \text{ [milliwatts per gram]}$$

$$\text{mW/g} = 0.382, \text{ [milliwatts per gram]}$$

Step 17. Calculate the core loss, P_{fe} , in watts.

$$P_{fe} = W_{fe} \left(\frac{mW}{g} \right) (10^{-3}), \text{ [watts]}$$

$$P_{fe} = 3.79(0.382)(10^{-3}), \text{ [watts]}$$

$$P_{fe} = 0.00145, \text{ [watts]}$$

Step 18. Calculate the induced core error in, %.

$$\text{Core loss induced error} = \frac{P_{fe}}{P_o} (100), \text{ [%]}$$

$$\text{Core loss induced error} = \frac{0.00145}{.07} (100), \text{ [%]}$$

$$\text{Core loss induced error} = 2.07, \text{ [%]}$$

Design Performance

A current transformer was built and the data recorded in Table 16-1. It was plotted in Figure 16-10, with an error of 3.4 %. The secondary winding resistance was 6.5 ohms.

Table 16-1

Current Transformer Electrical Data					
I_{in} amps	I_o volts	I_{in} amps	I_o volts	I_{in} amps	I_o volts
0.250	0.227	1.441	1.377	3.625	3.488
0.500	0.480	2.010	1.929	3.942	3.791
0.746	0.722	2.400	2.310	4.500	4.339
1.008	0.978	2.693	2.593	5.014	4.831
1.262	1.219	3.312	3.181	5.806	5.606

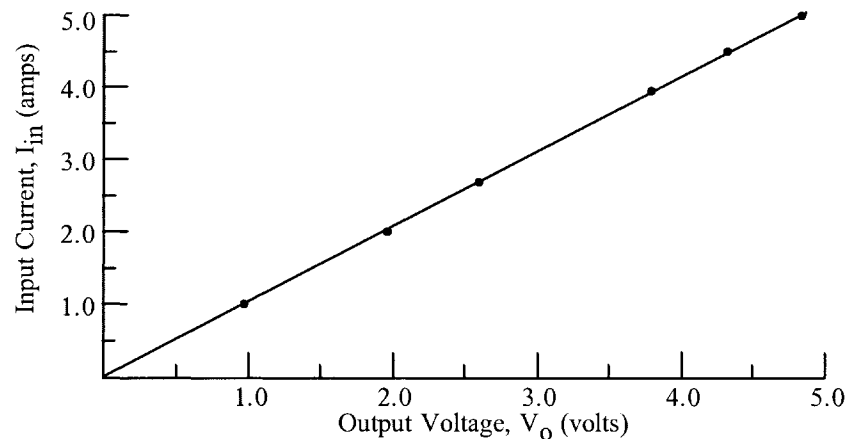


Figure 16-10. Current Transformer, Input Current versus Output Voltage.

Chapter 17

Winding Capacitance and Leakage Inductance

Table of Contents

1.	Introduction
2.	Parasitic Effects
3.	Leakage Flux
4.	Minimizing Leakage Inductance
5.	Winding Capacitance
6.	Winding Capacitance Turn-to-Turn
7.	Winding Capacitance Layer-to-Layer
8.	Capacitance Winding-to-Winding
9.	Stray Capacitance
10.	References

Introduction

Operation of transformers at high frequencies presents unique design problems due to the increased importance of core loss, leakage inductance, and winding capacitance. The design of high frequency power converters is far less stringent than designing high frequency, wide-band audio transformers. Operating at a single frequency requires fewer turns, and consequently, there is less leakage inductance and less capacitance with which to deal. The equivalent circuit for a two-winding transformer is shown in Figure 17-1.

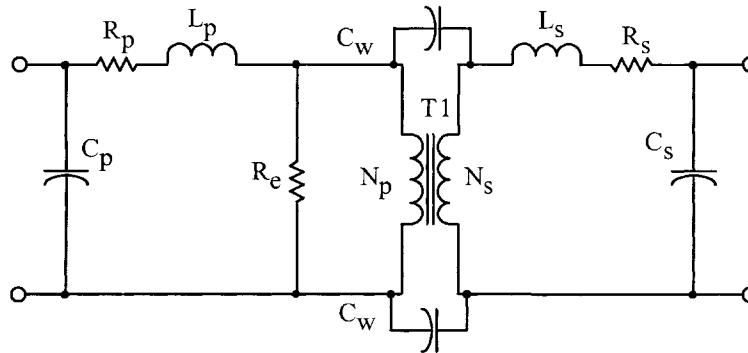


Figure 17-1. Equivalent Transformer Circuit.

High frequency designs require considerably more care in specifying the winding specification. This is because physical orientation and spacing of the windings determine leakage inductance and winding capacitance. Leakage inductance and capacitance are actually distributed throughout the winding in the transformer. However, for simplicity, they are shown as lumped constants, in Figure 17-1. The leakage inductance is represented by, L_p for the primary and, L_s for the secondary. The equivalent lumped capacitance is represented by, C_p and C_s for the primary and secondary windings. The dc winding resistance is, R_p , and R_s is for the equivalent resistance for the primary and secondary windings. C_w is the equivalent lumped, winding-to-winding capacitance. R_e is the equivalent core-loss shunt resistance.

Parasitic Effects

The effects of leakage inductance on switching power supplies' circuits are shown in Figure 17-2. The voltage spikes, shown in Figure 17-2, are caused by the stored energy in the leakage flux and will increase with load. These spikes will always appear on the leading edge of the voltage switching waveform.

$$Energy = \frac{L_{(Leakage)} (I_{(pk)})^2}{2}, \quad [\text{watt-seconds}] \quad [17-1]$$

Transformers designed for switching applications are normally designed to have minimum leakage inductance, in order to minimize the voltage spikes, as shown in Figure 17-2. Also, leakage inductance can be observed by the leading edge slope of the trapezoidal current waveform.

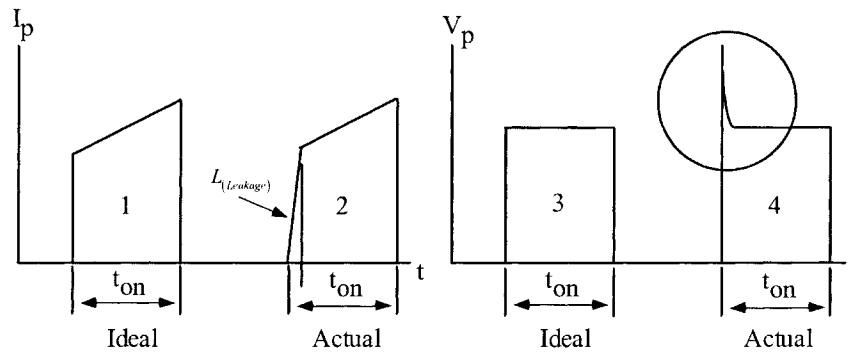


Figure 17-2. Switching Transistor Voltage and Current Waveforms.

Transformers designed for power conversion are normally being driven with a square wave, characterized by fast rise and fall times. This fast transition will generate high current spikes in the primary winding, due to the parasitic capacitance in the transformer. These current spikes, shown in Figure 17-3, are caused by the capacitance in the transformer; they will always appear on the lead edge of the current waveform and always with the same amplitude, regardless of the load. This parasitic capacitance will be charged and discharged every half cycle. Transformer leakage inductance and capacitance have an inverse relationship: if you decrease the leakage inductance, you will increase the capacitance; if you decrease the capacitance, you increase the leakage inductance. These are trade-offs that the power conversion engineer must make to design the best transformer for the application.

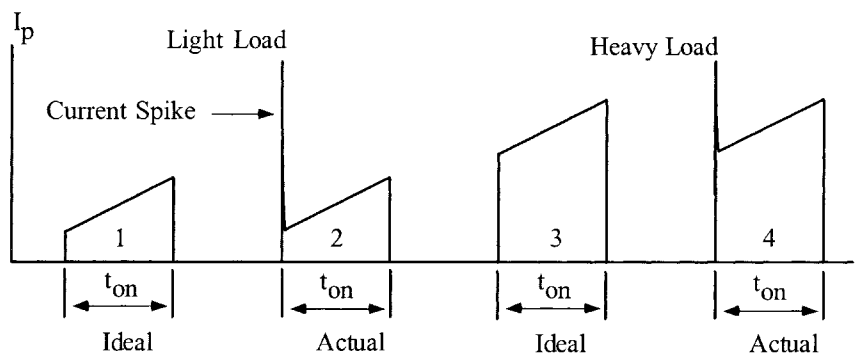


Figure 17-3. Transformer Capacitance Induced Current spike.

Leakage Flux

Leakage inductance is actually distributed throughout the windings of a transformer because of the flux set-up by the primary winding, which does not link the secondary, thus giving rise to leakage inductance in each winding without contributing to the mutual flux, as shown in Figure 17-4.

However, for simplicity, leakage inductance is shown as a lumped constant in Figure 17-1, where the leakage inductance is represented by L_p .

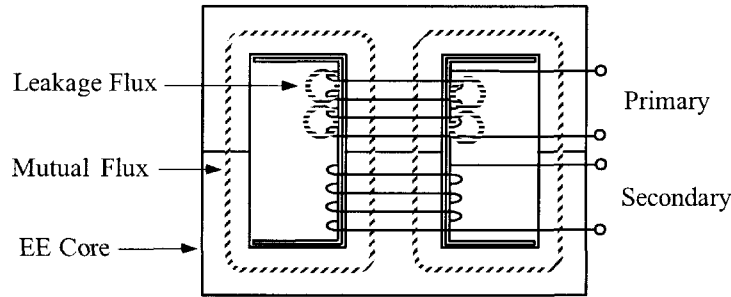


Figure 17-4. Leakage Flux.

In the layer-wound coil, a substantial reduction in leakage inductance, L_p and L_s , is obtained by interweaving the primary and secondary windings. The standard transformer, with a single primary and secondary winding, is shown in Figure 17-5, along with its leakage inductance, Equation [17-2]. Taking the same transformer and splitting the secondary on either side of the primary will reduce the leakage inductance, as shown in Figure 17-6, along with its leakage inductance, Equation [17-3]. The leakage inductance can be reduced even more, by interleaving the primary and secondary, as shown in Figure 17-7, along with its leakage inductance, Equation [17-4]. Transformers can also be constructed using the side-by-side, sectionalized bobbin as shown in Figure 17-8, along with its leakage inductance, Equation [17-5]. The modified three section, side-by-side bobbin is shown in Figure 17-9, along with its leakage inductance Equation [17-6].

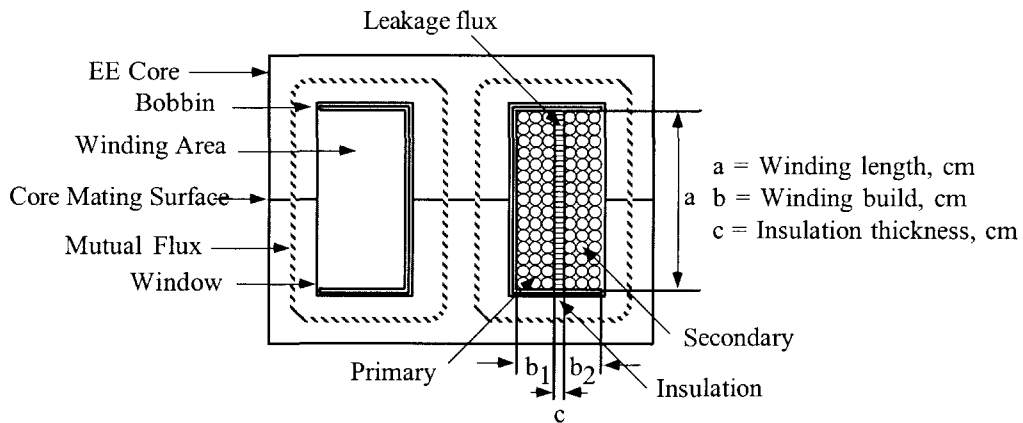


Figure 17-5. Conventional Transformer Configuration.

$$L_p = \frac{4\pi(MLT)N_p^2}{a} \left(c + \frac{b_1 + b_2}{3} \right) (10^{-9}), \text{ [henrys] [17-2]}$$

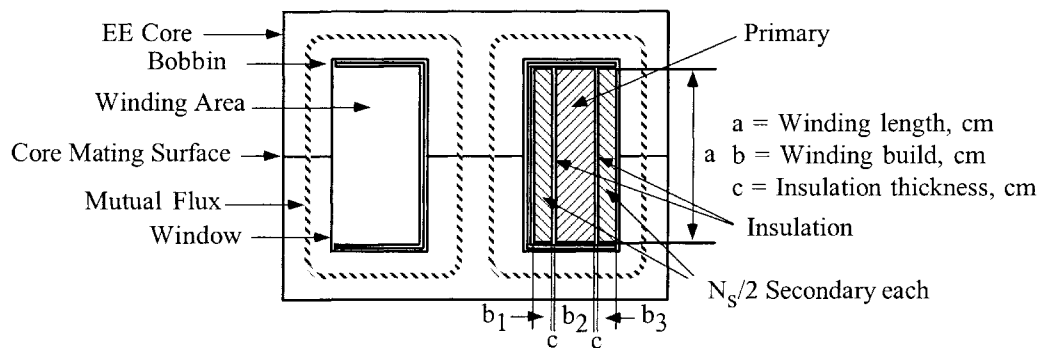


Figure 17-6. Conventional, Transformer Configuration with Simple Interleave.

$$L_p = \frac{\pi (MLT) N_p^2}{a} \left(\Sigma c + \frac{\Sigma b}{3} \right) (10^{-9}), \text{ [henrys]} \quad [17-3]$$

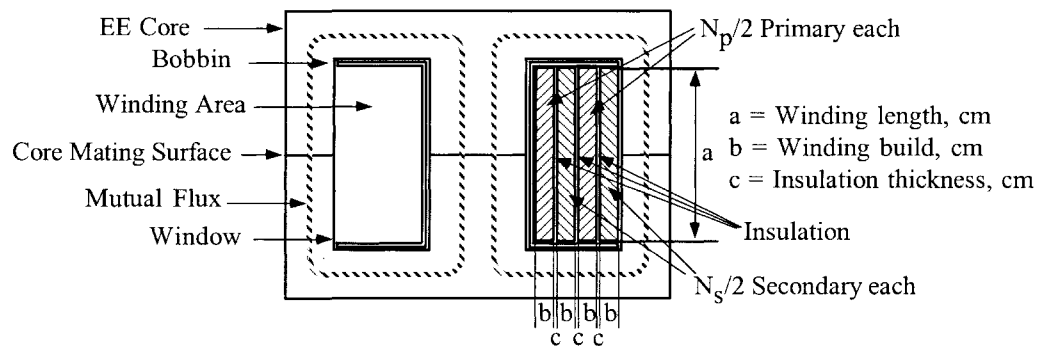


Figure 17-7. Sectionalized, Transformer Configuration Primary and Secondary Interleave.

$$L_p = \frac{\pi (MLT) N_p^2}{a} \left(\Sigma c + \frac{\Sigma b}{3} \right) (10^{-9}), \text{ [henrys]} \quad [17-4]$$

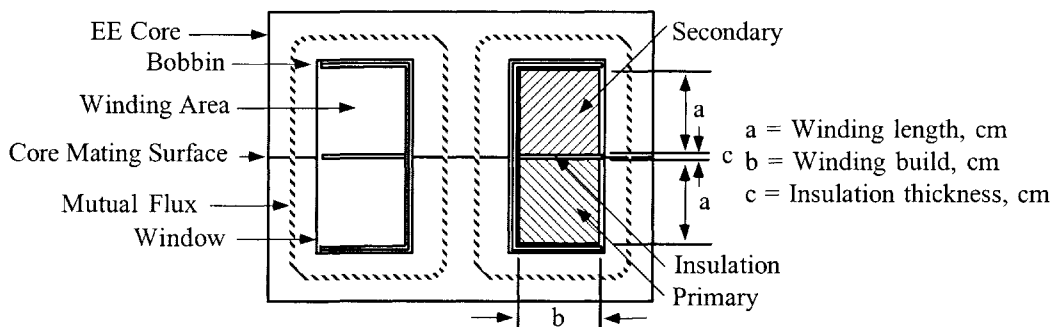


Figure 17-8. Pot Core, Sectionalized Transformer Configuration.

$$L_p = \frac{4\pi (MLT) N_p^2}{b} \left(c + \frac{\Sigma a}{3} \right) (10^{-9}), \text{ [henrys]} \quad [17-5]$$

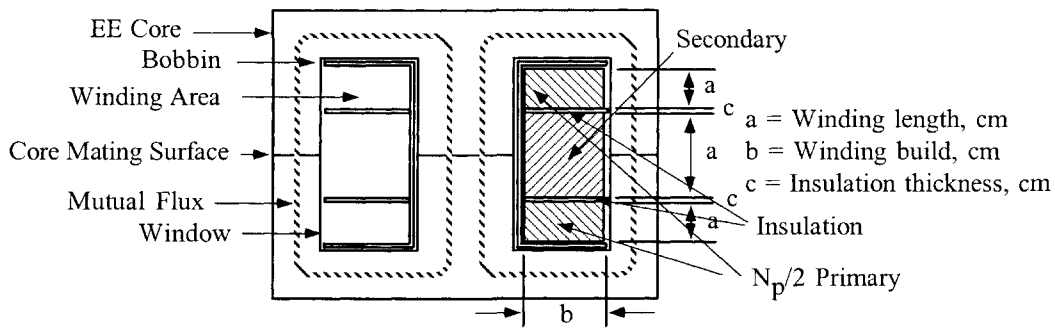


Figure 17-9. Modified, Pot Core Sectionalized, Transformer Configuration.

$$L_p = \frac{\pi(MLT)N_p^2}{b} \left(\Sigma c + \frac{\Sigma a}{3} \right) (10^{-9}), \text{ [henrys]} \quad [17-6]$$

Minimizing Leakage Inductance

Magnetic core geometry has a big influence on leakage inductance. To minimize leakage inductance, the primary winding should be wound on a long bobbin, or tube, with the secondary wound as close as possible, using a minimum of insulation. Magnetic cores can have identical rating, but one core will provide a lower leakage inductance than the other. A simple comparison would be two cores with the same window area, but one core has twice the winding length. Only half the winding build is shown in Figure 17-10.

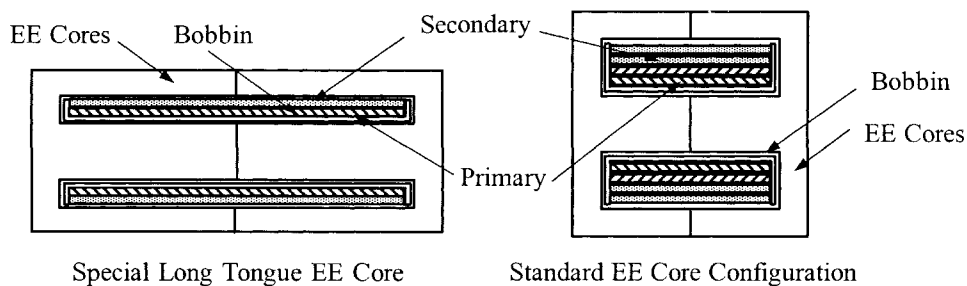


Figure 17-10. Comparing a Standard EE Core and a Special Long Tongue Core.

If layers must be used, the only way to reduce the leakage inductance is to divide the primary winding into sections, and then to sandwich the secondary winding between them, as shown in Figure 17-7. This can pose a real problem when designing around the European VDE specification, because of the required creepage distance and the minimum insulation requirements between the primary and secondary. Minimizing the leakage inductance on a push-pull converter design could be a big problem. A special consideration is required symmetry in both the leakage inductance and dc resistance; this is in order to get a balanced winding for the primary switching circuit to function properly.

The best way to minimize the leakage inductance, and to have a balanced dc resistance in a push-pull or center-tapped winding, is to wind bifilar. Bifilar windings will drastically reduce leakage inductance. This condition also exists on the secondary, when the secondary is a full-wave, center-tapped circuit. A bifilar winding is a pair of insulated wires, wound simultaneously and contiguously, (i.e., close enough to touch each other); Warning: do not use bifilar wire or the capacitance will go out of sight. Each wire constitutes a winding; their proximity reduces leakage inductance by several orders of magnitude, more than ordinary interleaving. This arrangement can be applied to the primary, to the secondary, or, it can be applied to the primary and secondary together. This arrangement will provide the minimum leakage inductance.

Winding Capacitance

Operating at high frequency presents unique problems in the design of transformers to minimize the effect of winding capacitance. Transformer winding capacitance is detrimental in three ways: (1) winding capacitance can drive the transformer into premature resonance; (2) winding capacitance can produce large primary current spikes when operating from a square wave source, (3) winding capacitance can produce electrostatic coupling to other circuits.

When a transformer is operating, different voltage gradients arise almost everywhere. These voltage gradients are caused by a large variety of capacitance throughout the transformer, due to the turns and how they are placed throughout the transformer. When designing high frequency converters, there are several factors that have a control over the turns: (1) the operating flux density or core loss; (2) the operating voltage levels in the primary and secondary; (3) the primary inductance.

Keeping turns to a minimum will keep the capacitance to a minimum. This capacitance can be separated into four categories: (1) capacitance between turns; (2) capacitance between layers; (3) capacitance between windings; and (4) stray capacitance. The net effect of the capacitance is normally seen by the lumped capacitance, C_p , on the primary, as shown in Figure 17-1. The lumped capacitance is very difficult to calculate by itself. It is much easier to measure the primary inductance and the resonant frequency of the transformer or inductor, as shown in Figure 17-11. Then, calculate the capacitance using Equation [17-7]. The test circuit, in Figure 17-11 functions as follows: The input voltage, V_1 , is held constant while monitoring the voltage, V_2 , sweep through the frequency with the power oscillator. When the voltage, V_2 , rises to a peak, and starts to decay at this peak voltage, the transformer or inductor is in resonance. At this point the phase angle is also 0 degrees at resonance when looking at both the curves of V_1 and V_2 .

$$C_p = \left(\frac{1}{(\omega_r)^2 L} \right) = \frac{1}{4\pi^2 f_r^2 L}, \text{ [farads] [17-7]}$$

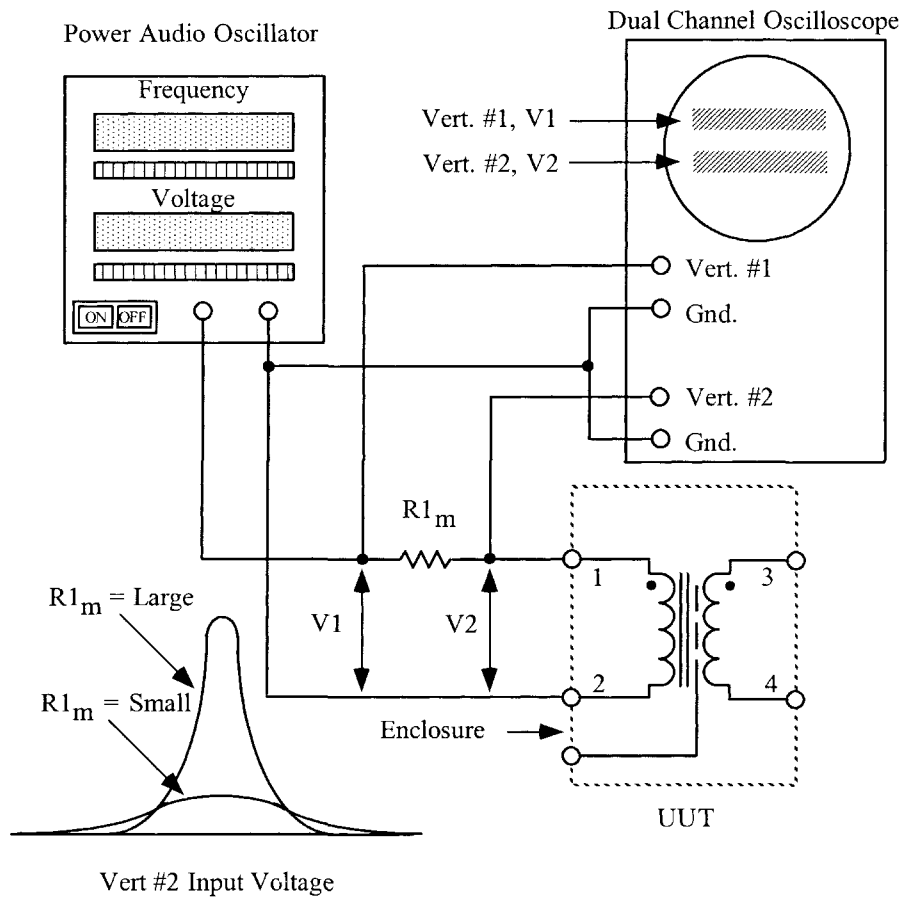


Figure 17-11. Circuit for Measuring either a Transformer or Inductor Self Resonates.

For transformers designed to operate with a square wave, such as dc-to-dc converter, leakage inductance, L_p , and the lumped capacitance, C_p , should be kept to a minimum. This is because they cause overshoot and oscillate, or ring, as shown in Figure 17-12. The overshoot oscillation, seen in Figure 17-12A, has a resonant frequency, f , that is controlled by, L_p and C_p . This resonant frequency could change and change drastically after potting, depending on the material and its dielectric constant, as shown Figure 17-12B.

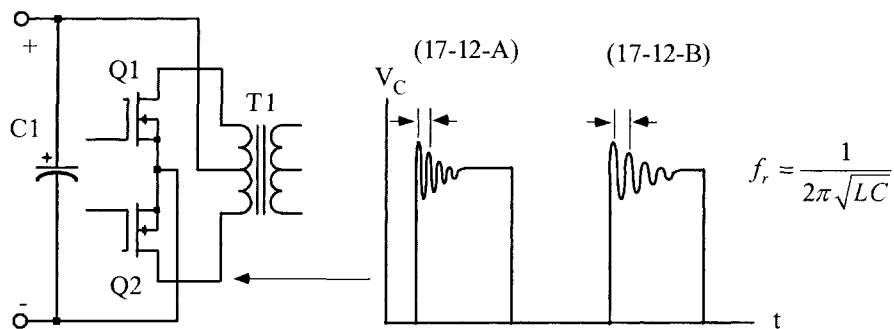


Figure 17-12. Primary Voltage with Leading Edge Ringing.

Winding Capacitance Turn-to-Turn

The turn-to-turn capacitance, C_t , shown in Figure 17-13, should not be a problem if you are operating at high frequency, low voltage power converters, due to the low number of turns. If the turn-to-turn capacitance is important, then change the magnet wire insulation to one with a lower dielectric constant. See Chapter 4.

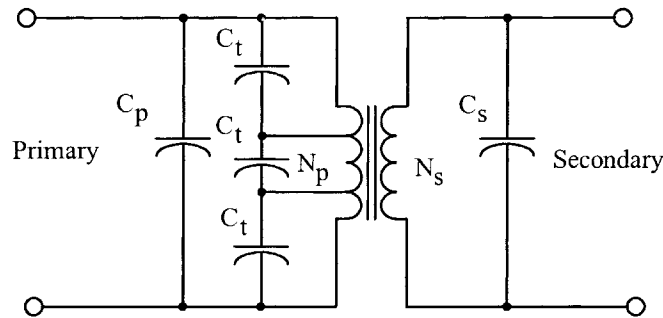


Figure 17-13. Capacitance Turn-to-Turn.

Winding Capacitance Layer-to-Layer

The capacitance between layers on the primary or secondary is the best contributor to the overall, lumped capacitance, C_p . There are three ways to minimize the layer capacitance: (1) Divide the primary and secondary windings into sections, and then sandwich the other winding between them, as shown in Figure 17-7; (2) The foldback winding technique, shown in Figure 17-14, is preferred to the normal U type winding, even though it takes an extra step before starting the next layer. The foldback winding technique will also reduce the voltage gradient between the end of the windings; (3) Increasing the amount of insulation between windings will decrease the amount of capacitance. But remember, this will increase the leakage inductance. If the capacitance is reduced, then the leakage inductance will go up. There is one exception to this rule, and that is, if the windings are sandwiched or interleaved, it will reduce the winding capacitance, but, it will increase the winding-to-winding capacitance.

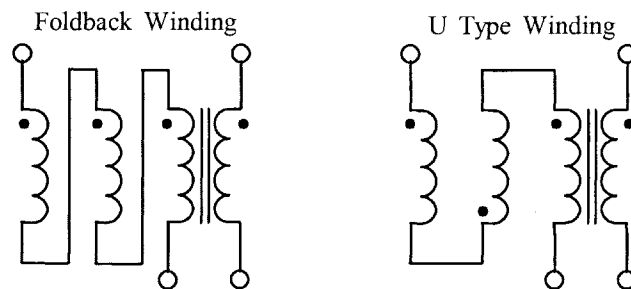


Figure 17-14. Comparing the Foldback to the U Type Winding.

Transformers and inductors wound on toroidal cores can have capacitance problems, just as much if care is not taken in the design at the beginning. It is difficult to control the winding capacitance on a toroidal core because of its odd configuration, but there are ways to control the windings and capacitance. The use of tape barriers to mark a zone for windings, as shown in Figure 17-15, offers a good way to control this capacitance.

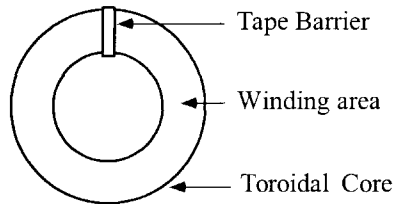


Figure 17-15. Tape Barrier for Winding Toroidal Core.

Another way to help reduce the capacitance effect on toroids is to use the progressive winding technique. The progressive winding technique example is shown in Figure 17-16 and 17-17: Wind 5 turns forward and wind 4 turns back, then wind 10 turns forward and keep repeating this procedure until the winding is complete.

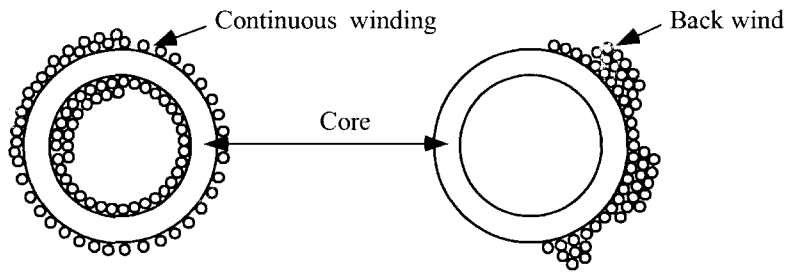


Figure 17-16. Progress Winding Top View.

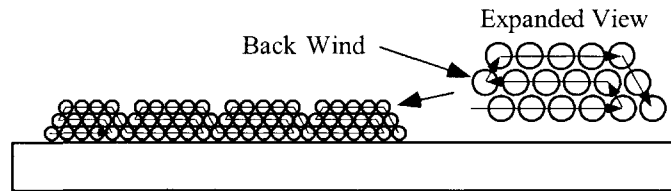


Figure 17-17. Progress Winding Side View.

Capacitance Winding-to-Winding

Balanced windings are very important in keeping down noise and common mode signals that could lead to in-circuit noise and instability problems later on. The capacitance, from winding-to-winding, shown in Figure 17-18, can be reduced, by increasing the amount of insulation between windings. This will decrease the amount of capacitance, but again, this will increase the leakage inductance. The capacitance effect

between windings can be reduced, without increasing the leakage inductance noticeably. This can be done, by adding a Faraday Shield or screen, as shown in Figure 17-19, between primary and secondary windings.

A Faraday Shield is an electrostatic shield, usually made of copper foil. The Faraday Shield is normally added along with the insulation between primary and secondary. In some designs, the Faraday Shield can consist of three independent insulated shields or just one. It all depends on the required noise rejection.

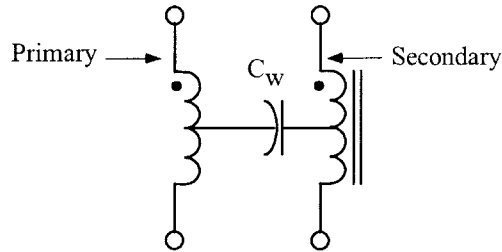


Figure 17-18. Capacitance, C_w , Winding-to-Winding.

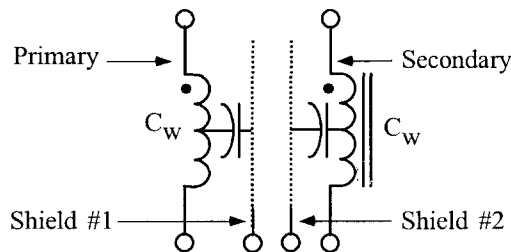


Figure 17-19. Transformer with a Primary and Secondary Shield.

Stray Capacitance

Stray capacitance is very important to minimize because it too, can generate asymmetry currents and could lead to high common mode noise. Stray capacitance is similar to winding-to-winding capacitance except that the capacitance is between the winding next to the core, C_c , and the outer winding next to the surrounding circuitry, C_s , as shown in Figure 17-20. Stray capacitance can be minimized by using a balanced winding, or using a copper shield over the entire winding. A means for measuring leakage current is shown in Figure 17-21. The winding-to-winding capacitance can be calculated, using Equations [17-8] and [17-9].

$$X_c = R1 \sqrt{\left(\frac{V_{in}}{V_o}\right) - 1}, \quad [\text{ohms}] \quad [17-8]$$

$$C_x = \frac{1}{2\pi f X_c}, \quad [\text{farads}] \quad [17-9]$$

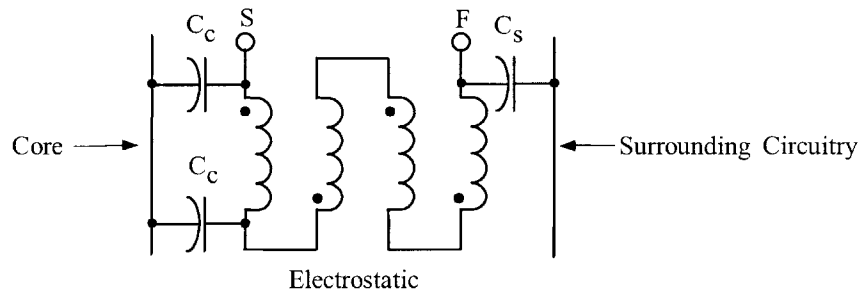


Figure 17-20. Transformer Winding with Stray Capacitance.

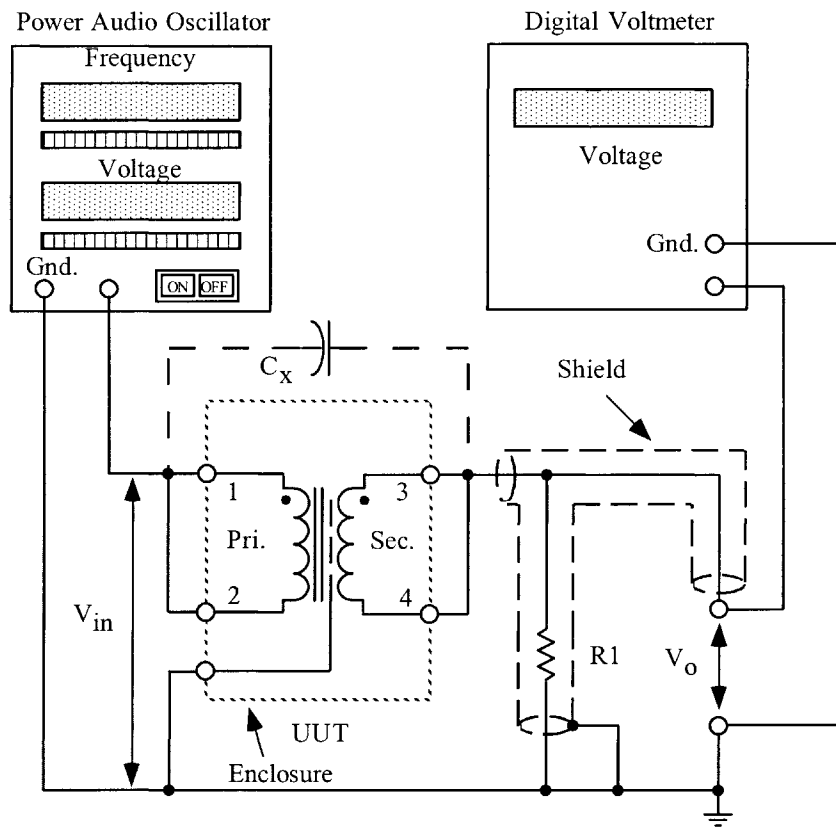


Figure 17-21. Test Circuit for Measuring Primary and Secondary, ac Leakage Current.

References

1. Grossner, N., "Transformer for Electronic Circuits." McGraw-Hill, New York, 1967.
2. Landee, R., Davis, D., and Albecht, A., "Electronic Designer's Handbook," McGraw-Hill, New York, 1957, p. 17-12.
3. Lee, R., "Electronic Transformer and Circuits," 2nd ed., John Wiley & Sons, New York, 1958.
"Reference Data for Radio Engineers," 4th ed., International Telephone and Telegraph Co., New York.
4. Richardson, I., The Technique of Transformer Design, Electro-Technology, January 1961, pp. 58-67.
Flanagan, W., "Handbook of Transformer Application." McGraw-Hill, New York, 1986.

Chapter 18

Quiet Converter Design

The author would like to thank **Dr. V. Vorperian**, Senior Engineer, Power and Sensor Electronics Group, Jet Propulsion Laboratory (JPL), for his help with the Quiet Converter design equations.

Table of Contents

1. Introduction	
2. The Voltage-fed Converter	
3. Regulating and Filtering	
4. The Current-fed Converter	
5. The Quiet Converter	
6. Regulating and Filtering	
7. Quiet Converter Waveforms	
8. Technology on the Move	
9. Window Utilization Factor, K_u	
10. Temperature Stability.....	
11. Calculating the Apparent Power, P_t	
12. Quiet Converter Design Equations	
13. Transformer Design, Using the Core Geometry, K_g , Approach	
14. Design Review	
15. References	

Introduction

A few designers have known about the Resonant Converter described here for many years. This type of Resonant Converter has been built mainly in the range of 200 watts to 2 kilowatts, and has been used as a static inverter. However, it has remained relatively obscure in the general literature. The Quiet Converter was developed at Jet Propulsion Laboratory (JPL), Division 38, to power very sensitive instruments. The Quiet Converter produces a sinusoidal voltage across a parallel resonant tank. The dc output voltage is obtained after rectification and filtering of the sinusoidal secondary voltage. The regulation is achieved by controlling the duty-cycle of the switching transistors. A comparison of the standard type of PWM control with the Quiet Converter and its amplitude modulation (AM), is shown in Figure 18-1. The inherent low noise from this converter is how the nickname, Quiet Converter, came about. The low noise can easily be reduced, even further, by the addition of a Faraday Shield and common-mode inductors. Programs at Jet Propulsion Laboratory (JPL) that have successfully used the low noise environment of the Quiet Converter are, WF/PC-II, Articulated Fold, Mirror Actuators, (Hubbell Space Telescope), MISR (Earth Orbiting System), Raman, and Mars 05 ONC, CCD Camera.

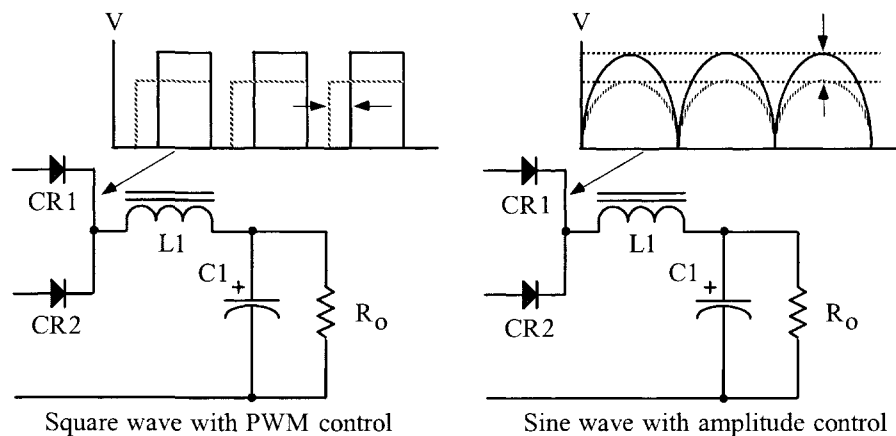


Figure 18-1. Comparing PWM and Amplitude Control.

The Voltage-fed Converter

The voltage-fed converter circuit is the most widely-used, converter topology. In a voltage-fed converter, the power source, V_{in} , is connected directly to the transformer through a transistor, Q1, as shown in Figure 18-2. When the transistor, Q1, is switched on, the full source voltage is applied to the transformer, T1, primary, (1-2). The transistor saturation will be ignored. Conversely, when Q2 is switched on, the full source voltage is applied to the other half of the transformer, T1, primary, (2-3).

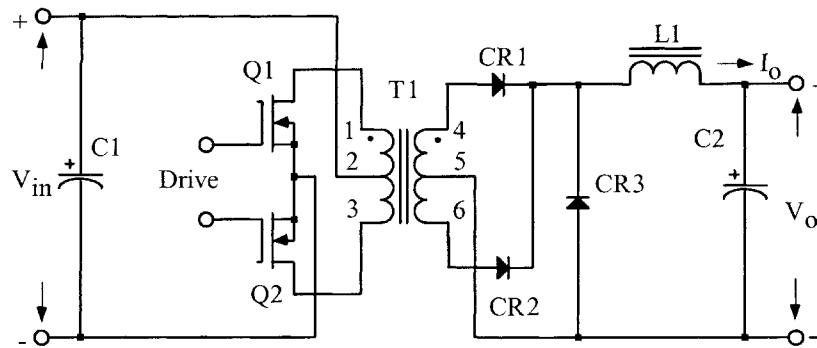


Figure 18-2. Typical, Voltage-fed Power Converter.

In Figure 18-2, the switching drive circuit alternately saturates and cuts off the semiconductors' switches, Q1 and Q2, causing an alternating voltage to be generated across the primary winding of transformer, T1, and then delivered to the secondary to be rectified and filtered before going to the load. The primary source voltage, V_{in} , is directly impressed onto the primary of the transformer, T1, and therefore, the voltage across the transformer, T1, is always a square wave.

Regulating and Filtering

The most effective method of regulation for a voltage-fed converter is pulse width modulation (PWM). A constant output voltage can be obtained for a changing input voltage, by reducing the on time, T_{on} of Q1 and Q2, as shown in Figure 18-3. The pulse width voltage is applied to the output filter, L1C2, averaging circuit to provide the proper output voltage, V_o .

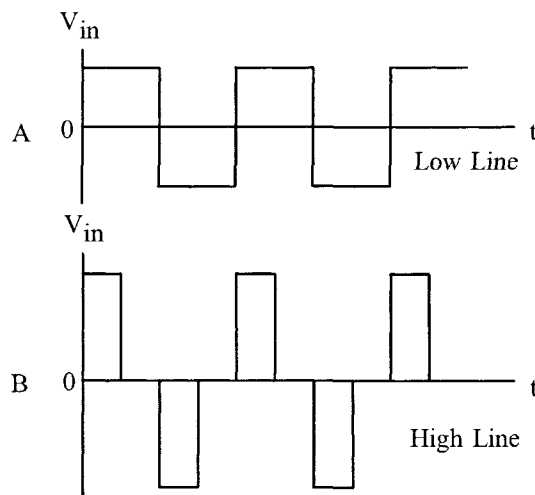


Figure 18-3. Primary Voltage of a PWM Controlled Converter.

The Current-fed Converter

The main difference between a voltage-fed converter and a current-fed converter is the series inductor, $L1$, shown in Figure 18-3. The inductor, $L1$, is commonly called a feed-choke or series inductor. It has an inductance large enough in value to maintain a continuous current through the circuit under all conditions of line and load.

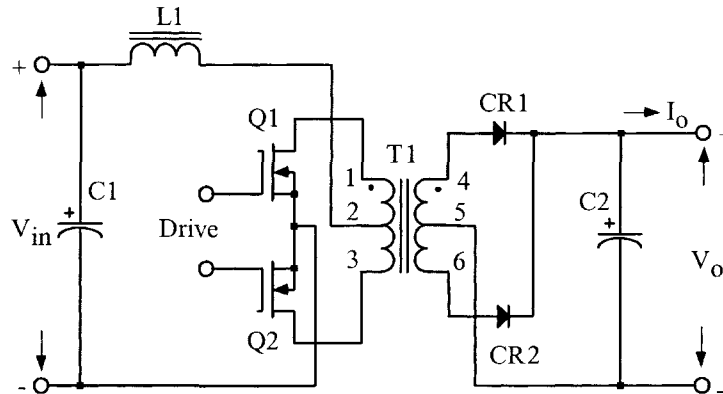


Figure 18-4. Typical Current-fed Power Converter Circuit.

The Quiet Converter

Simple additions to the circuit, in Figure 18-4, change the performance dramatically, and it becomes a whole new converter. The new converter is shown in Figure 18-5. The changes are: 1. The transformer, $T1$, core material has been changed to molypermalloy powder core, (MPP). The reason for using a powder core is because it has a built-in gap required for the tank circuit and these cores are available with temperature stabilized permeability. The use of a gap ferrite would perform just as well, but the design must be stable over temperature. 2. A commutating winding has been added to the series inductor, $L1$. 3. A capacitor, $C3$, was added for the required parallel tuned tank. The tuning capacitor, $C3$, should be of high quality with a low ESR and stable. The capacitors that were used in the flight power supplies, were plastic film, type CRH, to MIL-C-83421.

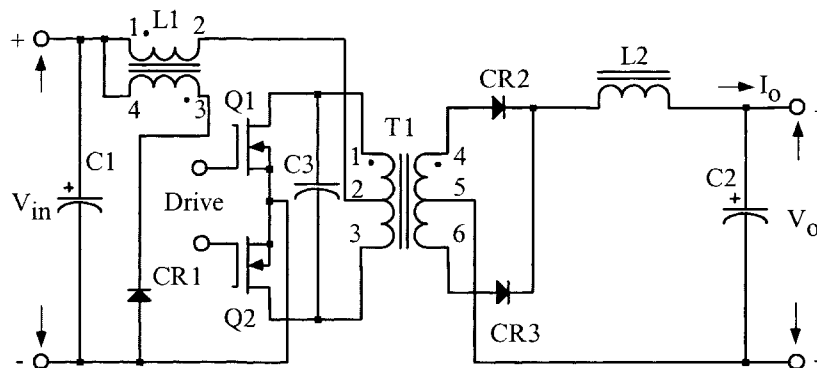


Figure 18-5. Current-fed Parallel Resonant Converter.

With properly designed components, the output voltage of transformer, T1, will always be a sine wave. The sine wave is accomplished by using a tuned parallel resonant tank circuit, (T1C3), to the natural running frequency of the converter. The series inductor, L1, isolates the input dc source from the sine wave voltage across the primary of the transformer, T1.

Regulating and Filtering

The current-fed resonant converter, shown in Figure 18-5, requires a minimum of dead time, (dwell), for the circuit to function properly. The series inductor, L1, when connected, as shown in Figure 18-4, requires continuous conduction of both Q1 and Q2, along with a small amount of overlap. In this way, there would always be continuous current flowing in L1. If there is any disruption of current in the series inductor, L1, no matter how small, it would destroy the switching transistors, Q1 and or Q2.

In order to incorporate pulse width modulation (PWM), or a drive circuit that has inherent dead time that neither transistor is conducting, there must be a means to commutate the current in the series inductor, L1. Adding a winding to the series inductor, L1, is a simple way to commutate the current. When the current flowing in winding, (1-2), is interrupted, the current will now be commutated to the added winding, (3-4). This is done when connected with proper phasing, through a diode CR1, then, back to the dc source to complete the path, as shown in Figure 18-5. Now, when either transistors, Q1 or Q2, are interrupted, the added winding of the series inductor, L1, commutates the current back into the dc source, thus preventing the destruction of the switching transistors Q1 and Q2.

Quiet Converter Waveforms

The current-fed, sine wave converter waveforms will be referenced from Figure 18-6. In Figure 18-7 through Figure 18-15, refer back to (A)–(J) points in Figure 18-6. The waveforms presented here are copies drawn from an actual photo taken with an oscilloscope camera.

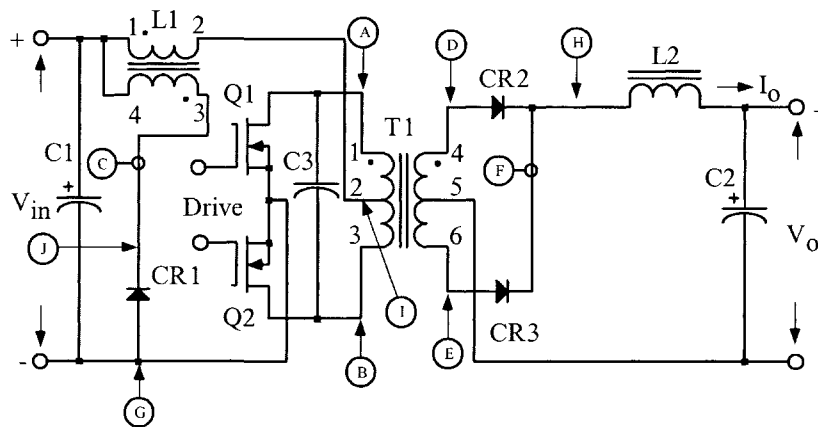


Figure 18-6. Quiet Converter Schematic with Reference Points.

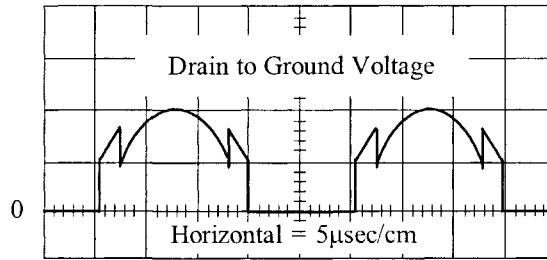


Figure 18-7. Drain to Ground, Voltage Waveform of Q1 and Q2.

The drain voltage waveform of Q1 is shown in Figure 18-7. Waveform is taken between points A and G. The converter is properly tuned to the natural frequency.

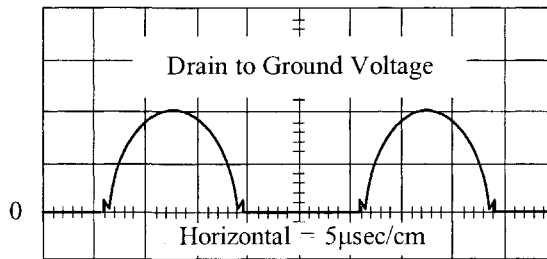


Figure 18-8. Drain to Ground, Voltage Waveform of Q1 and Q2.

The drain voltage waveform of Q1 is shown in Figure 18-8, with minimum dead time. Waveform is taken between points A and G. The converter is properly tuned to the natural frequency.

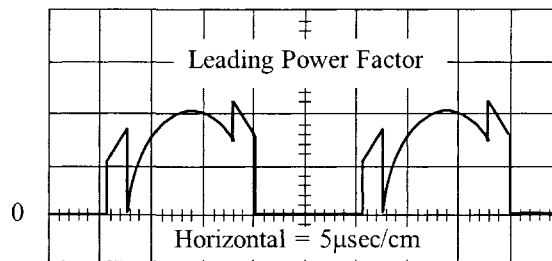


Figure 18-9. Drain to Ground, Voltage Waveform of Q1 and Q2.

The drain voltage waveform of Q1 is shown in Figure 18-9. Waveform is taken between points A and G. The converter is improperly tuned to the natural frequency. The resonant tank capacitor is too small in value.

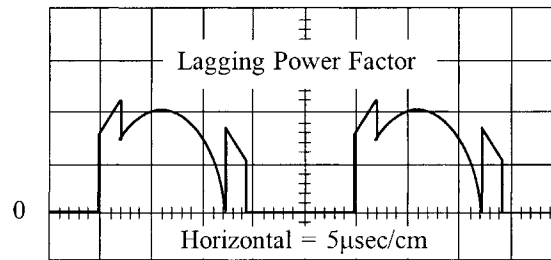


Figure 18-10. Drain to Ground, Voltage Waveform of Q1 and Q2.

The drain voltage waveform of, Q1, is shown in Figure 18-10. Waveform is taken between points A and G. The converter is improperly tuned to the natural frequency. The resonant tank capacitor is too large in value.

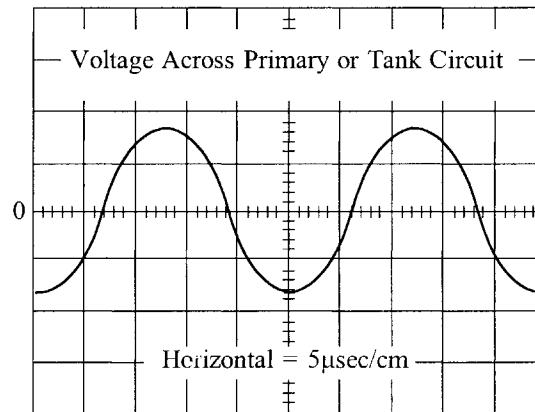


Figure 18-11. Voltage Waveform Across Transformer Primary.

The primary voltage waveform is shown in Figure 18-11, across transformer, T1. Waveform is taken between points A and B. The converter is properly tuned to the natural frequency.

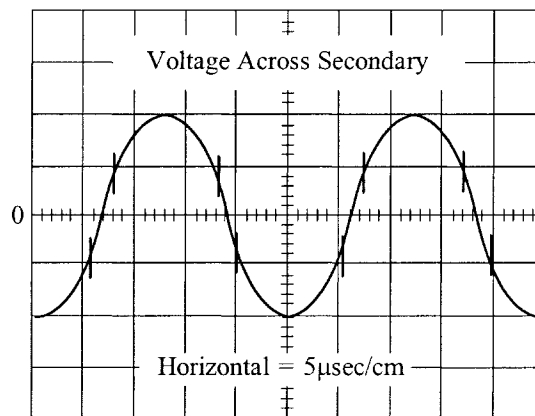


Figure 18-12. Voltage Waveform Across Transformer Secondary.

The secondary voltage waveform of transformer, T1, is shown in Figure 18-12. Waveform is taken between points D and E. The converter is properly tuned to the natural frequency.

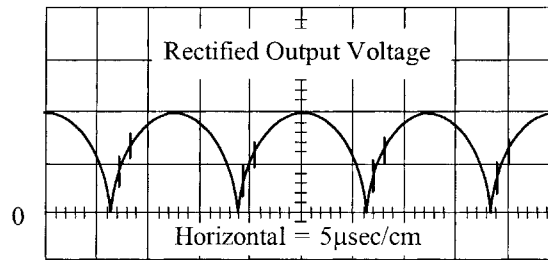


Figure 18-13. Secondary Rectified Voltage Waveform at CR2 and CR3.

The secondary, rectified voltage waveform, at the cathodes of, CR2 and CR3, is shown in Figure 18-13. Waveform is taken at point H. The converter is properly tuned to the natural frequency.

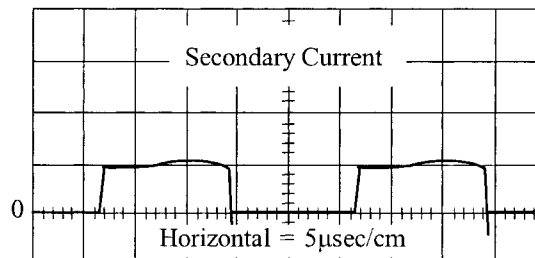


Figure 18-14. Secondary Current Waveform.

The secondary current waveform is shown in Figure 18-14. The current waveform is taken at point F.

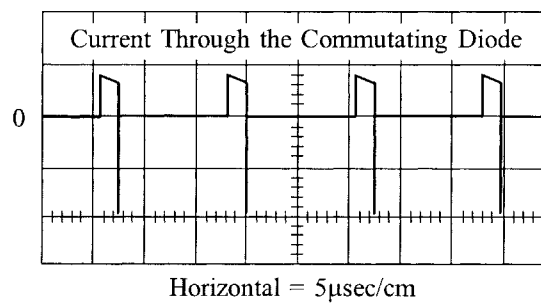


Figure 18-15. Current Through the Commutating Diode, CR1.

Commutating diode current waveform is shown in Figure 18-15. The current is through the series inductor L1 winding (3-4). Waveform is taken at point C. The converter is properly tuned to the natural frequency.

Technology on the Move

As technology moves ahead, instruments become more sophisticated, smaller in size, and require less power. Less power normally relates to lower current. Lower current requires smaller wire to carry the current. There is a practical point where the wire size can no longer be reduced, even though the current is very small. Reliability is affected when the wire size becomes very small. It becomes a handling and termination problem. If a larger wire size can be tolerated, and it does not impact the size a great deal, then, the larger wire should be used. The smallest wire size that seems to be tolerable, depending on the application, ranges from #35 to #39 AWG and this would be from a specialty house.

Window Utilization Factor, K_u

When designing a transformer or inductor, the window utilization factor, K_u , is the amount of copper that appears in the window area. See Chapter 4. The window utilization factor, K_u , is influenced by five main factors:

1. Wire insulation, S_1 .
2. Wire lay fill factor, S_2 .
3. Effective window area, S_3 .
4. Winding insulation, S_4 .
5. Workmanship.

These factors multiplied together will give a normalized window utilization factor of $K_u = 0.4$.

$$K_u = (S_1)(S_2)(S_3)(S_4) = 0.4 \quad [18-1]$$

The design of the current-fed sine wave converter is much more detailed and complex, compared to the simple voltage-fed, square wave converter. The sole reason to use the Quiet Converter is because of its inherent low noise, (EMI). The noise of the Quiet Converter can be, reduced even further by adding a primary and a secondary Faraday Shield. When a Faraday Shield is added between the primary and secondary, the transformer must be designed to accommodate the shield. Transformer size is, mainly determined by the loads. The window utilization, K_u , has to be adjusted during the design to accommodate the Faraday Shield. When the core size is selected for the transformer, it will be a little larger core, do to the added space required by the Faraday Shield.

After the preliminary design, the engineer will select the proper core size for the power transformer. The core geometry, K_g , will select the molypermalloy powder core size. After the molypermalloy powder core size has been selected, the engineer will now select a core with a permeability best-suited for the application. The molypermalloy powder cores come with a range of permeability from 14 to 550, all with the same core geometry, K_g .

Temperature Stability

For the Quiet Converter to function properly over a wide temperature range, the components must be stable over that temperature range. The components that control the oscillator frequency must be stable. The LC tank circuit must be stable and not drift with temperature. Molypermalloy powder cores are offered with stabilized permeability, with code letters M, W, and D from Magnetics, Inc. The W material temperature stability is shown in Figure 18-16.

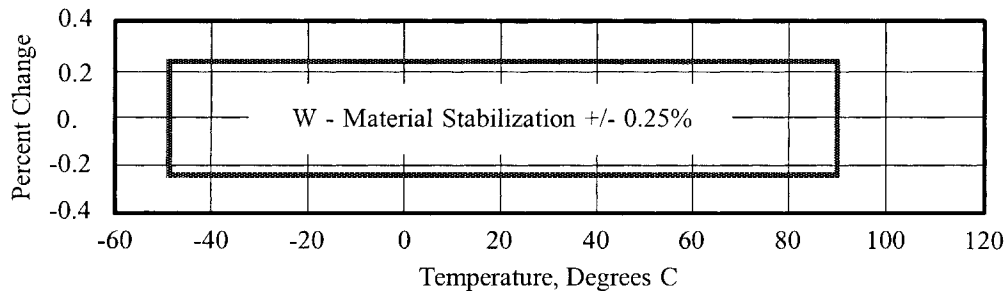


Figure 18-16. Typical, Stabilized Molypermalloy Material.

Calculating the Apparent Power, P_t

The apparent power, P_t , is the power associated with the geometry of the transformer. The designer must be able to make allowances for the rms power in each winding. The primary winding handles, P_{in} , the secondaries handle, P_o , to the load. Since the power transformer has to be designed to accommodate the primary power, P_{in} , and the secondary, P_o , then by definition,

$$P_t = P_{in} + P_{\Sigma}, \quad [\text{watts}]$$

$$P_{\Sigma} = P_{o1} + P_{o2} + \dots + P_{on}$$

$$P_{in} = \frac{P_{\Sigma}}{\eta}, \quad [\text{watts}] \quad [18-2]$$

$$P_t = \frac{P_{\Sigma}}{\eta} + P_{\Sigma}, \quad [\text{watts}]$$

$$\eta = \text{efficiency}$$

The designer must be concerned with the apparent power-handling capability, P_t , of the transformer core and winding. The apparent power, P_t , may vary by a factor ranging from 2 to 2.828 times the input power, P_{in} , depending upon the type of circuit in which the transformer is used. If the current in the transformer becomes interrupted, such as a center-tapped secondary or push-pull primary, its effective rms value changes. Transformer size is thus determined not only by the load demand, but also by application, because of the different copper losses incurred owing to current waveforms.

Because of the different winding configurations, the apparent power, P_t , of the transformer will have to be summed to reflect these differences. When the winding has a center tap and produces a discontinuous current, then the power in that winding, whether it is primary or secondary, has to be multiplied by the factor, U , to correct for the rms current in that winding. If the winding has a center tap, then, $U = 1.41$; if not, then, $U = 1$. Summing the output power of a multiple-output transformer would be:

$$P_{\Sigma} = P_{o1}(U) + P_{o2}(U) + \dots + P_{on}(U) \quad [18-3]$$

Quiet Converter Design Equations

The transformer secondary voltage, V_s , is:

V_o = Output voltage

V_d = Diode Drop

$$V_s = (V_o + V_d), \quad [\text{volts}] \quad [18-4]$$

The maximum secondary true power, $P_{s(\max)}$, is:

$$P_{s(\max)} = V_s (I_{o(\max)}), \quad [\text{watts}] \quad [18-5]$$

The minimum secondary true power, $P_{s(\min)}$, is:

$$P_{s(\min)} = V_s (I_{o(\min)}), \quad [\text{watts}] \quad [18-6]$$

The secondary apparent power, P_{sa} , is:

$U = 1.41$, center tapped winding

$U = 1.0$, single winding

$$P_{sa} = V_s (I_{o(\max)})(U), \quad [\text{watts}] \quad [18-7]$$

If, there is more than one output, then, sum the total secondary maximum apparent load power, $P_{sa\Sigma}$.

$$P_{sa\Sigma} = P_{sa01} + P_{sa02} + \dots, \quad [\text{watts}] \quad [18-8]$$

If, there is more than one output, then, sum the total secondary maximum load power, $P_{ot(\max)}$.

$$P_{ot(\max)} = P_{o01(\max)} + P_{o02(\max)} + \dots, \quad [\text{watts}] \quad [18-9]$$

If, there is more than one output, then, sum the total secondary minimum load power, $P_{ot(\min)}$.

$$P_{ot(\min)} = P_{o01(\min)} + P_{o02(\min)} + \dots, \quad [\text{watts}] \quad [18-10]$$

The maximum reflected secondary load resistance, $R_{(\max)}$, is:

$R_{(\max)}$ = Resistance Value

η = Efficiency

$$R_{(\max)} = \frac{(V_{in})^2 (\eta)}{P_{ot(\min)}}, \quad [\text{ohms}] \quad [18-11]$$

The required series inductor inductance, $L1$, is:

f = fundamental frequency

$$L1 = \frac{(R_{(\max)})}{3\omega}, \quad [\text{henrys}] \quad [18-12]$$

The total period, T , is:

$$T = \frac{1}{f}, \quad [\text{seconds}] \quad [18-13]$$

The maximum transistor on time, $t_{on(\max)}$, is:

Transistor drive circuits such as a pulse width modulator (PWM), will have a minimum of dead time, t_d .

Dead time or dwell is shown in Figure 18-17.

$$t_{on(\max)} = \left(\frac{T}{2}\right) - t_d, \quad [\mu\text{sec}] \quad [18-14]$$

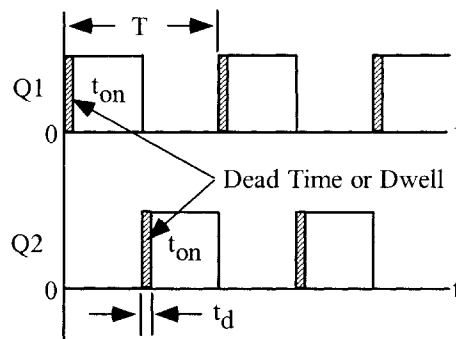


Figure 18-17. Transistor Drive Waveforms, Showing Dead Time or Dwell.

The conversion ratio, K_a , is:

$$K_a = \frac{(4t_{on(\max)} - T)}{T \text{Sin}\left(\frac{t_{on(\max)} 180}{T}\right)} \quad [18-15]$$

The peak voltage, $V_{c(pk)}$, on the resonant capacitor, C3, as shown in Figure 18-5, is:

$K_b = 2$, center tapped winding.

$K_b = 1$, single winding.

$$V_{c(pk)} = \frac{\pi(K_a V_{in} K_b)}{2}, \text{ [volts]} \quad [18-16]$$

The primary rms voltage, $V_{p(rms)}$, is:

$K_b = 2$, center tapped winding.

$K_b = 1$, single winding.

$$V_{p(rms)} = \frac{0.707(V_{c(pk)})}{K_b}, \text{ [volts]} \quad [18-17]$$

The primary maximum reflected secondary current, I_{ps} , is:

$$I_{ps} = \frac{P_{ot(max)}}{V_{p(rms)}\eta}, \text{ [amps]} \quad [18-18]$$

The secondary reflected loads to the primary, R_{SR} , is:

$K_b = 2$, center tapped winding.

$K_b = 1$, single winding.

$$R_{SR} = \frac{K_a V_{p(rms)} (K_b)^2}{I_{sp}}, \text{ [ohms]} \quad [18-19]$$

Note: The capacitance reactance affects the total percentage of harmonic distortion when:

$$\omega R_{SR} C = 1, \approx [12\%], \quad \omega R_{SR} C = 2, \approx [6\%], \quad \omega R_{SR} C = 3, \approx [4\%]$$

As a general rule:

$$C_x = \frac{2}{2\pi f (R_{SR})}, \text{ [farads]} \quad [18-20]$$

The resonant capacitance, C_x , is:

Q_T , is a variable that provides the engineer a little latitude with the capacitance value. ($1 < Q_T < 3$)

$$C_x = \frac{Q_T}{2\pi f (R_{SR})}, \text{ [farads]} \quad [18-21]$$

The reactance, X_{cx} , of capacitor, C_x , is:

Use a standard capacitor.

$$X_{cx} = \frac{1}{2\pi f C_x}, \text{ [ohms]} \quad [18-22]$$

The capacitor rms current, $I_{cx(rms)}$, is:

$$I_{cx(rms)} = \frac{(0.707)(V_{c(pk)})}{X_{cx}}, \quad [\text{amps}] \quad [18-23]$$

The total primary current, $I_{p(rms)}$, is:

$$I_{p(rms)} = \sqrt{\left((I_{p(rms)})^2 + (I_{cx(rms)})^2 \right)}, \quad [\text{amps}] \quad [18-24]$$

The primary tank inductance, L_x , is:

$$L_x = \frac{1}{(2\pi f)^2 C_x}, \quad [\text{henrys}] \quad [18-25]$$

The total transformer apparent power, P_t , is:

$$P_t = (\text{Primary VA}) + (\text{Secondary VA}) + (\text{Capacitor VA}), \quad [\text{watts}]$$

$$P_t = \left(\frac{P_{oi(\max)}(U)}{\eta} \right) + (P_{sa\Sigma}) + (K_b V_{p(rms)} I_{cx}), \quad [\text{watts}] \quad [18-26]$$

The core geometry, K_g , is:

K_f is the waveform factor = 4.44

B_{ac} is the operating flux density and its value is an engineering judgment based on the frequency and core material.

$$K_g = \left(\frac{P_t}{0.000029 (K_f)^2 (f)^2 (B_{ac})^2 \alpha} \right), \quad [\text{cm}^5] \quad [18-27]$$

Transformer Design, Using the Core Geometry, K_g , Approach

The following information is the Design specification for a 2.2 watt push-pull transformer, operating at 32kHz, using the K_g core geometry approach. For a typical design example, assume a push-pull, full wave bridge circuit, with the following specification:

1. Input voltage, $V_{(min)}$ = 22 volts
2. Output voltage #1, V_{s01} = 5.0 volts
3. Output current #1, $I_{s01(max)}$ = 0.2 amps
4. Output current #1, $I_{s01(min)}$ = 0.1 amps
5. Output voltage #2, V_{s02} = 12.0 volts
6. Output current #2, $I_{s02(max)}$ = 0.1 amps
7. Output current #2, $I_{s02(min)}$ = 0.05 amps
8. Frequency, f = 32 kHz
9. Switching dead time, t_d = 0.625 μ sec
10. Efficiency, η = 95%
11. Regulation, α = 1.0 %
12. Diode voltage drop, V_d = 0.5 volt
13. Operating flux density, B_{ac} = 0.05 tesla
14. Core Material = MPP
15. Window utilization, K_u = 0.4
16. Temperature rise goal, T_r = 15°C
17. Waveform coefficient, K_f = 4.44
18. Notes:

Using a center tapped winding, $U = 1.41$

Using a single winding, $U = 1.0$

Step 1. Calculate the total secondary voltage, V_s , for each output.

$$V_s = (V_o) + (2V_d), \quad [\text{volts}]$$

$$V_{s01} = (5.0) + (1.0) = 6.0, \quad [\text{volts}]$$

$$V_{s02} = (12) + (1.0) = 13.0, \quad [\text{volts}]$$

Step 2. Calculate the maximum secondary true power, $P_{s(max)}$.

$$P_{s(max)} = V_s (I_{o(max)}), \quad [\text{watts}]$$

$$P_{s01(max)} = 6.0(0.2) = 1.2, \quad [\text{watts}]$$

$$P_{s02(max)} = 13.0(0.1) = 1.3, \quad [\text{watts}]$$

Step 3. Calculate the minimum secondary true power, $P_{s(\min)}$.

$$P_{s(\min)} = V_s (I_{o(\min)}), \text{ [watts]}$$

$$P_{s01(\min)} = 6.0(0.1) = 0.6, \text{ [watts]}$$

$$P_{s02(\min)} = 13.0(0.05) = 0.65, \text{ [watts]}$$

Step 4. Calculate the secondary apparent power, P_{sa} .

$$P_{sa} = V_s (I_{o(\max)})(U), \text{ [watts]}$$

$$P_{sa01} = 6.0(0.2)(1.0) = 1.2, \text{ [watts]}$$

$$P_{sa02} = 13.0(0.1)(1.0) = 1.3, \text{ [watts]}$$

Step 5. Calculate the secondary total maximum apparent load power, $P_{sa\Sigma}$.

$$P_{sa\Sigma} = P_{sa01} + P_{sa02}, \text{ [watts]}$$

$$P_{sa\Sigma} = (1.2) + (1.3), \text{ [watts]}$$

$$P_{sa\Sigma} = 2.5, \text{ [watts]}$$

Step 6. Calculate the secondary total maximum load power, $P_{ot(\max)}$.

$$P_{ot(\max)} = P_{o01(\max)} + P_{o02(\max)}, \text{ [watts]}$$

$$P_{ot(\max)} = (1.2) + (1.3), \text{ [watts]}$$

$$P_{ot(\max)} = 2.5, \text{ [watts]}$$

Step 7. Calculate the secondary total minimum load power, $P_{ot(\min)}$.

$$P_{ot(\min)} = P_{o01(\min)} + P_{o02(\min)}, \text{ [watts]}$$

$$P_{ot(\min)} = (0.6) + (0.65), \text{ [watts]}$$

$$P_{ot(\min)} = 1.25, \text{ [watts]}$$

Step 8. Calculate the secondary maximum reflected load resistance, $R_{(\max)}$.

$R_{(\max)}$ = Resistance Value

η = Efficiency

$$R_{(\max)} = \frac{(V_{in})^2 (\eta)}{P_{ot(\min)}}, \text{ [ohms]}$$

$$R_{(\max)} = \frac{(22)^2 (0.95)}{1.25}, \text{ [ohms]}$$

$$R_{(\max)} = 368, \text{ [ohms]}$$

Step 9. Calculate the inductance of the series inductor, L1.

$$L1 = \frac{R_{(\max)}}{3\omega}, \text{ [henrys]}$$

$$L1 = \frac{(368)}{3(2(3.14)(32000))}, \text{ [henrys]}$$

$$L1 = 0.000610, \text{ [henrys]}$$

Step 10. Calculate the total period, T.

$$T = \frac{1}{f}, \text{ [seconds]}$$

$$T = \frac{1}{32,000}, \text{ [seconds]}$$

$$T = 31.25, \text{ [micro-seconds]}$$

Step 11. Calculate the maximum transistor on time, $T_{on(\max)}$. Dead time is shown in Figure 18-17.

$$t_{on(\max)} = \left(\frac{T}{2}\right) - t_d, \text{ [usec]}$$

$$t_{on(\max)} = \left(\frac{31.25}{2}\right) - 0.625, \text{ [usec]}$$

$$t_{on(\max)} = 15, \text{ [usec]}$$

Step 12. Calculate the conversion ratio, K_a .

$$K_a = \frac{(4t_{on(\max)} - T)}{T \sin\left(\frac{t_{on(\max)} 180}{T}\right)}$$

$$K_a = \frac{(4(15) - (32.25))}{(32.25) \sin\left(\frac{(15)180}{32.25}\right)}$$

$$K_a = 0.866$$

Step 13. Calculate the peak voltage, $V_{c(pk)}$, on the resonant capacitor, C3, as shown in Figure 18-5.

$K_b = 2$, center tapped winding.

$K_b = 1$, single winding.

$$V_{c(pk)} = \frac{\pi(K_a V_{in} K_b)}{2}, \text{ [volts]}$$

$$V_{c(pk)} = \frac{(3.1415)(0.866)(22)(2)}{2}, \text{ [volts]}$$

$$V_{c(pk)} = 59.85, \text{ [volts]}$$

Step 14. Calculate the primary rms voltage, $V_{p(rms)}$.

$K_b = 2$, center tapped winding.

$K_b = 1$, single winding.

$$V_{p(rms)} = \frac{0.707(V_{c(pk)})}{K_b}, \text{ [volts]}$$

$$V_{p(rms)} = \frac{0.707(59.85)}{2}, \text{ [volts]}$$

$$V_{p(rms)} = 21.2, \text{ [volts]}$$

Step 15. Calculate the primary maximum reflected secondary current, I_{ps} .

$$I_{ps} = \frac{P_{ot(max)}}{V_{p(rms)}\eta}, \text{ [amps]}$$

$$I_{ps} = \frac{2.5}{(21.2)(0.95)}, \text{ [amps]}$$

$$I_{ps} = 0.124, \text{ [amps]}$$

Step 16. Calculate the secondary reflected loads to the primary, R_{SR} .

$K_b = 2$, center tapped winding.

$K_b = 1$, single winding.

$$R_{SR} = \frac{K_a V_{p(rms)} (K_b)^2}{I_{sp}}, \text{ [ohms]}$$

$$R_{SR} = \frac{(0.866)(21.2)(2)^2}{0.124}, \text{ [ohms]}$$

$$R_{SR} = 592, \text{ [ohms]}$$

Note: The capacitance reactance effects the total percentage of harmonic distortion when:

$$\omega R_{SR} C = 1, \approx [12\%], \quad \omega R_{SR} C = 2, \approx [6\%], \quad \omega R_{SR} C = 3, \approx [4\%]$$

As a general rule:

$$C_x = \frac{2}{2\pi f (R_{SR})}, \text{ [farads]}$$

Step 17. Calculate the resonant capacitance, C_x .

$$C_x = \frac{2}{2\pi f (R_{SR})}, \text{ [farads]}$$

$$C_x = \frac{2}{(6.28)(32000)(592)}, \text{ [farads]}$$

$$C_x = 1.68(10^{-8}), \text{ [farads]}$$

$$C_x = 0.0168 \text{ use a } 0.015, \text{ [micro-farads]}$$

Step 18. Calculate the reactance, X_{cx} , of capacitor, C_x . Use a standard capacitor. Let, C_x , equal $0.015\mu\text{f}$.

$$X_{cx} = \frac{1}{2\pi f C_x}, \quad [\text{ohms}]$$

$$X_{cx} = \frac{1}{(6.28)(32,000)(0.015(10^{-6}))}, \quad [\text{ohms}]$$

$$X_{cx} = 332, \quad [\text{ohms}]$$

Step 19. Calculate the capacitor current, $I_{cx(rms)}$.

$$I_{cx(rms)} = \frac{(0.707)(V_{c(pk)})}{X_{cx}}, \quad [\text{amps}]$$

$$I_{cx(rms)} = \frac{(0.707)(59.85)}{332}, \quad [\text{amps}]$$

$$I_{cx(rms)} = 0.127, \quad [\text{amps}]$$

Step 20. Calculate the total primary current, $I_{p(rms)}$.

$$I_{p(rms)} = \sqrt{\left(I_{p(rms)}\right)^2 + \left(I_{cx(rms)}\right)^2}, \quad [\text{amps}]$$

$$I_{p(rms)} = \sqrt{\left(0.124\right)^2 + \left(0.127\right)^2}, \quad [\text{amps}]$$

$$I_{p(rms)} = 0.177, \quad [\text{amps}]$$

Step 21. Calculate primary tank inductance, L_x .

$$L_x = \frac{1}{(2\pi)^2 (f)^2 C_x}, \quad [\text{henrys}]$$

$$L_x = \frac{1}{(6.28)^2 (32000)^2 (0.015(10^{-6}))}, \quad [\text{henrys}]$$

$$L_x = 0.00165, \quad [\text{henrys}]$$

Step 22. Calculate the total transformer apparent power, P_t .

$$P_t = (\text{Primary VA}) + (\text{Secondary VA}) + (\text{Capacitor VA}), \quad [\text{watts}]$$

$$P_t = \left(\frac{P_{or(\max)}(U)}{\eta}\right) + (P_{sa\Sigma}) + (K_b V_{p(rms)} I_{cx}), \quad [\text{watts}]$$

$$P_t = \left(\frac{(2.5)(1.41)}{0.95}\right) + (2.5) + ((2)(21.2)(0.127)), \quad [\text{watts}]$$

$$P_t = 11.6, \quad [\text{watts}]$$

Step 23. Calculate the core geometry, K_g . B_{ac} is the operating flux density and its value is an engineering judgment based on the frequency and core material.

$$K_g = \left(\frac{P_t}{0.000029 (K_f)^2 (f)^2 (B_{ac})^2 \alpha} \right), \text{ [cm}^5\text{]}$$

$$K_g = \left(\frac{11.6}{0.000029 (4.44)^2 (32,000)^2 (0.05)^2 (1)} \right), \text{ [cm}^5\text{]}$$

$$K_g = 0.00793, \text{ [cm}^5\text{]}$$

Design Review

Conversion factor, K_a	0.866
Tank Capacitance, C_x	0.015 μ f
Tank Capacitance Peak Voltage, V_{cx}	59.85 volts
Tank Capacitance rms Current, $I_{cx(rms)}$	0.127 amps
Primary Inductance, L_x	0.00165 henrys
Series Inductor, L1	0.000610 henrys
Primary Reflected Current, $I_{ps(rms)}$	0.124 amps
Primary rms Voltage, $V_{p(rms)}$	21.2 volts
Primary Total rms Current, $I_{tp(rms)}$	0.177 amps
Secondary Total Load Power, $P_{ot(max)}$	2.5 watts
Transformer Total Apparent Power, P_t	11.6 watts
Transformer Core Geometry, K_g	0.0107 cm^2

Step 24. From Chapter 3, select a MPP powder core, comparable in core geometry, K_g .

Core part number	55848-W4
Manufacturer	Magnetics
Magnetic path length, MPL	= 5.09 cm
Core weight, W_{tfe}	= 9.4 gm
Copper weight, W_{tcu}	= 11.1 gm
Mean length turn, MLT	= 2.8 cm
Iron area, A_c	= 0.226 cm^2
Window area, W_a	= 1.11 cm^2
Area product, A_p	= 0.250 cm^4
Core geometry, K_g	= 0.008 cm^5
Surface area, A_t	= 22.7 cm^2
Permeability, μ	= 60
Millihenrys per 1000 turns, AL	= 32

Step 25. Calculate the total number of primary turns, N_{tp} .

$$N_{tp} = 1000 \sqrt{\frac{L_{(new)}}{L_{(1000)}}}, \text{ [turns]}$$

$$N_{tp} = 1000 \sqrt{\frac{1.65}{32}}, \text{ [turns]}$$

$$N_{tp} = 226, \text{ round-down [turns]}$$

$$N_p = 113, \text{ [each side center tap]}$$

Step 26. Calculate the operating flux density, B_{ac} .

$$B_{ac} = \frac{V_p(rms)(10^4)}{K_f N_p f A_c}, \text{ [tesla]}$$

$$B_{ac} = \frac{(21.2)(10^4)}{(4.44)(113)(32000)(0.226)}, \text{ [tesla]}$$

$$B_{ac} = 0.0587, \text{ [tesla]}$$

Step 27. Calculate the watts per kilogram, WK, using the MPP 60 perm loss equation in Chapter 2.

$$WK = 0.788(10^{-3})(f)^{(1.41)}(B_{ac})^{(2.24)}, \text{ [watts/kilogram]}$$

$$WK = 0.788(10^{-3})(32000)^{(1.41)}(0.0587)^{(2.24)}, \text{ [watts/kilogram]}$$

$$WK = 3.09, \text{ [watts/kilogram] or } 3.09, \text{ [milliwatts/gram]}$$

Step 28. Calculate the core loss, P_{fe} .

$$P_{fe} = \left(\frac{\text{milliwatts}}{\text{grams}} \right) W_{fe} (10^{-3}), \text{ [watts]}$$

$$P_{fe} = (3.09)(9.4)(10^{-3}), \text{ [watts]}$$

$$P_{fe} = 0.0290, \text{ [watts]}$$

Step 29. Calculate the volts per turn, $K_{N/V}$.

$$K_{N/V} = \frac{N_p}{V_p}, \text{ [turns/volt]}$$

$$K_{N/V} = \frac{(113)}{(21.2)}, \text{ [turns/volt]}$$

$$K_{N/V} = 5.33, \text{ [turns/volt]}$$

Step 30. Calculate the secondary number of turns N_s . α is regulation in percent. See Chapter 6.

$$K = \left(1 + \frac{\alpha}{100}\right) = 1.01$$

$$N_{s01} = K_{N/V} V_{s01} K = (5.33)(6.0)(1.01) = 32, \text{ [turns]}$$

$$N_{s02} = K_{N/V} V_{s02} K = (5.33)(13.0)(1.01) = 70, \text{ [turns]}$$

Step 31. Calculate the current density, J , using a window utilization, $K_u = 0.4$.

$$J = \frac{P_t 10^4}{A_p B_m f K_f K_u}, \text{ [amps per cm}^2\text{]}$$

$$J = \frac{(11.6)10^4}{(0.25)(0.0587)(32000)(4.44)(0.4)}, \text{ [amps per cm}^2\text{]}$$

$$J = 139, \text{ [amps per cm}^2\text{]}$$

Step 32. Calculate the secondary required wire area, A_{ws} .

$$A_{ws01} = \frac{I_{s(01)(rms)}}{J} = \frac{0.2}{139} = 1.44 \times 10^{-3}, \text{ [cm}^2\text{]}$$

$$A_{ws02} = \frac{I_{s(02)(rms)}}{J} = \frac{0.1}{139} = 0.719 \times 10^{-3}, \text{ [cm}^2\text{]}$$

Step 33. Then select the wire from the Wire Table, in Chapter 4. Record $\mu\Omega/cm$.

$$A_{ws01} = 1.44 \times 10^{-3}, \text{ use \#26} = 1.28 \times 10^{-3}, \text{ [cm}^2\text{]}$$

$$\#26, \frac{\mu\Omega}{cm} = 1345$$

$$A_{ws02} = 0.719 \times 10^{-3}, \text{ use \#29} = 0.647 \times 10^{-3}, \text{ [cm}^2\text{]}$$

$$\#29, \frac{\mu\Omega}{cm} = 2664$$

Step 34. Calculate the primary required wire area, A_{wp} .

$$A_{wp} = \frac{I_{ip(rms)}}{J}, \text{ [cm}^2\text{]}$$

$$A_{wp} = \frac{(0.177)}{139}, \text{ [cm}^2\text{]}$$

$$A_{wp} = 1.27 \times 10^{-3}, \text{ [cm}^2\text{]}$$

Step 35. Then select the wire from the Wire Table, in Chapter 4. Record $\mu\Omega/cm$.

$$A_{wp} = 1.27 \times 10^{-3}, \text{ use \#26} = 1.28 \times 10^{-3}, \text{ [cm}^2\text{]}$$

$$\#26, \frac{\mu\Omega}{cm} = 1345$$

Step 36. Calculate the total secondary window utilization, K_{us} .

$$K_{us01} = \frac{(N_{01} A_{w01})}{W_a} = \frac{(32)(0.00128)}{1.11} = 0.0369$$

$$K_{us02} = \frac{(N_{02} A_{w02})}{W_a} = \frac{(70)(0.000647)}{1.11} = 0.0408$$

$$K_{us} = K_{us01} + K_{us02} = 0.0777$$

Step 37. Calculate the primary window utilization, K_{up} .

$$K_{up} = \frac{(N_p A_w)}{W_a}$$

$$K_{up} = \frac{(226)(0.00128)}{1.11}$$

$$K_{up} = 0.261$$

Step 38. Calculate the total window utilization, K_u .

$$K_u = K_{up} + K_{us}$$

$$K_u = 0.261 + 0.0777$$

$$K_u = 0.339$$

Step 39. Calculate the primary, winding resistance, R_p .

$$R_p = \text{MLT}(N_p) \left(\frac{\mu\Omega}{\text{cm}} \right) (10^{-6}), \quad [\text{ohms}]$$

$$R_p = 2.80(113)(1345)(10^{-6}), \quad [\text{ohms}]$$

$$R_p = 0.426, \quad [\text{ohms}]$$

Step 40. Calculate the primary, copper loss, P_p .

$$P_p = (I_{p(\text{rms})})^2 R_p, \quad [\text{watts}]$$

$$P_p = (0.177)^2 (0.426), \quad [\text{watts}]$$

$$P_p = 0.0133, \quad [\text{watts}]$$

Step 41. Calculate the secondary, winding resistance, R_s .

$$R_s = \text{MLT}(N_s) \left(\frac{\mu\Omega}{\text{cm}} \right) (10^{-6}), \quad [\text{ohms}]$$

$$R_{s01} = 2.80(32)(1345)(10^{-6}) = 0.121, \quad [\text{ohms}]$$

$$R_{s02} = 2.80(70)(2664)(10^{-6}) = 0.186, \quad [\text{ohms}]$$

Step 42. Calculate the secondary, copper loss, P_s .

$$P_s = (I_{s(rms)})^2 R_s, \text{ [watts]}$$
$$P_{s01} = (0.2)^2 (0.121) = 0.00484, \text{ [watts]}$$
$$P_{s02} = (0.1)^2 (0.186) = 0.00186, \text{ [watts]}$$

Step 43. Calculate the total secondary, copper loss, P_{ts} .

$$P_{ts} = P_{s01} + P_{s02}, \text{ [watts]}$$
$$P_{ts} = 0.00484 + 0.00186, \text{ [watts]}$$
$$P_{ts} = 0.0067, \text{ [watts]}$$

Step 44. Calculate the total loss, core and copper, P_Σ .

$$P_\Sigma = P_p + P_{ts} + P_{fc}, \text{ [watts]}$$
$$P_\Sigma = (0.0133) + (0.0067) + (0.0290), \text{ [watts]}$$
$$P_\Sigma = 0.049, \text{ [watts]}$$

Step 45. Calculate the watts per unit area, ψ .

$$\psi = \frac{P_\Sigma}{A_t}, \text{ [watts per cm}^2\text{]}$$
$$\psi = \frac{(0.049)}{(22.7)}, \text{ [watts per cm}^2\text{]}$$
$$\psi = 0.00216, \text{ [watts per cm}^2\text{]}$$

Step 46. Calculate the temperature rise, T_r .

$$T_r = 450(\psi)^{(0.826)}, \text{ [}^\circ\text{C]}$$
$$T_r = 450(0.00216)^{(0.826)}, \text{ [}^\circ\text{C]}$$
$$T_r = 2.83, \text{ [}^\circ\text{C]}$$

Step 47. Calculate the, Q_t , of the tank.

$$Q_t = 2\pi f C_x R_{SR}$$
$$Q_t = (6.28)(32000)(0.015(10^{-6}))(592)$$
$$Q_t = 1.79$$

For more information see Equation [18-20].

References

1. V. Vorperian, and C. McLyman, "Analysis of a PWM-Resonant DC-to-DC Converter." IEEE transaction.
2. S. Lendena, "Current-Fed Inverter." 20th Annual Proceedings Power Sources Conference, May 24 1966.
3. S. Lendena, "Single Phase Inverter for a Three Phase Power Generation and Distribution System." Electro-Optical-System, Contract #954272, from Jet Propulsion Laboratory, January 1976.

Chapter 19

Rotary Transformer Design

Table of Contents

1. Introduction	
2. Basic Rotary Transformer	
3. Square Wave Technology	
4. Rotary Transformer Leakage Inductance	
5. Current-fed Sine Wave Converter Approach	
6. Rotary Transformer Design Constraints	
7. References	

Introduction

There are many requirements to transfer signals and power across rotary interfaces. Most things that use slip rings or brushes can be replaced with a rotary transformer. Science instruments, antennas and solar arrays are elements needing rotary power transfer for certain spacecraft (S/C) configurations, such as a spin, stabilized (S/C). Delivery of signals and power has mainly been done by slip rings. There are problems in using slip rings for long life and high reliability: contact wear, noise, and contamination. Contact wear will lead to a conductive path to ground. This conductive path will generate noise and upset the original designed common-mode noise rejection. A simple slip ring assembly and a rotary transformer are shown in Figure 19-1. High data rates and poor slip ring life forced the Galileo (S/C) to replace the signal interface with rotary transformers. The use of a rotary transformer to transfer power on the Galileo (S/C) was contemplated, but it was thought the impact on the (S/C) delivery was too great. The rotary transformers on the Galileo (S/C) lasted the life of the spacecraft, from 1989 to 2003 without a glitch.

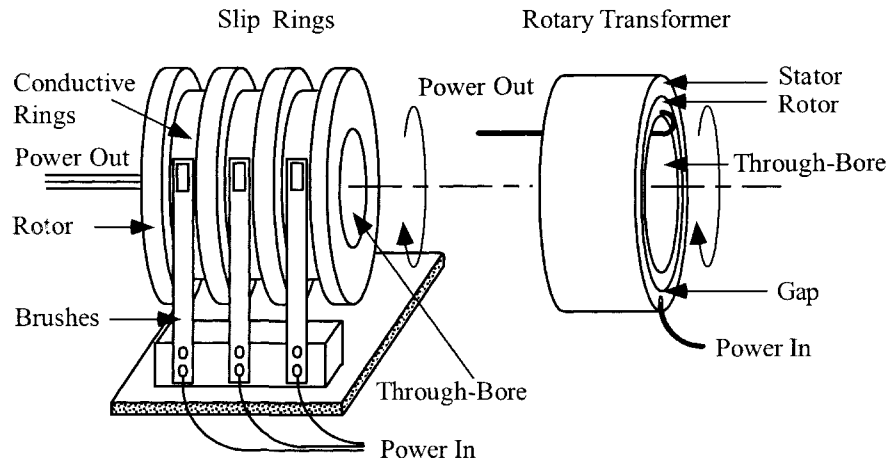


Figure 19-1. Comparing a Slip Ring Assembly and a Rotary Transformer.

Existing approaches to rotary power transfer use square wave converter technology. However, there are problems caused by the inherent gap in a rotary transformer, coupled with the fast rate of change in the square wave voltage. Undue stress is placed on the power electronics and the interface becomes a source of Electromagnetic Interference (EMI) that impacts the overall system's operating integrity.

Basic Rotary Transformer

The rotary transformer is essentially the same as a conventional transformer, except that the geometry is arranged so that the primary and secondary can be rotated, with respect to each other with negligible changes in the electrical characteristics. The most common of the rotary transformers are the axial rotary

transformer, shown in Figure 19-2, and the flat plane, (pot core type), rotary transformer, shown in Figure 19-3. The power transfer is accomplished, electro-magnetically, across an air gap. There are no wearing contacts, noise, or contamination problems due to lubrication or wear debris.

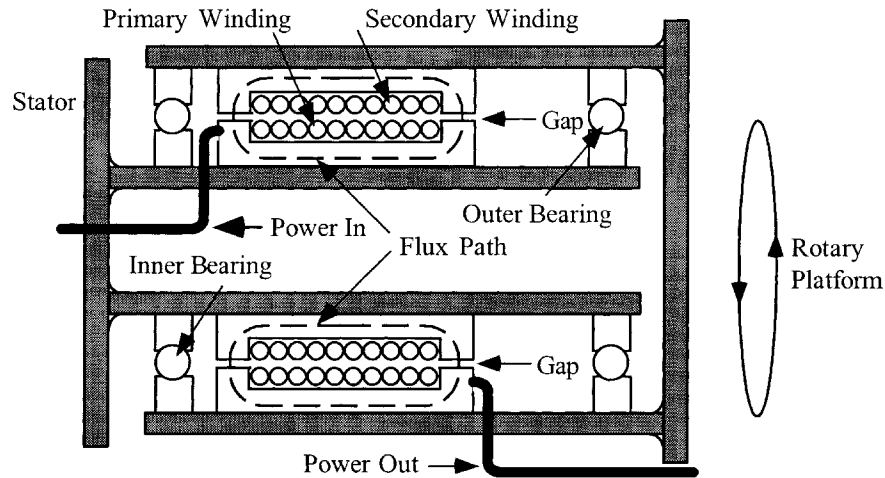


Figure 19-2. Pictorial of an Axial, type Rotary Transformer.

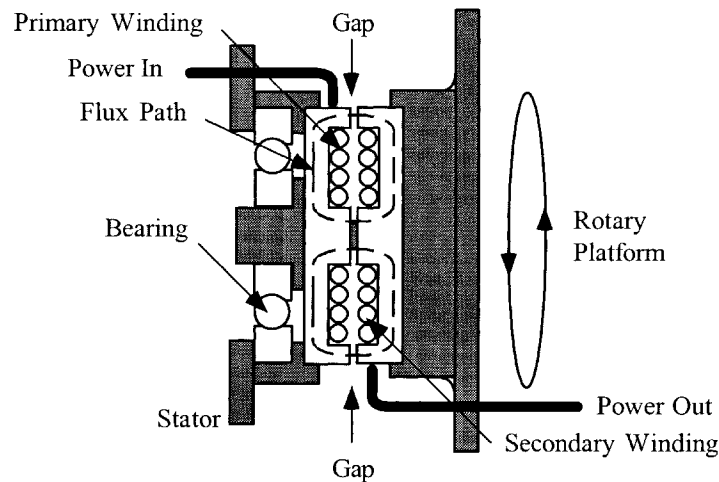


Figure 19-3. Pictorial of a Flat Plane, type Rotary Transformer.

Square Wave Technology

The ideal converter transformer would have a typical square B-H loop, as shown in Figure 19-4. A converter transformer is normally designed to have a minimum of leakage inductance. The voltage spikes that are normally seen on the primary of a square wave converter transformer are caused by the leakage inductance. To design a converter transformer to have a minimum of leakage inductance, the primary and secondary must have a minimum of distance between them. Minimizing the leakage inductance will

reduce the need for power-wasting, snubber circuits. Although there are rotary power transformers designed with the use of square wave converter technology, they are not, without problems.

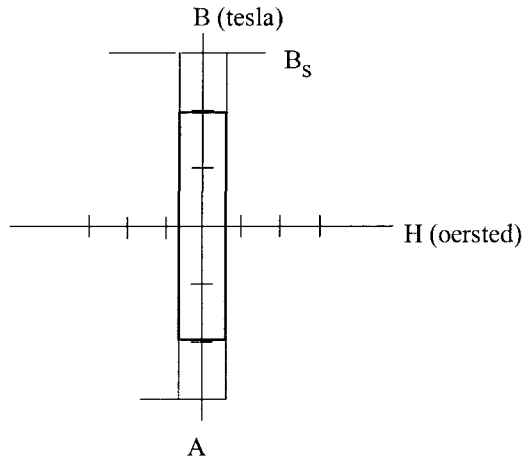


Figure 19-4. Typical, Transformer BH Loop.

There are two basic problems not found in the normal transformer: (1) the inherent gap in a rotary transformer is one problem, and (2) the required spacing between primary and secondary that leads to large leakage inductance is the other. These problems, along with a square wave drive, are what leads to a high loss, snubber circuit, and become a source of Electromagnetic Interference (EMI) that impacts the adjoining systems operating integrity. The rotary transformer, because of its inherent gap, has a B-H loop similar to an inductor, as shown in Figure 19-5. Basically, the transformer transforms power, and the inductor stores energy in the gap. The rotary transformer does not have any of the traits of an ideal transformer. It is, more accurately, a trans-inductor having a gap and a secondary, spaced away from the primary.

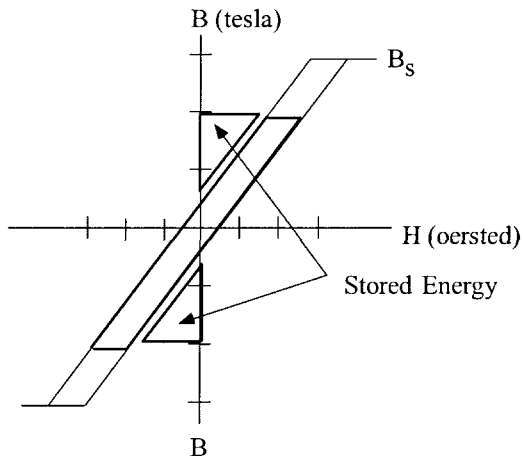


Figure 19-5. Typical, Rotary Transformer BH Loop.

Rotary Transformer Leakage Inductance

The rotary transformer has an inherent gap and spacing of the primary and secondary. The gap and spacing in the rotary transformer result in a low primary magnetizing inductance. This low primary inductance leads to a high magnetizing current. The leakage inductance, L_p , can be calculated for both axial and flat plane using Equation 19-1. The axial rotary transformer winding dimensions are shown in Figure 19-6. The flat plane rotary transformer winding dimensions are shown in Figure 19-7.

$$L_p = \frac{4\pi (MLT) N_p^2}{a} \left(c + \frac{b_1 + b_2}{3} \right) (10^{-9}), \text{ [henrys] [19-1]}$$

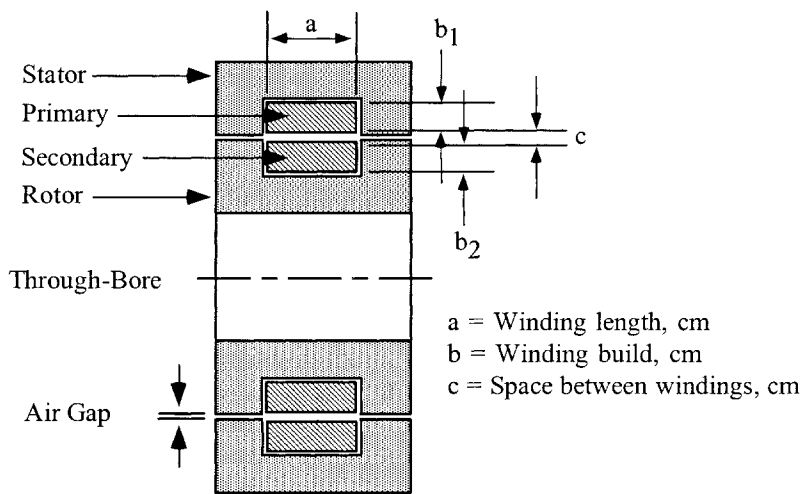


Figure 19-6. Axial Rotary Transformer, Showing Winding Dimensions.

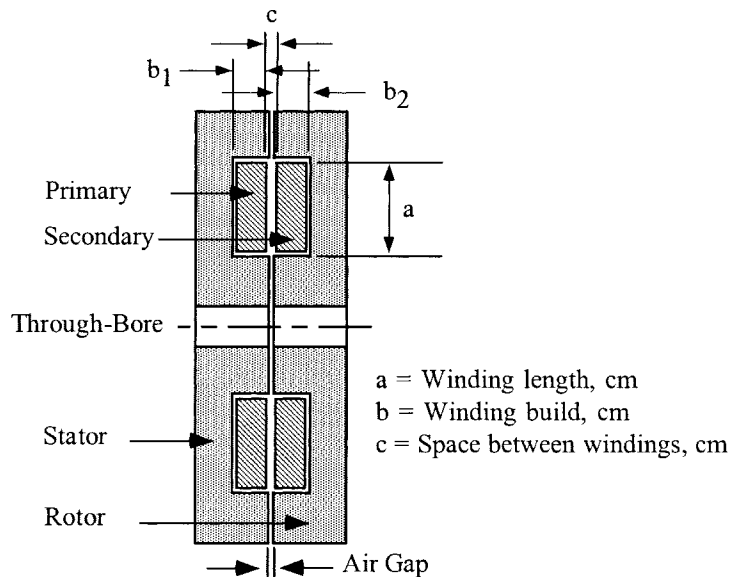


Figure 19-7. Flat Plane Rotary Transformer, Showing Winding Dimensions.

Current-fed Sine Wave Converter Approach

The current-fed, sine wave converter topology is a good candidate to power the rotary transformer. The design would be a current-fed, push-pull, tuned tank converter requiring a gapped transformer. A comparison between a standard, square wave converter, shown in Figure 19-8, and a current-fed, sine wave converter, is shown in Figure 19-9. Using the rotary transformer in this topology, the energy that is stored in the rotary gap that causes so much trouble in the standard square wave driving a rotary transformer, is recovered and is used in the tank circuit. There would not be any need of power-wasting snubbers using the rotary transformer approach. See Chapter 18.

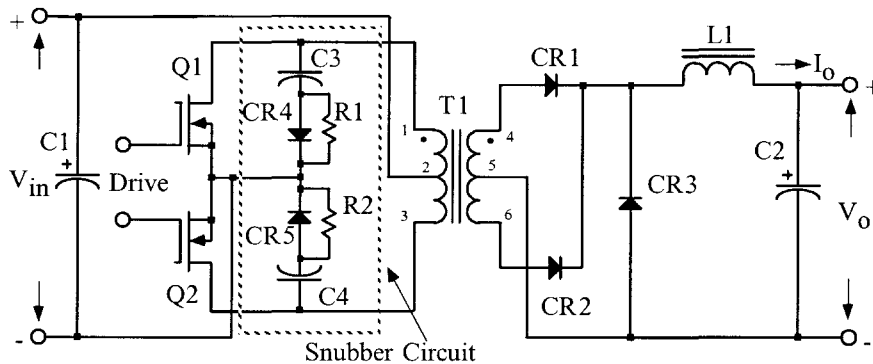


Figure 19-8. Typical, Voltage-fed, Square wave Converter Circuit with Snubbers.

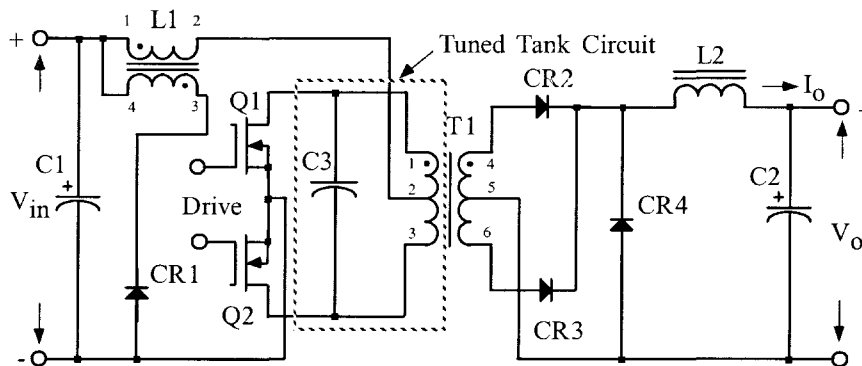


Figure 19-9. Typical, Current-fed, Resonant Converter Circuit.

The current-fed sine wave converter requires a resonant, LC, tank circuit to operate properly. The primary of the rotary transformer would be the ideal inductor, because of the inherent gap of the rotary transformer. There are several advantages to incorporating the resonant tank circuit into the rotary transformer. First, it minimizes the number of components in the power stage. Secondly, the output of the inverter is a natural sine wave, as shown in Figure 19-10, and usually requires no additional filtering. Thirdly, energy stored in the gap of the transformer is released when either power switch is turned off. This energy is commutated in the resonant tank circuit. This provides the capability for direct exchange of power between the tank circuit

and the load. There is not a noticeable drive torque in a rotary transformer. The tuning or tank capacitor must be of high quality, stable, and with low ESR.

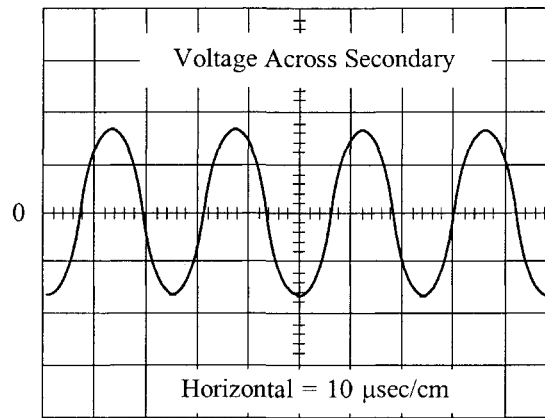


Figure 19-10. Current-fed Converter, Secondary Sine Wave Secondary Voltage.

Rotary Transformer Design Constraints

The rotary transformer requirements pose some unusual design constraints compared to the usual transformer design. The first is the relatively large gap in the magnetic circuit. This gap size depends on the eccentric dimension and the tolerance of the rotating shaft. The gap results in a low primary magnetizing inductance. Secondly, the large space separating primary and secondary windings results in an unusually high primary-to-secondary leakage inductance. Thirdly, the large through-bore requirement results in an inefficient utilization of the core material and copper, due to the fixed mean-length turn. This large diameter results in requiring more copper area for the same regulation. Finally, the core has to be more robust than the normal transformer because of the structural requirement. See Figure 19-11.

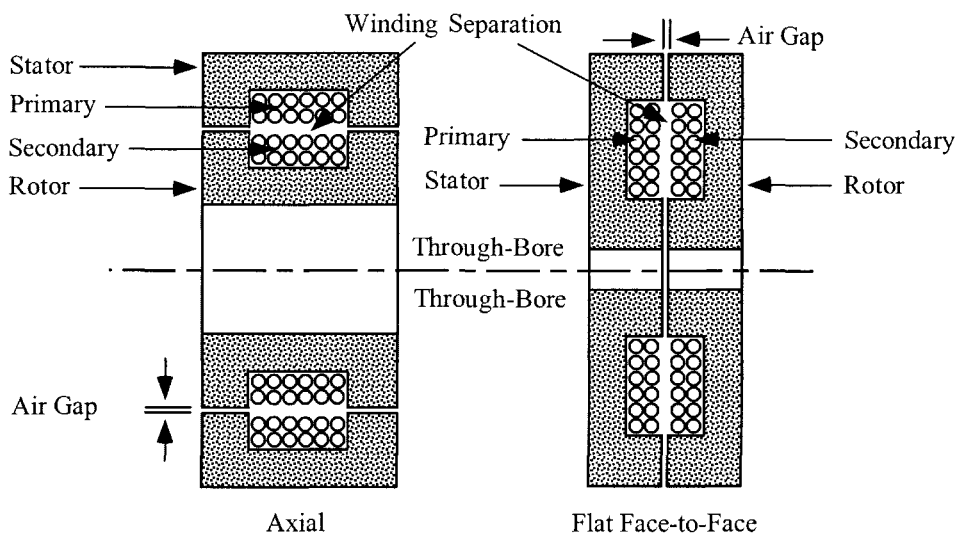


Figure 19-11. Geometries of the Basic Type Rotary Transformers.

Rotary transformer dimensions are usually governed by the mechanical interface, in particular the relatively large gap and the large through-bore, resulting in a long Mean Length Turn (MLT). The rotary transformer is not an ideal magnetic assembly. A toroidal core is an ideal magnetic assembly. Manufacturers use test data, taken from toroidal cores, to present magnetic material characteristics. The magnetic flux in a toroidal core travels through a constant core cross-section, A_c , throughout the whole Magnetic Path Length, MPL, as shown in Figure 19-12, and provides ideal magnetic characteristics. It can be seen that the core cross-section throughout the rotary transformers, shown in Figure 19-13 and Figure 19-14, does not provide constant flux density or an ideal magnetic assembly. The rotary transformers for the Galileo spacecraft were about 10 cm in diameter, and manufactured by CMI (Ref 4.)

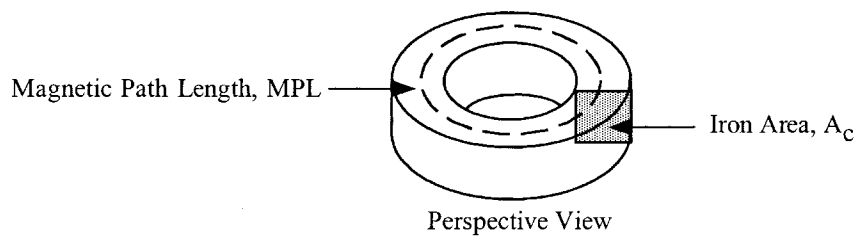


Figure 19-12. Typical Perspective View of a Toroidal Core.

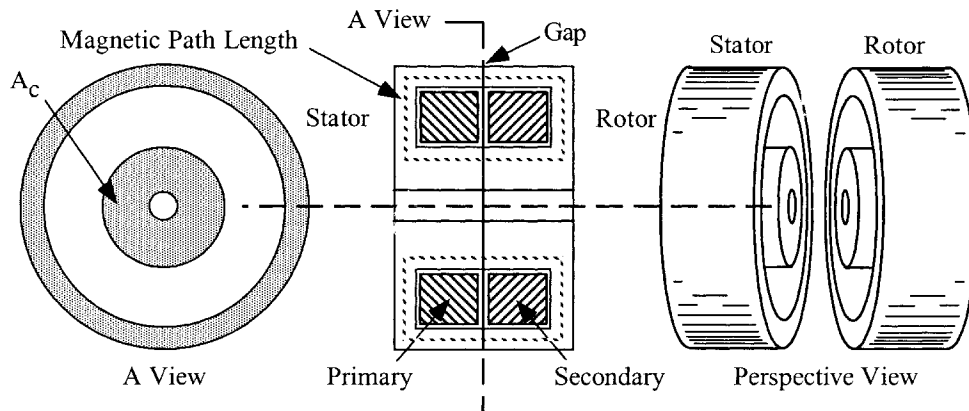


Figure 19-13. Open View of a Flat Plane, Type Rotary Transformers.

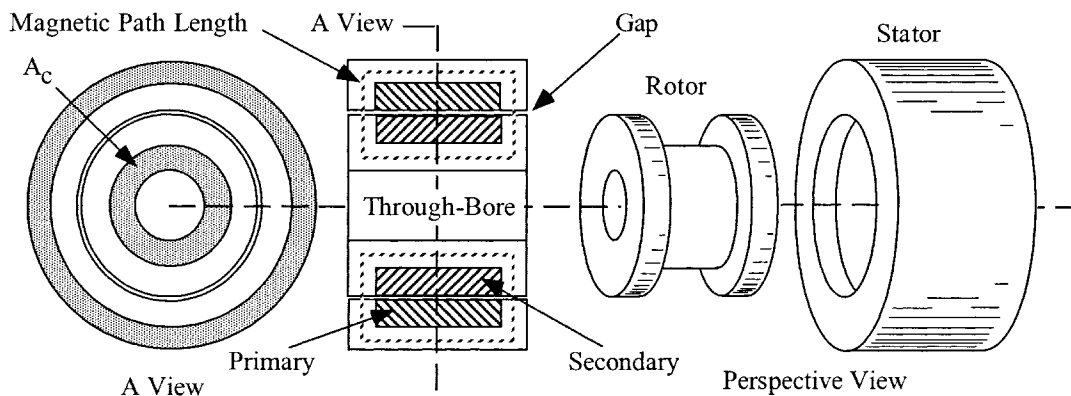


Figure 19-14. Open View of an Axial Type Rotary Transformers.

References

1. E. Landsman, "Rotary Transformer Design." Massachusetts Institute Technology, PCSC-70 Record, pp. 139-152
2. L. Brown, "Rotary Transformer Utilization in a Spin Stabilized Spacecraft Power System." General Electric, pp 373-376.
3. S. Marx, "A Kilowatt Rotary Power Transformer." Philco-Ford Corp., IEEE Transactions on Aerospace and Electronic Systems Vol. AES-7, No. 6 November 1971.
4. Ceramic Magnetics, Inc. 16 Law Drive Fairfield, NJ 07006. Tel. (973) 227-4222.

Chapter 20

Planar Transformers

Table of Contents

1. Introduction	
2. Planar Transformer Basic Construction	
3. Planar Integrated PC Board Magnetics.....	
4. Core Geometries	
5. Planar Transformer and Inductor Design Equations	
6. Window Utilization, K_u	
7. Current Density, J	
8. Printed Circuit Windings	
9. Calculating the Mean Length Turn, MLT	
10. Winding Resistance and Dissipation	
11. PC Winding Capacitance	
12. Planar Inductor Design.....	
13. Winding Termination	
14. PC Board Base Materials	
15. Core Mounting and Assembly	
16. References	

Introduction

The planar transformer, or inductor, is a low profile device that covers a large area, whereas, the conventional transformer would be more cubical in volume. Planar Magnetics is the new “buzz” word in the field of power magnetics. It took a few engineers with the foresight to come up with a way to increase the power density, while at the same time increasing the overall performance, and also, making it cost effective. One of the first papers published on planar magnetics was by Alex Estrov, back in 1986. After reviewing this paper, you really get a feeling of what he accomplished. A whole new learning curve can be seen on low profile ferrite cores and printed circuit boards if one is going to do any planar transformer designs. It is an all-new technology for the transformer engineer. The two basic items that made this technology feasible were the power, MOSFETs that increased the switching frequency and enabled the designer to reduce the turns, and the ferrite core, which can be molded and machined into almost any shape. After this paper was written the interest in planar magnetics seems to increase each year.

Planar Transformer Basic Construction

Here, shown in Figure 20-1 through Figure 20-4 are four views of a typical EE core, planar construction method. The assembled planar transformers have very unique characteristics in their finished construction. In the assembled planar transformer, every primary turn is at a precise location, governed by the PC board. The primary is always the same distance from the secondary. This provides a tight control over the primary to secondary leakage inductance. Using the same insulating material will always provide the same capacitance between primary and secondary; in this way, all parasitics will be the same from unit to unit. With this type of planar construction, the engineer will have a tight control over leakage inductance, the resonant frequency, and the common-mode rejection. A tight control is necessary on all materials used.

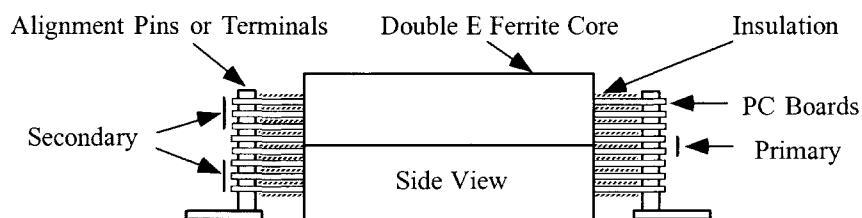


Figure 20-1. Side View of a Typical EE Planar Transformer.

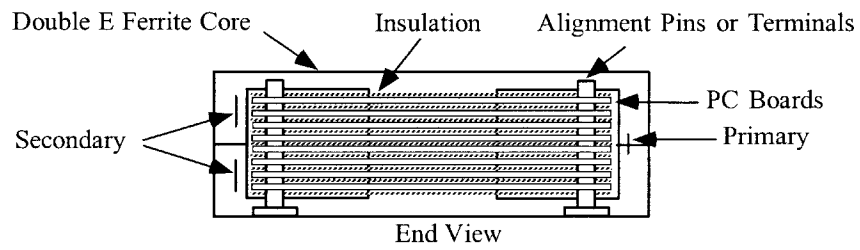


Figure 20-2. End View of a Typical EE Planar Transformer.

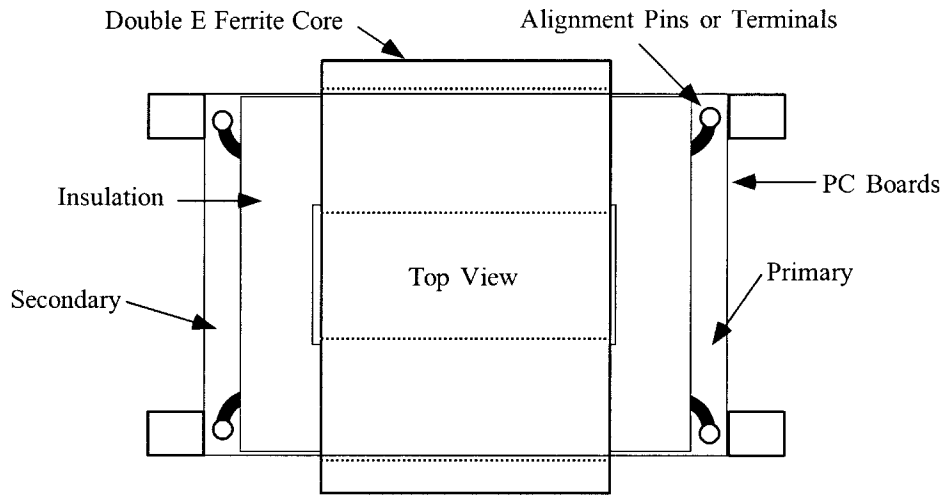


Figure 20-3. Top View of a Typical EE Planar Transformer.

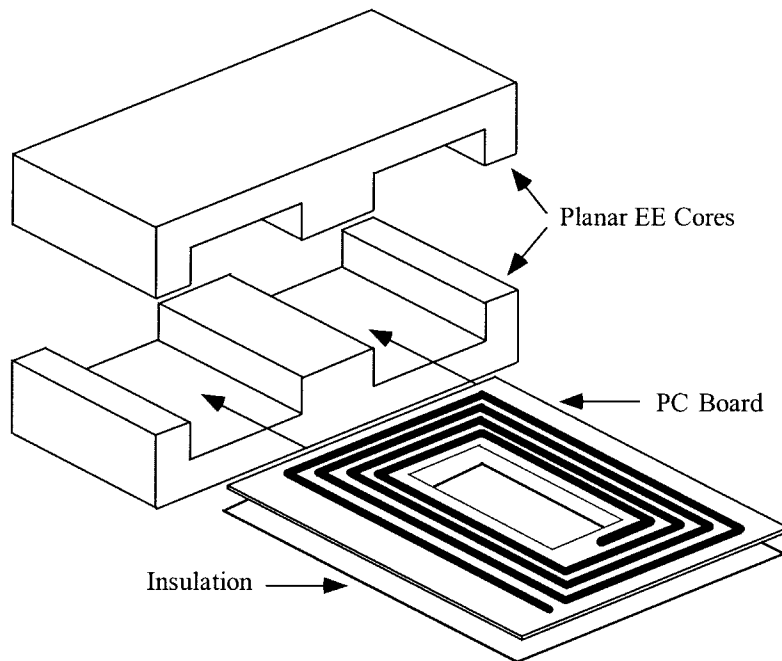


Figure 20-4. A Perspective View of a Typical EE Planar Transformer.

Planar Integrated PC Board Magnetics

Planar transformers and inductors are now being integrated right on the main PC board. Design engineers are pushing the operating frequency higher and higher to where it is commonplace to operate at frequency range between 250-500kHz. As the frequency increases the power supplies are getting smaller and smaller. To reduce the size of the power supply even further engineers are going to planar magnetics that are integrated into the main PC board. An exploded view to show the multi-layers PC board of a planar transformer that has been integrated into the main PC board is shown in Figure 20-5. The final assembly of the same planar transformer is shown in Figure 20-6.

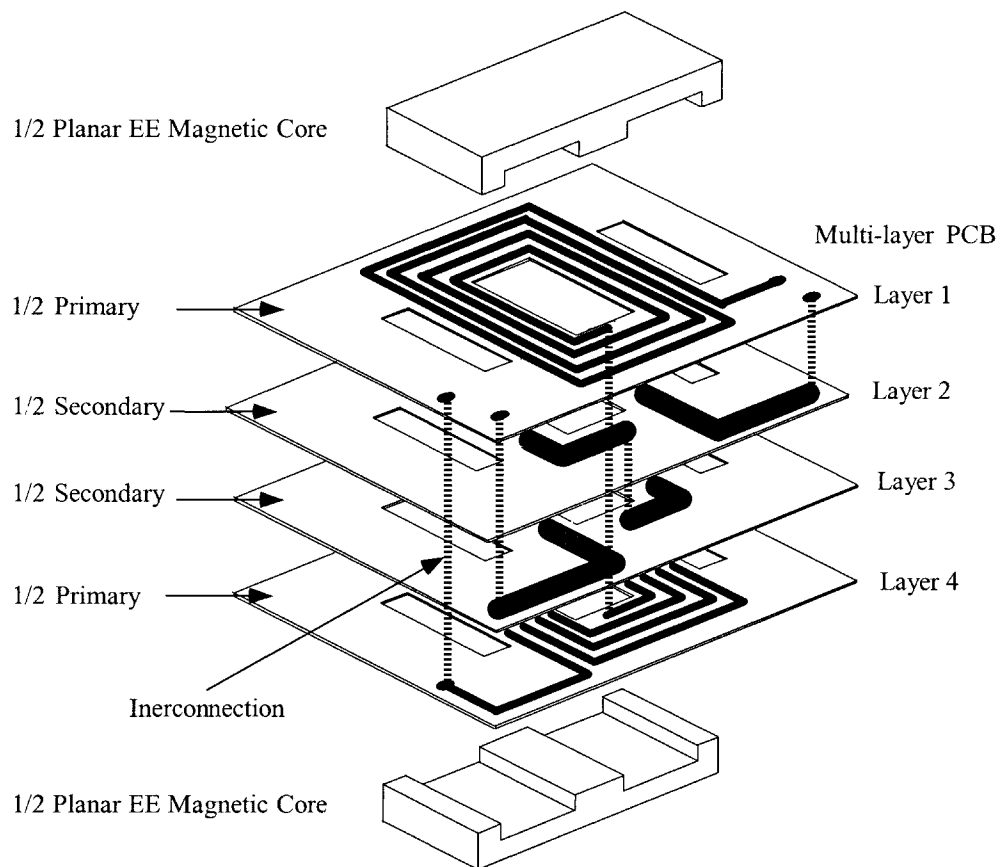


Figure 20-5. A Planar Transformer Integrated into the Main PC Board.

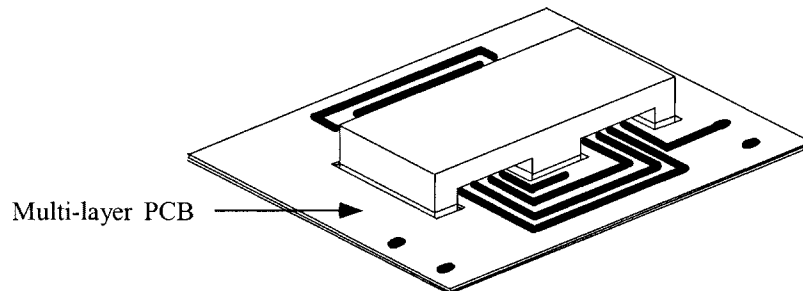


Figure 20-6. PC Board Planar Transformer in Final Assembly.

Core Geometries

The EE and EI are not the only planar geometries now available. There are a few firms in the ferrite industry that offer low profile versions of their standard cores, giving the engineer a few more choices in his design. There are EE and EI cores available from Magnetics Inc. as shown in Figure 20-7; there are ER cores available from Ferroxcube, as shown in Figure 20-8; there are ETD-lp cores available from Ferrite International, as shown in Figure 20-9; there are PQ-lp cores available from Ferrite International, as shown in Figure 20-10; and there are RM-lp cores available from Ferroxcube, as shown in Figure 20-11. There are several advantages, with cores with a round center post, such as PQ-lp, RM-lp, ETD-lp and ER. A round center post results in a more efficient use of copper and a more efficient use of board space. There is a company, Ceramic Magnetics, Inc. (CMI), that can modify any of these cores to your specification or machine a special core for your application. The IEC has a new standard 62313 for planar cores that supercedes standard 61860.

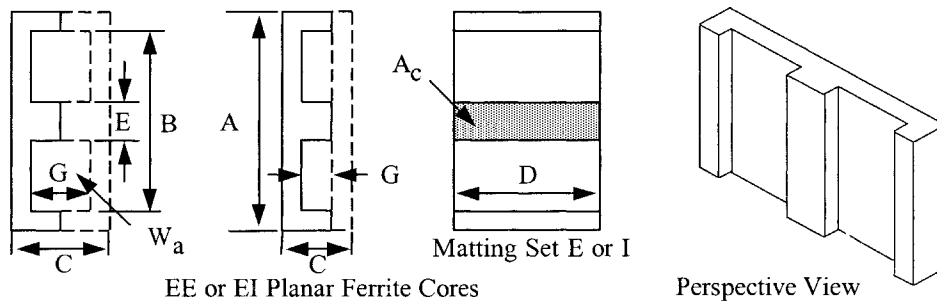


Figure 20-7. Magnetic Inc. EE and EI Low Profile Planar Cores.

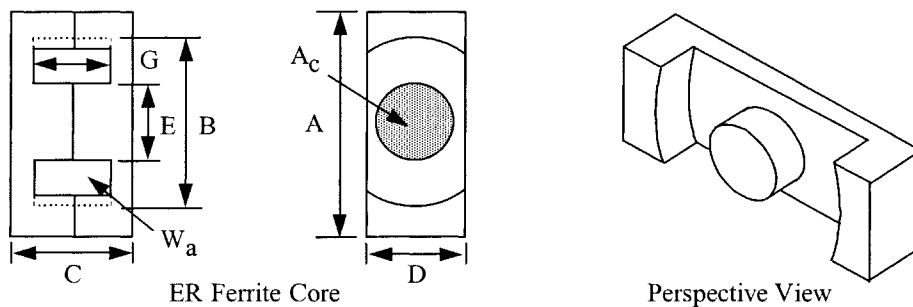


Figure 20-8. Ferroxcube ER Low Profile Planar Cores.

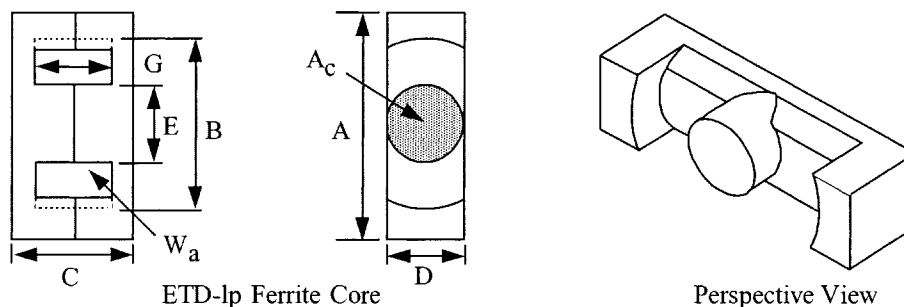


Figure 20-9. Ferrite International ETD Low Profile Planar Cores.

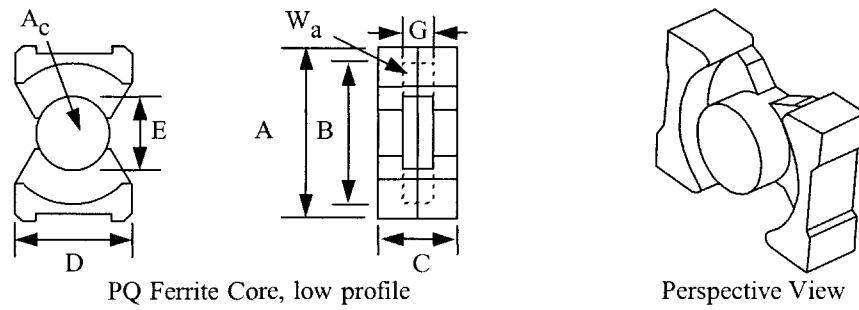


Figure 20-10. Ferrite International PQ Low Profile Planar Cores.

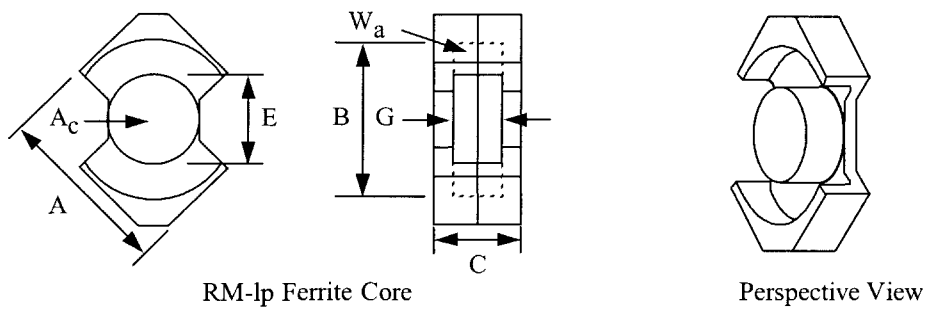


Figure 20-11. Ferroxcube RM Low Profile Planar Cores.

Planar Transformer and Inductor Design Equations

The same design equations are used, as well as the criteria used to select the proper core, to design a planar transformer as a conventional transformer. Faraday's Law is still used to calculate the required turns:

$$N = \frac{V_p (10^4)}{K_f f A_c B_{ac}}, \text{ [turns]} \quad [20-1]$$

The core power handling equation, A_p :

$$A_p = \frac{P_t (10^4)}{K_f K_u f A_c B_{ac} J}, \text{ [cm}^4\text{]} \quad [20-2]$$

The gapped inductor equation, L:

$$L = \frac{0.4\pi N^2 A_c (10^{-8})}{l_g + \left(\frac{MPL}{\mu_m}\right)}, \text{ [henrys]} \quad [20-3]$$

The core energy handling equation, A_p :

$$A_p = \frac{2(\text{Energy})}{K_u B_{ac} J}, \text{ [cm}^4\text{]} \quad [20-4]$$

Window Utilization, K_u

The window utilization factor in the conventional transformer is about 0.40. This means that 40% of the window is filled with copper, the other 60% of the area is devoted to the bobbin or tube, to the insulation both layer and wire, and to the winding technique. The window utilization is explained, in detail, in Chapter 4. Designing a planar transformer and using the PC winding technique, reduces the window utilization factor even further. The window utilization, K_u , comparison of the two different winding techniques is shown in Figure 20-12.

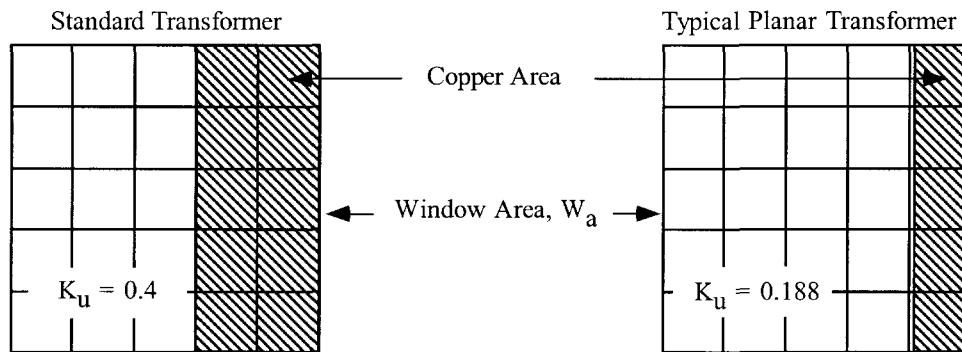


Figure 20-12. Comparing the Window Utilization of a Standard Transformer and a Planar Transformer.

A PC board window utilization, K_u , calculation example will be as follows:

The windings will be placed on a double-sided 2oz PC board 10 mils thick, giving a total thickness of 15.4 mils (0.0391 cm). The Mylar insulation material is between the PC boards, and between the PC boards, and the core will add another 4 mils (0.0102 cm) to the thickness. This will give 19.4 mils (0.0493 cm) per layer. There will be a 20 mil space (margin) between the edge of the board and the copper clad. The copper width will be the window width of 0.551cm minus 2x the margin of 0.102. This will give a total copper width of 0.449. The window utilization, K_u , will be summed in Table 20-1, using Figure 20-13 as a guide.

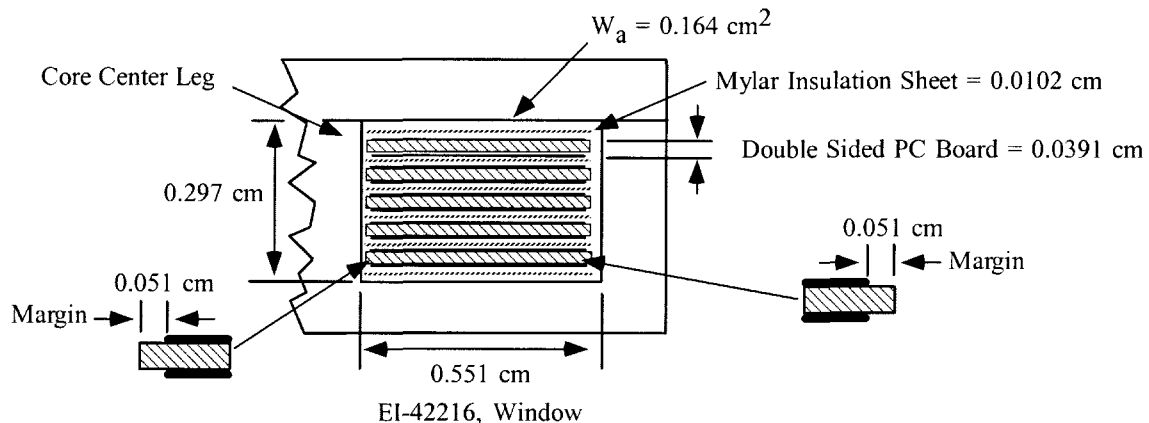


Figure 20-13. Window Utilization of a Typical EI Planar Transformer.

Table 20-1

EI-42216 Window Utilization	
Window Height, cm	0.2970
Window Width, cm	0.5510
Window Area, cm ²	0.1640
PC Board Thickness with Copper, cm	0.0391
Sheet Insulator, cm	0.0102
Total Insul. 5+1 Layers Thick, cm	0.0612
Total Thickness 5 Layers, cm	0.2570
Copper Thickness 5 Layers, cm	0.0686
Copper Width, cm	0.4494
Total Copper Area, cm ²	0.0308
Window Utilization, K _u	0.1878

Current Density, J

One of the unknown factors in designing planar transformers is the current density, J. The current density controls the copper loss (regulation) and the inherent temperature rise caused by the copper loss. The temperature rise is normally controlled by the surface dissipation of the transformer. The size of a transformer goes up by the cubic law, and the surface area goes up by the square law. Large transformers, such as 60 Hz, are designed with a low current density, while 400 Hz are designed with higher current density for the same temperature rise. There used to be an old rule of thumb, for a large transformer, you use 1000 circular mils per amp, and for a small transformer, you use 500 circular mils per amp:

$$500\text{CM/Amp} \approx 400\text{Amps/cm}^2, \quad [400 \text{ Hertz Aircraft}]$$

$$1000\text{CM/Amp} \approx 200\text{Amps/cm}^2, \quad [60 \text{ Hertz}]$$

Planar transformer designers handle the current density in a different way. When designing planar transformer PC windings, designers use the same technology used by the printed, circuit board designers, and that is the current rating for a given voltage drop and temperature rise. It is another way of saying the same thing. The printed circuit boards are covered with a copper clad. The thickness of this copper is called out in ounces, such as 1oz, 2oz, and 3oz. The weight in ounces comes from an area of one square foot of material. So 1oz of copper clad would be 1 square foot, and have a thickness of 0.00135 inch; 2oz would be 0.0027 inch; and 3oz would be 0.00405 inch. Tables have been made to show the current capacity for a constant temperature rise with different line width. The design data for 1oz copper is shown in Table 20-2. The 2oz copper is shown in Table 20-3, and 3oz copper is shown in Table 20-4. Planar transformer engineers are using the industrial guidelines for their selection of copper trace thickness and line width, based on temperature rise. The first effort for a planar transformer, PC winding should be around:

100CM/Amp \approx 2000Amps/cm², [500 kHz Planar Transformers]

If the current density is based on Table 20-1, with a line width of 0.06 inches, then use:

35CM/Amp \approx 5700Amps/cm², [500 kHz Planar Transformers]

Table 20-2. Design Data for 0.00135 Inch Thick Copper Clad.

*Printed Circuit Trace Data for 1oz Copper (Based on 10 Inches Long)							
Line Width Inches	Line Width mm	Resistance micro-ohm per-mm	Copper Weight 1oz Thickness 0.00135 cm ² **AWG		Temp. °C Increase above Amb. Vs. Current in Amperes		
					5°	20°	40°
0.0200	0.51	989.7	0.000174	35	1.00	3.00	4.00
0.0400	1.02	494.9	0.000348	32	2.25	5.00	6.50
0.0600	1.52	329.9	0.000523	30	3.00	6.50	8.00
0.0800	2.03	247.4	0.000697	29	4.00	7.00	9.50
0.1000	2.54	197.9	0.000871	28	4.50	8.00	11.00
0.1200	3.05	165.0	0.001045	27	5.25	9.25	12.00
0.1400	3.56	141.4	0.001219	26	6.00	10.00	13.00
0.1600	4.06	123.7	0.001394	26	6.50	11.00	14.25
0.1800	4.57	110.0	0.001568	25	7.00	11.75	15.00
0.2000	5.08	99.0	0.001742	25	7.25	12.50	16.60
*Data From: Handbook of Electronic Packaging.							
**This is a close approximation to an equivalent AWG wire size.							

Table 20-3. Design Data for 0.0027 Inch Thick Copper Clad.

*Printed Circuit Trace Data for 2oz Copper (Based on 10 Inches Long)							
Line Width Inches	Line Width mm	Resistance micro-ohm per-mm	Copper Weight 2oz Thickness 0.0027 cm ² **AWG		Temp. °C Increase above Amb. Vs. Current in Amperes		
					5°	20°	40°
0.0200	0.51	494.9	0.000348	32	2.00	4.00	6.25
0.0400	1.02	247.4	0.000697	29	3.25	7.00	9.00
0.0600	1.52	165.0	0.001045	27	4.25	9.00	11.25
0.0800	2.03	123.7	0.001394	26	5.00	10.25	13.25
0.1000	2.54	99.0	0.001742	25	5.25	11.00	15.25
0.1200	3.05	82.5	0.002090	24	5.75	12.25	17.00
0.1400	3.56	70.7	0.002439	23	6.25	13.25	18.50
0.1600	4.06	61.9	0.002787	23	6.50	14.25	20.50
0.1800	4.57	55.0	0.003135	22	7.00	15.25	22.00
0.2000	5.08	49.5	0.003484	22	7.25	16.25	24.00
*Data From: Handbook of Electronic Packaging.							
**This is a close approximation to an equivalent AWG wire size.							

Table 20-4. Design Data for 0.00405 Inch Thick Copper Clad.

*Printed Circuit Trace Data for 3oz Copper (Based on 10 Inches Long)							
Line Width Inches	Line Width mm	Resistance micro-ohm per-mm	Copper Weight 3oz Thickness 0.00405		Temp. °C Increase above Amb. Vs. Current in Amperes		
			cm ²	**AWG	5°	20°	40°
0.0200	0.51	329.9	0.000523	30	2.50	6.00	7.00
0.0400	1.02	165.0	0.001045	27	4.00	8.75	11.00
0.0600	1.52	110.0	0.001568	25	4.75	10.25	13.50
0.0800	2.03	82.5	0.002090	24	5.50	12.00	15.75
0.1000	2.54	66.0	0.002613	23	6.00	13.25	17.50
0.1200	3.05	55.0	0.003135	22	6.75	15.00	19.50
0.1400	3.56	47.1	0.003658	22	7.00	16.00	21.25
0.1600	4.06	41.2	0.004181	21	7.25	17.00	23.00
0.1800	4.57	36.7	0.004703	20	7.75	18.25	25.00
0.2000	5.08	33.0	0.005226	20	8.00	19.75	27.00

*Data From: Handbook of Electronic Packaging.
 **This is a close approximation to an equivalent AWG wire size.

Printed Circuit Windings

There will be a few paths of mystery along the way when engineers first get started in the design of a planar transformer. Therefore, it would be much easier to start on a simple design and use magnet wire, then convert that into a truly all planar approach, using a PC winding board design. In this way the engineer will slide up the learning curve slowly. There are several benefits to a printed circuit winding. Once the printed winding board is finished and the layout is fixed, the winding will not vary and all of the parasitics, including the leakage inductance, will be frozen. This is not necessarily true in conventional transformers. There are two basic core configurations available to the engineer for planar design. The first configuration is the EE or EI with the rectangular center post. A typical high current and low current winding PC board for E cores is shown in Figure 20-14.

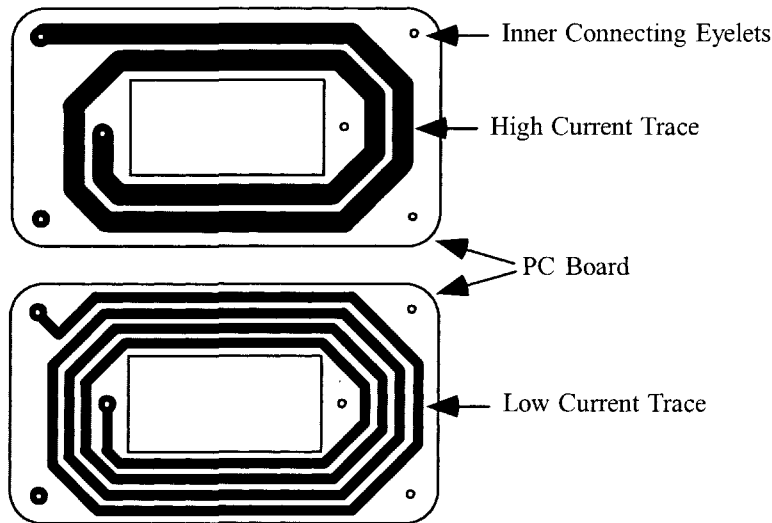


Figure 20-14. Typical Planar E Core Winding PC Board.

The second configuration is shown in Figure 20-15. These are four cores with round center legs. Winding PC boards with round center legs are used on PQ-lp, RM-lp, ETD-lp and ER cores. There is an advantage to cores with round center legs. Cores with round center leg will produce a round ID, OD resulting in a more efficient use of copper.

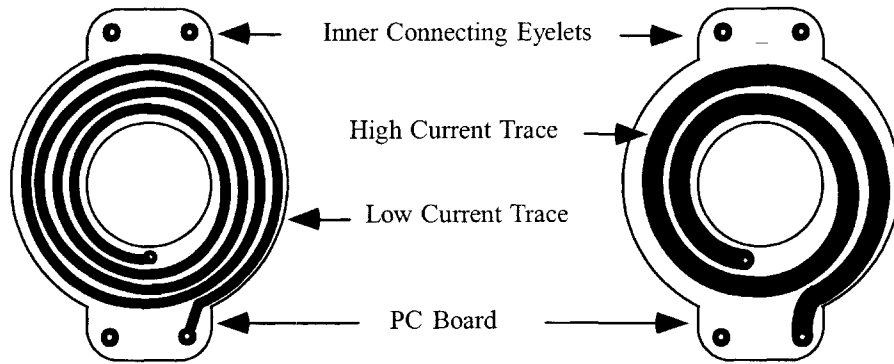
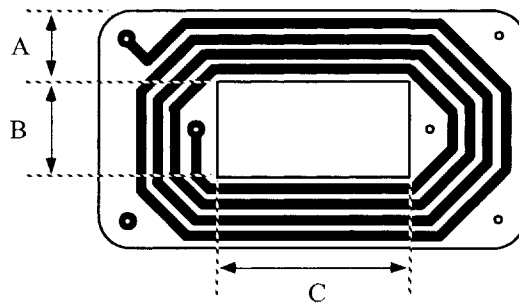


Figure 20-15. Typical Circular Winding PC Board for Cores with Round Center Leg.

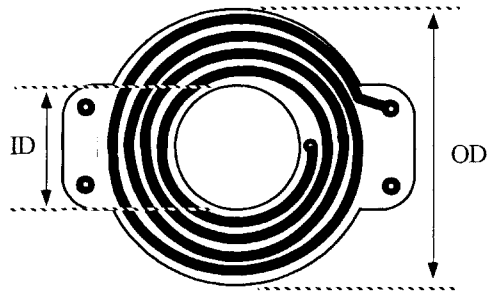
Calculating the Mean Length Turn, MLT

The Mean Length Turn (MLT), is required to calculate the dc winding resistance. With the winding resistance known, the winding voltage drop can be calculated at rated load. The winding dimensions, relating to the Mean Length Turn (MLT) for a rectangular winding, is shown in Figure 20-16, along with the MLT equation, and a circular winding is shown in Figure 20-17, along with the MLT equation.



$$MLT = 2B + 2C + 2.82A, \text{ [mm]} \quad [20-5]$$

Figure 20-16. Dimensions, Relating to a Rectangular Winding, Mean Length Turn (MLT).



$$MLT = \frac{\pi(OD + ID)}{2}, \text{ [mm]} \quad [20-6]$$

Figure 20-17. Dimensions, Relating to a Circular Winding, Mean Length Turn (MLT).

Winding Resistance and Dissipation

The winding dc resistance and voltage drop will be calculated as follows:

Calculate the Mean Length Turn (MLT) using the winding board configuration and Equation in Figure 20-17. Use the printed winding data in Table 20-5.

Table 20-5. PC Board Winding Data

PC Winding Data		
Item		Units
PC Board Turns Each Side	4	
Winding Trace Thickness	0.0027	inches
Winding Trace Width	2.54	mm
Trace Resistance	99	$\mu\Omega/\text{mm}$
Winding Board, OD	31.5	mm
Winding Board, ID	14.65	mm
Winding Current, I	3	amps
PC Board Thickness	0.5	mm
PC Board Dielectric Constant, K	4.7	

Step 1. Calculate the Mean Length Turn, MLT:

$$MLT = \frac{\pi(OD + ID)}{2}, \text{ [mm]}$$

$$MLT = \frac{3.14(31.5 + 14.65)}{2}, \text{ [mm]}$$

$$MLT = 72.5, \text{ [mm]}$$

Step 2. Calculate the winding resistance, R:

$$R = MLT(N) \left(\frac{\mu\Omega}{\text{mm}} \right) (10^{-6}), \text{ [ohms]}$$

$$R = (72.5)(8)(99.0)(10^{-6}), \text{ [ohms]}$$

$$R = 0.057, \text{ [ohms]}$$

Step 3. Calculate the winding voltage drop, V_w :

$$V_w = IR, \text{ [volts]}$$

$$V_w = (3.0)(0.057), \text{ [volts]}$$

$$V_w = 0.171, \text{ [volts]}$$

Step 4. Calculate the winding dissipation, P_w :

$$P_w = I^2 R, \text{ [watts]}$$

$$P_w = (3)^2 (0.057), \text{ [watts]}$$

$$P_w = 0.513, \text{ [watts]}$$

PC Winding Capacitance

The PC winding board traces will have capacitance, to the other side of the board as shown in Figure 20-18. This capacitance could be to another winding, or a Faraday shield to ground.

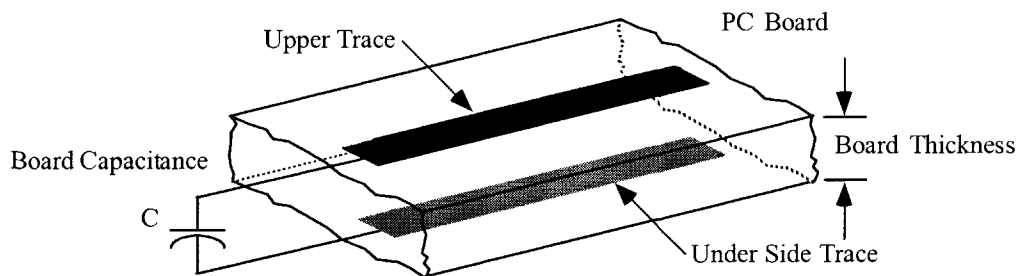


Figure 20-18. PC Board Trace Capacitance.

The formula for calculating the winding trace capacitance, to either another winding trace or ground plane, is given in Equation 20-7.

$$C_p = \frac{0.0085 K A}{d}, \text{ [pf]}$$

Where:

$$C_p = \text{capacitance, [pf]} \quad [20-7]$$

K = dielectric constant

A = area of the trace, [mm²]

d = thickness of the PC board, [mm]

A typical square wave power converter, operating at 250kHz, will have extremely fast rise and fall times in the order of 0.05 micro-seconds. This fast excursion will generate a fairly high current pulse depending on the capacitance and source impedance.

The calculation of the winding capacitance is as follows:

Use the PC board winding data in Table 20-5, the outline drawing in Figure 20-19, and Equation 20-7:

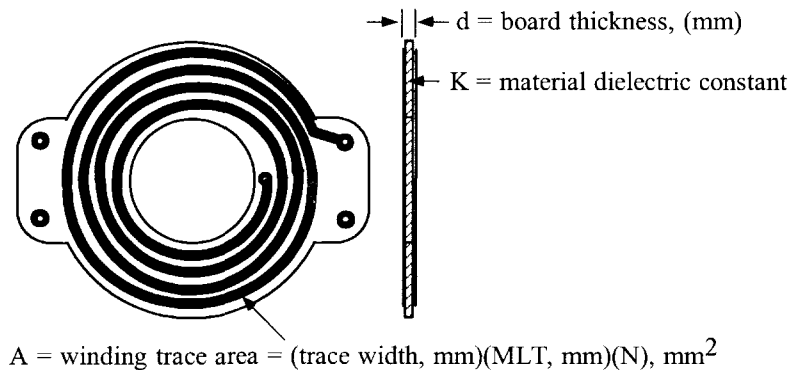


Figure 20-19. PC Board Winding Capacitance.

Step 1. Calculate the winding trace area, A .

$$A = (\text{trace width, mm})(\text{MLT, mm})(\text{turns, } N), \text{ [mm}^2\text{]}$$

$$A = (2.54)(72.5)(8), \text{ [mm}^2\text{]}$$

$$A = 1473, \text{ [mm}^2\text{]}$$

Step 2. Calculate the winding capacitance, C_p .

$$C_p = \frac{0.0085 K A}{d}, \text{ [pf]}$$

$$C_p = \frac{0.0085(4.7)(1473)}{(0.50)}, \text{ [pf]}$$

$$C_p = 118, \text{ [pf]}$$

Planar Inductor Design

Planar inductors are designed the same way as the conventional inductors. See Chapter 8. Planar inductors use the same planar cores and PC winding board techniques as the transformers. The main difference is the inductor will have a gap to prevent the dc current from prematurely saturating the core. It is normal to operate planar magnetics at a little higher temperature than conventional designs. It is important to check the maximum operating flux level at maximum operating temperature.

Fringing flux can be severe in any gapped ferrite inductor, but, even more so, on planar construction, because of the printed winding board, as shown in Figure 20-20. When the flux intersects the copper winding, eddy currents are generated, which produces hot spots and reduces the overall efficiency. The use of a PC winding board, (flat traces), can give the eddy currents an added degree of freedom. The resulting loss could be a disaster.

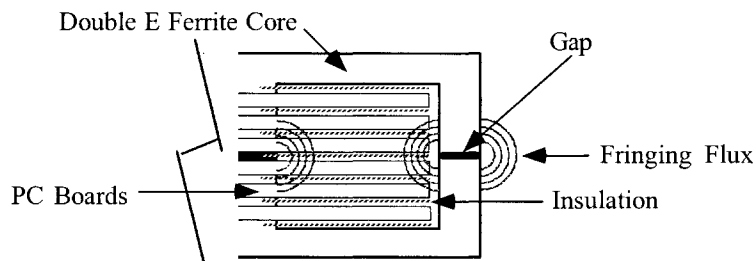


Figure 20-20. Fringing Flux Cutting Across PC Winding Boards.

Winding Termination

Making connections from a planar transformer to the outside world could be very clumsy, if not enough thought is put in for termination. It has to be remembered that this is a high frequency transformer, and skin effect, (ac resistance), has to be addressed. Because of the skin effect it is important the external leads of the planar transformer must be kept as short as possible. Terminations are very important for currents of one amp and above. A poor connection will only get worse. It is recommended to use plated-through holes and eyelets, where possible, but cost will control that. If the transformer has many interconnections, or only a few, there must be provisions made for those connections. When the PC winding boards are stacked, and because of the high density, all connections and interconnections have to be done with extended area pads, as shown in Figure 20-21. The PC winding boards require good artwork registry to make sure the interconnections can be made between boards. Interconnections are usually done, by passing a bus wire through a hole, and at the same time making the connection on the other board. If the solder terminations are to be made on the board, then it is important to leave as much room as possible especially if the connection is to be made with copper foil, as shown in Figure 20-22. When the PC windings have to be paralleled, because of the increased current, the interconnecting jumpers will also have to be increased.

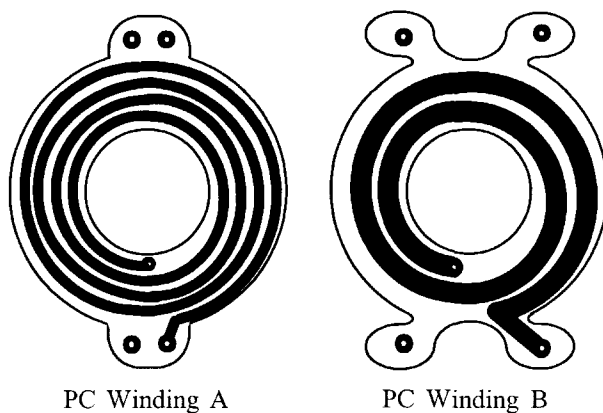


Figure 20-21. PC Winding Boards Showing Butterfly Pads.

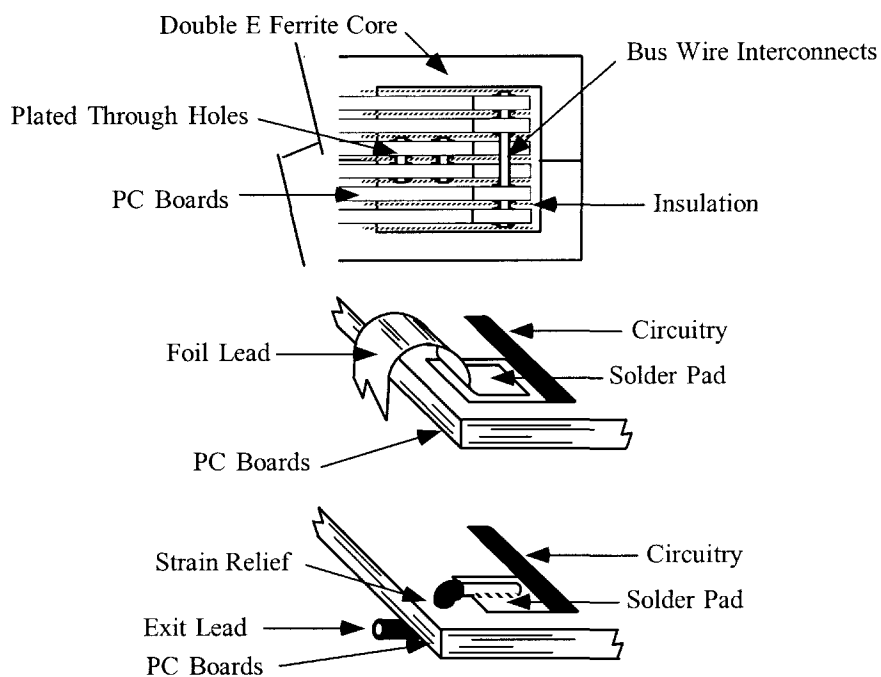


Figure 20-22. PC Winding Boards, Showing Interconnections and Exit Leads.

PC Board Base Materials

PC Board materials are available in various grades, as defined by the National Electrical Manufacturers Association (NEMA). The important properties for PC Board materials are tabulated in Table 20-6. It is very important to choose the correct PC board material for your application. Planar transformers are normally stressed to the last watt for a given temperature rise. This could give rise to hot spots at winding terminations and cause PC Board discoloration. Due to their inherent design Planar transformers will have a wide temperature delta, Δt . It would be wise to stay away from paper/phenolic materials and materials that absorb moisture.

Table 20-6. Properties of Typical Printer Circuit Board Materials

Properties of Typical Printed Circuit Board Materials							
Material/Comments	NEMA Grade						
	FR-1 Paper Phenolic	FR-2 Paper Phenolic	FR-3 Paper Epoxy	FR-4 Glass/Cloth Epoxy	FR-5 Glass/Cloth Epoxy	G10 Glass/Cloth Epoxy	G11 Glass/Cloth Epoxy
Mechanical Strength	good	good	good	excellent	excellent	excellent	excellent
Moisture Resistant	poor	good	good	excellent	excellent	excellent	excellent
Insulation	fair	good	good	excellent	excellent	excellent	excellent
Arc Resistance	poor	poor	fair	good	good	good	good
Tool Abrasion	good	good	good	poor	poor	poor	poor
Max. Cont. Temp. °C	105	105	105	130	170	130	170
Dielectric Constant, K	4.2	4.2	4.4	4.7	4.3	4.6	4.5

Core Mounting and Assembly

Core assembly and mounting should be strong and stable with temperature. One of the most viable methods for securing core halves together is epoxy adhesive. There is one epoxy adhesive that has been around a long time and that's 3M EC-2216A/B. This bonding technique is shown in Figure 20-23 and it seems to work quite well. When the core halves are properly bonded with epoxy adhesive, there will be little or no effect on the electrical performance. This means the epoxy adhesive added little or no gap to the mating surface. Large temperature excursions are normal in planar magnetics. Care should be taken into account for the coefficients of thermal expansion between the core and mounting surfaces. It has to be remembered ferrite is a ceramic and is very brittle. Planar cores have a low silhouette with thin sections that cannot absorb as much strain as other geometries. After the planar transformer has been assembled, there should be a small amount of play in the PC winding assembly to guarantee there will be a minimum of stress over temperature.

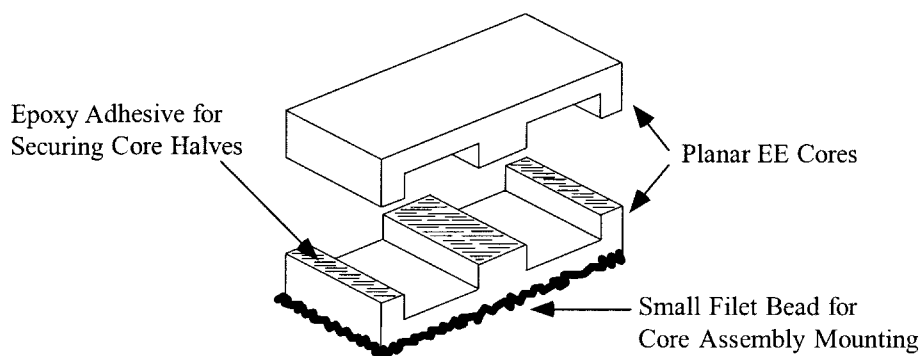


Figure 20-23. Epoxy Adhesive for Securing Transformer Assembly.

References

1. Designing with Planar Ferrite Cores, Technical Bulletin FC-S8, Magnetics, Division of Spang and Company 2001.
2. Brown, E., "Planar Magnetics Simplifies Switchmode Power Supply Design and Production," PCIM, June 1992, pp. 46-52.
3. Van der Linde, Boon, and Klassens, "Design of High-Frequency Planar Power Transformer in Multilayer Technology," IEEE Transaction on Industrial Electronics, Vol. 38, No. 2, April 1991, pp. 135-141.
4. Bloom, E., "Planar Power Magnetics: New Low Profile Approaches for Low-Cost Magnetics Design," Magnetic Business & Technology, June 2002, pp. 26,27.
5. Charles A. Harper, *Handbook of Electronic Packaging*, McGraw-Hill Book Company, pp. 1-51-1-53.
6. Reference Data for Radio Engineers, Fourth Edition, International Telephone and Telegraph Corp. March 1957, pp. 107-111.
7. PC Boards, Casco Circuits, Inc., 10039 D Canoga Ave., Chatsworth, CA 91311. Tel. (818) 882-0972.

Chapter 21

Derivations for the Design Equations

The author would like to thank **Richard Ozenbaugh** of Linear Magnetics for his help with the derivations.

Table of Contents

1. Output Power, P_o , Versus Apparent Power, P_t , Capability.....	
2. Transformer Derivation for the Core Geometry, K_g	
3. Transformer Derivation for the Area Product, A_p	
4. Inductor Derivation for the Core Geometry, K_g	
5. Inductor Derivation for the Area Product, A_p	
6. Transformer Regulation	

Output Power, P_o , Versus Apparent Power, P_t , Capability

Introduction

Output power, P_o , is of the greatest interest to the user. To the transformer designer, the apparent power, P_t , which is associated with the geometry of the transformer, is of greater importance. Assume, for the sake of simplicity, that the core of an isolation transformer has only two windings in the window area, a primary and a secondary. Also, assume that the window area, W_a , is divided up in proportion to the power-handling capability of the windings, using equal current density. The primary winding handles, P_{in} , and the secondary handles, P_o , to the load. Since the power transformer has to be designed to accommodate the primary, P_{in} , and P_o , then,

By definition:

$$\begin{aligned} P_t &= P_{in} + P_o, \quad [\text{watts}] \\ P_{in} &= \frac{P_o}{\eta}, \quad [\text{watts}] \end{aligned} \quad [21-A1]$$

The primary turns can be expressed using Faraday's Law:

$$N_p = \frac{V_p (10^4)}{A_c B_{ac} f K_f}, \quad [\text{turns}] \quad [21-A2]$$

The winding area of a transformer is fully utilized when:

$$K_u W_a = N_p A_{wp} + N_s A_{ws} \quad [21-A3]$$

By definition the wire area is:

$$A_w = \frac{I}{J}, \quad [\text{cm}^2] \quad [21-A4]$$

Rearranging the equation shows:

$$K_u W_a = N_p \left(\frac{I_p}{J} \right) + N_s \left(\frac{I_s}{J} \right) \quad [21-A5]$$

Now, substitute in Faraday's Equation:

$$K_u W_a = \frac{V_p (10^4)}{A_c B_{ac} f K_f} \left(\frac{I_p}{J} \right) + \frac{V_s (10^4)}{A_c B_{ac} f K_f} \left(\frac{I_s}{J} \right) \quad [21-A6]$$

Rearranging shows:

$$W_a A_c = \frac{[(V_p I_p) + (V_s I_s)] (10^4)}{B_{ac} f J K_f K_u}, \quad [\text{cm}^4] \quad [21-A7]$$

The output power, P_o , is:

$$P_o = V_s I_s, \quad [\text{watts}] \quad [21-A8]$$

The input power, P_{in} , is:

$$P_{in} = V_p I_p, \quad [\text{watts}] \quad [21-A9]$$

Then:

$$P_t = P_{in} + P_o, \quad [\text{watts}] \quad [21-A10]$$

Transformer Derivation for the Core Geometry, K_g

Introduction

Although most transformers are designed for a given temperature rise, they can also be designed for a given regulation. The regulation and power-handling ability of a core are related to two constants, K_g and K_e by the equation:

$$P_i = 2K_g K_e \alpha, \quad [\text{watts}] \quad [21-B1]$$

Where:

$$\alpha = \text{Regulation, } [\%]$$

The constant, K_g , is a function of the core geometry:

$$K_g = f(A_c, W_a, \text{MLT}) \quad [21-B2]$$

The constant, K_e , is a function of the magnetic and electrical operating conditions:

$$K_e = g(f, B_m) \quad [21-B3]$$

The derivation of the specific functions for, K_g and K_e , is as follows: First, assume there is a two-winding transformer with equal primary and secondary regulation, as schematically shown in Figure 21-B1. The primary winding has a resistance of, R_p , ohms, and the secondary winding has a resistance of, R_s , ohms:

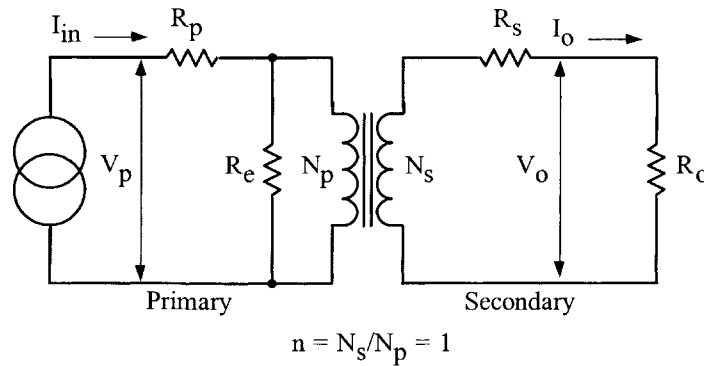


Figure 21-B1. Isolation Transformer.

$$\alpha = \frac{\Delta V_p}{V_p}(100) + \frac{\Delta V_s}{V_s}(100) \quad [21-B4]$$

The assumption, for simplicity, is that R_e is infinity (no core loss).

And:

$$I_{in} = I_o \quad [21-B5]$$

Then:

$$\Delta V_p = I_p R_p = \Delta V_s = I_s R_s, \quad [\text{volts}] \quad [21-B6]$$

$$\alpha = 2 \frac{I_p R_p}{V_p} (100) \quad [21-B7]$$

Multiply the numerator and denominator by V_p :

$$\alpha = 200 \frac{I_p R_p}{V_p} \left(\frac{V_p}{V_p} \right) \quad [21-B8]$$

$$\alpha = 200 \frac{R_p V A}{V_p^2} \quad [21-B9]$$

From the resistivity formula, it is easily shown that:

$$R_p = \frac{(\text{MLT}) N_p^2}{W_a K_p} \rho \quad [21-B10]$$

Where:

$$\rho = 1.724 (10^{-6}) \text{ ohm cm}$$

K_p is the window utilization factor (primary)

K_s is the window utilization factor (secondary)

$$K_p = \frac{K_u}{2} = K_s \quad [21-B11]$$

Faraday's Law expressed in metric units is:

$$V_p = K_f f N_p A_c B_m (10^{-4}) \quad [21-B12]$$

Where:

$K_f = 4.0$ for a square wave.

$K_f = 4.44$ for a sine wave.

Substituting Equation 21-B10 and 21-B12, for R_p and V_p , in Equation [21-B13]:

$$V A = \frac{E_p^2}{200 R_p} \alpha \quad [21-B13]$$

The primary VA is:

$$VA = \frac{(K_f f N_p A_c B_m (10^{-4})) (K_f f N_p A_c B_m (10^{-4}))}{200 \left(\frac{(\text{MLT}) N_p^2}{W_a K_p} \rho \right)} \alpha \quad [21-B14]$$

Simplify:

$$VA = \frac{K_f^2 f^2 A_c^2 B_m^2 W_a K_p (10^{-10})}{2(\text{MLT}) \rho} \alpha \quad [21-B15]$$

Inserting $1.724(10^{-6})$ for ρ :

$$VA = \frac{0.29 K_f^2 f^2 A_c^2 B_m^2 W_a K_p (10^{-4})}{\text{MLT}} \alpha \quad [21-B16]$$

Let primary electrical equal:

$$K_e = 0.29 K_f^2 f^2 B_m^2 (10^{-4}) \quad [21-B17]$$

Let the primary core geometry equal:

$$K_g = \frac{W_a A_c^2 K_p}{\text{MLT}}, \quad [\text{cm}^5] \quad [21-B18]$$

The total transformer window utilization factor is:

$$\begin{aligned} K_p + K_s &= K_u \\ K_p &= \frac{K_u}{2} = K_s \end{aligned} \quad [21-B19]$$

When this value for K_p is put into Equation [21-B16], then:

$$VA = K_e K_g \alpha \quad [21-B20]$$

Where:

$$K_e = 0.145 K_f^2 f^2 B_m^2 (10^{-4}) \quad [21-B21]$$

The above VA is the primary power, and the window utilization factor, K_u , includes both the primary and secondary coils.

$$K_g = \frac{W_a A_c^2 K_p}{MLT}, \quad [\text{cm}^5] \quad [21-B22]$$

Regulation of a transformer is related to the copper loss, as shown in Equation [21-B23]:

$$\alpha = \frac{P_{cu}}{P_o} (100), \quad [\%] \quad [21-B23]$$

The total VA of the transformer is primary plus secondary:

$$\begin{aligned} \text{Primary, } VA &= K_e K_g \alpha \\ \text{plus} & \hspace{15em} [21-B24] \\ \text{Secondary, } VA &= K_e K_g \alpha \end{aligned}$$

The apparent power, P_t , then is:

$$\begin{aligned} P_t &= (\text{Primary}) K_e K_g \alpha + (\text{Secondary}) K_e K_g \alpha \\ P_t &= 2 K_e K_g \alpha \end{aligned} \quad [21-B25]$$

Transformer Derivation for the Area Product, A_p

Introduction

The relationship between the power-handling capability of a transformer and the area product, A_p can be derived as follows.

Faraday's Law expressed in metric units is:

$$V = K_f f N_p A_c B_m (10^{-4}) \quad [21-C1]$$

Where:

$K_f = 4.0$ for a square wave.

$K_f = 4.44$ for a sine wave.

The winding area of a transformer is fully utilized when:

$$K_u W_a = N_p A_{wp} + N_s A_{ws} \quad [21-C2]$$

By definition the wire area is:

$$A_w = \frac{I}{J}, \quad [\text{cm}^2] \quad [21-C3]$$

Rearranging the equation shows:

$$K_u W_a = N_p \left(\frac{I_p}{J} \right) + N_s \left(\frac{I_s}{J} \right) \quad [21-C4]$$

Now, substitute in Faraday's Equation:

$$K_u W_a = \frac{V_p (10^4)}{A_c B_{ac} f K_f} \left(\frac{I_p}{J} \right) + \frac{V_s (10^4)}{A_c B_{ac} f K_f} \left(\frac{I_s}{J} \right) \quad [21-C5]$$

Rearranging shows:

$$W_a A_c = \frac{[(V_p I_p) + (V_s I_s)] (10^4)}{B_{ac} f J K_f K_u}, \quad [\text{cm}^4] \quad [21-C6]$$

The output power, P_o , is:

$$P_o = V_s I_s, \text{ [watts]} \quad [21-C7]$$

The input power, P_{in} , is:

$$P_{in} = V_p I_p, \text{ [watts]} \quad [21-C8]$$

Then:

$$P_t = P_{in} + P_o, \text{ [watts]} \quad [21-C9]$$

Therefore:

$$W_a A_c = \frac{P_t (10^4)}{B_{ac} f J K_f K_u}, \text{ [cm}^4\text{]} \quad [21-C10]$$

By definition:

$$A_p = W_a A_c \quad [21-C11]$$

Then:

$$A_p = \frac{P_t (10^4)}{B_{ac} f J K_f K_u}, \text{ [cm}^4\text{]} \quad [21-C12]$$

Inductor Derivation for the Core Geometry, K_g

Introduction

Inductors, like transformers, are designed for a given temperature rise. They can also be designed for a given regulation. The regulation and energy-handling ability of a core are related to two constants, K_g and K_e , by the equation:

$$(\text{Energy})^2 = K_g K_e \alpha, \quad [21-D1]$$

Where:

$$\alpha = \text{Regulation, } [\%]$$

The constant, K_g , is a function of the core geometry:

$$K_g = f(A_c, W_a, \text{MLT}) \quad [21-D2]$$

The constant, K_e , is a function of the magnetic and electrical operating conditions:

$$K_e = g(P_o, B_m) \quad [21-D3]$$

The derivation of the specific functions for, K_g and K_e , is as follows: First, assume a dc inductor could be an input or output as schematically shown in Figure 21-D1. The inductor resistance is R_L .

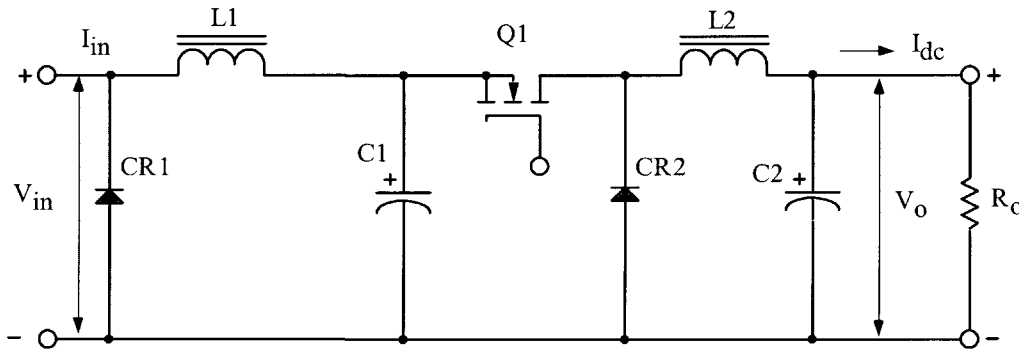


Figure 21-D1. Typical Buck Type Switching Converter.

The output power is:

$$P_o = I_{dc} V_o, \quad [\text{watts}] \quad [21-D4]$$

$$\alpha = \frac{I_{dc} R_L}{V_o} (100), \quad [\%] \quad [21-D5]$$

The inductance equation is:

$$L = \frac{0.4\pi N^2 A_c (10^{-8})}{l_g}, \quad [\text{henrys}] \quad [21-D6]$$

The inductor flux density is:

$$B_{dc} = \frac{0.4\pi N I_{dc} (10^{-4})}{l_g}, \quad [\text{tesla}] \quad [21-D7]$$

Combine Equations [21-D6] and [21-D7]:

$$\frac{L}{B_{dc}} = \frac{N A_c (10^{-4})}{I_{dc}} \quad [21-D8]$$

Solve for N:

$$N = \frac{L I_{dc} (10^4)}{B_{dc} A_c}, \quad [\text{turns}] \quad [21-D9]$$

From the resistivity formula, it is easily shown that:

$$R_L = \frac{(\text{MLT}) N_p^2}{W_a K_u} \rho, \quad [\text{ohms}] \quad [21-D10]$$

Where:

$$\rho = 1.724 (10^{-6}) \text{ ohm cm}$$

Combining Equations [21-D5] and [21-D10]:

$$\alpha = \left(\frac{I_{dc}}{V_o} \right) \left(\frac{(\text{MLT}) N_p^2}{W_a K_u} \rho \right) (100), \quad [\%] \quad [21-D11]$$

Take Equation [21-D9] and square it:

$$N^2 = \left(\frac{L I_{dc}}{B_{dc} A_c} \right)^2 (10^8) \quad [21-D12]$$

Combine Equations [21-D11] and [21-D12]:

$$\alpha = \left(\frac{I_{dc} (\text{MLT})}{V_o W_a K_u} \rho \right) \left(\frac{L I_{dc}}{B_{dc} A_c} \right)^2 (10^{10}) \quad [21-D13]$$

Combine and simplify:

$$\alpha = \left(\frac{I_{dc} (\text{MLT}) (L I_{dc})^2}{V_o W_a K_u B_{dc}^2 A_c^2} \rho \right) (10^{10}) \quad [21-D14]$$

Multiply the equation by I_{dc} / I_{dc} and combine:

$$\alpha = \left(\frac{(\text{MLT})(L I_{dc}^2)^2}{V_o I_{dc} W_a K_u B_{dc}^2 A_c^2} \rho \right) (10^{10}) \quad [21-D15]$$

The energy equation is:

$$\text{Energy} = \frac{L I_{dc}^2}{2}, \quad [\text{watt-second}] \quad [21-D16]$$

$$2\text{Energy} = L I_{dc}^2$$

Combine and simplify:

$$\alpha = \left(\frac{(2\text{Energy})^2}{P_o B_{dc}^2} \right) \left(\frac{\rho (\text{MLT})}{W_a K_u A_c^2} \right) (10^{10}) \quad [21-D17]$$

The resistivity is:

$$\rho = 1.724 (10^{-6}) \quad [\text{ohm cm}] \quad [21-D18]$$

Combine the resistivity:

$$\alpha = \left(\frac{6.89(\text{Energy})^2}{P_o B_{dc}^2} \right) \left(\frac{(\text{MLT})}{W_a K_u A_c^2} \right) (10^4) \quad [21-D19]$$

Solving for energy:

$$(\text{Energy})^2 = 0.145 P_o B_{dc}^2 \left(\frac{W_a A_c^2 K_u}{\text{MLT}} \right) (10^{-4}) \alpha \quad [21-D20]$$

The core geometry equals:

$$K_g = \frac{W_a A_c^2 K_u}{\text{MLT}}, \quad [\text{cm}^5] \quad [21-D21]$$

The electrical conditions:

$$K_e = 0.145 P_o B_{dc}^2 (10^{-4}) \quad [21-D22]$$

The regulation and energy-handling ability is:

$$(\text{Energy})^2 = K_g K_e \alpha \quad [21-D23]$$

The copper loss is:

$$\alpha = \frac{P_{cu}}{P_o} (100), \quad [\%] \quad [21-D24]$$

Inductor Derivation for the Area Product, A_p

Introduction

The energy-handling capability of an inductor can be determined by the area product, A_p . The area product, A_p , relationship is obtained by the following: (Note that symbols marked with a prime (such as H'), are mks (meter-kilogram-second) units.)

$$E = L \frac{dI}{dt} = N \frac{d\phi}{dt} \quad [21-E1]$$

Combine and simplify:

$$L = N \frac{d\phi}{dI} \quad [21-E2]$$

Flux density is:

$$\phi = B_m A_c' \quad [21-E3]$$

$$B_m = \frac{\mu_o NI}{I_g' + \left(\frac{MPL'}{\mu_m} \right)} \quad [21-E4]$$

$$\phi = \frac{\mu_o NI A_c'}{I_g' + \left(\frac{MPL'}{\mu_m} \right)} \quad [21-E5]$$

$$\frac{d\phi}{dI} = \frac{\mu_o N A_c'}{I_g' + \left(\frac{MPL'}{\mu_m} \right)} \quad [21-E6]$$

Combine Equations [21-E2] and [21-E6]:

$$L = N \frac{d\phi}{dI} = \frac{\mu_o N^2 A_c'}{I_g' + \left(\frac{MPL'}{\mu_m} \right)} \quad [21-E7]$$

The energy equation is:

$$\text{Energy} = \frac{LI^2}{2}, \quad [\text{watt-seconds}] \quad [21-E8]$$

Combine Equations [21-E7] and [21-E8]:

$$\text{Energy} = \frac{LI^2}{2} = \frac{\mu_o N^2 A_c' I^2}{2 \left(l_g' + \left(\frac{\text{MPL}'}{\mu_m} \right) \right)} \quad [21-E9]$$

If B_m is specified:

$$I = \frac{B_m \left(l_g' + \left(\frac{\text{MPL}'}{\mu_m} \right) \right)}{\mu_o N} \quad [21-E10]$$

Combine Equations [21-E7] and [21-E10]:

$$\text{Energy} = \frac{\mu_o N^2 A_c'}{2 \left(l_g' + \left(\frac{\text{MPL}'}{\mu_m} \right) \right)} \left(\frac{B_m \left(l_g' + \left(\frac{\text{MPL}'}{\mu_m} \right) \right)}{\mu_o N} \right)^2 \quad [21-E11]$$

Combine and simplify:

$$\text{Energy} = \frac{B_m^2 \left(l_g' + \left(\frac{\text{MPL}'}{\mu_m} \right) \right) A_c'}{2 \mu_o} \quad [21-E12]$$

The winding area of a inductor is fully utilized when:

$$K_u W_a' = N A_w' \quad [21-E13]$$

By definition the wire area is:

$$A_w' = \frac{I}{J'} \quad [21-E14]$$

Combining Equations [21-E13] and [21-E14]:

$$K_u W_a' = N \left(\frac{I}{J'} \right) \quad [21-E15]$$

Solving for I:

$$I = \frac{K_u W_a' J}{N} = \frac{B_m \left(l_g' + \left(\frac{\text{MPL}'}{\mu_m} \right) \right)}{\mu_o N} \quad [21-E16]$$

Rearrange Equation [21-E16]:

$$l'_g + \left(\frac{\text{MPL}'}{\mu_m} \right) = \frac{K_u W'_a J' \mu_o}{B_m} \quad [21-E17]$$

Now, substitute in Energy Equation [21-E11]:

$$\text{Energy} = \frac{B_m^2 \left(\frac{K_u W'_a J' \mu_o}{B_m} \right) A'_c}{2\mu_o} \quad [21-E18]$$

Rearrange Equation [21-E18]:

$$\text{Energy} = \left(\frac{B_m^2 A'_c}{2\mu_o} \right) \left(\frac{K_u W'_a J' \mu_o}{B_m} \right) \quad [21-E19]$$

Combine and simplify:

$$\text{Energy} = \left(\frac{B_m K_u W'_a J' A'_c}{2} \right) \quad [21-E20]$$

Now, multiply mks units to return cgs.

$$W'_a = W_a (10^{-4})$$

$$A'_c = A_c (10^{-4})$$

$$J' = J (10^4)$$

$$\text{MPL}' = \text{MPL} (10^{-2})$$

$$l'_g = l_g (10^{-2})$$

We can substitute into the energy equation to obtain:

$$\text{Energy} = \frac{B_m K_u W_a J A_c}{2} (10^{-4}) \quad [21-E21]$$

Solve for the area product:

$$A_p = W_a A_c$$

$$A_p = \frac{2(\text{Energy})}{B_m J K_u}, \quad [\text{cm}^4] \quad [21-E22]$$

Transformer Regulation

The minimum size of a transformer is usually determined either by a temperature rise limit, or by allowable voltage regulation, assuming that size and weight are to be minimized. Figure 21-F1 shows a circuit diagram of a transformer with one secondary.

Note that $\alpha = \text{regulation } (\%)$.

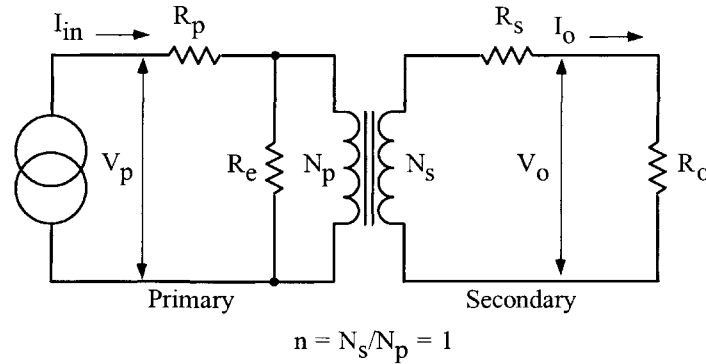


Figure 21-F1. Transformer Circuit Diagram.

The assumption is that distributed capacitance in the secondary can be neglected because the frequency and secondary voltage are not excessively high. Also, the winding geometry is designed to limit the leakage inductance to a level low enough to be neglected under most operating conditions. The transformer window allocation is shown in Figure 21-F2.

$$\frac{W_a}{2} = \text{Primary} = \text{Secondary} \quad [21-F1]$$

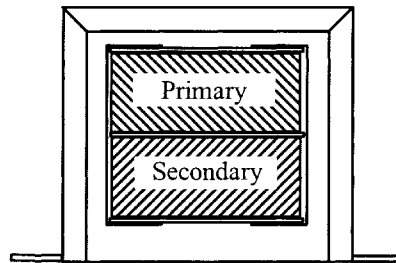


Figure 21-F2. Transformer Window Allocation.

Transformer voltage regulation can now be expressed as:

$$\alpha = \frac{V_o(\text{N.L.}) - V_o(\text{F.L.})}{V_o(\text{F.L.})} (100), \quad [\%] \quad [21-F2]$$

In which, $V_o(\text{N.L.})$ is the no load voltage, and $V_o(\text{F.L.})$ is the full load voltage. For the sake of simplicity, assume the transformer in Figure 21-F1 is an isolation transformer, with a 1:1 turns ratio, and the core impedance, R_e , is infinite.

If the transformer has a 1:1 turns ratio and the core impedance is infinite, then:

$$I_m = I_o, \quad [\text{amps}]$$

$$R_p = R_s, \quad [\text{ohms}] \quad [21-F3]$$

With equal window areas allocated for the primary and secondary windings, and using the same current density, J :

$$\Delta V_p = I_m R_p = \Delta V_s = I_o R_s, \quad [\text{volts}] \quad [21-F4]$$

Regulation is then:

$$\alpha = \frac{\Delta V_p}{V_p}(100) + \frac{\Delta V_s}{V_s}(100), \quad [\%] \quad [21-F5]$$

Multiply the equation by currents, I :

$$\alpha = \frac{\Delta V_p I_m}{V_p I_m}(100) + \frac{\Delta V_s I_o}{V_s I_o}(100), \quad [\%] \quad [21-F6]$$

Primary copper loss is:

$$P_p = \Delta V_p I_m, \quad [\text{watts}] \quad [21-F7]$$

Secondary copper loss is:

$$P_s = \Delta V_s I_o, \quad [\text{watts}] \quad [21-F8]$$

Total copper loss is:

$$P_{cu} = P_p + P_s, \quad [\text{watts}] \quad [21-F9]$$

Then, the regulation equation can be rewritten to:

$$\alpha = \frac{P_{cu}}{P_o}(100), \quad [\%] \quad [21-F10]$$